Metabolic phenotype analysis in patients with pulmonary hypertension

Thesis submitted for the degree of

Doctor of Philosophy

Imperial College London

By

Pavandeep Kaur Ghataorhe

2016

Centre for Pharmacology & Therapeutics

Imperial College London

Hammersmith Hospital

London W12 0NN

Declaration

I declare that this thesis was conducted and written by myself, and the work included is my own unless otherwise stated.

Copyright Declaration

'The copyright of this thesis rests with the author and is made available under a Creative Commons Attribution Non-Commercial No Derivatives licence. Researchers are free to copy, distribute or transmit the thesis on the condition that they attribute it, that they do not use it for commercial purposes and that they do not alter, transform or build upon it. For any reuse or redistribution, researchers must make clear to others the licence terms of this work'

Acknowledgements

I would like to extend my sincerest thanks to Chris Rhodes, John Wharton and Martin Wilkins for their never-ending support, guidance, wisdom and warmth in every aspect of this project. They have provided a wonderful environment for me to work in through their teaching, encouragement, laughter and regular pow-wows! I could not have hoped for a better team and had a happier, more supported experience. A huge and infinite thank you to Chris – you've been an awesome friend, mentor in all things stats/science, patient during my endless chatter, fabulous neighbour even when I crossed the desk line, lunch buddy and challenging debate partner, travel pal for le Paris, pizza/pasta and California dreamin' and the best partner in crime/science (high five!). My deepest thanks to John for always finding the positive (even through data normalisation), helping me strive to do better and for our delightful artistic discussions! Special thanks to Martin as my supervisor for his ongoing inspiration, boundless energy and encouragement through wit and wisdom.

I would like to thank everyone who was involved in the project including the volunteers and patients who donated their samples for this research and the Wellcome Trust for funding my fellowship. I am grateful to the clinical teams at Hammersmith Hospital, our collaborators in the UK and Europe, and Beatriz, Verena and Matt at the Clinical Phenome Centre. Special thanks go to Souad, George and Lavanya for their help obtaining clinical samples and data – you always do so with a smile. Many thanks to Lan Zhao and Ardeschir Ghofrani for their support and guidance during my project. A huge heartfelt thank you to Beata, Geoff, Alex, Kevin, Giusy, Lucie, Lulu, Eduardo, Olivier, Mark, Jerry, Moses, Lei, Waheedah, Ali and the department for their generous support and boosts of encouragement. It was because of you all that I was laughing so loudly in the open plan office!

My deepest thanks and love to my friends and family for their continuous support which kept me smiling and sane. Thank you to my friends, especially Shrina, Ian, Tracey, Shahbaz, Dot, Shelley, Anne-Catherine and Mary, who have shared coffees, calls and messages to keep me going and happy throughout. In particular, I could not have succeeded without my best friend and sister, Kiran who has been there for me throughout. We celebrated the good times with cocktails and university challenge and you listened, helped and encouraged me through every difficulty with love and grace (and sometimes potatoes). My deepest love and thanks to my brother Raj – you tell the best stories and make me laugh no matter what, and are wonderfully positive and kind. I would not be where I am without the love and belief of my parents, and my dad, to whom I am eternally grateful and who has worked so hard for us to succeed. I would like to especially thank Jasper, who became my fiancé during this process. You have been there for me through travels, engagements, successes and hardships, listening (or giving the impression!) to everything there is to know about metabolites and have been my absolute rock throughout.

Abstract

Pulmonary hypertension (PH) is a heterogeneous and progressive disorder leading to right ventricular dysfunction, and carries significant mortality. Diagnosis requires invasive cardiac catheterisation and the pathogenesis of the vascular biology is poorly understood. Metabolic dysregulation has been implicated in PH but there have been no high-throughput analyses of circulating metabolites in these patients.

Using nuclear magnetic resonance spectroscopy, abnormal plasma metabolite levels were identified in patients with pulmonary arterial hypertension (PAH), relating to energy metabolism and lipid regulation, with decreased large high-density lipoprotein subtypes associated with poor survival.

These findings were expanded using unbiased ultra-performance liquid chromatography mass spectrometry methodologies (including lipidomics), which identified novel changes including increased circulating fatty acid acylcarnitines and reduced sphingomyelins and phosphocholines.

To extend the identification of metabolites, samples were also analysed using a commercial metabolomics approach. Semi-quantitative assessment of 1416 metabolites in three cohorts of PAH patients identified metabolites that discriminated PAH patients from controls. These included increased levels of tRNA-specific modified nucleosides, tricarboxylic acid (TCA) cycle intermediates, glutamate, tryptophan and polyamine metabolites and decreased levels of steroids metabolites. The largest differences correlated with increased risk of death and correction of several metabolites over time was associated with better outcomes. Patients who responded to calcium channel blocker therapy had metabolic profiles similar to healthy controls. Metabolic profiling also discriminated patients with other sub-diagnoses of PH from controls.

Variant-metabolite associations published in control populations were validated in PAH patients using data from whole genome sequencing. Mendelian randomisation studies found that these variants did not relate to outcomes in PAH.

In conclusion, this study comprehensively describes metabolic abnormalities in patients with PAH and demonstrates alterations in pathophysiologically-relevant metabolites. Metabolic profiles are strongly related to outcomes and may be used to distinguish patients with poor prognosis or response to therapy and identify potential therapeutic targets.

Contents

Thesis title page 1

Declaration 2

Copyright Declaration 2

Acknowledgements 3

Abstract 4

Contents 5

Figures 10

Tables 13

Chapter 1 – Introduction 19

1.1 Pulmonary vasculature 19

1.2 Pathophysiology of pulmonary hypertension 20

1.2.1 Cellular and molecular changes in pulmonary arterial hypertension (PAH) 23

1.2.2 Right Ventricular (RV) dysfunction in pulmonary arterial hypertension 28

1.2.3 Genetic susceptibility to pulmonary arterial hypertension 29

1.3 Circulating biomarkers in pulmonary arterial hypertension 30

1.3.1 Prognostic markers in pulmonary arterial hypertension 31

1.4 Current treatment of pulmonary arterial hypertension 32

1.4.1 Targeted medical therapy 32

1.4.2 Interventional therapy 35

1.5 Mitochondrial Metabolism 36

1.6 Energy metabolism in pulmonary arterial hypertension 39

1.6.1 Pulmonary vasculature 39

1.6.2 Right ventricle 42

1.6.3 Fatty acid oxidation 42

1.6.4 TCA cycle intermediates 44

1.6.5 Global mitochondrial disturbances 44

1.7 Other metabolic abnormalities in pulmonary arterial hypertension 44
1.8 Metabolomics 53
1.8.1 Metabolomics technologies 53
1.8.2 Metabolomics in disease 54
1.8.3 Metabolomics in pulmonary arterial hypertension 56
1.8.4 Genetic variations associated with metabolite levels 57
1.9 Hypothesis 60
1.10 Objectives 60
Chapter 2 – Materials and methods 61
2.1 Declaration of responsibilities 61
2.2 Sample availability 61
2.3 Sample collection 62
2.3.1 Subjects 62
2.3.2 Samples 62
2.3.3 Outcome measures 62
2.3.4 Clinical Database 63
2.4 Nuclear magnetic resonance (NMR) spectroscopy 63
2.4.1 NMR data acquisition 64
2.4.2 NMR data processing and analysis 67
2.4.3 Identification of NMR signals 69
2.4.4 NMR lipoprotein subclass analysis 69
2.5 Ultra performance liquid chromatography mass-spectrometry (UPLC-MS) 70
2.5.1 Hydrophilic interaction chromatography (HILIC) 72
2.5.2 Lipidomics 73
2.5.3 UPLC-MS data processing and analysis 73
2.5.4 Identification of UPLC-MS peaks 78
2.5.5 Tandem mass spectrometry (MS/MS) 78
2.5.6 Analysis of pure standard compounds 78

2.5.7 Commercial platform (Metabolon) 79
2.6 Enzyme-linked immunosorbent assay (ELISA) 80
2.7 Immunohistochemistry 81
2.8 Targeted fluorometric assays 82
2.9 Whole genome sequencing 82
2.10 Statistical analysis 83
Chapter 3 - Metabolic phenotyping by nuclear magnetic resonance (NMR) spectroscopy in PAH 87
3.1 Introduction 87
3.2 Methods 88
3.3 Results 92
3.3.1 NMR peaks distinguishing between PAH and controls 93
3.3.2 Survival analysis of NMR peaks in PAH 104
3.3.3 High density lipoprotein (HDL) subclass levels and proteomic measures of apolipoprotein (Apo) A1 108
3.4 Discussion 110
Chapter 4 - Metabolic phenotyping using ultra-performance liquid chromatography mass-spectrometry in PAH 117
4.1 Introduction 117
4.2 Methods 118
4.3 Results 124
4.3.1 UPLC-MS peaks associated with drug therapy 126
4.3.2 UPLC-MS peaks distinguishing between PAH and controls 130
4.3.3 Discriminant analyses models to assess performance of best discriminating peaks 134
4.3.4 Survival analysis of UPLC-MS peaks in PAH 135
4.3.5 Identification of peaks of interest 138
4.4 Discussion 139
Chapter 5 - Investigation of metabolic abnormalities in PAH using the Metabolon platform 143
5.1 Introduction 143

5.2 Methods 144
5.2.1 Sample collection 144
5.2.2 Metabolomics 145
5.2.3 Angiogenin 146
5.2.4 Targeted fluorometric assays 146
5.2.5 Immunohistochemistry 146
5.2.6 Statistical analysis 147
5.3 Results 149
5.3.1 Metabolites distinguishing between PAH and controls 149
5.3.2 Discriminant analyses models to assess performance of best discriminating peaks 160
5.3.3 Survival analysis of plasma peaks of interest in PAH 162
5.3.4 Enrichment and clustering of metabolites of interest 166
5.3.5 Analysis of serial samples 169
5.3.6 Association of elevated modified nucleosides with elevated plasma angiogenin 172
5.3.7 Measurement of acetyl-coA and oxaloacetate with targeted fluorometric assays 173
5.3.8 Immunohistochemistry for antibody targets 1-methyladenosine, pseudouridine and angiogenin 174
5.4 Discussion 177
Chapter 6 - Metabolic phenotyping in other sub-diagnoses of pulmonary hypertension using the Metabolon platform 183
6.1 Introduction 183
6.1.1 Chronic thromboembolic pulmonary hypertension (CTEPH) 183
6.1.2 Pulmonary hypertension associated with left heart disease (LHD) 186
6.1.3 Pulmonary hypertension associated with congenital heart disease (CHD) 187
6.1.4 Pulmonary hypertension associated with connective tissue disease (CTD) 187
6.1.5 Metabolic phenotyping in PH sub-diagnoses 188
6.2 Methods 188
6.3 Results 192

6.3.1 Metabolites distinguishing CTEPH patients from controls 192

6.3.2 Metabolic alterations following pulmonary endarterectomy (PEA) surgery in patients with CTEPH 197

6.3.3 Metabolites distinguishing PAH patients, controls and CTEPH patients 202

6.3.4 Metabolites distinguishing other PH sub-diagnoses from controls, and metabolites specific to PAH 205

6.4 Discussion 212

Chapter 7 - Investigation of the genetic influences of metabolic dysregulation in PAH 215

7.1 Introduction 215

7.2 Methods 216

7.3 Results 218

7.4 Discussion 228

Chapter 8 – Conclusions and future work 231

8.1 Metabolic pathway abnormalities in PAH 231

8.2 Current methodology 232

8.3 Utility of metabolomics in PAH 234

8.4 Future studies 235

8.5 Final comments 239

References 241

Appendix 286

Figures

Figure 1.1 – Therapeutic targets in vasoreactive pathways in PAH. 33

Figure 1.2 – Mitochondrial energy metabolism. 37

Figure 1.3 – Steroid hormone biosynthesis. 45

Figure 1.4 – Tryptophan metabolism. 47

Figure 1.5 – Sphingolipid metabolism. 48

Figure 1.6 – Molecular phenotypes with associated genomic mapping. 58

Figure 1.7 – Principles of Mendelian Randomisation. 59

Figure 2.1 – ^{1}H NMR spectra from one dimensional radiofrequency pulse sequences. 66

Figure 2.2 – Multiplicity of NMR peaks. 67

Figure 2.3 – Superimposed ^{1}H NMR spectra from all plasma samples. 68

Figure 2.4 – Principles of high performance LC-MS. 70

Figure 2.5 – UPLC-MS raw spectra. 74

Figure 2.6 – Filtering of UPLC-MS peaks based on dilution series and coefficient of variation. 75

Figure 2.7 – Assessment of UPLC-MS peaks detected across all experimental runs. 77

Figure 2.8 – Assessment of plasma dilutions for angiogenin ELISA. 80

Figure 2.9 – Statistical analysis pipeline. 83

Figure 3.1 – NMR analysis of plasma samples from patients with PAH and controls. 91

Figure 3.2 – Citric acid NMR peak. 96

Figure 3.3 – Creatinine and 3-hydroxybutyrate peaks identified by NMR. 97

Figure 3.4 – Lipid NMR features between PAH patients on and off statin therapy. 102

Figure 3.5 - Prognostic NMR peaks and lipid features. 105

Figure 3.6 – Decreased HDL2a Apo-A2 is prognostic in PAH. 106

Figure 3.7 – Prognostic HDL lipid features. 107

Figure 3.8 – Levels of apolipoprotein A1 and HDL subclasses. 108

Figure 3.9 - High density lipoprotein (HDL) metabolism. 113

Figure 4.1 – UPLC-MS peaks for analysis. 119

Figure 4.2 – Retention time windows in lipidomics positive mode. 120

Figure 4.3 – Identification of palmitoylcarnitine peaks. 122

Figure 4.4 – UPLC-MS peaks representing Bosentan, Sildenafil and Imatinib. 128

Figure 4.5 – Volcano plot of drug metabolites in PAH patients. 130

Figure 4.6 – Analysis flow chart. 131

Figure 4.7 - Discriminant analysis models based on the best distinguishing metabolites between PAH patients and controls. 135

Figure 4.8 - Prognostic identified UPLC-MS peaks. 136

Figure 4.9 – Palmitoylcarnitine UPLC-MS peak which discriminates PAH patients from controls and is prognostic. 137

Figure 5.1 – Analysis flow chart. 152

Figure 5.2 - Dehydroisoandrosterone-sulphate (DHEA-S). 153

Figure 5.3 - Metabolite levels in BMPR2 (bone morphogenetic protein receptor, type 2) mutation carriers. 157

Figure 5.4 - Metabolites which discriminate PAH and control subjects. 158

Figure 5.5 – Network analysis of metabolites which discriminate PAH and control subjects. 159

Figure 5.6 - Discriminant analysis models based on low numbers of metabolites distinguish PAH patients from controls. 161

Figure 5.7 – Survival analysis of PAH patients. 163

Figure 5.8 - Prognostic metabolites independent of established risk factors. 165

Figure 5.9 – Hierarchical clustering of 19 discriminating and prognostic metabolites in PAH patients. 168

Figure 5.10 - Analysis of serial samples. 171

Figure 5.11 - Circulating angiogenin levels. 172

Figure 5.12 – Plasma oxaloacetate levels. 174

Figure 5.13 – Immunostaining for 1-methyladenosine in lung tissue from a PAH patient. 175

Figure 5.14 – Immunostaining for pseudouridine in lung tissue from a PAH patient. 176

Figure 6.1 – Factors influencing the pathogenesis of CTEPH. 185

Figure 6.2 – Principal component analysis (PCA) of metabolite levels in 40 bridging samples. 189

Figure 6.3 – Quantile normalisation. 190

Figure 6.4 - Metabolites which discriminate CTEPH and control subjects. 196

Figure 6.5 – Levels of 5 metabolites which are altered following PEA surgery. 198

Figure 6.6 – Levels of a sphingomyelin (SM) metabolite before and after PEA surgery in paired analysis. 200

Figure 6.7 – Metabolites which discriminate PH sub-diagnoses from controls. 209

Figure 6.8 – Principal component analysis (PCA) of metabolites which distinguish PH sub-diagnoses from controls. 210

Figure 6.9 – N1-methylinosine levels between control and patient groups. 211

Figure 7.1 – SNP-trait (single nucleotide polymorphism) associations with acylcarnitines in PAH patients. 224

Figure 7.2 – SNP-trait associations with steroid hormones in PAH patients. 225

Tables

Table 1.1 – Updated clinical classification of pulmonary hypertension. 22

Table 1.2 – Acylcarnitine carbon chain lengths. 43

Table 1.3 – Evidence for metabolic disturbances in PAH. 53

Table 3.1 – HDL classification and nomenclature. 87

Table 3.2 – NMR Cohort Characteristics. 93

Table 3.3 – NMR peaks distinguishing PAH from healthy and disease controls. 95

Table 3.4 – Lipid NMR features distinguishing PAH patients from healthy and disease controls. 101

Table 3.5 – PAH patients on statin therapy. 103

Table 3.6 – Correlation of HDL subclass levels to apolipoprotein A1. 109

Table 4.1 – Mass adduct calculator. 121

Table 4.2 – UPLC-MS Basic Cohort Characteristics. 124

Table 4.3 – UPLC-MS Cohort Characteristics – haemodynamics, functional status, pathology and drug therapy. 125

Table 4.4 – UPLC-MS peaks representing Bosentan and Sildenafil between PAH patients on and off therapy. 127

Table 4.5 – UPLC-MS peaks representing Bosentan, Sildenafil and Imatinib before and after therapy. 127

Table 4.6 – UPLC-MS peaks affected by Bosentan therapy. 129

Table 4.7 – UPLC-MS peaks distinguishing PAH from healthy controls, disease controls and CTEPH patients. 133

Table 4.8 – Identification of peaks based on tandem MS/MS fragmentation and mass/charge ratio. 138

Table 5.1 – Metabolon Cohort Characteristics. 151

Table 5.2 – Cohort Characteristics of PAH patients who are BMPR2 mutation carriers and non-carriers. 155

Table 5.3 - Pathway enrichment analysis results. 167

Table 5.4 – ROC (receiver operating characteristic) analysis of serial metabolite measurements. 170

Table 5.5 - Demographics and circulating factor levels in subjects used for angiogenin study. 172

Table 5.6 - Demographics and circulating factor levels in subjects used for acetyl-coA study. 173

Table 5.7 - Demographics and circulating factor levels in subjects used for oxaloacetate study. 173

Table 6.1 – Cohorts analysed using the Metabolon platform. 191

Table 6.2 – Cohort Characteristics for CTEPH analysis. 195

Table 6.3 – Cohort Characteristics for CTEPH sub-analysis. 197

Table 6.4 – 8 metabolites significantly different following pulmonary endarterectomy (PEA) surgery in paired analysis. 201

Table 6.5 – Cohort Characteristics of PH sub-diagnoses. 203

Table 6.6 - Metabolites distinguishing PAH from healthy controls, disease controls and CTEPH patients. 204

Table 6.7 - Metabolites distinguishing PH sub-diagnoses from healthy and disease controls. 208

Table 7.1 – Whole Genome Sequencing Cohort Characteristics. 219

Table 7.2 – 38 SNP-trait associations in PAH patients. 223

Table 7.3 – Number of variants associated with metabolites of interest from the Metabolomics GWAS (genome wide association study) server. 227

Appendix Table 2.1 – Products purchased and reference codes. 287

Appendix Table 3.1 – Identities of NMR peaks distinguishing PAH patients from healthy and disease controls. 290

Appendix Table 4.1 – Survival analysis of UPLC-MS peaks in PAH. 294

Appendix Table 5.1 - Metabolites distinguishing PAH from healthy and disease controls. 300

Appendix Table 5.2 - Survival analysis in PAH. 303

Appendix Table 6.1 - Metabolites distinguishing CTEPH from healthy and disease controls. 308

Abbreviations

5-HTT	Serotonin transporter
6MWD	Six minute walk distance
18F-FDG	18F-fluorodeoxyglucose
18F-FTHA	18F-fluoro-6-thioheptadecanoic acid
ABC	Adenosine triphosphate binding cassette transporter
AC	Acylcarnitine
ACADM	Acyl-coenzyme A dehydrogenase
ACE	Angiotensin converting enzyme
Acetyl-CoA	Acetyl co-enzyme A
ACN	Acetonitrile
ADMA	Asymmetric dimethylarginine
AF	Atrial fibrillation
ALK-1	Activin-like receptor kinase-1
AMP	Adenosine monophosphate
ANOVA	Analysis of variance
Anticoag.	Anticoagulation therapy
Apo	Apolipoprotein
ATP	Adenosine triphosphate
Bcl	B-cell lymphoma
BEH	Ethylene Bridged Hybrid
BMI	Body mass index
BMPR2	Bone morphogenetic protein receptor, type 2
BNP	Brain natriuretic peptide
BRC	Biomedical Research Centre
BRIDGE	Biomedical Research Centres Inherited Diseases Genetic Evaluation
BSA	Bovine Serum Albumin
CAD	Coronary artery disease
CAG	Confidentiality advisory group
cAMP	Cyclic adenosine monophosphate
CAV1	Caveolin-1
CBLN2	Cerebellin 2
CCB	Calcium channel blocker
CD20	B-lymphocyte antigen CD20
CETP protein	Cholesteryl ester transfer
cGMP	Cyclic guanosine monophosphate
CHD	Congenital heart disease
CMR	Cardiac magnetic resonance imaging
CoA	Co-enzyme A
Col18a1	Collagen type 18 alpha 1 Chain
COPD	Chronic obstructive pulmonary disease
COSY	Correlation Spectroscopy
COV	Coefficient of variation
CPC	Clinical Phenome Centre
CPMG	Carr–Purcell–Meiboom–Gill
CPT1/2	Carnitine palmitoyltransferase 1/2
CRP	C-reactive protein
CtBP1	C terminal binding protein 1
CTD	Connective tissue disease
CTED	Chronic thromboembolic disease
CTEPH	Chronic thromboembolic pulmonary hypertension
DAG	Diacylglycerol
DC	Disease controls
DCA	Dichloroacetate

DHE	Docosahexaenoyl
DHEA	Dehydroisoandrosterone
DHEA-S	Dehydroisoandrosterone sulphate
DM drugs	Antidiabetic drug therapy
DMSO	Dimethylsulfoxide
DNA	Deoxyribonucleic acid
DPE	Docosapentaenoyl
EDTA	Ethylenediaminetetraacetic acid
EIF	Eukaryotic initiation factor
ELISA	Enzyme-linked immunosorbent assay
ENG	Endoglin
eNOS	Endothelial nitric oxide synthase
EPC	Endothelial progenitor cells
EPE	Eicosapentaenoyl
eQTL	Expression quantitative trait locus
ERA	Endothelin receptor antagonists
ESI	Electrospray ionisation
FAIMS	High Field Asymmetric Waveform Ion Mobility Spectrometry
FAO	Fatty acid oxidation
FATP1	Fatty acid transport protein 1
FHR	Fawn hooded rat
G6P	Glucose-6-phosphate
GCN2	General control nonderepressible 2
GPC	Glycerophosphocholine
GLUT1	Glucose transporter 1
GWAS	Genome wide association studies
HC	Healthy controls
HDAC	Histone deacetylase
HDL	High density lipoprotein
HEPES	4-(2-hydroxyethyl)-1-piperazineethanesulfonic acid
HIF-1 α	Hypoxia inducible factor-1α
HILIC	Hydrophilic interaction chromatography
HK1/2	Hexokinase 1/2
HMDB	Human Metabolome Database
HPAH	Hereditary pulmonary arterial hypertension
hPMVECs	Human pulmonary microvascular endothelial cells
HRA	Health research authority
HSQC	Heteronuclear single quantum coherence
IDL	Intermediate density lipoprotein
IDO	Indoleamine 2,3-dioxygenase
IDO-TM	Indoleamine 2,3-dioxygenase tryptophan metabolites
IHD	Ischaemic heart disease
IL	Interleukin
IPAH	Idiopathic pulmonary arterial hypertension
IQR	Interquartile range
IsoProp	Isopropyl
JRES	J-resolved
KCNA5	Potassium voltage-gated channel subfamily A member 5
KCNK3	Potassium two pore domain channel subfamily K member 3
KEGG	Kyoto Encyclopaedia of Genes and Genomes
KM	Kaplan Meier

LCAT	Lecithin–cholesterol acyltransferase
LDL	Low density lipoprotein
LHD	Left heart disease
LIM	LIM kinases. Lin-11, Islet-1, Mec-3
Lneg	Lipidomics negative mode
Lowess	Locally weighted scatter plot smoothing
Lpos	Lipidomics positive mode
LV	Left ventricle
LXR	Liver X receptor
MCAD	Medium chain acyl coA dehydrogenase
MCT	Monocrotaline
mPAP	Mean pulmonary artery pressure
mQTL	Metabolite quantitative trait locus
MRC	Medical Research Council
MRI	Magnetic resonance imaging
mRNA	Messenger ribonucleic acid
MS	Mass spectrometry
MS/MS	Tandem mass spectrometry
MTA	5-methylthioadenosine
MWAS	Metabolome wide association study
m/z	Mass to charge ratio
NAA	N-acetylaspartate
NADH	Nicotinamide adenine dinucleotide
NFAT	Nuclear factor of activated T cells
NIHR	National Institute for Health Research
NMR	Nuclear magnetic resonance
NO	Nitric oxide
NOESY	1D nuclear Overhauser enhancement Spectroscopy
NT-proBNP	N-terminal brain natriuretic peptide
OPLS-DA	Orthogonal partial least squares discriminant analysis
PA	Pulmonary artery
PAB	Pulmonary artery banding
PAEC	Pulmonary artery endothelial cells
PAH	Pulmonary arterial hypertension
PASMC	Pulmonary artery smooth muscle cells
PAWP	Pulmonary arterial wedge pressure
PC	Phosphocholine
PCA	Principal component analysis
PCWP	Pulmonary capillary wedge pressure
PDE5	Phosphodiesterase type 5
PDGF	Platelet derived growth factor
PDH	Pyruvate dehydrogenase
PDK	Pyruvate dehydrogenase kinase
PE	Pulmonary embolism
PEA	Pulmonary endarterectomy
PET	Positron emission tomography
PFK	Phosphofructokinase
PGIS	Prostacyclin synthase
PH	Pulmonary hypertension
PPAR	Peroxisome proliferator-activated receptor
ppm	Parts per million
pQTL	Protein quantitative trait locus
PVR	Pulmonary vascular resistance

QC	Quality control
Q-Tof	Quadropole-time of flight
QTL	Quantitative trait locus
RAN	Ranolazine
RDW	Red cell distribution width
REC	Research ethics committee
REVEAL	Registry to Evaluate Early and Long-Term Pulmonary Arterial Hypertension Disease Management
RFU	Relative fluorescence units
RNA	Ribonucleic acid
ROC	Receiver operating characteristic
RSID	Reference SNP cluster identifications
RT	Retention time
RV	Right ventricle
RVEF	Right ventricular ejection fraction
RVF	Right ventricular failure
RVH	Right ventricular hypertrophy
SD	Standard deviation
SDMA	Symmetric dimethylarginine
Sig.	Significance
SIRT3	Sirtuin 3
SLC22A4	Solute carrier family 22 member 4
SLE	Systemic lupus erythematosus
SM	Sphingomyelin
Smad	Mothers against decapentaplegic homologue
SNP	Single nucleotide polymorphism
SOD2	Superoxide dismutase-2
SR-BI	Scavenger receptor BI
ST2	Soluble suppression of tumorigenicity
STAT3	Signal transducer and activator of transcription 3
STOCSY	Statistical total correlation spectroscopy
TCA	Tricarboxylic acid
TG	Triglyceride
TGF	Transforming growth factor
TMZ	Trimetazidine
TOCSY	Total Correlation Spectroscopy
TRIPHIC	Translational Research in Pulmonary Hypertension at Imperial College
tRNA	Transfer ribonucleic acid
TSP	Trimethylsilylpropionic acid
UPLC-MS	Ultra-performance liquid chromatography mass spectrometry
VCF	Variant call format
VEGF	Vascular endothelial growth factor
VIP	Vasoactive intestinal peptide
VLDL	Very low density lipoprotein
Vma	Vanillylmandelic acid
VOC	Volatile organic compounds
WGS	Whole genome sequencing
WHO-FC	World Health Organisation functional class

Chapter 1 – Introduction

1.1 Pulmonary vasculature

The pulmonary arterial system is a low pressure circulatory pathway which carries deoxygenated blood from the right ventricle of the heart to the lung, in order to facilitate gas exchange.

The pulmonary arterial trunk arises from the conus arteriosus of the right ventricle and subsequent pulmonary arteries run in parallel alongside conducting airways in the lung, changing their diameter and branching patterns with them (Huang, Yen et al. 1996). The tracheobronchial tree divides from the trachea to bronchi, bronchioles, terminal and respiratory bronchioli, and alveoli, where gas exchange occurs.

Pressure in the pulmonary system is low (mean pulmonary artery systolic pressure 14mmHg) relative to the systemic circulation (Leslie and Wick 2005). Due to this pressure differential, the muscular layer in systemic arteries is thicker than the pulmonary arteries. Pulmonary arteries consist of three distinct layers comprised of the tunica intima, media and adventitia. The tunica intima is the innermost layer and comprises endothelial cells and associated connective tissue, separated from the tunica media by an internal elastic lamina. The media forms the middle layer and comprises circumferentially-arranged pulmonary artery smooth muscle cells and elastic laminae enclosed by an external elastic lamina. The outermost tunica adventitia is comprised of collagen, elastic fibres, and matrix secreting fibroblasts, which provide stability for the blood vessel (Leslie and Wick 2005).

In the proximal pulmonary trunk and larger elastic pulmonary arteries, there are multiple layers of smooth muscle cells interspersed with elastic laminae (for distensibility), and collagen (for rigidity) (Hislop and Pierce 2000). Normally, where the arteries are not distended, the wall thickness is 5% of the external arterial diameter (Leslie and Wick 2005). Distal small pulmonary arteries (<0.1mm diameter) may be muscular or non-muscular and where the muscle is absent, a single elastic lamina separates the intima from the adventitia.

At the level of the alveolar ducts, arterioles subdivide giving rise to an extensive plexus of capillaries that supply each alveolus and make up the bulk of the alveolar wall. In the alveolar wall, the capillary endothelium is directly applied to the basement membrane supporting the alveolar epithelium, providing an interface of minimal thickness for gas exchange (Burri 2006). The alveolar capillary bed gives rise to the pulmonary venules and veins, which transport oxygenated blood back to the heart and systemic circulation (Leslie and Wick 2005). The pulmonary veins run in the interlobular septa

and converge to form larger veins that then accompany bronchi and pulmonary arteries to the hilum. The muscle layer in the pulmonary veins is relatively sparse and near their junction with the left atrium, extra-pulmonary veins are surrounded by a sheath of myocardium (Townsley 2012).

Developmentally, pulmonary arteries begin as endothelial tubes in the mesenchyme around airways and their growth is mediated by a process of vasculogenesis and angiogenesis (Hall, Hislop et al. 2000). Multiple factors regulate the development of the pulmonary vasculature such as platelet derived growth factor (PDGF), fibroblast growth factors and vascular endothelial growth factor (VEGF) (Stenmark and Mecham 1997). Smooth muscle cells grow onto vessels as they line up along the airways, originating from the bronchial smooth muscle layer, the mesenchyme around the arteries and potentially directly from endothelial cells (Hall, Hislop et al. 2000).

In fetal life, blood oxygenation is undertaken by the placenta and bypasses the high-pressure pulmonary circulation. A drop in pressure after birth and the initiation of spontaneous breathing, leads to dilatation and reduced pulmonary arterial pressures, allowing blood flow through the pulmonary vasculature (Hislop and Pierce 2000). With initiation of blood flow through the pulmonary arteries, increased shear stress acts on the endothelial layer to promote the release of vasodilators such as prostacyclin (Hislop and Pierce 2000) and nitric oxide (Hislop, Springall et al. 1995).

1.2 Pathophysiology of pulmonary hypertension

Pulmonary hypertension (PH) is a heterogeneous disease characterised by an imbalance of these vasoactive mediators and remodelling of the normal structure of the pulmonary vasculature (Humbert, Morrell et al. 2004, Rabinovitch 2012, Stacher, Graham et al. 2012). The global prevalence of PH is 1%, and in subjects over 65 years of age, it increases up to 10% (Hoeper, Humbert et al. 2016).

It is defined by a resting mean pulmonary artery pressure (mPAP) ≥25mmHg at rest during right heart catheterisation (Hoeper, Bogaard et al. 2013). Evidence of a mPAP ≥25mmHg is an independent predictor of worse outcomes (Aronson, Eitan et al. 2011, Maron, Hess et al. 2016), however, there is a continuum of risk with borderline PH, classified as mPAP between 19-24mmHg, associated with increased hospitalisations and mortality (Maron, Hess et al. 2016). In addition, patients with mPAP between 21-24mmHg showed an abnormal vascular response with exercise induced PH (mPAP>30mmHg and pulmonary vascular resistance, PVR >3 Wood Units at maximum

exercise), and worse functional parameters than subjects with mPAP<21mmHg (Lau, Godinas et al. 2016).

The 5 main subgroups of pulmonary hypertension are classified based on clinical features, such as the presence of a co-existing disease or genetic heritability, as well as haemodynamic features (Galie, Humbert et al. 2015) (Table 1.1). Most commonly, PH is associated with left heart disease or lung disease (Hoeper, Humbert et al. 2016). Patients present with non-specific symptoms and referral to a specialist centre can often be delayed by several years (Brown, Chen et al. 2011). Diagnosis requires detailed review and investigations, and is guided by a diagnostic algorithm (Galie, Humbert et al. 2015).

Pulmonary arterial hypertension (PAH) characterises a subgroup of PH patients with pre-capillary PH (mPAP≥25mmHg and pulmonary arterial wedge pressure (PAWP) ≤ 15mmHg) and pulmonary vascular resistance (PVR) >3 Wood units, without features of other forms of pre-capillary PH, such as chronic thromboembolic disease, lung disease and rare diseases (Galie, Humbert et al. 2015). Patients with idiopathic pulmonary arterial hypertension (IPAH) are the most common form of PAH and do not have any known risk factor or genetic susceptibility to PAH (Galie, Humbert et al. 2015). Environmental factors such as hypoxia, use of central nervous system stimulants such as cocaine and methamphetamine and anorexigens also contribute to an increased risk of developing PAH (Farber and Loscalzo 2004). The disease carries significant morbidity and mortality with 5 year survival rates of 65% for PAH patients (Farber, Miller et al. 2015).

A multi-centre US based registry for PAH (Registry to Evaluate Early and Long-Term Pulmonary Arterial Hypertension Disease Management -REVEAL registry) indicates an incidence and prevalence of 2.0 and 10.6 cases of PAH per million inhabitants respectively (McGoon, Benza et al. 2013). Registries from the UK show similar incidence and prevalence rates at 1.1 and 6.6 cases of PAH per million inhabitants respectively (Ling, Johnson et al. 2012).

Clinical Classification	Haemodynamic Classification
1. Pulmonary arterial hypertension	Pre-capillary
1.1 Idiopathic	
1.2 Heritable	
1.2.1 *BMPR2* mutation	
1.2.2 *ALK-1, ENG, SMAD9, CAV1, KCNK3* mutations	
1.2.3 Unknown	
1.3 Drugs and toxins induced	
1.4 Associated with:	
1.4.1 Connective tissue disease	
1.4.2 Human immunodeficiency virus (HIV) infection	
1.4.3 Portal hypertension	
1.4.4 Congenital heart disease	
1.4.5 Schistosomiasis	
1'. Pulmonary veno-occlusive disease and/or pulmonary capillary haemangiomatosis*	
1". Persistent pulmonary hypertension of the newborn	
2. Pulmonary hypertension due to left heart disease	Post-capillary
Including left ventricular systolic/diastolic dysfunction, valvular and congenital disease	
3. Pulmonary hypertension due to lung diseases and/or hypoxia	Pre-capillary
Including obstructive, restrictive, interstitial and developmental lung disease	
4. Chronic thromboembolic pulmonary hypertension and other pulmonary artery obstructions	Pre-capillary
4.1 Chronic thromboembolic pulmonary hypertension	
4.2 Other pulmonary artery obstructions	
5. Pulmonary hypertension with unclear and/or multifactorial mechanisms	Pre- & post-capillary

Table 1.1 – Updated clinical classification of pulmonary hypertension. Adapted from (Simonneau, Gatzoulis et al. 2013, Galie, Humbert et al. 2015). Haemodynamic features of each subgroup are also shown. Pre-capillary pulmonary hypertension is defined as mean pulmonary artery pressure (mPAP) ≥25mmHg and pulmonary arterial wedge pressure (PAWP) ≤ 15mmHg, whilst post-capillary pulmonary hypertension is mPAP ≥25mmHg and PAWP >15mmHg. *BMPR2,* bone morphogenetic protein receptor, type 2; *ALK-1*, activin-like receptor kinase-1; *ENG*, endoglin; *CAV1*, caveolin-1; *KCNK3*, potassium two pore domain channel subfamily K member 3. *includes the same subtypes as pulmonary arterial hypertension.

PAH is more commonly seen in women with a 4:1 female: male ratio in the REVEAL registry (Badesch, Raskob et al. 2010), and 72% female in a recent meta-analysis of 1550 PAH patients (Evans, Girerd et al. 2016). The landscape of PAH is changing with earlier registries showing the mean age of PAH patients at 36 years (Rich, Dantzker et al. 1987), whilst more recently, the disease is often seen in the elderly population, and current registries show a mean age between 50-65 years (Badesch, Raskob et al. 2010, Ling, Johnson et al. 2012, Hoeper, Huscher et al. 2013, Galie, Humbert

et al. 2015). Elderly patients diagnosed with PAH (median age 75) have less gender bias than younger patients and a higher mortality, following adjustment for age (Hoeper, Huscher et al. 2013).

1.2.1 Cellular and molecular changes in pulmonary arterial hypertension (PAH)

Pathology:

The pulmonary vasculature has 8 million small arteries of the type that can be affected by PAH, and a loss of more than half of these is required for the clinical and haemodynamic presentation of PAH (Peacock, Naeije et al. 2011). Pulmonary arterial hypertension is characterised by the narrowing of small pulmonary arteries through vasoconstriction, thrombosis, and proliferation and remodelling of the vessel wall (Jeffery and Morrell 2002, Farber and Loscalzo 2004, Humbert, Morrell et al. 2004, Rabinovitch 2012, Stacher, Graham et al. 2012, Tuder, Stacher et al. 2013). Occlusion of the lumen in small distal pulmonary arteries leads to increased pulmonary vascular resistance, and subsequently increased right ventricular (RV) afterload and RV failure, which is the most important determinant of survival in PAH (Humbert, Morrell et al. 2004).

Pulmonary arterial hypertension is characterised by neointimal and plexiform lesions, and intimal and medial hypertrophy, propagated by the proliferative and anti-apoptotic phenotypes of pulmonary endothelial cells, smooth muscle cells, fibroblasts and myofibroblasts (Stacher, Graham et al. 2012). Assessment of explanted lungs from PAH patients showed heterogeneity in the structural remodelling seen within the same lung or between lungs from different patients (Stacher, Graham et al. 2012). When compared to control lungs, intimal fractional thickening was the principal difference seen in PAH lungs, as well as perivascular inflammation and the accumulation of inflammatory and immune cells (Savai, Pullamsetti et al. 2012, Stacher, Graham et al. 2012).

Plexiform lesions are a hallmark of severe end-stage PAH and were seen in all cases of IPAH explanted lungs, and 50% of lungs with associated PAH due to collagen vascular disease (Stacher, Graham et al. 2012). Their distribution in the lung varies significantly in PAH, and the number of plexiform lesions does not relate to haemodynamic measures or the degree of remodelling in the intima and media (Stacher, Graham et al. 2012, Tuder, Stacher et al. 2013). The lesions represent complex vascular structures with disorganised angiogenesis (Cool, Stewart et al. 1999, Tuder, Chacon et al. 2001). This is reflected by endothelial cell proliferation and the incorporation of migrating and proliferating smooth muscle cells and circulating cells such as endothelial progenitor cells and macrophages (Runo and Loyd 2003). The development of these lesions may be triggered by

several factors including shear stress, hypoxia and defects in growth suppressive genes, such as transforming growth factor (TGF)- beta receptor 2 and the pro-apoptotic gene, *Bax* (Yeager, Halley et al. 2001).

The intimal layer is also subject to fibrosis through increased matrix deposition, endothelial cell injury and proliferation, and invasion by cells with myofibroblast characteristics (Schermuly, Ghofrani et al. 2011). Development of a 'neointima', consisting of a layer of extracellular matrix and myofibroblasts between the intimal endothelial cells and internal elastic lamina, is characteristic of severe PAH (Yi, Kim et al. 2000). There is some debate regarding the predominant origin of the cells in the neointima, with evidence of smooth muscle cells, endothelial cells (Qiao, Nishimura et al. 2014) and fibroblasts. Some studies suggest that fibroblasts in the adventitial later are the first cell type to respond to stimuli such as hypoxia, causing them to proliferate and migrate to the intima (Stenmark, Gerasimovskaya et al. 2002). There is also increasing evidence of a transition of pulmonary artery endothelial cells (PAECs) to smooth muscle like mesenchymal cells (endothelial-to-mesenchymal transitioning) due to dysfunctional bone morphogenic protein receptor type II (BMPR2) signalling (Ranchoux, Antigny et al. 2015, Hopper, Moonen et al. 2016, Stenmark, Frid et al. 2016), and these cells may be the source of α-smooth muscle actin expressing cells seen in vascular lesions in PAH. *BMPR2* mutations are the predominant cause of hereditary forms of PAH (HPAH) (Machado, Eickelberg et al. 2009, Soubrier, Chung et al. 2013), and will be discussed in section 1.2.3.

Another key feature of PAH is the muscularisation of small distal pulmonary arteries which normally do not have a muscular layer (Humbert, Morrell et al. 2004), and hyperplasia and proliferation of pulmonary artery smooth muscle cells (PASMCs) (Wagenvoort 1970).

The adventitial layer, and outermost parts of the tunica media, also undergo an increase in neovascularisation of the vaso vasorum, which carries circulating progenitor cells that may also contribute to vessel wall thickening (Davie, Crossno et al. 2004, Humbert, Morrell et al. 2004). Endothelial progenitor cells (EPCs) are important in neovascularisation and vascular repair in the lung (Diller, Thum et al. 2010). However, they may also promote disease progression, and have been localised to vascular lesions in lung tissue from PAH patients, with debate surrounding whether their role is protective or part of the pathogenesis of PAH (Diller, Thum et al. 2010).

It should be noted that in addition to small vessel disease, there are changes to large pulmonary arteries in PAH which exhibit decreased compliance and increased vascular stiffening (Fourie, Coetzee et al. 1992). This is mediated by narrowing and increased wall thickness of extralobar pulmonary arteries, rather than vasoconstriction (Tabima and Chesler 2010), and increased collagen

deposition (Tozzi, Christiansen et al. 1994, Ooi, Wang et al. 2010). Patients with PAH also have evidence of bronchial artery remodelling with angiogenesis and hypertrophy, as well as pulmonary venous involvement (Ghigna, Guignabert et al. 2016). Large lesions connecting the pulmonary artery, pulmonary venous and bronchial artery vasculature have been associated with haemoptysis, in particular in patients with *BMPR2* mutations (Ghigna, Guignabert et al. 2016, Voelkel and Bogaard 2016).

Regulation of vascular tone:

Pulmonary endothelium has a critical role in the regulation of vascular tone and pulmonary endothelial damage and dysfunction is considered to occur early in development of PAH and is associated with an imbalance in vasodilator and vasoconstrictor activity. The key vasoregulatory pathways in PAH included prostacyclin-cAMP (cyclic adenosine monophosphate), nitric oxide-cGMP-PDE5 (cyclic guanosine monophosphate- phosphodiesterase type 5) and endothelin.

Prostacyclins are released by endothelial cells into the pulmonary circulation, and act on G-protein coupled receptors on endothelial, smooth muscle and platelet cells to increase intracellular cAMP (Jakubowski, Utterback et al. 1994). Through this pathway, prostacyclins act to a) promote vasodilatation, b) reduce platelet aggregation (Jakubowski, Utterback et al. 1994) and c) decrease vascular smooth cell proliferation (Wharton, Davie et al. 2000). Pulmonary endothelial cells from patients with severe PAH show decreased expression of prostacyclin synthase (Tuder, Cool et al. 1999), and the use of prostacyclin (epoprostenol) was the first licensed therapy for patients with severe PAH. Thromboxane A2 is another arachidonic acid metabolite like prostacyclin but, in contrast, acts as a vasoconstrictor (Gerber, Voelkel et al. 1980). Metabolites of prostacyclin and thromboxane A2 measured in the urine of patients with PAH, show decreased prostacyclin and increased thromboxane A2 levels respectively (Christman, McPherson et al. 1992).

Nitric oxide is a potent vasodilator synthesised by endothelial nitric oxide synthase (eNOS), which has decreased expression in PAH lung tissue (Giaid and Saleh 1995). Nitric oxide stimulates soluble guanylate cyclase, which in turn activates cGMP signalling, leading to activation of cGMP dependent protein kinases (Chen, Watson et al. 2013). These protein kinases inhibit smooth muscle cell proliferation and cause vasorelaxation (Chen, Watson et al. 2013). In order to upregulate this pathway, cGMP breakdown can be inhibited by blocking phosphodiesterases, which regulate intracellular cGMP levels (Omori and Kotera 2007), in particular phosphodiesterase 5 which is highly expressed in the lung (Wharton, Strange et al. 2005). Phosphodiesterase 5 inhibitors, such as sildenafil, are a licensed treatment for patients with PAH (Galie, Humbert et al. 2015).

Endothelin-1 is mainly produced by endothelial cells and mediates its actions through endothelin receptor A on smooth muscle cells, and endothelin receptor B on both endothelial and smooth muscle cells (Galie, Manes et al. 2004, Shao, Park et al. 2011). In smooth muscle cells, this leads to increased intracellular calcium promoting vasoconstriction, and increased protein kinase C, mitogen activated protein kinase and phosphatidylinositol 3-kinase leading to smooth muscle cell proliferation (Chester and Yacoub 2014). Elevated circulating levels of endothelin-1 are seen in PAH patients (Stewart, Levy et al. 1991) and endothelin receptor antagonists are a key therapeutic strategy for patients with PAH (Galie, Humbert et al. 2015).

In addition, changes to vascular tone have also been attributed to other abnormalities such as down-regulation of potassium channels in PASMCs leading to opening of voltage gated calcium channels (Yuan, Wang et al. 1998), and decreased levels vasoactive intestinal peptide (VIP) (Petkov, Mosgoeller et al. 2003), all of which promote vasoconstriction and also directly promote cellular proliferation (Humbert, Morrell et al. 2004).

Involvement of growth factors and inflammatory cytokines and chemokines:

Several other factors contribute to pulmonary dysfunction in PAH including platelet dysfunction, thrombosis, tryptophan pathway dysregulation and inflammation.

Alterations in platelet function and thrombosis contribute to PAH, either causally or as a response to the disease process (Herve, Humbert et al. 2001, Humbert, Morrell et al. 2004, Johnson, Granton et al. 2006). Increased shear stress and vascular wall injury trigger a pro-thrombotic surface, with increased expression of von Willebrand factor (Collados, Sandoval et al. 1999). In parallel there is decreased fibrinolytic activity, with elevated circulating plasminogen activator inhibitor type 1, an inhibitor of tissue plasminogen activator, in PAH patients (Welsh, Hassell et al. 1996, Herve, Humbert et al. 2001). Increased circulating levels of fibrinopeptide A, a marker of thrombin activity, suggest an elevated intravascular coagulopathy in PAH (Eisenberg, Lucore et al. 1990).

Platelet dysfunction is triggered by vascular abnormalities in PAH to stimulate the release of pro-coagulant factors, as well as factors which mediate vasoconstriction and vascular remodelling such as serotonin, thromboxane A-2, PDGF, TGF-beta and VEGF (Herve, Humbert et al. 2001). Increased levels of serotonin are seen in patients with PAH (Herve, Launay et al. 1995), mediated by overexpression of the serotonin transporter (5-HTT) in PASMCs, platelets and lung tissue (Eddahibi, Humbert et al. 2001), leading to smooth muscle cell proliferation and hypertrophy (Lee, Wang et al. 1994). Increased expression of PDGF and its receptor have been seen in small pulmonary arteries from patients with IPAH and mediate proliferation and migration of PASMCs and fibroblasts (Perros,

Montani et al. 2008). Levels of VEGF and its receptors are increased in the lung in response to hypoxia (Tuder, Flook et al. 1995) and may contribute to abnormal angiogenic pathways underpinning the development of plexiform lesions (Cool, Stewart et al. 1999, Tuder, Chacon et al. 2001) and the pathophysiology of PAH (Farber and Loscalzo 2004).

Inflammation is a key feature of pulmonary hypertension (Rabinovitch 2012, Tuder, Stacher et al. 2013), with increased circulating cytokines, such as interleukin-1 (IL-1) and IL-6, seen in patients with PAH, and associated with worsening clinical outcomes (Soon, Holmes et al. 2010). Lung histology from animal models of severe PAH indicate inflammatory infiltrates in plexiform lesions, as well as increased expression of pro-inflammatory chemokines (Dorfmuller, Chaumais et al. 2011). In addition, patients with PAH associated with connective tissue disease, such as systemic lupus erythematosus (SLE), respond to immunosuppressive therapy (Morelli, Giordano et al. 1993).

Increasing evidence also exists about the role of the neuro-hormonal system both in the pathophysiology of PAH, and as a consequence of the disease process (Maron and Leopold 2015). Aldosterone and angiotensin are known to promote inflammation, vascular remodelling and reduce nitric oxide levels in endothelial cells, and increased levels are seen in the plasma and lungs of patients with PAH (Maron and Leopold 2014).

Understanding of the cellular and molecular basis of PAH requires animal models, such as hypoxia or monocrotaline (MCT) induced models of pulmonary hypertension, as well as studies from human subjects. These studies can be limited by the fact that few animal models can accurately represent the disease process in PAH (Stenmark, Meyrick et al. 2009, Schermuly, Ghofrani et al. 2011).

Exposure of mice and rats to hypoxia provide features of PAH but lack characteristic plexiform lesions and intimal fibrosis (Stenmark, Meyrick et al. 2009), whilst MCT exposure lacks intimal lesions in the distal pulmonary vasculature and leads to multiple off-target systemic effects in the cardiac, renal and hepatic systems (Stenmark, Meyrick et al. 2009, Schermuly, Ghofrani et al. 2011). *BMPR2* knockout mice models only exhibit a mild form of PAH and do not develop RVH (Maarman, Lecour et al. 2013). Fawn hooded rats are very sensitive to hypoxia and develop severe PAH with mild hypoxic exposure (Stenmark, Meyrick et al. 2009). These models have been used to study aerobic glycolysis in PAH (Bonnet, Michelakis et al. 2006, Rehman and Archer 2010), and have features of apoptosis resistance and PASMC proliferation, but also evidence of systemic hypertension, a feature not seen in human patients with PAH (Stenmark, Meyrick et al. 2009). Shunt models of PAH such as pulmonary artery banding show RVH but no features of pulmonary vasculature remodelling (Maarman, Lecour et al. 2013), whilst fetal shunt lamb models have increased pulmonary blood flow

and expression of lung eNOS (Black, Fineman et al. 1998). A rat model of PAH based on VEGF receptor blockade (SU5416) and chronic hypoxia (Sugen-hypoxia model) has shown promise as it develops severe PAH due to obliterative lesions in the pulmonary vasculature (Taraseviciene-Stewart, Kasahara et al. 2001) and shows similar features of drug resistance and RVH and RV failure as in humans (Gomez-Arroyo, Voelkel et al. 2012). In addition to the Sugen-hypoxia model, a combination of monocrotaline treatment and high shear stress through pneumonectomy in rats has also been reported to produce obliterative lesions (Okada, Tanaka et al. 1997). No one animal model fully replicates human PAH, and none have been developed to study other subtypes of PH such as chronic thromboembolic pulmonary hypertension (CTEPH) and left heart disease (LHD). The value of each model is that it provides the opportunity to study different pathways involved in the pathogenesis of PAH (Stenmark, Meyrick et al. 2009, Bonnet, Provencher et al. 2016).

1.2.2 Right Ventricular (RV) dysfunction in pulmonary arterial hypertension

A key feature of PAH is loss of RV function which is associated with poor outcomes and is a key determinant of survival in PAH patients (van de Veerdonk, Kind et al. 2011, Galie, Humbert et al. 2015). Initially RV hypertrophy begins as a means to compensate for increased pressure afterload and raised pulmonary vascular resistance, but it eventually leads to RV ischaemia, impaired RV ejection fraction (RVEF), and RV failure (Voelkel, Quaife et al. 2006). Acute right heart failure in patients with PAH results in hospitalisations requiring intensive care support (Sztrymf, Souza et al. 2010) and has a high mortality rate (Campo, Mathai et al. 2011).

The development of RV failure can vary between patients, despite having similar degrees of RV hypertrophy and pulmonary pressures, with the RV progressively dilating and decompensating more rapidly in some patients than others (Bogaard, Abe et al. 2009, Voeller, Aziz et al. 2011, Vonk-Noordegraaf, Haddad et al. 2013). This is categorised as an adaptive or maladaptive response of the RV – an adaptive response maintains relatively preserved RV ejection fraction with features of concentric hypertrophy and minimal dilatation, while the maladaptive response leads to a RV that is fibrosed, dilated and hypokinetic (Archer, Fang et al. 2013). Understanding the molecular basis for adaptation of the RV, predicting RV dysfunction clinically, and targeting it therapeutically forms a key aspect of the management and treatment of PAH.

1.2.3 Genetic susceptibility to pulmonary arterial hypertension

In cases of familial or heritable PAH (HPAH), mutations in the *BMPR2* gene, which encodes bone morphogenic protein receptor type II, are the predominant genetic cause of the disease (Deng, Morse et al. 2000). BMPR2 is a member of the TGF-beta family (Soubrier, Chung et al. 2013) and mutations in the kinase domain of BMPR2 lead to a detrimental effect on receptor function (Newman, Trembath et al. 2004). BMPR2 is the receptor for multiple bone morphogenic proteins, and acts to suppress vascular smooth muscle cell growth through the intracellular Smad and LIM kinase pathways (Foletta, Lim et al. 2003).

BMPR2 mutations account for more than 75% of familial cases of PAH and 25% of cases with idiopathic PAH (Machado, Eickelberg et al. 2009, Soubrier, Chung et al. 2013). A recent meta-analysis of 1550 patients with idiopathic, heritable or anorexigen forms of PAH, found *BMPR2* mutations in 29% of participants. In those with a known family history of PAH mutations were seen in 82% of patients, and in 17% of cases with no known family history of the disease (Evans, Girerd et al. 2016). *BMPR2* mutation carriers had an earlier onset of disease, higher mPAP and pulmonary vascular resistance, and those who presented earlier had poorer outcomes related to survival and transplantation (Evans, Girerd et al. 2016). Despite the importance of *BMPR2* mutations in the pathobiology of PAH, disease penetrance in carriers is only ~20% and has led to investigation of other genetic and/or environmental factors required for development of the phenotype. Mutations occur less commonly in other genes in the BMP/TGF-beta signalling pathways, including genes encoding activin A receptor type II-like kinase-1 (*ALK1/ACVRL1*), endoglin (*ENG*), *SMAD4* and *SMAD8* (Machado, Eickelberg et al. 2009, Soubrier, Chung et al. 2013). Exome sequencing has also led to the identification of other susceptibility genes, including caveolin-1 (*CAV1*), potassium channel *KCNK3* and cerebellin 2 (*CBLN2*) (Ma and Chung 2014), but mutations in non-BMPR2 genes account for < 5% of PAH cases (Graf & Morrell ERJ 2016).

Common polymorphisms could represent a 'second hit' that effect the manifestation and severity of the disease. For example, variants in the non-coding promoter region of the prostacyclin synthase (*PGIS*) gene may be protective in the development of PAH in unaffected *BMPR2* carriers (Stearman, Cornelius et al. 2014). Mutations in genes such as *KCNA5*, or in the non-coding regions of the *BMPR2* gene, also have the potential to effect the onset and severity of the disease process (Aldred, Machado et al. 2007, Wang, Li et al. 2009, Wang, Knight et al. 2014, Viales, Eichstaedt et al. 2015). In addition, variants in endostatin (collagen type 18 alpha 1 Chain, *Col18a1*) (Damico, Kolb et al. 2015) and the endothelin-1 pathway gene *GNG2* (Benza, Gomberg-Maitland et al. 2015) are associated with clinical outcomes in PAH and may influence the response to treatment.

There is also increasing interest in the non-coding regions such as micro-RNAs (Rhodes, Wharton et al. 2013, Boucherat, Potus et al. 2015) and epigenetic modifications such as DNA and histone methylation which regulate gene function (Huston and Ryan 2016).

1.3 Circulating biomarkers in pulmonary arterial hypertension

A biomarker is defined as "a characteristic that is objectively measured and evaluated as an indicator of normal biological processes, pathogenic processes, or pharmacologic responses to a therapeutic intervention" by the National Institutes of Health Biomarker Definitions Working Group (Biomarkers Definitions Working 2001). There are several criteria required for a vascular biomarker to qualify as a surrogate clinical endpoint – these include validation of the biomarker in a prospective group, additional predictive value above established markers, clinical utility in outcomes for trials or changing therapy and practical considerations such as cost, the ease of use and standardised methodologies to measure the biomarker (Hlatky, Greenland et al. 2009, Vlachopoulos, Xaplanteris et al. 2015).

Circulating biomarkers have multiple functions in clinical practice, from screening and risk management, to diagnosis, prognosis and treatment predictions (Gerszten and Wang 2008). A metabolic example of this in practice is the biomarker haemoglobin A1c, which is used to assess response to therapy in diabetic patients (Lyons and Basu 2012).

In pulmonary hypertension, biomarkers capable of predicting the development of RV dysfunction and prognosis could help target individual patient care, outline underlying disease pathways and provide potential therapeutic targets (Peacock, Naeije et al. 2011, Lewis 2014).

Multiple circulating factors have been proposed for risk stratification and as prognostic biomarkers in PAH. These include markers of inflammation (e.g. C-reactive protein), microRNAs (e.g. microRNA-150), markers of renal impairment (e.g. creatinine, cystatin 2), liver dysfunction (e.g. bilirubin), vascular remodelling (e.g. angiopoetin-2), oxidative stress (e.g. interleukin-6, soluble suppression of tumorigenicity (ST2)), and iron deficiency (e.g. red cell distribution width (RDW)) (Fijalkowska, Kurzyna et al. 2006, Shah, Thenappan et al. 2008, Quarck, Nawrot et al. 2009, Kumpers, Nickel et al. 2010, Takeda, Takeda et al. 2010, Rhodes, Wharton et al. 2011, Cracowski 2012, Rhodes, Wharton et al. 2013, Fenster, Lasalvia et al. 2014, Heresi, Aytekin et al. 2014, Zheng, Yang et al. 2014, Galie, Humbert et al. 2015, Pezzuto, Badagliacca et al. 2015).

Brain natriuretic peptide (BNP) and its N-terminal peptide (NT-proBNP) have been most widely studied, with circulating levels reflecting disease progression and the extent of functional and haemodynamic impairment in PAH patients (Nagaya, Nishikimi et al. 2000, Leuchte, Neurohr et al. 2004, Fijalkowska, Kurzyna et al. 2006, Nickel, Golpon et al. 2012, Fritz, Blair et al. 2013). However, measurement of BNP and NT-proBNP is currently the only circulating biomarker recommended for initial risk stratification and assessment of treatment effect in PAH (Galie, Humbert et al. 2015). Nonetheless, changes in the level of this cardiac-derived protein are affected by renal function and not specific to PAH and diagnosis still requires invasive cardiac catheterisation.

1.3.1 Prognostic markers in pulmonary arterial hypertension

Regular clinical assessment is required to evaluate disease progression, response to therapy and prognosis. Haemodynamic measurements, both at baseline (diagnosis) and during follow-up, are established predictors of disease severity and survival in PAH patients, with right atrial pressure, cardiac index and mixed venous oxygen saturation being the most robust haemodynamic indices of right ventricular function and prognosis (Sitbon, Humbert et al. 2002, McLaughlin, Sitbon et al. 2005, Nickel, Golpon et al. 2012, Rich, Thenappan et al. 2013). However, patients with PAH do not often receive follow up cardiac catheterisations, due to its invasive nature, therefore non-invasive markers that predict disease progression and survival are of key importance.

World Health Organisation functional class (WHO-FC) is a predictor of survival in PAH patients (Benza, Miller et al. 2010, Barst, Chung et al. 2013), and worsening WHO-FC is a marker of disease progression (Nickel, Golpon et al. 2012). Assessment of WHO-FC is made clinically and it is divided into 4 categories; class I are patients who are symptom free at rest or during activity, class II are symptom free at rest but develop symptoms with moderate activity, class III may be symptom free at rest but develop symptoms with light activity and class IV are symptomatic at rest. Assessment of WHO-FC is subjective and variable, however WHO-FC remains a prognostic marker in PAH patients (D'Alonzo, Barst et al. 1991). Six minute walk distance (6MWD) is readily measurable at a clinic visit, and is also a prognostic indicator in PAH (Benza, Miller et al. 2010), however it is limited by the effect of multiple confounding factors such as co-morbidities and age. In addition, a change in 6MWD also does not determine disease progression and survival (Savarese, Paolillo et al. 2012).

Prognosis in PAH is related to right ventricular dysfunction and parameters of RV function, or the presence of a pericardial effusion, based on imaging modalities such as cardiac magnetic resonance imaging (CMR) or echocardiography predict survival in PAH patients (Raymond, Hinderliter et al.

2002, Vonk-Noordegraaf, Haddad et al. 2013, Swift, Rajaram et al. 2014, Courand, Pina Jomir et al. 2015, Badagliacca, Poscia et al. 2016). Although many patients undergo CMR at diagnosis, due to the expense of the procedure it is not conducted regularly at follow-up. There remains scope for a robust and readily measurable circulating marker to predict survival in PAH.

1.4 Current treatment of pulmonary arterial hypertension

Patients with a diagnosis of pulmonary hypertension receive support therapies, comprising oral anticoagulants, diuretics, oxygen, digoxin and other cardiovascular drugs (Galie, Humbert et al. 2015, McLaughlin, Shah et al. 2015). Due to evidence of increased vascular thrombosis, in particular in IPAH (Fuster, Steele et al. 1984), patients with PAH are given oral anticoagulation therapy (Galie, Humbert et al. 2015, McLaughlin, Shah et al. 2015), although outcomes from various trials and registries are variable (Olsson, Delcroix et al. 2014, Preston, Roberts et al. 2015).

If patients show evidence of right ventricular dysfunction and fluid overload, they are given diuretic therapy, with close monitoring of renal function (Cohn 2001). In addition, if there is evidence of hypoxaemia, patients with PAH can be given ambulatory oxygen therapy (Galie, Humbert et al. 2015). Cardiac glycosides, such as digoxin, assist with atrial arrhythmias in PAH patients and can improve cardiac output when given in the acute setting (Rich, Seidlitz et al. 1998).

A substantial proportion of patients with IPAH have evidence of iron deficiency, which is associated with poor outcomes, independent of anemia (Rhodes, Wharton et al. 2011). As a result iron replacement is recommended for patients with evidence of iron deficiency (Galie, Humbert et al. 2015), and a clinical trial is currently ongoing for the use of intravenous iron replacement therapy in IPAH (Howard, Watson et al. 2013).

1.4.1 Targeted medical therapy

A small subset of patients (<10%) with IPAH exhibit pulmonary vasoreactivity when tested with short acting vasodilators during right heart catheterisation, demonstrating a decrease in mPAP ≥10mmHg to an overall mPAP≤40mmHg, and preserved cardiac output (Sitbon, Humbert et al. 2005, Galie, Humbert et al. 2015). These patients can show marked improvements in quality of life and survival and may maintain their haemodynamic response on long-term oral calcium channel blocker therapy, which is recommended (Sitbon, Humbert et al. 2005, Galie, Humbert et al. 2015).

Current approved therapies target the three main vasoactive pathways implicated in PAH, namely - prostacyclin-cAMP, nitric oxide-cGMP-PDE5 and endothelin (Figure 1.1).

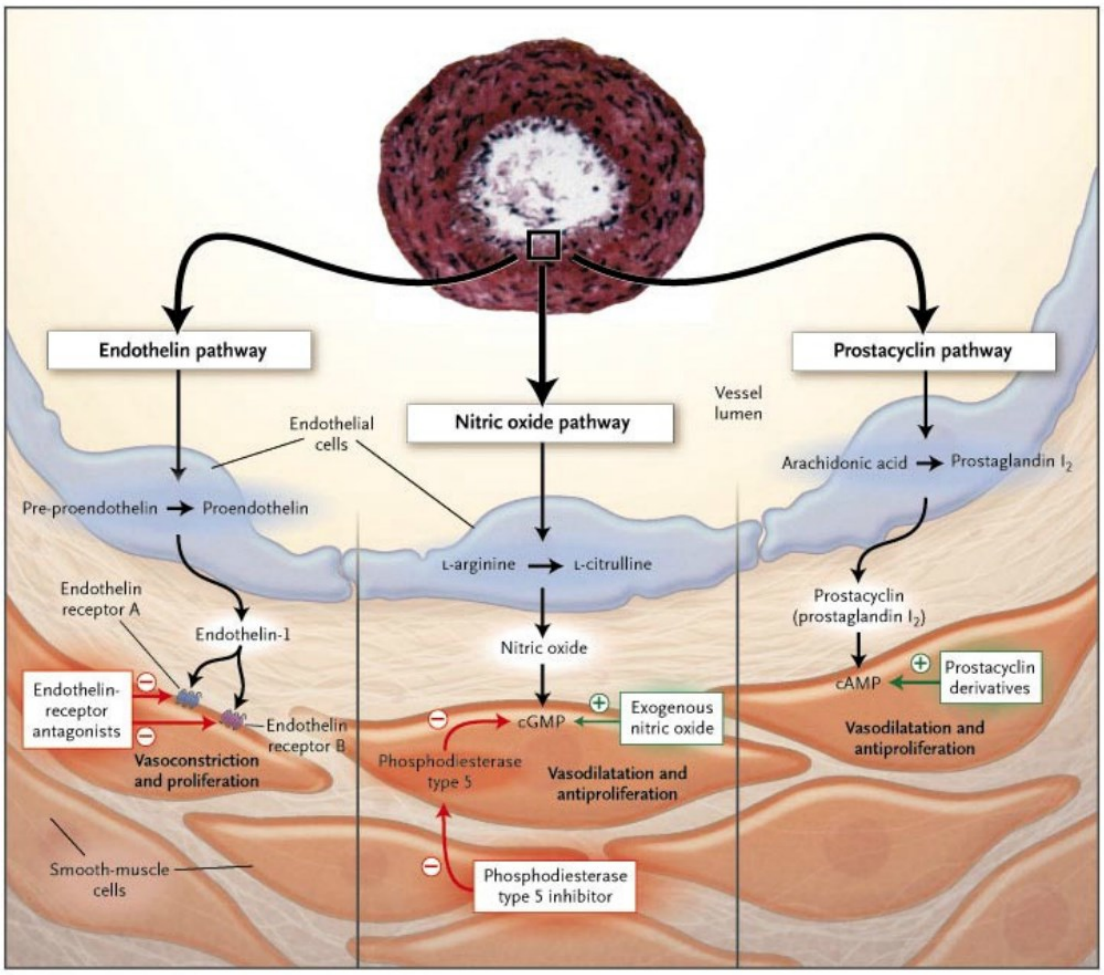


Figure 1.1 – Therapeutic targets in vasoreactive pathways in PAH. Figure from (Humbert, Sitbon et al. 2004) showing the 3 main vasoreactive pathways targeted in PAH. Abnormal and dysfunctional endothelial cells (blue) produce increased endothelin-1 and decreased nitric oxide and prostacyclin, which leads to vasoconstriction and abnormal proliferation of pulmonary artery smooth muscle cells (red). Drug targets are shown which inhibit endothelin receptors and cGMP breakdown (red minus signs) and promote cGMP and cAMP levels (green positive signs). Above, the cross section of a small pulmonary artery from a patient with severe PAH is shown with significant medial hypertrophy and intimal proliferation. cAMP, cyclic adenosine monophosphate; cGMP, cyclic guanosine monophosphate.

Use of prostacyclins is recommended in PAH (Galie, Humbert et al. 2015) and the most commonly used agent, epoprostenol, has shown improvements in haemodynamic measures, functional capacity and mortality in patients with PAH in randomised control trials (Barst, Rubin et al. 1996, Badesch, Tapson et al. 2000). Due to the short half-life of this synthetic agent (3-5 minutes), administration requires continuous intravenous infusion through a pump and can lead to complications from a long-term indwelling catheter such as obstruction and infection, including local and systemic sepsis (Doran, Ivy et al. 2008). Alternative administration routes include through inhalation (iloprost) (McLaughlin, Oudiz et al. 2006) or subcutaneously (treprostonil) (Simonneau, Barst et al. 2002), and both agents can also be given intravenously.

Phosphodiesterase type 5 (PDE5) inhibitors, including sildenafil (Sastry, Narasimhan et al. 2004, Galie, Ghofrani et al. 2005, Singh, Rohit et al. 2006), tadafanil (Galie, Brundage et al. 2009) and vardenafil (Jing, Yu et al. 2011) promote pulmonary vasodilation by inhibition of an enzyme (cyclic guanosine monophosphate, cGMP specific PDE5) that degrades cGMP to promote vasodilatation, as well as having anti-proliferative effects (Tantini, Manes et al. 2005, Wharton, Strange et al. 2005). The use of a direct soluble guanylate cyclase stimulator such as Riociguat has shown promise in animal models and a randomised control trial showed improvement in functional capacity (Ghofrani, Galie et al. 2013), however its use is contraindicated in combination with sildenafil due to hypotension (Galie, Muller et al. 2015).

Endothelin receptor antagonists (ERAs), such as bosentan and ambrisentan, target the pathogenic endothelin pathway in PAH, and are recommended for use based on several randomised control trials (Rubin, Badesch et al. 2002, Galie, Badesch et al. 2005, Galie, Olschewski et al. 2008, Galie, Rubin et al. 2008).

Meta-analysis suggests that the introduction of these therapies has improved the symptoms and clinical end-points of patients with PAH (Galie, Hoeper et al. 2009). More recently, guanylate cyclase stimulators, prostacyclin receptor agonists have been introduced and the efficacy of combination treatment examined (Humbert, Lau et al. 2014). Meta-analysis of 4095 patients enrolled in 17 trials demonstrated that a combination of these PAH-specific therapies is more effective than monotherapy in reducing clinical worsening and improving functional class and exercise capacity (Lajoie, Lauziere et al. 2016). However, a substantial number of patients do not respond to these vasodilator treatments and responsiveness declines with disease progression. There is a need for additional therapies targeting alternative pathways that can reverse pulmonary vascular remodelling, inhibit disease progression and improve survival.

Imatinib is an inhibitor of several tyrosine kinases, including PDGF receptors, and has been shown to inhibit PASMC proliferation and migration during in vitro experiments (Schermuly, Dony et al. 2005, Perros, Montani et al. 2008). Use of this drug was trialled in PAH but is not recommended due to a high rate of serious adverse events and side effects (Frost, Barst et al. 2015). Disappointing results have been found in trials examining other compounds such as statins, VIP and serotonin antagonists (Lythgoe, Rhodes et al. 2016), but greater understanding of the cellular and molecular mechanisms that underlie PAH has led to investigations examining a wide range of other therapeutic targets. These include compounds that target mitochondrial and metabolic function (e.g. dichloroacetate, an inhibitor of pyruvate dehydrogenase kinase, and proliferator-activator receptor agonists), inflammation (e.g. antibodies against B-lymphocyte antigen CD20 and IL-6), RhoA/Rho-kinase signalling, proteases and elastases, intracellular calcium, and epigenetic factors such as histone deacetylase (HDAC) activity and microRNAs (Humbert, Lau et al. 2014). In addition, drugs are being examined that may help restore BMPR2 signalling and there remains the tantalising prospect of gene therapy or stem/progenitor therapies.

1.4.2 Interventional therapy

In patients with advanced disease, interventional techniques can be used but largely as a palliative measure or a bridge to transplantation. These include the use of balloon atrial septostomy, to decreased pressure in the RV and improve cardiac output through a right-to-left heart shunt(Sandoval, Gaspar et al. 1998, Kurzyna, Dabrowski et al. 2007) or use of a veno-arterial extracorporeal membrane oxygenation to bypass the cardiopulmonary system (Olsson, Simon et al. 2010, Rosenzweig, Brodie et al. 2014). Catheter-based therapies are also in development for patients with medication-refractory PAH, including pulmonary artery denervation using radiofrequency ablation (Chen, Zhang et al. 2015, Rothman, Arnold et al. 2015).

Although medical and interventional strategies to target PAH have developed over the last three decades, mortality rates remain high with variable response to therapy. The 3 main therapeutic arms using PDE5 inhibitors, ERAs, and prostacyclins focus on specific molecular pathways in a complex and diverse disease process. In order to find novel treatment strategies, focus has shifted to other molecular pathways involved in PAH such as metabolic dysfunction, which has a pathogenic effect in the pulmonary vasculature, right ventricle and through global mitochondrial dysfunction.

1.5 Mitochondrial Metabolism

Metabolic changes are thought to be key features of the molecular pathophysiology of PAH, forming the 'metabolic theory of PAH', and may provide novel therapeutic targets (Cottrill and Chan 2013, Sutendra and Michelakis 2013, Paulin and Michelakis 2014, Sutendra and Michelakis 2014, Ryan and Archer 2015). Central to this has been the study of energy metabolism in the mitochondria, which also has a role as an oxygen sensor and in inflammation, epigenetic modifications, apoptosis and cellular growth (Sutendra and Michelakis 2014).

The three major pathways of energy metabolism are predominantly active in the mitochondria and comprise glucose oxidation, fatty acid oxidation, and glutaminolysis (Ryan and Archer 2015) (Figure 1.2). All three processes share certain properties; a) driving the tricarboxylic acid (TCA) cycle for adenosine triphosphate (ATP) production, b) requiring substrate transport from the cytosol to the mitochondria and c) being reciprocally related to one another (Ryan and Archer 2015).

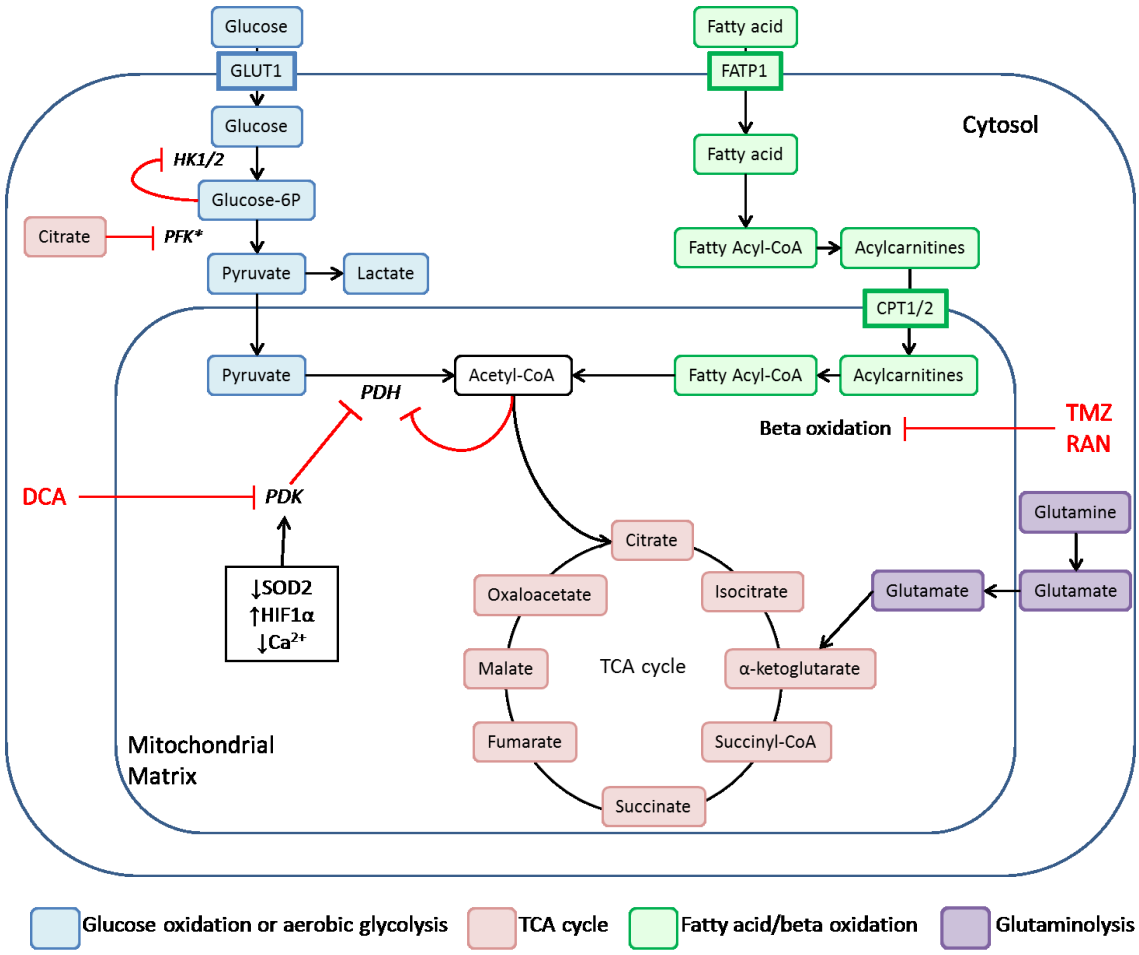


Figure 1.2 – Mitochondrial energy metabolism. Adapted from (Ryan and Archer 2015). The three main energy pathways in the mitochondria are shown including fatty acid/beta oxidation (green), glucose oxidation/aerobic glycolysis (blue) and glutaminolysis (purple) which feed into the tricarboxylic acid (TCA) cycle (pink). Acetyl-coA produces *citrate which is transported from the mitochondria to the cytosol where it inhibits phosphofructokinase (PFK) and glucose oxidation (Randle effect). Increased pyruvate dehydrogenase kinase (PDK) inhibits pyruvate dehydrogenase (PDH) and glucose oxidation, leading to aerobic glycolysis and the generation of lactate (Warburg effect). Dichloroacetate (DCA) directly inhibits PDK to restore glucose oxidation. Drugs such as ranolazine (RAN) and trimetazidine (TMZ) inhibit fatty acid oxidation. *citrate is transported from the mitochondria to the cytosol where it inhibits phosphofructokinase (PFK). GLUT1, glucose transporter 1; glucose-6P, glucose 6 phosphate; HK1/2, hexokinase 1/2; CoA, co-enzyme A; SOD2, superoxide dismutase-2 ; HIF-1 α, hypoxia inducible factor-1α; Ca2+, calcium; CPT1/2, carnitine palmitoyltransferase 1/2; FATP1, fatty acid transport protein 1.

Glucose oxidation is an efficient form of ATP generation in cells, and responsible for 48% of ATP produced in control rat models of the RV (Piao, Sidhu et al. 2013). The process begins in the cytosol, where glucose is converted to pyruvate and enters the mitochondria. Here it acts as a substrate for pyruvate dehydrogenase (PDH) which converts pyruvate to acetyl co-enzyme A (CoA), to enter the TCA cycle for ATP generation (Randle, Garland et al. 1965, Ryan and Archer 2015).

Fatty acid oxidation is the predominant source of energy in the heart. During this process, fatty acyl CoA converts fatty acids to long chain acyl coenzyme A esters, which are transported from the cytosol to the mitochondria. Here they are converted to long chain acylcarnitines by carnitine palmitoyltransferase, and produce acetyl CoA through the process of beta oxidation to enter the TCA cycle (Reuter and Evans 2012). Despite a high level of energy production, generating 48 ATPs for 6 carbons in the fatty acid chain (Ryan and Archer 2015), fatty acid oxidation carries a higher oxygen demand (10% greater) relative to glucose oxidation for the same level of ATP (Abozguia, Clarke et al. 2006). In the normal state, the RV can alternate it's energy source between either fatty acid or glucose oxidation (Archer, Fang et al. 2013).

In glutaminolysis, glutamine is converted to glutamate in the cytosol and transported to the mitochondria, where it is converted to alpha-ketoglutarate and enters the TCA cycle, providing minimal energy rewards to the cell (Piao, Fang et al. 2013).

Metabolic plasticity allows each of the energy pathways to influence one another. A key example is the Randle effect where fatty acid oxidation inhibits the process of glucose oxidation (Randle, Garland et al. 1965). Citrate, formed in fatty acid oxidation, causes accumulation of glucose-6-phosphate (G6P) by inhibiting phosphofructokinase. In turn, G6P inhibits hexokinase to reduce the production of pyruvate, a key substrate in glucose oxidation (Archer, Fang et al. 2013). In addition acetyl CoA generated from fatty acid oxidation, inhibits PDH to reduce the glucose oxidation pathway (Archer, Fang et al. 2013).

The Warburg effect describes the process where glucose oxidation becomes uncoupled from the TCA cycle into the less efficient 'aerobic glycolysis' (Warburg and Kaiser Wilhelm-Institut für Biologie (Berlin). 1926), generating only 2 ATPs per mole of glucose (Archer, Fang et al. 2013). The shift to aerobic glycolysis also leads to a concomitant increase in glutaminolysis (Ryan and Archer 2015). Initially described in cancer cells, the Warburg effect is driven by an inhibition of PDH by pyruvate dehydrogenase kinase (PDK) halting the process of glucose oxidation despite adequate oxygenation and leading to a build-up of pyruvate in the cytosol, and the generation of lactate (Warburg and Kaiser Wilhelm-Institut für Biologie (Berlin). 1926). Whilst giving cancerous cells an advantage to

survive and grow, aerobic glycolysis makes other cells more prone to hypertrophy and proliferation and encourages angiogenesis (Ryan and Archer 2015). Increased glutaminolysis also provides amino acid intermediates that support cell growth and proliferation (Piao, Fang et al. 2013).

1.6 Energy metabolism in pulmonary arterial hypertension

In pulmonary hypertension, there is a shift to aerobic glycolysis, mediated predominantly by PDK inhibition of PDH (Cottrill and Chan 2013), in both the pulmonary vasculature and the right ventricle (Archer, Fang et al. 2013). This has led to comparisons between the pathobiology of PAH and cancerous cells (Tuder, Stacher et al. 2013, Paulin and Michelakis 2014, Sutendra and Michelakis 2014) where cells which exhibit aerobic glycolysis in the pulmonary vasculature, with increased markers such as GLUT-1 and hexokinase-1, are hyperproliferative and apoptosis-resistant (Marsboom, Wietholt et al. 2012, Paulin and Michelakis 2014).

Reversal of this process to restore glucose oxidation, either directly or by exploiting the Randle cycle to decrease fatty acid oxidation and glutaminolysis, provides a potential therapeutic target for patients with PAH. Administration of dichloroacetate (DCA), to directly inhibit PDK, improves both pulmonary vascular disease and right ventricular function in animal models of PAH (Michelakis, McMurtry et al. 2002, McMurtry, Bonnet et al. 2004, Guignabert, Tu et al. 2009, Piao, Sidhu et al. 2013), and is currently under investigation in patients with PAH (http://www.clinicaltrials.gov; NCT01083524).

1.6.1 Pulmonary vasculature

A metabolic shift to aerobic glycolysis has been reported in the pulmonary vasculature in various cell types including endothelial cells (Xu, Koeck et al. 2007), smooth muscle cells (Bonnet, Michelakis et al. 2006) and fibroblasts (Li, Riddle et al. 2016).

Pulmonary artery endothelial cells from the lung of IPAH patients have an increased ^{3}H-glucose glycolytic rate and decreased oxygen consumption compared to healthy controls. In addition, increased 18F-fluorodeoxyglucose (18F-FDG) uptake, a glucose analog taken up by cells through the glucose transporter -1 (GLUT-1), is seen in pulmonary artery endothelial cells using positron emission tomography (PET) imaging in IPAH patients compared to controls, indicated a shift to aerobic glycolysis (Xu, Koeck et al. 2007).

Mitochondrial remodelling and a shift to aerobic glycolysis have multiple downstream effects in PASMCs including apoptosis-resistance, hyper-proliferation, effects on downstream cellular signalling and regulation of epigenetic mechanisms and inflammation (Sutendra and Michelakis 2013, Paulin and Michelakis 2014, Sutendra and Michelakis 2014).

An increase in the mitochondrial membrane potential and reduced mitochondrial reactive oxygen species, seen in PASMCs in PAH (Bonnet, Michelakis et al. 2006), leads to closure of the mitochondrial transition pore which would otherwise allow pro-apoptotic mediators into the mitochondria from the cytoplasm (Zamzami, Marchetti et al. 1996). Activation of the transcription factor nuclear factor of activated T cells (NFAT) may also stimulate anti-apoptotic mediators of the B-cell lymphoma (bcl)-2 group (Macian 2005).

In PASMCs, as well as a reduction in the levels of mitochondrial reactive oxygen species, there is also decreased alpha-ketoglutarate production, which affects multiple signalling pathways. These include a) inhibition of potassium channels and reduced calcium levels in the mitochondria (Michelakis, Thebaud et al. 2004, Archer, Gomberg-Maitland et al. 2008), b) activation of NFAT which, other than apoptosis-resistance, can activate proliferation, suppress potassium channels and promote mitochondrial suppression (Macian 2005) and c) activation of hypoxia inducible factor-1α (HIF-1α) which suppresses potassium channels and promotes cell proliferation (Bonnet, Michelakis et al. 2006).

A predominant cause of the shift to aerobic glycolysis is inhibition of PDH. In the pulmonary vasculature, this is in part mediated by the activation of HIF-1α (Papandreou, Cairns et al. 2006). Whilst oxygen availability is normal, reduced reactive oxygen species in the mitochondria of pulmonary artery smooth muscle cells, mediated by reduced mitochondrial superoxide dismutase-2 (SOD2) (Archer, Marsboom et al. 2010), lead to activation of HIF-1α and up-regulation of PDK in a 'pseudohypoxic' environment (Bonnet, Michelakis et al. 2006). Increased expression of HIF-1α has been demonstrated in PAECs from IPAH patients (Fijalkowska, Xu et al. 2010). In animal models, increased 18F-FDG PET uptake in the lung was localised to PASMCs and associated with activation of HIF-1α (Marsboom, Wietholt et al. 2012).

PDH is also inhibited by decreased levels of mitochondrial calcium, a feature of PAH, caused by endoplasmic reticulum stress from triggers such as hypoxia, inflammation (Hotamisligil 2010) and *BMPR2* mutations (Sobolewski, Rudarakanchana et al. 2008). A deficiency in uncoupling protein 2 in mice leads to decreased mitochondrial calcium, and the development of pulmonary hypertension (Dromparis, Paulin et al. 2013). In addition, mice lacking sirtuin 3 (*SIRT3*), an activator of PDH,

develop spontaneous PAH and have decreased PDH activity, and a loss of function polymorphism in *SIRT3* is found more frequency in IPAH patients versus controls (Paulin, Dromparis et al. 2014).

Adventitial fibroblasts from patients with PAH also show evidence of aerobic glycolysis, associated with an increase in free nicotinamide adenine dinucleotide (NADH) levels and expression of the NADH sensor C-terminal binding protein 1 (CtBP1) (Li, Riddle et al. 2016). Decreasing NADH in hypoxic mice decreased aerobic glycolysis, proliferation and vascular remodelling (Li, Riddle et al. 2016).

As well as the Warburg effect, there is also evidence of other metabolic shifts in the pulmonary vasculature, such as increased fatty acid oxidation. In mice models of hypoxia, an absence of malonyl-coenzyme-A-decarboxylase inhibits fatty acid oxidation, thus promoting glucose oxidation and halting the shift to aerobic glycolysis through the Randle cycle. This protects the pulmonary vasculature from abnormal proliferation and vasoconstriction seen in pulmonary hypertension (Sutendra, Bonnet et al. 2010).

Several other factors may also influence mitochondrial metabolism in the pulmonary vasculature in PAH including iron homeostasis, peroxisome proliferator activated receptor gamma (PPARγ) signalling, and mitochondrial fusion and fission (Paulin and Michelakis 2014, Gurtu and Michelakis 2015). Iron-sulphur clusters are formed in the mitochondria, and are required for the electron transport chain, as well as being components of TCA cycle enzymes (Rouault and Tong 2008). Iron deficiency without the presence of anaemia is seen in PAH patients and is prognostic (Rhodes, Wharton et al. 2011) and iron-deficient rats show evidence of pulmonary vascular remodelling, mitochondrial depolarisation, increased expression of HIF-1α and increased lung 18F-FDG uptake (Cotroneo, Ashek et al. 2015). PAH is associated with insulin resistance (Zamanian, Hansmann et al. 2009), and patients with PAH have decreased apolipoprotein E (ApoE) and PPARγ expression in the lungs. These are both associated with insulin resistance, and treatment of ApoE deficient mice with rosiglitazone (a PPARγ agonist) reverses PH (Hansmann, Wagner et al. 2007). Increased mitochondrial fission is mediated by dynamin related protein 1 in PASMCs, inhibition of which reduces smooth muscle cell proliferation (Marsboom, Toth et al. 2012). Mitochondrial fusion is reduced due to decreased expression of mitofusin-2 and PPARγ coactivator 1-α, and by increased mitofusin-2 expression in PASMCs, and by increasing mitofusin-2 expression, fusion was increased leading to increased apoptosis and decreased PASMC proliferation (Ryan, Marsboom et al. 2013). Changes to mitochondrial dynamics, including fusion and fission, influence mitochondrial function and may provide novel therapeutic targets in PAH (Ryan, Dasgupta et al. 2015).

1.6.2 Right ventricle

In the myocardium, metabolic remodelling is driven by coronary ischaemia due to right ventricular hypertrophy (Gomez, Bialostozky et al. 2001, Archer, Fang et al. 2013). This promotes a switch to aerobic glycolysis in RV myocytes (Piao, Marsboom et al. 2010, Ryan and Archer 2014), a process which is less efficient, but protects the cells from potential apoptosis and promotes rapid cell turnover for subsequent ventricular hypertrophy. However, through secondary lactate generation aerobic glycolysis leads to acidosis (Ryan and Archer 2015), electrical remodelling, and impaired RV contractility and cardiac output (Piao, Fang et al. 2010, Piao, Sidhu et al. 2013). Evidence suggests that the maladaptive RV phenotype is due to RV coronary ischaemia and increased aerobic glycolysis (Archer, Fang et al. 2013).

Increased aerobic glycolysis can be visualised in patients with PAH through increased RV 18F-FDG uptake during PET imaging (Oikawa, Kagaya et al. 2005), and an increased uptake ratio between the RV and left ventricle is prognostic in IPAH patients (Li, Wang et al. 2015). As well as increased 18F-FDG uptake, PAH patients show increased uptake of 18F-fluoro-6-thioheptadecanoic acid (FTHA), a marker of fatty acid oxidation, which is related to reduced RVEF (Ohira, deKemp et al. 2015). Through the Randle cycle, elevated fatty acid oxidation inhibits glucose oxidation, to promote aerobic glycolysis.

Inhibition of fatty acid oxidation in the right ventricle, to promote glucose oxidation, is beneficial in animal models of PAH (Guarnieri and Muscari 1988, Guarnieri and Muscari 1990). Use of ranolazine and trimetazidine, licensed anti-anginal and anti-ischaemic agents, in animal models of RVH reduce fatty acid oxidation, increase PDH activity and restored glucose oxidation to improve cardiac output and exercise capacity (Fang, Piao et al. 2012). A phase 1 trial for the use of ranolazine in PAH showed that it was safe but plasma concentrations of the drug did not reach levels considered to be therapeutic in PAH patients on background therapies (Gomberg-Maitland, Schulz et al. 2015). Inhibition of glutaminolysis, which is up-regulated in the myocardium in animal models of PAH, can also restore glucose oxidation, to reverse RVH and improve cardiac output (Piao, Fang et al. 2013).

1.6.3 Fatty acid oxidation

In addition to the Warburg effect, the hypertensive pulmonary vasculature and the right ventricle both exhibit evidence of elevated fatty acid oxidation. Disruption of carnitine homeostasis, with increased levels of acylcarnitines, has been associated with mitochondrial dysfunction and reduced

endothelial NO signalling in lung tissue from a fetal lamb shunt model of pulmonary hypertension (Sharma, Sud et al. 2008) and cultured pulmonary artery endothelial cells exposed to endothelin-1 (Sun, Kumar et al. 2014). Acylcarnitines vary in chain length and are formed when acyl groups are transferred from acyl-coA to carnitine (Table 1.2) (Sharma and Black 2009). Increased circulating levels of long chain acylcarnitines have been measured in PAH patients versus controls (Brittain, Talati et al. 2016).

Acylcarnitines	**Carbon chain length**
Short chain acylcarnitines (C1-C5)	
Acetylcarnitine	C2
Propionylcarnitine	C3
Butyrylcarnitine	C4
Isovalerylcarnitine	C5
Medium chain acylcarnitines (C6-C12)	
Hexanoylcarnitine	C6
Octanoylcarnitine	C8
Octenoylcarnitine	C8:1
Decanoylcarnitine	C10
Cecenoylcarnitine	C10:1
Lauroylcarnitine	C12
Long chain acylcarnitines (C14-C22)	
Myristoylcarnitine	C14
Myristoleylcarnitine	C14:1
Palmitoylcarnitine	C16
Palmitoleylcarnitine	C16:1
Stearoylcarnitine	C18
Oleoylcarnitine	C18:1
Hydroxymyristoylcarnitine	C14OH
Hydroxypalmitoylcarnitine	C16OH
Hydroxypalmitoleylcarnitine	C16:1OH
Hydroxyoleylcarnitine	C18:1OH

Table 1.2 – Acylcarnitine carbon chain lengths. Adapted from (Meyburg, Schulze et al. 2001). Acylcarnitines are grouped based on their carbon chain length into short-, medium- and long chain acylcarnitines.

1.6.4 TCA cycle intermediates

The TCA cycle is the key energy generator in the mitochondria. It links all 3 pathways of energy metabolism and is affected by shifts to aerobic glycolysis and increased fatty acid oxidation. This is reflected in circulating measurements of TCA cycle intermediates (Lewis, Farrell et al. 2010). Analysis of PAH lung tissue from humans has shown increased expression of metabolites in the TCA cycle, notably citrate and succinate (Zhao, Peng et al. 2014). Analysis of human pulmonary microvascular endothelial cells from patients with pathogenic *BMPR2* mutations showed depletion of TCA intermediates distal to citrate (Fessel, Hamid et al. 2012).

1.6.5 Global mitochondrial disturbances

Although multi-organ involvement in PAH may be secondary to reduced cardiac output and pulmonary dysfunction, there is evidence that global mitochondrial dysfunction can, in part, explain diffuse abnormalities in PAH – such as intrinsic RV dysfunction independent of increased afterload, insulin resistance, skeletal muscle abnormalities and generalised inflammatory responses (Paulin and Michelakis 2014). Rather than the current therapeutic strategies in PAH which target one specific pathogenic pathway (such as prostacyclins), an agent such as DCA can target global mitochondrial molecular disturbances in parallel (Paulin and Michelakis 2014). However, targeting mitochondrial disturbances non-specifically has an increased risk of toxicity and decreased efficacy.

1.7 Other metabolic abnormalities in pulmonary arterial hypertension

Several other metabolic pathways have been implicated in the pathobiology of pulmonary arterial hypertension, including steroid, arginine, polyamine, tryptophan and sphingolipid metabolism.

Reduced circulating levels of dehydroisoandrosterone sulfate (DHEA-S, also known as dehydroepiandrosterone sulfate) have been associated with PAH in a small cohort of 23 male patients compared to healthy controls (Ventetuolo, Baird et al. 2015). DHEA-S is the sulfated form of dehydroisoandrosterone (DHEA), which is the most abundant circulating steroid and an intermediate in the biosynthesis of androgen and estrogen sex steroids (Figure 1.3).

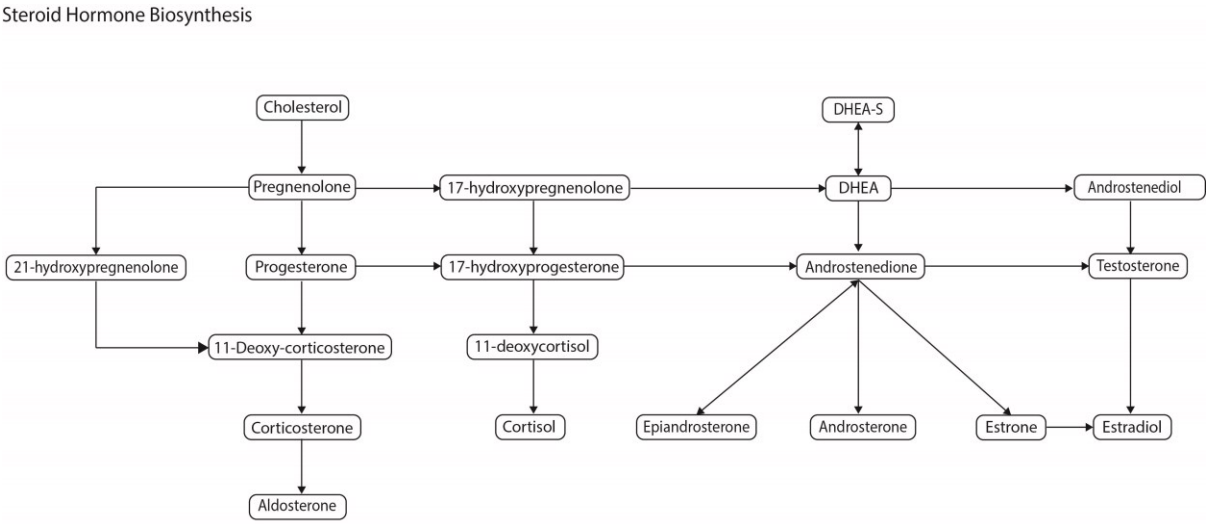


Figure 1.3 – Steroid hormone biosynthesis. Adapted from (Mostaghel 2014). Pathways leading to the production of the major steroid hormones and sex hormones are shown. DHEA, dehydroisoandrosterone; DHEA-S, dehydroisoandrosterone sulphate.

In keeping with the view that DHEA has a protective role in the cardiovascular system, treatment with DHEA or DHEA-S has repeatedly been shown to prevent and reverse pulmonary hypertension and cardiopulmonary remodelling in experimental rat models (Bonnet, Dumas-de-La-Roque et al. 2003, Hampl, Bibova et al. 2003, Homma, Nagaoka et al. 2008, Alzoubi, Toba et al. 2013). Inhibition of monocrotaline-induced PH and normalisation of RhoA/ROCK-associated proteins, a key pathway in the pathogenesis of PAH, were seen in monocrotaline-induced rat models of PAH treated with DHEA (Homma, Nagaoka et al. 2008). In chronic hypoxia rat models treated with DHEA, pulmonary artery tissue shows increased levels of soluble guanylate cyclase protein expression and improved pulmonary vasodilator response (Oka, Karoor et al. 2007).

In humans, a small population of eight patients with COPD associated PH were given 3 month treatment of DHEA orally and were noted to have improvements in the functional parameter, six-minute walk distance, and PVR (Dumas de La Roque, Savineau et al. 2012), with a larger double-blind placebo control trial in progress.

It is now apparent that DHEA and DHEA-S can act as ligands for nuclear receptors and plasma membrane G-protein-coupled receptors and affect a variety of cell types (Prough, Clark et al. 2016).

For example, *in vitro* studies have shown that DHEA activates endothelial nitric oxide synthases (eNOS) in human endothelial cells (Liu and Dillon 2002, Chen, Lin et al. 2008) and attenuates the proliferative and anti-apoptotic phenotype of PASMCs derived from PAH patients through the Src/STAT3 (signal transducer and activator of transcription 3) pathway (Paulin, Meloche et al. 2011). Enzymes responsible for the metabolism of DHEA are also expressed in peripheral tissues such as the lung (Labrie, Luu-The et al. 2001).

Decreased arginine bioavailability and increased plasma and tissue levels of asymmetric dimethylarginine (ADMA) and symmetric dimethylarginine (SDMA), endogenous nitric oxide synthase (eNOS) inhibitors, are associated with reduced nitric oxide signalling and vascular dysfunction in pulmonary hypertension (Budhiraja, Tuder et al. 2004, Pullamsetti, Kiss et al. 2005). Endothelial cells from PAH patients express raised levels of arginase II, which competes with eNOS for L-arginine (Xu, Kaneko et al. 2004). Increased levels of plasma ADMA have been reported in patients with IPAH and are associated with worsening clinical outcomes, including survival (Kielstein, Bode-Boger et al. 2005). Interestingly, exposure of lamb model pulmonary arterial endothelial cells to ADMA not only induces redistribution of eNOS to the mitochondria, but also increased acylcarnitine levels and subsequent mitochondrial dysfunction, which is reversed by the administration of L-arginine (Sun, Sharma et al. 2013). Administration of oral L-arginine to 19 patients with pre-capillary pulmonary hypertension showed improvement in haemodynamics and exercise capacity (Nagaya, Uematsu et al. 2001).

As well as nitric oxide, polyamines are also a product of L-arginine and several animal models of PAH have demonstrated evidence of increased polyamine levels and metabolism in lung tissue (Hoet and Nemery 2000). Administration of monocrotaline in rats led to significantly increased levels of polyamines and the development of PAH and RVH, which could be prevented by the administration of an inhibitor of polyamine biosynthesis (Olson, Atkinson et al. 1985).

The importance of serotonin, a tryptophan metabolite, in the pathophysiology of PAH has been well-studied (Herve, Launay et al. 1995, Eddahibi, Humbert et al. 2001, Guignabert, Raffestin et al. 2005), and there is increasing evidence that other metabolites of the tryptophan pathway (Figure 1.4) are also altered in PAH. Measurement of plasma concentrations of kynurenine, a tryptophan metabolite, showed significantly elevated levels in 26 PAH patients compared to healthy controls, and are related to adverse outcomes and altered immunity (Jasiewicz, Moniuszko et al. 2016).

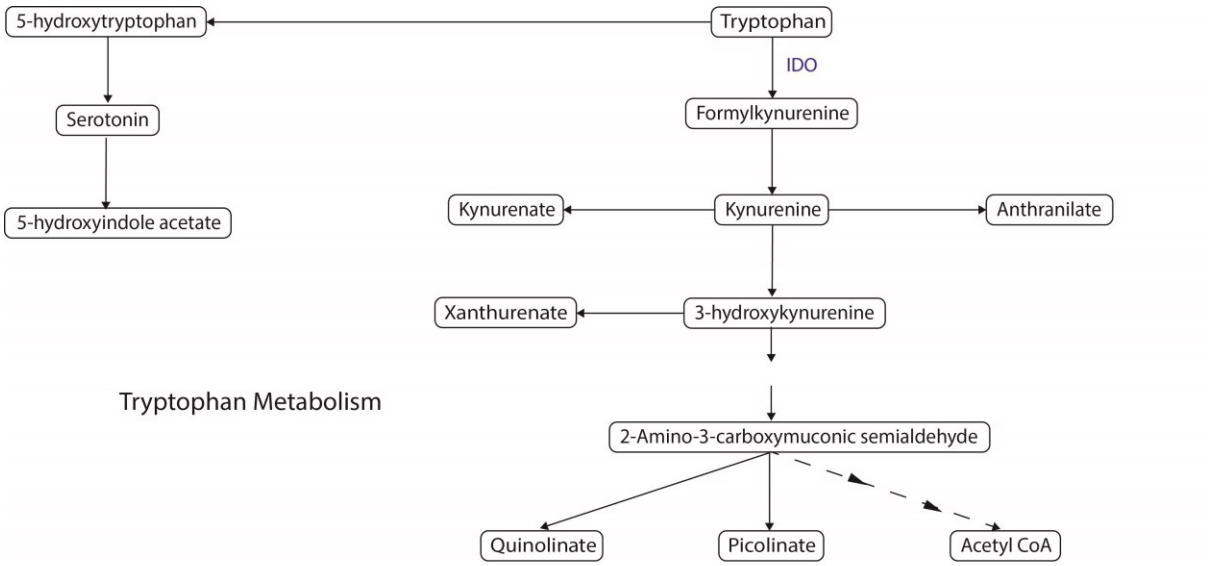


Figure 1.4 – Tryptophan metabolism. Adapted from (Chhabra 2013). The tryptophan metabolic pathway is shown including the generation of serotonin and kynurenine, which subsequently leads into the tricarboxylic acid cycle through acetyl co-enzyme A (CoA). IDO; indoleamine 2,3-dioxygenase. IDO-TM (tryptophan metabolites) include kynurenine, kynurenate, anthranilate and quinolinate (Lewis, Ngo et al. 2016).

Sphingomyelins are the most abundant subclass of sphingolipids, with other subclasses including sphinogosines, ceramides and glycosphingolipids (Figure 1.5) (Ogretmen and Hannun 2004, Hannun and Obeid 2008). Dysregulation of sphingolipid metabolism has been implicated in several cardiovascular and pulmonary disorders. In patients with COPD, low plasma levels of several sphingomyelins were inversely related to disease severity (Bowler, Jacobson et al. 2015). Up-regulation of the pulmonary sphingosine kinase 1/sphingosine-1-phosphate pathway has been found in patients with PAH, as well as being associated with increased PASMC proliferation *in vitro* and pulmonary vascular remodelling in experimental pulmonary hypertension (Chen, Tang et al. 2014).

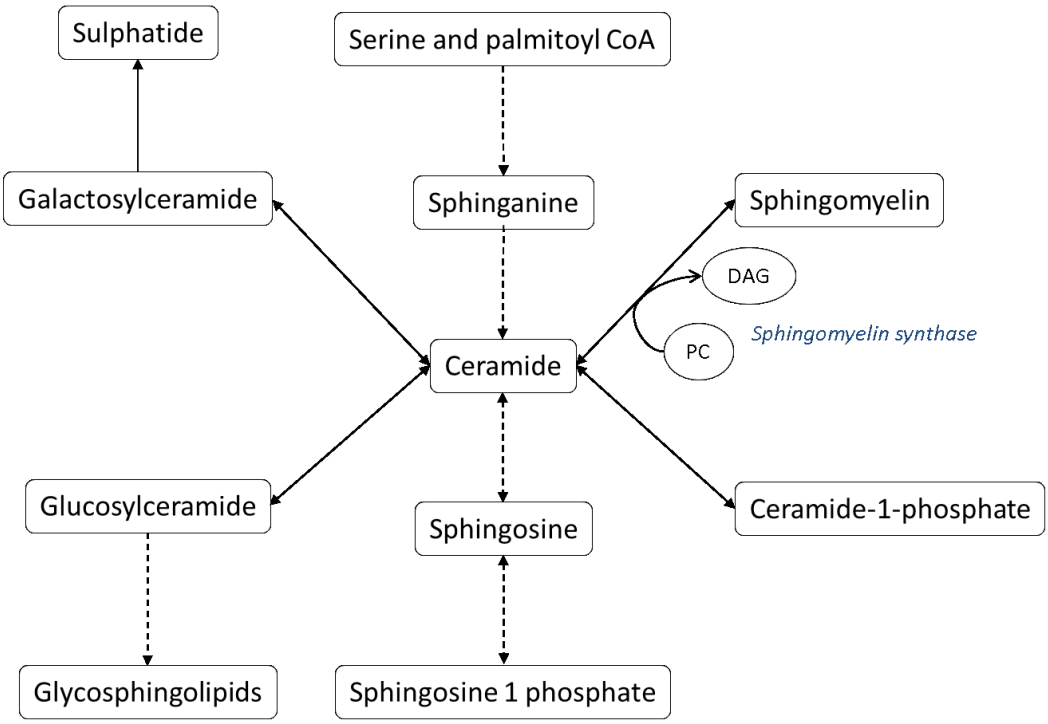


Figure 1.5 – Sphingolipid metabolism. Adapted from (Ogretmen and Hannun 2004). Sphingomyelins are the most common subclass of sphingolipid and produced from ceramide and the conversion of phosphatidylcholines (PC) to diacylglycerol (DAG) by sphingomyelin synthase.

Overall, a diverse range of metabolic abnormalities have been identified in PAH (Table 1.3). Many metabolomic changes occur in energy metabolism and the mitochondria and may be apparent in the circulation as well as affected tissues.

Metabolic pathway	***In vivo* evidence in PAH**	***In vitro* evidence in PAH**	**Evidence in PAH patients**
Energy (aerobic glycolysis)	-Prevention and reversal of RVH and PAH with DCA (PDK inhibitor) in over-expression of 5-HTT mice, FHR and chronic hypoxic and MCT rat models (Michelakis, McMurtry et al. 2002, McMurtry, Bonnet et al. 2004, Bonnet, Michelakis et al. 2006, Guignabert, Tu et al. 2009, Piao, Fang et al. 2010, Piao, Sidhu et al. 2013) -HIF1α up-regulation of PDK in FHR (Bonnet, Michelakis et al. 2006) -↓ Mitochondrial SOD2 and HIF1α up-regulation in FHR mediates PAH; reversed by DCA (Archer, Marsboom et al. 2010) -↑HIF1α mediated lung 18F-FDG PET uptake in MCT rat models (Marsboom, Wietholt et al. 2012) -Decreasing NADH in hypoxic mice decreases aerobic glycolysis, proliferation and vascular remodelling (Li, Riddle et al. 2016)	-↑Glycolytic rate in PAECs(Xu, Koeck et al. 2007) -↑HIF1α expression in PAECs (Fijalkowska, Xu et al. 2010) - ↓ Mitochondrial SOD2 in PASMCs; reversed by DCA (Archer, Marsboom et al. 2010) -↑Aerobic glycolysis in PA adventitial fibroblasts associated with increased NADH levels and CtBP1 expression (Li, Riddle et al. 2016)	-↑Lung 18F-FDG PET uptake (Xu, Koeck et al. 2007) - ↑RV 18F-FDG PET uptake(Oikawa, Kagaya et al. 2005) -↑RV/LV 18F-FDG PET uptake is prognostic in PAH (Li, Wang et al. 2015) -↑Exhaled acetaldehyde (by-product of shift to aerobic glycolysis) in PAH patients versus controls (Cikach, Tonelli et al. 2014) -↑Glucose, sorbitol, fructose and fructose-6-phosphate in lung tissue PAH patients versus controls (Zhao, Peng et al. 2014) -↑Plasma lactate and pyruvate in PAH patients versus controls (Bujak, Mateo et al. 2016)
Energy (fatty acid oxidation, FAO)	-Improved cardiac mitochondrial function, increased PDH, cardiac output and exercise capacity after FAO inhibition with trimetazide and ranolazine in MCT and PAB rat models (Guarnieri and Muscari 1988, Guarnieri and Muscari 1990, Fang, Piao et al. 2012) -↑Acylcarnitines in shunt lamb models(Sharma, Sud et al. 2008) -Knockout malonyl coenzyme-A decarboxylase (inhibiting FAO) protects from PAH(Sutendra, Bonnet et al. 2010) -↑Long chain fatty acids in *BMPR2* mutant mouse RV versus controls(Talati, Brittain et al. 2016)	-↑Acylcarnitines in PAECs exposed to endothelin-1(Sun, Kumar et al. 2014)	-↑RV 18F-FTHA PET uptake (Ohira, deKemp et al. 2015) -↑Plasma long chain acylcarnitines in PAH patients versus controls (Brittain, Talati et al. 2016) -↑Long chain fatty acids; tetradecanedioate, hexadecanedioate, octadecanedioate, adrenate, caproate, caprylate, myristate and palmitoleate in lung tissue PAH patients versus controls (Zhao, Peng et al. 2014) -↑Free fatty acids, glycerol and long chain acylcarnitines in PAH patients versus controls (Bujak, Mateo et al. 2016)
Energy (TCA cycle intermediates)		-↓Succinate, fumarate and malate in hPMVEC with pathogenic *BMPR2* mutations(Fessel, Hamid et al. 2012)	-↑Citrate and succinate in lung tissue PAH patients versus controls (Zhao, Peng et al. 2014) -↑Plasma malate, succinate, aconitate, isocitrate and α-ketoglutarate correlate to pulmonary haemodynamics (Lewis, Ngo et al. 2016)
Energy (glutamino-lysis)	-↑Glutaminolysis in RVH and improvement following inhibition of glutaminolysis in MCT rat model (Piao, Fang et al. 2013)		-↑Exhaled ammonia (by-product of glutamine breakdown) correlates to disease severity (Cikach, Tonelli et al. 2014) -↑Plasma glutamine PAH patients versus controls (Bujak, Mateo et al. 2016)

Metabolic pathway	*In vivo* evidence in PAH	*In vitro* evidence in PAH	Evidence in PAH patients
Steroid	-Improvement in RVH and PAH after DHEA treatment in chronic hypoxic, SUGEN and MCT rat models (Bonnet, Dumas-de-La-Roque et al. 2003, Hampl, Bibova et al. 2003, Oka, Karoor et al. 2007, Homma, Nagaoka et al. 2008, Alzoubi, Toba et al. 2013)	-DHEA activates eNOS in PAECs (Liu and Dillon 2002, Chen, Lin et al. 2008) -DHEA inhibits SrC/STAT3 pathway in PASMCs (Paulin, Meloche et al. 2011)	-↓Plasma DHEA-S in male PAH patients versus controls (Ventetuolo, Baird et al. 2015) -Haemodynamic and functional improvement with DHEA administration in COPD-associated PH (Dumas de La Roque, Savineau et al. 2012)
Arginine and nitric oxide	-↑ADMA/SDMA in plasma and lung tissue from MCT rat models (Pullamsetti, Kiss et al. 2005) -Exposure to ADMA induces mitochondrial dysfunction in lamb model (Sun, Sharma et al. 2013)	-↑Arginase II in PAECs (Xu, Kaneko et al. 2004) -ADMA pro-proliferative in PAECs (Chen, Strauch et al. 2014)	-↑ADMA/SMDA in plasma and lung tissue (Pullamsetti, Kiss et al. 2005) -↑Plasma ADMA, associated with worse survival(Kielstein, Bode-Boger et al. 2005) -L-arginine improves functional and haemodynamic parameters in pre-capillary pulmonary hypertension (Nagaya, Uematsu et al. 2001) -↓Arginine and ↑creatine, ornithine and urea in lung tissue from PAH patients versus controls (Zhao, Chu et al. 2015) -↓Plasma arginine and arginine/(ornithine+citrulline) ratio correlate to pulmonary haemodynamics (Lewis, Ngo et al. 2016)
Polyamine	-↑Polyamine levels and metabolism in lung tissue from chronic hypoxic and MCT rat models (Hoet and Nemery 2000) -MCT increases polyamine levels, RVH and PAH; reversed by inhibitor of polyamine biosynthesis (Olson, Atkinson et al. 1985)	-Spermine inhibits PASMC proliferation (Wei, Li et al. 2016)	-↑Putrescine in lung tissue from PAH patients versus controls (Zhao, Chu et al. 2015)
Tryptophan	-Inhibition of serotonin receptor in MCT rat models and knockout of tryptophan hydroxylase-1 in mice inhibits development of PAH (Guignabert, Raffestin et al. 2005, Izikki, Hanoun et al. 2007, Morecroft, Dempsie et al. 2007) -↑Endothelial indoleamine 2,3-dioxygenase expression protects from chronic hypoxic PAH in mice (Xiao, Christou et al. 2013)	-↑Serotonin leads to PASMC proliferation (Lee, Wang et al. 1994) -Overexpression of 5-HTT mediates increased PASMC proliferation; reversed by 5-HTT inhibitor (Eddahibi, Humbert et al. 2001) -Endothelial-derived indoleamine 2,3-dioxygenase is proapoptotic and antiproliferative in PASMCs (Xiao, Christou et al. 2013)	-↑Plasma serotonin PAH patients versus controls (Herve, Launay et al. 1995) -↑Plasma kynurenine in PAH patients versus controls (Jasiewicz, Moniuszko et al. 2016) -↓Plasma tryptophan in PAH patients versus controls (Bujak, Mateo et al. 2016) -↑Plasma kynurenine, anthralinate and quinolinate correlate to pulmonary haemodynamics (Lewis, Ngo et al. 2016)
Sphingolipid	-Sphingosine-1-phosphate knockout mice protected from hypoxic PAH (Chen, Tang et al. 2014)	-↑Sphingosine-1-phosphate in PASMCs, promoting proliferation (Chen, Tang et al. 2014)	-Trend to increased galactosylsphingosine, sphinganine, sphingosine and palmitoyl sphingomyelin in lung tissue from PAH patients versus controls (Zhao, Chu et al. 2015) -↑Plasma sphingosine in PAH patients versus controls (Bujak, Mateo et al. 2016)

Metabolic pathway	***In vivo* evidence in PAH**	***In vitro* evidence in PAH**	**Evidence in PAH patients**
			-↑Sphingosine-1-phosphate in lung tissue PAH versus controls (Chen, Tang et al. 2014)
Volatile organic compounds (VOCs)			-↑Exhaled VOCs, including ammonia, correlate with disease severity in PAH(Cikach, Tonelli et al. 2014) -↑Exhaled VOCs, including benzene, methane and propanoic acid, discriminate severe PAH and controls (Mansoor, Schelegle et al. 2014)
Heme		-Biliverdin reductase and bilirubin anti-apoptotic in PASMCs (Song, Wang et al. 2013)	-Iron deficiency (independent of anemia) prognostic in PAH (Rhodes, Wharton et al. 2011) -↑Plasma bilirubin prognostic in PAH (Takeda, Takeda et al. 2010) -↑Bile acid metabolites in lung tissue PAH patients versus controls (Zhao, Yun et al. 2014) -↑Bilirubin and biliverdin in lung tissue from PAH patients versus controls (Zhao, Chu et al. 2015)
Xylose			-↑Plasma threitol in PAH patients versus controls (Bujak, Mateo et al. 2016)
Fatty acid amides			-↑Plasma palmitamide, stearamide and oleamide in PAH patients versus controls (Bujak, Mateo et al. 2016)
Cholesterol			-↓Plasma HDL prognostic in PAH (Heresi, Aytekin et al. 2010, Zhao, Peng et al. 2012, Larsen, McCully et al. 2016) -↑Plasma cholesterol derived bile acids, glycochenodeoxycholate sulphate and deoxycholic acid 3-glucuronide in PAH patients versus controls (Bujak, Mateo et al. 2016)
Purine		-Uric acid leads to increased arginase activity and decreased NO in PAECs(Zharikov, Krotova et al. 2008)	-↑Plasma uric acid, associated with worse survival (Nagaya, Uematsu et al. 1999, Voelkel, Wynne et al. 2000, Bendayan, Shitrit et al. 2003) -↑Plasma xanthine, xanthosine, uric acid and inosine correlate to pulmonary haemodynamics (Lewis, Ngo et al. 2016)
Others			-↑Plasma aminomalonic acid in PAH patients versus controls (Bujak, Mateo et al. 2016) -↑Plasma ceraldehyde, glucuronate, cAMP, vma, aminoisobuytric acid and cystathionine correlate to pulmonary haemodynamics (Lewis, Ngo et al. 2016)

Table 1.3 – Evidence for metabolic disturbances in PAH. RV, right ventricle; LV, left ventricle; RVH right ventricular hypertrophy; DCA, dichloroacetate; PDK, pyruvate dehydrogenase kinase; PDH, pyruvate dehydrogenase; 5-HTT,serotonin transporter; FHR, fawn hooded rats; MCT, monocrotaline; CtBP1, C terminal binding protein 1; HIF1α, hypoxia inducible factor-1α; SOD2, superoxide dismutase-2; 18F-FDG, 18F-fluorodeoxyglucose; 18F-FTHA, 18F-fluoro-6-thioheptadecanoic acid; PET, positron emission tomography; PAEC, pulmonary artery endothelial cells; PASMCs, pulmonary artery smooth muscle cells; FAO, fatty acid oxidation; PAB, pulmonary artery banding; hPMVECs, human pulmonary microvascular endothelial cells; *BMPR2,* bone morphogenetic protein receptor, type 2; DHEA, dehydroisoandrosterone; DHEA-S dehydroisoandrosterone sulphate; eNOS, endothelial nitric oxide synthase; NO, nitric oxide; STAT3, signal transducer and activator of transcription 3; COPD, chronic obstructive pulmonary disorder; ADMA, asymmetric dimethylarginine; SDMA, symmetric dimethylarginine; VOC, volatile organic compounds; HDL, high density lipoprotein; cAMP, cyclic adenosine monophosphate; vma, vanillylmandelic acid; PAH, pulmonary arterial hypertension.

1.8 Metabolomics

1.8.1 Metabolomics technologies

'Metabolomics' describes the metabolic composition of a sample at a given time, whereas an alternative term 'metabonomics' has been used to describe the metabolic response to changes such as disease, nutrition and drug therapy over time (Nicholson, Holmes et al. 2012). Nevertheless, the two terms are now used interchangeably and I refer to metabolomics throughout this thesis.

Metabolomic technologies enable the simultaneous detection and semi-quantitative measurement of hundreds of unique metabolites, representing a broad range of metabolic pathways, in small volumes of biofluids (Holmes, Wilson et al. 2008, Nicholson and Lindon 2008, Evans, DeHaven et al. 2009, Dunn, Broadhurst et al. 2011). Experiments are most often conducted using nuclear magnetic resonance (NMR) spectroscopy and mass spectrometry (MS) (Nicholson and Lindon 2008). Use of these technologies on biofluids, such as plasma and urine samples, provides a 'metabolic phenotype' that reflects both genetic and environmental factors (Holmes, Wilson et al. 2008, Nicholson and Lindon 2008). Direct metabolomic profiling, using body fluids and tissue samples, can also provide *in vivo* information on disease processes and therapeutic interventions (Nicholson, Lindon et al. 1999).

Thus applications for the use of metabolomics include a) profiling in the population to assess for susceptibility to disease and the development of diagnostic biomarkers, b) profiling individuals for risk stratification and to predict outcomes and response to therapy and c) understanding molecular pathways in a disease for identification of novel therapeutic targets (Nicholson and Lindon 2008, Nicholson, Holmes et al. 2012).

Both NMR and MS require small amounts of sample (10 to 400 µL) to identify and quantify a range of small molecules (Nicholson, Holmes et al. 2012). ^{1}H NMR spectra are created by detecting hydrogen-containing molecules, encompassing nearly all metabolites, within a sample and untargeted profiling can typically identify ~200 high-abundance metabolites (Dumas, Kinross et al. 2014). NMR spectroscopy has a detection limit in the sub-micromolar range and is highly reproducible whereas MS has much lower detection limits, but is destructive and tends to be less reproducible (Nicholson, Holmes et al. 2012). There is also no pre-treatment to the biological fluid prior to NMR analysis, whereas in MS, chromatography is used to separate the metabolites from the rest of the biological fluid (Nicholson and Lindon 2008). Coupling of ultra-performance liquid chromatography with MS enables the measurement of more than 5000 uncharacterized metabolic features, but the identification of unassigned and potentially new metabolites remains challenging (Dumas, Kinross et al. 2014).

Untargeted metabolomics platforms provide a comprehensive, extensive and unbiased approach to metabolic profiling; however, targeted assays are increasingly used for semi-quantitative information on a smaller number of defined, identified metabolites (Dumas, Kinross et al. 2014). Untargeted metabolomics provides information on a large dataset and robust statistical approaches are required to analyse this data with consideration of confounding factors such as drug therapy. In addition, confirmation of identifies requires a targeted approach with analysis of authentic standards and fragmentation patterns (Baig, Pechlaner et al. 2016). However, an advantage of metabolomics over other systems biology approaches such as genomics and proteomics is the more readily available clinical samples such as plasma and urine, and the lower cost of the assays per sample (Nicholson, Holmes et al. 2012).

1.8.2 Metabolomics in disease

NMR and MS technologies have identified differences in circulating metabolites that distinguish physiological (Lewis, Farrell et al. 2010) and disease states (Lawton, Brown et al. 2014, Miller, Kennedy et al. 2015), and predict clinical outcomes. For example, differences in metabolites such as

arginine and steroid hormones distinguish patients with renal impairment (Shah, Townsend et al. 2013). Increased circulating levels of metabolites such as formate, isoleucine and mannose are seen in patients with inflammatory bowel disease compared to controls (Schicho, Shaykhutdinov et al. 2012). Metabolite profiles can also discriminate patients with various types of cancer (Carrola, Rocha et al. 2011, Oakman, Tenori et al. 2011) for example, elevated tissue lactate, phenylalanine and tyrosine, and reduced lipids and triglycerides, discriminate colorectal cancer from control tissue (Jimenez, Mirnezami et al. 2013). Metabolite changes in threonine, hydroxylamine and tagatose, amongst others, were found to be predictors of survival and disease progression in patients with lung cancer (Hao, Sarfaraz et al. 2016). A panel of ten circulating phospholipids were found to predict the onset of mild cognitive impairment or Alzheimer's disease over a 2-3 year period (Mapstone, Cheema et al. 2014). However, use of this panel as a predictor of preclinical Alzheimer's disease was not validated using the same platform in two larger cohorts of patients from different centres (Casanova, Varma et al. 2016). This highlights the need for validation of metabolomics results in independent cohorts of subjects, particularly where sample sizes are small.

Metabolomic profiling has also been used to predict the onset of diabetes using the amino acids isoleucine, leucine, valine, phenylalanine and tyrosine (Wang, Larson et al. 2011, Friedrich 2012), and branched chain amino acids, which were associated with insulin resistance and type 2 diabetes in large population studies (Menni, Fauman et al. 2013). Studies of metabolomics in cardiovascular disease (Shah, Kraus et al. 2012) show increased levels of acylcarnitines predict myocardial infarction and death in subjects with coronary artery disease (Shah, Bain et al. 2010), and a metabolite panel including amino acids, spermidine, butyrylcarnitine and the asymmetric methylarginine/arginine ratio was prognostic in patients with heart failure (Cheng, Wang et al. 2015).

The translational application of metabolomics in clinical practice can be seen by the development of the intelligent knife (iknife). This uses rapid evaporative ionization mass spectrometry technology to analyse the vapour from tissue samples directly in surgical operations and identify normal or cancerous tissue in real time (Balog, Sasi-Szabo et al. 2013). In addition, metabolomics can be used clinically to predict the response of a patient to drug therapy, identify influences on drug safety and efficacy, and predict pharmacokinetics in an approach known as pharmacometabonomics (Everett, Loo et al. 2013). This provides the opportunity for personalised treatment strategies based on predicting an individual's response to therapy (Nicholson, Wilson et al. 2011).

Translating metabolomics findings into clinical practice can be challenging due to variations in experimental protocols, statistical analysis and lack of standardisation (Klein and Shearer 2016). However, there is promise in the translational application of metabolomics, for example as a

predictive tool in diabetes, where a panel of 19 metabolites classified high risk patients who would have otherwise been missed by standard clinical tests (Varvel, Voros et al. 2014). To date, few metabolomics profiling studies have been undertaken in patients with pulmonary vascular disease to assess their potential applications in pulmonary hypertension.

1.8.3 Metabolomics in pulmonary arterial hypertension

Analysis of breath samples has shown elevated exhaled acetaldehyde in PAH patients relative to healthy controls, which may form as a by-product of the shift to aerobic glycolysis from glucose oxidation (Cikach, Tonelli et al. 2014). Elevated ammonia levels also correlate with disease severity in PAH patients (Cikach, Tonelli et al. 2014). Ammonia is a product of glutamine breakdown (Wu, Haynes et al. 2000), and may represent increased glutaminolysis in these patients. Altered volatile organic compounds, measured by gas chromatography MS, in exhaled breath condensate also discriminate between severe IPAH and healthy volunteers (Mansoor, Schelegle et al. 2014).

Evidence of increased metabolites from the TCA cycle and fatty acid oxidation, and altered arginine and sphingosine pathways have been found from mass spectrometry analysis of lung tissue from PAH patients (Zhao, Peng et al. 2014, Zhao, Chu et al. 2015). A small study of 20 PAH patients and controls used an untargeted metabolomics platform and showed changes in circulating metabolites such as increased lactate, free fatty acids and glutamine in PAH patients supporting a shift to aerobic glycolysis (Bujak, Mateo et al. 2016).

A targeted analysis of 105 circulating plasma metabolites in PAH, primarily amino acids, nucleosides and their derivatives, showed abnormal levels of tryptophan, purine and tricarboxylic acid cycle metabolites correlated to haemodynamic measures (Lewis, Ngo et al. 2016). In this study, 105 circulating metabolites were measured in a discovery cohort of 71 subjects with shortness of breath, and assessed against 5 haemodynamic markers of right ventricular-pulmonary vascular (RV-PV) dysfunction, including resting right atrial pressure, PAP, PVR, change in mean pulmonary artery pressure and exercise PVR. They found 21 metabolites associated with at least 2 markers of RV-PV dysfunction after correction for multiple testing, including cystathionine, inosine, urate, xanthine, glyceraldehyde, vanillylmandelic acid, aminoisobutyric acid, cyclic adenosine monophosphate, TCA cycle intermediates, arginine and tryptophan metabolites of the indoleamine 2,3-dioxygenase (IDO) pathway (Figure 1.4). In particular, multimarker scores indicated a strong association between the 5 markers of RV-PV dysfunction and 4 IDO metabolites (kynurenine, kynurenate, anthranilate and quinolinate), which were also elevated in a hypoxic mouse model of PAH and validated in another

cohort of 71 subjects. In addition, a third cohort of 30 subjects including both PAH patients and controls, showed 3 IDO metabolites discriminated patients and controls. This study was limited by the small number of metabolites measured and shows an association to RV-PV dysfunction in subjects with shortness of breath without a definitive diagnosis of PAH in the first two cohorts, and is not related to outcomes.

To date, no large scale metabolomics studies have assessed circulating metabolite changes in PAH and their relationship with clinical outcomes such as survival and response to therapy.

1.8.4 Genetic variations associated with metabolite levels

The integration of data obtained from so-called '-omics' technologies such as proteomics, metabolomics, transcriptomics and genomics, combined with clinical phenotype information, allows a comprehensive review of the molecular basis of a disease process, and the opportunity to assess potential therapeutic targets and predict and monitor an individuals response to therapy (Chambliss and Chan 2016).

In particular, the contribution of a genetic locus to a complex phenotypic trait (quantitative trait locus-QTL), has been well studied (Doerge 2002). QTLs have also been mapped to expression profiles (eQTLs) (Schadt, Monks et al. 2003), protein levels (pQTLs) (Sun, Kechris et al. 2016), and metabolite levels (mQTLs) (Dumas 2012) (Figure 1.6).

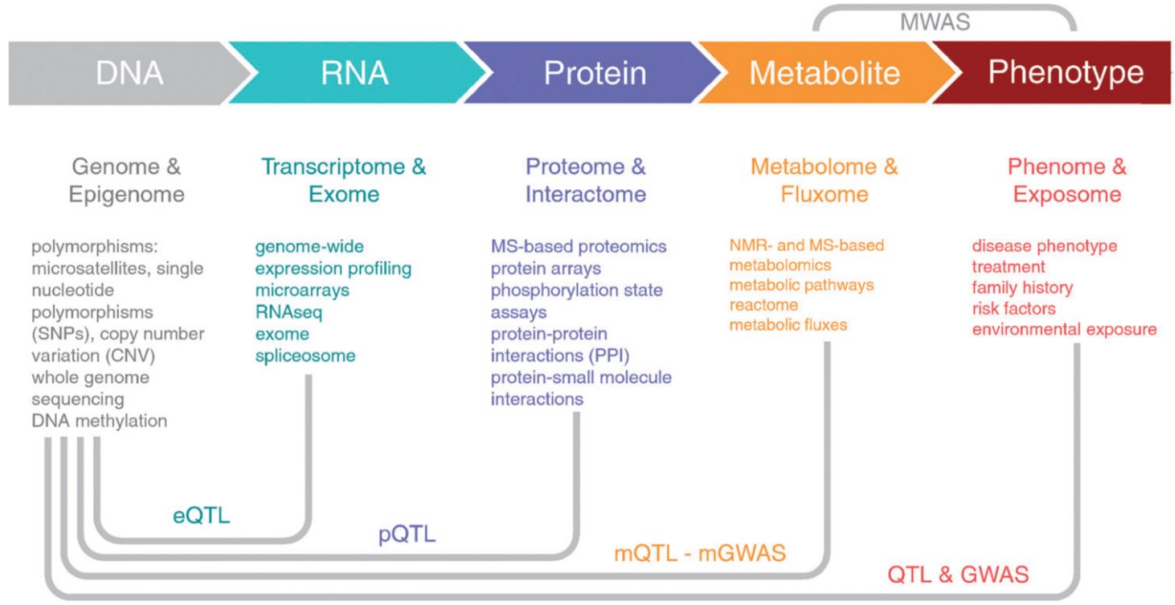


Figure 1.6 – Molecular phenotypes with associated genomic mapping. Figure from (Dumas 2012). Horizontal axis represents the biomolecular phenotype from genome to clinical phenotype, where the genome can be mapped to each stage. QTL, quantitative trait locus; eQTL, expression quantitative trait locus; pQTL, protein quantitative trait locus; mQTL, metabolite quantitative trait locus; GWAS, genome wide association study; MWAS, metabolome wide association study.

Genome wide association studies (GWAS) have been used to identify the loci of metabolic traits, using association between metabolites identified by metabolomics profiling and single nucleotide polymorphisms (SNPs) (Gieger, Geistlinger et al. 2008, Suhre, Shin et al. 2011, Hong, Karlsson et al. 2013, Draisma, Pool et al. 2015, Kastenmuller, Raffler et al. 2015, Raffler, Friedrich et al. 2015, Kettunen, Demirkan et al. 2016). In a large scale study of over 7500 healthy individuals, metabolite levels or metabolite ratios measured by UPLC-MS were associated with SNPs from GWAS, with 299 robust SNP-trait associations (Shin, Fauman et al. 2014).

By identifying gene variants associated with metabolite levels (i.e. polymorphisms in gene regions encoding enzymes that regulate these metabolites) a causal genetic link can be implicated for metabolic changes in a disease process. The link to the pathophysiology of a disease process may be verified by Mendelian randomisation, where both the SNP and trait are associated with an outcome such as survival (Figure 1.7). For example, elevated circulating interleukin 6 (IL-6) is associated with an increased risk of coronary disease and a SNP linked to IL-6 receptor was associated with a decreased risk of coronary events, implicating a causal relationship of IL-6 signalling and coronary

disease (Interleukin-6 Receptor Mendelian Randomisation Analysis 2012). In addition, a variant in carbamoyl-phosphate synthase 1 encoding an enzyme in the urea cycle is associated with reduced levels of metabolites in the urea cycle and decreased coronary artery disease risk in females (Hartiala, Tang et al. 2016).

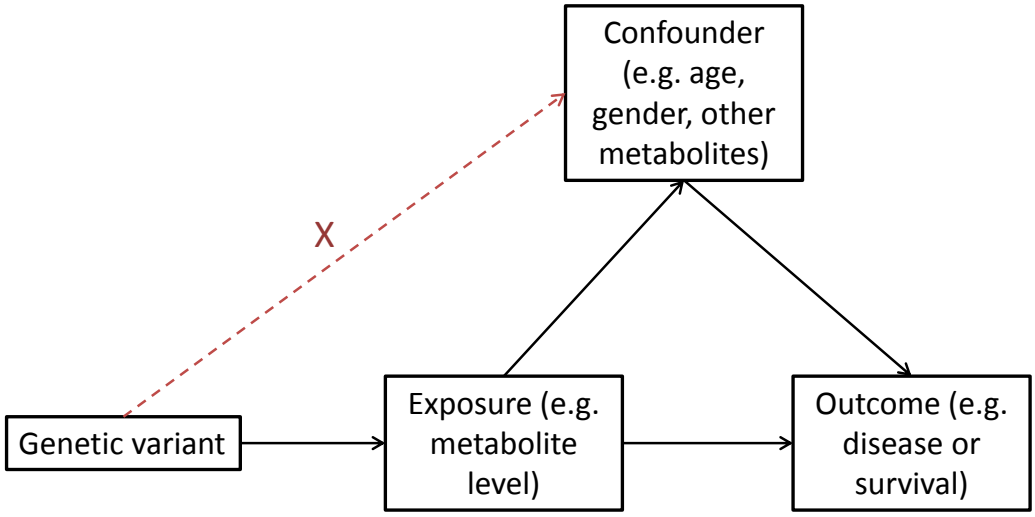


Figure 1.7 – Principles of Mendelian Randomisation. Adapted from (Swerdlow, Kuchenbaecker et al. 2016). The principle of Mendelian randomisation is that the exposure (for example a metabolite level) is associated with the outcome, based on a) the genetic variant being associated with the exposure, b) the genetic variant only being associated to the outcome through the exposure and c) the genetic variant being associated with the outcome independent of any potential confounding factors (red dashed line and X).

1.9 Hypothesis

Pulmonary arterial hypertension is caused by vascular remodelling of the distal pulmonary arteries and despite current therapeutic strategies, outcomes remain poor. Evidence is growing that metabolic dysregulation contributes to the pathophysiology of the disease process. Studies to date have focused on energy metabolism and as yet, broad spectrum metabolomics studies in large populations of PAH patients have not been conducted.

I hypothesise that measurement of circulating metabolites can distinguish PAH patients from controls, predict outcomes such as response to therapy and survival, and that metabolomics technologies may be used to identify novel metabolic disturbances and potential therapeutic targets in PAH.

1.10 Objectives

1. To document changes in energy metabolism and novel metabolic disturbances in patients with pulmonary arterial hypertension
2. To investigate the prognostic value of circulating metabolite levels in patients with pulmonary arterial hypertension
3. To establish if metabolic changes are specific to pulmonary arterial hypertension or present in other pulmonary hypertension subtypes
4. To investigate if genetic variants contribute to metabolic changes in pulmonary arterial hypertension

Chapter 2 – Materials and methods

2.1 Declaration of responsibilities

Patients were diagnosed and managed by the clinical team at the National Pulmonary Hypertension service at Hammersmith Hospital, under the guidance of Dr Simon Gibbs, Dr Luke Howard and Dr Rachel Davies, and the PH nurses. Plasma samples were collected from patients by the research nurses in the National Institute for Health Research (NIHR) /Wellcome Trust-Imperial College Clinical Research Facility. Samples were also collected from collaborating centres at the University Hospital of Giessen and Marburg, and from other UK national centres as part of the National Cohort Study of Idiopathic and Heritable Pulmonary Arterial Hypertension (ClinicalTrials.gov NCT01907295).

Metabolomics experiments were conducted in collaboration with the National Institute for Health Research (NIHR) Biomedical Research Centre (BRC) Imperial College Clinical Phenome Centre (CPC), with Dr Jeremy Nicholson and his group. A commercial platform was also used called the Discovery HD4^{TM} Global Metabolomics platform, Metabolon, Inc. (Durham, NC, USA), which will be referred to as the Metabolon platform.

Whole-genome sequencing data was used from the UK National Institute of Health Research Biomedical Research Centres Inherited Diseases Genetic Evaluation (BRIDGE) consortium.

The remaining data was produced and analysed by myself. I planned the metabolomics experiments, prepared the samples, and conducted the statistical analysis and interpretation of the results.

2.2 Sample availability

Although animal models are available for PAH, lung samples from patients represent the only precise description of the human disease process. However, suitable samples of the diseased lung are scarce, since they are only available at the end stage of disease during lung or heart/lung transplantation. Furthermore, very few patients with PAH now undergo transplantation, most being managed medically. In the case CTEPH, the surgical procedure of choice is pulmonary endarterectomy. In order to compare explanted diseased tissue samples with nominally healthy lung, specimens are obtained from unused donor lung tissue or patients undergoing other surgical procedures such as lobectomies for lung cancer. Blood samples are more readily available and can be collected at regular intervals when patients attend clinic appointments.

2.3 Sample collection

2.3.1 Subjects

Patients were recruited from the National Pulmonary Hypertension Service at Hammersmith Hospital, London between 2002-2015, other UK national centres as part of the National Cohort Study of Idiopathic and Heritable Pulmonary Arterial Hypertension (ClinicalTrials.gov NCT01907295) between 2013-2015, and the University Hospital of Giessen and Marburg between 2004 – 2014.

Control subjects included healthy controls (HC) and disease controls (DC), the latter being symptomatic patients presenting to the service but in whom pulmonary hypertension was excluded by cardiac catheterisation. Disease control subjects had similar comorbidities to patients with PAH (Tables 3.2, 4.3, 5.1, 6.5, 7.1). The diagnosis of PAH, PH secondary to left heart disease (LHD) and CTEPH was based on standard criteria from the most recent guidelines (Galie, Humbert et al. 2015). PAH patients with idiopathic or heritable disease were compared to healthy controls, disease controls and patients with CTEPH, PH secondary to LHD and PAH associated with congenital heart disease (CHD) and connective tissue disease (CTD).

Vasoresponders were defined as those who dropped their mean pulmonary artery pressure >10 mmHg to <40 mmHg, with preserved cardiac output, in response to an acute pulmonary vasodilator challenge and remained stable on calcium channel blocker therapy alone for at least 1 year (Galie, Humbert et al. 2015).

2.3.2 Samples

Venous blood samples were drawn from the antecubital fossa and collected in EDTA- and lithium-heparin Vacutainer tubes (BD, Oxford, UK), immediately put on ice, centrifuged (1,300g, 15 minutes) within 30 minutes and stored at -80°C until required.

2.3.3 Outcome measures

World Health Organisation functional class (WHO-FC) and six minute walk distance (6MWD) data was obtained at the sample date. World Health Organisation functional class (WHO-FC) is assessed

clinically and is a prognostic indicator in PAH patients (Benza, Miller et al. 2010, Barst, Chung et al. 2013), and worsening WHO-FC is a marker of disease progression (Nickel, Golpon et al. 2012). Six minute walk distance (6MWD) is readily measurable at a clinic visit, and is also a prognostic indicator in PAH (Benza, Miller et al. 2010). Clinical biochemical data, such as creatinine and bilirubin, were recorded within 30 days of the sample date.

Local research ethics committee approval (REC 11/LO/0395) was obtained for the collection, storage and use of plasma samples as well as access to their clinical data and all subjects provided informed written consent.

2.3.4 Clinical Database

Patient information, including cardiopulmonary haemodynamic data, imaging, therapy, co-morbidity, hospitalisation and mortality, was obtained using the TRIPHIC (Translational Research in Pulmonary Hypertension at Imperial College) database. The TRIPHIC system received both research ethics committee (13/LO/0695) and HRA-CAG (health research authority – confidentiality advisory group) approval (CAG 4-09(a) 2013) approval, providing pseudonymised clinical data for research purposes and an integrated secure source of information on samples stored in the pulmonary hypertension biorepository at Imperial College.

2.4 Nuclear magnetic resonance (NMR) spectroscopy

To assess circulating metabolite levels in PAH patients, NMR spectroscopy was employed initially. This technique is based on the principle that certain NMR active nuclei such as hydrogen (^{1}H) or carbon (^{13}C), are electrically charged and when placed in an external magnetic field, align predominantly in line with the magnetic field in a low energy state, or less commonly against the field in a high energy state. In the presence of radio waves, nuclei in the low and preferred energy state, move into a high energy state by absorbing this energy. Measurement can subsequently be made of the absorption of the radiofrequency waves or relaxation back into the low energy state. The frequency at which this absorption or relaxation occurs, is based on the chemical environment of the nuclei such as their chemical bonds, which provides a distinct chemical shift (δ, parts per million, ppm) signal for each nuclei within a molecule.

NMR technology is highly reproducible and quantitative (Dumas, Maibaum et al. 2006, Bictash, Ebbels et al. 2010), with relatively established means to characterise and identify several hundred metabolites. Although less sensitive than mass spectrometry, the metabolites that can be detected by NMR feature in key metabolic pathways (Elliott, Posma et al. 2015), and therefore assessment in PAH patients could be used to validate current metabolic dysregulation in PAH, as well as highlight novel metabolic pathways involved in the disease process.

A short acquisition time of 4-5 minutes is needed to measure a variety of metabolites with concentrations in the low micromolar range (Beckonert, Keun et al. 2007). In NMR spectroscopy, samples do not undergo any pre-treatment and signals from proteins and macromolecules are suppressed using the Carr–Purcell–Meiboom–Gill (CPMG) sequence(Beckonert, Keun et al. 2007). This methodology filters out signals from macromolecules, as the protons in these molecules have a fast relaxation (Beckonert, Keun et al. 2007).

The use of intact plasma in NMR has some limitations including the number of metabolites detected, which is substantially less than the estimated total number of circulating metabolites (Psychogios, Hau et al. 2011), and the binding of metabolites to proteins which underestimates their concentration (Nicholson and Gartland 1989), distorts the CPMG baseline and broadens the NMR peaks(Nagana Gowda, Gowda et al. 2015). Efforts are being made to expand the number of metabolites detected by NMR, for example with the use of ultrafiltration(Nagana Gowda, Gowda et al. 2015).

2.4.1 NMR data acquisition

Plasma samples were thawed, vortexed, centrifuged at 16,000g for 5 minutes at 4^0C and aliquoted (500 µL) in Riplate™ 96-well 1ml plates (Ritter, GmbH, Schwabmünchen, Germany). Aliquots of plasma (300µl per well) were mixed with 300 µL 0.9% saline in flow-injection plates and mixed with phosphate buffer (pH 7.4), containing the reference standard trimethylsilylpropionic acid (TSP). A representative quality control sample was included in all plates at regular sample intervals. NMR data was acquired at 36.9^{o}C, using a 600 MHz Avance III NMR Spectrometer equipped with a SampleJet sample handler which stores samples at 4°C (Bruker Biospin, Billerica, Massachusetts, USA).

Data was acquired with a standard one-dimensional solvent suppression pulse sequence; one dimensional 1D nuclear Overhauser enhancement Spectroscopy (NOESY), the Carr–Purcell–

Meiboom–Gill (CPMG) pulse sequence and a two dimensional J-resolved (JRES) experiment (Figure 2.1) (Beckonert, Keun et al. 2007).The NOESY pulse sequence is used for general profiling for a comprehensive view of all molecules within the plasma sample, while the CPMG experiment filters macromolecules based on their relaxation time, as discussed. Finally, JRES creates a pseudo two dimensional spectrum, providing information on the chemical shift on one axis and multiplicity on another axis, i.e. singlet, doublet, triplet or multiplet peaks. Multiplicity refers to the number of adjacent hydrogen atoms immediately next to the hydrogen atoms that are creating a peak. For example, a methyl group (CH_3) without any neighbouring hydrogens appears on the spectrum as a singlet, if there is one neighbour (CH_3CHCl_2) as a doublet and 2 neighbour hydrogens (CH_3CH_2Cl) as a triplet (Figure 2.2). This information can be used to characterise which molecule the NMR peak at a given chemical shift represents. A line broadening of 0.3 Hz was used and the spectra were calibrated based on the anomeric glucose resonance at δ^1H 5.233ppm.

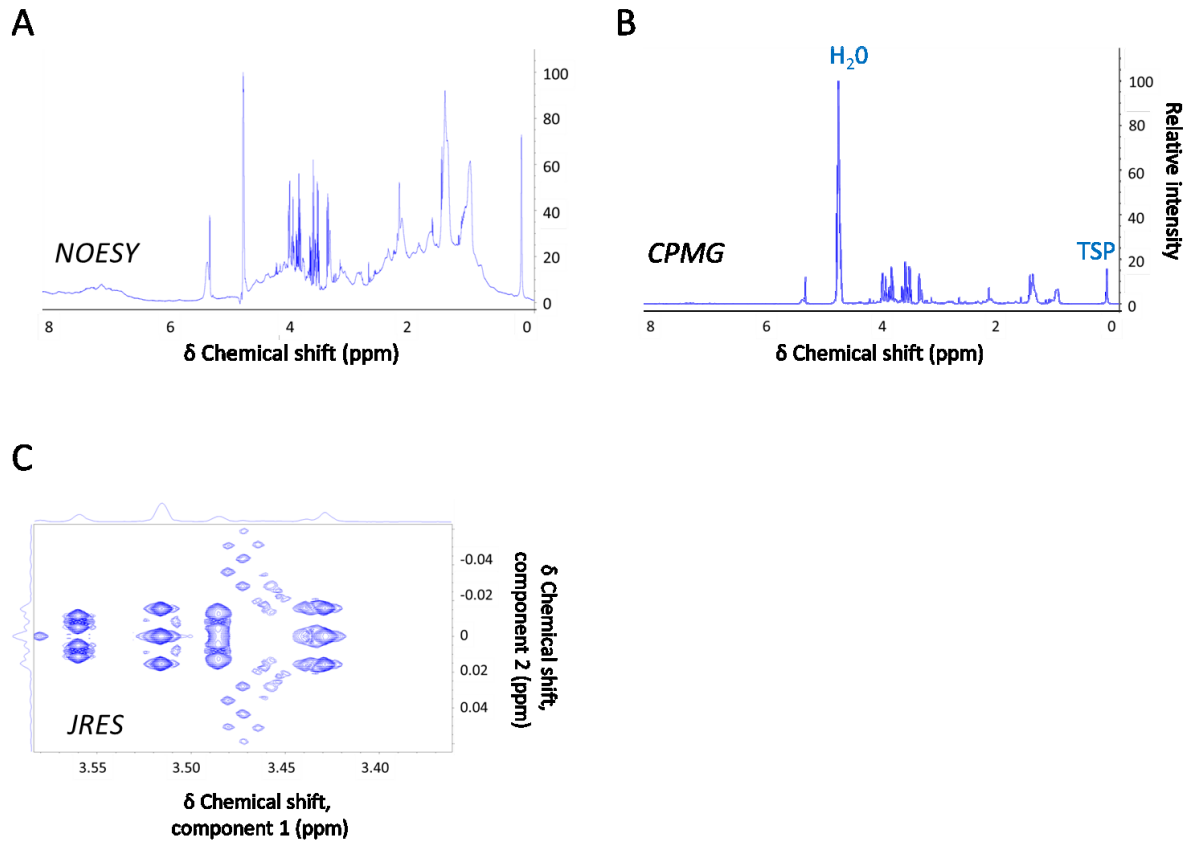


Figure 2.1 – ^{1}H NMR spectra from one dimensional radiofrequency pulse sequences. Raw spectra are shown for a single plasma sample. Chemical shift in parts per million (ppm) and relative intensity are shown. **A)** One dimensional nuclear Overhauser enhancement Spectroscopy (NOESY) provides a comprehensive view of all molecules in the sample, **B)** Carr–Purcell–Meiboom–Gill (CPMG) pulse sequence filters out signals from macromolecules to show small molecule signals more clearly - peaks for a reference standard, trimethylsilylpropionic acid (TSP) and water are shown, and **C)** Two dimensional J-resolved (JRES) experiment uncouples the spectra to provide more detailed information on peaks at a given resonance, for example a doublet at 3.57ppm and triplet at 3.43 and 3.52ppm.

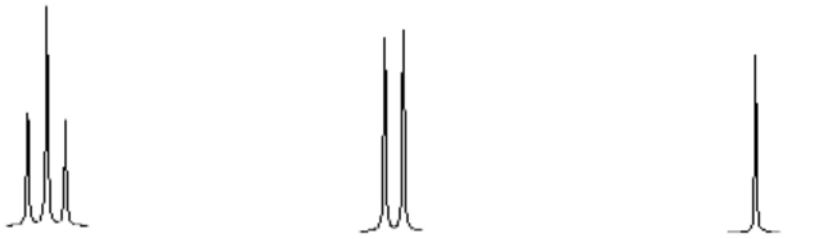


Figure 2.2 – Multiplicity of NMR peaks. NMR spectra are shown for a singlet, doublet and triplet with examples for a methyl group (CH_3) with no adjacent hydrogens (singlet), 1 adjacent hydrogen (doublet) and 2 adjacent hydrogens (triplet).

To advance the identification of NMR peaks, additional two dimensional experiments were acquired for a subset of 8 plasma samples, providing one axis for information on ^{1}H and another for the ^{13}C isotope. Two dimensional experiments were conducted using heteronuclear single quantum coherence (HSQC) spectroscopy (Bodenhausen 1980), Correlation Spectroscopy (COSY) and Total Correlation Spectroscopy (TOCSY) (W. P. Aue 1976). The HSQC experiment was used to visualise the ^{13}C-^{1}H connectivities while the COSY and TOCSY experiments display protons that are coupled to one another, either directly or indirectly.

2.4.2 NMR data processing and analysis

A ^{1}H NMR CPMG spectra contains sharp lines which represent features of low molecular weight metabolites, with broader signals coming from lipoproteins and proteins (Beckonert, Keun et al. 2007). These signals are superimposed on one another, and represent multiple metabolites in a single sample, with chemical shift on the x axis and intensity on the y axis (Figure 2.3). The chemical shift of each signal represents the resonant frequency of a nucleus in a magnetic field, determined by the bonds of the nucleus and its chemical environment. The intensity is proportional to the molar concentration of the compound, therefore a more dilute sample will give a smaller (weak intensity) signal. The relative intensities within a sample are dependent on the number of hydrogen atoms – as an example, cyclohexane gives a signal twice as intense as benzene due to the fact that it has twice as many hydrogens in the molecule.

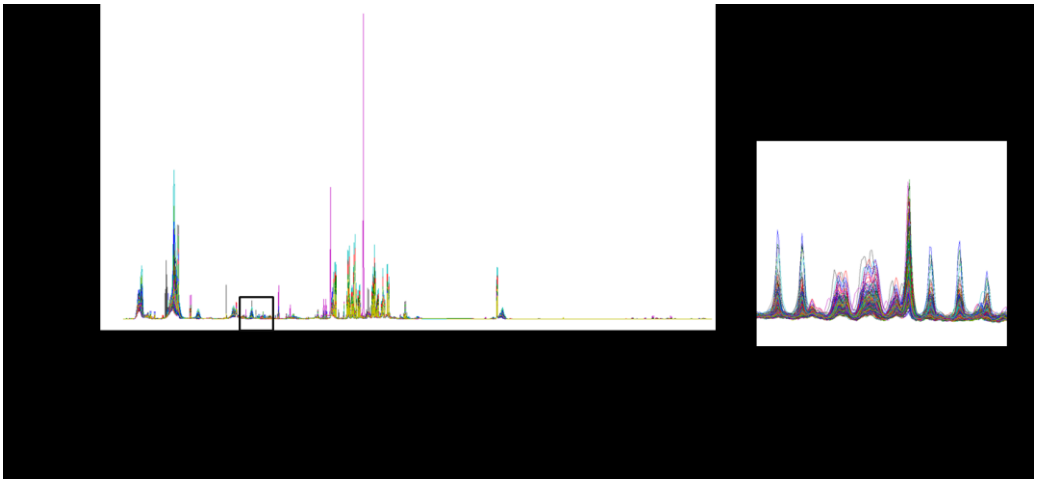


Figure 2.3 – Superimposed ^{1}H NMR spectra from all plasma samples. Spectra are shown after removal of trimethylsilylpropionic acid (TSP), water and empty regions, chemical shift in parts per million (ppm) and relative intensity are shown. A zoomed in region is shown between 2.1-2.5ppm.

Raw spectra per sample were reviewed using TopSpin™ software (Bruker, Billerica, Massachusetts, USA) and data from all samples loaded into MetaSpectra (http://otm.illinois.edu/technologies/metaspectra-software-storage-and-retrieval-spectra) via Matlab (Matrix Laboratory, MathWorks, Natick, Massachusetts, USA).

NMR profiles were recorded as 20000 data points spaced by 0.00055ppm, as per other published studies (Holmes, Loo et al. 2007, Jimenez, Mirnezami et al. 2013, Mirnezami, Jimenez et al. 2014) and calibrated to the expected chemical shift of glucose. Regions containing TSP (less than 0.65ppm), H_2O (4.33-4.90ppm), ethylenediaminetetraacetic acid (EDTA) (2.51-2.58, 3.06-3.17ppm), paracetamol (2.15-2.16, 3.61-3.63, 5.08-5.10, 7.15-7.16, 7.34-7.37ppm) and background noise (above 7.87ppm) were removed from the spectra, leaving a total of 12089 data points (ppm) for each sample. Spectral data points were normalised to the median intensity value at each ppm.

Each of the 12089 data points from NMR analysis were assessed by Mann Whitney U-test and areas of interest were defined by significant consecutive points ($p<0.01$) in any of the 4 group comparisons between patients (PAH or CTEPH) and controls (HC or DC), leaving 201 regions for further analysis. Distinct peaks within these regions of interest were compared between PAH patients and healthy controls, disease controls and CTEPH patients (Mann Whitney U-test, $p<0.05$).

2.4.3 Identification of NMR signals

STOCSY (statistical total correlation spectroscopy) (Cloarec, Dumas et al. 2005) was used to indicate regions of the spectrum with correlating intensities to areas of interest across the entire sample set. This technique identifies several correlated regions or peaks to a potential peak of interest to create a 'pseudo-spectrum' of that chemical molecule which can be used to identify it.

To identify the molecules, NMR peaks of interest were cross-referenced to information in the Human Metabolome Database (HMDB) (Wishart, Tzur et al. 2007) and literature (Nicholson, Foxall et al. 1995). AMIX software (Bruker, Billerica, Massachusetts, USA) was used, containing a reference database (SpectraBase) of spectra from multiple metabolites. Samples with high peak intensities were searched (including regions found to correlate to the peak using STOCSY). If a metabolite was suspected, other regions of the reference spectra were compared to the sample spectra. In addition, the ^{1}H and 2D ^{13}C-^{1}H chemical shift were cross referenced to the same databases to confirm the identity of potential metabolites.

2.4.4 NMR lipoprotein subclass analysis

In depth NMR lipoprotein subclass analysis was conducted by Bruker (Billerica, Massachusetts, USA) to provide quantitative levels of 105 lipid subgroups. Briefly, data from a training sample set produced by Bruker (Biospin 2015) was used to construct a linear regression model on ultra-centrifugation based lipoprotein data with ^{1}H NMR spectra from a training sample set of the study (Mihaleva, van Schalkwijk et al. 2014). The prediction component of this model was applied to the NMR dataset from controls and PAH patients to provide lipoprotein analyte information based on the ^{1}H NMR spectrum. This data provides information on very low density lipoprotein (VLDL), 6 VLDL subclasses, intermediate density lipoprotein (IDL), low density lipoprotein (LDL), 6 LDL subclasses, high density lipoprotein (HDL) and 4 HDL subclasses. For each of these, the lipoprotein content (cholesterol, free cholesterol, phospholipids, apolipoprotein (Apo) A1, A2 and triglycerides) is also given.

2.5 Ultra performance liquid chromatography mass-spectrometry (UPLC-MS)

In order to expand the range of circulating metabolites detected, a non-targeted and unbiased UPLC-MS experiment was conducted (Broeckling, Heuberger et al. 2013). This technique couples liquid chromatography to mass spectrometry, and has a high degree of sensitivity, using small sample volumes for high-throughput assessment of thousands of metabolites in the picomolar range and above (Bictash, Ebbels et al. 2010). Complimentary information based on the separation of analytes with LC and detection of analytes by MS is used to help identify the metabolites (Figure 2.4) (Pitt 2009, Want, Masson et al. 2013).

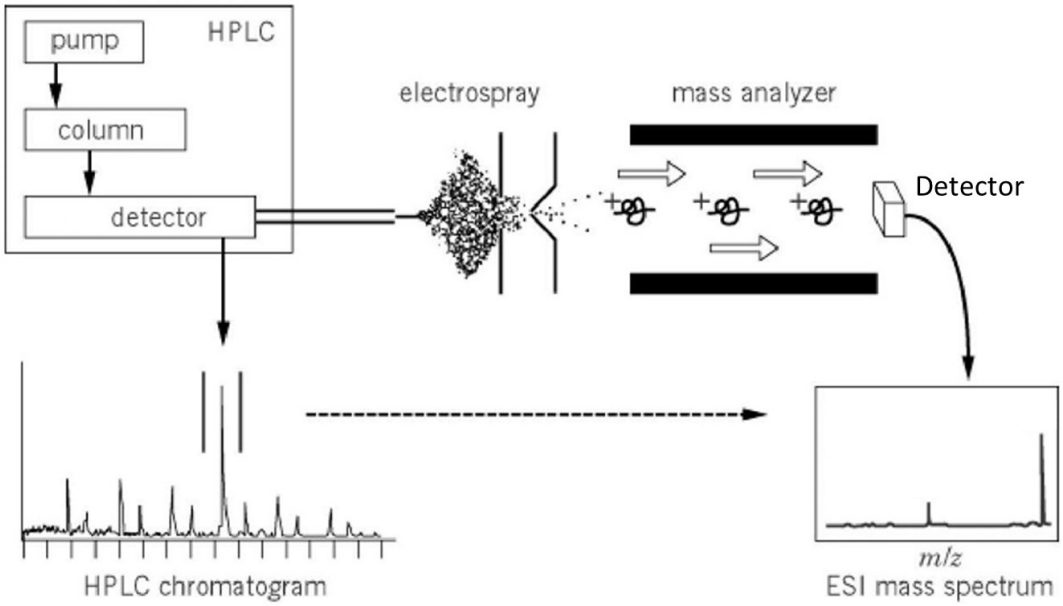


Figure 2.4 – Principles of high performance LC-MS. Adapted from (Scripps Center for Metabolomics and Mass Spectrometry). Initially the sample is separated based on the time taken for it to move through a column (retention time) recorded in a chromatogram. The sample is then ionised using electrospray ionisation (ESI) and sorted in the mass analyser based on the mass to charge ratio and deflection in an electromagnetic field. HPLC, high performance liquid chromatography; MS, mass spectrometry.

Liquid chromatography is used to separate a sample into its component parts (or analytes) by the sample moving through a column. The column has a stationary phase or adsorbent, consisting of a substance that stays fixed in the column, for example silica gel. Once the sample enters the column, it adheres to the stationary phase. In UPLC, the mobile phase involves a liquid based solvent moving through the column under pressure, rather than slowly moving through the column by gravity. As different analytes within the sample adhere to the stationary phase with different affinity, analytes move through the column at different speeds, and the time taken for an analyte to move through the column to the mass spectrometry detector can be recorded as the retention time. The mobile phase can be delivered continuously with the same solvent, or as a gradient, for example becoming increasingly hydrophilic, which will alter the adherence of analytes to the stationary phase.

Two approaches were used - Hydrophilic interaction chromatography (HILIC) and lipidomics. HILIC separates analytes based on their polarity, and is a variation of normal phase liquid chromatography where the stationary phase is more polar (or hydrophilic) than the mobile phase (Alpert 1990, Buszewski and Noga 2012). In this technique a polar stationary phase such as silica is used and the mobile phase is a hydrophobic solvent, most commonly acetonitrile. Highly polar analytes within the sample will have a greater affinity to the stationary aqueous phase, thus a longer retention time. Lipidomics uses a similar form of chromatography as HILIC and soft ionisation during mass spectrometry, so that the chemical nature of the lipid is not destroyed.

Following chromatography, the sample solution is sprayed from a small tube into a strong electric field to ionise the molecules (electrospray ionisation, ESI). Ionised molecules are then sorted in the MS analyser based on their mass to charge ratio (m/z) by their deflection in an electromagnetic field. Ions which have a heavier mass are deflected less than lighter ones, and those with a greater charge are deflected more. These features are detected by the machine to provide information on the mass to charge ratio.

Samples were prepared and experiments conducted in line with the protocols of the Medical Research Council (MRC)-NIHR National Phenome Centre and in collaboration with the Clinical Phenotyping Centre at Imperial College.

Mass spectrometry was performed on high-resolution Q-Tof (quadropole-time of flight) instruments from Waters Limited, Manchester, UK (Synapt and Xevo G2-XS) in both positive and negative ion electrospray ionization (ESI + and ESI–) modes. The MS parameters were set as follows: capillary voltage 1.0-2.0 kV, sample cone voltage 20-25 V, source offset 80, source temperature 120°C, desolvation temperature 600°C, desolvation gas flow 1000 L/h, and cone gas flow 150 L/h.

Data were collected in centroid mode with a scan range of 50-1200 m/z for small molecule profiling with HILIC chromatography and of 50–2000 m/z for lipidomics and a scan time of 0.07-0.15 seconds, respectively. For mass accuracy, LockSpray™ (patented ion source, Waters Corporation, Milford, U.S.A.), ion source) mass correction was employed using a 200 pg/µL leucine enkephalin (m/z 556.2771 in ESI+, m/z 554.2615 in ESI−) solution in water/acetonitrile solution (50:50) at a flow rate of 10 µL/minute. Lockmass scans from a reference solution of a known compound were collected every 60 seconds and averaged over 3 scans as advised by the manufacturer.

2.5.1 Hydrophilic interaction chromatography (HILIC)

50 µl of sample was aliquoted in 96-well plates, mixed with 1:3 high-grade LC-MS acetonitrile (Sigma) for protein precipitation, vortexed, kept at 4 ^{o}C for 2 hours and centrifuged (16000g for 10 minutes). For each experiment, 75 µl of the supernatant was transferred into a fresh 96-well plate (Eppendorf) for analysis and 25 µl of the supernatant were pooled to create a quality control (QC) sample which was injected repeatedly every 11 sample throughout the whole LC-MS run. The heat-sealed sample plates were stored at 4°C for immediate, or at -80°C for later analysis. HILIC chromatography employed an Acquity Ethylene Bridged Hybrid (BEH) HILIC (1.7 micrometer(µm), 2.1 × 150 mm) column (Waters Corporation, Milford, U.S.A.) kept at 40 °C by a Waters Acuity UPLC system (Waters Corporation, Milford, MA, USA). Gradient elution was used for separation, using 0.1% (v/v) formic acid and 20mmol/L ammonium formate in high-grade LC-MS water (Fisher) for mobile phase A and 0.1% (v/v) formic acid in high-grade LC-MS acetonitrile (Sigma) for mobile phase B at a flow rate of 0.6 ml/minute. For the discovery study following 15 minute gradient run was applied: Starting condition 95% B were kept for 0.1minute followed by a decrease to 50% from 0.1 to 6.85 minutes. These conditions were kept till 8 minutes before the gradient was set back to initial condition of 95% B at 8.1 minutes where it was kept for the remaining run time. Two µl were used for injection of all samples.

The gradient used for chromatography in the validation differed from the discovery experimental run due to a change in protocols by the Clinical Phenome Centre and this was taken into consideration during the data processing step. For the validation study the following 15 gradient run was applied: Starting condition 95% B were kept for 0.1 minutes followed by a first decrease to 80% B from 0.1 to 4.60 minutes and a second decrease to 50% B from 4.6 to 5.50 minutes. These conditions were kept till 7 minutes before the gradient was set back to initial condition of 95% B at 7.1 minutes where it remained till end of the run time. Two µl were used for injection of all samples.

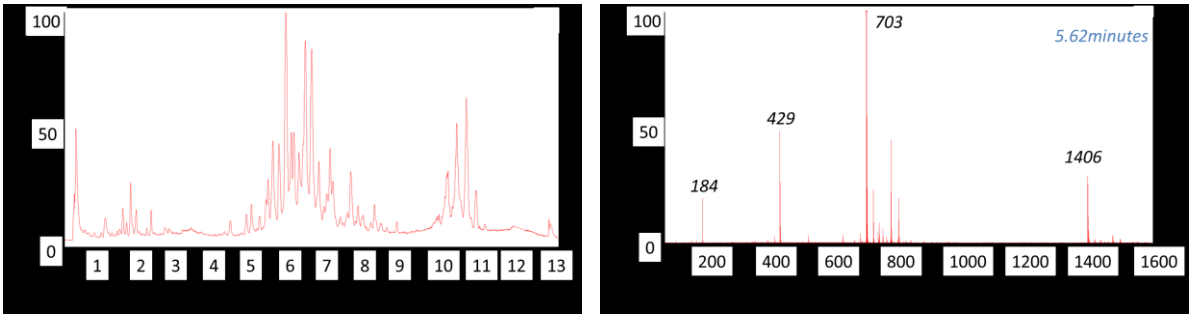
2.5.2 Lipidomics

50 µl of plasma samples was aliquoted in 96-well plates, mixed with 1:4 high-grade LC-MS isopropanol (Sigma) for protein precipitation, vortexed, kept at 4 ^{o}C for 2 hours and centrifuged (16000g for 10 minutes). For each experiment, 75 µl of the supernatant was transferred into a fresh 96-well plate (Eppendorf) for analysis and 25 µl of the supernatant were pooled to create a quality control (QC) sample which was injected repeatedly every 11 sample throughout the whole LC-MS run. The heat-sealed sample plates were stored at 4°C for immediate or at -80°C for later analysis. HILIC chromatography employed an Acquity BEH C8 (1.7 µm, 2.1 × 100 mm) column (Waters Corporation, Milford, U.S.A.) kept at 40 °C by a Waters Acuity UPLC system (Waters Corporation, Milford, MA, USA). Gradient elution with a flow rate of 0.6 ml/minutes was used for separation. Mobile phase A consisted of following mixture: water/isopropanol/acetonitrile (all high grade LC-MS from Fisher or Sigma) in a 50:25:25 ratio with the addition of 5 mmol/L ammonium acetate, 0.05% acetic acid, and 20 µM phosphoric acid (all from Sigma). Mobile phase B consisted of isopropanol:acetonitrile (both high grade LC-MS solvents from Sigma) in a ratio of 50:50 with 5 mmol/L ammonium acetate and 0.05% acetic acid as modifiers. Following 15 minutes, gradient run was applied: Starting conditions of 1% B were kept for 0.1minutes followed by an increase to 30% from 0.1 to 2.0 minutes and to 90% B till 11.5 minutes. At 12 minutes 99.9% B was used for washing out till 12.55 minutes. After that initial conditions were re-established for the remaining run time. Two µl were used for injection of all samples. The same chromatographic protocol was used for the discovery and validation experimental runs.

2.5.3 UPLC-MS data processing and analysis

Data were aligned and peaks selected and normalised using Progenesis QI software (Nonlinear Dynamics, Waters Company, North Carolina, USA). Raw spectra were reviewed using MassLynx MS Software (Waters, Milford, MA, USA) (Figure 2.5).

A



B

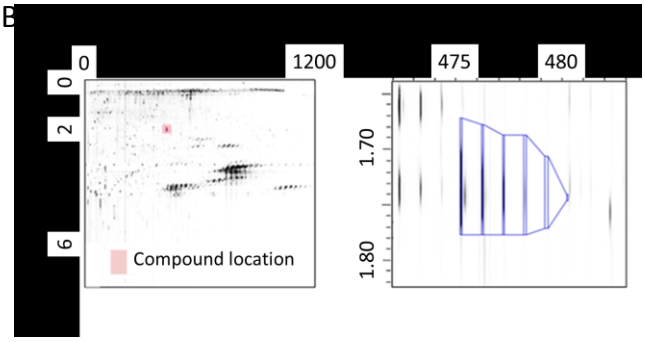


Figure 2.5 – UPLC-MS raw spectra. A) Raw data is shown for a single plasma sample, with the entire chromatogram and the masses detected at 5.62 minutes, reviewed in MassLynx. Peaks were annotated based on the retention time and mass to charge ratio for example 5.62_703.5778m/z. **B)** Overall retention time and mass to charge ratio (m/z) data is shown for a single plasma sample, highlighting all the peaks detected, and zoomed in to a region between 1.65-1.8 minutes, where a peak and its isotopes can be seen, as generated by Progenesis. UPLC-MS, ultra performance liquid chromatography mass-spectrometry.

A quality control (QC) sample was produced by pooling all plasma samples that underwent experimentation, and was measured on each plate throughout the experiment. Peaks whose signal did not dilute in a quality control dilution series (using a mixture of pooled samples and buffer, Spearman's Rho>0.7) were excluded. For example, as the QC dilution sample was diluted, if the intensity of the peak did not decrease in proportion, it was excluded from further analysis (Figure 2.6A). Peaks whose intensity values were inconsistent, measured by the extent of variation, in the QC sample which was measured throughout the experiment, were excluded based on a coefficient of variation (COV>0.6) (Figure 2.6B).

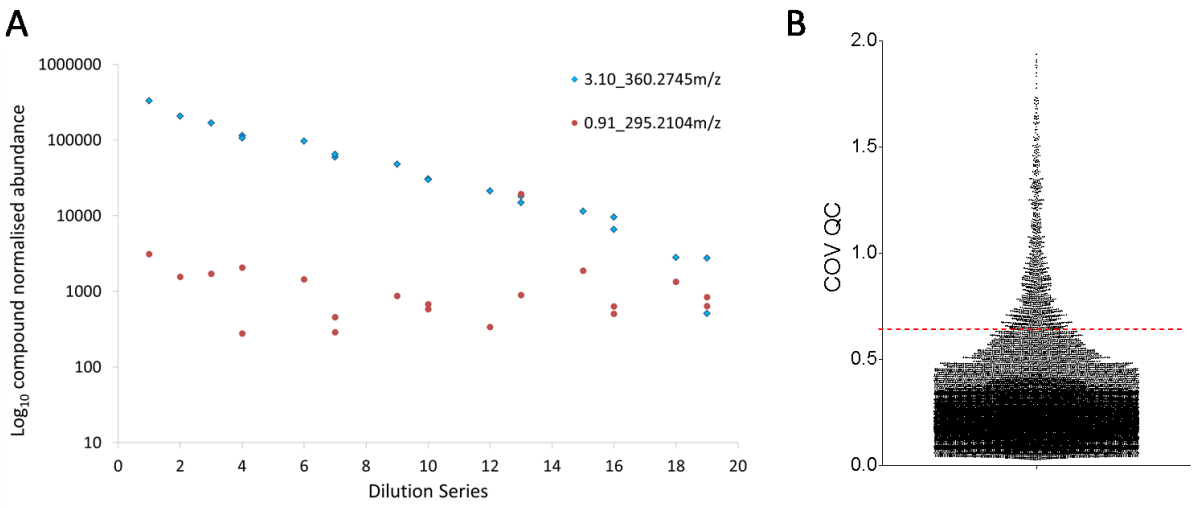


Figure 2.6 – Filtering of UPLC-MS peaks based on dilution series and coefficient of variation. A) Log normalised abundance of two example peaks from a quality control of pooled samples is shown. The abundance of the peak in blue decreases appropriately as the sample is diluted (Spearman's Rho>0.7), whilst the metabolite in red shows high variation as the sample dilutes, therefore it was excluded from further analysis. **B)** Coefficient of variation (COV) is shown for all peaks detected in lipidomics mode in a quality control (QC) of pooled samples. Peaks with a COV greater than 0.6 were excluded from further analysis. m/z, mass to charge ratio; UPLC-MS, ultra performance liquid chromatography mass-spectrometry.

Only peaks detected across all experimental runs were considered. This was defined as peaks with the same mass (+/-10ppm) between discovery and validation runs. A predicted retention time was calculated for the discovery peaks based on a locally weighted scatter plot smoothing (lowess) regression model (HILIC) and linear regression model (lipidomics). A linear model was used for the lipidomics experiments as the same chromatographic protocol was used in the discovery and validation experiments. A non-linear regression model was used for the HILIC experimentation due to a different chromatographic protocol used in the validation experiment, where the overall chromatographic run was longer (Figure 2.7A).

In order to create this model, peaks were chosen with the same mass (+/- 10ppm) between the discovery and validation experiment and the ratio between the retention times in each experiment was calculated. For the HILIC model, the interquartile range of the retention time ratio was 0.629-1.15 minutes and any peaks outside of this range were excluded for the model generation. A lowess

model was fitted to the remaining peaks and used to calculate the predicted retention time for all the HILIC discovery peaks.

For the lipidomics model, any peaks where the ratio of retention times was not within the range of 0.94-1.06 minutes were excluded and a linear regression model fitted to the remaining peaks. This was used to calculate the predicted retention time for all discovery lipidomics peaks.

Based on the standard deviation of the difference between the predicted and actual retention time in the validation experiment, a range of 0.3 minutes was chosen. Peaks where the difference in predicted retention time and detected retention time in the validation experiment was less than 0.3 minutes were considered for further analysis (Katajamaa and Oresic 2005, Vaughan, Dunn et al. 2012) (Figure 2.7B).

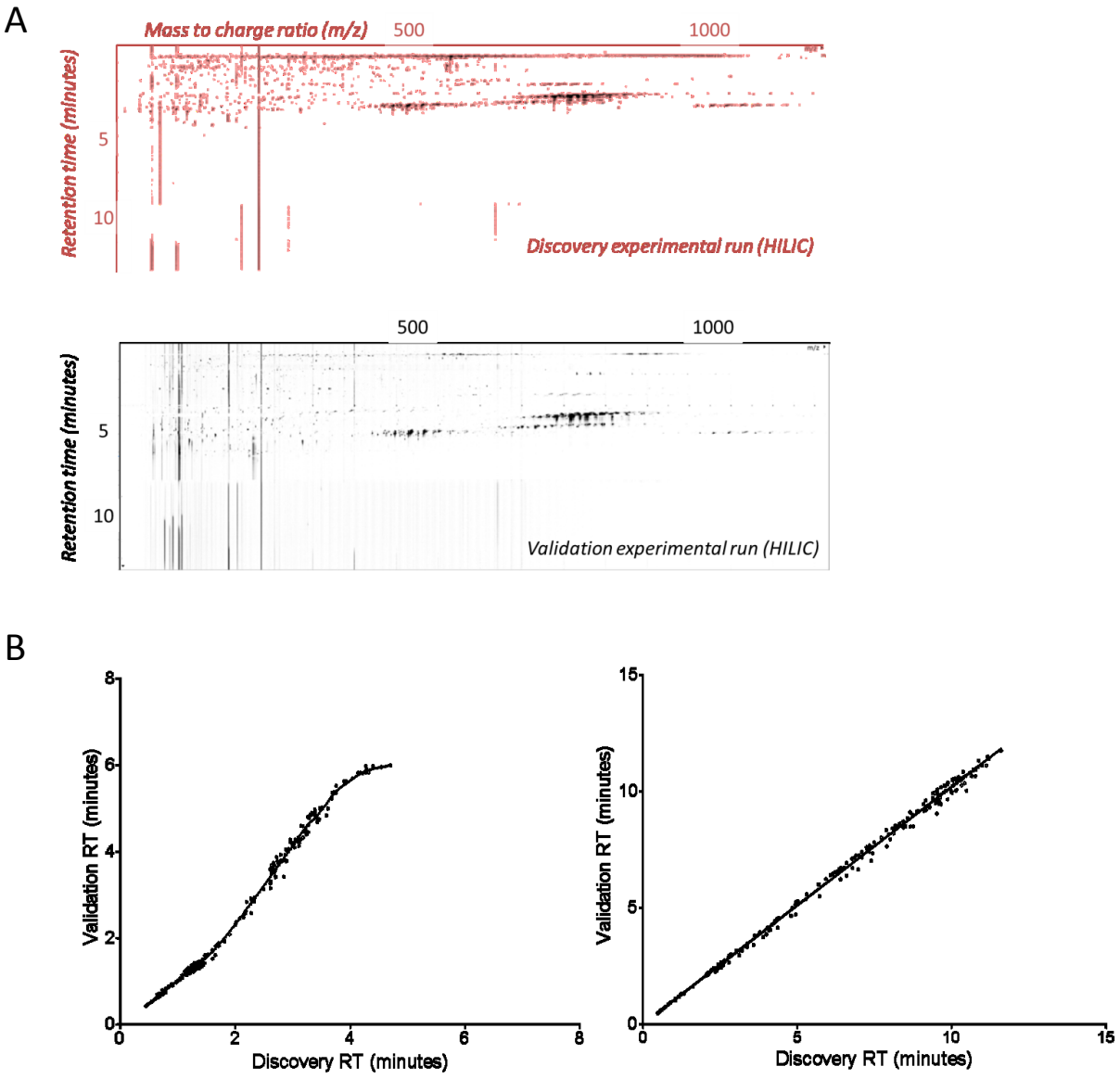


Figure 2.7 – Assessment of UPLC-MS peaks detected across all experimental runs. A) Peaks detected between the discovery and validation experimental runs using HILIC chromatography in a quality control of pooled samples are shown. Due to a change in protocol at the Clinical Phenome Centre, a different gradient run was used for the validation experiment where overall the chromatographic run is longer (6 minutes rather than 5 minutes) and after 2 minutes, there is a non-linear relationship with the same peaks detected later in the validation experiment. The relationship between the time at which peaks were detected between the experimental runs could be modelled using lowess non-linear regression. **B)** Peaks detected within 0.3 minutes between the discovery and validation experimental runs are shown for HILIC and lipidomics mode experiments, based on a lowess and linear regression model respectively. UPLC-MS, ultra performance liquid chromatography mass-spectrometry; HILIC, hydrophilic interaction chromatography; Lowess, locally weighted scatter plot smoothing; RT, retention time.

2.5.4 Identification of UPLC-MS peaks

The identities of peaks of interest were investigated through comparisons of m/z values with published databases including HMDB, and Metlin (Scripps Center for Metabolomics and Mass Spectrometry, La Jolla, CA, U.S.A), to provide putative identities for peaks of interest. In order to confirm these identities, tandem mass spectrometry (MS/MS) analysis was conducted to provide fragmentation patterns for a peak of interest, where both the parent ion and the fragments could be compared to reference databases. In addition, pure standard compounds representing the chemical identities of the peaks of interest were purchased (Appendix Table 2.1) and underwent UPLC-MS in order to compare the retention time and mass to the peak of interest under the same experimental conditions.

2.5.5 Tandem mass spectrometry (MS/MS)

Tandem mass spectrometry is conducted to aid in the identification on a metabolite of interest, by providing high accuracy data on both the parent and daughter ions by fragmenting the parent ion of interest. This data can be compared to databases such as HMBD and Metlin, but ideally to the fragmentation data of an authentic standard (Want, Masson et al. 2013).

Sample preparation was the same as for UPLC-MS experimentation, and conducted on high-resolution Q-Tof instruments from Waters Limited, Manchester, UK (Synapt and Xevo G2-XS), using lipidomics chromatography in positive ion mode. Due to time constraints and machine availability, it was not conducted in negative ion mode or using HILIC chromatography.

Peaks of interest were isolated, using XCalibur software (ThermoFisher Scientific, MA, USA) to define a mass/charge window, and the collision energy gradually increased (from 10eV to maximum of 40eV) until the peak fragmented. The resultant spectra were stored, fragment regions of the peak recorded and cross referenced against published databases of metabolites, and the fragmentation pattern of a subset of pure standard compounds.

2.5.6 Analysis of pure standard compounds

Chemical standards for candidate metabolites of interest were purchased from Sigma Aldrich (Missouri, USA), Santa Cruz Biotechnology (Texas, USA), Ambinter (Orleans, France), Elastin Products

(Missouri, USA), Berry and Associates (Missouri, USA), Enamine (New Jersey, USA) and Avanti Polar Lipids (Alabama, USA) (Appendix Table 2.1). Comparison of the mass and retention time, as well as fragmentation patterns in some cases was made between compound standard and metabolites of interest to confirm their identity.

2.5.7 Commercial platform (Metabolon)

Metabolomic profiling by UPLC-MS was also conducted by a commercial approach using the Discovery HD4^{TM} Global Metabolomics platform, Metabolon, Inc. (Durham, NC, USA) (Evans AM1 2009), who provided semi-quantitative assessment of 949 named and 467 unnamed metabolite levels, annotated with pathways. This commercial platform was used to validate metabolites we had found to be associated with PAH from the unbiased UPLC-MS approach. As it also provided information on named metabolites which were not identified by the initial UPLC-MS approach, it allowed assessment of novel metabolites and metabolic pathways associated with PAH.

Plasma EDTA samples (200µL) were maintained at -80^{0}C prior to processing, and were prepared with use of an automated MicroLab STAR system (Hamilton Company, Reno, NV, USA). For quality control (QC), a pooled sample from all experimental samples was used throughout the experiment, and a mixture of Metabolon QC standards were spiked into all experimental samples to monitor instrument performance and chromatographic alignment. Samples were randomised prior to experimentation.

Experiments were conducted on Waters Acuity ultra-performance liquid chromatography (UPLC) systems (Waters Corporation, Milford, MA, USA) using Thermo Scientific Q-Exactive high resolution/accurate mass spectrometer interfaced with a heated electrospray ionization (HESI-II) source and Orbitrap mass analyser (Thermo Fisher Scientific, MA, USA).

The analysis platform used four methods for Ultrahigh Performance Liquid Chromatography-Tandem Mass Spectroscopy (UPLC-MS/MS) including a) positive ion mode electrospray ionisation (ESI), b) positive ion mode optimised for hydrophobic compounds, c) negative ion mode ESI and d) negative ionisation following elution from a hydrophilic interaction chromatography (HILIC) column. Scan time varied between methods and covered 70-1000m/z.

The resulting spectra were compared to the in-house Metabolon standard library using retention time, mass, adducts and MS/MS spectra. A subset of metabolites were named compounds identified

based on mass and fragmentation analysis but yet to be confirmed with standards, and are indicated by asterisks. Metabolon provided raw data with the quantitative abundance of 1416 metabolites in all plasma samples.

Analysis using this platform has been applied to measure metabolite levels in human plasma in control (Shin, Fauman et al. 2014, Guo, Milburn et al. 2015) and disease populations (Lawton, Brown et al. 2014, Miller, Kennedy et al. 2015).

2.6 Enzyme-linked immunosorbent assay (ELISA)

To assess levels of circulating proteins which may be associated with, or act on, metabolites of interest, ELISA based experiments were conducted. An example of this was the assessment of plasma angiogenin levels, which were determined by ELISA (Ref:DAN00, R&D Systems, Abingdon, UK) as per manufacturer's guidelines, with 200 µL EDTA plasma samples diluted 1:800 before assay after testing several dilution options (Figure 2.8).

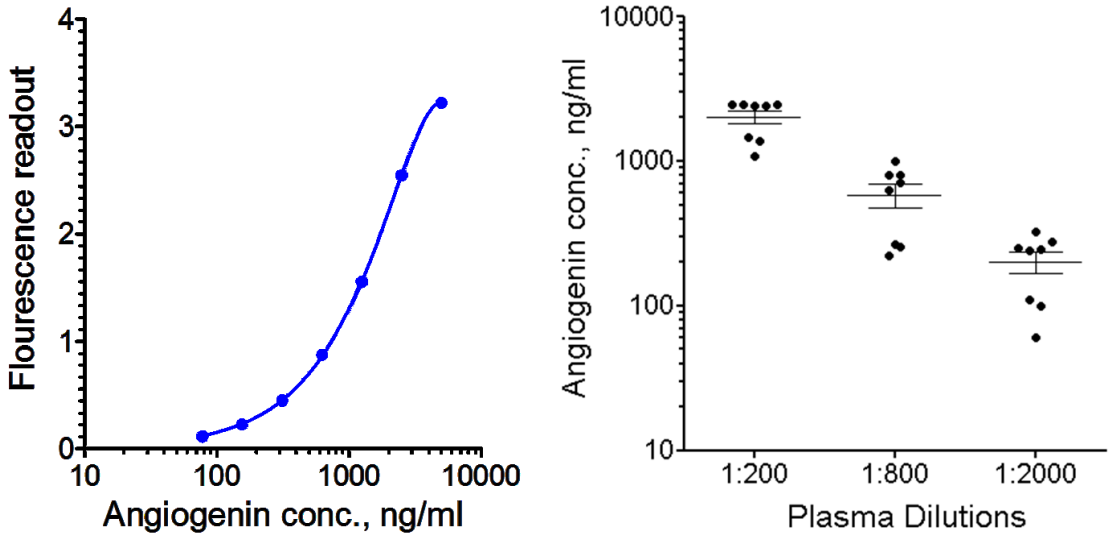


Figure 2.8 – Assessment of plasma dilutions for angiogenin ELISA. Representative standard curve is shown. Angiogenin levels are shown for different plasma dilutions with a dilution of 1:800 chosen to provide values of angiogenin within the standard curve range. conc., concentration.

This assay used a sandwich ELISA technique, which is highly sensitive and provides quantitative values against a standard curve. Here the antigen angiogenin is bound to pre-coated capture antibodies on the surface of the plate, and after incubation any unbound materials are removed. The antigen is then sandwiched between the capture antibody and a specific detecting antibody which is added to the sample. Following this, an enzyme linked secondary antibody binds to the detecting antibody and a substrate solution is added and converted to a detectable form (colour signal) by the enzyme. This signal can be measured by absorbance at 450/540nm. This assay has been used to measure circulating angiogenin levels in diseases such as cancer(Landt, Mordelt et al. 2011) and cardiovascular disease (Idriss, Lip et al. 2010).

2.7 Immunohistochemistry

To investigate the potential source of metabolites associated with PAH, immunohistochemistry experiments were conducted with lung tissue from PAH patients. Antibody targets included 1-methyladenosine, pseudouridine and angiogenin, and were purchased from MBL International Corporation (Massachusetts, USA) and Sigma Aldrich (Missouri, USA), (Appendix Table 2.1) with experiments conducted as per manufacturers guidelines.

Briefly, formalin-fixed paraffin embedded sections were dewaxed and rehydrated, washed in phosphate buffer saline and immersed in hydrogen peroxide to block endogenous peroxidase and minimise non-specific background staining. After application and wash with a blocking buffer (20mmol/L 4-(2-hydroxyethyl)-1-piperazineethanesulfonic acid-HEPES/1% Bovine Serum Albumin-BSA/135mmol/L NaCl (pH 7.3)), the primary antibody was applied and incubated. Dilutions of 1:10000, 1:1000 and 1:400 were used for anti-1-methyladenosine, anti-pseudouridine and anti-angiogenin antibodies respectively, with an incubation period of 1 hour at room temperature. This was followed by a secondary antibody (Histostar (Ms+Rb), MBL code 8460) for 30 minutes at room temperature. Visualisation was conducted by immersing the sections in 3,3'-Diaminobenzidine substrate solution (Histostar DAB Substrate Solution, MBL code 8469) targeting the secondary antibody and counterstaining with haemotoxylin. Use of these antibodies and methodology have previously been conducted in renal tissue from animal models (Mishima, Inoue et al. 2014) and resected human cancer tissue (Masuda, Nishihira et al. 1993).

2.8 Targeted fluorometric assays

To investigate a subset of metabolites which were not identified using the unbiased UPLC-MS approach, or the commercial Metabolon platform, targeted flourometric assays were used. This approach focused specifically on metabolites involved in pathways which were found to be abnormal in PAH. Metabolites measured with these assays included oxaloacetate and acetyl co-A, with plasma EDTA samples diluted 1:5 and 1:800 for each experiment respectively, after testing different plasma dilutions.

Assays were purchased from Abcam (Cambridge, UK), AAT Bioquest (Sunnyvale, CA, USA) and Stratech Scientific Limited (Suffolk, UK) with experiments conducted as per manufacturers guidelines. The Amplite™ Fluorimetric Oxaloacetate Assay Kit (AAT Bioquest, Ref:13841) involves the conversion of oxaloacetate to pyruvate, which produces hydrogen peroxide that can be measured by the fluorescence reader. The PicoProbe Acetyl CoA Assay Kit (fluorometric) (Abcam, Ref:ab87546) converts acetyl Co-A to Co-A, and generates fluorescence through the interaction of a PicoProbe with Nicotinamide adenine dinucleotide (NADH), formed by a reaction of Co-A.

2.9 Whole genome sequencing

Whole-genome sequencing data were available from the UK National Institute of Health Research Biomedical Research Centres Inherited Diseases Genetic Evaluation (BRIDGE) consortium, to investigate variants underlying rare diseases.

Whole-genome sequencing was undertaken by Illumina (San Diego, CA, USA) with a target of sequencing 1250 PAH patients, as well as sequencing other rare disorders including bleeding and platelet disorders, primary immune disorders, steroid resistant nephrotic syndrome and Ehlers-Danlos syndromes.

Whole-genome sequencing data was used to determine which patients had known pathogenic mutations in the gene encoding the bone morphogenetic protein type II receptor (BMPR2) (Machado, Eickelberg et al. 2009). Variants with known associations with metabolites based on published data in human control subjects (Shin, Fauman et al. 2014), were tested for variant-metabolite associations in the PAH population.

2.10 Statistical analysis

Data are presented as absolute numbers, percentages, mean or median (±standard deviation, SD) and percentile range. The principles of the statistical approach applied can be found in Figure 2.9.

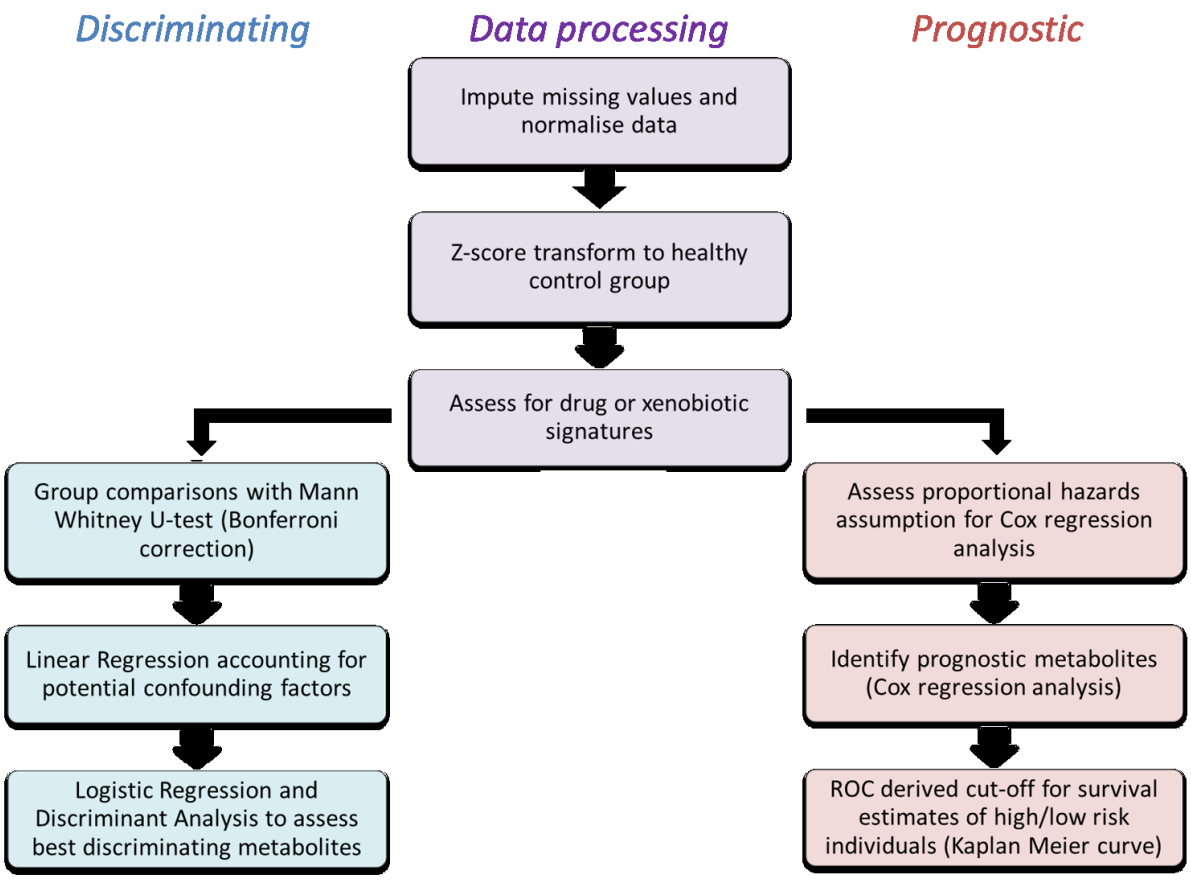


Figure 2.9 – Statistical analysis pipeline. Principles behind metabolomics statistical analysis are shown. These include data processing and identification of metabolites which are discriminating between PAH and controls, and prognostic in PAH. Linear regression accounts for potential confounders including age, gender, ethnicity, body mass index, renal and hepatic dysfunction and drug therapy. ROC; receiver operating characteristics.

Samples where metabolites were undetected were imputed with the minimum detected level for the metabolite. Prior to modelling, metabolites detected by UPLC-MS whose distribution was not normal were transformed either by $\log_{10}$ or power transformations (x^Y, with Y from -2 to 2 in 0.5 steps, as performed for Box-Cox transformations (Box and Cox 1964), whichever best normalised the data based on Kolmogorov-Smirnov tests (i.e. with the largest p value), or ranked if no test met $p>0.05$. Data were z-score transformed based on healthy control data for ease of comparisons between different cohorts and experimental runs. This was conducted by subtracting the mean and dividing by the standard deviation of the healthy control group. In some experiments, bridging samples from controls and patients were used in order to account for between-experiment variability.

Comparisons of peaks between PAH patients who were or were not prescribed specific drug therapies (including anticoagulants, PDE5 inhibitors, ERAs, diuretics, aldosterone antagonists, statins, calcium channel blockers, cardiac glycosides, antidiabetic drugs, prostanoids, iron replacement therapy and ACE inhibitors) at the time of sampling were conducted using the Mann Whitney U test and post-hoc Bonferroni correction applied. Peaks significantly different between PAH patients on and off specific therapies (following correction for multiple testing), or those with a known identity of a drug or xenobiotic were classified as 'drug-related'.

The remaining peaks were analysed for comparisons between diagnostic groups using the Mann Whitney U test and post-hoc Bonferroni correction applied. Either univariate or multivariate statistical approaches can be applied for metabolomics data (Cambiaghi, Ferrario et al. 2016), and the combination of the two approaches is highly recommended (Vinaixa, Samino et al. 2012). Univariate analysis involves assessment of a single variable at a time, with correction for multiple testing recommended (Cambiaghi, Ferrario et al. 2016), and allows you to retain information about variables that would otherwise be filtered out by multivariate approaches (Vinaixa, Samino et al. 2012). Multivariate analysis involves assessment of multiple variables at the same time, and is frequently conducted in metabolomics (Worley and Powers 2013). However, this approach can have difficulties with overfitting due to the model too closely reporting on a limited number of data points and instead reporting on noise and error, leading to decreased predictive power of the model (Vinaixa, Samino et al. 2012). Whilst univariate approaches provide information on the independent change in a variable, multivariate assesses the relationship of variables and other biological factors to one another (Saccenti, Hoefsloot et al. 2013).

To prevent skewing of results by outliers, and to retain information on discriminating metabolites, initial group comparisons between controls and patients were performed using univariate non-

parametric Mann Whitney U tests. Subsequent regression models were used to assess potential confounding factors and to identify metabolites which best discriminated between PAH and controls.

Linear regression analysis was conducted to assess the relationships between metabolite levels, diagnoses and potential confounders including age, gender, ethnicity, body mass index, renal and hepatic dysfunction and drug therapy. In the disease control, PAH and CTEPH cohorts, preserved renal function was defined as creatinine <75 µmol/L, and liver function as bilirubin <21 µmol/L. In the healthy control group, preserved renal and hepatic function was assumed as clinical assay data was unavailable. Logistic regression was conducted to determine metabolites that independently distinguished between diagnostic groups. Orthogonal partial least squares discriminant analysis (OPLS-DA) modelling was used to test the performance of these metabolites. R^2 scores indicate model performance and Q^2 scores estimate reproducibility, based on cross validation. Pathway enrichment analysis was conducted on discriminating and prognostic metabolites using Fisher's exact test.

Survival analyses were performed using time from sampling to death/census. In a secondary analysis, transplantation or death (all-causes) was used as a composite endpoint. Cox regression analysis was used to identify prognostic predictors, with proportional hazard assumptions tested. A proportional hazards assumption in Cox regression analysis indicates that a step change in a metabolite from any value has the equivalent hazard ratio over time. Metabolites found to predict survival were tested against established prognostic indicators – namely, N-terminal pro-brain natriuretic peptide (NT-proBNP) (Nagaya, Nishikimi et al. 2000), six minute walk distance (6MWD) (Fritz, Blair et al. 2013)and red cell distribution width (RDW) (Rhodes, Wharton et al. 2011). Kaplan-Meier plots were used to illustrate events from time of sampling in relation to metabolite levels. Receiver Operating Characteristic (ROC) curves were used to assess discriminating and prognostic value of metabolites against diagnosis and all-cause mortality respectively. Hierarchical clustering based on Euclidean distances was used to assess if metabolites and patients clustered by functional pathways and phenotypes, respectively.

Network analysis was performed to assess the relationship between metabolites. Here metabolite information is imported into a software package which assesses the correlation between metabolites by calculating second order Spearman's rank correlations using ParCorA (http://www.comp-sys-bio.org/software.html), where 2 variables in the dataset correlate with one another after correction for at least 2 other variables (second order), in order to create a causal link between them (de la Fuente, Bing et al. 2004). Network analysis was visualised using Cytoscape

(http://www.cytoscape.org/). ‘Hub’ nodes are metabolites with the most ‘edges’ (correlations) to other metabolites.

Statistical analysis was performed using IBM SPSS Statistics 22 (International Business Machines Corporation, New York, USA), Matlab (Matrix Laboratory, MathWorks, Natick, Massachusetts, USA), Microsoft Excel (Microsoft, Redmond, Washington, USA), SIMCA-P software, (Umetrics, Umea, Sweden) and R with RStudio and associated packages (http://CRAN.R-project.org/).

Chapter 3 - Metabolic phenotyping by nuclear magnetic resonance (NMR) spectroscopy in PAH

3.1 Introduction

NMR spectroscopy is a highly reproducible technique and has been used to measure metabolite changes in a number of disease states such as colorectal cancer (Jimenez, Mirnezami et al. 2013) and coronary artery disease (Malik, Sharma et al. 2015). In addition, NMR can be used to assess lipoprotein subclasses (Mihaleva, van Schalkwijk et al. 2014, Flote, Vettukattil et al. 2016) including high density lipoprotein (HDL) and HDL subclasses (Table 3.1). Recent studies have indicated that circulating HDL levels are decreased and prognostic in PAH patients (Zhao, Peng et al. 2012), although this has been contested by other groups (Cracowski, Labarere et al. 2012). This study represents the first to use NMR spectroscopy to measure both lipid subclasses and metabolite levels in patients with PAH.

NMR HDL subpopulation nomenclature	HDL subclass	Size group	Size range (nm)	Density range (g/mL)
HDL-1	HDL3c	Very small (preβHDL)	7.2-7.8	1.154-1.210
HDL-2	HDL3b	Small	7.8-8.2	1.129-1.154
HDL-3	HDL3a	Medium	8.2-8.8	1.110-1.129
HDL-4	HDL2a	Large	8.8-9.7	1.088-1.110
HDL-5*	HDL2b	Very large	9.7-12.9	1.063-1.087

Table 3.1 – HDL classification and nomenclature. Adapted from (Barter, Kastelein et al. 2003, Rosenson, Brewer et al. 2011, Hafiane and Genest 2015). HDL subclasses are defined based on their density (ultracentrifugation) into HDL2 and HDL3 and sub-fractionated based on their size (gel electrophoresis) (Camont, Chapman et al. 2011). Density range is shown from density gradient ultracentrifugation, and size range from gradient gel electrophoresis and NMR spectroscopy. HDL, high density lipoprotein. *HDL-5 is not measured by Bruker.

I hypothesised that NMR spectroscopy could be used to measure circulating metabolite levels in PAH. I set out to a) validate published changes in metabolite levels related to energy metabolism

such as increased citrate, succinate (Lewis, Ngo et al. 2016), lactate, pyruvate and glutamine (Bujak, Mateo et al. 2016); b) identify novel metabolite changes; c) assess changes in lipid subgroup levels; and d) assess metabolite changes in relation to survival.

3.2 Methods

See Chapter 2 for detailed experimental methods and protocols.

Samples were obtained from healthy controls (HC), disease controls (DC) and patients with idiopathic or heritable PAH and CTEPH, and examined following randomisation and an unbiased approach to ensure that each plate was representative of all sample groups. World Health Organisation functional class (WHO-FC) and six minute walk distance (6MWD) data was obtained at the sample date. Clinical biochemical data, such as bilirubin and red cell distribution width (RDW), were recorded within 30 days of the sample date.

NMR profiles were recorded as 20000 data points and calibrated to glucose. Prior to analysis, regions containing TSP (less than 0.65ppm), H_2O (4.33-4.90ppm), ethylenediaminetetraacetic acid (EDTA) (2.51-2.58, 3.06-3.17ppm), paracetamol (2.15-2.16, 3.61-3.63, 5.08-5.10, 7.15-7.16, 7.34-7.37ppm) and background noise (above 7.87ppm) were removed. This left 12089 data points (ppm) from each sample for further analysis, and all of these spectral data points were z-score transformed based on healthy control data for ease of comparisons.

Mann Whitney U test was used to compare each of the 12089 data points in the 4 group comparisons between controls (healthy controls or disease controls) and patients (PAH or CTEPH) and areas of interest defined by significant consecutive points ($p<0.01$), leaving 201 regions for further analysis (Figure 3.1A). Distinct peaks within areas of interest, and data from lipoprotein subclass analysis for 105 lipid NMR features, were compared between PAH patients and healthy controls by Mann Whitney U-test ($p<0.05$). For clarity, HDL lipid features are referred to based on their subclass nomenclature throughout the chapter (Table 3.1).

Linear regression analysis was conducted to assess the relationships between metabolite levels, diagnoses and potential confounders including age, gender, ethnicity, BMI, renal and hepatic dysfunction and drug therapy. Patients taking any type of statin therapy or dose were considered to be on statins. In the disease control, PAH and CTEPH cohorts, preserved liver function was defined as bilirubin <21 µmol/L. In the healthy control group, preserved hepatic function was assumed as

clinical assay data was unavailable. Renal function was defined based on a NMR peak at 3.039ppm which was identified as creatinine. This was used instead of clinical assay data for creatinine because it was available for all patients and controls, whilst the clinical creatinine assay levels were not available for healthy controls.

In order to help identify peaks that were significantly different between PAH and controls, STOCSY (statistical total correlation spectroscopy) (Cloarec, Dumas et al. 2005) was used to indicate regions of the spectrum with correlating intensities to areas of interest across the entire sample set (Figure 3.1B). To identify the molecules, NMR peaks of interest were cross-referenced to information in available reference databases (SpectraBases-AMIX software, HMDB, Metlin). Spectra from samples with high intensities of the peak of interest and regions found to correlate to the peak from STOCSY analysis were cross-referenced to the databases. If a metabolite was suspected, other regions of the spectra were compared to the sample spectra. In addition, the ^{1}H and 2D ^{13}C-^{1}H chemical shift were cross referenced to the same databases to confirm the identity of potential metabolites (Figure 3.1C-D).

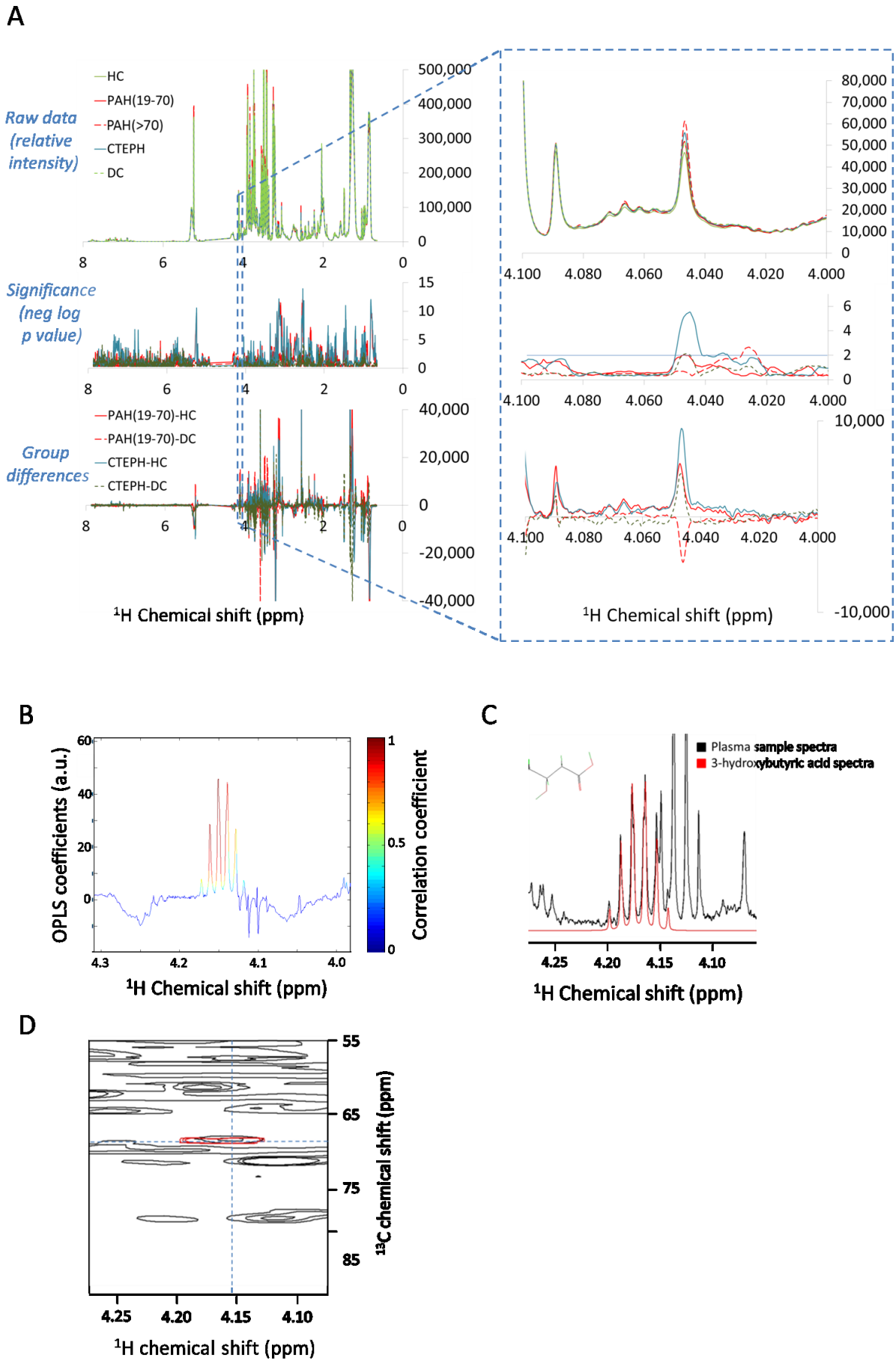

A
Raw data (relative intensity)
HC
PAH(19-70)
PAH(>70)
CTEPH
DC
Significance (neg log p value)
Group differences
PAH(19-70)-HC
PAH(19-70)-DC
CTEPH-HC
CTEPH-DC
¹H Chemical shift (ppm)
¹H Chemical shift (ppm)
B
OPLS coefficients (a.u.)
Correlation coefficient
¹H Chemical shift (ppm)
C
Plasma sample spectra
3-hydroxybutyric acid spectra
¹H Chemical shift (ppm)
D
¹³C chemical shift (ppm)
¹H chemical shift (ppm)

Figure 3.1 – NMR analysis of plasma samples from patients with PAH and controls. (A) NMR profiles of plasma samples. First panel shows the average intensity for each group at a given chemical shift. Each line represents a 'pseudo-spectra' of the average intensity for each group. Second panel shows the negative log p value based on a Mann Whitney U test between different group comparisons at a given chemical shift. Each line represents a 'pseudo-spectra' of the significance of different group comparisons. Third panel shows the difference in intensity values (based on subtraction) between different group comparisons. Each line represents a 'pseudo-spectra' of the fold difference between groups. **(B)** Statistical total correlation spectroscopy (STOCSY) analysis from a peak of interest at 2.31ppm, showing one region of the spectrum with correlating intensities to this peak across the entire sample set. Line colour represents the strength of correlation. **(C)** ^{1}H NMR data and **(D)** 2D ^{13}C-^{1}H NMR data from a PAH patient (black) and the reference NMR spectrum representing 3-hydroxybutyric acid (red). HC, healthy controls; DC, disease controls; PAH, pulmonary arterial hypertension; CTEPH, chronic thromboembolic pulmonary hypertension; OPLS, Orthogonal partial least squares.

Survival analysis was conducted using Cox regression analysis. Metabolites found to predict survival were tested against established prognostic indicators – namely, NT-proBNP (Nagaya, Nishikimi et al. 2000), 6MWD (Fritz, Blair et al. 2013) and RDW (Rhodes, Wharton et al. 2011). Kaplan-Meier plots were used to illustrate events from time of sampling in relation to metabolite levels. Receiver Operating Characteristic (ROC) curves were used to assess the prognostic value of metabolites against all-cause mortality respectively.

For healthy controls and PAH patients who had undergone NMR spectroscopy, measures of apolipoprotein A1 were available for plasma samples (120µL EDTA plasma) from a proteomic experiment contemporary to this study (Rhodes, Wharton et al. manuscript submitted). The proteomic assay was conducted using SOMAscanV3 (Somalogic Inc. Boulder, CO, USA), which uses DNA-based aptamer reagents known as SOMAmers (Gold, Ayers et al. 2010).

3.3 Results

Analysis using ^{1}H NMR profiling was performed on samples from healthy controls (HC, n=63), disease controls (DC, n=47), PAH patients (n=131) and CTEPH patients (n=152). PAH patients were divided into those aged 19-70 (n=103) and >70 years (n=28). Healthy controls were age- and sex-matched to the PAH 19-70 year group, to minimise the confounding factors of age and gender, only this group was compared to healthy controls.

60/152 CTEPH patients had previously undergone pulmonary endarterectomy (PEA) surgery at the time of sampling. 14/152 had their sample taken prior to PEA surgery, 18/152 declined surgery but were operable, and the remaining were deemed inoperable due to distal disease (n=34), age/co-morbidities/borderline PH (n=17) or unknown reasons (n=9). Baseline characteristics and laboratory data are shown in Table 3.2.

	HC (n=63)	DC (n=47)	PAH (19-70) (n=103)	PAH (>70) (n=28)	CTEPH (n=152)
Age at sampling	47.5 +/-13.2	58.1 +/-17.7	48.1 +/-13.7	75.5 +/- 4.8	65.8 +/- 15.0
Sex, Female:Male (ratio)	42:21 (2:1)	30:17 (1.76:1)	74:29 (2.55:1)	19:9 (2.11:1)	69:83 (0.83:1)
Ethnicity, % non-caucasian	22.0	40.4	13.6	10.7	14.5
BMI, kg/m^2	30.0+/-10.0	26.0+/-5.6	28.8+/-7.8	28.3+/-7.6	28.2+/-6.0
BMPR2 mutation carriers (%)			7.8	3.6	
Treatment naïve cases (%)			11.7	17.9	
Baseline Haemodynamics at diagnosis					
Pulmonary capillary wedge pressure, mmHg		11.3 +/- 4.1	11.9 +/- 5.8	12.3 +/- 4.5	13.5 +/- 5.2
Mean pulmonary artery pressure, mmHg		21.2 +/- 9.2	54.2 +/- 15.3	45.6 +/- 14.6	44.7 +/- 12.5
Pulmonary vascular resistance, Woods units		2.2 +/- 2.7	12.2 +/- 5.8	8.3 +/- 4.7	9.2 +/- 6.3
Mean right atrial pressure, mmHg		7.1 +/- 4.1	9.8 +/- 5.5	9.3 +/- 5.2	11.2 +/- 5.5
Cardiac output, L/min			4.0 +/- 1.6	4.8 +/- 1.4	4.0 +/- 1.2
Functional status and pathology					
6MWD (m)			297 +/- 152	209 +/- 154	282 +/- 150
WHO Functional Class - I / II / III / IV		11/10/26/0	6/23/63/11	0/4/22/2	12/34/98/8
RDW, %			15.0 +/- 2.1	15.1 +/- 1.2	15.2 +/- 1.7
NT-proBNP (pmol/L)			640 +/- 807	919 +/- 887	
Creatinine, umol/L		81.9 +/- 36.2	79.7 +/- 27.9	104 +/- 37.0	94.3+/-67.4
Bilirubin, umol/L		13.2 +/- 16.5	15.1 +/- 10.4	11.4 +/- 7.1	13.9 +/- 9.2
Comorbidities					
Asthma/COPD		8.5	9.7	10.7	11.2
Diabetes		10.6	14.6	42.9	9.2
CAD/IHD		14.9	10.7	32.1	27
AF/flutter		12.8	13.6	28.6	23
Systemic hypertension		23.4	18.4	71.4	32.9

	HC (n=63)	DC (n=47)	PAH (19-70) (n=103)	PAH (>70) (n=28)	CTEPH (n=152)
Hypercholesterolaemia/lipidaemia		10.6	13.6	21.4	16.4
Drug therapy					
Anticoagulation			75.7	82.1	100.0
PDE5 inhibitors			78.6	67.9	40.1
ERAs			62.1	46.4	29.6
Prostanoids			21.4	3.6	1.3
Diuretics			39.8	71.4	51.3
Aldosterone antagonists			37.9	32.1	25.0
Statins/lipid lowering drugs			24.3	50.0	38.2
CCBs			20.4	32.1	9.2
Cardiac glycosides			19.4	25.0	8.6
Antidiabetic drugs			11.7	35.7	9.9
Iron replacement therapy			13.6	28.6	9.2
ACE inhibitors			11.7	32.1	30.9

Table 3.2 – NMR Cohort Characteristics. Means and standard deviations or counts are given. Clinical pathology parameters are shown within 30 days of the sample date. Co-morbidities and drug therapy are shown as the percentage of patients with those co-morbidities or on each agent (%).BMI, body mass index; NT-proBNP, N-terminal brain natriuretic peptide at time of sample; RDW, red cell distribution width; HC, healthy controls; DC, disease controls; PAH, pulmonary arterial hypertension; CTEPH, chronic thromboembolic pulmonary hypertension; BMPR2, bone morphogenetic protein receptor, type 2; COPD, chronic obstructive pulmonary disease; CAD, coronary artery disease; IHD, ischaemic heart disease; AF, atrial fibrillation; PDE5, phosphodiesterase type 5; ERA, endothelin receptor antagonists; CCB, calcium channel blocker; ACE, angiotensin converting enzyme. Ethnicity is shown for subjects who self-declared. 10 PAH patients were on calcium channel blocker therapy as vasoresponders.

3.3.1 NMR peaks distinguishing between PAH and controls

^{1}H NMR profiles of plasma samples identified 201 areas of interest in clinical group comparisons (Figure 3.1A). Of these 201 regions, 65 contained distinct peaks able to distinguish PAH patients from healthy controls ($p<0.05$) and 40/65 were identified using STOCSY analysis and cross referencing the ^{1}H and 2D ^{13}C-^{1}H chemical shifts to available reference databases (Figure 3.1B-D, Table 3.3, Appendix Table 3.1). These include markers of abnormal oxidation pathways (citric acid, glutamine), renal impairment (creatinine), ketosis (3-hydroxybutyric acid/3-hydroxybutyrate), amino acids (valine, lysine) and several lipid regions.

Peak (^{1}H shift, ppm)	Identity	Group average (z-score relative to healthy controls)	Linear Regression		Confounder
		PAH (19-70)	HC vs PAH	HC+DC vs PAH	HC vs PAH
Increased in PAH vs HC and DC (independent of confounding factors)					
2.65	Citric Acid	0.68 (-0.19 - 1.34)	4.62E-04	1.46E-03	
2.143	Unknown	0.54 (-0.16 - 1.16)	1.97E-02	3.58E-02	
2.366	Unknown	0.91 (-0.32 - 1.77)	4.04E-02	3.53E-02	
Increased in PAH vs HC					
5.757	Lipid region	0.46 (-0.45 - 0.97)	6.66E-01	3.71E-01	Diuretics
5.728	Lipid region	0.43 (-0.56 - 1.06)	5.02E-01	2.31E-01	Diuretics
6.926	Unknown	0.48 (-0.22 - 1.24)	5.48E-01	9.79E-01	ERAs
7.668	Unknown	0.45 (-0.44 - 1.16)	5.75E-01	8.66E-01	Creatinine
6.968	Unknown	0.37 (-0.28 - 1.09)	8.90E-01	9.83E-01	Ald. antag.
2.861	Unknown	0.61 (0.07 - 1.16)	1.08E-01	4.71E-01	PDE5 inhib.
7.734	Unknown	0.41 (-0.47 - 1.08)	7.30E-01	7.69E-01	Age
6.979	Unknown	0.43 (-0.31 - 1.06)	6.17E-01	7.51E-01	Age
4.93	Unknown	0.47 (-0.24 - 1.26)	1.59E-01	2.28E-01	ACE inhib.
3.304	Unknown	0.52 (-0.16 - 1.06)	2.73E-01	4.29E-01	Bilirubin
3.371	Unknown	0.55 (-0.09 - 0.94)	3.43E-01	2.56E-01	Statin
3.333	Unknown	0.47 (-0.06 - 0.97)	1.11E-01	1.80E-01	Anticoag.
2.188	VLDL-4 - Phospholipids	0.67 (-0.41 - 1.40)	3.54E-01	2.90E-01	Creatinine
1.77	Unknown	0.42 (-0.52 - 1.24)	6.37E-01	9.51E-01	Bilirubin
3.581	Glycerol	0.74 (-0.12 - 1.35)	5.99E-01	9.08E-01	Creatinine
3.348	Unknown	0.38 (-0.39 - 1.07)	6.28E-02	5.75E-03	DM drugs
3.567	Glycerol	0.59 (-0.46 - 1.36)	9.50E-01	6.87E-01	Age
3.282	Unknown	0.66 (-0.56 - 1.40)	1.08E-01	1.89E-02	Creatinine
1.4	Unknown	0.60 (-0.27 - 1.37)	8.60E-01	7.49E-01	Bilirubin
2.061	Glutamine related	0.74 (-0.25 - 1.59)	6.33E-01	2.73E-01	Cardiac glycosides
2.052	VLDL-1 - Phospholipids	0.55 (-0.34 - 1.32)	8.53E-01	5.64E-01	Ethnicity
3.039	Creatinine	0.53 (-0.31 - 1.05)	7.01E-01	6.65E-01	Creatinine
3.639	Glycerol	0.48 (-0.51 - 1.11)	7.84E-01	9.64E-01	Age
4.046	Creatinine	0.50 (-0.49 - 1.19)	7.90E-01	7.25E-01	Creatinine
3.785	Unknown	0.43 (-0.43 - 1.14)	8.54E-01	8.90E-01	Bilirubin
2.087	Unknown	0.24 (-0.31 - 0.81)	6.08E-01	2.01E-01	Iron therapy
3.935	Unknown	0.47 (-0.55 - 1.36)	3.16E-01	4.08E-01	Iron therapy
3.678	Background related to glucose	0.51 (-0.36 - 0.93)	7.41E-01	8.18E-01	ERAs
2.32	3-hydroxybutyric acid	0.34 (-0.36 - 0.41)	1.41E-01	1.37E-01	Bilirubin
2.31	3-hydroxybutyric acid	0.28 (-0.34 - 0.32)	1.40E-01	1.50E-01	BMI
2.41	3-hydroxybutyric acid	0.18 (-0.33 - 0.44)	1.70E-01	1.68E-01	BMI
2.104	Unknown	0.19 (-0.54 - 0.95)	4.86E-01	4.05E-01	Ethnicity
5.834	Unknown	0.28 (-0.50 - 0.78)	7.89E-01	4.86E-01	DM drugs
Decreased in PAH vs HC					
7.054	1-methylhistamine	-0.38 (-1.16 - 0.36)	7.85E-01	5.00E-01	Prostanoids
0.794	HDL - Phospholipids	-0.86 (-1.33 - -0.29)	1.05E-01	6.72E-01	Ethnicity
3.199	HDL3a - Cholesterol	-0.95 (-1.66 - -0.35)	9.76E-02	5.54E-01	Ethnicity

Peak (^{1}H shift, ppm)	Identity	Group average (z-score relative to healthy controls)	Linear Regression		Confounder
		PAH (19-70)	HC vs PAH	HC+DC vs PAH	HC vs PAH
2.736	Lipid region	-0.83 (-1.69 - -0.14)	9.19E-02	3.24E-01	ERAs
1.03	Valine	-0.56 (-1.2 - 0.07)	7.80E-01	3.33E-01	Diuretics
2.466	Glutamine	-0.32 (-1.05 - 0.46)	7.68E-01	2.34E-01	Prostanoids
1.047	Valine	-0.56 (-1.17 - 0.15)	8.01E-01	4.16E-01	Diuretics
5.264	HDL3a - Phospholipids	-0.9 (-1.78 - -0.12)	2.60E-01	8.34E-01	Creatinine
3.23	Background related to glucose	-0.47 (-1.11 - -0.06)	8.18E-01	5.26E-01	Ethnicity
1.214	HDL3a - Apo-A1	-0.61 (-1.2 - -0.03)	4.90E-01	8.97E-01	Creatinine
2.455	Glutamine	-0.3 (-0.9 - 0.52)	8.11E-01	4.68E-01	Prostanoids
2.442	Glutamine	-0.38 (-1.17 - 0.4)	7.05E-01	7.44E-01	Creatinine
1.004	Valine	-0.46 (-1.19 - 0.13)	8.09E-01	3.31E-01	Diuretics
5.215	Lipid region	-0.42 (-0.88 - 0.1)	3.87E-01	4.44E-01	Creatinine
4.3	HDL3b - Phospholipids	-0.41 (-1.01 - 0.22)	5.66E-01	7.96E-01	Bilirubin
1.473	Unknown	-0.54 (-1.28 - -0.06)	6.44E-01	7.87E-01	DM drugs
0.942	Valine	-0.94 (-1.75 - -0.3)	2.05E-01	1.76E-01	Diuretics
1.906	Unknown	-0.41 (-1.21 - 0)	8.36E-01	8.52E-01	Prostanoids
3.25	Background related to glucose	-0.26 (-0.94 - 0.27)	9.56E-01	5.89E-01	Age
1.882	Lysine	-0.41 (-1.1 - 0.26)	8.16E-01	6.69E-01	Anticoag.
1.502	Lipid region	-0.39 (-1.36 - 0.26)	9.93E-01	5.79E-01	Bilirubin
1.719	Lysine	-0.43 (-1.26 - 0.31)	6.91E-01	7.00E-01	Anticoag.
3.178	Unknown	-0.63 (-1.42 - 0.3)	2.35E-01	2.16E-01	Age
3.02	Lysine	-0.41 (-1.27 - 0.39)	2.36E-01	2.53E-01	Creatinine
1.194	Lipid	-0.65 (-1.29 - 0.01)	1.06E-01	8.44E-02	Creatinine
1.448	Unknown	-0.75 (-1.42 - -0.05)	2.09E-01	2.34E-01	Anticoag.
1.951	Lipid region	-0.34 (-1.07 - 0.2)	8.16E-01	4.04E-01	Creatinine
1.691	Lysine	-0.31 (-1.22 - 0.69)	2.21E-01	2.41E-01	Iron therapy
1.182	Lipid	-0.41 (-1.24 - 0.22)	1.61E-01	8.90E-02	Creatinine

Table 3.3 – NMR peaks distinguishing PAH from healthy and disease controls. 65 NMR peaks that are significantly different between PAH and healthy controls are shown ($p<0.05$). Mean values are given and the data is scaled to the healthy control group. Significance from linear regression is shown (p value) and for metabolites with $p>0.05$ in PAH HC linear regression, the significant confounder is shown. Identities are shown for 40/65 NMR peaks. HC, healthy controls; DC, disease controls; PAH, pulmonary arterial hypertension; HDL, high density lipoprotein; VLDL, very low density lipoprotein; Apo-A1, apolipoprotein A1; Anticoag., Anticoagulation therapy; DM drugs, antidiabetic drug therapy; ERAs, endothelin receptor antagonists; PDE5 inhib., phosphodiesterase type 5 inhibitors; ACE inhib., angiotensin converting enzyme inhibitors; BMI, body mass index; Ald. antag., aldosterone antagonists.

Of these 65 NMR peaks, 3 distinguished PAH patients from healthy controls and disease controls after correcting for potential confounders including age, gender, ethnicity, BMI, renal and hepatic dysfunction and drug therapy ($p<0.05$, Table 3.3). This included increased citric acid (Figure 3.2) and increased levels of 2 unidentified NMR peaks. These 3 NMR peaks did not discriminate PAH and CTEPH patients following correction for potential confounders ($p>0.05$).

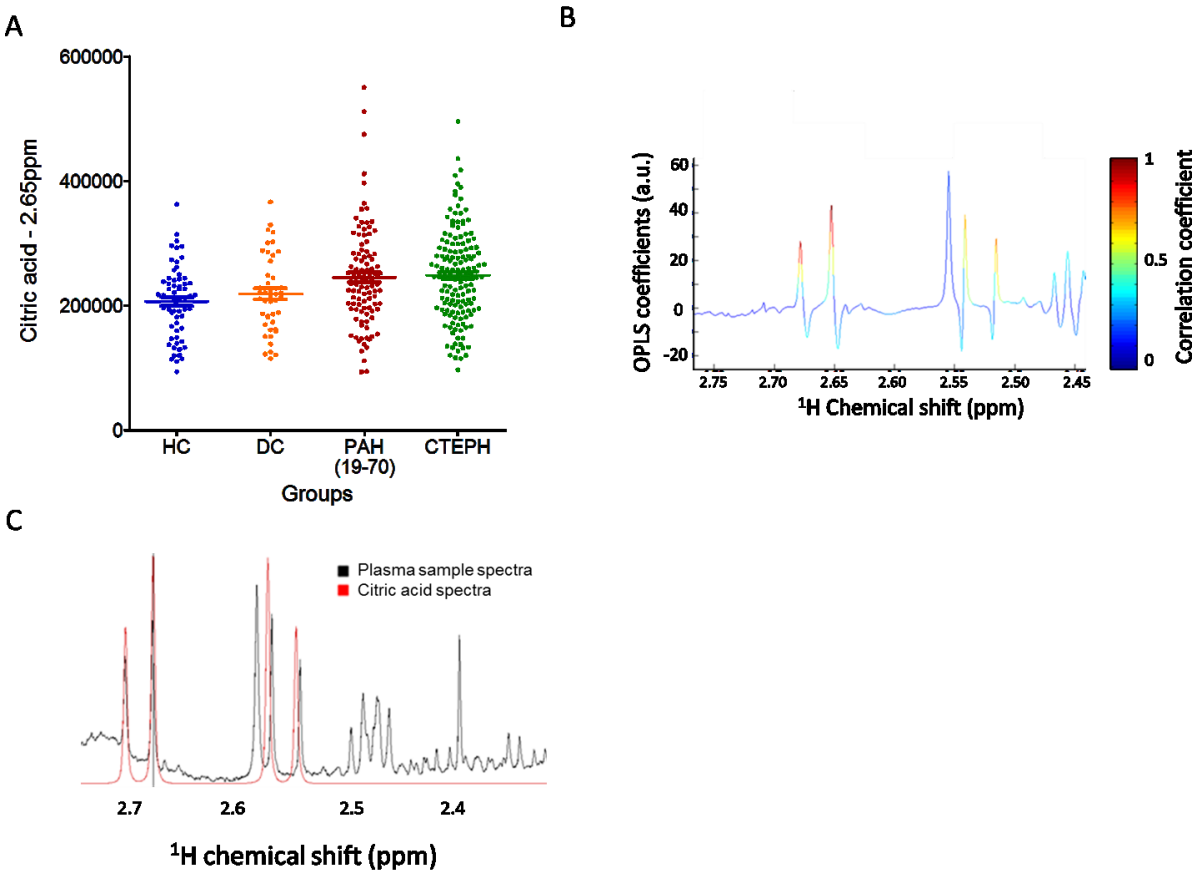


Figure 3.2 – Citric acid NMR peak. (A) Normalised abundance of a ^{1}H NMR peak at 2.65ppm representing citric acid is shown between different groups. Levels were significantly different between PAH patients aged 19-70 against healthy controls (HC) and disease controls (DC) independent of confounding factors ($p<0.05$) but not with chronic thromboembolic pulmonary hypertension (CTEPH). Bar represents mean and standard error of the mean. **(B)** Statistical total correlation spectroscopy (STOCSY) analysis from a peak of interest at 2.65ppm. Line colour represents the strength of correlation. **(C)** ^{1}H NMR data from a PAH patient (black) and the reference NMR spectrum representing citric acid (red) is shown.

The identity of NMR peaks was verified with available clinical assay data, the peak for creatinine correlating with the clinical assay levels of creatinine (Rho=0.655, p<0.001, Figure 3.3A-B). Another NMR peak was identified as 3-hydroxybutyric acid, and another associated peak seen through STOCSY analysis was identified by comparison with reference databases as acetoacetate. Levels of the acetoacetate peak correlated with 3-hydroxybutyrate, a reduced form of acetoacetate (Figure 3.3C). None of the 3 NMR peaks representing 3-hydroxybutyric acid were influenced by diabetic therapy (p>0.05 linear regression analysis).

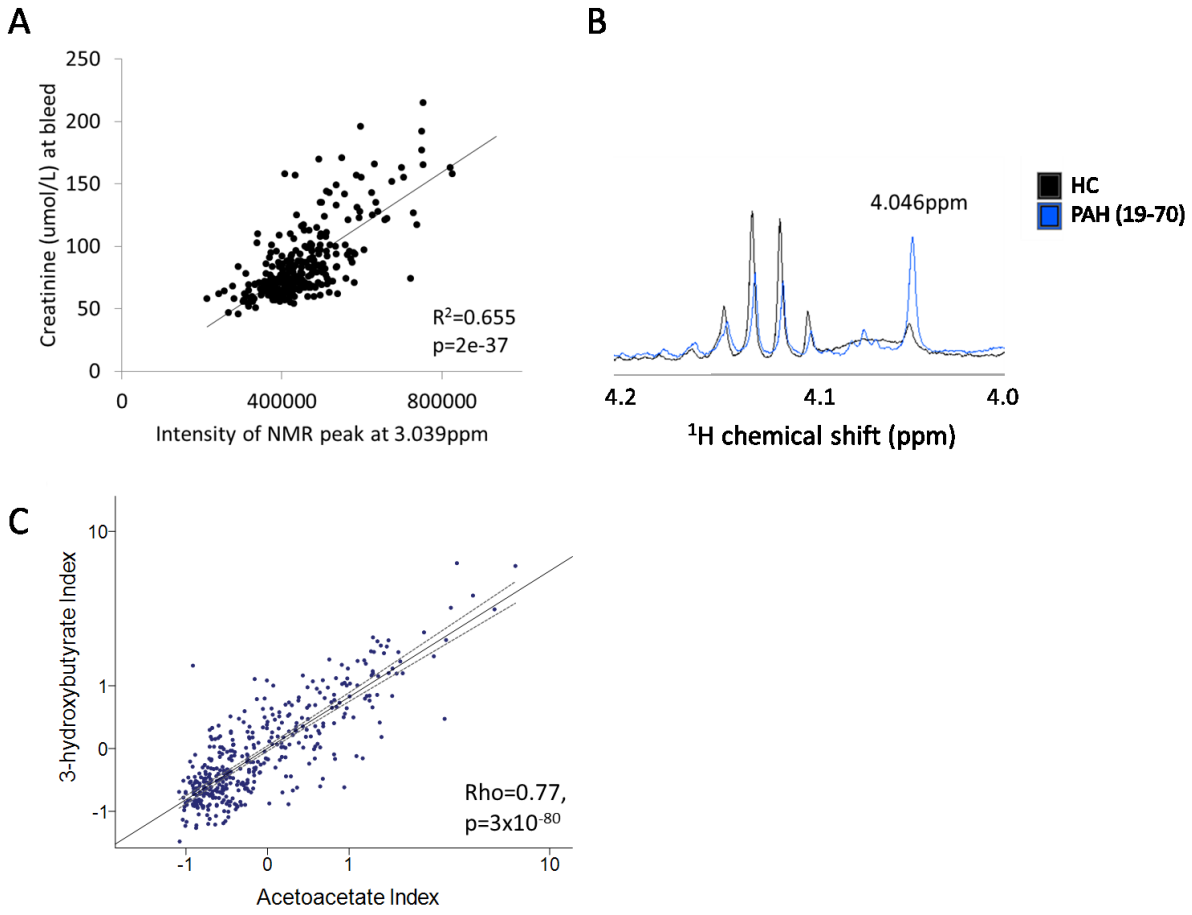


Figure 3.3 – Creatinine and 3-hydroxybutyrate peaks identified by NMR. (A) Scatterplot comparing levels of serum creatinine quantified by clinical assay against quantitation of ^{1}H NMR peak at 4.046ppm, identified as creatinine. **(B)** Creatinine peak at 4.046ppm is shown for one healthy control (HC) and one PAH subject. **(C)** Scatterplot comparing average standardized abundance of NMR peaks identified as acetoacetate (n=2) and 3-hydroxybutyrate (n=4) in plasma samples from PAH patients.

In order to further assess the lipid regions which discriminate PAH patients from controls, NMR profiles known to represent 105 lipid species were compared. 67/105 lipid NMR features were significantly different between healthy controls and PAH patients aged 19-70 years ($p<0.05$, Table 3.4). Of these, 5/67 distinguished PAH from healthy and disease controls after correcting for potential confounders ($p<0.05$, Table 3.4). These changes included increased LDL-Triglycerides and decreased HDL2a Apolipoprotein (Apo) A1, A2 and HDL-cholesterol (Table 3.4). None of these 5 lipid NMR features were significantly different between PAH and CTEPH patients.

	Group Median (IQR)		Linear Regression		Confounder
Lipid NMR Feature	HC	PAH (19-70)	HC vs PAH	HC+DC vs PAH	HC vs PAH
Increased in PAH vs HC and DC (independent of confounding factors)					
LDL-1 - Triglycerides	3.48 (2.31 - 4.18)	5.41 (3.61 - 6.95)	7.46E-03	3.03E-03	
LDL-2 - Triglycerides	2.03 (1.56 - 2.53)	2.4 (1.78 - 2.94)	2.94E-02	1.27E-03	
Decreased in PAH vs HC and DC (independent of confounding factors)					
HDL2a - Apo-A2	24.2 (22.28 - 27.5)	20.62 (17.77 - 24.38)	1.21E-02	1.86E-02	
HDL2a - Apo-A1	87.03 (78.54 - 97.05)	74.84 (63.87 - 86.83)	2.07E-02	4.05E-02	
HDL2a - Cholesterol	22.99 (20.28 - 26.24)	18.76 (14.27 - 22.53)	2.10E-02	3.34E-02	
Increased in PAH vs HC (independent of confounding factors)					
IDL - Apo-B	2.75 (1.77 - 3.25)	3.81 (2.52 - 4.43)	4.37E-02	1.27E-01	
Decreased in PAH vs HC (independent of confounding factors)					
Total Plasma - Apo-A2	41 (37.13 - 43.51)	35.91 (32.4 - 40.16)	1.45E-02	2.10E-01	
HDL - Apo-A2	41.22 (37.21 - 43.7)	36.14 (32.7 - 40.05)	1.52E-02	2.13E-01	
Increased in PAH vs HC					
LDL - Triglycerides	22.13 (19.24 - 25.17)	24.8 (20.68 - 28.79)	7.73E-02	4.68E-03	Ald. antag.
IDL - Free Cholesterol	2.25 (1.36 - 3.02)	3.1 (1.5 - 3.93)	8.61E-02	2.35E-01	Creatinine
LDL-3 - Triglycerides	2.3 (1.8 - 2.77)	2.62 (1.91 - 3.19)	8.73E-02	3.26E-03	Diuretics
IDL - Cholesterol	9.82 (5.34 - 11.61)	13.18 (7.65 - 15.68)	1.08E-01	2.30E-01	Creatinine
VLDL-5 - Free Cholesterol	0.09 (-0.13 - 0.37)	0.3 (-0.04 - 0.49)	1.18E-01	4.69E-01	PDE5 inhib.
LDL-1 - Apo-B	6.57 (4.96 - 7.61)	7.36 (5.17 - 8.92)	1.24E-01	3.44E-02	Creatinine
IDL - Phospholipids	6.33 (4.26 - 8.25)	8.23 (5.67 - 10.1)	1.84E-01	2.48E-01	Creatinine
IDL - Triglycerides	10.57 (7.32 - 13.52)	14.55 (8.35 - 16.56)	2.35E-01	2.50E-01	Creatinine
VLDL-4 - Cholesterol	4.16 (2.29 - 5.38)	5.91 (3.52 - 7.82)	2.45E-01	6.45E-01	DM drugs
VLDL-4 - Free Cholesterol	1.81 (1.08 - 2.43)	2.54 (1.4 - 3.41)	2.70E-01	5.49E-01	Creatinine
VLDL-4 - Phospholipids	4.68 (3.22 - 5.91)	5.92 (3.91 - 7.52)	3.79E-01	7.37E-01	DM drugs
VLDL - Apo-B	5.65 (3.73 - 7.21)	7.09 (4.54 - 9.13)	3.86E-01	7.38E-01	Creatinine
HDL3b - Triglycerides	2.19 (1.73 - 2.52)	2.55 (1.88 - 2.96)	3.96E-01	1.61E-01	Creatinine
HDL3a - Triglycerides	2.2 (1.71 - 2.58)	2.55 (1.89 - 3.02)	3.98E-01	2.57E-01	Creatinine
HDL3c - Triglycerides	4.07 (2.73 - 5.49)	4.91 (3.41 - 5.65)	4.23E-01	1.04E-01	ACE inhib.
HDL - Triglycerides	12.39 (10.02 - 13.6)	14.29 (11.05 - 16.44)	4.55E-01	2.04E-01	Creatinine
Decreased in PAH vs HC					
HDL2a - Free Cholesterol	5.26 (4.48 - 5.96)	4.45 (3.62 - 5.39)	6.68E-02	1.19E-01	Creatinine
Total Plasma - Apo-A1	177.92 (157.95 - 193.31)	156.45 (141.27 - 171.43)	6.91E-02	7.30E-01	Creatinine
HDL - Cholesterol	71.16 (59.32 - 81.29)	59.5 (49.85 - 68.77)	8.29E-02	6.58E-01	Age
HDL - Apo-A1	177.37 (155.95 - 195)	155.13 (138.88 - 171.51)	8.31E-02	7.78E-01	Creatinine
LDL-5 - Free Cholesterol	6.05 (4.8 - 7.39)	4.49 (3.36 - 6.05)	1.01E-01	3.49E-01	ACE inhib.
LDL-5 - Cholesterol	22.34 (15.94 - 28.47)	15.59 (10.19 - 21.82)	1.05E-01	2.65E-01	Bilirubin
LDL-4 - Free Cholesterol	6.29 (5 - 7.74)	4.61 (3.01 - 6.01)	1.13E-01	6.97E-01	ACE inhib.
LDL-5 - Phospholipids	12.22 (8.97 - 15.22)	8.97 (6.22 - 12.1)	1.32E-01	3.40E-01	Iron therapy
HDL3a - Cholesterol	13.05 (10.95 - 14.59)	10.83 (9.22 - 12.15)	1.36E-01	7.44E-01	Creatinine
HDL3a - Free Cholesterol	3.53 (2.84 - 4.28)	2.91 (2.38 - 3.49)	1.73E-01	6.31E-01	Creatinine
LDL-5 - Apo-B	11.7 (8.64 - 14.48)	8.88 (6.22 - 12.07)	1.98E-01	4.29E-01	Iron therapy
LDL-6 - Free Cholesterol	8.28 (6.32 - 9.63)	6.81 (5.37 - 8.38)	2.00E-01	4.03E-01	Diuretics
LDL-4 - Cholesterol	21.15 (16.31 - 27.67)	14.85 (7.1 - 21.11)	2.02E-01	7.12E-01	Statin

	Group Median (IQR)		Linear Regression		Confounder
Lipid NMR Feature	HC	PAH (19-70)	HC vs PAH	HC+DC vs PAH	HC vs PAH
HDL3b - Cholesterol	11.66 (9.13 - 13.66)	9.71 (7.96 - 11.39)	2.24E-01	9.44E-01	Bilirubin
LDL-4 - Phospholipids	11.89 (9.27 - 15.13)	8.86 (5.04 - 12.13)	2.43E-01	8.27E-01	Statin
HDL2a - Phospholipids	30.8 (27.21 - 34.54)	26.62 (22.04 - 30.96)	2.66E-01	2.66E-01	ERAs
HDL3a - Apo-A2	8.11 (6.91 - 9.08)	7.2 (6.25 - 8.24)	2.75E-01	9.97E-01	Creatinine
LDL - Cholesterol	133.74 (106.99 - 160.98)	109.5 (88.07 - 130.57)	3.29E-01	9.89E-01	Statin
LDL-6 - Cholesterol	31.26 (23.35 - 36.75)	25.63 (19.63 - 31.95)	3.35E-01	4.80E-01	Diuretics
LDL-4 - Apo-B	9.76 (7.39 - 12.18)	7.46 (4.79 - 10.1)	3.51E-01	9.57E-01	Statin
LDL-3 - Free Cholesterol	6.3 (5 - 7.66)	4.91 (3.29 - 6.31)	3.55E-01	6.97E-01	Age
LDL-6 - Phospholipids	16.91 (12.93 - 19.97)	14.09 (11.15 - 17.36)	4.07E-01	6.30E-01	Diuretics
HDL - Free Cholesterol	17.82 (14.39 - 20.88)	14.96 (12.13 - 17.77)	4.16E-01	6.88E-01	Ethnicity
HDL3a - Apo-A1	32.15 (27.7 - 36.02)	27.84 (23.84 - 31.29)	4.50E-01	8.83E-01	Creatinine
HDL3b - Apo-A1	26.68 (21.15 - 30.47)	23.46 (19.99 - 26.95)	5.05E-01	5.10E-01	Bilirubin
Total Plasma - Cholesterol	223.12 (191.54 - 251.61)	195.03 (167.39 - 220.71)	5.13E-01	7.43E-01	Creatinine
LDL - Free Cholesterol	38.08 (31.48 - 44.69)	32.28 (26.08 - 38.08)	5.32E-01	6.16E-01	Statin
Total Plasma - Free Cholesterol	68.05 (61.34 - 75.97)	61 (53.13 - 67.55)	5.36E-01	6.18E-01	Creatinine
HDL3b - Free Cholesterol	2.98 (2.35 - 3.57)	2.54 (2.12 - 2.99)	5.36E-01	4.88E-01	Age
HDL3c - Free Cholesterol	6.41 (4.57 - 7.35)	5.28 (3.52 - 6.44)	5.39E-01	3.37E-01	Bilirubin
LDL-3 - Cholesterol	23.3 (18.38 - 28.78)	19.27 (12.47 - 23.86)	5.48E-01	5.83E-01	DM drugs
LDL - Phospholipids	72.74 (60.74 - 85.6)	61.99 (50.74 - 72.73)	5.64E-01	6.41E-01	Statin
HDL3c - Cholesterol	20.65 (13.53 - 25.14)	17.46 (11.87 - 22.21)	5.92E-01	3.01E-01	Bilirubin
HDL3a - Phospholipids	20.4 (16.82 - 22.71)	17.62 (15.01 - 19.76)	6.18E-01	6.37E-01	Creatinine
HDL - Phospholipids	94.08 (76.14 - 104.59)	82.83 (72.13 - 94.36)	6.18E-01	4.33E-01	Creatinine
LDL-3 - Phospholipids	12.73 (10.23 - 15.23)	10.84 (7.37 - 13.1)	6.63E-01	4.45E-01	Age
LDL-6 - Apo-B	18.43 (13.83 - 21.4)	15.84 (12.13 - 19.5)	7.05E-01	8.62E-01	Diuretics
LDL-2 - Cholesterol	17.05 (12.08 - 21.07)	14.97 (9.98 - 18.89)	7.51E-01	2.87E-01	Gender
LDL-3 - Apo-B	9.96 (8.12 - 12.11)	8.71 (6.25 - 10.57)	7.66E-01	3.29E-01	ERAs
LDL - Apo-B	60.92 (49.09 - 70.77)	52.62 (41.66 - 61.54)	8.34E-01	4.58E-01	Statin
HDL3b - Phospholipids	16.18 (12.5 - 19.57)	14.17 (11.71 - 16.69)	8.48E-01	3.01E-01	Ald. antag.
LDL-2 - Free Cholesterol	5.57 (4.15 - 6.63)	4.8 (3.28 - 6.07)	9.49E-01	3.64E-01	Gender
Total Plasma - Apo-B	76.31 (62.59 - 87.08)	70.07 (56.52 - 82.58)	9.55E-01	4.79E-01	Creatinine

Table 3.4 – Lipid NMR features distinguishing PAH patients from healthy and disease controls. 67 lipid NMR features that are significantly different between PAH and healthy controls are shown ($p<0.05$). Median and interquartile range (IQR) for diagnostic groups is shown (mg/dL). Significance from linear regression is shown (p value) and for metabolites with $p > 0.05$ in PAH HC linear regression, the significant confounder is shown. HC, healthy controls; DC, disease controls; PAH, pulmonary arterial hypertension; HDL, high density lipoprotein; IDL, intermediate density lipoprotein; LDL, low density lipoprotein; VLDL, very low density lipoprotein; Apo, apolipoprotein; Anticoag., Anticoagulation therapy; DM drugs, antidiabetic drug therapy; ERAs, endothelin receptor antagonists; PDE5 inhib., phosphodiesterase type 5 inhibitors; ACE inhib., angiotensin converting enzyme inhibitors; BMI, body mass index; Ald. antag., aldosterone antagonists.

The main confounding factors were renal dysfunction and statin therapy. In a sub-analysis, 27/105 lipid features, predominantly low density lipoprotein (LDL) subtypes, were significantly decreased in PAH patients on statin therapy (n=39) versus those off therapy (n=92) ($p<0.05$, Figure 3.4). Of the 39 PAH patients on statin therapy, 44% were on simvastatin 40mg once daily (Table 3.5).

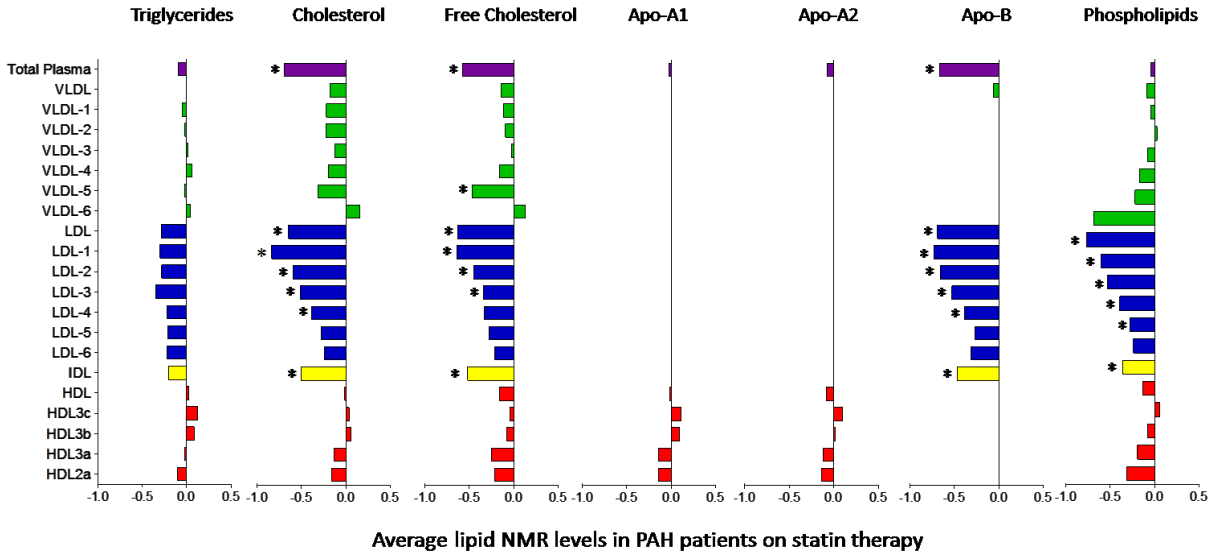


Figure 3.4 – Lipid NMR features between PAH patients on and off statin therapy. Average metabolite levels in PAH patients on statin therapy are shown. Values plotted are z-scores calculated based on mean in PAH patients off statin therapy - negative values indicate lipid features with lower levels in PAH patients on statin therapy and positive values indicate higher levels of lipid features on statins. * indicates 27 lipid features that are significantly different between PAH patients on and off statin therapy by Mann Whitney U test ($p<0.05$). Data is shown in lipoprotein groups – total plasma (purple); VLDL, very low density lipoprotein (green); LDL, low density lipoprotein (blue); IDL, intermediate density lipoprotein (yellow); HDL, high density lipoprotein (red) – and analytes. Apo, apolipoprotein.

Type of statin	Dose daily (mg)	No PAH patients on therapy
Simvastatin		
	10	1
	20	7
	40	17
	80	2
Atorvastatin		
	10	3
	20	2
	40	3
	80	1
Others		
Fluvastatin	80	1
Pravastatin	20	1
Rosuvastatin	10	1

Table 3.5 – PAH patients on statin therapy. Type of statin therapy and dose are shown for all PAH patients on statins.

3.3.2 Survival analysis of NMR peaks in PAH

I hypothesised that metabolites related to the disease pathophysiology would be associated with clinical outcomes, in particular survival. 28/131 PAH patients died with a median follow-up of 3.3 years (+/- 0.8). Creatinine and diuretic use were incorporated into the Cox regression analysis to assess metabolites which predict survival independent of these markers. Creatinine was the most common confounder in the linear regression model between PAH patients and controls and is known to be prognostic in PAH (Shah, Thenappan et al. 2008). Diuretic use was also a common confounder and affects circulating blood volume which may alter metabolite levels. Due to the small number of events in this group, it was not possible to assess all other potential confounders for their prediction of survival.

All 65 NMR peaks and 67 lipid NMR features that discriminate PAH patients and controls met the proportional hazards assumptions of Cox regression analysis. Overall, 31 NMR peaks or lipid NMR features were prognostic after accounting for creatinine and diuretic use (Figure 3.5). 3 PAH cases underwent transplantation. In a sub-analysis, where these patients were excluded, 26/31 metabolites NMR peaks or lipid NMR features remained prognostic ($p<0.05$). The five which did not remain prognostic were LDL-5 free cholesterol and Apo-B, LDL phospholipid and total plasma free cholesterol and Apo-B.

I compared these metabolites to established prognostic indicators - NT-proBNP, 6MWD and RDW - and found that 11/31 NMR peaks and lipid NMR features were independent of these measures ($p<0.05$ by Cox regression analysis, Figure 3.5), including HDL2a Apo-A2 (Figure 3.6).

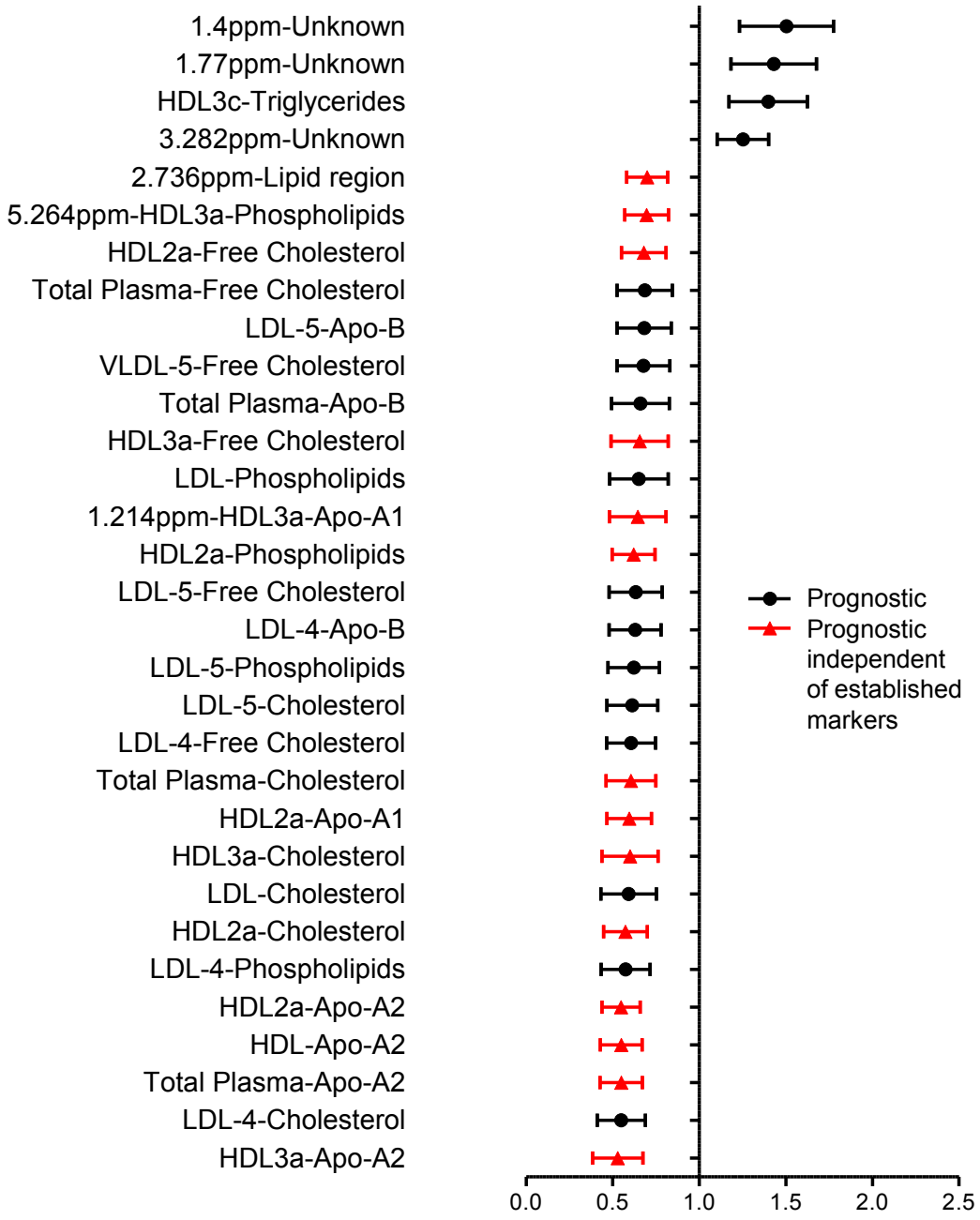


Figure 3.5 - Prognostic NMR peaks and lipid features. Hazard ratios after correcting for creatinine and diuretic use are shown for 31 NMR peaks and lipid features significantly different between PAH survivors and non-survivors. 11 features which are also independent of established prognostic markers, NT-proBNP (N-terminal brain natriuretic peptide), 6MWD (six minute walk distance) and RDW (red cell distribution width) are shown in red. For NMR peaks, the ^{1}H chemical shift is shown in ppm. HDL, high density lipoprotein; Apo, Apolipoprotein; LDL, low density lipoprotein.

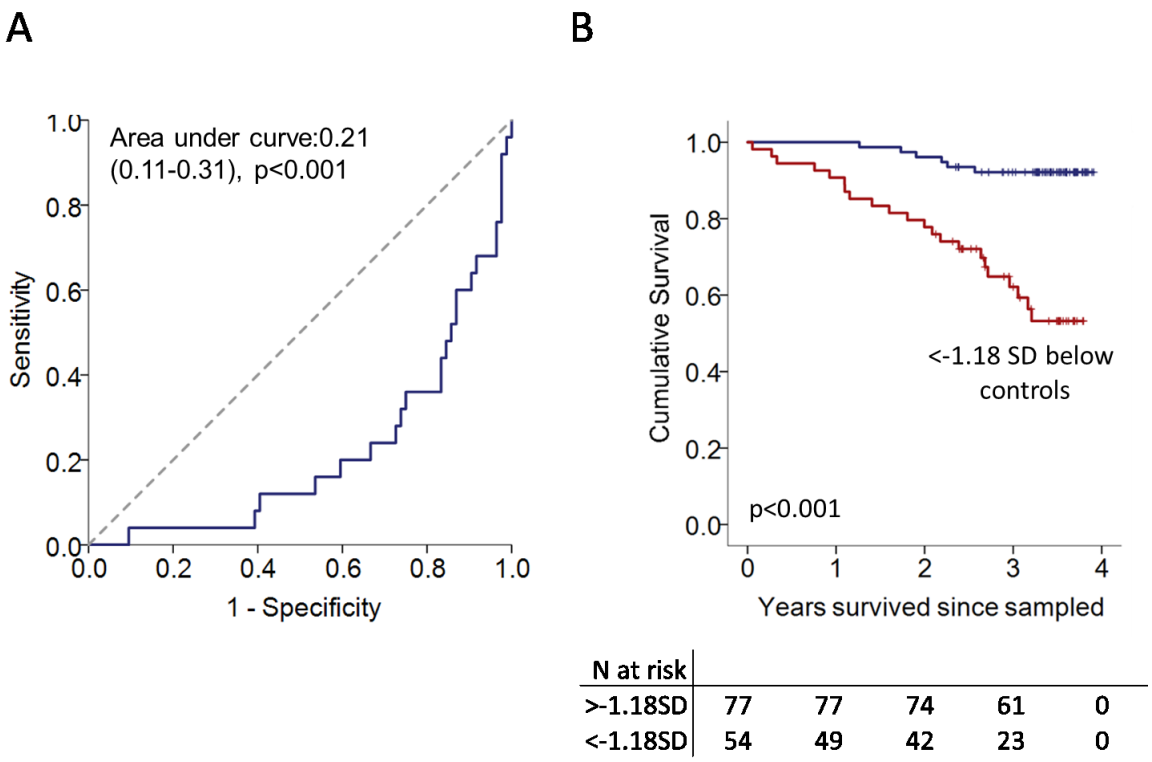


Figure 3.6 – Decreased HDL2a Apo-A2 is prognostic in PAH. (A) Receiver operating curve (ROC) for HDL2a Apo-A2 analysis at 3 years of follow up. The optimal cut off for high/low risk levels of HDL2a Apo-A2 was derived from this **(A)**. Kaplan Meier **(B)** survival estimates in PAH patients with high and low risk levels of HDL2a Apo-A2. HDL, high density lipoprotein; Apo, Apolipoprotein; SD, standard deviation.

In general, decreased HDL2a and HDL3a, and increased HDL3c levels were prognostic in PAH patients (Figure 3.7).

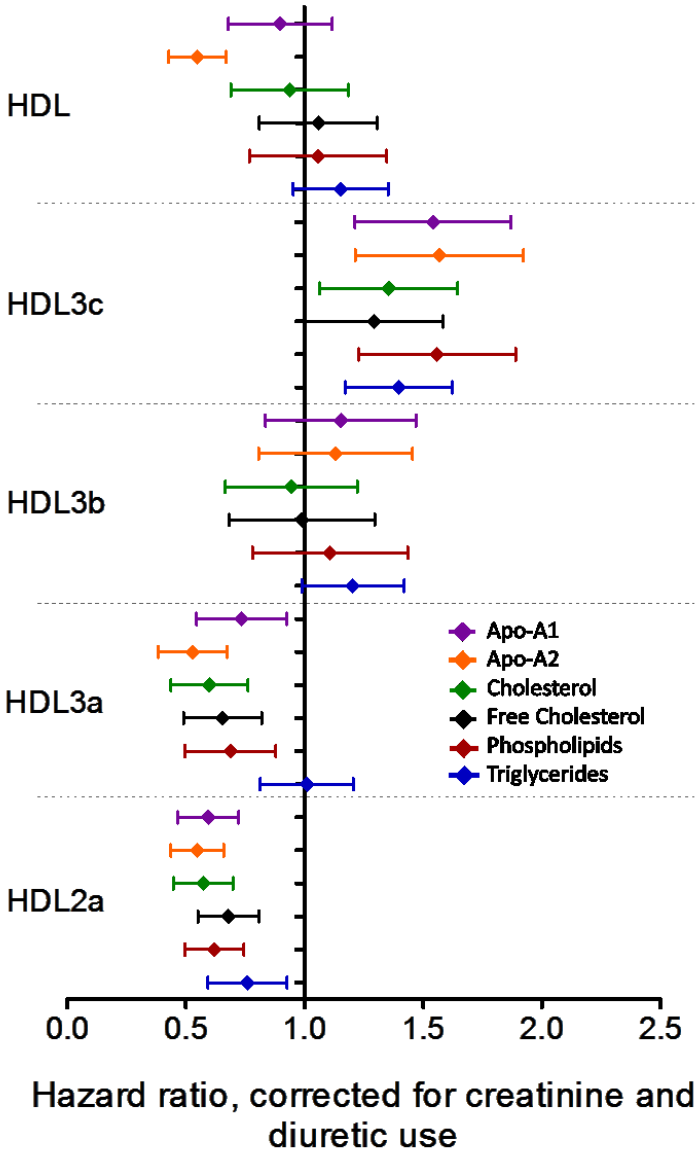


Figure 3.7 – Prognostic HDL lipid features. Hazard ratios after correcting for creatinine and diuretic use are shown for the 5 HDL groups measured, and their associated analytes. Hazard ratios indicate the risk of a change in each metabolite of 1 standard deviation, for ease of comparison. HDL, high density lipoprotein; Apo, Apolipoprotein.

3.3.3 High density lipoprotein (HDL) subclass levels and proteomic measures of apolipoprotein (Apo) A1

Proteomic measurements of Apo-A1 were available for 129/131 PAH patients and 62/63 health controls. Plasma levels of Apo-A1 were significantly decreased in PAH patients aged 19-70 and healthy controls ($p<0.001$). Levels of Apo-A1 correlated with 17/30 HDL subtypes, and most significantly with HDL2a Apo-A1 and Apo-A2 ($p<0.05$, Figure 3.8, Table 3.6). The HDL2a and HDL3a subclasses had a positive correlation to Apo-A1, whilst HDL3b and HDL3c subclasses had a predominantly negative correlation (Table 3.6).

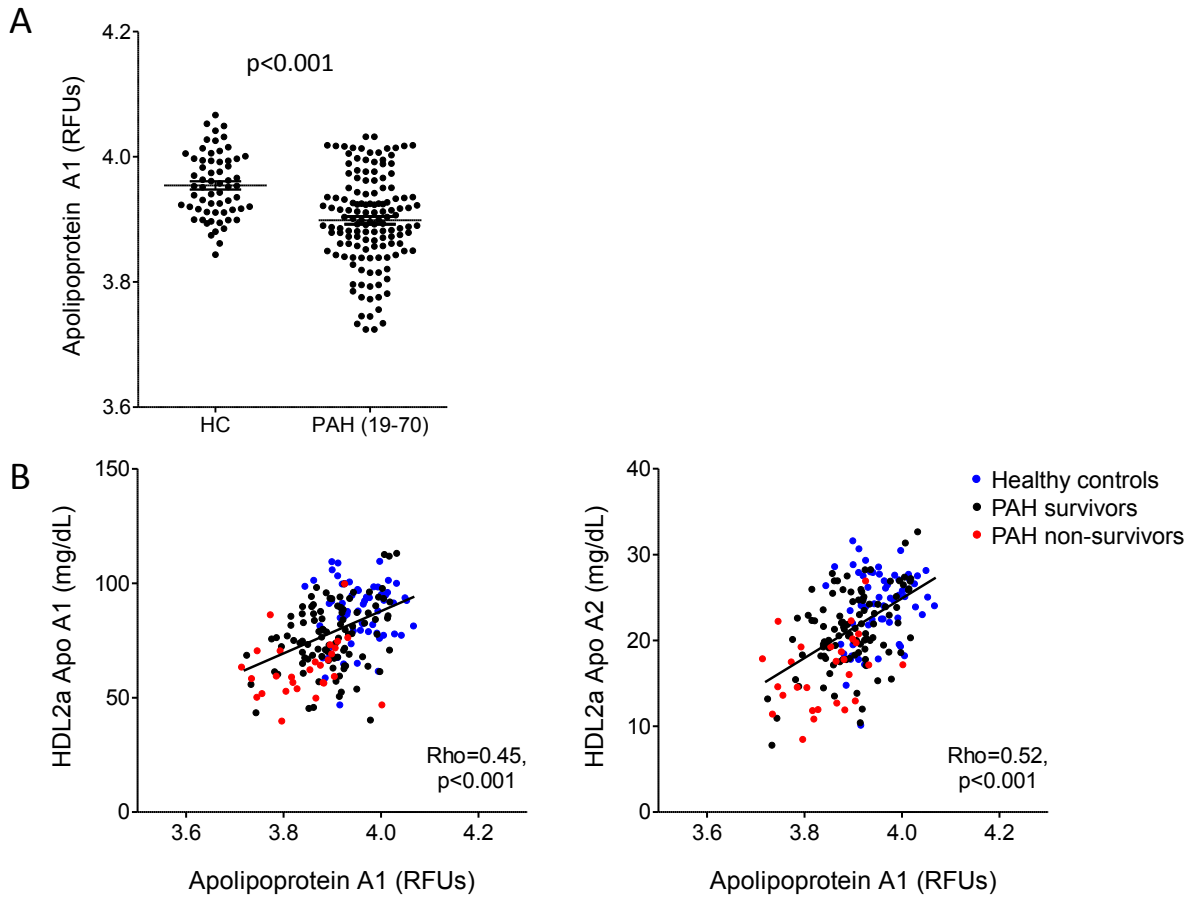


Figure 3.8 – Levels of apolipoprotein A1 and HDL subclasses. (A) Levels of apolipoprotein (Apo) A1 from plasma proteomic measurements are shown between healthy controls (HC) and PAH patients aged 19-70. Bar represents mean and standard error of the mean. **(B)** Scatter plot of Apo-A1 versus HDL2a Apo-A1 and A2 in healthy controls, PAH survivors and non-survivors. Statistics shown are from Spearman's Rank test. RFU, relative fluorescence units; HDL, high density lipoprotein

Lipid NMR feature (HDL)	Rho	Sig.
Positive correlation to Apo-A1		
HDL2a - Apo-A2	0.52	1.47E-14
HDL2a - Apo-A1	0.45	3.22E-11
HDL2a - Cholesterol	0.44	1.46E-10
HDL2a - Phospholipids	0.35	6.12E-07
HDL - Apo-A2	0.34	1.80E-06
HDL2a - Free Cholesterol	0.32	4.89E-06
HDL2a - Triglycerides	0.22	2.09E-03
HDL3a - Free Cholesterol	0.18	1.09E-02
HDL - Apo-A1	0.15	3.79E-02
Negative correlation to Apo-A1		
HDL3c - Apo-A2	-0.31	1.05E-05
HDL3c - Triglycerides	-0.30	3.12E-05
HDL3b - Triglycerides	-0.25	3.75E-04
HDL3b - Apo-A2	-0.25	5.30E-04
HDL3c - Phospholipids	-0.24	7.80E-04
HDL3c - Apo-A1	-0.16	2.34E-02
HDL3b - Phospholipids	-0.14	4.60E-02
HDL - Triglycerides	-0.14	4.95E-02

Table 3.6 – Correlation of HDL subclass levels to apolipoprotein A1. 17/30 high density lipoprotein (HDL) subclasses with a significant correlation with proteomic measurements of apolipoprotein (Apo) A1 are shown ($p<0.05$). Rho value and significance (Sig.) are shown from Spearman's rank correlation.

3.4 Discussion

This study represents a comprehensive analysis of circulating metabolites and lipid subclasses using NMR spectroscopy in patients with PAH.

I found increased levels of circulating citric acid in PAH patients compared to healthy and disease controls, independent of confounding factors. Levels were not significantly different between PAH and CTEPH indicating that citric acid may be a marker of pulmonary hypertension, rather than specific to the PAH subtype. Citric acid is an intermediate in the TCA cycle and acts to inhibit glucose oxidation through phosphofructokinase (Archer, Fang et al. 2013). Increased levels have been reported in lung tissues from PAH patients (Zhao, Peng et al. 2014), which may represent a potential source of the increased circulating citric acid concentration. Increased circulating levels of other TCA cycle intermediates such as malate and succinate correlate to haemodynamic measurements in PAH (Lewis, Ngo et al. 2016), and citric acid was significantly different between PAH patients and controls in this study. However, citrate levels were not prognostic in the current analysis, indicating that it is not a marker of disease severity in relation to survival.

Increased circulating citric acid may represent a build-up of TCA cycle intermediates and reflect dysfunction of this cycle. In addition, by inhibiting glucose oxidation, raised citric acid could contribute to the increased aerobic glycolysis observed in PAH (Cottrill and Chan 2013, Ryan and Archer 2015). In order to further address this, measurement of other TCA cycle intermediates and the precursors to the cycle from both glucose and fatty acid oxidation are needed.

Glutamine is one of the precursors to the TCA cycle, and circulating levels were found to be decreased in PAH patients versus controls. Glutamine is the amino acid with the highest circulating concentration and a major energy source and nitrogen donor for proliferating cells (Dang 2012). It is a precursor for the synthesis of many biologically important molecules, including amino acids, proteins, nucleotides, and has a number of significant regulatory roles (Smith 1990). In stressful disease states, there is increased catabolic metabolism and concentrations of glutamine decrease while tissue glutamine metabolism increases (Smith 1990). A reduction in plasma glutamine has been documented in disease processes such as sepsis and critical illness, and is an independent predictor of mortality for patients in intensive care (Oudemans-van Straaten, Bosman et al. 2001). In cardiovascular disease, models of ischemia in the rat heart demonstrate increased glutaminase activity, with high rates of glutamine conversion to glutamate, and supplementation with glutamine had a cardioprotective role (Khogali, Harper et al. 1998).

My finding of reduced plasma glutamine levels in PAH patients may be significant as the hypertrophic RV in the monocrotaline rat model of PAH displays a marked increase in glutamine metabolism and glutamine transporter expression (Piao, Fang et al. 2013). As with the shift to aerobic glycolysis, cardiac glutaminolysis was implicated in the maladaptive response of the RV and postulated to be a novel therapeutic target in PAH (Piao, Fang et al. 2013). Plasma and erythrocyte levels of glutamine have been assessed in patients with sickle cell disease (using high pressure liquid chromatography linked tandem MS), with a significant decrease occurring in patients with PH that also inversely correlated with tricuspid regurgitation, an early marker of mortality (Morris, Suh et al. 2008). The effect of glutamine therapy on haemolysis-associated pulmonary hypertension is now being evaluated (ClinicalTrials.gov – NCT01048905). Glutamine supplementation is postulated to reduce oxidative stress and haemolysis, improve arginine availability and endothelial function and alleviated endothelial cell dysfunction and associated metabolic changes in a mouse model of pulmonary hypertension (Addabbo, Chen et al. 2013). It should be noted however that, in contrast to these findings, another study using mass spectrometry reported increased circulating levels of glutamine in PAH patients compared to controls (Bujak, Mateo et al. 2016). The numbers of PAH patients (n=20) and healthy controls (n=20) used was small (Bujak, Mateo et al. 2016) compared to the present study, nonetheless a more targeted assessment of glutamine levels is required in a larger cohort of PAH patients in order to robustly test the findings.

Increased levels of circulating 3-hydroxybutyric acid, a ketone body and marker of ketoacidosis, was seen in PAH patients versus controls. Measurement of increased 3-hydroxybutric acid levels is used to diagnose diabetic ketoacidosis (Misra and Oliver 2015), the levels of 3-hydroxybutyric acid accumulating due to a lack of insulin and shift away from glucose oxidation. This results in acetyl-coA being diverted away from the TCA cycle to create acetoacetate and its reduced form, 3-hydroxybutyric acid (Wallace and Matthews 2004). Measurement of 3-hydroxybutyric acid has not previously been conducted in PAH and the 3 NMR peaks representing 3-hydroxybutyric acid were not influenced by diabetic therapy. It should be noted that 3-hydroxybutric acid, and indeed glutamine, were not significantly different between PAH patients and disease controls when taking into account confounding factors and may therefore reflect a general disease state, with up-regulation of glutaminolysis and mild ketosis, rather than being specific to PH.

Three of the most robust distinguishing and prognostic differences in PAH patients were decreased HDL2a cholesterol, Apo-A1, and Apo-A2. Lipid dysregulation has previously been demonstrated in PAH patients, with low plasma levels of HDL cholesterol associated with worsening clinical outcomes and increased mortality rates (Heresi, Aytekin et al. 2010, Zhao, Peng et al. 2012). However, other

studies have suggested HDL cholesterol is not prognostic in incident cases of PAH (Cracowski, Labarere et al. 2012). The data indicate that total HDL is not prognostic except for HDL Apo-A2. It is specific subtypes of HDL that are prognostic with increased HDL3b/3c (small HDL) and decreased HDL2a/3a (medium-large HDL) predicting worse survival in PAH patients (Figure 3.7). In addition, HDL2a/3a had a positive correlation to Apo-A1, whilst HDL3b/c had a negative correlation, indicating that both levels of large HDL and its major protein constituent Apo-A1 are decreased in PAH patients. Several studies have shown that the larger HDL2 subclass is more strongly associated with cardiovascular disease, stroke and diabetes than HDL cholesterol (Johansson, Carlson et al. 1991, Drexel, Amann et al. 1992, Mueller, Chang et al. 2008, Xian, Ma et al. 2009, Zeljkovic, Vekic et al. 2010, Blackburn, Lemieux et al. 2012), however assessment of these HDL subtypes has not previously been conducted in PAH patients.

The main role of HDL is to promote cholesterol efflux by mediating the transfer of cholesterol back to the liver from peripheral tissue, predominantly macrophages, where lipid efflux is mediated by adenosine triphosphate binding cassette transporters (ABC) A1 and G1 (Figure 3.9) (Glomset 1968). Measurements of HDL levels provide a marker of how efficient this process of 'reverse cholesterol transport' is (Glomset 1968, Rosenson, Brewer et al. 2012). Free cholesterol is converted to cholesteryl esters by LCAT (Lecithin–cholesterol acyltransferase), which aids in cholesterol efflux by preventing the reverse exchange of cholesterol back into peripheral cells from HDL and essentially trapping it in HDL (Glomset and Wright 1964, Glomset 1968). Cholesteryl ester transfer protein (CETP) is involved in the transfer of cholesteryl esters in HDL to other lipoproteins such as LDL/VLDL (Tall 1993), reducing the ability of HDL to perform its role in cholesterol clearance.

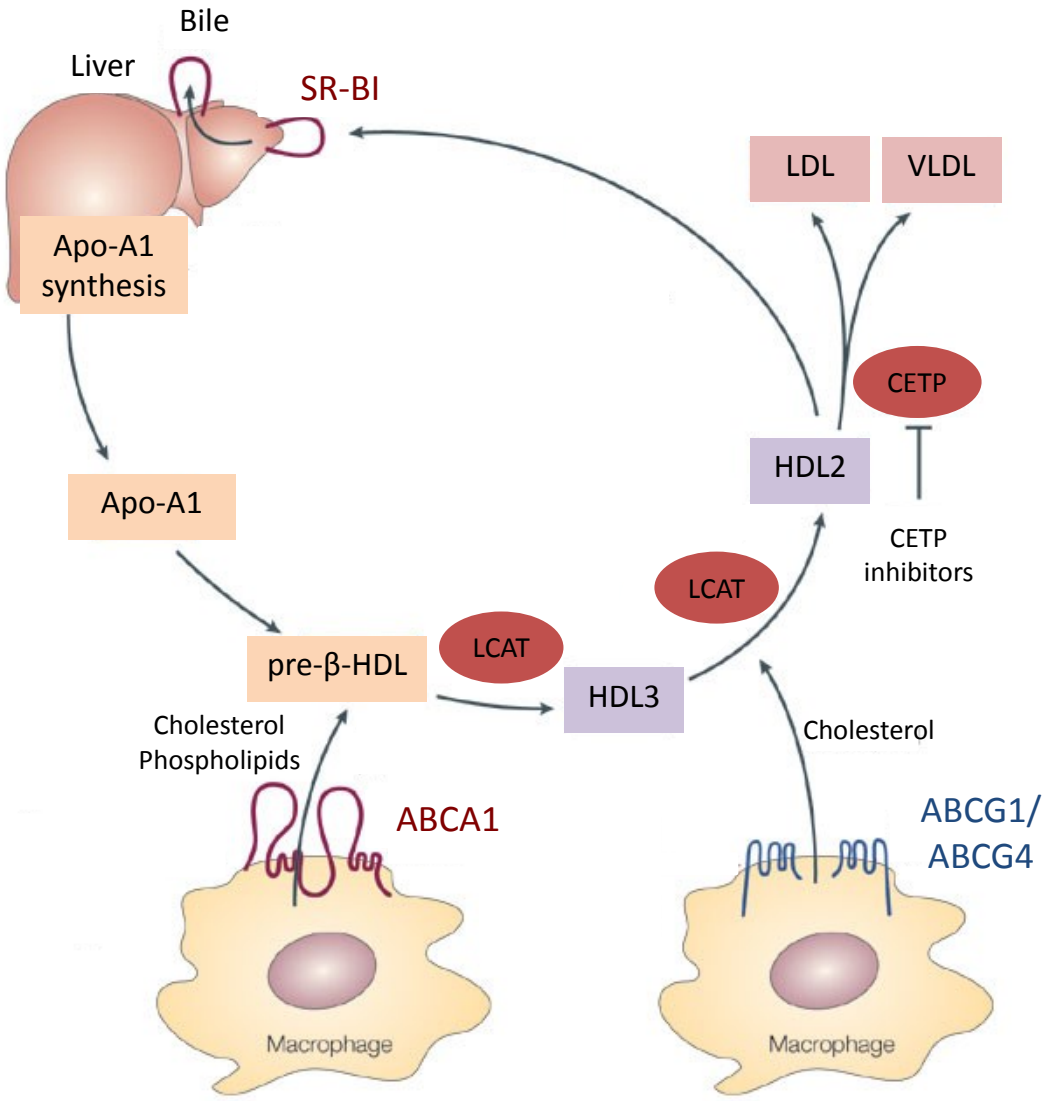


Figure 3.9 - High density lipoprotein (HDL) metabolism. Adapted from (Linsel-Nitschke and Tall 2005). HDL particles are formed from the secretion of apolipoprotein (Apo) A1 from the liver. Efflux of lipids from macrophages is mediated by adenosine triphosphate binding cassette transporter A1 (ABCA1), and uptake of cholesterol and phospholipids into Apo-A1 from macrophages leads to the formation of pre beta HDL particles. These are matured and converted initially to the smaller HDL3, and subsequently larger HDL2 subclasses by lecithin-cholesterol acyltransferase (LCAT) which also converts free cholesterol into cholesteryl esters. HDL2 and HDL3 subclasses accept further cholesterol from macrophages, where lipid efflux is mediated by ABCG1/G4 transporters. Cholesteryl ester transfer protein (CETP) mediates the transfer of cholesteryl esters from HDL to other lipoproteins such as low density and very low density lipoproteins (LDL, VLDL). HDL and cholesteryl esters are transferred back to liver for secretion through bile and HDL catabolism by scavenger receptor BI (SR-BI).

Mendelian randomization studies have shown that variants in genes associated with increased HDL cholesterol and ABCA1 transporter are not associated with improvements in cardiovascular risk (Voight, Peloso et al. 2012, Consortium, Deloukas et al. 2013, Global Lipids Genetics, Willer et al. 2013), questioning the causal relationship between HDL cholesterol and reverse cholesterol efflux and cardiovascular disease (Holmes, Asselbergs et al. 2015, Rosenson, Brewer et al. 2016).

HDL has several other roles which are protective as well as cholesterol clearance, including upregulation of endothelial nitric oxide synthase promoting vasodilatation (Yuhanna, Zhu et al. 2001), anti-inflammatory effects on the endothelium through decreased adhesion molecule expression, decreased oxidation of LDL and anti-apoptotic effects (Rosenson, Brewer et al. 2016). Increased cardiovascular risk is associated with dysfunction of HDL when Apo-A1 is oxidized by myeloperoxidase, leading to impaired cholesterol clearance by ABCA1 (Huang, DiDonato et al. 2014, Rosenson, Brewer et al. 2016) and pro-inflammatory actions of HDL (Rosenson, Brewer et al. 2016).

The importance of HDL subtypes and apolipoproteins, as well as HDL cholesterol, is being increasingly demonstrated in cardiovascular and respiratory disease. Subjects with coronary artery disease and evidence of endothelial dysfunction have decreased large HDL, associated with impaired cholesterol efflux, independent of HDL cholesterol (Monette, Hutchins et al. 2016), implying that large HDL is more important in determining cholesterol efflux than smaller HDL subclasses. Apolipoprotein A1 is the predominant protein constituent of HDL (Rosenson, Brewer et al. 2016) and mediates cholesterol transport through interactions with the ABCA1 transporter, and is also expressed in the lung, where it exerts anti-inflammatory and anti-oxidant properties, leading to apolipoprotein mimetics proposed as potential drug treatments for respiratory diseases including PH (Yao, Gordon et al. 2016, Yao, Gordon et al. 2016).

Several drug targets have been proposed in different parts of the HDL metabolic pathway to increase HDL cholesterol. Current drugs used to increase HDL cholesterol levels include niacin, which acts by increasing hepatic production of Apo-A1 and decreasing HDL breakdown in the liver, and fibrates which induce the transcription of Apo-A1 through PPARα (Remaley, Norata et al. 2014). Direct inhibition of cholesteryl ester transfer protein (CETP) (McTaggart and Jones 2008, Barter, Brandrup-Wognsen et al. 2010) has been proposed as a means for specifically increasing HDL-cholesterol and HDL2 subclass levels in cardiovascular disease (Pirillo, Norata et al. 2013).

Clinical trials have taken place with several CETP inhibitors (torcetrapib, dalcetrapib, evacetrapib and anacetrapib) with no improvements seen in cardiovascular outcomes (Barter, Caulfield et al. 2007, Cannon, Shah et al. 2010, Nicholls, Brewer et al. 2011, Schwartz, Olsson et al. 2012, McLain, Alsterda

et al. 2016). Other agents proposed to act on the HDL pathway include drugs that inhibit SR-BI mediated HDL catabolism, induction of Apo-A1, transcriptional upregulation of ABCA1/G1 transporters by liver X receptor (LXR) agonists, infusion of recombinant LCAT and HDL/Apo-A1 mimetics (Remaley, Norata et al. 2014). However, to date these have had limited success in human studies of cardiovascular disease (Remaley, Norata et al. 2014). Several steps have been proposed prior to initiating clinical trials to assess the potential efficacy of HDL targeting therapies including a) increase in the overall HDL numbers, b) assessment of HDL subtypes and proteomic and lipidomic components, c) assessment of HDL function by a macrophage cholesterol efflux assay and d) using Mendelian randomization to establish a causal link between the target and outcome (cardiovascular disease) (Rosenson 2016).

Targeting the lipid pathway therapeutically in PAH has been investigated with statin therapy, however, despite animal models demonstrating statin modulation of RV hypertrophy, clinical trials have not demonstrated a sustained reduction of RV mass in PAH patients on simvastatin (Wilkins, Ali et al. 2010). Recent meta-analyses of randomized control trials indicated that statin therapy had no effect on exercise capacity, cardiac output, (Zhang, Zeng et al. 2016), and mortality in PH (Anand, Garg et al. 2016). In the current dataset, statin therapy had a significant impact on LDL but not HDL subtypes. Some studies have shown that statins confer moderate increases in levels of HDL-cholesterol and Apo-A1 (Nicholls, Tuzcu et al. 2007, McTaggart and Jones 2008), independent of LDL changes (Barter, Brandrup-Wognsen et al. 2010). When looking more specifically at HDL subclasses, some studies have shown that the use of atorvastatin significantly increases large HDL, but not medium or small HDL subtypes (Schaefer, McNamara et al. 2002).

My findings indicate that large HDL subtypes are decreased in PAH and prognostic in keeping with other forms of cardiovascular disease. The present findings require validation in other cohorts of PAH patients, but specific agents that increase HDL levels, particularly large HDL, could be considered as a potential therapy in patients with PAH. In addition, comparing HDL levels to proteomic measures of Apo-A1 showed that Apo-A1 correlates to levels of large HDL and is reduced in PAH. This may provide a potential therapeutic target where Apo-A1 mimetics are being assessed in lung diseases such as asthma and emphysema (Yao, Gordon et al. 2016). In rat MCT and hypoxia models of PH, Apo-A1 mimetics decreased oxidized lipid levels and prevented the development of PH (Sharma, Umar et al. 2014). In addition, assessment of genetic variants encoding enzymes and proteins such as Apo-A1 involved in HDL metabolism, with levels of HDL subclasses and survival in PAH, may provide a causal link between decreased large HDL and PAH disease pathobiology. Although this has been conducted with HDL cholesterol and cardiovascular disease, it has not been

assessed with the HDL subtypes, and not with PAH. Agents that specifically act on HDL2a cholesterol, Apo-A1 and Apo-A2 are likely to be most beneficial, as these were the most discriminating and prognostic markers.

Limitations of this study include the lack of a validation cohort and a heterogenous population of PAH and CTEPH patients, the majority of whom were prevalent PAH cases, and CTEPH patients at different stages around PEA surgery. Due to the nature of PH as a rare disease, there is difficultly obtaining sufficient numbers of a homogenous population to study and this has been considered with the interpretation of the results.

A significant limitation has been in the identification of the NMR features of interest. NMR peaks at 3.039 and 4.046ppm, identified as creatinine, were validated with significant correlations demonstrated between these peaks and the clinical assay for creatinine (Rho values 0.613 and 0.578 respectively, p-values<0.0001), and increased plasma creatinine levels have been previously demonstrated in PAH and relate to mortality (Shah, Thenappan et al. 2008, Mielniczuk, Chandy et al. 2012). However, from the 65 NMR peaks that distinguish PAH patients from controls, several were not identified and many that were represent the same metabolite. Excluding lipid regions, only 8 distinct metabolites were identified - 1-methylhistidine, 3-hydroxybutyric acid, citric acid, creatinine, glutamine, glycerol, lysine and valine. Identification of metabolites using NMR spectroscopy can be challenging due to peaks with low intensities or regions that overlap; similar challenges have been seen in other studies (Elliott, Posma et al. 2015).

In summary, I measured circulating metabolites and lipid features using NMR spectroscopy in PAH patients and controls. In keeping with published findings I found increased citric acid in PAH patients versus controls. I also found novel metabolite changes with increased 3-hydroxybutyrate and decreased HDL subtypes in PAH patients, with HDL2a significantly related to poor outcomes. In order to improve the sensitivity of these analyses and to detect a broader range of metabolites, including more lipid features, I next used a high sensitivity UPLC-MS approach with the capacity to measure thousands of metabolic and lipidomic features.

Chapter 4 - Metabolic phenotyping using ultra-performance liquid chromatography mass-spectrometry in PAH

4.1 Introduction

Ultra-performance liquid chromatography mass spectrometry (UPLC-MS) allows the simultaneous measurement of thousands of metabolic features with a high degree of sensitivity (Bictash, Ebbels et al. 2010). In addition, untargeted lipid profiling (lipidomics) can be employed for in depth examination of lipophilic molecules, for example in coronary artery disease (Vorkas, Isaac et al. 2015). Lipid dysregulation is of interest in PAH based on my findings from NMR spectroscopy and lipidomic analysis would provide a more detailed assessment of lipid features in PAH patients.

LC-MS can also be used for the quantitative measurement of plasma drug levels, for example sildenafil (Paul, Gibbs et al. 2005). Current treatment for PAH involves the use of 3 pharmacological classes of therapy comprising phosphodiesterase (PDE5) inhibitors, endothelin receptor antagonists (ERAs), and prostanoids (Galie, Humbert et al. 2015). Imatinib is an inhibitor of several tyrosine kinases and its use in PAH patients is not recommended due to adverse events during a randomised control trial (Frost, Barst et al. 2015). However, a subset of patients within these studies who had not responded to conventional therapy had favourable outcomes on chronic imatinib and understanding their molecular profile may help to define potential responders and choose appropriate therapy for patients on an individual basis (Lythgoe, Rhodes et al. 2016).

Metabolomics experiments using mass spectrometry have previously been conducted in PAH. Abnormal sphingosine, arginine and oxidation pathways have been demonstrated in lung tissue from PAH patients (Zhao, Peng et al. 2014, Zhao, Chu et al. 2015). Changes in circulating levels of tryptophan, purine and tricarboxylic acid cycle metabolites have been found to correlate to haemodynamic measures in PAH using targeted LC-MS approaches (Lewis, Ngo et al. 2016). In addition, an untargeted study in a small set of 20 healthy controls and 20 PAH patients has shown increased levels of circulating lactate, pyruvate, free fatty acids, long chain acylcarnitines, glutamine, sphingosine and decreased tryptophan in PAH patients (Bujak, Mateo et al. 2016). Untargeted metabolomics studies to assess circulating metabolite levels have not been performed in a large population of PAH patients and associated with outcome data such as survival.

Using ^{1}H NMR spectroscopy, I found altered levels of metabolites related to oxidation pathways (citric acid and glutamine) and lipid metabolism in PAH patients, which relate to poor survival. I

hypothesised that UPLC-MS could be used to measure a greater variety and number of circulating metabolite levels, including drug therapies, in patients with PAH which relate to clinical outcomes.

I set out to a) measure levels of PAH therapies in patients before and after initiation of therapy and assess metabolites influenced by these therapies, b) validate changes from NMR analysis in abnormal oxidation and lipid metabolism in PAH, c) identify novel metabolic changes in PAH, d) assess metabolite changes in relation to outcomes (survival and response to therapy) and e) validate these findings in an independent cohort of PAH patients and controls.

4.2 Methods

See Chapter 2 for detailed experimental methods and protocols.

Samples were obtained from healthy controls, disease controls and patients with idiopathic or heritable PAH or CTEPH attending the National Pulmonary Hypertension Service at Hammersmith Hospital, London. In addition samples were obtained from the University Hospital of Giessen and Marburg, before and after the initiation of drug therapy including bosentan, sildenafil and patients on imatinib during the Imatinib in Pulmonary Arterial Hypertension, a Randomized, Efficacy Study (IMPRES) trial (Hoeper, Barst et al. 2013).

Samples were examined following randomisation to ensure that each plate was representative of all sample groups. World Health Organisation functional class (WHO-FC) and six minute walk distance (6MWD) data was obtained at the sample date for the discovery cohort and within 12 months of the sample date for the validation cohort, due to data availability. Clinical biochemical data, such as creatinine and bilirubin were recorded within 30 days of the sample date.

Data were aligned and peaks selected and normalised using Progenesis QI software (Nonlinear Dynamics, Waters Company, North Carolina, USA). Peaks whose signal did not dilute in a quality control dilution series (using a mixture of pooled samples and buffer, Spearman's Rho >0.7) were excluded. Peaks where the intensity levels were not consistent, assessed by the extent of variability (coefficient of variation, COV >0.6), in a quality control sample run throughout the experiment were also excluded from further analysis, leaving 55052 peaks for further analysis (Figure 4.1).

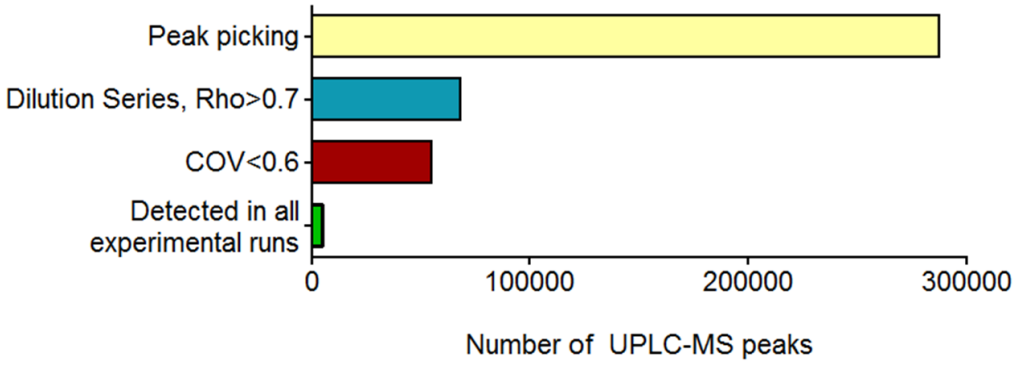


Figure 4.1 – UPLC-MS peaks for analysis. Number of ultra-performance liquid chromatography mass spectrometry (UPLC-MS) peaks for analysis are shown from a) peak picking, where peaks are selected from Progenesis QI software, b) those that correlated to a dilution series of pooled samples (Spearman's Rho >0.7), c) those that met the coefficient of variation (COV) across quality control samples (COV <0.6) and d) were detected across all experimental runs.

Only peaks detected across all experimental runs were considered. This was defined as peaks with the same mass (+/-10ppm) and where the difference in predicted retention time and detected retention time in the validation experiment was less than 0.3 minutes, leaving 4657 peaks for further analysis.

Comparisons of peaks between PAH patients who were or were not prescribed specific drug therapies (including anticoagulants, PDE5 inhibitors, ERAs, diuretics, aldosterone antagonists, statins, calcium channel blockers, cardiac glycosides, antidiabetic drugs, prostanoids, iron replacement therapy and ACE inhibitors) at the time of sampling were conducted in the discovery cohort. Peaks not related to drug therapy were analysed between diagnostic groups. Comparisons were made using the Mann Whitney U test and post-hoc Bonferroni correction applied. In a sub-analysis comparisons were made between PAH patients on sildenafil monotherapy who were responders and non-responders to treatment (defined as death or change in therapy within 1 year from the sample date).

The identities of peaks of interest were investigated through comparisons of m/z values with published databases (HMDB, Metlin) and retention time windows provided indications of which metabolite group the peak belonged to, in particular in lipidomics positive mode (Figure 4.2). The mass/charge ratio detected reflects the compound mass +/- any adduct, losses or replacement for example hydrogen or sodium adducts (Table 4.1).

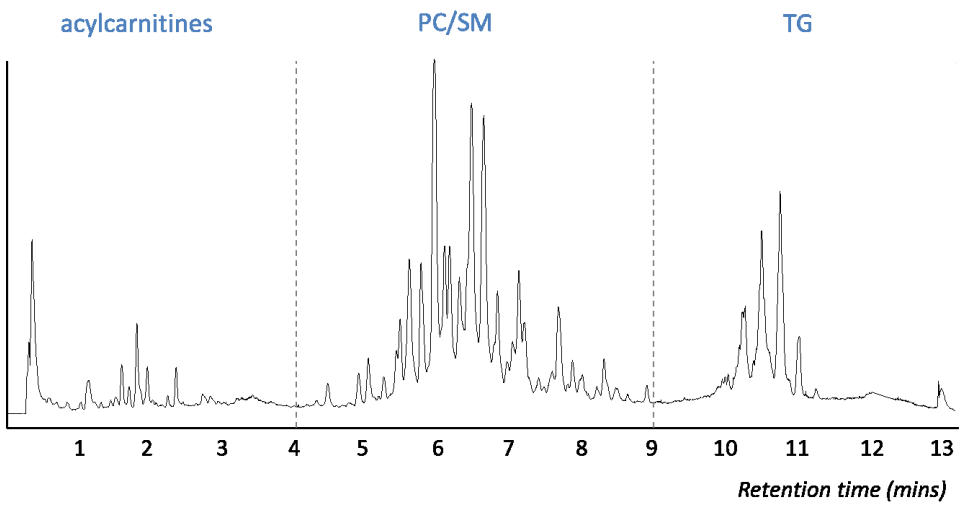


Figure 4.2 – Retention time windows in lipidomics positive mode. Chromatogram from a representative sample from a PAH patient is shown. Retention times below 4 minutes indicate metabolites potentially within the acylcarnitine family, 4-9 minutes phosphocholines (PC) or sphingomyelins (SM) and over 9 minutes triglycerides (TG).

Positive Ion Mode			Negative ion mode		
Ion Name	Ion Mass	Charge	Ion Name	Ion Mass	Charge
M+3H	M/3 + 1.007276	3+	M-3H	M/3 - 1.007276	3-
M+2H+Na	M/3 + 8.334590	3+	M-2H	M/2 - 1.007276	2-
M+H+2Na	M/3 + 15.7661904	3+	M-H2O-H	M- 19.01839	1-
M+3Na	M/3 + 22.989218	3+	M-H	M - 1.007276	1-
M+2H	M/2 + 1.007276	2+	M+Na-2H	M + 20.974666	1-
M+H+NH4	M/2 + 9.520550	2+	M+Cl	M + 34.969402	1-
M+H+Na	M/2 + 11.998247	2+	M+K-2H	M + 36.948606	1-
M+H+K	M/2 + 19.985217	2+	M+FA-H	M + 44.998201	1-
M+ACN+2H	M/2 + 21.520550	2+	M+Hac-H	M + 59.013851	1-
M+2Na	M/2 + 22.989218	2+	M+Br	M + 78.918885	1-
M+2ACN+2H	M/2 + 42.033823	2+	M+TFA-H	M + 112.985586	1-
M+3ACN+2H	M/2 + 62.547097	2+	2M-H	2M - 1.007276	1-
M+H	M + 1.007276	1+	2M+FA-H	2M + 44.998201	1-
M+NH4	M + 18.033823	1+	2M+Hac-H	2M + 59.013851	1-
M+Na	M + 22.989218	1+	3M-H	3M - 1.007276	1-
M+CH3OH+H	M + 33.033489	1+			
M+K	M + 38.963158	1+			
M+ACN+H	M + 42.033823	1+			
M+2Na-H	M + 44.971160	1+			
M+IsoProp+H	M + 61.06534	1+			
M+ACN+Na	M + 64.015765	1+			
M+2K-H	M + 76.919040	1+			
M+DMSO+H	M + 79.02122	1+			
M+2ACN+H	M + 83.060370	1+			
M+IsoProp+Na+H	M + 84.05511	1+			
2M+H	2M + 1.007276	1+			
2M+NH4	2M + 18.033823	1+			
2M+Na	2M + 22.989218	1+			
2M+K	2M + 38.963158	1+			
2M+ACN+H	2M + 42.033823	1+			
2M+ACN+Na	2M + 64.015765	1+			

Table 4.1 – Mass adduct calculator. Adapted from (Huang, Siegel et al. 1999). The potential adducts for a peak detected by mass spectrometry are shown in positive and negative ion mode. ACN, acetonitrile; IsoProp, isopropyl; DMSO, dimethylsulfoxide.

In order to further identify a peak of interest, fragmentation patterns from tandem mass spectrometry (MS/MS) analysis were assessed, and UPLC-MS analysis of pure standard compounds was conducted. For example, palmitoylcarnitine was purchased and run using the HILIC protocol and the mass and retention time of the authentic standard matched 2 peaks from our HILIC dataset - 2.77_398.3264m/z and 2.76_400.3424m/z (hydrogen adduct) (Figure 4.3A-B). These peaks also correlated to another peak with the same mass in lipidomics positive (Lpos) mode (1.72_400.3427m/z) (Figure 4.3C). In addition, fragmentation of this peak in Lpos mode revealed a pattern consistent with an acylcarnitine (Figure 4.3D).

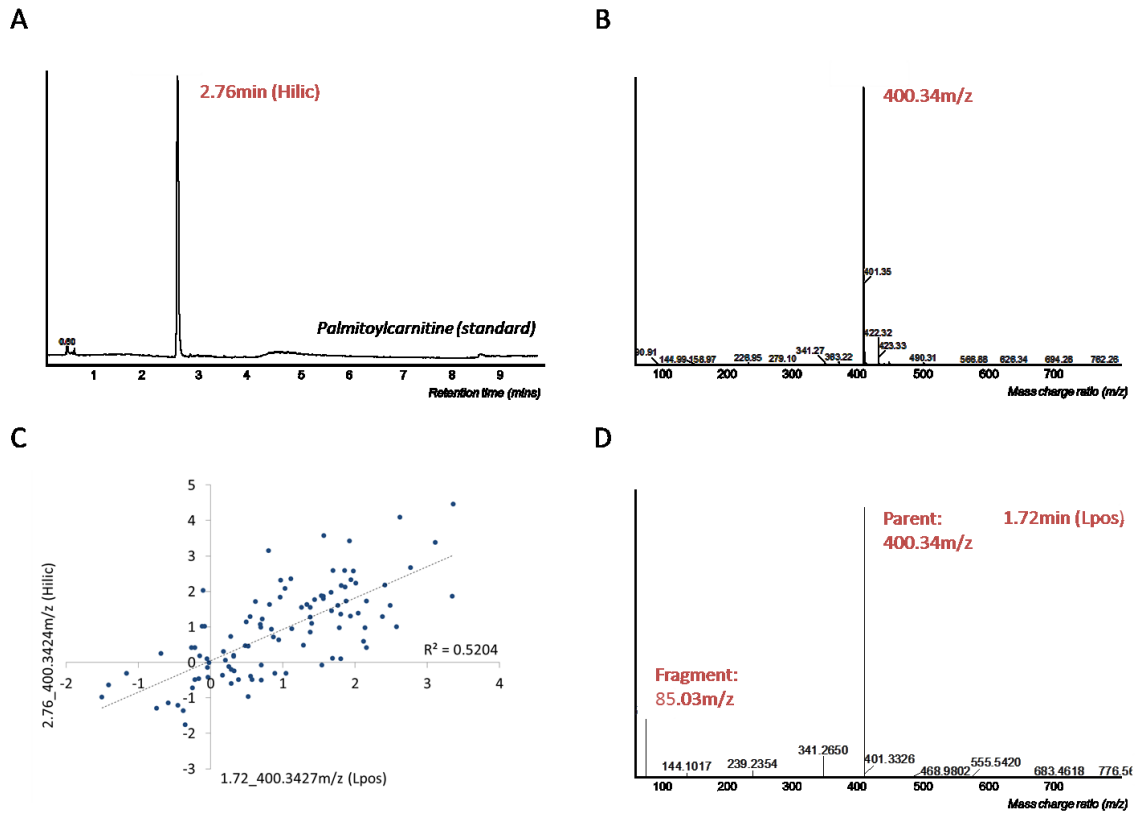


Figure 4.3 – Identification of palmitoylcarnitine peaks. The spectrum for an authentic standard of palmitoylcarnitine is shown with a retention time of 2.76 minutes **(A)** and mass of 400.34m/z **(B)** in HILIC UPLC-MS, corresponding to a peak 2.76_400.3424m/z. **(C)** This peak correlates to a peak from lipidomics positive mode (Lpos) which was isolated and fragmented producing a characteristic fragment **(D)** of the acylcarnitine metabolite group at 85.03m/z.

Prior to modelling, metabolites detected by UPLC-MS whose distribution was not normal were transformed either by $\log_{10}$ or power transformations (x^Y, with Y from -2 to 2 in 0.5 steps, as performed for Box-Cox transformations (Box and Cox 1964), whichever best normalised the data based on Kolmogorov-Smirnov tests, or ranked if no test met $p>0.05$. All UPLC-MS data were z-score transformed based on healthy control data for ease of comparisons between data from the discovery and validation experiments.

Linear regression analysis was conducted to assess the relationships between metabolite levels, diagnoses and potential confounders. In the disease control, PAH and CTEPH cohorts, preserved renal function was defined as creatinine <75 μmol/L, and liver function as bilirubin <21 μmol/L. In the healthy control group, preserved renal and hepatic function was assumed as clinical assay data was unavailable. Logistic regression was conducted to determine metabolites that independently distinguished between diagnostic groups. Orthogonal partial least squares discriminant analysis (OPLS-DA) modelling was used to test the performance of these metabolites. R^2 scores indicate model performance and Q^2 scores estimate reproducibility, based on cross validation.

Survival analyses were performed using time from sampling to death/census. In a secondary analysis, transplantation or death (all-causes) was used as a composite endpoint. Cox regression analysis was used to identify prognostic predictors, with proportional hazard assumptions tested. Metabolites which were found to predict survival were tested against established prognostic indicators – namely, NT-proBNP (Nagaya, Nishikimi et al. 2000), 6MWD (Fritz, Blair et al. 2013) and RDW (Rhodes, Wharton et al. 2011). Kaplan-Meier plots were used to illustrate events from time of sampling in relation to metabolite levels. Receiver Operating Characteristic (ROC) curves were used to assess discriminating and prognostic value of metabolites against diagnosis and all-cause mortality respectively.

4.3 Results

Discovery analysis using UPLC-MS profiling was performed using healthy controls (HC, n=63) and disease controls (DC, n=47); and disease groups of PAH (n=131) and CTEPH (n=152) , - the same groups analysed by ^{1}H NMR spectroscopy in Chapter 3. In the discovery cohort, HC were compared to age and gender matched patients with PAH (aged 19-70) (n=103). Validation analysis utilised 250 plasma samples including healthy controls (n=63) and disease groups of PAH (n=111) and CTEPH patients (n=76). Samples were not available from disease controls patients for the validation analysis. 22/76 CTEPH patients had previously undergone pulmonary endarterectomy (PEA) surgery at the time of sampling. 20/76 had their sample taken prior to PEA surgery, 12/76 declined surgery but were operable, and the remaining were deemed inoperable due to distal disease (n=8), age/co-morbidities/borderline PH (n=12) or unknown reasons (n=2).

A sub-analysis of PAH patients sampled before and after treatment initiation underwent UPLC-MS profiling. This included paired samples from PAH patients treated with the experimental drug imatinib (n=12), and PAH therapies bosentan (n=13) and sildenafil (n=16). Baseline characteristics and laboratory data are shown in Tables 4.2 and 4.3.

	Discovery					Validation			Paired PAH subjects before and after drug therapy		
	HC (n=63)	DC (n=47)	PAH (19-70) (n=103)	PAH (>70) (n=28)	CTEPH (n=152)	HC (n=63)	PAH (n=111)	CTEPH (n=76)	Bosentan (n=13)	Sildenafil (n=16)	Imatinib (n=12)
Age at sampling	47.5 +/-13.2	58.1 +/-17.7	48.1 +/-13.7	75.5 +/-4.8	65.8+/-15.0	49.1+/-16.1	56.6+/-16.7	63.6+/-15.6	57.6 +/-19.8	60.2 +/-12.9	45.4 +/-17.9
Sex, Female:Male	42:21 (2:1)	30:17 (1.76:1)	74:29 (2.55:1)	19:9 (2.11:1)	69:83 (0.83:1)	40:23 (1.74:1)	69:42 (1.64:1)	39 / 37 (1.05:1)			
Ethnicity, % non-caucasian	22.0	40.4	13.6	10.7	14.5	38.1	20.0	15.8			
BMI, kg/m^2	30.0+/-10.0	26.0+/-5.6	28.8+/-7.8	28.3+/-7.6	28.2+/-6.0	26.0+/-4.1	28.9+/-6.7	29.0+/-5.8			
BMPR2 mutation carriers (%)			7.8	3.6			2.7				
Treatment naïve cases (%)			11.7	17.9			18.9				

Table 4.2 – UPLC-MS Basic Cohort Characteristics. Means and standard deviations or counts are given. BMI, body mass index; HC, healthy controls; DC, disease controls; PAH, pulmonary arterial hypertension; CTEPH, chronic thromboembolic pulmonary hypertension; BMPR2, bone morphogenetic protein receptor, type 2. Ethnicity is shown for subjects who self-declared.

	Discovery				Validation	
	DC (n=47)	PAH (19-70) (n=103)	PAH (>70) (n=28)	CTEPH (n=152)	PAH (n=111)	CTEPH (n=76)
Baseline Haemodynamics at diagnosis						
Pulmonary capillary wedge pressure, mmHg	11.3+/-4.1	11.9+/-5.8	12.3+/4.5	13.5 +/-5.2	11.2+/-5.5	13.0 +/-5.6
Mean pulmonary artery pressure, mmHg	21.2+/-9.2	54.2+/-15.3	45.6+/14.6	44.7 +/-12.5	49.5+/-12.1	42.6 +/-12.7
Pulmonary vascular resistance, Woods units	2.2+/-2.7	12.2+/-5.8	8.3+/-4.7	9.2 +/-6.3	10.5+/-5.2	8.1 +/-4.8
Mean right atrial pressure, mmHg	7.1+/-4.1	9.8+/-5.5	9.3+/-5.2	11.2 +/-5.5	11.3+/-6.0	10.9 +/-5.7
Cardiac output, L/min		4.0 +/- 1.6	4.8 +/- 1.4	4.0 +/- 1.2	3.9+/-1.5	4.0+/-1.5
Functional status and pathology						
6MWD (m)		297+/-152	209+/-154	282+/-150	271+/-161	277+/-156
WHO Functional Class - I / II / III / IV	11/10/26/0	6/23/63/11	0/4/22/2	12/34/98/8	8/16/39/12	13/17/61/20
RDW, %		15.0+/-2.1	15.1+/-1.2	15.2+/-1.7	16.1+/-3.2	15.4+/-2.2
NT-proBNP (pmol/L)		640+/-807	919+/-887		1295+/1371	
Creatinine, umol/L	81.9+/-36.2	79.7+/-27.9	104+/37.0	94.3+/-67.4	97.9+/-52.6	99.7+/-87.1
Bilirubin, umol/L	13.2+/-16.5	15.1+/-10.4	11.4+/-7.1	13.9+/-9.2	17.7+/-10.1	14.3+/-10.3
Drug therapy						
Anticoagulation		75.7	82.1	100.0	55.9	84.2
PDE5 inhibitors		78.6	67.9	40.1	43.2	23.7
ERAs		62.1	46.4	29.6	35.1	19.7
Prostanoids		21.4	3.6	1.3	9.0	1.3
Diuretics		39.8	71.4	51.3	49.5	42.1
Aldosterone antagonists		37.9	32.1	25.0	34.2	18.4
Statins/lipid lowering drugs		24.3	50.0	38.2	22.5	34.2
CCBs		20.4	32.1	9.2	9.9	3.9
Cardiac glycosides		19.4	25.0	8.6	18.9	6.6
Antidiabetic drugs		11.7	35.7	9.9	16.2	5.3
Iron replacement therapy		13.6	28.6	9.2	9.0	13.2
ACE inhibitors		11.7	32.1	30.9	25.2	32.9

Table 4.3 – UPLC-MS Cohort Characteristics – haemodynamics, functional status, pathology and drug therapy. Means and standard deviations or counts are given. Clinical pathology parameters are shown within 30 days of the sample date. NT-proBNP, N-terminal brain natriuretic peptide at time of sample; RDW, red cell distribution width; HC, healthy controls; DC, disease controls; PAH, pulmonary arterial hypertension; CTEPH, chronic thromboembolic pulmonary hypertension; PDE5, phosphodiesterase 5; ERA, endothelin receptor antagonists; CCB, calcium channel blocker; ACE, angiotensin converting enzyme. 10 PAH patients in the discovery cohort and 2 PAH patients in the validation cohort were on calcium channel blocker therapy as vasoresponders.

4.3.1 UPLC-MS peaks associated with drug therapy

604/4657 UPLC-MS peaks were significantly different between PAH patients on and off drug therapies (including anticoagulants, PDE5 inhibitors, ERAs, diuretics, aldosterone antagonists, statins, calcium channel blockers, cardiac glycosides, anti-diabetic drugs, prostanoids, iron replacement therapy and ACE inhibitors) following correction for multiple testing ($p<1.07e-5$).

Metabolites of the PAH therapies bosentan and sildenafil and the experimental drug imatinib were detected and identified by comparing m/z values to available reference databases, and were significantly different between patients who were or were not prescribed them at the time of sampling ($p<1.07e-5$, Table 4.4, Figure 4.4A-B), as well as between paired samples from patients before and after initiating these therapies (Table 4.5, Figure 4.4C-E).

Peak, Retention Time-mass/charge (m/z) or neutral mass (n)	Discovery Median (IQR)		Validation Median (IQR)		Discovery Significance	Validation Significance
	On therapy	Off therapy	On therapy	Off therapy	On/off therapy	On/off therapy
Bosentan						
1.20_574.1743m/z	1.05 (0.47-1.05)	-0.76 (-0.90--0.58)	1.43 (0.53-1.94)	-0.61 (-0.61--0.61)	3.58E-11	3.30E-12
0.74_551.1865n	1.19 (1.11-1.19)	-0.86 (-0.94--0.75)	1.05 (0.17-2.00)	-0.57 (-0.72--0.36)	1.00E-12	2.32E-13
0.84_551.1847n	1.19 (1.01-1.19)	-0.86 (-0.92--0.78)	1.42 (1.23-1.52)	-0.63 (-0.88--0.41)	7.23E-13	6.88E-17
Sildenafil						
1.99_474.2038n	0.51 (0.26-0.87)	-1.47 (-1.55--1.40)	0.95 (0.62-1.36)	-0.84 (-0.95--0.75)	5.12E-11	5.41E-20
2.94_460.1899n	0.44 (-0.12-0.86)	-1.34 (-1.59--0.95)	0.97 (0.54-1.26)	-0.92 (-1.06--0.59)	2.74E-10	8.30E-20

Table 4.4 – UPLC-MS peaks representing Bosentan and Sildenafil between PAH patients on and off therapy. Normalised scaled abundances for 3 bosentan and 2 sildenafil hydrophilic interaction chromatography (HILIC) peaks between PAH patients on and off respective therapies, in both discovery and validation cohorts. Median with interquartile range (IQR) and significance (p value) is shown.

Peak, Retention Time-mass/charge (m/z) or neutral mass (n)	Median (IQR)		Sig
	Baseline before therapy	Following Initiation therapy	Baseline/Follow-up
Bosentan			
0.74_573.1695n	-0.88 (-0.85-1.06)	1.06 (0.86-1.41)	3.52E-07
Sildenafil			
2.35_230.0948n	-0.83 (-0.76-0.82)	0.82 (0.56-1.14)	4.79E-07
Imatinib			
3.03_479.2438n	-1.07 (-0.99-1.21)	1.21 (1.07-1.39)	3.73E-07

Table 4.5 – UPLC-MS peaks representing Bosentan, Sildenafil and Imatinib before and after therapy. Normalised scaled abundances for bosentan, sildenafil and imatinib hydrophilic interaction chromatography (HILIC) peaks between paired samples from PAH patients before and following initiation of respective therapies. Median with interquartile range (IQR) and significance (p value) is shown.

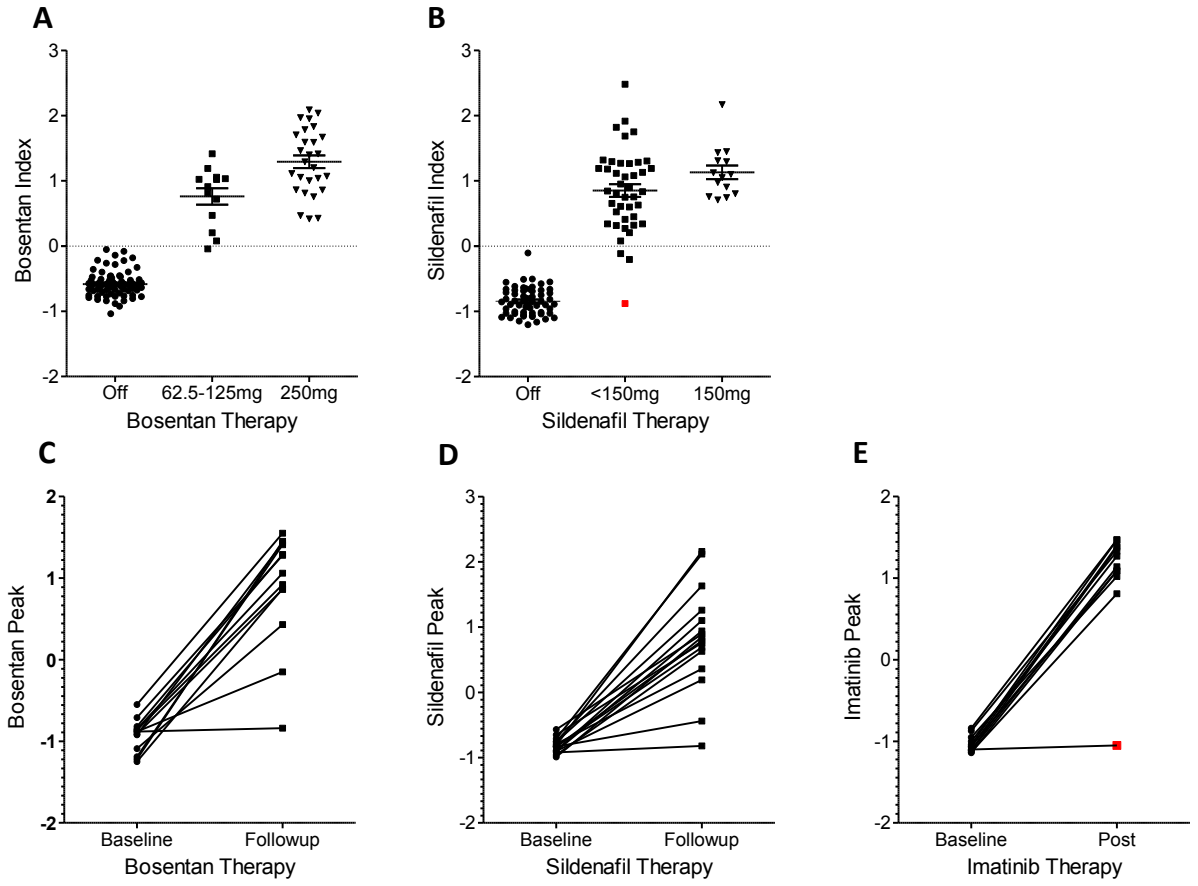


Figure 4.4 – UPLC-MS peaks representing Bosentan, Sildenafil and Imatinib. Normalised average abundance for 3 bosentan **(A)** and 2 sildenafil **(B)** metabolites in PAH patients off therapy and on different dosing regimens. Bar represents the mean and standard error of the mean. A bosentan **(C)**, sildenafil **(D)** and imatinib metabolite **(E)** are shown in IPAH patients before and after initiation of therapy. A patient with documented adherence issues is highlighted in red.

16 metabolites were decreased in patients on bosentan therapy, which may represent the effect of the drug itself, and the identities of these peaks are unknown (Table 4.6, Figure 4.5).

Peak, Retention Time-mass/charge (m/z) or neutral mass (n)	Platform	On therapy	Off therapy	Sig.
0.75_637.2918m/z	HILIC	-1.18 (-1.31 - -1.15)	-0.67 (-0.66 - -0.6)	6.99E-12
0.75_513.3168m/z	HILIC	-0.97 (-1.08 - -0.86)	-0.59 (-0.45 - -0.52)	1.05E-10
0.75_373.2162m/z	HILIC	-1.47 (-1.56 - -1.38)	-1.22 (-0.94 - -1.19)	1.80E-09
0.75_500.1836m/z	HILIC	-0.16 (-0.84 - 0.06)	0.21 (0.26 - 0.35)	1.70E-08
0.76_635.2823m/z	HILIC	-0.62 (-0.78 - -0.6)	-0.23 (-0.22 - -0.28)	2.56E-08
0.75_349.2160m/z	HILIC	0.04 (0.15 - 0.12)	0.22 (0.41 - 0.25)	4.75E-08
0.74_300.2885m/z	HILIC	0.2 (0.31 - 0.26)	0.41 (0.57 - 0.46)	7.27E-08
0.74_387.2527m/z	HILIC	0.38 (0.49 - 0.4)	0.55 (0.69 - 0.58)	1.08E-07
0.76_343.1741m/z	HILIC	-0.11 (-0.08 - -0.18)	0.29 (0.1 - 0.27)	3.57E-07
0.75_237.1463m/z	HILIC	-0.98 (-0.95 - -0.91)	-0.82 (-0.6 - -0.78)	3.84E-07
0.75_269.1347m/z	HILIC	-0.67 (-0.6 - -0.62)	-0.42 (-0.3 - -0.36)	4.81E-07
0.63_327.1378m/z	Lpos	-0.49 (-1.15 - -1.32)	-0.16 (-0.93 - -1.19)	1.40E-06
0.75_181.0934m/z	HILIC	-0.76 (-0.57 - -0.74)	-0.63 (-0.41 - -0.65)	2.24E-06
0.75_363.2169m/z	HILIC	1.19 (1.2 - 1.27)	1.4 (1.45 - 1.46)	2.46E-06
0.60_253.1426m/z	Lpos	-0.96 (-0.76 - -0.92)	-0.8 (-0.58 - -0.81)	8.54E-06
0.74_411.2161n	HILIC	0.21 (0.4 - 0.24)	0.32 (0.52 - 0.33)	9.54E-06

Table 4.6 – UPLC-MS peaks affected by Bosentan therapy. Normalised scaled abundances for 16 UPLC-MS peaks that are significantly decreased on bosentan therapy ($p<1.07e-5$). Experimental platforms are shown. Median with interquartile range (IQR) and significance (p value) is shown for PAH patients on and off bosentan in the discovery cohort. HILIC, hydrophilic interaction chromatography; Lpos, lipidomics positive mode.

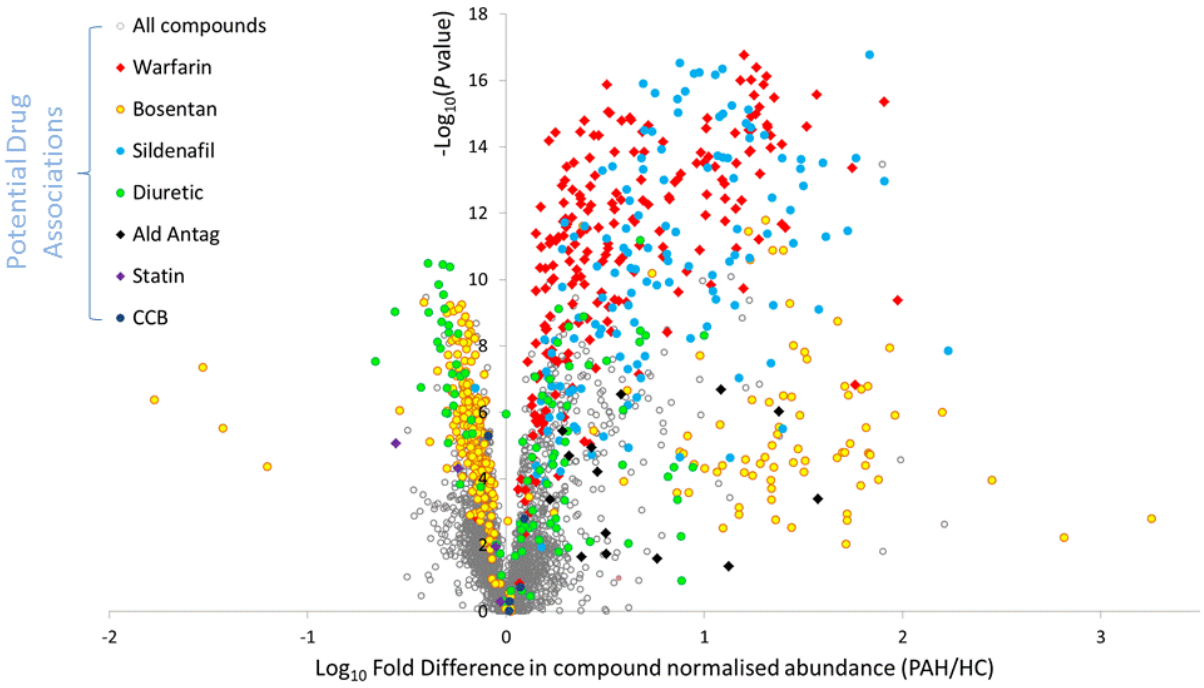


Figure 4.5 – Volcano plot of drug metabolites in PAH patients. Plot shows the fold difference and statistical significance (negative log p value, Mann Whitney U test) of UPLC-MS peaks in a comparison between PAH patients (aged 19-70) and healthy controls (HC). Peaks which are significantly different between PAH patients on and off respective drug therapies ($p<1.07e-5$) are colour coded. Peaks related to drug therapies are increased in PAH patients and some peaks (e.g. for bosentan) are decreased in PAH indicating they may be associated with the effect of the drug therapy. Ald antag, aldosterone antagonists; CCB, calcium channel blocker.

4.3.2 UPLC-MS peaks distinguishing between PAH and controls

Following exclusion of 604 'drug related' peaks, 4053 non-drug related peaks were compared between groups and 67 discriminated PAH and healthy controls in the discovery and validation cohorts following correction for multiple testing ($p<1.23e-5$, Table 4.7, Figure 4.6).

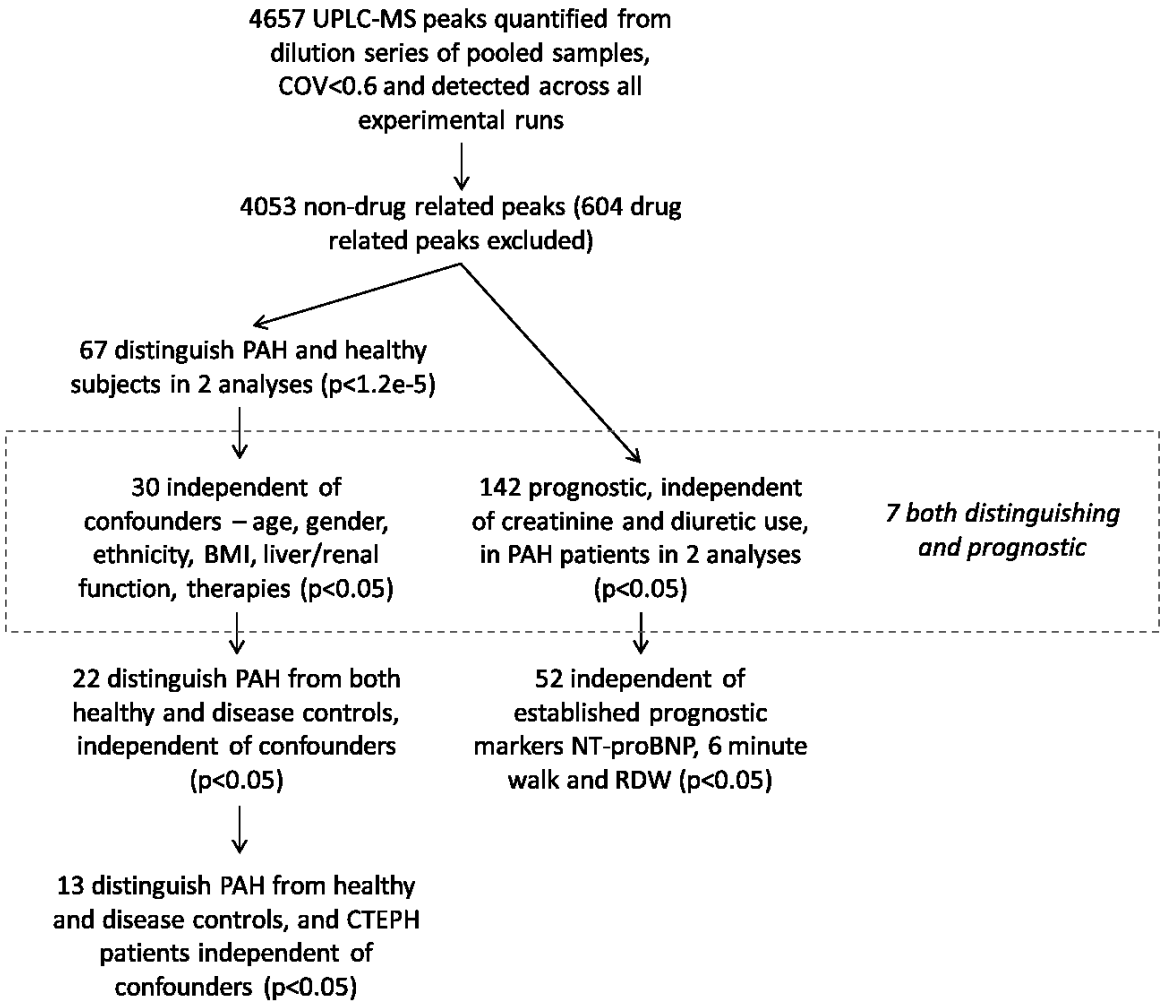


Figure 4.6 – Analysis flow chart. Summary of analytical workflow showing numbers of UPLC-MS peaks that distinguish PAH from controls, and/or are prognostic in PAH. BMI, body mass index; NT-proBNP, N-terminal brain natriuretic peptide; RDW, red cell distribution width; UPLC-MS, ultra-performance liquid chromatography mass spectrometry; COV, coefficient of variation.

Of these 67 peaks, 30 distinguished healthy controls and PAH subjects after correcting for potential confounders, including age, gender, ethnicity, body mass index, creatinine, bilirubin and drug therapies ($p<0.05$, Table 4.7). Of the 67 peaks, 5 were identified and include increased acylcarnitines (myristoylcarnitine, palmitoylcarnitine), N4-acetylcytidine and decreased sphingomyelins (d18:1/24:0 and 18:1/23.0) (peak identification will be detailed in section 4.3.5). Among the 67 peaks, 22 were prioritised as they discriminated PAH patients from disease controls after correction for potential confounders ($p<0.05$, Table 4.7). In addition, 13/22 discriminated PAH patients from CTEPH patients after correcting for potential confounders and therefore may represent 'PAH-specific' differences ($p<0.05$, Table 4.7).

Peak, Retention Time-mass/charge (m/z) or neutral mass (n)	Platform	Identity	Group averages (z-score relative to healthy controls)	Linear Regression		Confounder
			PAH (19-70)	HC vs PAH	HC+DC vs PAH	HC vs PAH
Increased in PAH vs HC, DC and CTEPH (independent of confounders)						
1.26_397.3102m/z	Lpos	Unknown	0.87 (0.03 - 1.64)	5.31E-10	6.78E-10	
Decreased in PAH vs HC, DC and CTEPH (independent of confounders)						
8.08_814.6940n	Lpos	SM(d18:1/24:0)	-1.18 (-1.71 - -0.59)	4.58E-03	3.92E-02	
1.66_564.3302m/z	Lneg	Unknown	-0.99 (-1.98 - 0.1)	2.01E-02	3.76E-02	
7.72_810.6826n	Lneg	Unknown	-0.81 (-1.22 - -0.25)	1.25E-03	4.82E-03	
8.32_838.7161n	Lneg	Unknown	-1.27 (-2.21 - -0.45)	2.19E-03	1.08E-02	
7.50_787.9067m/z	Lpos	Unknown	-1.15 (-2.32 - -0.09)	5.39E-03	2.33E-02	
7.81_831.6590m/z	Lneg	Unknown	-1.23 (-1.79 - -0.61)	2.88E-05	2.62E-04	
7.49_750.5768m/z	Lpos	Unknown	-1.14 (-1.91 - -0.47)	3.52E-03	4.13E-02	
8.30_799.6693m/z	Lneg	Unknown	-1.34 (-2.31 - -0.57)	9.44E-04	8.91E-03	
5.80_902.5333m/z	Lneg	Unknown	-0.77 (-1.19 - -0.1)	1.07E-03	2.08E-04	
7.25_843.6593m/z	Lneg	Unknown	-0.84 (-1.33 - -0.16)	4.53E-03	1.61E-02	
8.09_1077.5975m/z	Lpos	Unknown	-1.01 (-1.74 - -0.29)	1.44E-03	5.55E-03	
7.49_929.6091m/z	Lpos	Unknown	-1.06 (-1.76 - -0.41)	3.52E-03	3.16E-02	
Increased in PAH vs HC and DC (independent of confounders)						
1.25_372.3112m/z	Lpos	myristoylcarnitine~	0.71 (0.04 - 1.46)	2.05E-03	8.38E-03	
1.72_400.3427m/z	Lpos	palmitoylcarnitine~	0.91 (0.23 - 1.77)	1.41E-04	1.53E-03	
0.93_412.3046m/z	Lpos	Unknown	0.79 (0.18 - 1.56)	4.40E-05	2.28E-04	
Decreased in PAH vs HC and DC (independent of confounders)						
1.66_579.3524n	Lneg	Unknown	-0.96 (-2.02 - 0.26)	2.53E-02	4.69E-02	
7.45_817.6388m/z	Lneg	Unknown	-0.96 (-1.54 - -0.38)	1.02E-02	3.52E-02	
7.50_832.6448m/z	Lneg	Unknown	-1.02 (-1.42 - -0.52)	9.21E-03	2.84E-02	
7.17_743.6010m/z	Lneg	Unknown	-0.99 (-1.4 - -0.57)	1.89E-03	5.33E-03	
3.30_1062.6670n	HILIC	Unknown	-0.89 (-1.46 - -0.18)	2.37E-03	3.99E-03	
1.66_504.3081m/z	Lneg	Unknown	-0.97 (-2.03 - 0.19)	1.92E-02	3.39E-02	
Increased in PAH vs HC (independent of confounders)						
0.84_458.3469m/z	Lpos	Unknown	0.99 (-0.2 - 2.28)	3.61E-02	9.23E-02	
Decreased in PAH vs HC (independent of confounders)						
7.79_800.6783n	Lpos	SM(d18:1/23:0)	-0.9 (-1.47 - -0.31)	9.81E-03	6.23E-02	
7.46_831.6551m/z	Lneg	Unknown	-0.83 (-1.39 - -0.27)	1.95E-02	5.28E-02	
7.25_736.5598m/z	Lpos	Unknown	-0.88 (-1.45 - -0.23)	2.36E-02	1.11E-01	
7.26_590.5873m/z	Lpos	Unknown	-0.97 (-1.71 - -0.17)	2.59E-02	9.29E-02	
8.08_184.0746m/z	Lpos	Unknown	-1.04 (-1.65 - -0.11)	1.81E-02	1.25E-01	
8.08_957.6400m/z	Lpos	Unknown	-1.3 (-2.11 - -0.69)	2.63E-02	1.90E-01	
7.79_764.5927m/z	Lpos	Unknown	-1.31 (-2.02 - -0.59)	2.20E-02	7.77E-02	
Increased in PAH vs HC						
1.27_112.0510m/z	HILIC	N4-acetylcytidine~	1.35 (0.32 - 2.31)	9.83E-01	7.77E-01	Cardiac glycosides
1.69_187.1337m/z	HILIC	Unknown	0.8 (0.12 - 1.54)	8.48E-01	7.41E-01	DM drugs
1.69_98.0609m/z	HILIC	Unknown	1.08 (0.27 - 2.16)	1.53E-01	4.00E-01	Ethnicity
1.25_120.0452m/z	HILIC	Unknown	0.59 (-0.05 - 1.13)	3.58E-01	2.99E-01	PDE5 inhib.

			Group averages (z-score relative to healthy controls)	Linear Regression		Confounder
Peak, Retention Time-mass/charge (m/z) or neutral mass (n)	Platform	Identity	PAH (19-70)	HC vs PAH	HC+DC vs PAH	HC vs PAH
5.27_800.5788m/z	Lpos	Unknown	0.99 (-0.03 - 2.05)	7.37E-01	7.65E-01	ACE inhib.
1.78_408.3218m/z	Lpos	Unknown	1.01 (-0.2 - 2.31)	7.70E-02	2.13E-01	Cardiac glycosides
1.54_194.1053m/z	HILIC	Unknown	1.6 (0.37 - 2.81)	9.18E-01	8.47E-01	CCBs
Decreased in PAH vs HC						
6.35_800.5828m/z	Lneg	Unknown	-0.78 (-1.4 - -0.07)	4.60E-01	5.41E-01	ACE inhib.
0.33_449.1226m/z	Lneg	Unknown	-1.06 (-2.07 - -0.14)	1.70E-01	2.61E-01	DM drugs
0.33_351.1642m/z	Lneg	Unknown	-1.08 (-2.08 - -0.11)	1.67E-01	3.51E-01	Diuretics
0.34_351.1595m/z	Lneg	Unknown	-1.1 (-2.17 - -0.19)	1.77E-01	4.39E-01	DM drugs
0.33_414.1583n	Lneg	Unknown	-1.13 (-2.08 - -0.2)	8.09E-02	2.06E-01	DM drugs
0.41_449.1636m/z	Lneg	Unknown	-1.34 (-2.41 - -0.4)	2.48E-01	3.26E-01	Ethnicity
0.33_351.1556m/z	Lneg	Unknown	-1.02 (-1.98 - -0.13)	1.62E-01	2.54E-01	Ethnicity
0.88_449.2501m/z	Lneg	Unknown	-0.93 (-1.9 - -0.02)	2.06E-01	1.22E-01	Diuretics
0.53_283.2415m/z	HILIC	Unknown	-0.88 (-1.54 - -0.31)	2.74E-01	2.88E-01	Anticoagulants
0.49_370.1696m/z	Lneg	Unknown	-1.35 (-2.45 - -0.22)	5.09E-01	9.86E-01	DM drugs
0.46_367.1572m/z	Lneg	Unknown	-1.22 (-2.31 - -0.19)	8.08E-01	9.43E-01	ACE inhib.
0.52_271.2062m/z	HILIC	Unknown	-1.48 (-2.43 - -0.47)	1.12E-01	1.44E-01	BMI
0.58_459.1806m/z	HILIC	Unknown	-0.81 (-1.41 - -0.03)	4.36E-01	1.74E-01	PDE5 inhib.
8.64_843.7288m/z	Lpos	Unknown	-0.95 (-1.66 - 0.05)	1.47E-01	5.08E-01	ACE inhib.
2.98_493.3344m/z	Lneg	Unknown	-0.76 (-1.37 - -0.17)	2.01E-01	4.01E-01	ERAs
2.97_591.3148m/z	Lneg	Unknown	-0.76 (-1.49 - -0.13)	8.48E-02	2.13E-01	ERAs
4.82_566.4139m/z	Lpos	Unknown	-0.8 (-1.63 - 0.02)	1.26E-01	5.40E-01	Prostanoids
1.13_158.1185m/z	HILIC	Unknown	-0.82 (-1.39 - 0.25)	5.29E-01	3.75E-01	Gender
2.95_590.3862n	Lpos	Unknown	-0.83 (-1.89 - 0.11)	8.68E-01	9.51E-01	Creatinine
3.61_345.2571m/z	Lpos	Unknown	-0.92 (-1.76 - -0.19)	2.24E-01	2.23E-01	Creatinine
7.63_813.9255m/z	Lpos	Unknown	-0.92 (-1.82 - -0.19)	1.58E-01	3.89E-01	BMI
4.10_476.3643m/z	Lpos	Unknown	-0.94 (-1.61 - -0.27)	6.53E-01	7.04E-01	Bilirubin
3.66_566.4119m/z	Lpos	Unknown	-0.94 (-1.62 - -0.26)	5.90E-01	6.83E-01	DM drugs
4.10_550.4155n	Lpos	Unknown	-0.95 (-1.78 - -0.21)	3.47E-01	3.58E-01	DM drugs
3.66_549.4139m/z	Lpos	Unknown	-0.96 (-1.6 - -0.2)	9.19E-01	7.14E-01	Bilirubin
0.88_438.2975m/z	Lpos	Unknown	-1.01 (-1.58 - -0.27)	2.10E-01	8.98E-02	ACE inhib.
3.62_550.4180n	Lpos	Unknown	-1.02 (-1.77 - -0.2)	6.22E-01	4.84E-01	Statin
0.66_175.1488m/z	HILIC	Unknown	-1.05 (-1.92 - -0.29)	4.50E-01	9.29E-01	ERAs
3.62_458.3485n	Lpos	Unknown	-1.15 (-1.9 - -0.16)	9.23E-01	6.11E-01	ERAs
0.52_565.1305m/z	Lneg	Unknown	-1.32 (-2.31 - -0.33)	3.95E-01	6.08E-01	Ethnicity

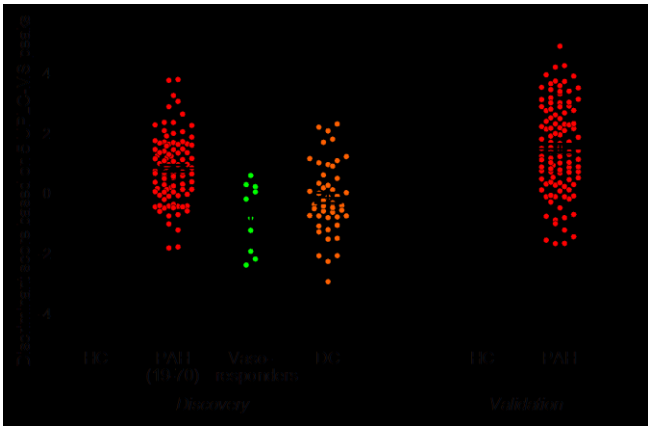
Table 4.7 – UPLC-MS peaks distinguishing PAH from healthy controls, disease controls and CTEPH patients. 67 UPLC-MS peaks that are significantly different between PAH and healthy controls in the discovery and validation cohort (p<1.07e-5) are shown. Experimental platforms hydrophilic interaction chromatography (HILIC) and lipidomics positive (Lpos) and negative (Lneg) mode are

shown. Mean values are given and the data is scaled to the healthy control group. Significance from linear regression is shown (p value) and for metabolites with p>0.05 in PAH HC linear regression, the significant confounder is shown. Identities are shown where known. HC, healthy controls; DC, disease controls; PAH, pulmonary arterial hypertension; CTEPH; chronic thromboembolic pulmonary hypertension; Anticoag., Anticoagulation therapy; DM drugs, antidiabetic drug therapy; ERAs, endothelin receptor antagonists; PDE5 inhib., phosphodiesterase type 5 inhibitors; ACE inhib., angiotensin converting enzyme inhibitors; BMI, body mass index; CCBs, calcium channel blockers; SM, sphingomyelin. ~indicates peaks where the identity was confirmed by analysis of a pure standard compound, the remaining were confirmed by assessment of tandem MS/MS fragmentation patterns.

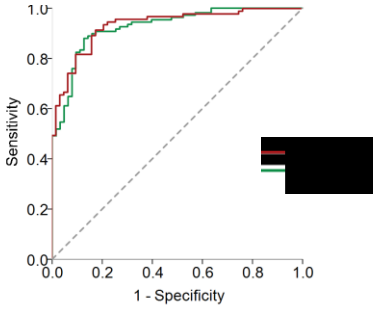
4.3.3 Discriminant analyses models to assess performance of best discriminating peaks

To identify a minimal set of metabolites which could in combination best distinguish PAH patients from healthy controls, I performed logistic regression analysis on the 30 peaks which distinguished PAH patients from healthy controls after correcting for confounders. I found 5/30 UPLC-MS peaks – palmitoylcarnitine (1.72_400.3427m/z) and four unidentified peaks (3.30_1062.6670n, 7.26_590.5873m/z, 8.09_1077.5975m/z, 8.30_799.6693m/z) - independently distinguished PAH patients (aged 19-70) and healthy subjects in the discovery analysis, with 82% accuracy in an orthogonal partial least squares discriminant analysis (OPLS-DA, R^2=0.65, Q^2=0.48). This model classified healthy and PAH subjects in the validation analyses with 85% accuracy. In addition, 60% (6/10) of PAH vasoresponders in the discovery cohort had metabolite levels typical of healthy controls (Figure 4.7).

A



B



Analysis	AUC	Sig.	95% CI
Discovery	0.933	5E-20	0.895 - 0.971
Validation	0.926	2E-20	0.888 - 0.965

Figure 4.7 - Discriminant analysis models based on the best distinguishing metabolites between PAH patients and controls. (A) Dot-plots showing individual subjects' model scores in healthy controls (HC), PAH patients, vasoresponders and disease controls (DC) in discovery and validation analyses. Bar represents the mean and standard error of the mean. Metabolites were selected by logistic regression of PAH versus HC**. (B)** ROC curves showing performance of models in distinguishing PAH versus HC with area under the curve (AUC), significance (Sig.) and 95% confidence intervals (CI) shown**.**

4.3.4 Survival analysis of UPLC-MS peaks in PAH

I hypothesised that metabolites closely related to the disease pathology would be associated with worsening survival. In the discovery cohort, 28/131 IPAH patients died with a median follow-up of 3.3 years (+/- 0.8) and 64/111 IPAH patients died with an average follow up of 2.3 years (+/- 2.6) in the validation cohort. Of the 4053 non-drug related UPLC-MS peaks, 3819 met the proportional hazards assumptions of Cox regression analysis, and 142 of these were prognostic after accounting for creatinine and diuretic use in both analyses. 7/142 prognostic peaks were identified with increased acylcarnitines and decreased triglycerides/phosphocholines predicting worse survival in PAH patients ($p<0.05$, Figure 4.8, Appendix Table 4.1) (peak identification will be detailed in section 4.3.5). 9 cases underwent transplantation (3 in the discovery cohort and 6 in the first validation cohort). In a sub-analysis, where these patients were excluded, 112/142 metabolites remained prognostic in both the discovery and validation cohorts ($p<0.05$, Appendix Table 4.1).

I assessed metabolite levels relative to established prognostic markers - NTproBNP, 6MWD and RDW - and found 52/142 were independent of these markers ($p<0.05$, Appendix Table 4.1).

In a sub-analysis, PAH patients on sildenafil monotherapy were classified as responders (n=18) or non-responders (n=11, defined as death or change in PAH drug therapy within 1 year). 43/142 prognostic peaks were significantly different between the two groups; all are unidentified ($p<0.05$, Appendix Table 4.1).

A subset of 7 metabolites both discriminated PAH patients from healthy controls, and were prognostic – namely palmitoylcarnitine (1.72_400.3427m/z) (Figure 4.9), myristoylcarnitine (1.25_372.3112m/z) and five unidentified peaks (1.26_397.3102m/z, 0.84_458.3469m/z, 1.54_194.1053m/z, 2.98_493.3344m/z, 2.97_591.3148m/z).

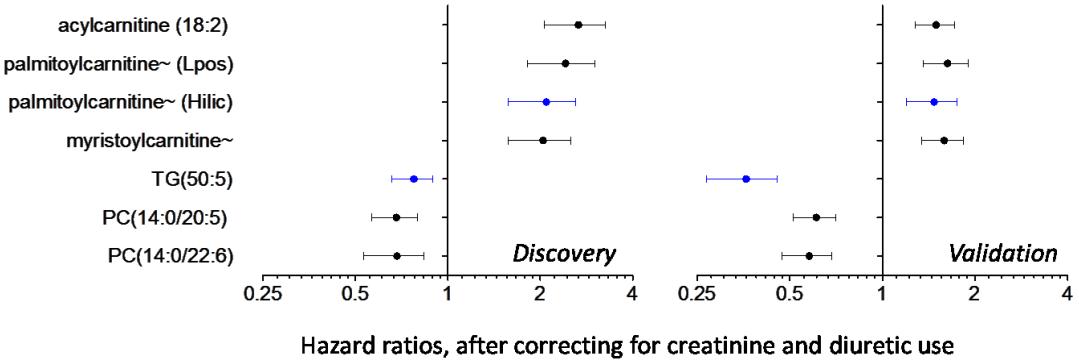


Figure 4.8 - Prognostic identified UPLC-MS peaks. Hazard ratios after correcting for creatinine and diuretic use of 7 UPLC-MS peaks which have been identified are shown in the discovery and validation cohorts.Those independent of established prognostic markers (N-terminal brain natriuretic peptide, six minute walk distance and red cell distribution width) are shown in black. Hazard ratios indicate the risk of change in each peak of 1 standard deviation, for ease of comparison. The palmitoylcarnitine peaks were detected from the HILIC and lipodomics positive (Lpos) UPLC-MS experiments. TG, triglyceride; PC, phosphocholine. ~indicates peaks where the identity was confirmed by analysis of a pure standard compound, the remaining were confirmed by assessment of tandem MS/MS fragmentation patterns, or assessment of retention time and neutral mass.

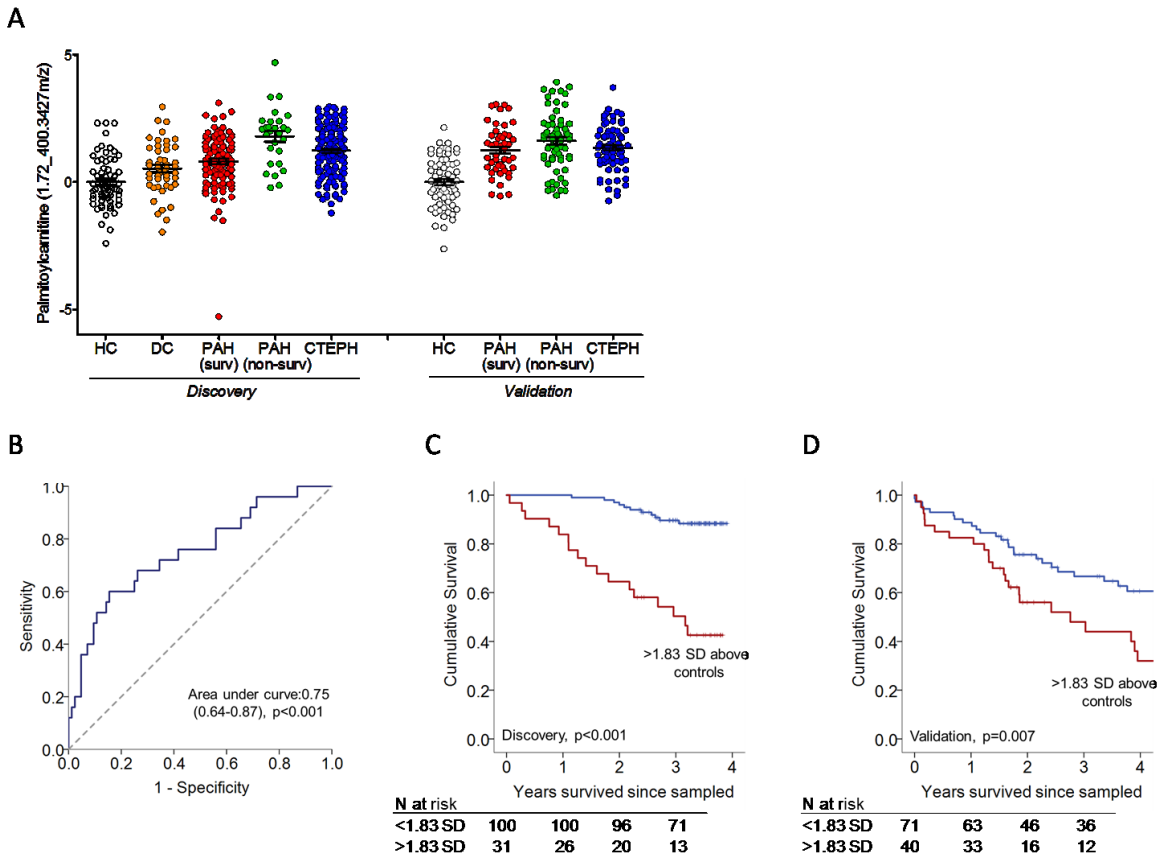


Figure 4.9 – Palmitoylcarnitine UPLC-MS peak which discriminates PAH patients from controls and is prognostic. Normalised abundance of a UPLC-MS peak identified as palmitoylcarnitine is shown between diagnostic groups **(A)** in the discovery and validation cohort. Data is scaled to the healthy control groups, and is shown for healthy controls (HC), disease controls (DC), PAH survivors (surv) and non-survivors (non-surv) and CTEPH patients. Bar represents mean and standard error of the mean. **(B)** Receiver operating characteristic (ROC) curve for palmitoylcarnitine in the discovery cohort and survival at 3 years of follow-up. The optimal cut-off for high/low risk levels of palmitoylcarnitine was derived from this for **C&D**. Kaplan Meier survival estimates in PAH patients in the discovery **(B)** and validation **(C)** cohorts.

4.3.5 Identification of peaks of interest

Overall, the identity of 5/67 discriminating and 7/142 prognostic peaks were identified by review of the retention times, comparison of the mass to charge ratio and fragmentation patterns to available reference databases, and analysis of pure standard compounds. The key fragments detected in lipidomics positive mode tandem MS/MS were 85.03m/z and 184.08m/z representing fragments of acylcarnitines and sphingomyelins or phosphocholines respectively. Additional fragmentation patterns were used to decipher the chain lengths of the metabolites these peaks represented (Table 4.8). Peaks identified by analysis to pure standard compounds include palmitoylcarnitine (1.72_400.3427m/z, 2.77_398.3264m/z), myristoylcarnitine (1.25_372.3112m/z) and N4-acetylcytidine (1.27_112.0510m/z).

Peak, Retention Time-mass/charge (m/z) or neutral mass (n)	Platform	Identity	Key Fragment (m/z)	Additional fragments (m/z) and chain length
1.54_424.3423m/z	Lpos	acylcarnitine (18:2)	85.03	297 (18:2)
8.08_814.6940n	Lpos	SM(d18:1/24:0)	184.08	264.25 (18:1)
7.79_800.6783n	Lpos	SM(d18:1/23:0)	184.08	264.27 (18:1)
4.65_751.5156n	Lpos	PC(14:0/20:5)	184.07	524 (14:0), 468 and 450 (20:5)
4.95_777.5321n	Lpos	PC(14:0/22:6)	184.07	568 and 550 (14:0), 468 (22:6)
9.54_824.6886n	Lpos	TG(50:5)		

Table 4.8 – Identification of peaks based on tandem MS/MS fragmentation and mass/charge ratio. Identification of 6 UPLC-MS peaks from lipidomics positive mode (Lpos) is shown based on a key fragment seen from the parent ion using MS/MS fragmentation pointing to an acylcarnitine group (85.03m/z) and sphingomyelin (SM) or phosphocholine (PC) (184.08/184.07m/z). Additional fragments that were used to identify the chain lengths are also shown. Triglyceride peak was identified based on late retention time, and chain length based on the neutral mass.

4.4 Discussion

This study represents a comprehensive analysis of circulating metabolites using UPLC-MS in patients with PAH, with data validated in a second independent cohort.

I was able to detect and identify UPLC-MS peaks of bosentan, sildenafil and imatinib after the initiation of drug therapy. Levels of bosentan and sildenafil were related to the dose of the treatment and, in patients on sildenafil and imatinib, highlighted patients who did not adhere with therapy. In addition, metabolites which were significantly decreased on bosentan therapy were detected and may inform on how the drug itself is acting, but as yet remain unidentified.

With many chronic diseases, adherence to therapy remains a significant challenge (Cramer 2002) and regimes which require once a day dosing tend to fare better rather than 2-3 times a day (Frishman 2007). Lack of adherence influences the effectiveness of a drug therapy (Cramer 2002) and in PAH, despite current therapies, may contribute to the poor outcomes that persist in the modern era.

In a study of 2143 patients, adherence to PDE5 inhibitors in PAH patients over a 6 month period was only 46.8%, with better adherence to once daily regimes (Waxman, Chen et al. 2013). Adherence to therapy was assessed based on 'proportion of days covered' defined as the number of days medication was available over the 6 month period (Waxman, Chen et al. 2013). Assessing patient adherence based on an objective measure such as UPLC-MS may allow more studies of adherence to other PAH related therapies and could translate into clinical practice to improve patient adherence.

A subset of prognostic peaks were significantly different between PAH responders and non-responders on sildenafil monotherapy, however these have not been identified. This assessment was also limited by small numbers of patients in each group. Prospective longitudinal assessment of metabolite profiles before the initiation of therapy and after therapy in the same patients would allow assessment of metabolic profiles that predict outcomes and response to therapy based on changes in biochemical signatures. For example, metabolic profiles have been shown to predict the response to rituximab therapy in patients with rheumatoid arthritis (Sweeney, Kavanaugh et al. 2016) or a response to angiotensin II receptor blockers in diabetes (Pena, Heinzel et al. 2016).

The most robust distinguishing and prognostic difference in PAH patients were increased acylcarnitines, in particular palmitoylcarnitine and myristoylcarnitine, consistent with previous reports of increased levels of circulating long chain acylcarnitines in PAH (Brittain, Talati et al. 2016, Bujak, Mateo et al. 2016).

An accumulation of acylcarnitines may represent an increase in fatty acid oxidation, which is seen in the pulmonary vasculature (Sutendra, Bonnet et al. 2010) and RV (Fang, Piao et al. 2012) in PAH, suggesting these tissues may be the source in this disease. Through the Randle effect, increased fatty acid oxidation inhibits glucose oxidation to promote aerobic glycolysis. Inhibition of fatty acid oxidation has been proposed as a potential therapeutic target in PAH and improves functional and haemodynamic parameters in animal models of PAH (Guarnieri and Muscari 1988, Fang, Piao et al. 2012).

Increased acylcarnitine levels may also represent dysfunction of the TCA cycle, leading to subsequent build-up of acylcarnitines and TCA cycle intermediates. From NMR analysis, increased citric acid was noted in PAH patients however, intermediates of the TCA cycle and glutaminolysis were not identified in this UPLC-MS experiment to validate or expand these findings. Further assessment of these features would be needed for a more detailed understanding of energy metabolism changes in PAH.

The accumulation of acylcarnitines may itself be detrimental, effecting cardiac electrophysiological changes and causing arrhythmias (DaTorre, Creer et al. 1991). There is also increasing evidence that accumulation of long chain acylcarnitines may contribute to insulin resistance (Schooneman, Vaz et al. 2013), which is itself common and associated with prognosis in PAH (Zamanian, Hansmann et al. 2009).

Multiple sphingomyelin and phosphatidylcholine lipid species were significantly reduced in PAH patients, relating to increased mortality. Sphingomyelins are the most abundant subclass of sphingolipids, with other subclasses including sphinogosines, ceramides and glycophospholipids (Hannun and Obeid 2008). In patients with chronic obstructive pulmonary disease (COPD), low plasma levels of several sphingomyelins relate to disease severity (Bowler, Jacobson et al. 2015). As a membrane constituent, sphingomyelins are implicated in trans-membrane signalling and are generated from phosphatidylcholine and ceramide by sphingomyelin synthase, knockout of which leads to mitochondrial dysfunction and reduced insulin release (Yano, Watanabe et al. 2011). Sphingomyelins may also be considered a source of ceramide, which directly (and indirectly through other active lipid products) regulates cell proliferation, apoptosis, cell migration and autophagy (Taniguchi and Okazaki 2014).

Reduced lineoyl glycerophosphocholine has been shown to be an early marker of insulin resistance in non-diabetics (Ferrannini, Natali et al. 2013), and decreased circulating levels of several phosphatidylcholines were seen in patients with severe heart failure (Cheng, Wang et al. 2015).

Phospholipids are also sources of multiple cellular signalling molecules including eicosanoids such as prostacyclin (Wymann and Schneiter 2008), levels of which are known to be reduced in pulmonary hypertension, with replacement an established treatment option.

A key limitation and difficulty of this study has been identifying UPLC-MS peaks of interest, a known difficulty with mass spectrometry based metabolomics (Dunn, Broadhurst et al. 2011, Lynn, Cheng et al. 2015). Based on mass to charge ratio alone, each peak can often have up to 100 putative identities matched in available databases and the availability of databases themselves are limited (Xiao, Zhou et al. 2012).

In order to confirm identities from these lists, analysis of pure standard compounds was undertaken, but this was only conducted using HILIC experimentation. In the future with increased availability of authentic lipid standards, this would be useful to conduct in lipidomics mode. For a definitive identification, authentic standards should also be subject to tandem MS/MS experimentation in parallel with the sample and peak of interest. These techniques are labour intensive and require a high degree of technical expertise, cost, sample availability, authentic standard availability and time. In this study, the majority of UPLC-MS peaks of interest remain unidentified however, with better tools, databases and identification pipelines, it may be possible to identify these features in the future.

In this study I was able to measure levels of PAH therapies in patients after initiation of therapy that were dose-related and highlighted non-adherent patients. In addition, features influenced by these therapies were detected but remain unidentified. Novel metabolite abnormalities affecting acylcarnitines, sphingomyelins and phosphocholines were detected and associated with worse clinical outcomes. However, changes in abnormal oxidation found in NMR were not validated and the majority of interesting UPLC-MS peaks remain unidentified. Improved identification of UPLC-MS is required and in parallel, use of an alternative broad metabolomics platform containing identified metabolites would allow a more detailed assessment of metabolic dysregulation in PAH.

Chapter 5 - Investigation of metabolic abnormalities in PAH using the Metabolon platform

5.1 Introduction

I initially found increased citric acid, 3-hydroxybutyric acid, and decreased glutamine and HDL subtypes using NMR spectroscopy in PAH patients. In order to validate these findings and expand the number of metabolites detected, in particular lipids, an unbiased UPLC-MS approach was applied on a discovery and validation cohort of distinct patients and controls. This identified increased acylcarnitines and decreased sphingomyelins and phosphocholines in PAH patients but was limited by techniques to identify several metabolite features which were discriminating and prognostic in PAH.

The major advantage of Metabolon's commercial approach is access to their extensive chemical reference library. This comprises more than 4,500 known metabolites, as well as 9,000 novel metabolites without an identified chemical structure, providing the most comprehensive metabolomics coverage currently available. The use of Metabolon's technology also gives semi-quantitative information on hundreds of named metabolites with annotated pathways. This offers the opportunity to validate the findings from the previous NMR and UPLC-MS studies, explore other metabolites in pathways such as energy metabolism and lipid regulation, and assess novel metabolic changes in PAH. Metabolomic profiling by Metabolon has previously been used to assess circulating metabolite levels in control subjects (Shin, Fauman et al. 2014) and diseases such as amyotrophic lateral sclerosis (Lawton, Brown et al. 2014), inborn errors of metabolism (Miller, Kennedy et al. 2015), systemic hypertension (Menni, Graham et al. 2015), heart failure in the African-American population (Zheng, Yu et al. 2013) and diabetes (Yengo, Arredouani et al. 2016). Metabolites contributing to the risk of developing diabetes included a glycerophosphocholine, glucose, isoleucine, mannose and pro-hydroxy-pro (Yengo, Arredouani et al. 2016) and increased hexadecanedioate was reported in systemic hypertension (Menni, Graham et al. 2015).

This study also provides the opportunity to look at subtypes of IPAH and HPAH patients, including those with *BMPR2* mutations. Several genetic mutations have been reported in hereditary and isolated idiopathic presentations of PAH, providing insight into perturbed signalling pathways (Machado, Eickelberg et al. 2009, Ma and Chung 2014), and genome sequencing of clinically well characterised patient cohorts is underway in anticipation of finding new mutations. PAH patients who are *BMPR2* mutation carriers have an earlier onset of disease, higher mPAP and pulmonary

vascular resistance, and those who present earlier have poorer outcomes (Evans, Girerd et al. 2016). Understanding the metabolic profile of *BMPR2* mutation carriers may provide insight into the molecular drivers of PAH.

Another subset of PAH patients are those who have favourable outcomes with oral calcium channel blocker therapy (vasoresponders) with improvements to quality of life and survival (Sitbon, Humbert et al. 2005, Galie, Humbert et al. 2015). Understanding the metabolic profile of patients who are responders to therapy, in addition to those with poor survival, provides information on whether disturbances in metabolic profiles are linked to outcomes and are modifiers of disease progression.

In this study I set out to a) validate findings from NMR and UPLC-MS in abnormal energy metabolism (citric acid, glutamine, acylcarnitines), sphingomyelin metabolism and lipid regulation in PAH, b) identify novel metabolic abnormalities in PAH, c) assess metabolic profiles in patients who are *BMPR2* mutation carriers, d) identify patients at high risk of early death and e) identify patients who respond well to treatment (vasoresponders).

5.2 Methods

See Chapter 2 for detailed experimental methods and protocols.

5.2.1 Sample collection

Samples were obtained from patients with idiopathic or heritable PAH attending the National Pulmonary Hypertension Service at Hammersmith Hospital, London between 2002-2015 and from patients recruited from other UK national centres as part of the National Cohort Study of Idiopathic and Heritable Pulmonary Arterial Hypertension (ClinicalTrials.gov NCT01907295) between 2013-2015. Control plasma samples were obtained from healthy subjects and disease controls, the latter being symptomatic patients presenting to the service but in whom pulmonary hypertension was excluded by cardiac catheterisation. Whole-genome sequencing data from the UK National Institute of Health Research Biomedical Research Centres Inherited Diseases Genetic Evaluation (BRIDGE) consortium were used to determine which patients had known pathogenic mutations in the gene encoding the bone morphogenetic protein type II receptor (BMPR2) (Machado, Eickelberg et al. 2009). WHO functional class and six minute walk distance at sample date and clinical biochemical

data (within 30 days) were recorded. A subset of patients consented to provide additional samples at later dates whilst attending follow-up clinical appointments.

5.2.2 Metabolomics

Metabolomic profiling by ultra-performance liquid chromatography mass spectrometry was conducted on the Discovery HD4^{TM} Global Metabolomics platform by Metabolon, Inc. (Durham, NC, USA) (Evans, DeHaven et al. 2009, Dehaven, Evans et al. 2010). Metabolon has several commercial platforms including the Discovery HD4^{TM} for metabolomics assessment, a Complex Lipid Platform for lipidomics assessment, and targeted metabolite panels for fatty acids, acylcarnitine, bile acid, cholesterol and biomarker assays. The Discovery HD4^{TM} platform was chosen as it provides the most comprehensive assessment of metabolite features.

Briefly, samples were prepared by Metabolon using the MicroLab STAR system (Hamilton Company, Reno, NV, USA). Methanol was added to the samples to remove protein and protein bound molecules and following centrifugation, the remaining extract used for subsequent investigations. Standards were spiked into all experimental samples for quality control and assessment of instrument performance and chromatographic alignment (Miller, Kennedy et al. 2015). A further quality control, comprising a pooled sample of all the experimental samples, was used throughout the assay and water was used as sample blanks. All the samples were also randomised prior to UPLC-MS/MS analysis.

The assay was performed using four UPLC-MS/MS techniques including a) positive ion mode electrospray ionisation (ESI), b) positive ion mode optimised for hydrophobic compounds, c) negative ion mode ESI and d) negative ionisation following elution from a hydrophilic interaction chromatography (HILIC) column. The initial separation was conducted on Waters Acuity ultra-performance liquid chromatography (UPLC) systems (Waters Corporation, Milford, MA, USA). Sample ionisation and sorting was conducted using a Thermo Scientific Q-Exactive high resolution/accurate mass spectrometer interfaced with a heated electrospray ionization (HESI-II) source and Orbitrap mass analyser (Thermo Fisher Scientific, MA, USA). The scan time varied between methods and covered 70-1000m/z.

The resulting spectra were compared to a Metabolon standard library which contains 4500 annotated metabolite features, including the mass to charge ratio, retention time and chromatographic data of chemical standards. The library was established using LC-MS and GC-MS

techniques in positive and negative ion mode to document all ions detected from chemical standards.

Ion features were compared to the chemical reference library by Metabolon using their own Metabolyzer^{TM} software. Identification required that a) the retention time of the detected ion to be within a narrow retention time window of the proposed biochemical, b) a mass match within +/- 10ppm of the detected and proposed biochemical and c) assessment of the 'MS/MS' score which reflects a comparison between the ions present in the experimental run to the reference library. Metabolon use interpretation and visualisation software to confirm the identities of ions for every compound in every sample, and although multiple ions may be detected for each metabolite, only the abundance of a representative peak is provided. A subset of metabolites were named, based on mass and fragmentation analysis, but their identity has yet to be confirmed with standards, and these are indicated by asterisks.

In this study, Metabolon provided raw data with the quantitative abundance of 1416 metabolites (949 with metabolite identities and 467 without chemical identities) annotated with pathways.

5.2.3 Angiogenin

Plasma angiogenin levels were determined by ELISA (Ref:DAN00, R&D Systems, Abingdon, UK) as per manufacturer's guidelines, with EDTA plasma diluted 1:800 before assay.

5.2.4 Targeted fluorometric assays

To investigate a subset of metabolites which were not identified using the unbiased UPLC-MS approach, or the commercial Metabolon platform, targeted flourometric assays were used. Metabolites measured with these assays included oxaloacetate and acetyl co-A, with plasma EDTA samples of 50uL and 10uL diluted 1:5 and 1:800 for each experiment respectively.

5.2.5 Immunohistochemistry

To investigate the possible pulmonary source of circulating metabolites associated with PAH, immunohistochemistry experiments were conducted on sections of lung tissue obtained at the

transplantation of 3 PAH patients. Antibody targets included 1-methyladenosine, pseudouridine and angiogenin with experiments conducted as per manufacturers guidelines. Antibodies for 1-methyladenosine and pseudouridine have previously been used to study oesophageal carcinoma (Masuda, Nishihira et al. 1993) and renal disease (Mishima, Inoue et al. 2014).

5.2.6 Statistical analysis

To prevent skewing of results by outliers, initial group comparisons between controls and patients were performed using non-parametric Mann Whitney U tests. Prior to modelling, metabolites whose distribution was not normal were transformed either by log10 or power transformations (xY, with Y from -2 to 2 in 0.5 steps, as performed for Box-Cox transformations (Box and Cox 1964), whichever best normalised the data based on Kolmogorov-Smirnov tests, or ranked if no test met $p>0.05$. Samples where metabolites were undetected were imputed with the minimum detected level for the metabolite. All data were z-score transformed based on healthy control data for ease of comparisons, between the discovery and validation experiments.

Linear regression analysis was conducted to assess the relationships between metabolite levels, diagnoses and potential confounders. In the disease control and PAH cohorts, preserved renal function was defined as creatinine <75 μmol/L, and liver function as bilirubin <21 μmol/L. In the healthy control group, preserved renal and hepatic function was assumed as clinical assay data was unavailable. Logistic regression was conducted to determine metabolites that independently distinguished between diagnostic groups. Orthogonal partial least squares discriminant analysis (OPLS-DA) modelling was used to test the performance of these metabolites. R^2 scores indicate model performance and Q^2 scores estimate reproducibility, based on cross validation. Pathway enrichment analysis was conducted on discriminating and prognostic metabolites using Fisher's exact test.

Survival analyses were performed using time from sampling to death/census. In a secondary analysis, transplantation or death (all-causes) was used as a composite endpoint. Cox regression analysis was used to identify prognostic predictors, with proportional hazard assumptions tested. Metabolites which were prognostic were assessed against established prognostic indicators – NT-proBNP (Nagaya, Nishikimi et al. 2000), 6MWD (Fritz, Blair et al. 2013) and RDW (Rhodes, Wharton et al. 2011). Kaplan-Meier plots used to illustrate events from time of sampling in relation to metabolite levels. Receiver Operating Characteristic (ROC) curves were used to assess discriminating and prognostic value of metabolites against diagnosis and all-cause mortality respectively.

Hierarchical clustering based on Euclidean distances was used to assess if metabolites and patients clustered by functional pathways and phenotypes, respectively.

Network analysis was performed by calculating second order Spearman's rank correlations using ParCorA (http://www.comp-sys-bio.org/software.html) (de la Fuente, Bing et al. 2004) and visualised using Cytoscape (http://www.cytoscape.org/). 'Hub' nodes are metabolites with the most 'edges' (correlations) to other metabolites.

5.3 Results

5.3.1 Metabolites distinguishing between PAH and controls

I first compared plasma metabolite profiles from 116 consecutive patients with idiopathic or heritable PAH attending Hammersmith Hospital between November 2011 and August 2013 and 58 healthy controls. To minimise confounding factors, only PAH patients aged 19-70 were compared with age- and sex-matched healthy controls in this analysis. Results were validated in 75 PAH patients recruited between 2002 and 2015 against a separate control group (n=63). A second validation analysis used 174 PAH patients recruited from other specialist centres in the UK from August 2013 to June 2015 and compared to all controls. Baseline characteristics and laboratory data are shown in (Table 5.1). Metabolites identified as xenobiotics or detected in less than 95% of samples were excluded from the analysis, leaving 686 well-quantified biological metabolites.

	Discovery				Validation 1			Validation 2
	HC (n=58)	DC (n=70)	PAH (19-70) (n=88)	PAH (>70) (n=28)	HC (n=63)	DC (n=69)	PAH (n=75)	PAH-2 (n=174)
Age at sampling, years	48+/-13.5	56.5+/-15.9	48.1+/-13.8	75.9 +/-4.8	49.1+/-16.1	55.9+/-18.5	52+/-16.3	52+/-15
Sex, Female:Male (ratio)	38:20 (1.9:1)	48:22 (2.2:1)	61:27 (2.3:1)	19:9 (2.1:1)	40:23 (1.7:1)	48:21 (2.3:1)	52:23 (2.3:1)	127:47 (2.7:1)
Ethnicity, % non-Caucasian	32.5	56.9	17	14.8	38.1	44.1	18.6	8.1
BMI, kg/m^2	30.5+/-10.5	27.9+/-6	28.7+/-8.2	27.9+/-5.7	26+/-4.1	27.4+/-5.9	30.1+/-7.2	29.2+/-7
BMPR2 mutation carriers (%)			8.0	3.6			5.3	
Treatment naïve cases (%)			12.5	21.4			30.7	
Baseline haemodynamics at diagnosis								
Pulmonary capillary wedge pressure, mmHg		11.6+/-4.5	11.9+/-6	12.1+/-4.6		10.8+/-3.5	10.8+/-4.9	9.4+/-3.8
Mean pulmonary artery pressure, mmHg		19.3+/-4.1	53.1+/-14.3	46.3+/-14.6		19.1+/-4.7	53.7+/-11.1	56.2+/-15.2
Pulmonary vascular resistance, Woods units			12.3+/-5.7	8.6+/-4.7			12.4+/-5.8	13+/-6.4
Mean right atrial pressure, mmHg		7.3+/-3.4	10.0+/-5.7	9.3+/-4.9		6.3+/-3.2	11.8+/-5.8	9.2+/-5.3
Cardiac output, L/min			4.4+/-1.7	4.5+/-1.8			4.0+/-1.7	4.0+/-1.3
Functional status and pathology								
Six minute walk distance, m			279.4+/-153.4	197.9+/-158.7			271.3+/-169.5	334.8+/-119.0
WHO Functional Class, I/II/III/IV			2/11/65/10	0/2/23/1			0/7/52/9	2/24/119/18
RDW, %			14.8+/-2.1	15.0+/-1.1			16.0+/-2.9	14.7+/-3.3
NT-proBNP, pmol/L			735+/-882	1137+/-1123				895+/-1244
Creatinine, umol/L		76.3+/-21.8	81.2+/-29.1	107.6+/-35.7		87+/-40.6	92.7+/-32.6	89.9+/-25.1
Bilirubin, umol/L		13.9+/-13.9	15.6+/-10.7	12.4+/-8.5		16.3+/-22.8	17.2+/-10.4	12.1+/-9.0
Comorbidities								
Asthma/COPD		17.1	11.4	11.1		11.6	17.1	17.6
Diabetes		8.6	17	48.1		13	24.3	14.2
CAD/IHD		10	12.5	37		11.6	12.9	8.3
AF/flutter		14.3	18.2	25.9		17.4	8.6	5.9
Systemic hypertension		22.9	19.3	77.8		36.2	22.9	17.2
Hypercholesterolaemia/ lipidaemia		12.9	12.5	22.2		10.1	15.7	6.5
Drug therapy								
Anticoagulation		32.9	71.6	78.6		34.8	65.3	66.7
PDE5 inhibitors		0	65.9	67.9		0	48	77.8
ERA		0	48	30.8		0	33.8	64.3
Prostanoids		0	9.1	0		0	6.7	33.3
Diuretics		12.9	37.5	75		21.7	53.3	54.4
Aldosterone antagonists		7.1	31.8	21.4		1.4	34.7	8.2
Statins/lipid lowering drugs		25.7	22.7	57.1		33.3	24	24
CCB		10	14.8	28.6		24.6	14.7	21.1
Cardiac glycosides		7.1	17	14.3		8.7	21.3	9.4

	Discovery				Validation 1			Validation 2
	HC (n=58)	DC (n=70)	PAH (19-70) (n=88)	PAH (>70) (n=28)	HC (n=63)	DC (n=69)	PAH (n=75)	PAH-2 (n=174)
Antidiabetic drugs		8.6	12.5	35.7		10.1	18.7	9.4
Iron replacement therapy		4.3	13.6	25		5.8	4	10.5
ACE inhibitors		27.1	17	60.7		37.7	28	16.4

Table 5.1 – Metabolon Cohort Characteristics. Means and standard deviations or counts are given. Clinical pathology parameters are shown within 30 days of the sample date. Co-morbidities and drug therapy are shown as the percentage of patients with those co-morbidities or on each agent (%).BMI, body mass index; NT-proBNP, N-terminal brain natriuretic peptide at time of sample; RDW, red cell distribution width; HC, healthy controls; DC, disease controls; COPD, chronic obstructive pulmonary disease; CAD, coronary artery disease; IHD, ischaemic heart disease; AF, atrial fibrillations; PDE5, phosphodiesterase 5; ERA, endothelin receptor antagonists; CCB, calcium channel blocker; ACE, angiotensin converting enzyme. 10 PAH patients in the discovery cohort and 3 in the validation cohort are on CCB therapy as vasoresponders. Ethnicity is shown for subjects who self-declared.

Circulating levels of 97 metabolites distinguished PAH from healthy subjects in all three analyses following Bonferroni correction ($p<7.3e-5$). Of these metabolites, 53 distinguished healthy and PAH subjects after correcting for potential confounders, including age, gender, ethnicity, body mass index, creatinine, bilirubin and drug therapies ($p<0.05$, Appendix Table 5.1, Figure 5.1).

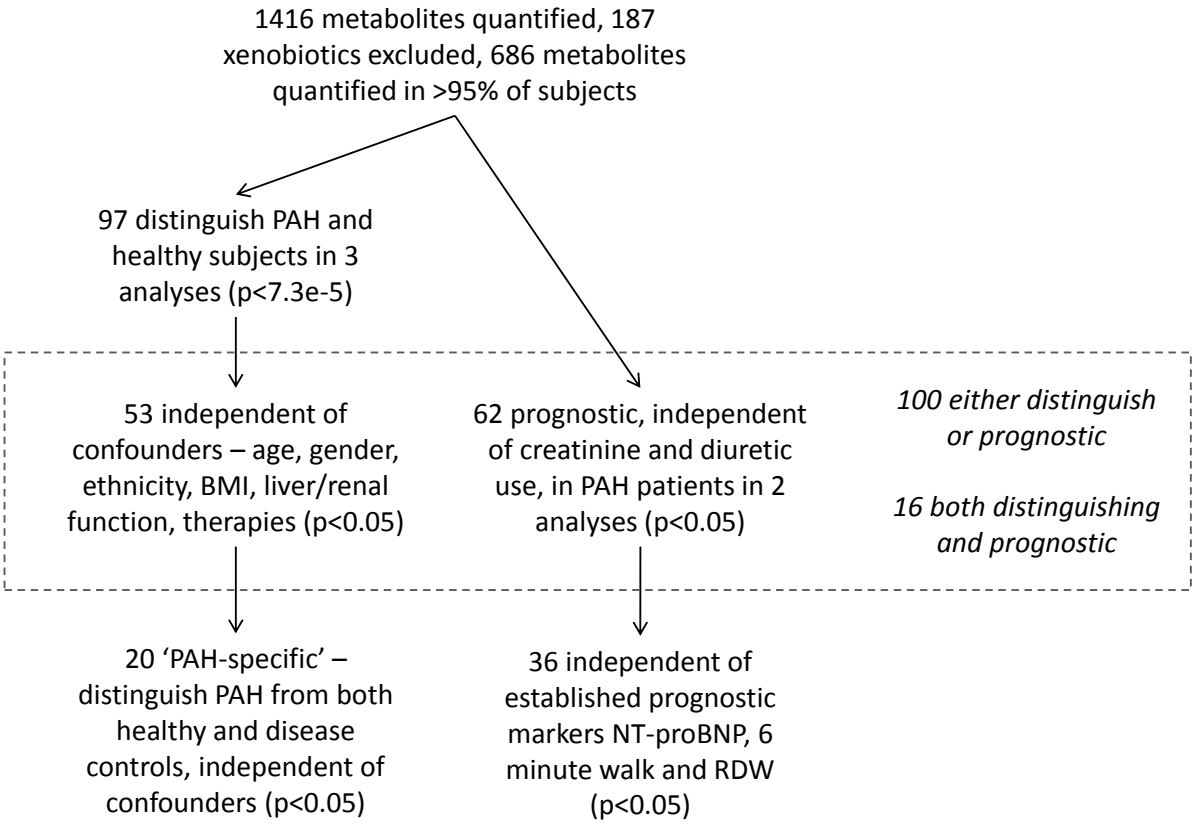


Figure 5.1 – Analysis flow chart. Summary of analytical workflow showing numbers of metabolites that distinguish PAH from controls, and/or are prognostic in PAH. BMI, body mass index; NT-proBNP, N-terminal brain natriuretic peptide; RDW, red cell distribution width.

The most common confounders associated with metabolite levels were liver function (bilirubin) and renal function (creatinine). Although several metabolites were related to confounders such as age and gender, differences between PAH and control groups remained significant after correction for these factors (Figure 5.2).

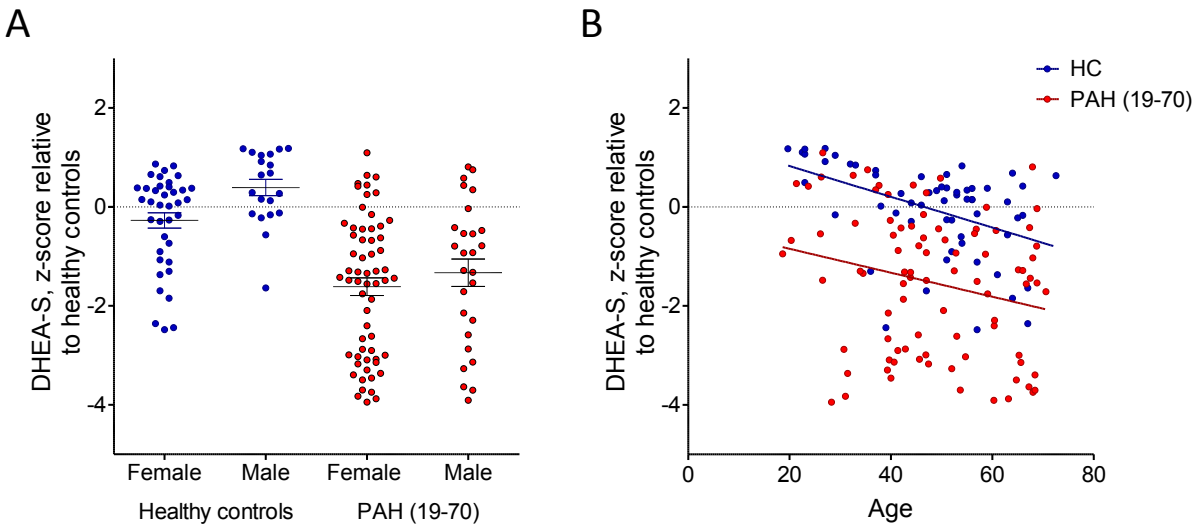


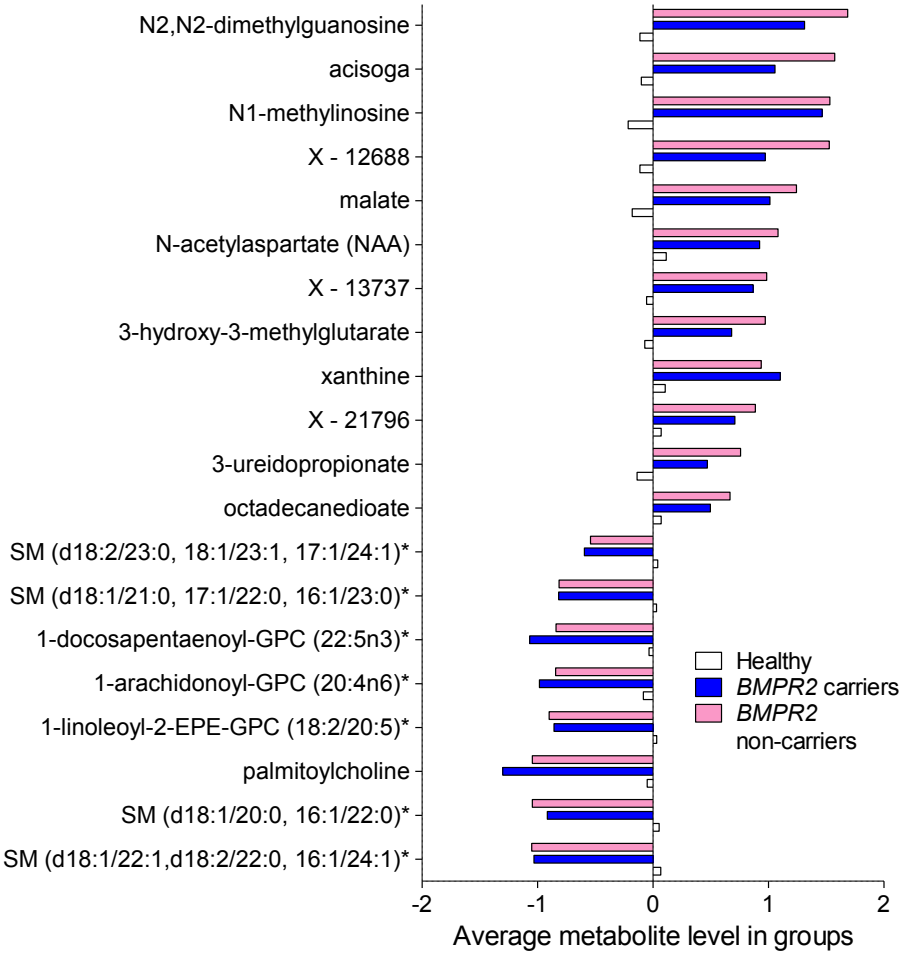
Figure 5.2 - Dehydroisoandrosterone-sulphate (DHEA-S). Plasma DHEA-S levels in the discovery cohort are shown for healthy controls (HC) and PAH (19-70) with **(A)** separation by gender and **(B)** against age. Bar represents mean and standard error of the mean in **(A)**.

To determine whether these metabolite differences could be detected prior to initiation of PAH therapies, I performed a sub-analysis comparing 40 patients who were treatment naïve at the time of sampling and all 53 metabolites distinguished this group from healthy controls ($p<0.05$, Appendix Table 5.1). Patients with pathogenic *BMPR2* mutations (n=42) had similar metabolite levels to PAH non-mutation carriers from all three cohorts (n=323) (Table 5.2, Figure 5.3, Appendix Table 5.1). Patients who were *BMPR2* mutation carriers had higher mPAP and PVR at baseline ($p<0.0001$) but had a similar duration of time survived from the diagnosis to sample date ($p>0.05$).

	BMPR2 mutation carriers (n=42)	Non-BMPR2 mutation carriers (n=323)
Age at sampling, years	46.0+/-14.1	53.8 +/- 16.0
Sex, Female:Male (ratio)	26:16 (1.6:1)	233:90 (2.6:1)
Ethnicity, % non-Caucasian	11.9	12.7
BMI, kg/m^2	28.7+/- 6.3	29.2 +/- 7.4
Time from diagnosis to sample date (years)	3.8 +/- 3.9	4.4 +/- 3.9
Baseline haemodynamics at diagnosis		
Pulmonary capillary wedge pressure, mmHg	10.4 +/- 3.7	10.4 +/- 4.9
Mean pulmonary artery pressure, mmHg	62.5 +/-12.4	53.1 +/- 14.4
Pulmonary vascular resistance, Woods units	17.0 +/- 7.3	11.7 +/- 5.6
Mean right atrial pressure, mmHg	9.6 +/- 4.8	9.0 +/- 5.6
Cardiac output, L/min	3.5 +/- 1.1	4.1 +/- 1.4
Functional status and pathology		
Six minute walk distance, m	373.6+/- 117.0	321.1 +/- 173.9
WHO Functional Class, I/II/III/IV	1/14/22/2	21/76/182/22

Table 5.2 – Cohort Characteristics of PAH patients who are BMPR2 mutation carriers and non-carriers. Means and standard deviations or counts are given. BMI, body mass index. Ethnicity is shown for subjects who self-declared.

A


N2,N2-dimethylguanosine
acisoga
N1-methylinosine
X - 12688
malate
N-acetylaspartate (NAA)
X - 13737
3-hydroxy-3-methylglutarate
xanthine
X - 21796
3-ureidopropionate
octadecanedioate
SM (d18:2/23:0, 18:1/23:1, 17:1/24:1)*
SM (d18:1/21:0, 17:1/22:0, 16:1/23:0)*
1-docosapentaenoyl-GPC (22:5n3)*
1-arachidonoyl-GPC (20:4n6)*
1-linoleoyl-2-EPE-GPC (18:2/20:5)*
palmitoylcholine
SM (d18:1/20:0, 16:1/22:0)*
SM (d18:1/22:1,d18:2/22:0, 16:1/24:1)*
Healthy
BMPR2 carriers
BMPR2 non-carriers
-2
-1
0
1
2
Average metabolite level in groups

B

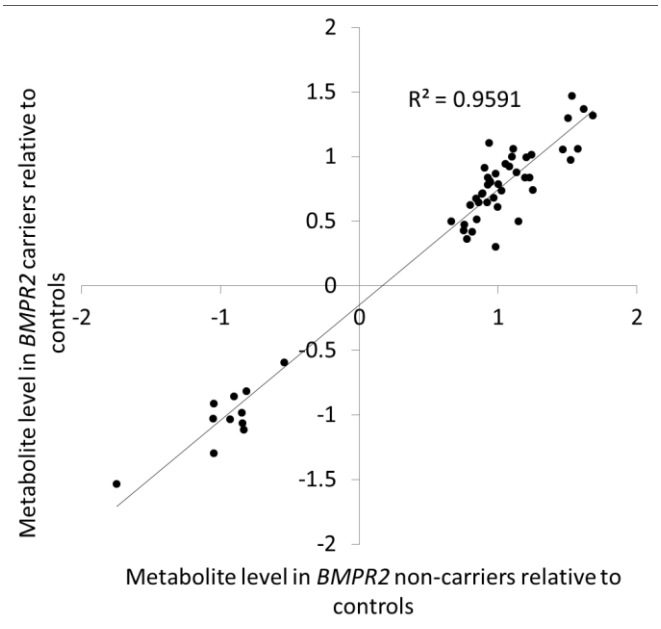

R² = 0.9591
2
1.5
1
0.5
0
-0.5
-1
-1.5
-2
-2
-1
0
1
2
Metabolite level in BMPR2 carriers relative to controls
Metabolite level in BMPR2 non-carriers relative to controls

Figure 5.3 - Metabolite levels in BMPR2 (bone morphogenetic protein receptor, type 2) mutation carriers. (A) Average metabolite levels in PAH *BMPR2* mutation carriers, non-carriers and healthy control subjects for 20 metabolites found to significantly distinguish PAH and both healthy and disease controls, independent of potential confounders. SM, sphingomyelin; GPC, glycerophosphocholine; EPE, eicosapentaenoyl. *probable metabolite identity, but unconfirmed (see methods). **(B)** Correlation of average metabolite levels in *BMPR2* mutation carriers and non-carriers relative to controls for 53 metabolites that distinguish PAH from healthy controls, independent of potential confounders. Values plotted are z-scores calculated based on mean and standard deviation of all healthy volunteers in study - negative values indicate metabolites at lower levels in patients versus healthy controls and positive values indicate higher levels of metabolites in patients.

Given that many metabolic alterations might occur in a chronic disease such as PAH, I set out to prioritise more disease-specific metabolites by comparing the PAH patients with disease controls. A subset (20/53) of the metabolites distinguished PAH patients from disease controls after correcting for potential confounders ($p<0.05$, Appendix Table 5.1). These 'PAH-specific' differences in metabolites included increases in purine, polyamine and tricarboxylic acid (TCA) cycle metabolites, and decreases in phosphocholines and sphingomyelins (Figure 5.4), with network analysis showing the importance of 'hub' metabolites N2,N2-dimethylguanosine and malate (Figure 5.5).

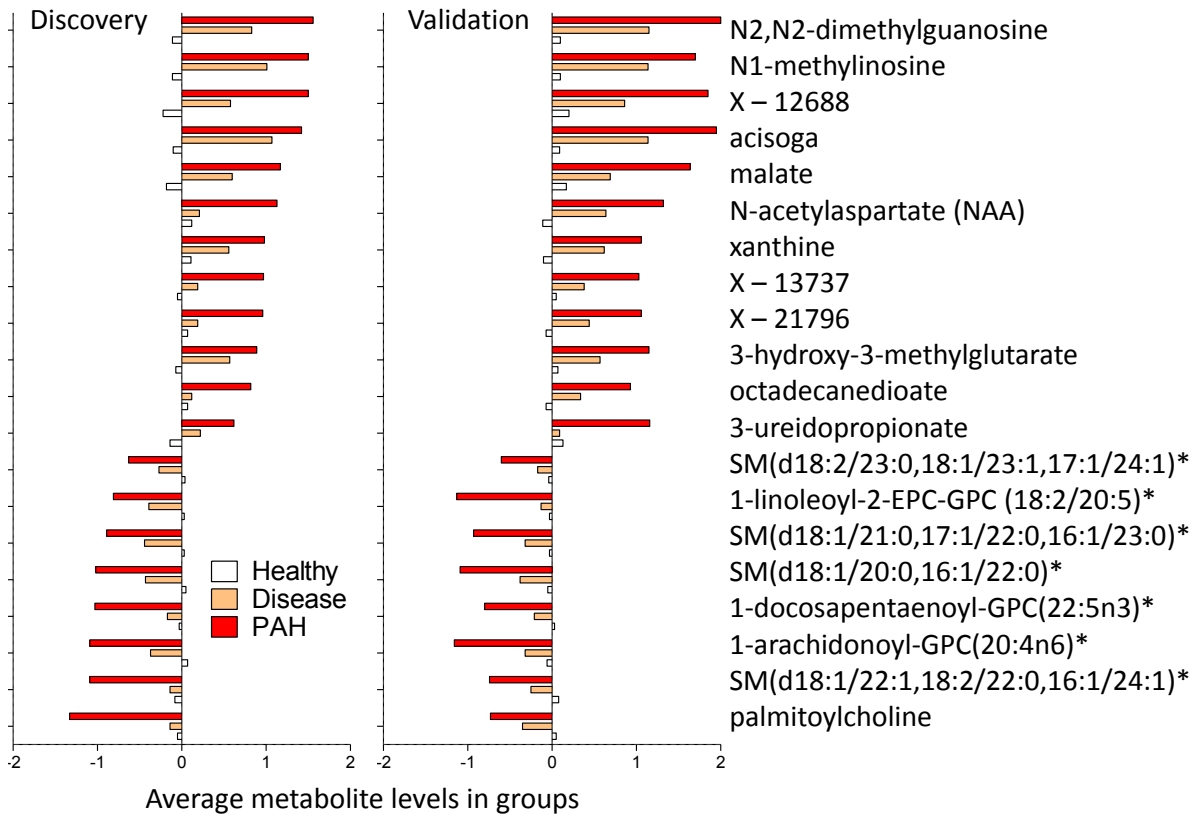


Figure 5.4 - Metabolites which discriminate PAH and control subjects. Average metabolite levels in PAH and control subjects for 20 metabolites found to significantly distinguish PAH and both healthy and disease controls, independent of potential confounders. Values plotted are z-scores calculated based on mean and standard deviation of all healthy volunteers in study - negative values indicate metabolites at lower levels in patients versus healthy controls and positive values indicate higher levels of metabolites in patients. *probable metabolite identity, but unconfirmed (see methods). EPE, eicosapentaenoyl; DHE, docosahexaenoyl; DPE, docosapentaenoyl; DHEA-S, dehydroisoandrosterone sulphate; GPC, glycerophosphocholine; SM, sphingomyelin.

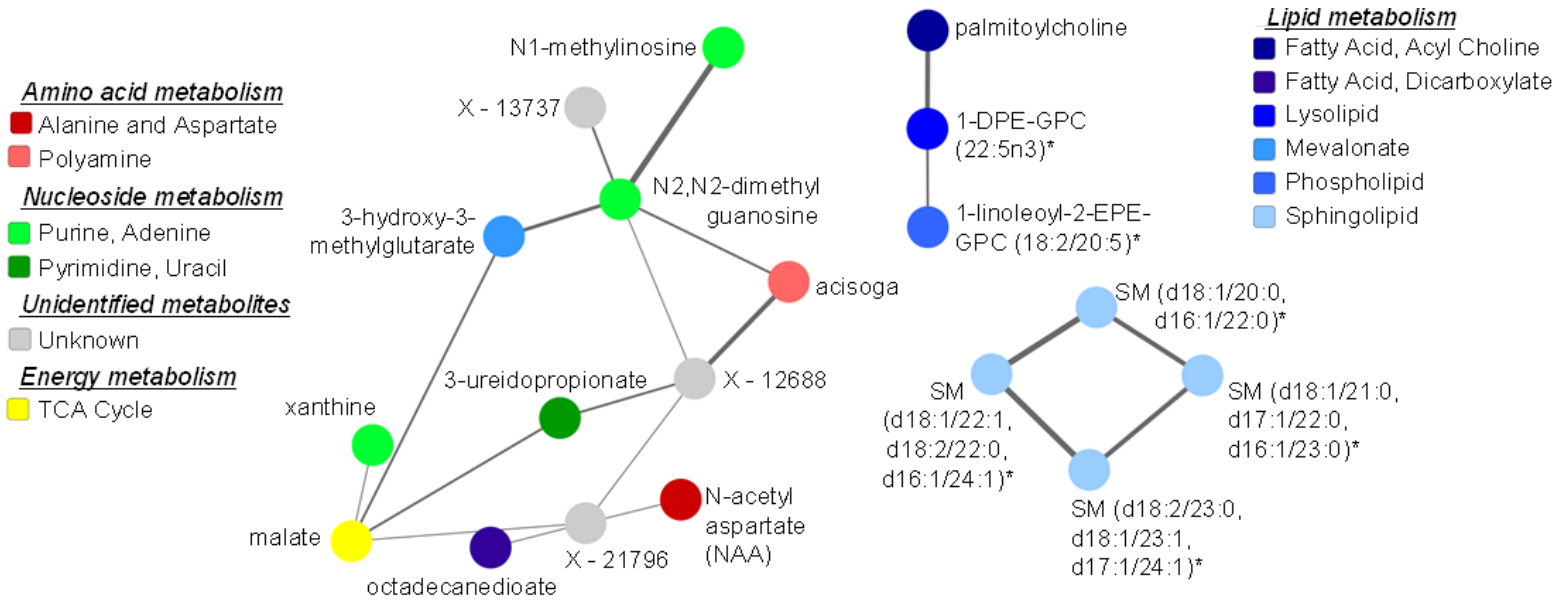
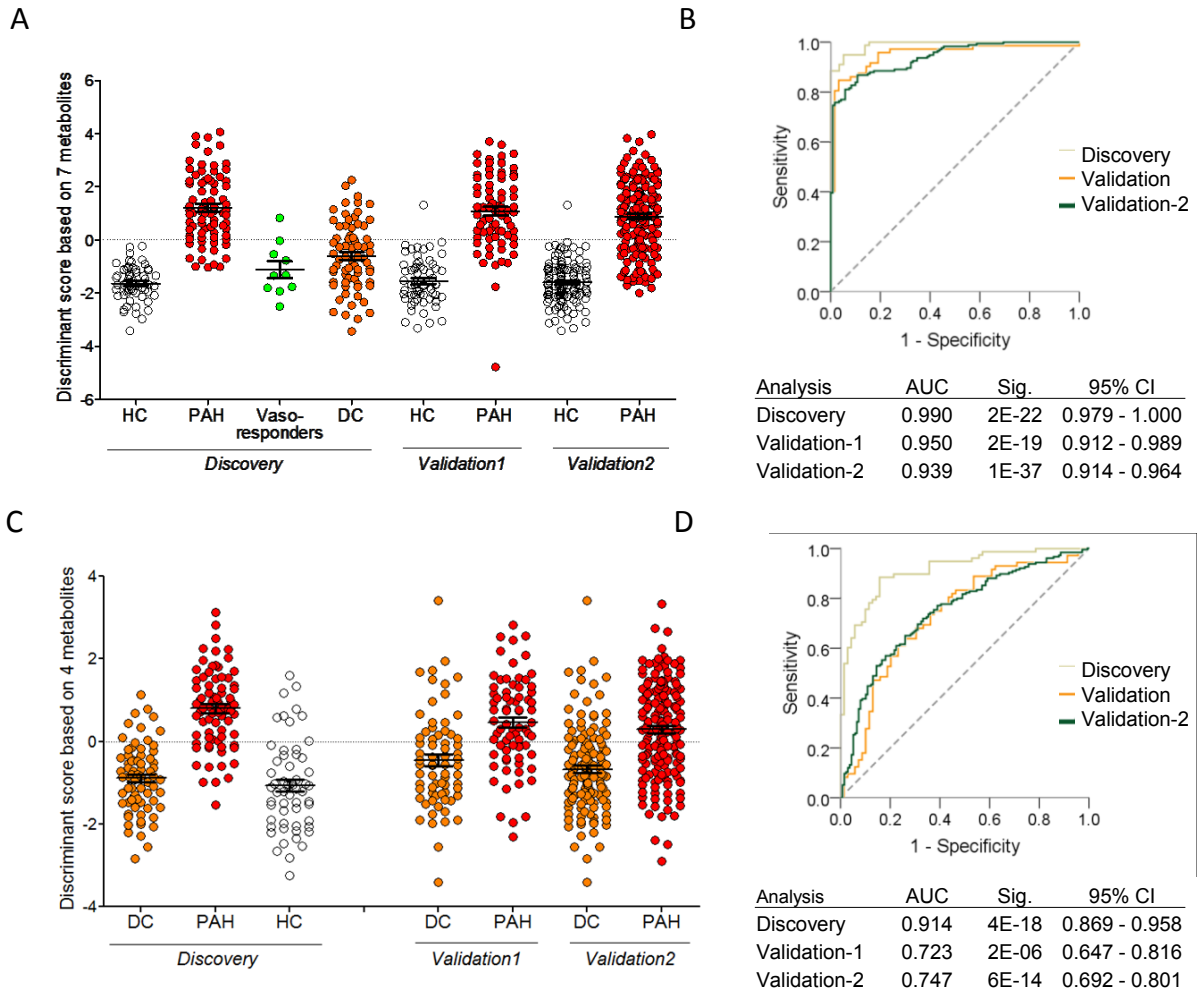


Figure 5.5 – Network analysis of metabolites which discriminate PAH and control subjects. Network analysis of 20 metabolites found to significantly distinguish PAH and both healthy and disease controls, independent of potential confounders, based on second order correlations. Line thickness indicates strength of correlations (all p<0.0001). *probable metabolite identity, but unconfirmed (see methods). EPE, eicosapentaenoyl; DHE, docosahexaenoyl; DPE, docosapentaenoyl; DHEA-S, dehydroisoandrosterone sulphate; GPC, glycerophosphocholine; SM, sphingomyelin.

5.3.2 Discriminant analyses models to assess performance of best discriminating peaks

To identify a minimal set of metabolites which could in combination best distinguish PAH patients, I performed logistic regression analysis. We found 7/53 metabolites – DHEA-S, methionine sulfone, N1-methylinosine, oleoylcarnitine, palmitoylcholine, sphingomyelin (d18:1/20:0, d16:1/22:0)* and X-24513 – independently distinguished PAH (aged 19-70) and healthy subjects in the discovery analysis, with 90% accuracy in an orthogonal partial least squares discriminant analysis (OPLS-DA, R^2=0.64, Q^2=0.61). This model classified healthy and PAH subjects in the two validation analyses with 89% and 84% accuracy, respectively. In addition, 90% (9/10) of PAH vasoresponders in the discovery cohort had metabolite levels typical of healthy controls (Figure 5.6A-B).

Out of the 20 'PAH-specific' metabolites, four – N-acetylaspartate, octadecanedioate, palmitoylcholine and X-13737 – distinguished PAH patients and disease controls with 83% accuracy in the discovery analysis (R^2=0.49, Q^2=0.47). This model classified disease controls and PAH subjects in the two validation analyses with 69% and 67% accuracy, respectively (Figure 5.6C-D).



Analysis	AUC	Sig.	95% CI
Discovery	0.990	2E-22	0.979 - 1.000
Validation-1	0.950	2E-19	0.912 - 0.989
Validation-2	0.939	1E-37	0.914 - 0.964

Analysis	AUC	Sig.	95% CI
Discovery	0.914	4E-18	0.869 - 0.958
Validation-1	0.723	2E-06	0.647 - 0.816
Validation-2	0.747	6E-14	0.692 - 0.801

Figure 5.6 - Discriminant analysis models based on low numbers of metabolites distinguish PAH patients from controls. (**A&C**) Dot-plots showing individual subjects' model scores in healthy controls (HC), PAH patients, vasoresponders and disease controls (DC) in discovery and validation analyses. Bar represents mean and standard error of mean. Metabolites were selected by logistic regression of PAH-HC **(A)** and PAH-DC **(C)** comparisons, respectively. (**B&D**) ROC curves showing performance of models in distinguishing PAH and HC **(B)** and DC **(D)** subjects.

5.3.3 Survival analysis of plasma peaks of interest in PAH

I hypothesised that metabolites most closely related to the disease pathobiology would be associated with clinical outcomes. To identify metabolites associated with disease progression and mortality, we performed survival analyses. 28/116 and 25/75 patients died in the discovery and first validation PAH groups, with a median follow-up of 3.2±1.6 and 2.4±4.0 years, respectively. The length of patient follow-up in the second validation cohort was insufficient to permit analysis. Of the 686 metabolites quantified in over 95% of subjects, 640 met the proportional hazards assumptions of Cox regression analysis, and 62 of these were prognostic after accounting for creatinine and diuretic use in both analyses (Appendix Table 5.2). ROC analysis at 3 years of follow-up confirmed these metabolites were prognostic and identified optimal cut-offs (Figure 5.7, $p<0.05$). 6 cases underwent transplantation (3 in the discovery cohort and 3 in the first validation cohort). In a sub-analysis, where these patients were excluded, 55/62 metabolites remained prognostic in both the discovery and validation cohorts ($p<0.05$).

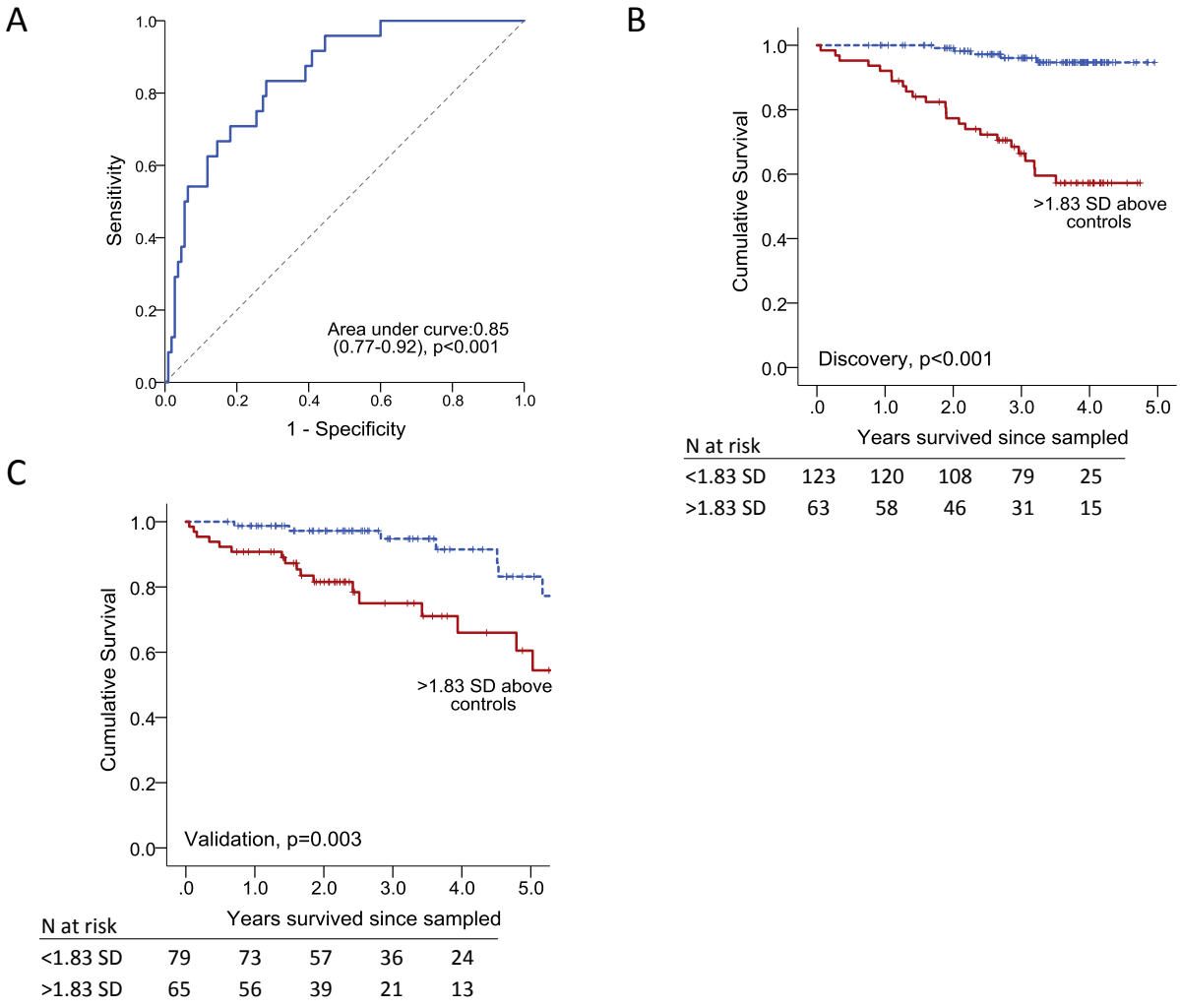
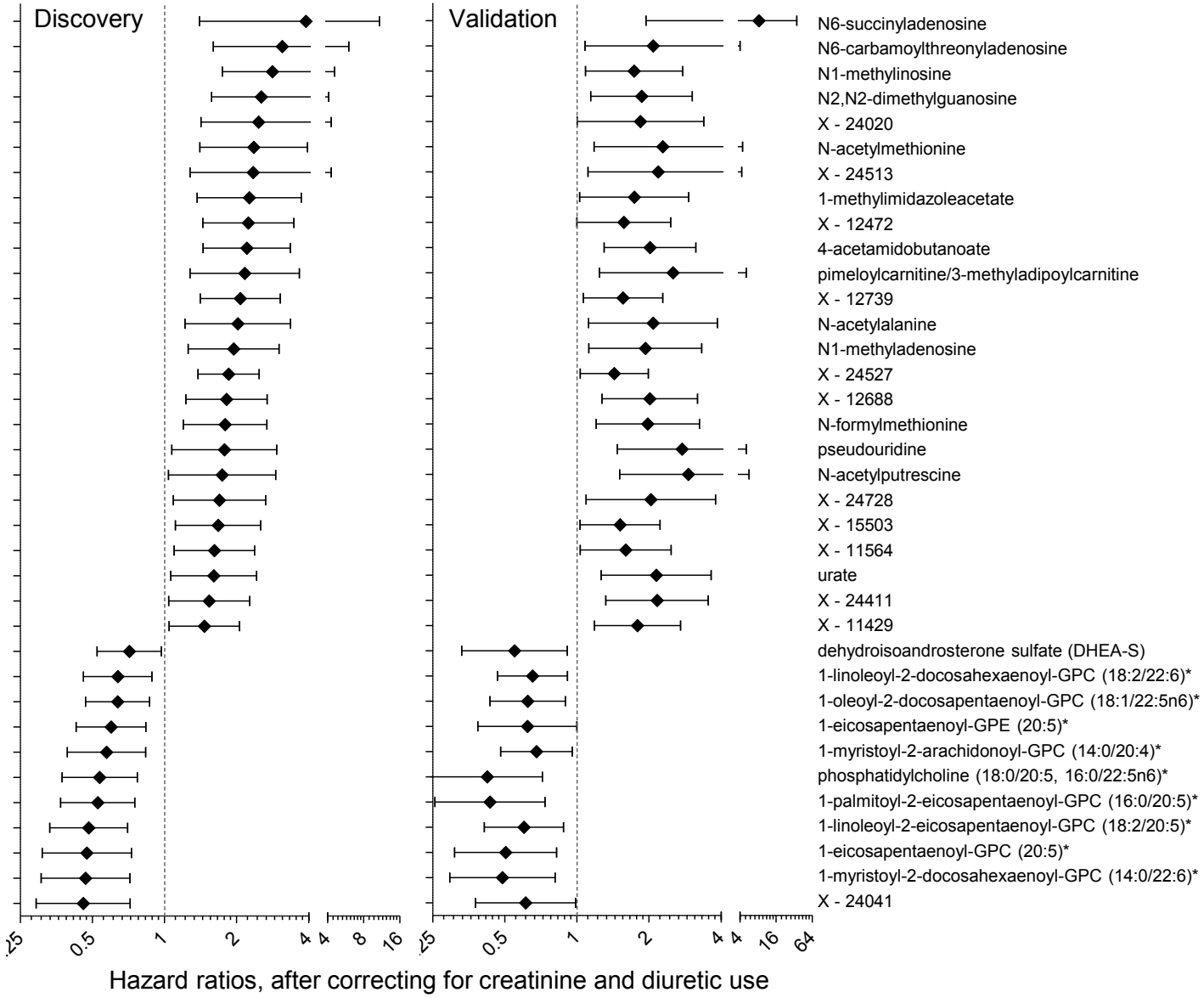


Figure 5.7 – Survival analysis of PAH patients. (**A**) Receiver operating characteristic (ROC) curve for N2,N2-dimethylguanosine in the discovery cohort at 3 years of follow-up. The optimal cut-off for high/low risk levels of N2,N2-dimethylguanosine was derived from this for **B&C.** Kaplan Meier survival estimates in PAH patients in the discovery (**B**) and first validation (**C**) cohorts. SD, standard deviation.

To identify metabolites that report on novel pathways independent of current prognostic estimates, I compared the 62 prognostic metabolites with three markers previously found to best predict survival in our patients – namely, NT-proBNP, 6MWD and RDW. 36/62 of the metabolites were independent of these measures ($p<0.05$, Figure 5.8A, Appendix Table 5.2) and network analysis indicated two main clusters with 'hub' metabolites including again, among others, N2,N2-dimethylguanosine (Figure 5.8B).

A


Discovery
Validation
N6-succinyladenosine
N6-carbamoylthreonyladenosine
N1-methylinosine
N2,N2-dimethylguanosine
X - 24020
N-acetylmethionine
X - 24513
1-methylimidazoleacetate
X - 12472
4-acetamidobutanoate
pimeloylcarnitine/3-methyladipoylcarnitine
X - 12739
N-acetylalanine
N1-methyladenosine
X - 24527
X - 12688
N-formylmethionine
pseudouridine
N-acetylputrescine
X - 24728
X - 15503
X - 11564
urate
X - 24411
X - 11429
dehydroisoandrosterone sulfate (DHEA-S)
1-linoleoyl-2-docosahexaenoyl-GPC (18:2/22:6)*
1-oleoyl-2-docosapentaenoyl-GPC (18:1/22:5n6)*
1-eicosapentaenoyl-GPE (20:5)*
1-myristoyl-2-arachidonoyl-GPC (14:0/20:4)*
phosphatidylcholine (18:0/20:5, 16:0/22:5n6)*
1-palmitoyl-2-eicosapentaenoyl-GPC (16:0/20:5)*
1-linoleoyl-2-eicosapentaenoyl-GPC (18:2/20:5)*
1-eicosapentaenoyl-GPC (20:5)*
1-myristoyl-2-docosahexaenoyl-GPC (14:0/22:6)*
X - 24041
.25
0.5
1
2
4
4
8
16
.25
0.5
1
2
4
4
16
64
Hazard ratios, after correcting for creatinine and diuretic use

B

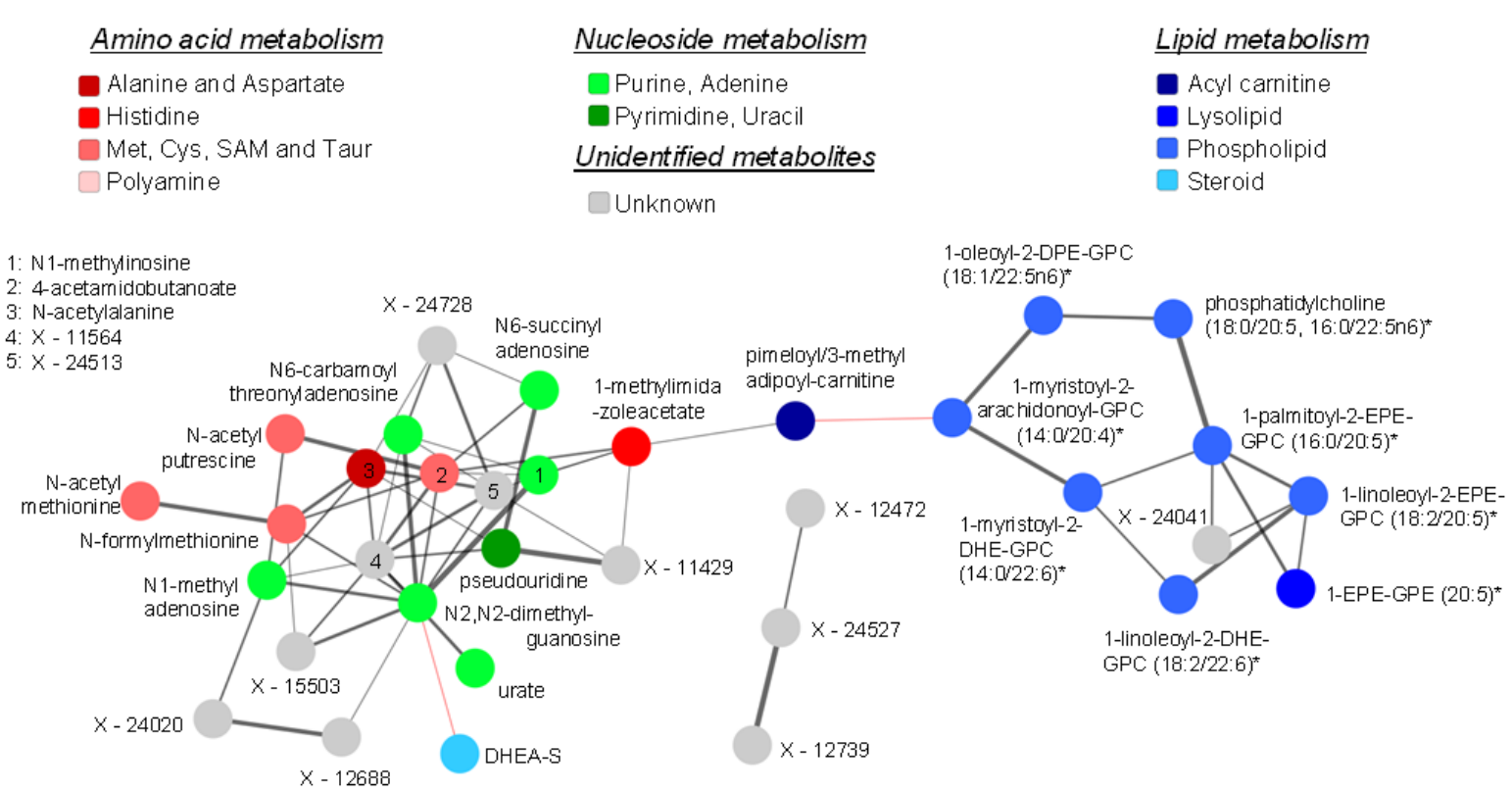


Figure 5.8 - Prognostic metabolites independent of established risk factors. (A) Hazard ratios after correcting for creatinine and diuretic use of 36 metabolites which were prognostic in PAH patients independent of red cell distribution width, N-terminal brain natriuretic peptide and six minute walk distance. Hazard ratios indicate the risk of a change in each metabolite of 1 standard deviation, for ease of comparison. **(B)** Network analysis of the same 36 metabolites based on second order correlations. Line thickness indicates strength of correlations (all $p<0.0001$). Red lines indicate negative correlations. *probable metabolite identity, but unconfirmed (see methods). EPE, eicosapentaenoyl; DHE, docosahexaenoyl; DPE, docosapentaenoyl; DHEA-S, dehydroisoandrosterone sulphate; GPC, glycerophosphocholine; GPE, glycerophosphoethanolamine.

5.3.4 Enrichment and clustering of metabolites of interest

The above analyses identified and validated, after controlling for confounders, a total of 100 metabolites that were either discriminating or prognostic in PAH, representing twenty five metabolic pathways. Six pathways in particular were enriched with metabolites of interest, including fatty acid (acylcarnitines), polyamine and nucleoside metabolism (Table 5.3, $p<0.05$). Sixteen of these metabolites both discriminated PAH and were prognostic; these, along with the peaks selected by logistic regression modelling to best distinguish PAH and healthy subjects, clustered into defined metabolic pathways (Figure 5.9). Four metabolites - DHEA-S, N1-methylinosine, sphingomyelin (d18:1/20:0, d16:1/22:0)* and X – 24527 – overlapped and were part of the logistic regression model, and discriminating and prognostic metabolites (Figure 5.9).

Pathway	Result	Metabolite	HC v PAH	Prognosis
Fatty Acid Metabolism(Acyl Carnitine)	4.5E-05	3-hydroxybutyrylcarnitine (1)	***6E-05***	0.3499
		pimeloylcarnitine/3-methyladipoylcarnitine	NA	***0.0006***
		suberoylcarnitine	***0.0071***	***0.0044***
		3-hydroxybutyrylcarnitine (2)	***0.0047***	***0.0046***
		palmitoleoylcarnitine*	***0.0085***	0.3042
		adipoylcarnitine	***0.0464***	***0.0106***
		acetylcarnitine	***0.0118***	0.141
		myristoleoylcarnitine*	***0.0165***	0.6142
		oleoylcarnitine	***0.0176***	0.0598
		myristoylcarnitine	***0.0412***	0.2631
		palmitoylcarnitine	0.0604	0.1959
		linoleoylcarnitine*	NA	0.0615
		hexanoylcarnitine	NA	0.5981
		stearoylcarnitine	NA	0.6611
		octanoylcarnitine	NA	0.8074
		laurylcarnitine	NA	0.8641
		decanoylcarnitine	NA	0.912
		cis-4-decenoyl carnitine	NA	0.9541
Polyamine Metabolism	0.01079	N-acetylputrescine	0.5825	***2E-05***
		4-acetamidobutanoate	0.8618	***3E-05***
		acisoga	***0.0002***	***0.0003***
		5-methylthioadenosine (MTA)	NA	***0.0433***
Alanine and Aspartate Metabolism	0.02412	N-acetylaspartate (NAA)	***0.0002***	0.2634
		asparagine	***0.0009***	0.9422
		N-acetylalanine	0.9901	***0.009***
		alanine	NA	0.6529
		aspartate	NA	0.9677
Purine Metabolism, (Hypo)Xanthine/Inosine containing	0.04317	xanthine	***2E-07***	0.438
		urate	NA	***0.0004***
		N1-methylinosine	***0.0008***	***0.0144***
		AICA ribonucleotide	NA	***0.0066***
		allantoin	NA	0.0934
		hypoxanthine	NA	0.6652
Purine Metabolism, Adenine containing	0.04317	N6-carbamoylthreonyladenosine	0.1735	***7E-05***
		N6-succinyladenosine	0.1452	***0.0005***
		N1-methyladenosine	0.8632	***0.0006***
		adenine	NA	0.4835
		adenosine	NA	0.5677
		adenosine 5'-monophosphate (AMP)	NA	0.5988
Pyrimidine Metabolism, Uracil containing	0.04317	pseudouridine	0.1506	***6E-05***
		N-acetyl-beta-alanine	NA	***0.0002***
		3-ureidopropionate	***0.0175***	***0.0024***
		uridine	NA	0.2684
		5-methyluridine (ribothymidine)	NA	0.5196
		beta-alanine	NA	0.8665

Table 5.3 - Pathway enrichment analysis results. Pathways analysed and enrichment p-values are given, as well as metabolites within each pathway and significance values from tests used to select metabolites considered to be disease-associated. HC v PAH, significance of PAH on metabolite levels after controlling for potential confounders by linear regression; Prognosis, weakest significance of metabolite association with survival by Cox analysis in discovery or validation cohorts. Values in bold have a p value <0.05. *probable metabolite identity, but unconfirmed (see methods).

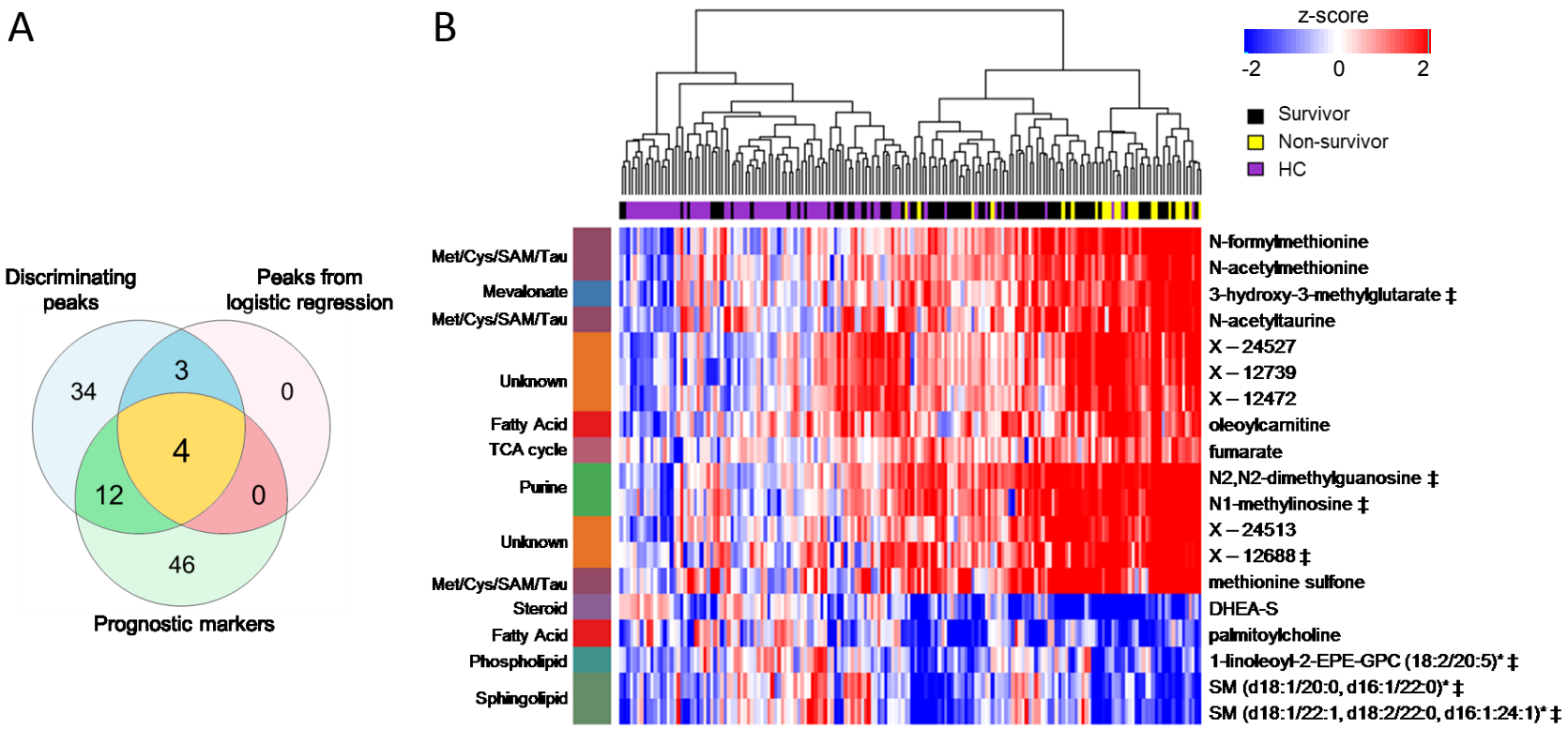


Figure 5.9 – Hierarchical clustering of 19 discriminating and prognostic metabolites in PAH patients. (**A**) Venn diagram shows overlap between metabolites that discriminate PAH from healthy controls in all 3 cohorts, from logistic regression between PAH and healthy controls and prognostic metabolites in the discovery and first validation cohorts. (**B**) Clustering of the 19 overlapping metabolites from A. is shown between healthy controls (n=58), PAH survivors (n=110, alive at 3 years post-sample) and non-survivors (n=24) in the discovery analysis. Red indicates metabolite levels that are increased (and blue levels that are decreased) in PAH versus controls. *probable metabolite identity, but unconfirmed (see methods), ‡metabolites also distinguish PAH from disease controls. GPC, glycerophosphocholine; EPE, eicosapentaenoyl; SM, sphingomyelin; DHEA-S, dehydroisoandrosterone sulphate.

5.3.5 Analysis of serial samples

Changes in metabolite levels in individuals over time may indicate pathways that report clinical improvement or whose correction itself leads to improved outcomes. I analysed serial samples from 86 patients who were followed up for a minimum of 1 year (median 1.50, interquartile range 1.33-2.95 years) after the second sample. Twenty nine patients died during follow-up. Changes in metabolite levels between the two samples (median time between samples 1.75, IQR 1.07-2.58 years) were compared between 'survivors' and 'non-survivors'.

Changes in 27/100 metabolites were significantly different between survivors and non-survivors ($p<0.05$), including several modified amino acids and nucleosides. ROC analysis confirmed these associations (Table 5.4) and identified prognostic cut-offs (Figure 5.10).

Metabolites	AUC	Sig.	95% CI
3-hydroxy-3-methylglutarate	0.75	0.0002	0.63 - 0.86
3-hydroxybutyrylcarnitine (2)	0.67	0.01096	0.54 - 0.79
4-acetamidobutanoate	0.67	0.0084	0.56 - 0.79
acetylcarnitine	0.65	0.02803	0.52 - 0.77
C-glycosyltryptophan	0.66	0.01821	0.53 - 0.78
erythronate*	0.65	0.02008	0.54 - 0.77
hexadecanedioate	0.65	0.02321	0.52 - 0.78
malate	0.69	0.00332	0.58 - 0.81
N-acetylalanine	0.67	0.01013	0.55 - 0.79
N-acetylglucosamine/N-acetylgalactosamine	0.71	0.0017	0.6 - 0.82
N-acetylmethionine	0.76	6.9E-05	0.66 - 0.87
N-acetylneuraminate	0.73	0.00049	0.62 - 0.84
N-acetylputrescine	0.69	0.00407	0.57 - 0.81
N-acetylserine	0.65	0.02008	0.53 - 0.77
N-acetyltaurine	0.68	0.0064	0.56 - 0.8
N-formylmethionine	0.67	0.00863	0.56 - 0.79
N1-methyladenosine	0.69	0.00362	0.57 - 0.81
N2,N2-dimethylguanosine	0.69	0.0047	0.57 - 0.8
X - 11564	0.65	0.0216	0.53 - 0.77
X - 12026	0.64	0.03369	0.52 - 0.76
X - 12688	0.68	0.00526	0.57 - 0.8
X - 13737	0.66	0.01454	0.54 - 0.78
X - 15503	0.68	0.00589	0.56 - 0.8
X - 24020	0.67	0.01155	0.55 - 0.78
X - 24527	0.67	0.00863	0.55 - 0.79
X - 12127	0.65	0.02434	0.53 - 0.77
X - 24766	0.67	0.01068	0.55 - 0.78
5,6-dihydrothymine	0.67	0.0104	0.55 - 0.79
X - 12472	0.65	0.02321	0.53 - 0.77
X - 21796	0.7	0.00303	0.59 - 0.8
fumarate	0.67	0.01013	0.55 - 0.79
orotidine	0.7	0.00322	0.58 - 0.81
X - 12739	0.68	0.00775	0.56 - 0.79

Table 5.4 – ROC (receiver operating characteristic) analysis of serial metabolite measurements. Area under the curve values for the association between metabolite level changes (i.e. sample 1 subtracted from sample 2) and survival during follow-up are shown for significantly associated metabolites. *probable metabolite identity, but unconfirmed (see methods).

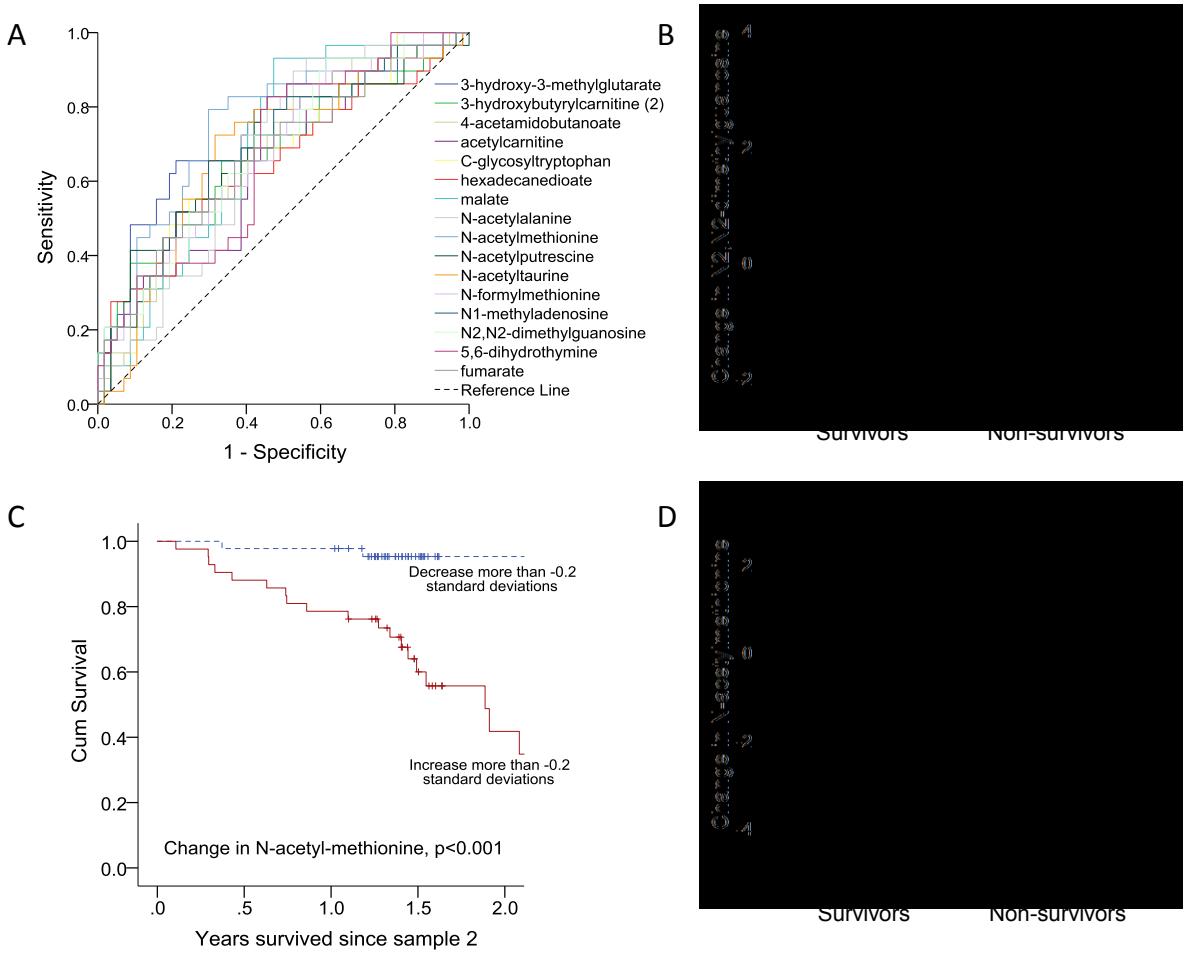


Figure 5.10 - Analysis of serial samples. (**A**) ROC analysis of changes in metabolite levels and survival during follow-up. (**B&D**) Changes in individual patient metabolite levels, grouped by survival during follow-up. (**C**) Kaplan-Meier analysis illustrating survival over time in PAH patients divided into groups according to the changes in N-acetyl-methionine levels between serial samples.

5.3.6 Association of elevated modified nucleosides with elevated plasma angiogenin

Modified nucleosides can be released into the circulation during stress following cleavage of tRNAs by the ribonuclease angiogenin (Kirchner and Ignatova 2015). To determine whether this mechanism was relevant to PAH, I measured plasma angiogenin in a representative subset of age- and sex-matched healthy controls and PAH patients from the discovery analysis (Table 5.5). Angiogenin levels were elevated in plasma from PAH patients and correlated with N2,N2-dimethylguanosine levels (Rho:0.49, p<0.001, Figure 5.11).

	Healthy controls (n=30)	PAH (19-70) (n=69)	PAH (>70) (n=8)
Female:Male ratio	2.0	2.3	3.0
Age	48.5 +/- 13.1	48.3 +/- 14.1	75.6 +/- 8.1
Angiogenin conc., ng/ml	360 +/- 110.3	479.7 +/- 176.6	554.9 +/- 234.2
N2,N2-dimethylguanosine	-0.1 +/- 1	1.6 +/- 1.2	2.7 +/- 1.4

Table 5.5 - Demographics and circulating factor levels in subjects used for angiogenin study. Mean +/- standard deviation is shown for continuous variables.

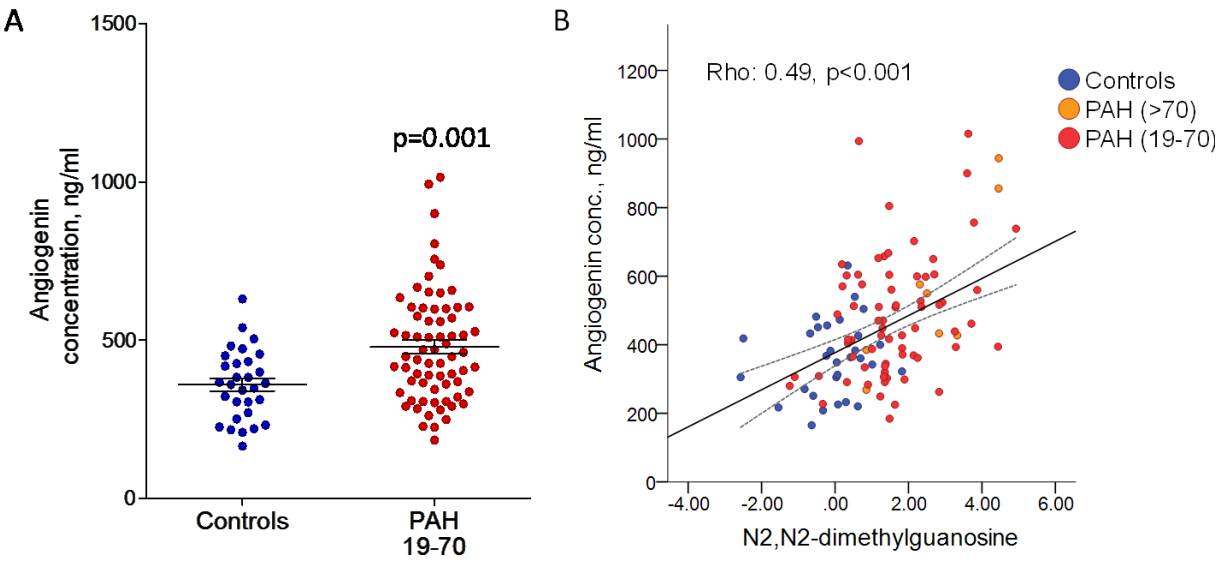


Figure 5.11 - Circulating angiogenin levels. (**A**) Plasma angiogenin levels determined by ELISA in healthy controls and PAH patients. Bar represents mean and standard error of the mean. (**B**) Scatter-plot of plasma N2,N2-dimethylguanosine versus plasma angiogenin in controls and PAH patients. Statistics shown are from Spearman's Rank test.

5.3.7 Measurement of acetyl-coA and oxaloacetate with targeted fluorometric assays

Key intermediates of the TCA cycle, acetyl-coA and oxaloacetate were not measured on the Metabolon platform. To determine whether these were relevant to PAH, and related to acylcarnitines, I measured plasma acetyl-coA and oxaloacetate in a representative subset of healthy controls and PAH patients with high and low levels of oleoylcarnitine, a representative acylcarnitine (Table 5.6). Levels of acetyl-CoA were below the limit of detection in 16/36 samples and not significantly different between controls and PAH patients ($p>0.05$, Table 5.6). Oxaloacetate levels did not correlate with oleoylcarnitine (Rho=0.015) and were not significantly different between healthy controls and PAH patients with high and low acylcarnitine levels ($p>0.05$, Table 5.7, Figure 5.12).

	Healthy controls (n=9)	PAH (Low AC) (n=9)	PAH (High AC) (n=18)
Female:Male ratio	3.5	3.5	3
Age	41.7 +/- 11.3	44.1 +/- 14.4	53.6 +/- 15.5
Oleoylcarnitine	-1.14 +/- 1.4	-0.32 +/- 0.2	2.44 +/- 0.5
acetyl-CoA (uM)	0.009	0.003	0.003

Table 5.6 - Demographics and circulating factor levels in subjects used for acetyl-coA study. Mean +/- standard deviation is shown for continuous variables. PAH patients are divided based on low and high acylcarnitine (AC) levels.

	Healthy controls (n=18)	PAH (Low AC) (n=16)	PAH (High AC) (n=33)
Female:Male ratio	2	2.2	1.2
Age	41.7 +/- 11.9	41.2 +/- 15.0	53.7 +/- 13.6
Oleoylcarnitine	-0.51 +/- 1.3	-0.55 +/- 0.5	2.13 +/- 0.6
oxaloacetate (uM)	19.5 +/- 11.3	15.8 +/- 9.5	16.7 +/- 9.2

Table 5.7 - Demographics and circulating factor levels in subjects used for oxaloacetate study. Mean +/- standard deviation is shown for continuous variables. PAH patients are divided based on low and high acylcarnitine (AC) levels.



Figure 5.12 – Plasma oxaloacetate levels. Levels of oxaloacetate are shown between healthy controls (HC) and PAH patients with low and high levels of an acylcarnitine (AC) – oleoylcarnitine. Bar represents mean and standard error of the mean.

5.3.8 Immunohistochemistry for antibody targets 1-methyladenosine, pseudouridine and angiogenin

Preliminary immunohistochemistry studies were conducted on sections of lung tissue obtained at the transplantation of 3 PAH patients. For each antibody three dilutions were tested and an optimum dilution of 1:10000, 1:1000 and 1:400 chosen for anti-1-methyladenosine, anti-pseudouridine and anti-angiogenin antibodies respectively. 1-methyladenosine showed localised staining of the endothelium in proximal pulmonary arteries (compared with the negative underlying smooth muscle), distal branches, the vaso vasorum, lymphatic vessels and macrophages (Figure 5.13). Pseudouridine immunostaining was evident in the endothelium of pulmonary arteries and microvasculature, but was also prominent in the bronchial and bronchiolar epithelium, and weaker immunostaining was observed in both vascular and airway smooth muscle (Figure 5.14). No specific staining seen with the angiogenin antibodies, although I lacked a positive control such as sections of oesophageal or renal tissue (Masuda, Nishihira et al. 1993, Mishima, Inoue et al. 2014).

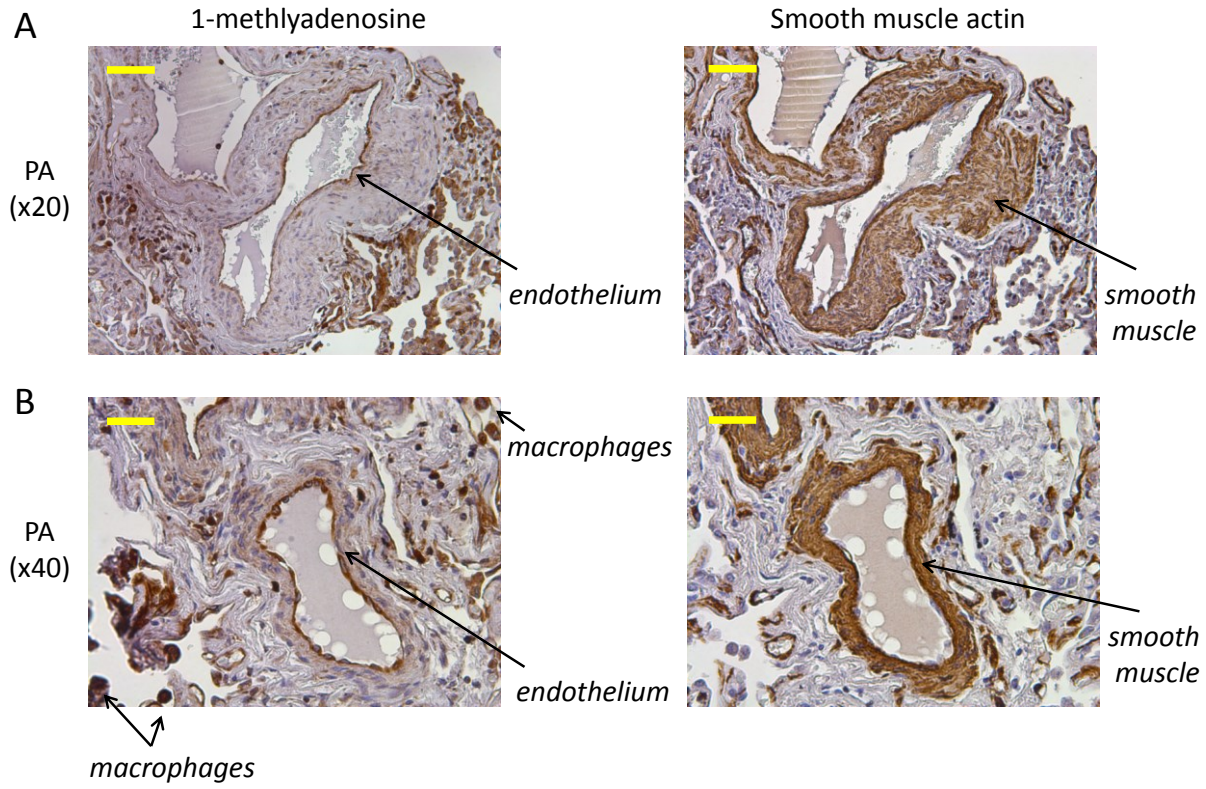


Figure 5.13 – Immunostaining for 1-methyladenosine in lung tissue from a PAH patient. Staining for 1-methyladenosine (1:10000 dilution) and smooth muscle actin in lung tissue from a PAH patient is shown in the pulmonary artery (PA). The yellow bar represents 500µm in **(A)** and 250µM in **(B)** and the magnification is also shown.

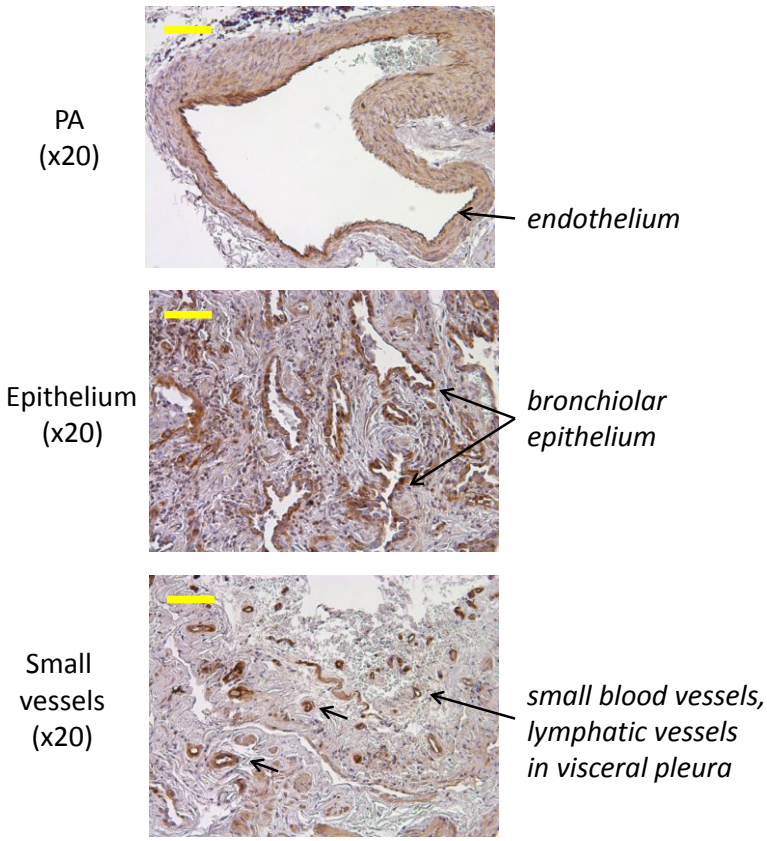


Figure 5.14 – Immunostaining for pseudouridine in lung tissue from a PAH patient. Staining for pseudouridine (1:1000 dilution) is localised in the endothelium amd smooth muscle of a pulmonary artery (PA), bronchiolar epithelium and small blood vessels or lympatic vessels in the pleura. The yellow bar represents 500µm and the magnification is also shown.

5.4 Discussion

This study represents a comprehensive analysis of circulating metabolites with known identities in patients with PAH. Results from this study identify novel metabolic dysregulation in PAH such as increased modified nucleosides, and validate findings from NMR and unbiased UPLC-MS approaches indicating changes in energy metabolism, increased circulating acylcarnitines, and decreased sphingomyelins and phosphocholines in patients with IPAH and HPAH.

Differences in metabolites in PAH were identified and validated in comparisons to both healthy and disease controls, and associated with outcomes in PAH, strengthening the evidence that the pathways identified could be important modifiers of disease progression. Changes in the levels of metabolites over time were associated with survival in a direction that suggests that correction of these disturbances is linked to improved outcomes. In agreement with this, patients defined as vasoresponders, who have excellent outcomes on calcium channel blocker therapies, demonstrated metabolic profiles more similar to healthy controls than other patients. Metabolic profiles seen in incident cases were similar to those with established PAH, emphasising that metabolic dysregulation is not corrected in the majority of cases by current therapy.

Patients who were *BMPR2* mutation carriers had similar metabolic profiles to non-carriers. Although they had more severe haemodynamic measures with increased mPAP and PVR at baseline, their survival from the diagnosis to time of sampling was similar and may be reflected by the similar metabolite profiles seen between carriers and non-carriers.

Energy metabolism

Significant alterations were observed in several pathways related to cellular energy production, with accumulation of multiple acylcarnitines, glutamate and TCA cycle intermediates. As well as validating the finding of increased myristoylcarnitine and palmitoylcarnitine in PAH, other acylcarnitines such as acetylcarnitine, oleoylcarnitine and 3-hydroxybutyrylcarnitine were notably increased in PAH. The accumulation in PAH patients may represent a failed attempt to increase utility of fatty acids as an energy source, perhaps reflecting the inability of fatty acid beta-oxidation to keep pace with the demands of the overburdened right ventricle.

Glutamine levels previously measured by NMR spectroscopy were decreased in PAH patients and levels measured using this platform showed decreased glutamine levels in both validation cohorts ($p<0.05$) but not the discovery cohort. Levels of glutamate however, were significantly increased in PAH patients in all 3 cohorts ($p<7.3e-5$) independent of confounding factors. Glutaminolysis is an

alternative energy production pathway to glucose oxidation, with the product glutamate entering the TCA cycle as alpha-ketoglutarate. Inhibition of glutaminolysis and restoration of glucose oxidation has beneficial effects in rat models of right ventricular hypertrophy (Piao, Fang et al. 2013). Increased circulating glutamate levels have previously been seen in cancer patients (Koochekpour, Majumdar et al. 2012), however, anti-glutaminolysis therapeutic targets have demonstrated toxic side effects (Tennant, Duran et al. 2010). Glutamine levels may be depleted in PAH in an attempt to increase glutamate production and upregulate glutaminolysis to enter the TCA cycle.

Increased levels of several TCA cycle intermediates (malate, alpha-ketoglutarate and fumarate) were observed in PAH patients, and increased fumarate levels relate to worse survival in PAH. Previously increased levels of succinate and citrate have been observed from the lung tissue of PAH patients (Zhao, Peng et al. 2014) and levels of malate, succinate, isocitrate and alpha-ketoglutarate correlate to pulmonary haemodynamics in PAH (Lewis, Ngo et al. 2016). Citrate levels measured by NMR spectroscopy in our previous experiment showed significantly increased levels in one cohort of PAH patients. Although citrate levels measured by this platform were increased in all 3 cohorts ($p<0.05$), significance levels only met Bonferroni correction in the discovery cohort ($p<7.3e-5$). Succinate levels were not significantly different in PAH patients relative to controls, and isocitrate was not measured on this platform. Levels of oxaloacetate measured by a targeted assay showed no significant difference between PAH patients and controls ($p>0.05$), however, these findings were in a small group of subjects and not validated.

The build-up of TCA intermediates and the precursors to the molecules that enter the cycle (acylcarnitines and glutamate) may indicate dysfunction of this cycle, or at least the inability to keep pace with the demands of the most active cells, such as proliferating pulmonary vascular cells. Restoration of glucose oxidation by dichloroacetate therapy is under investigation as a treatment for PAH (Piao, Fang et al. 2010), and maximising the capacity of the TCA cycle to process the acetyl-CoA produced may be a complementary therapeutic approach. Measurements of acetyl-CoA were unsuccessful using a targeted assay where a significant proportion of readings were below the limits of detection. This assay has previously been used to measure intracellular acetyl-coA (Teng, Wu et al. 2015) and concentrations of acetyl-coA in liver tissue (Le, Urasaki et al. 2014) but not circulating plasma levels, and attempts to use another more sensitive assay may be required in the future.

Modified nucleosides

Two of the most robust distinguishing and prognostic differences identified in PAH patients were increased levels of N1-methylinosine and N2,N2-dimethylguanosine. These are recognised

epigenetic, post-transcriptional modifications of transfer RNA (tRNA) (Slotkin and Nishikura 2013, Torres, Batlle et al. 2014, Kirchner and Ignatova 2015), and other tRNA modifications also found to be increased and prognostic included pseudouridine, N6-carbamoylthreonyladenosine and N1-methyladenosine. N2,N2-dimethylguanosine is found in the majority of tRNAs at position 26, upstream of the anticodon sequence at positions 34-36, and promotes the folding of tRNAs towards the classical clover-leaf structure (Steinberg and Cedergren 1995). N1-methylinosine is found 3' adjacent to the anticodon at position 37 of eukaryotic tRNAs and is formed from inosine by a specific S-adenosylmethionine-dependent methylase (Grosjean, Auxilien et al. 1996). Increased serum and urine levels of N2,N2-dimethylguanosine, as well as pseudouridine and 1-methylinosine, have been observed in multiple solid tumour malignancies (Waalkes, Gehrke et al. 1975) and may reflect the general upregulation of the translational apparatus, including tRNA turnover, in hyperproliferative cancerous cells (Anderson and Ivanov 2014). Increased circulating 1-methyladenosine has also been shown to be an early indicator of oxidative stress, cell damage and mortality in kidney disease (Mishima, Inoue et al. 2014).

Intracellular tRNA pools are dynamically regulated. For example under stress, tRNAs required for the translation of stress response proteins are preferentially expressed (Kirchner and Ignatova 2015). The altered levels of specific nucleoside modifications in PAH patients may reflect preferential expression of tRNAs that harbour them, as part of a switch towards translation of disease-related proteins. In addition, stress-induced cleavage of tRNA produces fragments that propagate the stress response and interfere with eukaryotic initiation factor (eIF)-4G and eIF4F (Kirchner and Ignatova 2015). Furthermore, eIF2α kinase-4 (also known as general control nondepressible 2, GCN2), which prevents eIF2α interacting with the initiating Met-tRNA, suppressing general protein synthesis and activating stress-inducible transcription factors, is mutated and causally implicated in some cases of pulmonary vascular disease (Eyries, Montani et al. 2014). Mutations in tRNA genes themselves have also been reported to cause pulmonary hypertension driven by mitochondrial dysfunction (Sproule, Dyme et al. 2008). These findings suggest that increased circulating modified nucleosides in PAH represent; a) a stress response that leads to increased translation of disease related proteins, b) a hyperproliferative state with an increase in overall tRNA levels and c) subsequent fragments which interfere with translation.

The initial cleavage of tRNAs is mediated by angiogenin (Kirchner and Ignatova 2015), which we showed to be elevated in the plasma of PAH patients in concert with elevated levels of modified nucleosides. Angiogenin is also up-regulated in cancer cells, mediating angiogenesis, cell proliferation and protection from apoptosis (Saikia and Hatzoglou 2015), and is increased in breath

condensates from patients with pulmonary hypertension (Seyfarth, Sack et al. 2015), indicating a possible pulmonary origin in this disease. Angioproliferative plexiform vascular lesions are characteristic of advanced PAH and the pro-angiogenic activity of angiogenin is inhibited by mutation of its ribonuclease active site (Shapiro and Vallee 1989), suggesting that elevated angiogenin and nucleoside levels may report patients developing this type of pulmonary vascular remodelling.

I sort to explore the potential pulmonary origin of increased circulating nucleosides and angiogenin in PAH patients by the immunohistochemical localization of 1-methyladenosine, pseudouridine and angiogenin in sections of explanted lung tissues. The preliminary results indicate that 1-methyladenosine and pseudouridine is present in the diseased pulmonary vasculature, as well as other regions of the lung. But further studies are required to confirm these observations and determine whether the tissue levels of these metabolites differ from that seen in healthy lung tissue.

Alterations in tRNA biology appear to be capable of driving the development of rare forms of pulmonary hypertension and are closely linked to the progression of PAH, and circulating levels of modified nucleosides may reflect increases in both pulmonary vascular cell proliferation and stress.

Steroids, polyamines and tryptophan metabolites

Circulating levels of DHEA-S and its metabolites (androsterone, epiandrosterone and androstenediol/4-androsten-3beta, 17beta-diol disulfate) were reduced in PAH patients compared to healthy controls, consistent with a recent report of reduced circulating levels of DHEA-S in a small cohort of 23 male PAH patients compared to healthy controls (Ventetuolo, Baird et al. 2015). Differences in DHEA-S between PAH and controls were independent of the more subtle effects of both gender and age (Figure 5.2), and lower DHEA-S levels were independently associated with mortality. Treatment with DHEA or DHEA-S has repeatedly been shown to prevent and reverse pulmonary hypertension in experimental rat models (Alzoubi, Toba et al. 2013), with clinical trials ongoing in COPD-associated pulmonary hypertension (Dumas de La Roque, Savineau et al. 2012).

I found increased levels of a breakdown product of N1-acetylspermidine, acisoga. Other metabolites of polyamine metabolism (4-acetamidobutanoate and N-acetylputrescine) were increased in PAH in relation to bilirubin levels and were prognostic in 2 distinct PAH cohorts, independent of established prognostic markers. Several animal models of pulmonary hypertension have demonstrated evidence of increased polyamine levels and metabolism in lung tissue (Hoet and Nemery 2000). Administration of monocrotaline to rats led to significantly increased levels of polyamines and the development of pulmonary hypertension and right ventricular hypertrophy, which could be

prevented by the administration of an inhibitor of polyamine biosynthesis (Olson, Atkinson et al. 1985), suggesting these molecules may be novel therapeutic targets.

I validated findings of elevated circulating tryptophan metabolites (Lewis, Ngo et al. 2016) with increased C-glycosyltryptophan and kynurenine in PAH patients compared to healthy controls, but changes in kynurenine were related to increased bilirubin levels. Levels of tryptophan and its other major metabolite, serotonin, were not significantly altered in our analysis.

In this study I found increased circulating modified nucleosides (N2,N2-dimethylguanosine, N1-methylinosine), TCA cycle intermediates (malate, fumarate), glutamate, fatty acid acylcarnitines and polyamine metabolites and decreased levels of steroids, sphingomyelins and phosphatidylcholines characteristic of patients with PAH (Rhodes, Ghataorhe et al. 2016). These findings validated those from experiments using NMR spectroscopy and unbiased UPLC-MS approaches, as well as identified key novel metabolic disturbances in PAH. Improvements in circulating metabolite levels are associated with a better prognosis and could be used to monitor response to PAH treatments. Targeting alterations in energy metabolism in PAH or correcting translational regulation in PAH may provide future therapeutic options in PAH.

In order to assess whether these changes are specific to PAH, or present in all PH subtypes, I set out to compare the results of the Metabolon analysis in IPAH/HPAH with plasma from patients with CTEPH, PH associated with left heart disease (PAH-LHD), and other subtypes of PAH associated with either congenital heart disease (PAH-CHD) or connective tissue disease (PAH-CTD).

Chapter 6 - Metabolic phenotyping in other sub-diagnoses of pulmonary hypertension using the Metabolon platform

6.1 Introduction

Using NMR spectroscopy, unbiased UPLC-MS and the Metabolon platform, increased circulating modified nucleosides (N2,N2-dimethylguanosine, N1-methylinosine), TCA cycle intermediates (malate, fumarate, citrate), glutamate, fatty acid acylcarnitines and polyamine metabolites, and decreased levels of steroids, sphingomyelins, HDL sub-diagnoses and phosphatidylcholines have been associated with clinical outcomes in PAH patients.

These changes distinguish PAH patients from symptomatic patients without pulmonary hypertension, however their specificity to PAH, compared to other PH sub-diagnoses has not been ascertained.

Comparisons of metabolite profiles in PAH patients with other forms of PAH such as congenital heart disease (CHD) and connective tissue disease (CTD), as well as other forms of PH such as CTEPH and left heart disease (LHD), the metabolomics of which have not previously been studied, would provide the opportunity to explore metabolic disturbances in different sub-diagnoses of PH and those specific to PAH.

6.1.1 Chronic thromboembolic pulmonary hypertension (CTEPH)

CTEPH is distinguished from PAH by the presence of chronic thromboembolic vascular obstruction, confirmed by radiological criteria with organized thrombi replacing the normal intima and occluding the lumen in elastic pulmonary arteries (Hoeper, Madani et al. 2014, Matthews and Hemnes 2016). Patients with CTEPH present with non-specific symptoms of decreased exercise tolerance and worsening dyspnoea and the pathophysiology of the disease remains unclear, but is likely multifactorial (Matthews and Hemnes 2016).

The most widely accepted theory of CTEPH is the ‘embolic hypothesis’, with single or recurrent thromboembolic events underlying disease progression (Humbert 2010). The incidence of CTEPH after acute pulmonary embolism (PE) ranges from 0.6 to 9.1% and many patients have a history of venous thromboembolism (Cannon and Pepke-Zaba 2013). Assessment of acute PE specimens from

pulmonary thrombectomy surgery show red blood cells, fibrin and inflammatory cells, whilst specimens from the pulmonary artery of CTEPH patients are more complicated (Matthews and Hemnes 2016). These sections show the presence of organised thrombi, collagen, inflammation and myofibroblasts (Blauwet, Edwards et al. 2003) and thrombotic, neointimal, atherosclerotic and re-canalised lesions (Quarck, Wynants et al. 2015).

The presence of haemostatic risk factors, such as increased factor VIII (Bonderman, Turecek et al. 2003) and plasma lipoprotein (a) levels (Ignatescu, Kostner et al. 1998) create a hypercoagulable state for the formation of in situ thrombus. Fibrin in CTEPH patients has also been shown to be resistant to plasmin mediated lysis (Morris, Marsh et al. 2006). The ability of fibrin to resist lysis has also been demonstrated in patients with PAH and previous PE (Miniati, Fiorillo et al. 2010). Genetic variants associated with prothrombotic conditions occur with the same frequency in CTEPH and PE and genetic variants of fibrinogen have been identified in patients with CTEPH (Morris 2013).

In situ thrombosis could also be driven by local factors such as endothelial dysfunction and arteriopathy, with small vessel remodelling occurring in regions of the lung obstructed and non-obstructed by thrombus. These structural changes are indistinguishable from those found in PAH (Galie and Kim 2006) and include medial hypertrophy, intimal proliferation, adventitial thickening, perivascular inflammatory infiltration and formation of complex plexiform lesions (Moser and Bloor 1993, Galie and Kim 2006). CTEPH is also associated with other risk factors, including previous splenectomy, ventriculoatrial shunt, chronic inflammatory disease (Kim and Lang 2012), autoimmune conditions (systemic lupus erythrematosus, antiphospholipid antibody syndrome, inflammatory bowel disease), chronic venous ulcers and malignancy (Figure 6.1) (Matthews and Hemnes 2016).

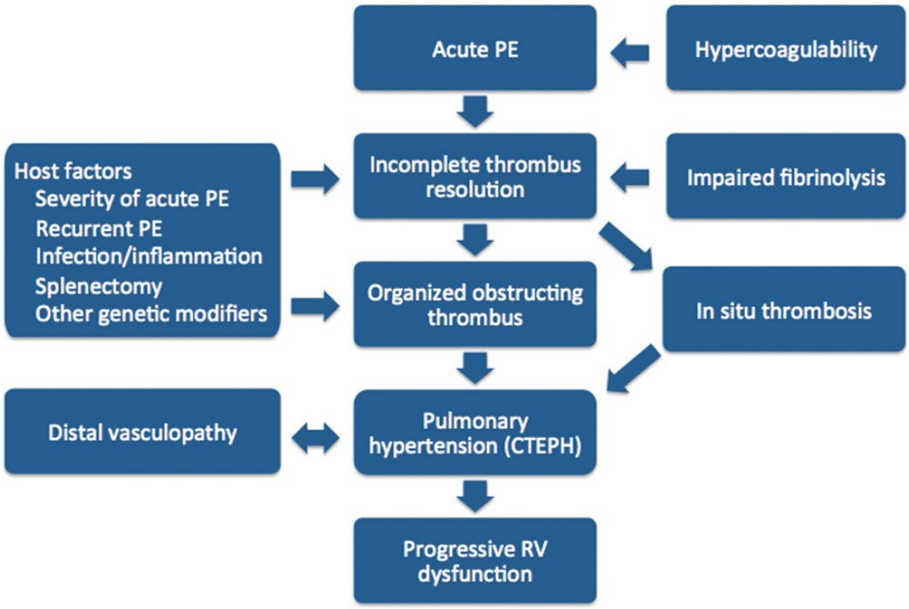


Figure 6.1 – Factors influencing the pathogenesis of CTEPH. Figure from (Matthews and Hemnes 2016). Factors influencing the development of CTEPH and subsequent right ventricular (RV) dysfunction are shown. These include pro-thrombotic factors and the presence of pulmonary embolism (PE).

CTEPH is a potentially curable form of PH and pulmonary endarterectomy (PEA) is the treatment of choice for surgically accessible chronic thromboembolic disease (Rahnavardi, Yan et al. 2011). However, up to one third of patients develop persistent pulmonary hypertension after PEA surgery – although this may be due to co-existing distal and small vessel disease, the reason for unsuccessful outcomes following PEA surgery in some patients is not fully understood (Mayer, Jenkins et al. 2011). In 17 CTEPH cases undergoing PEA surgery, pathological features of pulmonary arteriopathy (medial hypertrophy, intimal thickening but no plexiform lesions) and pulmonary venopathy were observed, and subjects with increased pulmonary arterial obstruction had higher mPAP and PVR following PEA which may explain persistent PH in some subjects following surgery (Jujo, Sakao et al. 2015). In addition, up to 40% of patients at evaluation are not deemed suitable for PEA surgery, often due to either the distribution of disease burden or significant co-morbidities (Kim and Lang 2012). In those who are suitable for surgery, referrals are recommended without delay with no evidence for bridging medical therapy (Kim, Delcroix et al. 2013).

All patients with a diagnosis of CTEPH are anti-coagulated lifelong to treat in situ pulmonary artery thrombosis and prevent recurrence of venous thromboembolic disease (Hoeper, Barbera et al. 2009). Patients with inoperable CTEPH or persistent PH post-PEA can be treated with Riociguat, a

stimulator of soluble guanylate cyclase, which has been shown to improve exercise capacity and pulmonary vascular resistance in this patient group (Ghofrani, D'Armini et al. 2013). Evidence for agents used in PAH such as prostanoids, endothelin receptor antagonists and phosphodiesterase 5 inhibitors is growing in the CTEPH group, but the outcomes remain mixed (Kim, Delcroix et al. 2013). If medical therapy is ineffective, other options include lung transplantation (Dartevelle, Fadel et al. 2004) or percutaneous transluminal pulmonary angioplasty (Sugimura, Fukumoto et al. 2012).

It is known that the reduction in RV afterload post-PEA leads to an improvement in RV dimensions and function (Surie, Bouma et al. 2011) and examination of patients before and after surgery offers an opportunity to study the response of the RV to changes in afterload. There is great scope to aid the diagnosis of CTEPH and to identify and risk-stratify patients regarding variable outcomes following PEA surgery. In addition, in depth assessment of metabolite profile of CTEPH allows better understanding of the molecular pathophysiology of the disease and whether these changes are reflected in correction of metabolite profiles after PEA surgery.

6.1.2 Pulmonary hypertension associated with left heart disease (LHD)

Pulmonary hypertension associated with left heart disease (LHD) (group 2 PH) (Galie, Humbert et al. 2015) can be caused by LV systolic dysfunction, diastolic dysfunction or valvular disease (Fang, DeMarco et al. 2012). Patients with PH secondary to heart failure with preserved ejection fraction are older than PAH patients and with higher rates of impaired renal function, decreased exercise capacity and co-morbidities (Thenappan, Shah et al. 2011).

In the context of left heart disease, pulmonary venous congestion leads to a reactive pulmonary vasoconstriction, which if uncorrected causes structural changes similar to PAH including medial hypertrophy and intimal fibrosis (Fang, DeMarco et al. 2012). There is evidence of impaired NO signalling and increased pulmonary endothelin contributing to pulmonary vascular remodelling in PH associated with heart failure (Moraes, Colucci et al. 2000, Fang, DeMarco et al. 2012). Treatment of PH associated with LHD is focused on targeting the underlying cause (Galie, Humbert et al. 2015). Small studies show some improvement in functional status and haemodynamics using PAH targeted therapies and larger studies are underway, however their use is currently not recommended in this patient group (Galie, Humbert et al. 2015).

6.1.3 Pulmonary hypertension associated with congenital heart disease (CHD)

PH associated with congenital heart disease (CHD) encompasses a heterogeneous group of PAH patients (group 1.4.4 PH) (Galie, Humbert et al. 2015) with underlying conditions such as Eisenmenger's syndrome, systemic-pulmonary shunts and septal defects (Simonneau, Gatzoulis et al. 2013, Galie, Humbert et al. 2015). Increased pulmonary blood flow due to a left-to-right shunt leads to increased shear stress, vascular remodelling, and endothelial dysfunction with altered endothelin-1, NO and prostacyclin promoting pulmonary vasoconstriction (Adatia, Kothari et al. 2010, D'Alto and Mahadevan 2012). In addition, there is evidence of smooth muscle proliferation and hypertrophy mediated by increased expression of fibroblast and endothelial growth factors (Adatia, Kothari et al. 2010, D'Alto and Mahadevan 2012). Increased PVR leads to RV remodelling and in patients where the RV pressure matches the systemic arterial pressure, the shunt is reversed to right-to-left (Eisenmenger's syndrome) in response to the raised pulmonary arterial pressure (Hopkins 2005). Surgical operations are not indicated for Eisenmenger's syndrome or if the PVR is greater than 4.6 Wood Units in a left-to-right shunt (Galie, Humbert et al. 2015). Bosentan used in patients with Eisenmenger's syndrome demonstrated improved functional capacity compared to placebo (Gatzoulis, Beghetti et al. 2008), and use of sildenafil and epoprostenol has also had favourable outcomes in these patients (Galie, Humbert et al. 2015).

6.1.4 Pulmonary hypertension associated with connective tissue disease (CTD)

PH associated with connective tissue disease are patients with PAH (group 1.4.1 PH) due to conditions such as systemic lupus erythematosus, scleroderma, systemic sclerosis and mixed connective tissue disease amongst others (Galie, Humbert et al. 2015). Patients with PAH associated with systemic sclerosis have evidence of inflammatory cells in pulmonary vascular lesions with pulmonary venous involvement (Dorfmuller, Humbert et al. 2007), as well as characteristic medial hypertrophy and intimal hyperplasia without plexiform lesions (Condliffe and Howard 2015). Patients with PH associated with CTD have favourable outcomes on PAH targeted therapies, and also with the use of immunosuppressant therapy (Galie, Humbert et al. 2015).

6.1.5 Metabolic phenotyping in PH sub-diagnoses

Patients with CTEPH and PH associated with LHD are older than PAH patients with a median age of 63 years (Lang and Madani 2014) and over 65 years (Galie, Humbert et al. 2015) at diagnosis respectively. In a registry of PH patients from the University of Sheffield, CTEPH patients had less gender bias (54% female) and patients with PAH and CTEPH had higher mPAP and PVR relative to PH patients associated with LHD (Hurdman, Condliffe et al. 2012). In addition, PCWP was higher in patients with PH-LHD (Hurdman, Condliffe et al. 2012).

Similar remodelling within the pulmonary vasculature is seen in different sub-diagnoses of PAH but also from other sub-diagnoses of PH such as CTEPH and LHD, where pulmonary vascular changes are triggered by in situ thrombosis or pulmonary venous congestion respectively. Assessing the molecular profile of these sub-diagnoses may provide insight into whether metabolic profiles represent universal changes across PH sub-diagnoses or provides a specific signature for PAH patients. In addition, use of PEA surgery as a curative intervention in CTEPH allows assessment of whether metabolite profiles are corrected after surgery and represent modifiers of disease progression.

In this study I set out to a) assess metabolic dysregulation in patients with CTEPH, b) assess whether metabolite changes are altered following PEA surgery in these patients and c) assess metabolic dysregulation in other sub-diagnoses of PH including PH associated with LHD and PAH associated with CHD and CTD, to assess whether metabolite changes are specific to PAH.

6.2 Methods

See Chapter 2 for detailed experimental methods and protocols.

Samples were obtained from patients attending the National Pulmonary Hypertension Service at Hammersmith Hospital, London between 2002-2016, with diagnoses of CTEPH, PAH (idiopathic or heritable), pulmonary hypertension associated with left heart disease (LHD), and pulmonary arterial hypertension associated with congenital heart disease (CHD) and connective tissue disease (CTD), as well as additional control samples from patients with pulmonary embolism (PE) and chronic thromboembolic disease (CTED).

Metabolomic profiling by ultra-performance liquid chromatography mass spectrometry was again conducted on the Discovery HD4^{TM} Global Metabolomics platform by Metabolon, Inc. (Durham, NC,

USA) (Evans, DeHaven et al. 2009), who provided semi-quantitative assessment of 985 named and 390 unnamed metabolite levels (total 1375), annotated with pathways.

For the metabolites which overlapped between the 2 experiments (n=1176) data was combined with that from healthy controls, disease controls and PAH patients in the first experiment using the Metabolon platform detailed in Chapter 5 (Table 6.1). In order to account for any between-experiment variability between the 2 experimental runs, bridging samples were included from healthy controls (n=15) and PAH patients (n=25). Bridging samples are representative samples from the first experiment, which are re-analysed in the second experimental run to assess for variability between the two experiments.

Metabolite intensities were compared for the bridging samples in the two experimental runs. This was conducted by calculating the ratio of metabolite intensities measured in experiment 1 to the intensity in the same sample measured in experiment 2. Metabolite levels in the second experiment were divided by the 10% trimmed mean of the average ratio between bridged samples, in order to correct for between-experiment variability (Figure 6.2).

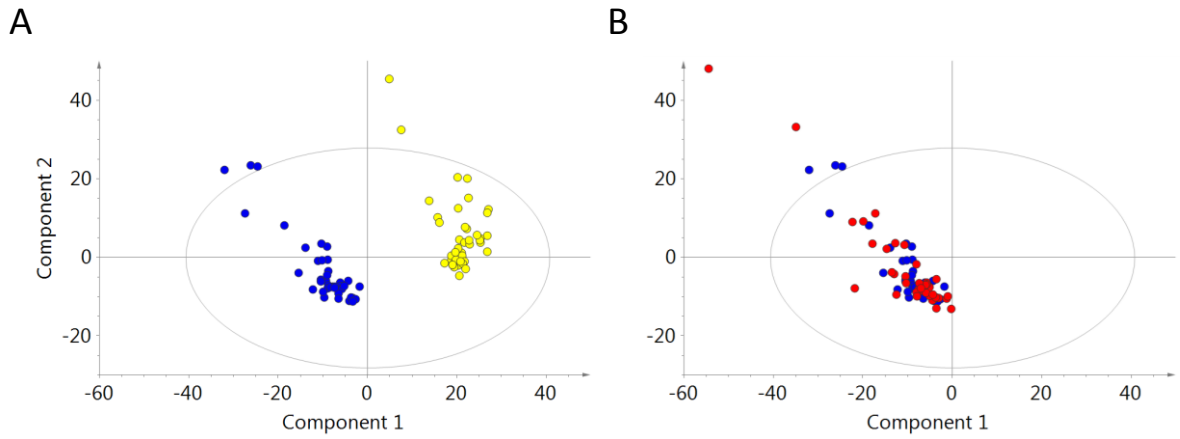


Figure 6.2 – Principal component analysis (PCA) of metabolite levels in 40 bridging samples. First and second component scores are shown for 40 samples run in both Metabolon experiments **(A)** prior to and **(B)** following correction, by dividing by the 10% trimmed mean of the average ratio between bridged samples. PCA scores are shown from the first experimental run in blue, and from the second experiment in yellow (pre-correction) and red (post-correction).

In order to further reduce the variability between experiments, a quantile normalisation approach was utilised, which sets the distribution of metabolite levels in each sample to the average distribution of all samples, making them directly comparable (Ejigu, Valkenborg et al. 2013) (Figure 6.3). This has previously been used in metabolomics LC-MS data to minimise experimental variation due to a variety of causes, including experiments being conducted at different times (Ejigu, Valkenborg et al. 2013), using more than one instrument use and different sample processing procedures (Lee, Park et al. 2012).

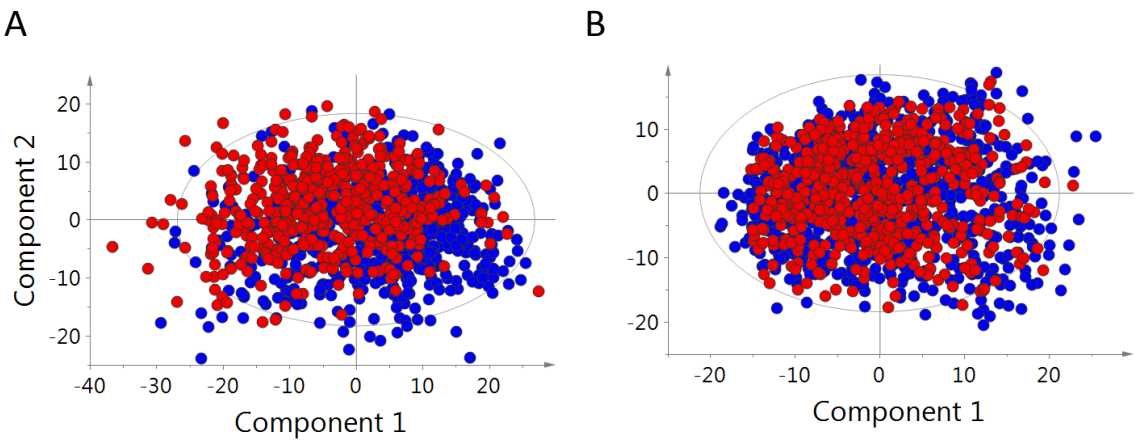


Figure 6.3 – Quantile normalisation. Principal component analysis (PCA) of all detected metabolites in the first (blue) and second (red) experimental runs are shown before **(A)** and following **(B)** quantile normalisation.

Initial group comparisons between controls and patients were performed using non-parametric Mann Whitney U tests. Comparisons before and after PEA surgery in paired samples was conducted using the Wilcoxon signed rank test. Comparisons of demographic features between PH sub-diagnoses were conducted using the Kruskal-Wallis (continuous data) or Chi-squared (categorical data) tests. Prior to modelling, metabolites were normalised using the same transformation applied during analysis of the first dataset for consistency and ease of comparisons. Samples where metabolites were undetected were imputed with the minimum detected level for the metabolite. All data were z-score transformed based on healthy control data.

Linear regression analysis was conducted to assess the relationships between metabolite levels, diagnoses and potential confounders. In the DC, CTED, PAH, CTEPH, LHD, CHD and CTD patients,

preserved renal function was defined as creatinine <75 µmol/L, and liver function as bilirubin <21 µmol/L. In the healthy control group, preserved renal and hepatic function was assumed as clinical assay data was unavailable. Clinical assay data was also not available for the PE cohort; here patients with comorbidities of diabetes and hypertension, or left ventricular impairment were excluded from regression analysis (n=4) as these were most likely to be associated with renal and hepatic dysfunction, and the remaining were assumed to have preserved renal and hepatic function.

Group	Number of subjects analysed	Metabolon Experiment
Controls		
HC	121	1
DC	132	1
CTED	13	1 & 2
PE	28	2
Bridging samples		
HC	15	1 & 2
PAH	25	1 & 2
PH groups		
PAH	365 & 68	1 & 2
CTEPH (before PEA/inoperable)	174	2
CTEPH (post PEA)	82	2
CTEPH (paired before and after PEA)	17	2
LHD	83	2
CHD	30	2
CTD	48	2

Table 6.1 – Cohorts analysed using the Metabolon platform. Number of subjects analysed are shown for control and patients groups from the first experiment detailed in Chapter 5 and the current experimental run (experiment 2). HC, healthy controls; DC, disease controls (symptomatic patients in whom pulmonary hypertension has been excluded); CTED, chronic thromboembolic disease; PE, pulmonary embolism; PAH, pulmonary arterial hypertension; CTEPH, chronic thromboembolic pulmonary hypertension; LHD, left heart disease; CHD, congenital heart disease; CTD, connective tissue disease; PEA, pulmonary endarterectomy.

6.3 Results

6.3.1 Metabolites distinguishing CTEPH patients from controls

I compared plasma metabolite levels from 82 consecutive CTEPH patients who attended Hammersmith Hospital between November 2011 and August 2013 to 58 healthy controls from the initial discovery cohort. The findings were validated in a second cohort of 92 CTEPH patients recruited from 2003 to 2015, and compared to a distinct healthy control group (n=63). Metabolite levels were also compared to control groups including disease controls (n=132) and patients with PE (n=28) or CTED (n=13).

The CTEPH cohort of patients did not include those that had undergone PEA surgery. In the discovery cohort, 33/82 were deemed operable for surgery and the remaining non-operable due to distal disease (n=26), age/co-morbidities/borderline PH (n=16) or unknown reasons (n=7). In the validation cohort, 48/92 were deemed operable for surgery and the remaining non-operable due to distal disease (n=15), age/co-morbidities/borderline PH (n=13) or unknown reasons (n=16). Overall, 81/174 CTEPH patients from the discovery and validation cohorts were deemed operable for PEA surgery.

Baseline characteristics and laboratory data are shown in Table 6.2. CTEPH patients were older than controls groups with less gender bias. The presence of co-morbidities was similar between groups except for coronary artery disease and the use of anticoagulants, PAH targeted therapies, aldosterone antagonists and diuretic use, which were higher in CTEPH patients reflecting treatment for pulmonary hypertension, embolic disease and right heart failure. Patients with CTEPH had higher mPAP and mRAP and lower CO than disease controls and CTED patients.

	HC - Discovery (n=58)	HC - Validation (n=63)	DC (n=132)	CTED (n=13)	PE (n=28)	CTEPH-Discovery (n=82)	CTEPH-Validation (n=92)	Sig.
Age at sampling	48+/-13.5	49.1+/-16.1	56.7+/-16.8	55.1+/-20.8	49.9+/-19	65.2+/-16.1	64.3+/-14.5	3.62E-04
Sex, Female:Male	38:20 (1.9:1)	40:23 (1.7:1)	90:42 (2.1:1)	8:5 (1.6:1)	15:13 (1.2:1)	33:49 (0.7:1)	56:36 (1.6:1)	5.00E-03
Ethnicity, % non-Caucasian	32.5	38.1	51.3	36.4	50.0	23.7	15.0	5.00E-06
BMI, kg/m^2	30.5+/-10.5	26+/- 4.1	27.8+/-5.8	26.8+/-6.5	30.1+/-6.8	27.8+/-6.2	28.7+/-5.9	0.41
Baseline haemodynamics								
Pulmonary capillary wedge pressure, mmHg			11+/-4	11.8+/-3.5		12.3+/-4.3	11+/-3.7	0.06
Mean pulmonary artery pressure, mmHg			19.3+/-4.5	19.3+/-3.4		42.9+/-13	44.8+/-13.4	6.78E-28
Pulmonary vascular resistance, Woods units				1.5+/-0.4		9.6+/-7.3	8.9+/-5.9	4.68E-04
Mean right atrial pressure, mmHg			6.8+/-3.4	6.8+/-2.6		10.3+/-5.7	9.7+/-5.2	7.00E-03
Cardiac Output, L/min			5.1+/-2.2	5.3+/-1.5		4+/-1.2	4.1+/-1.4	5.53E-07
Functional status and pathology								
Six minute walk distance, m				330.5+/-136.5		256+/-168.2	229.7+/-145.3	0.27
WHO Functional Class, I/II/III/IV				1/1/2/0		2/19/52/7	7/13/53/6	0.35
Creatinine, umol/L			81.7+/-33.2	86.3+/-34	73.7+/-16.8	89.3+/-27.7	91.7+/-27.5	2.00E-06
Bilirubin, umol/L			15.2+/-19.9	9.3+/-4.2	10.7+/-9.9	15.3+/-10.2	16.2+/-11.8	0.24
Comorbidities								
Asthma/COPD			15.2	7.7		9.8	13.0	0.65
Diabetes			11.4	7.7		9.8	8.7	0.91
CAD/IHD			10.6	7.7		32.9	18.5	4.87E-04
AF/flutter			16.7	0.0		19.5	23.9	0.17
Systemic hypertension			29.5	15.4		35.4	28.3	0.46
Hypercholesterolaemia/lipidaemia			12.1	7.7		15.9	15.2	0.76
Drug therapy								
Anticoagulation			33.3	61.5		95.1	85.9	1.56E-23
PDE5 inhibitors			0.0	0.0		47.6	37.0	1.36E-17
ERAs			0.0	0.0		32.9	22.8	6.11E-11
Prostanoids			0.0	0.0		2.4	1.1	0.34
Diuretics			18.2	0.0		50.0	50.0	7.48E-09
Aldosterone antagonists			4.5	0.0		26.8	28.3	7.86E-07
Statins/lipid lowering drugs			30.3	15.4		36.6	38.0	0.29
CCBs			16.7	15.4		4.9	9.8	0.06
Cardiac glycosides			8.3	0.0		8.5	8.7	0.75
Antidiabetic drugs			9.8	7.7		11.0	8.7	0.96
Iron replacement therapy			5.3	0.0		9.8	6.5	0.46
ACE inhibitors			33.3	15.4		34.1	28.3	0.48

Table 6.2 – Cohort Characteristics for CTEPH analysis. Means and standard deviations or counts are given. Significance is shown using Kruskal-Wallis (continuous) and Chi-squared tests (categorical) between all groups for baseline characteristics and between DC, CTED and CTEPH patients for haemodynamics, functional status, co-morbidities and drug therapy. Co-morbidities and drug therapy are shown as the percentage of patients with those co-morbidities or on each agent (%) and BMI, body mass index; HC, healthy controls; DC, disease controls; CTED; chronic thromboembolic disease; PE; pulmonary embolism; CTEPH, chronic thromboembolic pulmonary hypertension; COPD, chronic obstructive pulmonary disease; CAD, coronary artery disease; IHD, ischaemic heart disease; AF, atrial fibrillations; PDE5, phosphodiesterase 5; ERA, endothelin receptor antagonists; CCB, calcium channel blocker; ACE, angiotensin converting enzyme. Ethnicity is shown for subjects who self-declared.

Plasma levels of 87 metabolites distinguished CTEPH patients from healthy controls in both cohorts following Bonferroni correction ($p<8.94e-5$, Appendix Table 6.1). 42 of these metabolites distinguished CTEPH from healthy controls after correcting for potential confounders such as age, gender, ethnicity, body mass index, creatinine, bilirubin and drug therapies ($p<0.05$, Appendix Table 6.1).

To assess whether these changes were related to a general chronic disease process, I compared CTEPH patients to disease controls (n=132). Of the 42 metabolites, a subset of 12 distinguished CTEPH from disease controls after correcting for potential confounders ($p<0.05$, Appendix Table 6.1). Eleven of the metabolites were increased, including modified nucleosides, fatty acid acylcarnitines, monohydroxy- fatty acids and metabolites of polyamine and methionine metabolism, and one was decreased gamma-glutamyl amino acid (Figure 6.4).

In order to evaluate if these metabolic changes were reflective of an underlying embolic phenomenon, I compared CTEPH patients to those with chronic thromboembolic disease (CTED, n=13) and pulmonary embolism (PE, n=28). Of the 12 metabolites which discriminate CTEPH from healthy and disease controls, none discriminated between CTEPH and CTED, but the raised levels of 8 metabolites were significantly different between CTEPH and PE patients ($p<0.05$, Appendix Table 6.1, Figure 6.4).

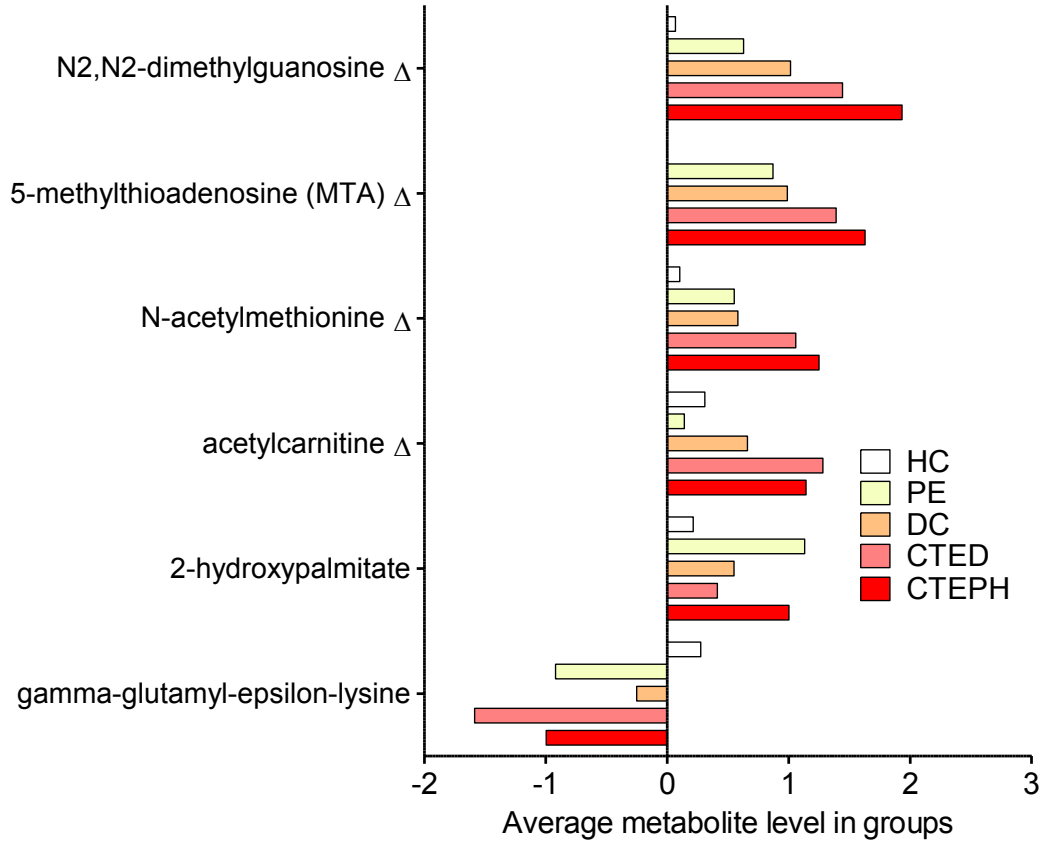


Figure 6.4 - Metabolites which discriminate CTEPH and control subjects. Average metabolite levels in CTEPH and control subjects for 6/12 representative metabolites from different metabolic pathways are shown, which were found to significantly distinguish CTEPH and both healthy and disease controls, independent of potential confounders ($p<0.05$). Values plotted are z-scores calculated based on mean and standard deviation of all healthy volunteers in study - negative values indicate metabolites at lower levels in patients versus healthy controls and positive values indicate higher levels of metabolites in patients. Δ indicates 4/8 metabolites that also discriminate patients with CTEPH from PE. HC, healthy controls; PE, pulmonary embolus; DC, disease controls; CTED, chronic thromboembolic disease; CTEPH, chronic thromboembolic pulmonary hypertension.

6.3.2 Metabolic alterations following pulmonary endarterectomy (PEA) surgery in patients with CTEPH

I hypothesised that metabolites which represent raised pulmonary pressures and are altered in CTEPH would be changed following PEA surgery, and would reflect the outcome of surgical intervention. To assess this, I compared CTEPH patients from the discovery and validation cohorts who were deemed suitable for PEA surgery (operable) but had not undergone surgery (i.e. those pending surgery or who had declined intervention, n=81) with patients sampled after PEA surgery (n=82, Table 6.3).

	Operable (n=81)	Post PEA (n=82)	Paired samples (n=17)	Sig.
Age at sampling	60.4+/-15.5	64.1+/-14.1	62.3+/-13.8	0.34
Sex, Female:Male	30:51 (0.6:1)	37:45 (0.8:1)	7:10 (0.7:1)	0.58
Ethnicity, % non-Caucasian	27	10.4	23.5	0.03
BMI, kg/m^2	29+/-6.2	29.5+/-5.9	29.9+/-4.2	0.61
Baseline haemodynamics				
Pulmonary capillary wedge pressure, mmHg	9.2+/-6.1	10.4+/-7.2	7.6+/-5.6	0.23
Baseline mean pulmonary artery pressure, mmHg	43.3+/-14.5	47.1+/-12.1	42.1+/-17.0	0.07
Mean pulmonary artery pressure 3-12 months post PEA, mmHg		30.9+/-11	28.8+/-11.9	
Pulmonary vascular resistance, Woods units	8.9+/-6.6	9.4+/-5.1	8.5+/-5.0	0.33
Mean right atrial pressure, mmHg	9.4+/-5.4	10.7+/-5.7	10.0+/-5.6	0.38
Cardiac Output, L/min	3.8+/-1.8	3.2+/-2.6	3.7+/-1.5	0.42
Functional status and pathology				
Six minute walk distance, m	251.7+/-155.2	367.5+/-110.3	270.3+/-173.6	
WHO Functional Class, I/II/III/IV	5/19/49/4	12/29/35/4	1/4/10/2	0.16
Creatinine, umol/L	91+/-27.3	82.3+/-18	82.9+/-14.8	0.36
Bilirubin, umol/L	16.2+/-11.8	11.9+/-6.3	18.2+/-13	3.00E-03

Table 6.3 – Cohort Characteristics for CTEPH sub-analysis. Significance is shown using Kruskal-Wallis (continuous) and Chi-squared tests (categorical) showing similar baseline characteristics between groups. Means and standard deviations or counts are given. BMI, body mass index; PEA, pulmonary endarterectomy. Ethnicity is shown for subjects who self-declared.

Of the 42 metabolites which were significantly altered in CTEPH compared to healthy controls independent of confounding factors, 5 were significantly altered following PEA surgery ($p<0.05$, Figure 6.5). N2,N2-dimethylguanosine and alpha-ketoglutarate levels are increased in CTEPH patients but decrease following PEA surgery and levels of three types of sphingomyelin which are decreased in CTEPH patients, increase following surgery, indicating reversal of these metabolic changes following surgical intervention.

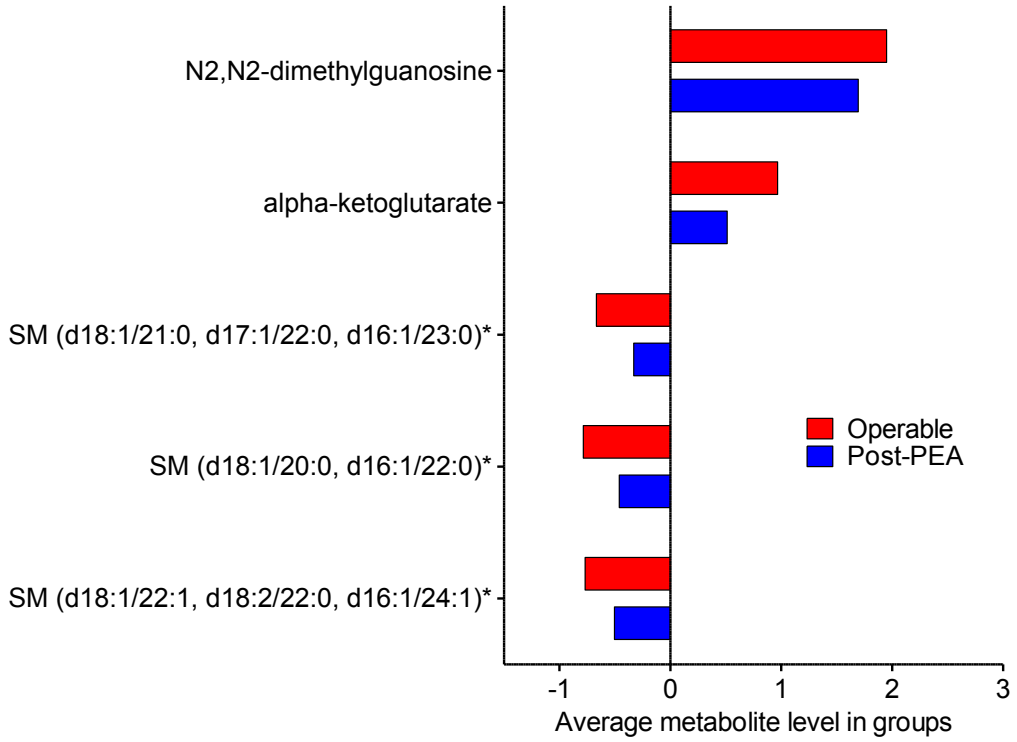


Figure 6.5 – Levels of 5 metabolites which are altered following PEA surgery. Average metabolite levels in CTEPH patients who are operable for pulmonary endarterectomy (PEA) surgery (n=81), and those following surgery (n=82) are shown. 42 metabolites which were significantly altered in CTEPH versus HC independent of confounding factors were tested and 5 which were significantly altered following PEA surgery are shown ($p<0.05$, Mann Whitney U-test). Metabolites which are increased in CTEPH patients compared to controls decrease following surgery and vice versa. N2,N2-dimethylguanosine also discriminates CTEPH patients from disease controls and patients with pulmonary embolism. Values plotted are z-scores calculated based on mean and standard deviation of all healthy volunteers in study - negative values indicate metabolites at lower levels in patients versus healthy controls and positive values indicate higher levels of metabolites in patients. HC, healthy controls; SM, sphingomyelin. *probable metabolite identity, but unconfirmed (see methods).

In order to review whether metabolite changes following PEA surgery reflect a response to surgery, I performed a sub-analysis comparing patients who were deemed responders (n=42, mPAP<30mmHg 3-12 months after surgery) and non-responders (n=40, mPAP>30mmHg 3-12 months after surgery). Of the 5 metabolites significantly altered following PEA surgery, none were significantly different between PEA responders compared to non-responders ($p>0.05$).

In a separate analysis I also compared 17 paired samples taken from the same patient before and after PEA surgery (Table 6.3). Of the 42 metabolites which were altered in CTEPH, 8 were significantly altered before and after surgery (Figure 6.6, Table 6.4, $p<0.05$). Except for an increase in 3-methylcytidine, the levels of the 7 other metabolites changed towards that of healthy controls following PEA surgery (Table 6.4). The altered metabolites include three sphingomyelins increased after PEA surgery and N2,N2-dimethylguanosine decreased following surgery, which validate the previous findings in comparisons between operable and post-PEA CTEPH patients.

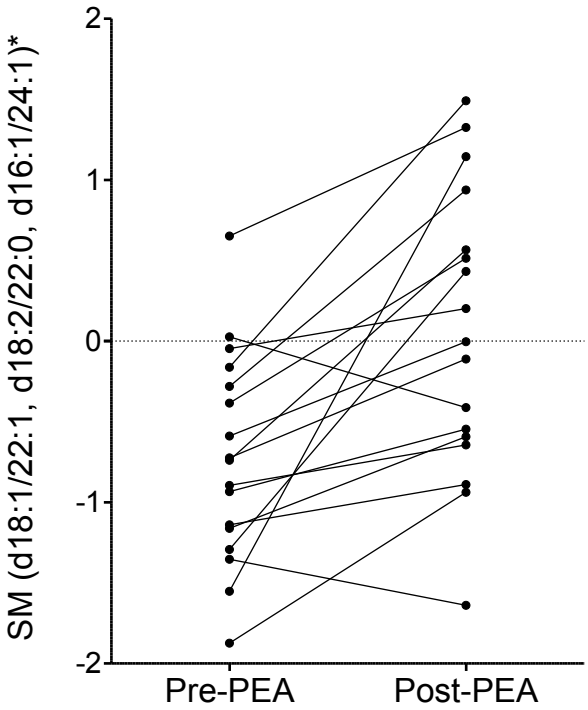


Figure 6.6 – Levels of a sphingomyelin (SM) metabolite before and after PEA surgery in paired analysis. Levels of a representative metabolite significantly different between 17 paired samples taken before and after pulmonary endarterectomy (PEA) surgery are shown ($p<0.05$). *probable metabolite identity, but unconfirmed (see methods).

Metabolite	Metabolic Pathway	Group averages (z-score relative to healthy control levels)		Sig.
		Pre-PEA	Post-PEA	
Decreased following PEA surgery				
C-glycosyltryptophan	Tryptophan Metabolism	1.48	1.09	0.03
myristoleoylcarnitine*	Fatty Acid Metabolism(Acyl Carnitine)	1.11	0.62	0.05
N2,N2-dimethylguanosine	Purine Metabolism, Guanine containing	2.07	1.81	0.04
palmitoylcarnitine	Fatty Acid Metabolism(Acyl Carnitine)	1.61	1.04	0.03
Increased following PEA surgery				
3-methylcytidine	Pyrimidine Metabolism, Cytidine containing	1.52	2.19	0.01
SM (d18:1/20:0, d16:1/22:0)*	Sphingolipid Metabolism	-0.83	-0.21	0.01
SM (d18:1/21:0, d17:1/22:0, d16:1/23:0)*	Sphingolipid Metabolism	-0.62	-0.01	0.01
SM (d18:1/22:1, d18:2/22:0, d16:1/24:1)*	Sphingolipid Metabolism	-0.73	0.05	8.22E-04

Table 6.4 – 8 metabolites significantly different following pulmonary endarterectomy (PEA) surgery in paired analysis. Metabolites that are significantly different between 17 CTEPH patients with paired sample before and surgery PEA surgery are shown ($p<0.05$). Mean values are given and the data is scaled to the healthy control group. Significance from Wilcox signed rank test is shown (p value). SM, sphingomyelin. *probable metabolite identity, but unconfirmed (see methods).

6.3.3 Metabolites distinguishing PAH patients, controls and CTEPH patients

In order to assess whether metabolites which distinguish PAH from healthy and disease controls, also discriminate PAH patients from CTEPH, I compared metabolite levels from 174 CTEPH patients from the discovery (n=82) and validation (n=92) cohorts, with 433 PAH (IPAH and HPAH) patients. CTEPH patients sampled after PEA surgery were excluded from the CTEPH group. Baseline characteristics and laboratory data are shown in Table 6.5, and will be described in more detail in section 6.3.4.

	HC (n=121)	DC (n=132)	PAH (n=433)	CTEPH-Discovery (n=82)	CTEPH-Validation (n=92)	LHD (n=83)	CHD (n=30)	CTD (n=48)	Sig.
Age at sampling	48.6+/-14.8	56.7+/-16.8	53.4+/-16.2	65.2+/-16.1	64.3+/-14.5	70.2+/-11.8	49.5+/-16.2	59.5+/-13.5	9.21E-25
Sex, Female:Male	78:43 (1.8:1)	90:42 (2.1:1)	305:128 (2.4:1)	33:49 (0.7:1)	56:36 (1.6:1)	49:34 (1.4:1)	21:9 (2.3:1)	37:11 (3.4:1)	4.87E-05
Ethnicity, % non-Caucasian	35.9	51.3	14.8	23.7	15.0	37.3	32	29.3	5.8E-5
BMI, kg/m^2	28+/-8	27.8+/-5.8	28.9+/-7.2	27.8+/-6.2	28.7+/-5.9	29.1+/-7.1	25.2+/-6.4	26.5+/-6.1	2.64E-03
BMPR2 mutation carriers (%)			9.93						
Treatment naïve cases (%)			17.1						
Baseline haemodynamics									
Pulmonary capillary wedge pressure, mmHg		11+/-4	10.5+/-5	12.3+/-4.3	11+/-3.7	20.2+/-4.5	11.3+/-3.7	10.9+/-4.9	1.06E-16
Mean pulmonary artery pressure, mmHg		19.3+/-4.5	53.8+/-14.5	42.9+/-13	44.8+/-13.4	37.2+/-10.3	48.4+/-17.4	42.3+/-11.5	9.08E-24
Pulmonary vascular resistance, Woods units			11.6+/-6.6	9.6+/-7.3	8.9+/-5.9	4.4+/-3.6	5.3+/-6.5	8.5+/-5.1	5.89E-12
Mean right atrial pressure, mmHg		6.8+/-3.4	9.9+/-5.6	10.3+/-5.7	9.7+/-5.2	13.9+/-4.8	12.2+/-12.4	8.7+/-4.6	9.96E-07
Cardiac Output, L/min		5.1+/-2.2	4+/-1.4	4+/-1.2	4.1+/-1.4	4.5+/-2.1	9.2+/-6.4	4+/-1.2	0.04
Functional status and pathology									
Six minute walk distance, m			263.8+/-158.9	256+/-168.2	229.7+/-145.3	231.7+/-177.1	251.1+/-157.3	220.8+/-150	0.38
WHO Functional Class, I/II/III/IV			9/31/170/34	2/19/52/7	7/13/53/6	2/12/58/5	0/6/19/4	1/12/24/9	0.09
Creatinine, umol/L		81.7+/-33.2	91.5+/-35.9	89.3+/-27.7	91.7+/-27.5	100.1+/-65.7	76.3+/-23.4	83.1+/-26.4	2.12E-03
Bilirubin, umol/L		15.2+/-19.9	15.9+/-10.8	15.3+/-10.2	16.2+/-11.8	16.9+/-10.4	13.8+/-5	12.8+/-8.7	0.17
Comorbidities									
Asthma/COPD		15.2	15.0	9.8	13.0	8.4	16.7	4.2	0.12
Diabetes		11.4	18.9	9.8	8.7	22.9	13.3	4.2	1.76E-03
CAD/IHD		10.6	13.6	32.9	18.5	32.5	16.7	10.4	5.96E-05
AF/flutter		16.7	13.2	19.5	23.9	57.8	16.7	22.9	2.67E-17
Systemic hypertension		29.5	23.8	35.4	28.3	56.6	23.3	29.2	2.75E-07
Hypercholesterolaemia/lipidaemia		12.1	10.2	15.9	15.2	16.9	3.3	8.3	0.10

	HC (n=121)	DC (n=132)	PAH (n=433)	CTEPH-Discovery (n=82)	CTEPH-Validation (n=92)	LHD (n=83)	CHD (n=30)	CTD (n=48)	Sig.
Drug therapy									
Anticoagulation		33.3	67.2	95.1	85.9	56.6	53.3	39.6	1.49E-13
PDE5 inhibitors		0.0	65.4	47.6	37.0	4.8	43.3	56.3	1.46E-23
ERAs		0.0	53.6	32.9	22.8	1.2	56.7	43.8	7.84E-20
Prostanoids		0.0	18.0	2.4	1.1	0.0	3.3	4.2	1.63E-10
Diuretics		18.2	52.7	50.0	50.0	69.9	26.7	41.7	3.56E-04
Aldosterone antagonists		4.5	24.0	26.8	28.3	26.5	13.3	29.2	0.47
Statins/lipid lowering drugs		30.3	25.9	36.6	38.0	47.0	16.7	27.1	2.12E-04
CCBs		16.7	17.3	4.9	9.8	16.9	13.3	27.1	5.12E-03
Cardiac glycosides		8.3	15.7	8.5	8.7	14.5	13.3	8.3	0.16
Antidiabetic drugs		9.8	14.3	11.0	8.7	19.3	3.3	2.1	0.01
Iron replacement therapy		5.3	11.5	9.8	6.5	13.3	10.0	25.0	0.03
ACE inhibitors		33.3	23.1	34.1	28.3	67.5	16.7	25.0	3.62E-14

Table 6.5 – Cohort Characteristics of PH sub-diagnoses. Means and standard deviations or counts are given. Clinical pathology parameters are shown within 30 days of the sample date. Significance is shown using Kruskal-Wallis (continuous) and Chi-squared tests (categorical) between the PH sub-diagnoses (PAH, CTEPH, LHD, CHD and CTD). Co-morbidities and drug therapy are shown as the percentage of patients with those co-morbidities or on each agent (%). BMI, body mass index; HC, healthy controls; DC, disease controls; PAH, pulmonary arterial hypertension; CTEPH, chronic thromboembolic pulmonary hypertension; LHD, pulmonary hypertension associated with left heart disease; CHD, PAH associated with congenital heart disease; CTD, PAH associated with connective tissue disease; COPD, chronic obstructive pulmonary disease; CAD, coronary artery disease; IHD, ischaemic heart disease; AF, atrial fibrillations; PDE5, phosphodiesterase 5; ERA, endothelin receptor antagonists; CCB, calcium channel blocker; ACE, angiotensin converting enzyme. 16 PAH patients are on CCB therapy as vasoresponders. Ethnicity is shown for subjects who self-declared.

From the analysis in Chapter 5, 20 metabolites were found to distinguish PAH patients from healthy and disease controls independent of confounding factors (Appendix Table 5.1). Of these, 10 (4 increased and 6 decreased) also distinguished PAH and CTEPH patients after correcting for potential confounders, including age, gender, ethnicity, BMI, renal and hepatic dysfunction and drug therapy (Table 6.6). In CTEPH patients, the levels of 9/10 of the metabolites were closer to healthy controls than patients with PAH (Table 6.6).

Metabolite	Metabolic Pathway	Group averages (z-score relative to healthy control levels)		Linear Regression PAH vs CTEPH
		PAH (n=433)	CTEPH (n=174)	
Increased PAH vs HC,DC and CTEPH (independent confounders)				
3-ureidopropionate	Pyrimidine Metabolism, Uracil containing	0.73	0.31	0.01
acisoga	Polyamine Metabolism	1.48	1.09	3.2E-05
N-acetylaspartate (NAA)	Alanine and Aspartate Metabolism	1.11	0.41	7.5E-03
X - 21796	Unknown	0.82	0.36	6.7E-07
Decreased IPAH vs HC, DC and CTEPH (independent confounders)				
1-arachidonoyl-GPC (20:4n6)*	Lysolipid	-0.70	-0.47	0.03
1-docosapentaenoyl-GPC (22:5n3)*	Lysolipid	-0.74	-0.24	0.01
1-linoleoyl-2-eicosapentaenoyl-GPC (18:2/20:5)*	Phospholipid Metabolism	-1.07	-1.89	8.1E-05
palmitoylcholine	Fatty Acid Metabolism (Acyl Choline)	-0.89	-0.63	0.03
SM (d18:1/20:0, d16:1/22:0)*	Sphingolipid Metabolism	-0.98	-0.65	0.04
SM (d18:1/22:1, d18:2/22:0, d16:1/24:1)*	Sphingolipid Metabolism	-0.97	-0.66	0.02
Increased PAH vs HC and DC (independent confounders)				
3-hydroxy-3-methylglutarate	Mevalonate Metabolism	0.88	0.90	0.24
malate	TCA Cycle	1.28	1.34	0.43
N1-methylinosine	Purine Metabolism, (Hypo)Xanthine/Inosine containing	1.54	1.85	0.13
N2,N2-dimethylguanosine	Purine Metabolism, Guanine containing	1.68	1.91	0.32
octadecanedioate	Fatty Acid, Dicarboxylate	0.58	0.61	0.12
X - 12688	Unknown	1.53	1.39	0.07
X - 13737	Unknown	1.07	1.17	0.30
xanthine	Purine Metabolism, (Hypo)Xanthine/Inosine containing	0.98	0.42	0.19
Decreased IPAH vs HC and DC (independent confounders)				
SM (d18:1/21:0, d17:1/22:0, d16:1/23:0)*	Sphingolipid Metabolism	-0.72	-0.51	0.14
SM (d18:2/23:0, d18:1/23:1, d17:1/24:1)*	Sphingolipid Metabolism	-0.44	-0.30	0.10

Table 6.6 - Metabolites distinguishing PAH from healthy controls, disease controls and CTEPH patients. 20 metabolites that are significantly different between PAH patients and healthy and disease controls are shown. 11 metabolites also distinguish PAH and CTEPH patients independent of confounding factors ($p<0.05$). Mean values are given and the data is scaled to the healthy control group. Significance from linear regression is shown (p value). PAH, pulmonary arterial hypertension; CTEPH, chronic thromboembolic pulmonary hypertension; GPC, glycerophosphocholine; TCA, tricarboxylic acid; SM, sphingomyelin. *probable metabolite identity, but unconfirmed (see methods).

6.3.4 Metabolites distinguishing other PH sub-diagnoses from controls, and metabolites specific to PAH

In an exploratory analysis of other PH sub diagnoses where validation cohorts were not available, metabolite levels were compared between all healthy controls (n=121) and patients with PH secondary to left heart disease (LHD, n=83), and PAH secondary to congenital heart disease (CHD, n=30) and connective tissue disease (CTD, n=48) respectively. Baseline characteristics and laboratory data are shown in Table 6.5.

Patients with CTEPH and LHD were generally older than other PH sub-diagnoses with less gender bias. Patients with PH associated with LHD had a higher PCWP (post-capillary PH), whilst those with PAH had higher mPAP and PVR at baseline. In addition, patients with CHD had a higher cardiac output. The degree of coronary disease was similar in LHD to the discovery CTEPH cohort indicating that the cause of LV impairment in this group may not only be due to ischaemic heart disease, but also due to other factors such as diastolic heart failure.

I identified circulating metabolites which distinguished LHD (n=14), CHD (n=9) and CTD (n=14) from both healthy and disease controls following correction for potential confounders ($p<0.05$). Overall, 54 metabolites distinguished PAH (n=20), CTEPH (n=12), LHD, CHD or CTD from healthy and disease controls independent of confounding factors (Table 6.7). No metabolites discriminated every PH sub-diagnosis from healthy and disease controls independent of confounding factors and each metabolite had varying degrees of significance by which they were distinguished from controls. For example, N2,N2-dimethylguanosine was increased in all PH sub-diagnoses relative to controls, but in PAH and CTEPH was increased compared to both healthy and disease controls independent of confounders, and in LHD, CHD and CTD met Bonferroni correction but was not independent of confounding factors in linear regression analysis.

Metabolite	Metabolic Pathway	Group averages (z-score relative to healthy control levels)					
		DC	PAH	CTEPH	LHD	CHD	CTD
Increased in PH subgroup versus controls							
16-hydroxypalmitate	Fatty Acid, Monohydroxy	0.64	0.70*	0.88****	0.91**	0.85*	1.15**
2-hydroxypalmitate	Fatty Acid, Monohydroxy	0.55	0.59	0.98****	1.01**	1.00*	0.97**
3-hydroxy-3-methylglutarate	Mevalonate Metabolism	0.59	0.88****	0.90**	0.84**	0.69*	0.53*
3-methylcytidine	Pyrimidine Metabolism, Cytidine containing	0.41	-0.43	0.99****	0.41	1.60****	1.42**
3-ureidopropionate	Pyrimidine Metabolism, Uracil containing	0.17	0.73****	0.31	0.82**	0.18	0.41*
5-methylthioadenosine (MTA)	Polyamine Metabolism	0.99	0.57	1.57****	1.65**	1.40**	1.88****
acetylcarnitine	Fatty Acid Metabolism(Acyl Carnitine)	0.66	0.80***	1.10****	1.09**	0.93*	0.98**
dimethylarginine (SDMA + ADMA)	Urea cycle; Arginine and Proline Metabolism	0.68	0.84*	1.29***	1.68***	1.17**	1.63****
kynurenine	Tryptophan Metabolism	0.44	1.13**	1.40***	1.62**	1.03*	1.66****
malate	TCA Cycle	0.70	1.28****	1.34**	1.10**	0.74*	1.11**
N1-methyladenosine	Purine Metabolism, Adenine containing	0.84	0.99**	1.69****	1.69***	1.65**	1.67**
N1-methylinosine	Purine Metabolism, (Hypo)Xanthine/Inosine containing	0.73	1.54****	1.85****	1.42**	1.08**	0.96**
N2,N2-dimethylguanosine	Purine Metabolism, Guanine containing	1.02	1.68****	1.91****	1.85**	1.40**	1.70**
N6-carbamoylthreonyladenosine	Purine Metabolism, Adenine containing	0.76	1.29**	1.45**	1.72**	1.12**	1.56****
N-acetylaspartate (NAA)	Alanine and Aspartate Metabolism	0.53	1.11****	0.41*	0.72**	0.94*	0.88***
N-acetylglucosamine/N-acetylgalactosamine	Aminosugar Metabolism	0.73	0.78**	0.93*	1.24****	0.81*	1.25**
N-acetylmethionine	Methionine, Cysteine, SAM and Taurine Metabolism	0.58	0.91***	1.21****	1.38****	1.37**	1.30**
N-formylmethionine	Methionine, Cysteine, SAM and Taurine Metabolism	0.58	1.11***	1.54****	1.57***	1.40**	1.47****
N-palmitoyl-sphingosine (d18:1/16:0)	Sphingolipid Metabolism	0.52	0.30	0.59	-0.05	1.05**	1.52****
octadecanedioate	Fatty Acid, Dicarboxylate	0.30	0.58****	0.61*	0.45*	0.67*	0.78**
oleoylcarnitine	Fatty Acid Metabolism(Acyl Carnitine)	0.75	1.33***	1.16***	1.00**	1.29****	1.27**
pseudouridine	Pyrimidine Metabolism, Uracil containing	0.95	1.44**	1.69**	1.96***	1.33**	1.74****
vanillylmandelate (VMA)	Phenylalanine and Tyrosine Metabolism	0.34	1.15**	1.38**	1.32**	1.24****	1.03**
X - 11429	Unknown	1.21	1.80**	1.98***	2.20***	1.46***	2.13****
X - 12688	Unknown	1.10	1.53****	1.39***	1.74**	1.68****	1.53**
X - 13737	Unknown	0.31	1.07****	1.17**	1.07**	0.92**	1.00**
X - 24020	Unknown	0.77	0.72*	1.04***	1.27****	1.20**	1.23***
X - 24527	Unknown	1.15	1.17***	1.20****	1.38***	1.21***	1.21**
xanthine	Purine Metabolism, (Hypo)Xanthine/Inosine containing	0.71	0.98****	0.42	0.52*	0.85*	0.50

Metabolite	Metabolic Pathway	Group averages (z-score relative to healthy control levels)					
		DC	PAH	CTEPH	LHD	CHD	CTD
Decreased in PH subgroup versus controls							
1-(1-enyl-palmitoyl)-2-docosahexaenoyl-GPE (P-16:0/22:6)*	Plasmalogen	0.16	-0.80*	-0.43	-0.61****	-0.53*	-0.39*
1-arachidonoyl-GPC (20:4n6)*	Lysolipid	-0.08	-0.70****	-0.47*	-0.36*	-0.81****	-0.46*
1-docosapentaenoyl-GPC (22:5n3)*	Lysolipid	-0.09	-0.74****	-0.24*	-0.56**	-0.91****	-0.40*
1-myristoyl-2-docosahexaenoyl-GPC (14:0/22:6)*	Phospholipid Metabolism	0.08	-0.60*	-0.31	-0.90****	-0.42*	-0.28*
1-oleoyl-2-docosahexaenoyl-GPC (18:1/22:6)*	Phospholipid Metabolism	0.01	-0.38	-0.34	-0.59****	-0.34*	-0.32*
1-palmitoyl-2-docosahexaenoyl-GPC (16:0/22:6)	Phospholipid Metabolism	0.11	-0.50*	-0.52*	-0.68****	-0.58**	-0.30*
1-palmitoyl-2-eicosapentaenoyl-GPC (16:0/20:5)*	Phospholipid Metabolism	0.07	-0.49*	-0.33*	-0.75****	-0.59**	-0.38*
1-pentadecanoyl-2-docosahexaenoyl-GPC (15:0/22:6)*	Phospholipid Metabolism	0.07	-0.51*	-0.37	-0.61****	-0.29*	0.11
1-stearoyl-2-docosahexaenoyl-GPC (18:0/22:6)	Phospholipid Metabolism	0.19	-0.43	-0.40*	-0.51****	-0.41*	-0.30*
1-stearoyl-GPC (18:0)	Lysolipid	-0.28	-0.48*	-0.78**	-0.86**	-0.78****	-0.79**
2-palmitoyl-GPC (16:0)*	Lysolipid	0.16	-0.33	-0.53*	-0.82**	-0.88****	-0.42*
4-androsten-3beta,17beta-diol disulfate (1)	Steroid	-0.51	-0.90**	-1.02***	-0.77**	-0.83**	-1.29****
4-androsten-3beta,17beta-diol disulfate (2)	Steroid	-0.48	-0.62*	-0.86*	-0.20*	-0.35*	-1.07****
androsterone sulfate	Steroid	-0.65	-1.22**	-1.19***	-1.14***	-0.93**	-1.69****
dehydroisoandrosterone sulfate (DHEA-S)	Steroid	-1.04	-1.66***	-1.54**	-1.54**	-1.03**	-2.11****
gamma-glutamyl-epsilon-lysine	Gamma-glutamyl Amino Acid	-0.25	0.05	-0.91****	-0.92**	-0.92**	-0.99****
isovalerylcarnitine	Leucine, Isoleucine and Valine Metabolism	-0.15	-0.41	-0.36*	-0.53****	-0.58*	-0.68*
palmitoylcholine	Fatty Acid Metabolism (Acyl Choline)	-0.18	-0.89****	-0.63**	-0.58**	-1.03****	-0.55*
SM (d18:1/20:0, d16:1/22:0)*	Sphingolipid Metabolism	-0.33	-0.98****	-0.65***	-0.97**	-0.74***	-0.65**
SM (d18:1/21:0, d17:1/22:0, d16:1/23:0)*	Sphingolipid Metabolism	-0.29	-0.72****	-0.51***	-0.81**	-0.53*	-0.56**
SM (d18:1/22:1, d18:2/22:0, d16:1/24:1)*	Sphingolipid Metabolism	-0.26	-0.97****	-0.66***	-0.92**	-0.62*	-0.58**
SM (d18:2/23:0, d18:1/23:1, d17:1/24:1)*	Sphingolipid Metabolism	-0.09	-0.44****	-0.30*	-0.59***	-0.27*	-0.18*
X - 02269	Unknown	-0.13	-0.69*	-0.70*	-0.80****	-0.53*	-0.55*
X - 21364	Unknown	-0.37	-0.41	-0.75*	-0.18*	-0.37*	-0.86****
X - 24831	Unknown	-0.25	-0.62*	-0.98**	-1.17****	-0.69*	-0.80**

Table 6.7 - Metabolites distinguishing PH sub-diagnoses from healthy and disease controls. 54 metabolites that are significantly different between PH sub-diagnoses and both healthy and disease controls, independent of confounders, are shown. Mean values are given and the data is scaled to the healthy control group. Values are coded based on significance in Mann Whitney U-test between the PH sub-diagnosis and healthy controls (* p<0.05, ** Bonferroni correction) and linear regression between PH sub-diagnosis and healthy controls (***p<0.05) and disease controls (****p<0.05) independent of confounding factors. *probable metabolite identity, but unconfirmed (see methods). GPC, glycerophosphocholine; SM, sphingomyelin; HC, healthy controls; DC, disease controls; PAH, pulmonary arterial hypertension; CTEPH, chronic thromboembolic pulmonary hypertension; LHD, left heart disease; CHD, Congenital heart disease; CTD, connective tissue disease.

Several approaches were undertaken to assess if metabolites which distinguish PH patients from controls were specific to a PH sub-diagnosis. To begin with, I focused on the 54 metabolites which discriminate each PH sub-diagnosis from healthy and disease controls independent of confounding factors (Table 6.7). The differences in metabolite levels which discriminated one PH sub-diagnosis from controls also showed similar variation in other PH sub-diagnoses (Figure 6.7). In addition, although principal component analysis of these 54 metabolites was visually able to discriminate PH sub diagnoses from controls, and components 1 and 2 discriminated between all groups (p<0.001, Kruskall Wallis test), there was a significant degree of overlap (Figure 6.8).

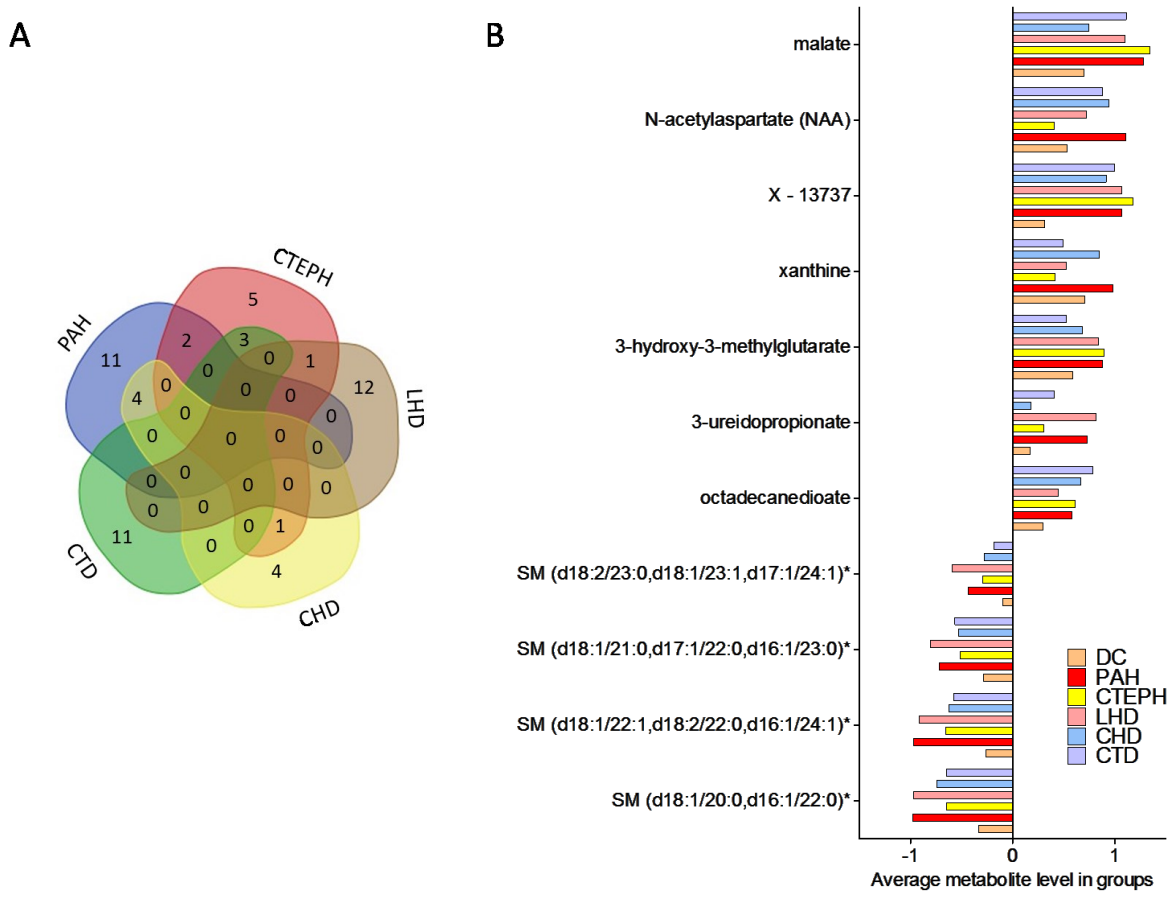


Figure 6.7 – Metabolites which discriminate PH sub-diagnoses from controls. (A) Venn diagram shows overlap between the 54 metabolites that discriminate PH sub-diagnoses from healthy and disease controls independent of confounding factors. 11 metabolites discriminate PAH patients from controls and do not overlap with metabolites discriminating other PH sub-diagnoses from controls. **(B)** Average metabolite levels in PH sub-diagnoses and control subjects for 11 metabolites which distinguish PAH from controls and do not overlap with other PH sub-diagnoses, showing similar trend in levels of metabolites in all PH sub-diagnoses. Values plotted are z-scores calculated based on mean and standard deviation of all healthy volunteers in study - negative values indicate metabolites at lower levels in patients versus healthy controls and positive values indicate higher levels of metabolites in patients. HC, healthy controls; DC, disease controls; PAH, pulmonary arterial hypertension; CTEPH, chronic thromboembolic pulmonary hypertension; LHD, left heart disease; CHD, congenital heart disease; CTD, connective tissue disease; SM, sphingomyelin; GPC, glycerophosphocholine. *probable metabolite identity, but unconfirmed (see methods).

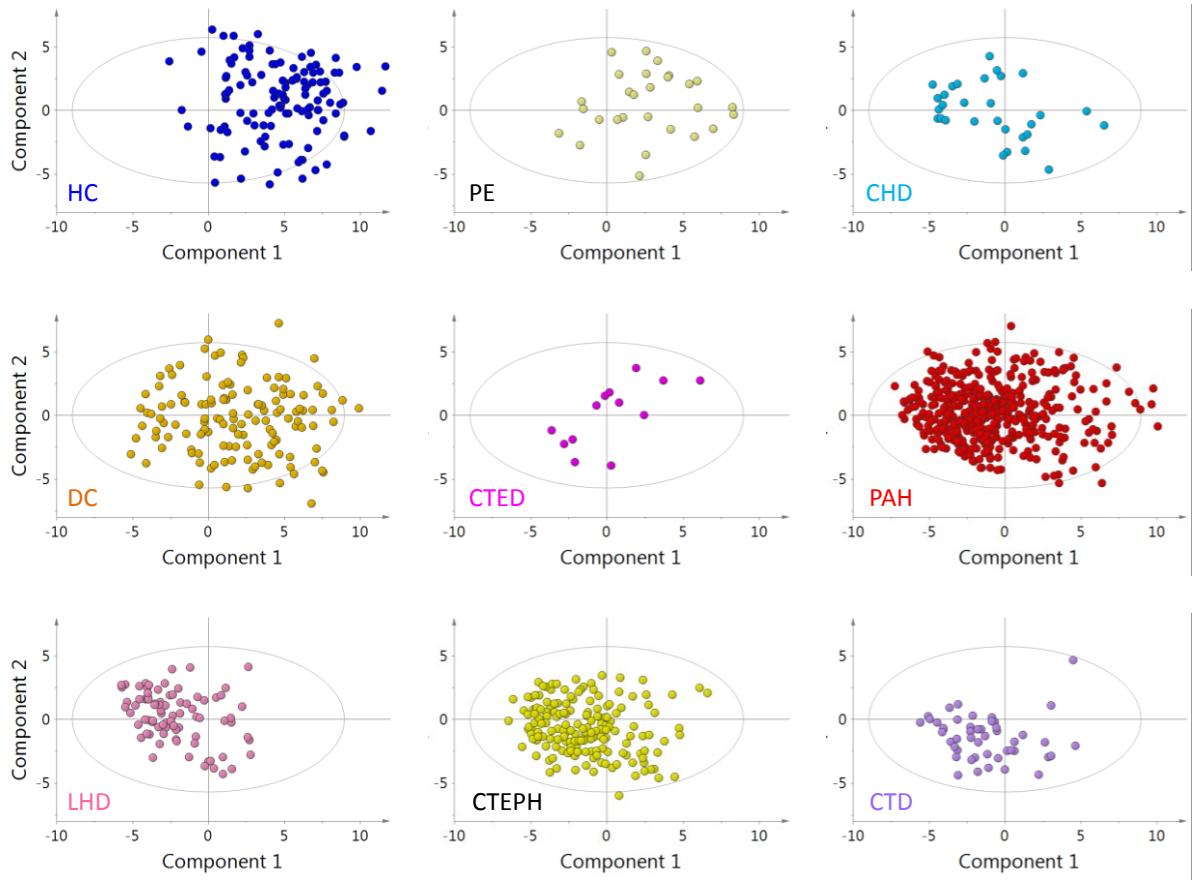


Figure 6.8 – Principal component analysis (PCA) of metabolites which distinguish PH sub-diagnoses from controls. First and second component scores are shown for control and PH sub-diagnoses from a PCA of 76 metabolites which are known to distinguish PH sub-diagnoses from healthy and disease controls independent of confounding factors. HC, healthy controls; DC, disease controls; LHD, left heart disease; PE, pulmonary embolus; CTED, chronic thromboembolic disease; CTEPH, chronic thromboembolic pulmonary hypertension; CTD, connective tissue disease; PAH, pulmonary arterial hypertension; CHD, congenital heart disease.

A linear regression model was used to assess metabolites specific to PAH, taking into account potentially confounding factors including age, gender, ethnicity, BMI, drug therapy, renal and hepatic dysfunction and PH disease severity (PVR). Of the 54 metabolites which discriminate each PH sub-diagnosis from healthy and disease controls independent of confounding factors, 16 including 5-methylthioadenosine (MTA), 3-methylcytidine, N1-methyladenosine, N1-methylinosine, N2,N2-dimethylguanosine, N-acetylaspartate (NAA), 3-ureidopropionate, palmitoylcholine, 1-arachidonoyl-GPC (20:4n6)*, 1-docosapentaenoyl-GPC (22:5n3)*, sphingomyelin (d18:1/22:1, d18:2/22:0, d16:1/24:1)*, sphingomyelin (d18:2/23:0, d18:1/23:1, d17:1/24:1)*, gamma-glutamyl-epsilon-lysine, X – 21364, X – 24020 and X - 11429 were significantly different between PAH versus all controls and PH sub diagnoses (non PAH) in this model ($p<0.05$). However, levels of these metabolites showed similar differences across all PH sub-diagnoses (Figure 6.9).

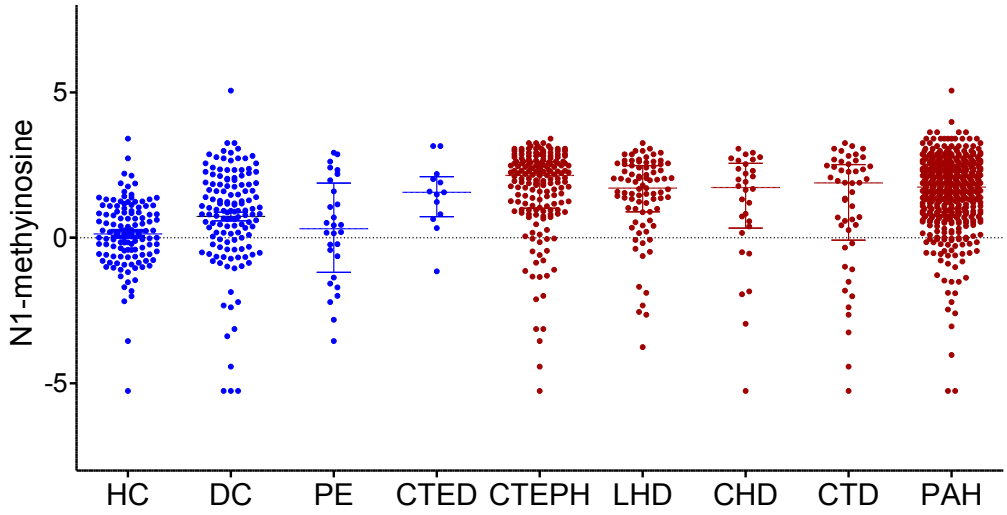


Figure 6.9 – N1-methylinosine levels between control and patient groups. Levels of N1-methylinosine are shown in each diagnostic group including controls (blue) and patients (red). Bar represents mean and standard error of the mean. Levels are significantly increased in PAH versus controls, but show similar trends across all PH sub-diagnoses. Values are z-scored to healthy controls. HC, healthy controls; DC, disease controls; PE, pulmonary embolism; CTED, chronic thromboembolic disease; PAH, pulmonary arterial hypertension; CTEPH, chronic thromboembolic pulmonary hypertension; LHD, left heart disease; CHD, congenital heart disease; CTD, connective tissue disease.

6.4 Discussion

In this study I assessed circulating metabolite levels in different sub-diagnoses of PH, with particular focus on CTEPH where results were validated in a second independent cohort. Discovery analyses were also conducted in PH associated with LHD and PAH due to CHD and CTD, and showed similar differences in metabolic changes across all PH sub-diagnoses.

Patients with CTEPH had significantly increased levels of modified nucleosides, fatty acid acylcarnitines, long/medium chain and monohydroxy- fatty acids, sphingomyelins and metabolites of polyamine and methionine metabolism. Some of these changes, in particular in modified nucleosides and acylcarnitines are similar to those seen in PAH, and also discriminate CTEPH from PE patients indicating they are not a reflection of generalised embolic disease. Following PEA surgery, levels of alpha-ketoglutarate and N2,N2-dimethyguanosine were decreased and levels of sphingomyelins increased. Changes in sphingomyelin levels following PEA surgery were validated in analysis of paired samples taken before and after surgery, but their levels did not relate to a haemodynamic response to surgical intervention.

Changes seen in other PH sub-diagnoses were similar to those observed in PAH with increased modified nucleosides, fatty acid acylcarnitines, TCA cycle intermediates, mono hydroxy fatty acids, tryptophan, polyamine and arginine metabolites, and decreased sphingomyelin, phosphocholines and steroid metabolites across PH sub-diagnoses. Although alterations in metabolite levels could be more pronounced in a specific sub-diagnosis, the overall differences were similar across the various subtypes of PH. This may indicate that the metabolic disturbances reflect changes in cardiopulmonary structure and function which are common to the different sub-diagnoses of PH CTEPH (Wilkins 2012, Matthews and Hemnes 2016) and PH with LHD (Fang, DeMarco et al. 2012). Indeed similarities between CTEPH and PAH with pulmonary arterial remodelling and endothelial cell dysfunction, as well as subsequent RV remodelling are well documented (Humbert 2010, Matthews and Hemnes 2016).

Models of RVH secondary to pulmonary arterial banding show increased fatty acid oxidation in the RV (Fang, Piao et al. 2012). In CTEPH patients the use of a fatty acid tracer (123I-β-methyl iodophenyl pentadecanoic acid (BMIPP)) in scintigraphy imaging showed increased fatty acid uptake in the RV, which was decreased after PEA surgery (Sakao, Miyauchi et al. 2015). Levels of fatty acid acylcarnitines were decreased following PEA surgery in our analysis of paired samples, and may indicate restoration of fatty acid oxidation following an improvement in pulmonary pressure and RV strain following surgery.

In addition, isolated myofibroblast-like cells and endothelial-like cells present in pulmonary vascular tissue surrounding fibrous clots from endarterectomy surgery have reduced mitochondrial numbers, SOD-2 and reactive oxygen species indicating a shift to aerobic glycolysis (Sakao, Hao et al. 2011). Isolated PASMCs from thrombotic tissue following PEA surgery show evidence of PASMC proliferation, apoptosis-resistance and features of aerobic glycolysis, with increased glucose and lactate consumption (Wang, Gan et al. 2013). These findings indicate a detrimental metabolic shift to aerobic glycolysis in CTEPH, similar to that seen in PAH (Archer, Marsboom et al. 2010), is also present in patients with CTEPH. Accumulation of acylcarnitines and TCA cycle intermediates may reflect the general inability of the TCA cycle and beta oxidation to maintain pace with proliferating pulmonary vascular cells and right ventricular overload in turn promoting aerobic glycolysis, which I proposed in idiopathic and heritable PAH but may also be the case in CTEPH, PH-LHD and other PAH sub-diagnoses. Alpha-ketoglutarate levels were decreased following PEA surgery, which may indicate a shift away from aerobic glycolysis following surgical intervention.

Patients with CTEPH had decreased sphingomyelin levels, which increased in patients following PEA surgery. Metabolic disturbances in sphingolipids have not previously been reported in CTEPH. Increased sphingosine (Bujak, Mateo et al. 2016) and sphingosine-1-phosphate (Chen, Tang et al. 2014) have been reported in PAH patients from plasma samples and lung tissue respectively, but levels of these metabolites were not significantly different in the current analysis. Changes to sphingomyelin levels were seen across the PH sub-diagnoses and may represent markers of disease progression – decreased levels are prognostic in PAH, near normal in treated PAH vasoresponders, and more like healthy controls in CTEPH patients following surgery. Levels of ceramide were not measured on this platform but would be useful to study in the future as both precursors to sphingomyelins, or produced by sphingomyelins, (Ogretmen and Hannun 2004) and key mediators of cellular function (Taniguchi and Okazaki 2014). Both ceramide and sphingomyelins have roles in cell proliferation, apoptosis and survival (Taniguchi and Okazaki 2014), relevant to changes seen in pulmonary vascular cells in PH.

Increased levels of symmetric and asymmetric dimethylarginine (SDMA + ADMA) were seen in PH patients versus controls, in particular CTEPH, LHD and CTD. ADMA acts as an endogenous inhibitor of nitric oxide synthase (Dweik 2007) and the reduced bioavailability of vasodilators such as nitric oxide are an important determinant in the pathophysiology of PH and endothelial dysfunction (Cooper, Landzberg et al. 1996). Plasma ADMA levels are known to correlate with severity and outcomes in both PAH and CTEPH (Skoro-Sajer, Mittermayer et al. 2007). My findings of increased

dimethylarginine levels may indicate endothelial dysfunction and impaired NO signalling across several PH sub-diagnoses.

Increased levels of modified nucleosides are seen across the PH sub-diagnoses and are prognostic in PAH, and may reflect pulmonary vascular remodelling, proliferation and stress in all PH sub-diagnoses. Levels of angiogenin have not been measured in patients with CTEPH and would be of interest to assess whether angiogenin mediates tRNA cleavage in these patients.

In order to assess response to PEA surgery, larger cohorts of paired samples would be required which are taken prospectively with follow up in both haemodynamic and functional response to surgery. In addition, comparisons made with patients with LHD, CHD and CTD were in small numbers of subjects and require validation. Although these metabolite changes are not specific to PAH, they still provide potential therapeutic targets for the treatment of these PH sub-diagnoses particularly in energy metabolism and translational regulation.

In order to ascertain whether the metabolite disturbances are causally related to outcomes and mediators of disease progression, an approach assessing genetic variants which determine the levels of these metabolites would be informative.

Chapter 7 - Investigation of the genetic influences of metabolic dysregulation in PAH

7.1 Introduction

Analyses of metabolite levels using NMR spectroscopy, unbiased UPLC-MS and the Metabolon platform have shown increased modified nucleosides, fatty acid acylcarnitines, TCA cycle intermediates, tryptophan and polyamine metabolites and decreased sphingomyelin, phosphocholines and steroid metabolites in PAH and in different diagnoses of PH. Assessment of genetic variants which could underlie these metabolic changes could help determine whether these disturbances are causative in the disease pathophysiology, using techniques such as Mendelian randomisation analyses.

Mendelian randomisation is used to assess whether a variable is causally related to a disease process (Lawlor, Harbord et al. 2008), using the principle that both a genetic variant and variable (such a metabolite or protein) are associated to an outcome and with one other (Swerdlow, Kuchenbaecker et al. 2016). Examples include the use of Mendelian randomisation to show that a variant encoding C reactive protein (CRP) was associated with levels of CRP but not with the risk of cardiovascular disease itself (Collaboration, Wensley et al. 2011). Variants in the low-density lipoprotein receptor gene were found to be associated with elevated risk of coronary artery disease through increased levels of LDL cholesterol, indicating a causal link between LDL cholesterol and coronary disease (Linsel-Nitschke, Gotz et al. 2008). Limited studies have been conducted with Mendelian randomisation in metabolomics. Levels of epiandrosterone sulphate were found to be associated with chronic widespread musculoskeletal pain and highly associated with a variant (rs1581492), however mendelian randomisation using this variant indicated epiandrosterone sulphate was not causally related to the disease process (Livshits, Macgregor et al. 2015).

Several studies have been conducted to assess genetic variants associated with changes in metabolite levels, using metabolomics with genome wide association studies (GWAS) (Kastenmuller, Raffler et al. 2015). The first study was conducted in 2008 in 284 healthy subjects comparing 363 metabolite levels to variant information from GWAS data. This study highlighted four associations between variants and metabolite levels such as glycerophosphocholine, sphingomyelin and acylcarnitines, where the variants were in genes encoding enzymes known to have a biological association to the metabolite (Gieger, Geistlinger et al. 2008).

To date, the largest association studies between metabolite levels and genetic variants have been conducted using a GWAS with metabolite data from the Metabolon platform in large populations of healthy controls from the KORA and TwinsUK studies (Suhre, Shin et al. 2011, Shin, Fauman et al. 2014). Genotyping for the KORA study was conducted using the Affymetrix (Santa Clara, CA, USA) GeneChip array 6.0 and TwinsUK using several Illumina (San Diego, CA, USA) arrays (Illig, Gieger et al. 2010, Suhre, Shin et al. 2011, Shin, Fauman et al. 2014). In the most recent study, 529 metabolite levels, as well as metabolite ratios, were assessed in 7824 healthy controls with 299 SNP-trait associations reaching genome wide significance (Shin, Fauman et al. 2014). Results from these studies have been made available in the Metabolomics GWAS server (Suhre, Shin et al. 2011, Shin, Fauman et al. 2014) and provide information on all genetic variants that associate with metabolite levels in these patients.

Use of Mendelian randomisation in this study as evidence for a causal link between metabolic changes and outcomes in PAH would require that a) the genetic variant is associated with the metabolite level, b) the variant is associated with the outcome (such as disease or survival) via the metabolite, and c) the variant is associated with the outcome, independent of potential confounders.

I set out to investigate a) the association between metabolite levels and genetic variants in PAH patients with a biological association between the affected gene and metabolite, b) the frequency of variants associated with metabolites of interest in the PAH and non-PAH population and c) whether variants associated with prognostic metabolites were themselves associated with survival in PAH patients.

7.2 Methods

See Chapter 2 for detailed experimental methods and protocols.

Whole-genome sequencing data were available from the UK National Institute of Health Research Biomedical Research Centres Inherited Diseases Genetic Evaluation (BRIDGE) consortium, to investigate variants underlying rare diseases. In addition to patients with idiopathic, heritable or anorexigen-induced PAH, the consortium is seeking to undertake whole-genome sequencing in several other rare diseases, including bleeding and platelet disorders, primary immune disorders, paediatric neuro-metabolic diseases, inherited retinal dystrophy, steroid resistant nephrotic

syndrome and Ehlers-Danlos syndromes. Patients with these other rare diseases were used as a control (non-PAH) population to compare with PAH.

Sequencing was conducted by Illumina (San Diego, CA, USA), providing an average coverage above 30X. Data were aligned and quality control conducted by Illumina in order to generate variant call format (VCF) files, a file format used to encode single nucleotide polymorphisms (SNPs). Further quality control analysis and merging of individuals' VCF files to allow comparisons of variant calls between subjects was performed by Dr Stefan Graf and colleagues in the NIHR BRIDGE consortium at the University of Cambridge, which aims to sequence 10,000 whole genomes of people with rare genetic diseases. All the sequencing data were securely stored and analysed on the University of Cambridge High Performance Computing service Darwin cluster.

Variants with known associations with metabolites (also referred to as 'traits') based on published data in human control subjects (Suhre, Shin et al. 2011, Shin, Fauman et al. 2014), were tested for SNP-trait associations in the PAH population. Reference SNP cluster identifications (rsid) were available in the published database (Suhre, Shin et al. 2011, Shin, Fauman et al. 2014) and the Biomart GRCh37 (Ensembl) (Yates, Akanni et al. 2016) database was used to obtain the chromosome locations for these variants. The chromosome location was used to filter the VCF files using bcftools (https://github.com/samtools/bcftools) for the variants that would be analysed in PAH and non-PAH patients.

Initially, 299 of the most robust SNP-trait associations with genome wide significance ($p<1e-13$) in a discovery and validation cohort of 7824 healthy controls were selected from a published dataset (Shin, Fauman et al. 2014). Variants associated with metabolites found to be discriminating (n=97) or prognostic (n=67) in PAH from our previous analysis (detailed in Chapter 5, Appendix Tables 5.1, 5.2), representing 131 unique metabolites, were selected for further analysis.

In a secondary analysis, variant information from human controls with SNP-trait associations ($p<1e-5$) available from the Metabolomics GWAS server (Suhre, Shin et al. 2011, Shin, Fauman et al. 2014) was used to obtain all available variant associations to discriminating or prognostic metabolites in PAH. Variants not present in at least 10 of the PAH samples with metabolite data available were excluded in order to select common variants.

In the published studies, variants had been associated to either metabolite levels or metabolite ratios (Suhre, Shin et al. 2011, Shin, Fauman et al. 2014), therefore variants were compared to corresponding metabolites or ratios.

Associations between variants and metabolite levels or ratios were conducted using analysis of variance (ANOVA) or linear regression with age and gender as covariates. Frequency testing was conducted to assess whether a variant was present more in the PAH group compared to non-PAH group using the Fishers exact test. Survival analysis of variants was conducted using Cox regression analysis on PAH patients with survival outcome data.

Statistical analysis was performed using R with RStudio and associated packages (http://CRAN.R-project.org/).

7.3 Results

At the time of analysis, whole genome sequencing (WGS) data were available for 781 PAH patients and 5906 patients with other rare diseases (non-PAH). Of these 781 PAH patients, 325 also had metabolite data available from the Metabolon platform. Baseline characteristics and laboratory data for these patients are shown in Table 7.1. Patients without PAH did not have the same gender bias as PAH patients. PAH patients with WGS and metabolite data represented a typical cohort of PAH patients with baseline characteristics similar to patients in Chapter 6 (Table 6.5).

	PAH patients with WGS and metabolite data (n=325)	PAH patients with WGS data (n=781)	non-PAH patients with WGS data (n=5906)
Age at sampling, years	52.7 +/- 15.9		
Sex, Female:Male (ratio)	229:96 (2.4:1)	541:240 (2.3:1)	3222:2666 (1.2:1)
Ethnicity, % non-Caucasian	10.5	12.2	11.5
BMI, kg/m^2	29.3 +/- 7.2		
BMPR2 mutation carriers (%)	12.0		
Treatment naïve cases (%)	11.1		
Baseline haemodynamics at diagnosis			
Pulmonary capillary wedge pressure, mmHg	10.0 +/- 5.0		
Mean pulmonary artery pressure, mmHg	54.5 +/- 14.5		
Pulmonary vascular resistance, Woods units	12.2 +/- 6.0		
Mean right atrial pressure, mmHg	9.8 +/- 5.5		
Cardiac output, L/min	4.1 +/- 1.4		
Functional status and pathology			
Six minute walk distance, m	331.1 +/- 163.0		
WHO Functional Class, I/II/III/IV	20/83/180/18		
RDW, %	15.2+/-2.7		
NT-proBNP, pmol/L	868+/-1087		

	PAH patients with WGS and metabolite data (n=325)	PAH patients with WGS data (n=781)	non-PAH patients with WGS data (n=5906)
Creatinine, umol/L	90.0+/-29.0		
Bilirubin, umol/L	13.8+/-10.1		
Comorbidities			
Asthma/COPD	9		
Diabetes	18		
CAD/IHD	11		
AF/flutter	10		
Systemic hypertension	22		
Hypercholesterolaemia/lipidaemia	9		
Drug therapy			
Anticoagulation	68		
PDE5 inhibitors	68		
ERA	56		
Prostanoids	20		
Diuretics	51		
Aldosterone antagonists	19		
Statins/lipid lowering drugs	25		
CCB	19		
Cardiac glycosides	15		
Antidiabetic drugs	13		
Iron replacement therapy	11		
ACE inhibitors	22		

Table 7.1 – Whole Genome Sequencing Cohort Characteristics. Means and standard deviations or counts are given. non-PAH patients are those with other rare diseases. Clinical pathology parameters are shown within 30 days of the sample date. Co-morbidities and drug therapy are shown as the percentage of patients with those co-morbidities or on each agent (%). BMI, body mass index; *BMPR2*, bone morphogenetic protein receptor type 2; WGS, whole genome sequencing; PAH, pulmonary arterial hypertension; COPD, chronic obstructive pulmonary disease; CAD, coronary artery disease; IHD, ischaemic heart disease; AF, atrial fibrillations; PDE5, phosphodiesterase 5; ERA, endothelin receptor antagonists; CCB, calcium channel blocker; ACE, angiotensin converting enzyme. 12 PAH patients with metabolite and WGS data are on CCB therapy as vasoresponders. Ethnicity is shown for subjects who self-declared. Information on gender and ethnicity was not available for 18 non-PAH patients.

Of the 299 SNP-trait associations previously published in healthy controls (Shin, Fauman et al. 2014), 38 associations were related to metabolites which were either discriminating or prognostic in PAH patients from our analysis in Chapter 5.

18/38 SNP-trait associations in healthy controls were validated in PAH patients when accounting for age and gender using linear regression analysis ($p<0.05$) and 11 were significant following Bonferroni correction ($p<0.001$) (Table 7.2). These all had the same effect direction as previously published and included variants associated with acetylcarnitine, steroid metabolites, 4-acetamidobutanoate, valine, hexadecanedioate and kynurenine (Table 7.2).

Locus ID and name (Cytoband)	*SNP and chromosome location*	*Metabolite or ratio with SNP-trait association*	*Biological significance*	*Linear regression (Sig.)*	*Cox regression (Sig.)*	*Frequency testing (Sig.)*
11 SNP-trait associations in PAH (p<0.001)						
60. CYP3A5 (7q22.1)	rs10278040 7_99141373_G _A	androsterone sulfate	*CYP3A5* - encodes P450 which has 6beta-hydroxylation activity against steroids, including progesterone and testosterone (Yamakoshi, Kishimoto et al. 1999).	1.98E-07	0.01	0.67
60. CYP3A5 (7q22.1)	rs7809615 7_99184778_G _T	androsterone sulfate/4-androsten-3beta,17beta-diol disulfate 2*	see above	8.51E-06	0.11	0.51
60. CYP3A5 (7q22.1)	rs11974702 7_99163951_A _G	epiandrosterone sulfate	see above	6.47E-04	0.32	0.34
66. NAT2 (8p22)	rs4921913 8_18272377_C_ T	4-acetamidobutanoate Δ/N1-methyladenosine Δ	*NAT2* encodes arylamine N-acetyltransferase (Sim, Walters et al. 2008). 4-acetamidobutanoate might related to a product , or a product of the enzyme (Shin, Fauman et al. 2014).	8.74E-06	0.27	0.09
66. NAT2 (8p22)	rs721399 8_18259366_C_ T	4-acetamidobutanoate Δ	see above	3.65E-04	0.36	0.29
7. ACADM (1p31.1)	rs4949874 1_76161889_T_ C	acetylcarnitine/hexanoylcarnitine	*ACADM* encodes medium-chain acyl-CoA dehydrogenase, which has enzyme has activity against acyl-CoAs, including hexanoyl-CoA (Finocchiaro, Ito et al. 1987).	1.74E-05	0.33	0.47
94. SLCO1B1 (12p12.1)	rs1871395 12_21352315_ A_G	hexadecanedioate Δ	*SLCO1B1* encodes organic anion transporter (OATP2, OATP-C) (Tamai, Nezu et al. 2000). Polymorphism of the gene has an effect on the ability of HMG CoA reductase inhibitors to decrease lipid levels (Tachibana-Iimori, Tabara et al. 2004).	7.64E-04	0.13	0.07
43. SLC22A4 (5q31.1)	rs274567 5_131714409_C _T	acetylcarnitine	*SLC22A4 & SLC22A5* encode the organic cation transporters OCTN1 and OCTN2 respectively (Shin, Fauman et al. 2014), which are involved in carnitine transport (Xu, Flanagan et al. 2010).	1.22E-03	0.38	0.93

Locus ID and name (Cytoband)	*SNP and chromosome location*	*Metabolite or ratio with SNP-trait association*	*Biological significance*	*Linear regression (Sig.)*	*Cox regression (Sig.)*	*Frequency testing (Sig.)*
62. ZCWPW1 (7q22.1)	rs132225437_100015457_C_T	androsterone sulfate/4-androsten-3beta,17beta-diol disulfate 2*		6.76E-04	0.72	0.92
62. ZCWPW1 (7q22.1)	rs132225437_100015457_C_T	androsterone sulfate		6.76E-04	0.72	0.92
62. ZCWPW1 (7q22.1)	rs132225437_100015457_C_T	epiandrosterone sulfate		6.76E-04	0.72	0.92
7 SNP-trait associations in PAH (p<0.05)						
136. SULT2A1 (19q13.32)	rs29639619_48365523_T_C	4-androsten-3beta,17beta-diol disulfate 1	*SULT2A1* is involved in the sulfation of hormones such as steroids (Weinshilboum, Otterness et al. 1997). Genetic variants close to or at the *SULT2A1* gene are associated with levels of DHEA-S (Zhai, Teumer et al. 2011).	8.07E-03	0.91	0.11
141. PRODH (22q11.21)	rs254064722_18966617_G_A	valine Δ/proline	*PRODH* encodes proline dehydrogenase, involved in proline degradation (Hu, Donald et al. 2007). Subsequent valine changes may be to correct overall amino acid pool levels (Shin, Fauman et al. 2014).	1.06E-02	0.89	0.68
76. AKR1C4 (10p15.1)	rs1713458510_5256272_T_C	androsterone sulfate/epiandrosterone sulfate	*AKR1C4* encodes 3 alpha-hydroxysteroid dehydrogenase (HSD) isoform which acts on androsterone and is expressed in the liver (Penning, Jin et al. 2004).	3.09E-02	0.70	0.91
78. SLC16A9 (10q21.1)	rs117161410_61469538_T_C	acetylcarnitine	*SLC16A9* encodes carnitine efflux transporter (Suhre, Shin et al. 2011)	3.90E-03	0.20	0.40
124. SLC7A5 (16q24.2)	rs805114916_87878822_G_A	kynurenine	*SLC7A5* encodes LAT1, a transporter which mediates tryptophan/kynurenine exchange (Kaper, Looger et al. 2007).	2.82E-02	0.06	0.11
95. SLCO1B1 (12p12.1)	rs1282970412_21388621_G_A	octadecanedioate	see *SLC01B1* above	4.90E-02	0.22	0.47
98 SH2B3 (12q24.12)	rs318450412_111884608_T_C	kynurenine		8.59E-03	0.50	0.11
20 SNP-trait associations in PAH (p>0.05)						
33. SLC2A9 (4p16.1)	rs9385544_9925692_C_G	urate Δ		1.23E-01	0.37	0.50
58. DDC (7p12.2)	rs78092347_50610379_A_T	indoleacetate/N2,N2-dimethylguanosine Δ		1.33E-01	0.14	0.40
49. SLC17A3 (6p22.2)	rs27623536_25794431_A_G	4-androsten-3beta,17beta-diol disulfate 2*		1.59E-01	0.20	0.41
73. CRAT (9q34.11)	rs78492709_131874641_A_G	C-glycosyltryptophan*/ succinylcarnitine		2.18E-01	0.38	0.41
33. SLC2A9 (4p16.1)	rs68380214_9927620_T_C	urate Δ/histidine		3.17E-01	0.58	0.47

Locus ID and name (Cytoband)	*SNP and chromosome location*	*Metabolite or ratio with SNP-trait association*	*Biological significance*	*Linear regression (Sig.)*	*Cox regression (Sig.)*	*Frequency testing (Sig.)*
4. CYP4A11 (1p33)	rs66637311_47347427_A_T	hexadecanedioate Δ		4.15E-01	0.33	0.25
96. GLS2 (12q13.2)	rs269491712_56912864_T_C	glutamine/histidine		4.17E-01	0.52	0.54
136. SULT2A1 (19q13.32)	rs29639619_48365523_T_C	dehydroisoandrosterone sulfate (DHEA-S) Δ		4.60E-01	0.91	0.11
49. SLC17A3 (6p22.2)	rs11855676_25818588_A_G	dehydroisoandrosterone sulfate (DHEA-S) /4-androsten-3beta,17beta-diol disulfate 2*		4.64E-01	0.20	0.43
70. ADHFE1 (8q13.1)	rs1011257448_67381268_G_A	X-04499--3,4-dihydroxybutyrate/C-glycosyltryptophan* (tested C-glycosyltryptophan*)		5.01E-01	0.32	0.50
65. ABP1 (7q36.1)	rs10053907_150543721_T_G	4-acetamidobutanoate/ X-03056--N-[3-(2-Oxopyrrolidin-1-yl)propyl]acetamide (tested 4-acetamidobutanoate))		5.01E-01	0.68	0.45
43. SLC22A4 (5q31.1)	rs2728895_131665378_A_G	valine Δ/ isovalerylcarnitine		5.47E-01	0.44	0.87
105. ASPG (14q32.33)	rs414402714_104357638_T_C	asparagine		5.54E-01	0.32	0.62
27. TKT (3p21.1)	rs468771753282188_T_C	phosphate/ erythronate*		5.80E-01	0.44	0.70
136. SULT2A1 (19q13.32)	rs18242019_48372195_C_T	androsterone sulfate		7.07E-01	0.81	0.54
35. PPM1K (4q22.1)	rs14405814_89226422_T_C	valine Δ		7.54E-01	0.24	0.48
136. SULT2A1 (19q13.32)	rs254723119_48385057_C_A	X-11440/4-androsten-3beta,17beta-diol disulfate 2 (tested 4-androsten-3beta,17beta-diol disulfate (2))		7.71E-01	0.82	0.11
33. SLC2A9 (4p16.1)	rs1686824649978305_C_G	histidine		8.59E-01	0.34	0.42
27. TKT (3p21.1)	rs468771753282188_T_C	erythronate*		8.84E-01	0.44	0.70
43. SLC22A4 (5q31.1)	rs2739145_131660431_A_T	oleoylcarnitine		9.10E-01	0.50	0.98

Table 7.2 – 38 SNP-trait associations in PAH patients. 38 SNP-trait associations from analysis of healthy controls (Shin, Fauman et al. 2014) assessed in PAH patients are shown. For the variant/SNP (single nucleotide polymorphism), the reference SNP cluster identification (rsid) and chromosome location is shown. Significance (Sig.) from linear regression analysis between the SNP and metabolite taking into account age and gender, Cox regression analysis of the variant in PAH patients, and frequency testing between PAH (n=781) and non-PAH patients (n=5906) using Fishers exact test are shown. Significant associations with a biological link between the metabolite and locus identification (ID) are shown. Δ indicates metabolites which are prognostic in PAH patients. If metabolite information for a ratio was not available, the metabolite tested in shown. PAH, pulmonary arterial hypertension; HMG-CoA, 3-hydroxy-3-methyl-glutaryl-coenzyme A; *ACADM*, acyl-coenzyme A dehydrogenase; DHEA-S, dehydroisoandrosterone sulfate.

A plausible biological association between the gene affected and the metabolite could be found for 14/18 SNP-trait associations (Table 7.2). For example, acetylcarnitine was associated with the *SLC22A4* gene which encodes a carnitine transporter (Xu, Flanagan et al. 2010, Shin, Fauman et al. 2014) (Figure 7.1), and androsterone sulfate was associated with the *CYP3A5* gene which encodes an enzyme involved in steroid hormone metabolism (Yamakoshi, Kishimoto et al. 1999) (Figure 7.2).

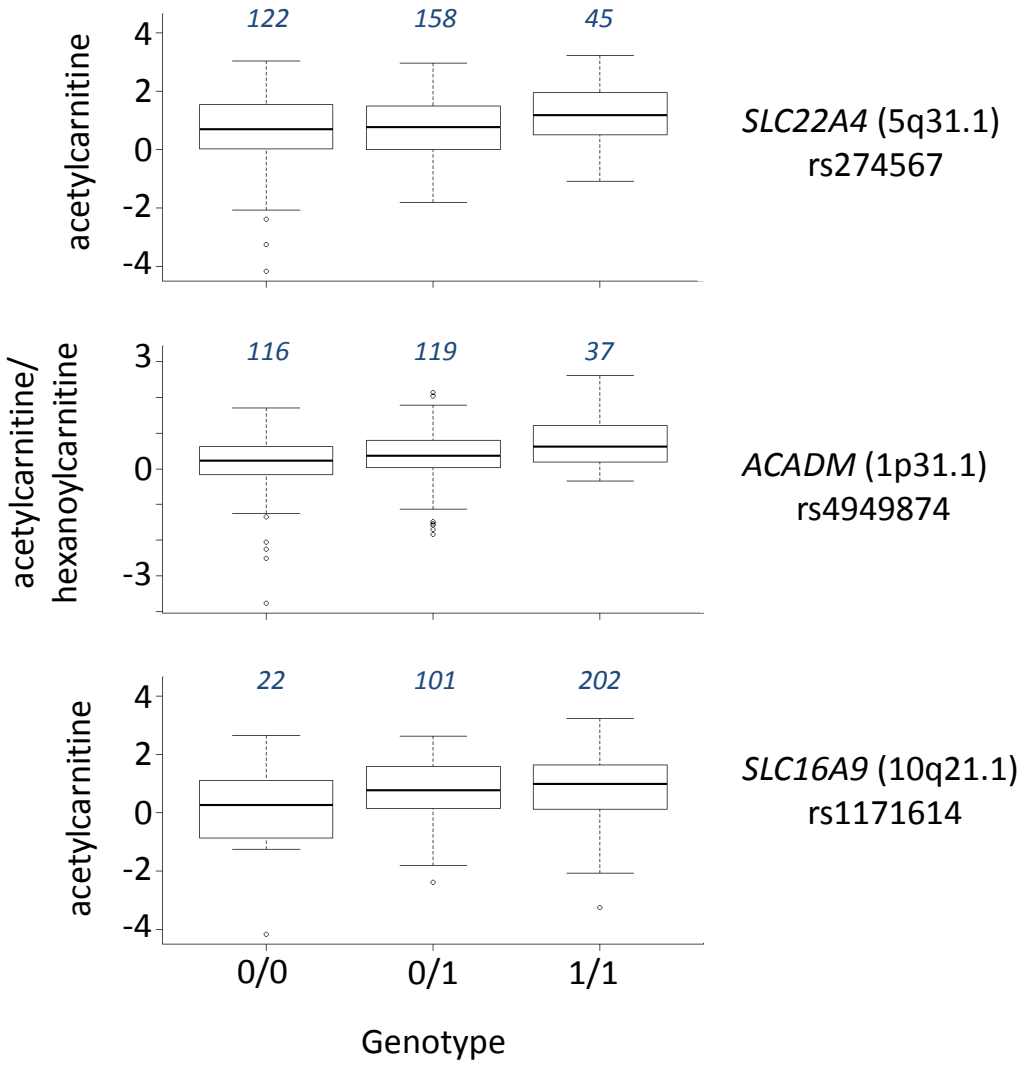


Figure 7.1 – SNP-trait (single nucleotide polymorphism) associations with acylcarnitines in PAH patients. Three examples of significant associations between variants and acylcarnitines are shown where the genetic locus has a biological association to the metabolite. Levels of acylcarnitines or ratios are shown for different genotypes – 0/0 homozygous for the reference, 0/1 heterozygous for the reference and 1/1 homozygous for the alternate allele. The number of subjects with each genotype for a given variant are shown in blue. Locus identities for the gene and reference SNP cluster identification (rsid) are shown.

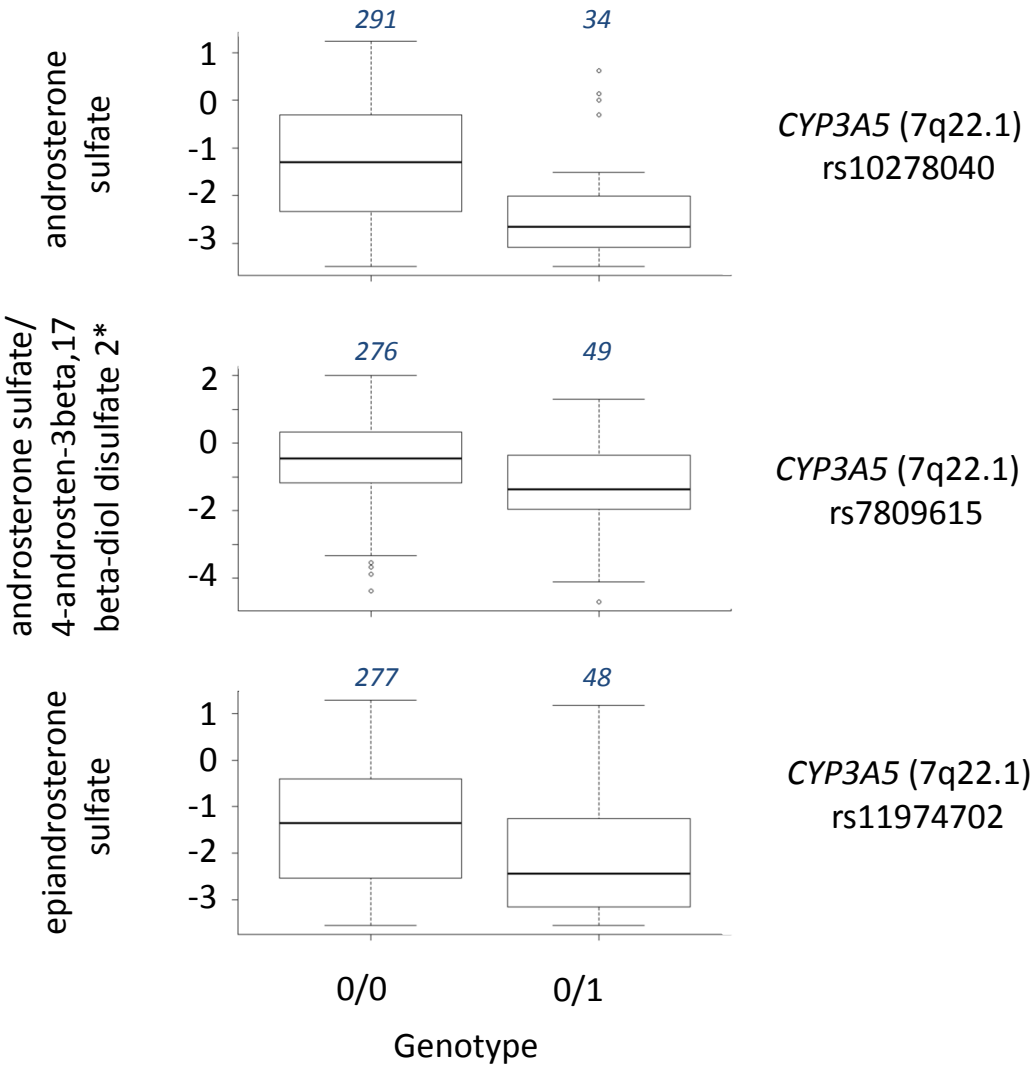


Figure 7.2 – SNP-trait associations with steroid hormones in PAH patients. Three examples of significant associations between variants in the CYP3A5 locus and steroid hormones are shown where the genetic locus has a biological association to the metabolite. Levels of steroid hormones are shown for different genotypes - 0/0 homozygous for the reference and 0/1 heterozygous for the reference allele. The number of subjects with each genotype for a given variant are shown in blue. Locus identities for the gene and reference SNP cluster identification (rsid) are shown.

None of the 38 variants were significantly associated with PAH after frequency testing between PAH and non-PAH patients (all p>0.05).

Complete survival information was available at the time of analysis for 284/781 PAH patients irrespective of whether these patients had metabolite information. 81/284 PAH patients died with a median follow up of 3.7+/-1.6 years. 1/38 variants were prognostic in PAH patients (p<0.05) but did not meet Bonferroni correction (p<0.003). This variant was associated with a metabolite (androsterone sulphate) which was not prognostic in PAH patients.

In my initial approach I focused on published variants which were associated with metabolite levels and had met genome wide significance (p<1e-13). In an alternative approach to broaden the number of variants assessed I looked at published variants associated with metabolites with a significance level of p<1e-5 from the Metabolomics GWAS server focusing again on metabolites found to be discriminating or prognostic in PAH. Information for 28/131 of these metabolites was available in the Metabolomics GWAS server represented by associations to 14011 variants (Table 7.3). Variants not present in at least 10 subjects were excluded leaving 13060 variants for further analysis, equivalent to a minor allele frequency of 1.5%. 938 variants had a significant association to the metabolite level (p<0.05 by ANOVA) however none met Bonferroni correction (p>3.8e-6) and therefore were not pursued for associations with disease status or severity.

Metabolite	Metabolic Pathway	Number of associated variants in GWAS server (p<1e-5)
4-acetamidobutanoate	Polyamine Metabolism	990
acetylcarnitine	Fatty Acid Metabolism(Acyl Carnitine)	589
alpha-ketoglutarate	TCA Cycle	321
androsterone sulfate	Steroid	495
arginine	Urea cycle; Arginine and Proline Metabolism	463
asparagine	Alanine and Aspartate Metabolism	937
C-glycosyltryptophan*	Tryptophan Metabolism	321
dehydroisoandrosterone sulfate (DHEA-S)	Steroid	391
epiandrosterone sulfate	Steroid	403
erythronate*	Aminosugar Metabolism	906
glutamate	Glutamate Metabolism	204
hexadecanedioate	Fatty Acid, Dicarboxylate	681
histidine	Histidine Metabolism	323
kynurenine	Tryptophan Metabolism	989
malate	TCA Cycle	490
N1-methyladenosine	Purine Metabolism, Adenine containing	144
N2,N2-dimethylguanosine	Purine Metabolism, Guanine containing	947
N-acetylalanine	Alanine and Aspartate Metabolism	358
N-acetylthreonine	Glycine, Serine and Threonine Metabolism	268
octadecanedioate	Fatty Acid, Dicarboxylate	468
oleoylcarnitine	Fatty Acid Metabolism(Acyl Carnitine)	351
palmitoylcarnitine	Fatty Acid Metabolism(Acyl Carnitine)	315
pro-hydroxy-pro	Urea cycle; Arginine and Proline Metabolism	483
pseudouridine	Pyrimidine Metabolism, Uracil containing	383
urate	Purine Metabolism, (Hypo)Xanthine/Inosine containing	1212
valine	Leucine, Isoleucine and Valine Metabolism	137
X-12100	Unknown	830
xanthine	Purine Metabolism, (Hypo)Xanthine/Inosine containing	136

Table 7.3 – Number of variants associated with metabolites of interest from the Metabolomics GWAS (genome wide association study) server. 28/131 discriminating or prognostic metabolites in PAH which have associated variants in the Metabolomics GWAS server are shown with the number of associated variants per metabolite.

7.4 Discussion

In this study I validated associations between genetic variants and plasma metabolites, found in healthy control populations, in patients with PAH. This included variants associated with acetylcarnitine, steroid metabolites, 4-acetamidobutanoate, valine, hexadecanedioate and kynurenine, where the gene locus had a biological link to the metabolites affected. For example, a variant (rs274567) in the *SLC22A4* gene, which is involved in carnitine transport (Xu, Flanagan et al. 2010) was associated with increased levels of acetylcarnitine, a metabolite which is increased in PAH patients compared to controls. However, these variants were not found to be more frequent in PAH patients compared to non-PAH patients or associated with outcomes such as survival.

A variant in the *ACADM* (acyl-coenzyme A dehydrogenase) gene was related to metabolite levels of acylcarnitines in the dataset and is known to encode medium chain acyl coA dehydrogenase (MCAD), an enzyme involved in the conversion of acyl-coA to acetyl-coA. Children with MCAD deficiency have increased levels of plasma acylcarnitines (Matern and Rinaldo 1993) and increased expression of *ACADM* has been demonstrated in lung tissue from patients with severe PAH (Zhao, Peng et al. 2014). Patients with PAH may overexpress the *ACADM* gene in the lung tissue, where a variation in the gene leads to impaired conversion of acyl-coA to acetyl-coA which would normally enter the TCA cycle and leads to a subsequent build-up of acylcarnitines.

A difficulty in Mendelian randomisation analyses is limited power to detect a causal link between a variable and an outcome (Smith and Ebrahim 2004, Burgess, Butterworth et al. 2016). In a rare disease such as PAH there are limited numbers of patients to obtain sequencing and metabolite data, and there is also limited information on outcomes such as survival. The present study may have been underpowered to establish a causal link between metabolite levels and outcomes. In the future, increased numbers of PAH patients with whole genome sequencing data and outcome information on survival would increase the power to assess causal links in this population, although numbers available in PAH will always be limited compared to more common diseases.

In this study I focused on SNP-trait associations established in a large population of healthy controls (Suhre, Shin et al. 2011, Shin, Fauman et al. 2014). These only represented a subset of metabolites we have found to be discriminating or prognostic in PAH patients. With increased studies of variants associated with metabolites studies in larger populations taking place, more information will be available on established SNP-trait associations which can be assessed in the PAH population.

This analysis describes preliminary assessment of metabolomics and WGS data in PAH which has validated SNP-trait associations, discovered in healthy controls, in this disease population. This

suggests that these genes, and associated proteins, are potential therapeutic targets if the impact of the associated metabolite disturbances in PAH is confirmed through an alternative approach such as in vivo experimentation.

Chapter 8 – Conclusions and future work

This thesis began with NMR spectroscopy of plasma detailing differences in energy metabolism (citric acid, glutamine), 3-hydroxybutyrate and HDL subtypes in PAH patients that were related to clinical outcomes. Experimentation with unbiased UPLC-MS found metabolite signatures of PAH targeted therapies relating to drug dosage and identified non-adherent patients. In addition, I identified novel metabolic abnormalities such as increased acylcarnitines and decreased sphingomyelins and phosphocholines that also related to adverse outcomes in PAH patients. Due to difficulties in identifying some key metabolic signatures using these methodologies, a commercial approach (DiscoveryHD4™, Metabolon Inc. USA) was also used. This provided access to an extensive library of metabolites, enabling both the validation of many of the earlier findings and the identification of novel changes in modified nucleosides, tryptophan, polyamine and steroid metabolites in PAH that both distinguish PAH patients from controls and are prognostic (Rhodes, Ghataorhe et al. 2016). While most of the investigations were cross sectional in nature, changes in an individual patient's metabolite levels over time were also associated with improved survival. In support of this, patients defined as PAH vasoresponders or CTEPH patients following PEA surgery, had metabolic profiles comparable with those seen in the healthy control population.

8.1 Metabolic pathway abnormalities in PAH

Several metabolic pathways were found to be dysregulated in PAH and provide potential therapeutic targets.

A key example is decreased levels of large HDL subtypes which are prognostic in PAH. These results require validation in a distinct cohort of patients and controls, but suggest an agent which specifically increases levels of large HDL, rather than total HDL levels, may have promise as a therapeutic drug in PAH. In addition, several changes to energy metabolism were seen in PAH patients including increased fatty acid acylcarnitines, TCA cycle intermediates (malate, fumarate, citrate) and glutamate. Correction of the rate limiting step within the TCA cycle may provide a means to restore function of the TCA cycle, and subsequent build-up of acylcarnitines, glutamate and acetyl-coA which promote aerobic glycolysis. Levels of acetyl-coA were below the limit of detection in several samples using a targeted fluorometric approach and may require a more sensitive assay in the future. One of the most robust discriminating and prognostic markers were modified nucleosides. These include N2,N2-dimethylguanosine, which was decreased following PEA surgery.

The correction of altered translational regulation is being investigated as a therapeutic strategy in cancer (Bhat, Robichaud et al. 2015) and similar approaches could also be explored for their utility in PAH.

8.2 Current methodology

Metabolomics technologies applied in this thesis include NMR spectroscopy, unbiased UPLC-MS profiling, a commercial UPLC-MS approach through Metabolon and the combination of metabolomics data with analysis of whole genome sequencing data in PAH patients and controls.

The samples used in these experiments were donated by patients over a broad period (2002-2015), during which treatment strategies have changed. For example, the recommendation to use PDE5 inhibitors in PAH patients was introduced in 2005 (Galie, Ghofrani et al. 2005). In addition, the demographics of the disease have altered from a younger to older population of patients diagnosed with PAH (Hoeper and Gibbs 2014). In the analyses of patients with PAH and CTEPH, the discovery cohorts were age- and sex-matched with the control group and recruited consecutively from 2011 to 2013. In contrast, the validation cohort comprised a more diverse, heterogenous population of non-consecutive patients recruited from 2002 to 2015. The design of this study is however in keeping with recommendations for biomarker studies where the discovery population should comprise a homogenous population with a well-defined phenotype, while the validation group can be more diverse and represent the reality of clinical situations (de Lemos, Rohatgi et al. 2015).

The majority of patients included in this study were prevalent cases on established treatments. Corrections were made for potential confounding effects in the main analyses, including PAH-specific drugs and therapies related to comorbidities, as well as demographics and renal/hepatic function. Further prospective studies, enrolling new referrals with incident disease are required in order to validate changes in circulating metabolites following therapeutic interventions and distinguish responders from non-responders.

Patients and controls were sampled in a non-fasting state and information on insulin resistance was not available for all cases. Insulin resistance is frequently observed in PAH patients and is prognostic (Zamanian, Hansmann et al. 2009). Metabolic disturbances in diabetes and insulin resistance include alterations in branch chain amino acids, fructose, glucose, pro-hydroxy-pro, and metabolite changes seen in PAH including DHEA-S, acylcarnitines and 1-lineoyl-GPC (Newgard, An et al. 2009, Yengo, Arredouani et al. 2016). I cannot exclude the possibility that metabolite levels were altered by

diabetes in this study, but correction was made for subjects on anti-diabetic therapy. Further correction using circulating markers such as glucose and glycated haemoglobin may improve future studies.

A large proportion of metabolites measured through the unbiased UPLC-MS platform could not be identified with current annotation techniques. Although the use of a commercial metabolomics approach allowed assessment of several hundred named metabolite features, this was limited by the metabolites that had been annotated in the Metabolon reference library and may not be representative of all circulating metabolites. Analysis of metabolomics data requires standardisation as differences between studies may lead to discrepancies when examining the same disease process (Kelly, Dahlin et al. 2016).

Measurements of metabolites using technology such as LC-MS are biased to the detection of highly abundant metabolites, and signals from low-abundant metabolites cannot always be determined (Dutta, Shetty et al. 2012). Metabolite signals are not only endogenous, but may include exogenous metabolites from food or medications (Wang, Byun et al. 2010), and corrections were made where possible for exogenous signatures in the analysis of datasets in this thesis.

Another important factor in determining an individuals metabolite levels is the gut microbiome (Holmes, Li et al. 2012). Several studies have been conducted to assess the human microbiome (Qin, Li et al. 2010, Human Microbiome Project 2012), and in particular the gut microbiome (Li, Jia et al. 2014) which contains over a thousand species of bacteria (Lozupone, Stombaugh et al. 2012). Changes to the gut microbiome are associated with metabolic conditions such as obesity (Ley, Turnbaugh et al. 2006), systemic hypertension (Yang, Santisteban et al. 2015) and cardiovascular disease through dietary phosphatidylcholines (Wang, Klipfell et al. 2011). The gut microbiome may also influence vascular function and the development of pulmonary vascular disease through regulating inflammatory responses (Prakash, Sundar et al. 2015) and smooth muscle cell proliferation (Kinlay, Michel et al. 2016). In the future, studies could take into consideration the effect of the gut microbiome on metabolite levels and whether the microbiome could be targeted to alter metabolite levels and vascular pathology in PAH.

In Chapter 7, preliminary analysis validated associations between genetic variants and metabolite levels from healthy controls in PAH patients, such as the relationship between variants on the *ACADM* gene, which encodes medium chain acyl coA dehydrogenase and is up-regulated in the lung tissue of PAH patients (Zhao, Peng et al. 2014), and levels of acylcarnitines. These variants were not associated with outcomes, perhaps reflecting a lack of power in the study. Nevertheless, the findings

suggest that these genes and their associated proteins could be potential therapeutic targets for modulation of metabolism in PAH.

8.3 Utility of metabolomics in PAH

This study suggests that metabolomics can be used to discriminate PH patients from controls, predict survival in PAH patients and potentially be used to monitor response to therapy.

Caution is required for the use of metabolomics as a diagnostic tool (Ala-Korpela 2016, Ala-Korpela and Davey Smith 2016). For translation into clinical practice the metabolites should a) be specific to the disease itself and not represent an overall 'disease' pathology, b) discriminate subtypes of the disease and arguably most importantly, c) predict outcomes (Kelly, Dahlin et al. 2016). In this study, metabolic signatures were found to discriminate PAH patients from disease control groups, and predict outcomes such as survival and response to therapy, but did not distinguish between the subtypes of PH that were studied.

A commercial UPLC-MS metabolomics approach was also used to assess circulating metabolite levels in PH sub-diagnoses, in particular CTEPH. Metabolic signatures were found to be similar in a preliminary (un-validated) assessment of PH due to left heart disease and PAH associated with connective tissue or congenital heart disease. These findings indicate that although metabolic changes distinguish PH patients from disease controls with similar cardiovascular co-morbidities such as coronary disease, diabetes and hypertension, they may be common to different sub-diagnoses of PH. Nevertheless, the predictive power of differences in metabolite levels is considered to be of greater value than the ability to discriminate between disease sub-phenotypes (Kelly, Dahlin et al. 2016). This study supports the use of metabolic signatures as prognostic indicators in PAH.

Another translational application of metabolite measurements is the ability to assess drug levels for PAH targeted therapies and identify issues with adherence. This may provide an important tool for clinicians and in particular, an objective measure for research studies and clinical trials to assess adherence.

In this thesis, I showed that correction of metabolites over time was related to improved survival. In order to fully establish whether metabolite changes reflect a response to PAH targeted therapy, measurements are required before and after the initiation of therapy with subsequent longitudinal measures compared to markers of response such as 6MWD, NT-proBNP, haemodynamics and

mortality (Peacock, Naeije et al. 2009). This would allow assessment of whether continuous monitoring of metabolite levels indicates a clinical response in PAH patients.

8.4 Future studies

Future studies may allow improved assessment of a broader range of named metabolites. In addition, prospective studies can be used to assess longitudinal changes in metabolite levels related to alternative measures of survival and response to therapy in PAH. Identifying the source of these metabolite changes, and their pathogenic implication in PAH could be achieved through transpulmonary sampling and integration of different 'omics' platforms. This could be used to identify potential therapeutic targets and consider translational applications, such as metabolic imaging, for the clinical use of metabolomics in PAH.

Several discriminating and prognostic metabolic features were not identified using the unbiased UPLC-MS approach and increased availability of authentic standards, reference databases and analysis pipelines may allow these features to be annotated in the future. In addition, identified metabolites from the Metabolon dataset could be used to help identify unannotated UPLC-MS peaks.

In this study, lipid features were measured using NMR spectroscopy, unbiased lipidomic UPLC-MS profiling, and the Metabolon UPLC-MS analysis. Results from lipid NMR spectroscopy require validation using samples from distinct healthy controls and PAH patients. Improved identification through analysis of a larger library of lipid standards would allow annotation of several lipidomic features which were unidentified from unbiased UPLC-MS. Another approach may be a detailed lipidomic study conducted using Metabolon's TrueMass^{TM} Complex Lipid Panel which can identify around 1000 lipid features such as triacylglycerols, phosphatidylethanolamines, sphingomyelins, free fatty acids, cholesteryl esters and phosphatidylcholines.

The main outcome measure assessed in this thesis was survival due to all-cause mortality, although patients with PAH often have co-morbidities that could also affect mortality. Metabolite levels were compared to established predictors of survival, namely NT-proBNP (Nagaya, Nishikimi et al. 2000), 6MWD (Fritz, Blair et al. 2013) and RDW (Rhodes, Wharton et al. 2011). The predictive value of metabolite changes could also be compared with other prognostic indicators in PAH. Large-scale registries of patients with PAH have led to the development of prognostic equations which combine several clinical parameters to define a prognostic risk score for PAH patients (McGoon, Benza et al.

2013) using algorithms such as the REVEAL equation (Benza, Miller et al. 2012). This equation includes information on sub-diagnosis, age, gender, renal insufficiency, WHO functional class, systolic blood pressure, heart rate, 6MWD, NT-proBNP, presence of pericardial effusion, predicted diffusing capacity for carbon monoxide, mean right atrial pressure and pulmonary vascular resistance. The equation was established in PAH patients with predominantly prevalent disease (Benza, Miller et al. 2010) and was subsequently validated in an incident cohort (Benza, Miller et al. 2012). However, equations such as this were designed to assess risk at diagnosis rather than for serial assessment during follow up (Raina and Humbert 2016). The prospective collection of plasma samples before and after the initiation of therapy, together with detailed clinical phenotypic characterisation and longitudinal assessment of patients' outcomes, would enable a direct comparison between metabolic profiling and established predictors of survival.

PAH patients who are *BMPR2* mutation carriers were found to have comparable metabolic profiles to non-mutations carriers. This was unexpected as patients with pathogenic *BMPR2* mutations have been shown to have more severe clinical phenotypes and poorer outcomes (Evans, Girerd et al. 2016). However, this was not the case in this study suggesting this relatively small group may not be representative of the *BMPR2* mutation carrier population. Future studies, focussing recruitment on PAH patients at diagnosis would include incident *BMPR2* mutation carriers presenting at an earlier stage with more severe disease, whose metabolite profiles could be assessed longitudinally and related to outcomes.

While plasma is readily accessible, it comprises a pool of metabolites that reflects the integrated input and output of many tissues and biological systems and the vast majority are not tissue specific. It is therefore difficult to derive insights into tissue- and cellular-level mechanisms when using plasma alone. In order to localise the source of differences in plasma metabolite levels, sampling can be conducted across specific vascular beds or metabolic imaging may be used to localise metabolite changes to the diseased lung tissue or myocardium. Transpulmonary sampling at different locations across the cardiopulmonary system during right heart catheterisation would allow assessment of whether the levels of metabolites are changing across the pulmonary vascular bed in PAH, providing tissue-specific evidence of production or consumption (Gutierrez, Venbrux et al. 2007). The direct measurement of lung tissue levels and immunohistochemical localisation of metabolites in tissue sections may also help to corroborate the pulmonary source of circulating metabolites that are altered in PAH.

A key tool for validating the causal and pathogenic importance of metabolic dysregulation is Mendelian randomisation. To identify more genetic variants associated with the levels of

metabolites of interest, published databases such as KEGG (Kyoto Encyclopaedia of Genes and Genomes) (Kanehisa, Sato et al. 2016) can be interrogated to investigate enzymes associated with these metabolic pathways and the genes encoding them. Variants within these genes can subsequently be assessed in PAH patients to identify their association with metabolite levels in corresponding pathways, and with outcomes such as survival. For example, CPT1 is an enzyme involved in the formation of acylcarnitines from acyl-coA and the mitochondrial translocation of acylcarnitines (McGarry and Brown 1997). Neonates with *CPT1A* deficiency have decreased synthesis and levels of acylcarnitines (Bennett and Santani 1993). Variants in the gene encoding CPT1, carnitine palmitoyltransferase 1A (*CPT1A*), could be tested for associations with the levels of plasma acylcarnitines and survival in PAH.

Variants in genes encoding enzymes involved in HDL metabolism, for example CETP, might be predicted to relate to levels of HDL subclasses in PAH. Subjects with homozygous *CETP* deficiency have increased levels of the HDL2 subclass and an improved ability for cholesterol efflux when compared to control HDL2 (Matsuura, Wang et al. 2006). Variants in or near to the *CETP* gene (16q21) are associated with increased HDL cholesterol levels and reduced risk of myocardial infarction, indicating a causal link between CETP, HDL cholesterol and coronary artery disease (Thompson, Di Angelantonio et al. 2008, Ridker, Pare et al. 2009). Mutations in the *ABCA1* gene lead to decreased or absent HDL cholesterol levels and premature coronary disease in an autosomal recessive disorder called Tangiers disease (Rust, Rosier et al. 1999). Subjects with mutations in genes encoding ApoA1 have decreased HDL cholesterol, increased endothelial dysfunction and coronary artery disease risk, similar to the phenotype of subjects with familial hypercholesterolaemia (Hovingh, Brownlie et al. 2004). A Mendelian randomisation approach to assess variants in genes encoding CETP, ABCA1, LCAT and ApoA1 has not been conducted in relation to HDL subclass levels and outcomes in PAH patients.

As well as Mendelian randomisation, future studies involving *in vivo* experimentation could provide further information as to whether the metabolic changes identified are pathological disturbances in PAH. For example, knockout animal models for key genes which encode rate limiting enzymes in metabolic pathways of interest would provide information on whether these disturbances are pathogenic in PAH, and would act as potential therapeutic targets.

Preliminary analysis of whole genome sequencing data and measurement of targeted proteins (e.g. ApoA1 and angiogenin) has been conducted in this study. The integration of genomics, transcriptomics, proteomics, and metabolomics data may also be informative, providing a comprehensive insight into the underlying biological changes and disease process (Wanichthanarak,

Fahrmann et al. 2015, Ala-Korpela and Davey Smith 2016, Cambiaghi, Ferrario et al. 2016). Indeed, the analysis of circulating metabolite data alone may be limited due to the complex regulation of metabolites by cellular and tissue-specific processes, mRNA, epigenetic and post translational proteomic modifications (Wanichthanarak, Fahrmann et al. 2015).

However, the integration of multiple 'omics' datasets remains a challenge (Wanichthanarak, Fahrmann et al. 2015, Cambiaghi, Ferrario et al. 2016). While several software tools are available such as MetaCore™ (Thomson Reuters, NY, USA) and MetaboAnalyst (Xia, Sinelnikov et al. 2015), with large reference databases of molecular interactions, they have limitations such as lack of proteomic input and incomplete biological pathway annotation (Cambiaghi, Ferrario et al. 2016).

Network analysis provides another means of prioritising metabolites for pharmacological targeting, by integrated assessment of metabolic pathway dysregulation in relation to the entire metabolic, proteomic, transcriptomic and genomic network. PAH comprises a heterogeneous disease group, involving numerous molecular and pathological mechanisms, and multiple organs. Patients with similar clinical manifestations (sub-diagnoses) also vary markedly in their outcomes and responses to therapy. A systems wide approach is required to understand the complex genetic, epigenetic and environmental influences and interaction of molecular pathways that underlie these differences. This involves computational analysis of multiple datasets and modelling of the dynamic interactions of genes, proteins and metabolites through networks in an 'interactome' (Lusis and Weiss 2010, Barabasi, Gulbahce et al. 2011, Vidal, Cusick et al. 2011, Menche, Sharma et al. 2015). This has led to various research initiatives such as the MAPGen program (http://www.mapgenprogram.org/) and the Human Interactome Project (http://interactome.dfci.harvard.edu/H_sapiens/) at the Centre for Cancer and Systems Biology, Boston USA.

The application of system wide network analysis in the field of pulmonary vascular disease has been limited and probably reflects the shortage of available data (Brittain and Chan 2016). An example of where this approach has been applied is in the analysis of the role of microRNAs in controlling vascular tone and pulmonary hypertension (Parikh, Jin et al. 2012, Bertero, Lu et al. 2014, Bertero, Cottrill et al. 2015). A similar approach can be applied to the current metabolomics data, to prioritise key metabolite changes in pulmonary hypertension and to identify focal proteomic or genetic changes related to metabolic disturbances, and could provide potential therapeutic targets.

Two major barriers to the translational application of metabolomics are the expensive equipment and level of expertise required to operate the complex equipment and undertake statistical analysis of the data. A commercially available bench-top metabolomics instrument called the High Field

Asymmetric Waveform Ion Mobility Spectrometry (FAIMS) device (Lonestar from Owlstone Ltd., Cambridge) (Arasaradnam, McFarlane et al. 2014) has shown promise as a clinical application for metabolite assessment in real time. FAIMS technology allows point of care testing at the bedside, which can be operated by research nurses, and measures signatures from volatile organic compounds that emanate from clinical samples such as urine. FAIMS technology has already been shown to distinguish between control groups and patients with lung and colorectal cancer (Arasaradnam, McFarlane et al. 2014). This device can be used to investigate whether metabolites of interest from this study can be measured in urine. In addition, novel metabolic signatures from volatile organic compounds which distinguish patients from controls can be investigated for their clinical utility.

Evidence of increased aerobic glycolysis has been localised to the lung (Xu, Koeck et al. 2007) and RV (Oikawa, Kagaya et al. 2005) of PAH patients using 18F-FDG PET imaging, however this technique has the disadvantage of radiation use. Metabolic MR imaging, using hyperpolarised tracers such as ^{13}C pyruvate as a marker of aerobic glycolysis, can also be used to assess tissue metabolism *in situ* and has been conducted in pre-clinical studies of the myocardium (Schroeder, Clarke et al. 2011, Tyler and Neubauer 2016), and more recently in four human healthy controls (Cunningham, Lau et al. 2016). This non-invasive, non-irradiating technique has the potential to identify myocardial ischaemia and cardiomyopathies (Schroeder, Clarke et al. 2011). This has promise in PAH to assess whether changes in energy metabolism are seen in the right ventricle, in a way that could be readily translated to clinical practice. Further advances require the development of new tracers that represent metabolic pathways in addition to energy metabolism. There is also scope to integrate metabolite information with machine learning based analysis of high resolution CMR imaging and correlate circulating metabolite levels to regions of RV wall stress (Schafer, de Marvao et al. 2016).

8.5 Final comments

In conclusion, this study has demonstrated metabolic dysregulation in PAH involving several pathways including increased circulating modified nucleosides (N2,N2-dimethylguanosine, N1-methylinosine), TCA cycle intermediates (malate, fumarate, citrate), glutamate, fatty acid acylcarnitines, polyamine and tryptophan metabolites and decreased levels of large HDL subtypes, steroids, sphingomyelins and phosphatidylcholines, which predict poor survival. Many alterations also remain unidentified. Key metabolic derangements are seen in different sub-diagnoses of PH, and improvements in circulating metabolite levels are associated with a better prognosis, and reflect

response to PEA surgery in CTEPH patients. These findings require further investigation through validation experiments, network analysis, *in vivo* experimentation and integration with proteomics and genomics data to investigate potential therapeutic targets. These results have scope for translational application in assessing metabolite levels as part of the deep phenotypic characterisation of PAH patients, for diagnosis, treatment monitoring, and assessment of outcomes in both the clinical setting and for clinical research trials.

References

Abozguia, K., K. Clarke, L. Lee and M. Frenneaux (2006). "Modification of myocardial substrate use as a therapy for heart failure." Nat Clin Pract Cardiovasc Med **3**(9): 490-498.

Adatia, I., S. S. Kothari and J. A. Feinstein (2010). "Pulmonary hypertension associated with congenital heart disease: pulmonary vascular disease: the global perspective." Chest **137**(6 Suppl): 52S-61S.

Addabbo, F., Q. Chen, D. P. Patel, M. Rabadi, B. Ratliff, F. Zhang, J. F. Jasmin, M. Wolin, M. Lisanti, S. S. Gross and M. S. Goligorsky (2013). "Glutamine supplementation alleviates vasculopathy and corrects metabolic profile in an in vivo model of endothelial cell dysfunction." PLoS One **8**(6): e65458.

Ala-Korpela, M. (2016). "Metabolomics in cardiovascular medicine: Not personalised, not diagnostic." Eur J Prev Cardiol **23**(17): 1821-1822.

Ala-Korpela, M. and G. Davey Smith (2016). "Metabolic profiling-multitude of technologies with great research potential, but (when) will translation emerge?" Int J Epidemiol **45**(5): 1311-1318.

Aldred, M. A., R. D. Machado, V. James, N. W. Morrell and R. C. Trembath (2007). "Characterization of the BMPR2 5'-untranslated region and a novel mutation in pulmonary hypertension." Am J Respir Crit Care Med **176**(8): 819-824.

Alpert, A. J. (1990). "Hydrophilic-interaction chromatography for the separation of peptides, nucleic acids and other polar compounds." J Chromatogr **499**: 177-196.

Alzoubi, A., M. Toba, K. Abe, K. D. O'Neill, P. Rocic, K. A. Fagan, I. F. McMurtry and M. Oka (2013). "Dehydroepiandrosterone restores right ventricular structure and function in rats with severe pulmonary arterial hypertension." American Journal of Physiology: Heart and Circulatory Physiology **304**(12): H1708-1718.

Anand, V., S. Garg, S. Duval and T. Thenappan (2016). "A systematic review and meta-analysis of trials using statins in pulmonary arterial hypertension." Pulm Circ **6**(3): 295-301.

Anderson, P. and P. Ivanov (2014). "tRNA fragments in human health and disease." FEBS letters **588**(23): 4297-4304.

Arasaradnam, R. P., M. J. McFarlane, C. Ryan-Fisher, E. Westenbrink, P. Hodges, M. G. Thomas, S. Chambers, N. O'Connell, C. Bailey, C. Harmston, C. U. Nwokolo, K. D. Bardhan and J. A. Covington (2014). "Detection of colorectal cancer (CRC) by urinary volatile organic compound analysis." PLoS One **9**(9): e108750.

Archer, S. L., Y. H. Fang, J. J. Ryan and L. Piao (2013). "Metabolism and bioenergetics in the right ventricle and pulmonary vasculature in pulmonary hypertension." Pulm Circ **3**(1): 144-152.

Archer, S. L., M. Gomberg-Maitland, M. L. Maitland, S. Rich, J. G. Garcia and E. K. Weir (2008). "Mitochondrial metabolism, redox signaling, and fusion: a mitochondria-ROS-HIF-1alpha-Kv1.5 O2-sensing pathway at the intersection of pulmonary hypertension and cancer." Am J Physiol Heart Circ Physiol **294**(2): H570-578.

Archer, S. L., G. Marsboom, G. H. Kim, H. J. Zhang, P. T. Toth, E. C. Svensson, J. R. Dyck, M. Gomberg-Maitland, B. Thebaud, A. N. Husain, N. Cipriani and J. Rehman (2010). "Epigenetic attenuation of mitochondrial superoxide dismutase 2 in pulmonary arterial hypertension: a

basis for excessive cell proliferation and a new therapeutic target." Circulation **121**(24): 2661-2671.

Aronson, D., A. Eitan, R. Dragu and A. J. Burger (2011). "Relationship between reactive pulmonary hypertension and mortality in patients with acute decompensated heart failure." Circ Heart Fail **4**(5): 644-650.

Badagliacca, R., R. Poscia, B. Pezzuto, S. Papa, F. Pesce, G. Manzi, E. Giannetta, C. Raineri, M. Schina, S. Sciomer, D. Parola, M. Francone, I. Carbone, F. Fedele and C. D. Vizza (2016). "Right ventricular concentric hypertrophy and clinical worsening in idiopathic pulmonary arterial hypertension." J Heart Lung Transplant **35**(11): 1321-1329.

Badesch, D. B., G. E. Raskob, C. G. Elliott, A. M. Krichman, H. W. Farber, A. E. Frost, R. J. Barst, R. L. Benza, T. G. Liou, M. Turner, S. Giles, K. Feldkircher, D. P. Miller and M. D. McGoon (2010). "Pulmonary arterial hypertension: baseline characteristics from the REVEAL Registry." Chest **137**(2): 376-387.

Badesch, D. B., V. F. Tapson, M. D. McGoon, B. H. Brundage, L. J. Rubin, F. M. Wigley, S. Rich, R. J. Barst, P. S. Barrett, K. M. Kral, M. M. Jobsis, J. E. Loyd, S. Murali, A. Frost, R. Girgis, R. C. Bourge, D. D. Ralph, C. G. Elliott, N. S. Hill, D. Langleben, R. J. Schilz, V. V. McLaughlin, I. M. Robbins, B. M. Groves, S. Shapiro and T. A. Medsger, Jr. (2000). "Continuous intravenous epoprostenol for pulmonary hypertension due to the scleroderma spectrum of disease. A randomized, controlled trial." Ann Intern Med **132**(6): 425-434.

Baig, F., R. Pechlaner and M. Mayr (2016). "Caveats of Untargeted Metabolomics for Biomarker Discovery." J Am Coll Cardiol **68**(12): 1294-1296.

Balog, J., L. Sasi-Szabo, J. Kinross, M. R. Lewis, L. J. Muirhead, K. Veselkov, R. Mirnezami, B. Dezso, L. Damjanovich, A. Darzi, J. K. Nicholson and Z. Takats (2013). "Intraoperative tissue identification using rapid evaporative ionization mass spectrometry." Sci Transl Med **5**(194): 194ra193.

Barabasi, A. L., N. Gulbahce and J. Loscalzo (2011). "Network medicine: a network-based approach to human disease." Nat Rev Genet **12**(1): 56-68.

Barst, R. J., L. J. Rubin, W. A. Long, M. D. McGoon, S. Rich, D. B. Badesch, B. M. Groves, V. F. Tapson, R. C. Bourge, B. H. Brundage, S. K. Koerner, D. Langleben, C. A. Keller, S. Murali, B. F. Uretsky, L. M. Clayton, M. M. Jobsis, S. D. Blackburn, D. Shortino, J. W. Crow and G. Primary Pulmonary Hypertension Study (1996). "A comparison of continuous intravenous epoprostenol (prostacyclin) with conventional therapy for primary pulmonary hypertension." N Engl J Med **334**(5): 296-301.

Barter, P., J. Kastelein, A. Nunn, R. Hobbs and B. Future Forum Editorial (2003). "High density lipoproteins (HDLs) and atherosclerosis; the unanswered questions." Atherosclerosis **168**(2): 195-211.

Barter, P. J., G. Brandrup-Wognsen, M. K. Palmer and S. J. Nicholls (2010). "Effect of statins on HDL-C: a complex process unrelated to changes in LDL-C: analysis of the VOYAGER Database." J Lipid Res **51**(6): 1546-1553.

Barter, P. J., M. Caulfield, M. Eriksson, S. M. Grundy, J. J. Kastelein, M. Komajda, J. Lopez-Sendon, L. Mosca, J. C. Tardif, D. D. Waters, C. L. Shear, J. H. Revkin, K. A. Buhr, M. R. Fisher, A. R. Tall, B. Brewer and I. Investigators (2007). "Effects of torcetrapib in patients at high risk for coronary events." N Engl J Med **357**(21): 2109-2122.

Beckonert, O., H. C. Keun, T. M. Ebbels, J. Bundy, E. Holmes, J. C. Lindon and J. K. Nicholson (2007). "Metabolic profiling, metabolomic and metabonomic procedures for NMR spectroscopy of urine, plasma, serum and tissue extracts." Nature protocols **2**(11): 2692-2703.

Bendayan, D., D. Shitrit, M. Ygla, M. Huerta, G. Fink and M. R. Kramer (2003). "Hyperuricemia as a prognostic factor in pulmonary arterial hypertension." Respir Med **97**(2): 130-133.

Bennett, M. J. and A. B. Santani (1993). Carnitine Palmitoyltransferase 1A Deficiency. GeneReviews(R). R. A. Pagon, M. P. Adam, H. H. Ardinger et al. Seattle (WA).

Benza, R. L., M. Gomberg-Maitland, T. Demarco, A. E. Frost, A. Torbicki, D. Langleben, T. Pulido, P. Correa-Jaque, M. J. Passineau, H. W. Wiener, M. Tamari, T. Hirota, M. Kubo and H. K. Tiwari (2015). "Endothelin-1 Pathway Polymorphisms and Outcomes in Pulmonary Arterial Hypertension." Am J Respir Crit Care Med **192**(11): 1345-1354.

Benza, R. L., D. P. Miller, R. J. Barst, D. B. Badesch, A. E. Frost and M. D. McGoon (2012). "An evaluation of long-term survival from time of diagnosis in pulmonary arterial hypertension from the REVEAL Registry." Chest **142**(2): 448-456.

Benza, R. L., D. P. Miller, M. Gomberg-Maitland, R. P. Frantz, A. J. Foreman, C. S. Coffey, A. Frost, R. J. Barst, D. B. Badesch, C. G. Elliott, T. G. Liou and M. D. McGoon (2010). "Predicting survival in pulmonary arterial hypertension: insights from the Registry to Evaluate Early and Long-Term Pulmonary Arterial Hypertension Disease Management (REVEAL)." Circulation **122**(2): 164-172.

Bertero, T., K. Cottrill, A. Krauszman, Y. Lu, S. Annis, A. Hale, B. Bhat, A. B. Waxman, B. N. Chau, W. M. Kuebler and S. Y. Chan (2015). "The microRNA-130/301 family controls vasoconstriction in pulmonary hypertension." J Biol Chem **290**(4): 2069-2085.

Bertero, T., Y. Lu, S. Annis, A. Hale, B. Bhat, R. Saggar, R. Saggar, W. D. Wallace, D. J. Ross, S. O. Vargas, B. B. Graham, R. Kumar, S. M. Black, S. Fratz, J. R. Fineman, J. D. West, K. J. Haley, A. B. Waxman, B. N. Chau, K. A. Cottrill and S. Y. Chan (2014). "Systems-level regulation of microRNA networks by miR-130/301 promotes pulmonary hypertension." J Clin Invest([Epub ahead of print]).

Bhat, M., N. Robichaud, L. Hulea, N. Sonenberg, J. Pelletier and I. Topisirovic (2015). "Targeting the translation machinery in cancer." Nat Rev Drug Discov **14**(4): 261-278.

Bictash, M., T. M. Ebbels, Q. Chan, R. L. Loo, I. K. Yap, I. J. Brown, M. de Iorio, M. L. Daviglus, E. Holmes, J. Stamler, J. K. Nicholson and P. Elliott (2010). "Opening up the "Black Box": metabolic phenotyping and metabolome-wide association studies in epidemiology." J Clin Epidemiol **63**(9): 970-979.

Biomarkers Definitions Working, G. (2001). "Biomarkers and surrogate endpoints: preferred definitions and conceptual framework." Clin Pharmacol Ther **69**(3): 89-95.

Biospin, B. (2015). "Study on NMR based Lipoprotein Subclass Analysis."

Black, S. M., J. R. Fineman, R. H. Steinhorn, J. Bristow and S. J. Soifer (1998). "Increased endothelial NOS in lambs with increased pulmonary blood flow and pulmonary hypertension." Am J Physiol **275**(5 Pt 2): H1643-1651.

Blackburn, P., I. Lemieux, B. Lamarche, J. Bergeron, P. Perron, G. Tremblay, D. Gaudet and J. P. Despres (2012). "Angiographically-assessed coronary artery disease associates with HDL particle size in women." Atherosclerosis **223**(2): 359-364.

Blauwet, L. A., W. D. Edwards, H. D. Tazelaar and C. G. McGregor (2003). "Surgical pathology of pulmonary thromboendarterectomy: a study of 54 cases from 1990 to 2001." Hum Pathol **34**(12): 1290-1298.

Bodenhausen, G., ; Ruben, D. (1980). "Natural abundance nitrogen-15 NMR by enhanced heteronuclear spectroscopy." Chemical Physics Letters **69**(1): 185-189.

Bonderman, D., P. L. Turecek, J. Jakowitsch, A. Weltermann, C. Adlbrecht, B. Schneider, M. Kneussl, L. J. Rubin, P. A. Kyrle, W. Klepetko, G. Maurer and I. M. Lang (2003). "High prevalence of elevated clotting factor VIII in chronic thromboembolic pulmonary hypertension." Thromb Haemost **90**(3): 372-376.

Bonnet, S., E. Dumas-de-La-Roque, H. Begueret, R. Marthan, M. Fayon, P. Dos Santos, J. P. Savineau and E. E. Baulieu (2003). "Dehydroepiandrosterone (DHEA) prevents and reverses chronic hypoxic pulmonary hypertension." Proc Natl Acad Sci U S A **100**(16): 9488-9493.

Bonnet, S., E. D. Michelakis, C. J. Porter, M. A. Andrade-Navarro, B. Thebaud, S. Bonnet, A. Haromy, G. Harry, R. Moudgil, M. S. McMurtry, E. K. Weir and S. L. Archer (2006). "An abnormal mitochondrial-hypoxia inducible factor-1alpha-Kv channel pathway disrupts oxygen sensing and triggers pulmonary arterial hypertension in fawn hooded rats: similarities to human pulmonary arterial hypertension." Circulation **113**(22): 2630-2641.

Bonnet, S., S. Provencher, C. Guignabert, F. Perros, O. Boucherat, R. T. Schermuly, P. M. Hassoun, M. Rabinovitch, M. R. Nicolls and M. Humbert (2016). "Translating Research into Improved Patient Care in Pulmonary Arterial Hypertension." Am J Respir Crit Care Med.

Boucherat, O., F. Potus and S. Bonnet (2015). "microRNA and Pulmonary Hypertension." Adv Exp Med Biol **888**: 237-252.

Bowler, R. P., S. Jacobson, C. Cruickshank, G. J. Hughes, C. Siska, D. S. Ory, I. Petrache, J. E. Schaffer, N. Reisdorph and K. Kechris (2015). "Plasma sphingolipids associated with chronic obstructive pulmonary disease phenotypes." American Journal of Respiratory and Critical Care Medicine **191**(3): 275-284.

Box, G. and D. Cox (1964). "An Analysis of Transformations." Journal of the Royal Statistical Society **26**(No. 2): 211-252.

Brittain, E. L. and S. Y. Chan (2016). "Integration of complex data sources to provide biologic insight into pulmonary vascular disease (2015 Grover Conference Series)." Pulm Circ **6**(3): 251-260.

Brittain, E. L., M. Talati, J. P. Fessel, H. Zhu, N. Penner, M. W. Calcutt, J. West, M. Funke, G. D. Lewis, R. E. Gerszten, R. Hamid, M. E. Pugh, E. D. Austin, J. H. Newman and A. R. Hemnes (2016). "Fatty Acid Metabolic Defects and Right Ventricular Lipotoxicity in Human Pulmonary Arterial Hypertension." Circulation **133**(20): 1936-1944.

Broeckling, C. D., A. L. Heuberger and J. E. Prenni (2013). "Large scale non-targeted metabolomic profiling of serum by ultra performance liquid chromatography-mass spectrometry (UPLC-MS)." J Vis Exp(73): e50242.

Brown, L. M., H. Chen, S. Halpern, D. Taichman, M. D. McGoon, H. W. Farber, A. E. Frost, T. G. Liou, M. Turner, K. Feldkircher, D. P. Miller and C. G. Elliott (2011). "Delay in recognition of pulmonary arterial hypertension: factors identified from the REVEAL Registry." Chest **140**(1): 19-26.

Budhiraja, R., R. M. Tuder and P. M. Hassoun (2004). "Endothelial dysfunction in pulmonary hypertension." Circulation **109**(2): 159-165.

Bujak, R., J. Mateo, I. Blanco, J. L. Izquierdo-Garcia, D. Dudzik, M. J. Markuszewski, V. I. Peinado, M. Laclaustra, J. A. Barbera, C. Barbas and J. Ruiz-Cabello (2016). "New Biochemical Insights into the Mechanisms of Pulmonary Arterial Hypertension in Humans." PLoS One **11**(8): e0160505.

Burgess, S., A. S. Butterworth and J. R. Thompson (2016). "Beyond Mendelian randomization: how to interpret evidence of shared genetic predictors." J Clin Epidemiol **69**: 208-216.

Burri, P. H. (2006). "Structural aspects of postnatal lung development - alveolar formation and growth." Biol Neonate **89**(4): 313-322.

Buszewski, B. and S. Noga (2012). "Hydrophilic interaction liquid chromatography (HILIC)--a powerful separation technique." Anal Bioanal Chem **402**(1): 231-247.

Cambiaghi, A., M. Ferrario and M. Masseroli (2016). "Analysis of metabolomic data: tools, current strategies and future challenges for omics data integration." Brief Bioinform.

Camont, L., M. J. Chapman and A. Kontush (2011). "Biological activities of HDL subpopulations and their relevance to cardiovascular disease." Trends Mol Med **17**(10): 594-603.

Cannon, C. P., S. Shah, H. M. Dansky, M. Davidson, E. A. Brinton, A. M. Gotto, M. Stepanavage, S. X. Liu, P. Gibbons, T. B. Ashraf, J. Zafarino, Y. Mitchel, P. Barter, E. Determining the and I. Tolerability (2010). "Safety of anacetrapib in patients with or at high risk for coronary heart disease." N Engl J Med **363**(25): 2406-2415.

Cannon, J. E. and J. Pepke-Zaba (2013). "Is distal chronic thromboembolic pulmonary hypertension treatable with PAH targeted drugs?" Semin Respir Crit Care Med **34**(5): 620-626.

Carrola, J., C. M. Rocha, A. S. Barros, A. M. Gil, B. J. Goodfellow, I. M. Carreira, J. Bernardo, A. Gomes, V. Sousa, L. Carvalho and I. F. Duarte (2011). "Metabolic signatures of lung cancer in biofluids: NMR-based metabonomics of urine." J Proteome Res **10**(1): 221-230.

Casanova, R., S. Varma, B. Simpson, M. Kim, Y. An, S. Saldana, C. Riveros, P. Moscato, M. Griswold, D. Sonntag, J. Wahrheit, K. Klavins, P. V. Jonsson, G. Eiriksdottir, T. Aspelund, L. J. Launer, V. Gudnason, C. Legido Quigley and M. Thambisetty (2016). "Blood metabolite markers of preclinical Alzheimer's disease in two longitudinally followed cohorts of older individuals." Alzheimers Dement **12**(7): 815-822.

Chambliss, A. B. and D. W. Chan (2016). "Precision medicine: from pharmacogenomics to pharmacoproteomics." Clin Proteomics **13**: 25.

Chen, B., K. Strauch, Y. Jin, H. Cui, L. D. Nelin and L. G. Chicoine (2014). "Asymmetric dimethylarginine does not inhibit arginase activity and is pro-proliferative in pulmonary endothelial cells." Clin Exp Pharmacol Physiol **41**(7): 469-474.

Chen, C. N., G. Watson and L. Zhao (2013). "Cyclic guanosine monophosphate signalling pathway in pulmonary arterial hypertension." Vascul Pharmacol **58**(3): 211-218.

Chen, H., A. S. Lin, Y. Li, C. E. Reiter, M. R. Ver and M. J. Quon (2008). "Dehydroepiandrosterone stimulates phosphorylation of FoxO1 in vascular endothelial cells via phosphatidylinositol 3-kinase- and protein kinase A-dependent signaling pathways to regulate ET-1 synthesis and secretion." J Biol Chem **283**(43): 29228-29238.

Chen, J., H. Tang, J. R. Sysol, L. Moreno-Vinasco, K. M. Shioura, T. Chen, I. Gorshkova, L. Wang, L. S. Huang, P. V. Usatyuk, S. Sammani, G. Zhou, J. U. Raj, J. G. Garcia, E. Berdyshev, J. X. Yuan, V. Natarajan and R. F. Machado (2014). "The sphingosine kinase 1/sphingosine-1-phosphate

pathway in pulmonary arterial hypertension." Am J Respir Crit Care Med **190**(9): 1032-1043.

Chen, S. L., H. Zhang, D. J. Xie, J. Zhang, L. Zhou, A. M. Rothman and G. W. Stone (2015). "Hemodynamic, functional, and clinical responses to pulmonary artery denervation in patients with pulmonary arterial hypertension of different causes: phase II results from the Pulmonary Artery Denervation-1 study." Circ Cardiovasc Interv **8**(11): e002837.

Cheng, M. L., C. H. Wang, M. S. Shiao, M. H. Liu, Y. Y. Huang, C. Y. Huang, C. T. Mao, J. F. Lin, H. Y. Ho and N. I. Yang (2015). "Metabolic Disturbances Identified in Plasma Are Associated With Outcomes in Patients With Heart Failure: Diagnostic and Prognostic Value of Metabolomics." Journal of the American College of Cardiology **65**(15): 1509-1520.

Chester, A. H. and M. H. Yacoub (2014). "The role of endothelin-1 in pulmonary arterial hypertension." Glob Cardiol Sci Pract **2014**(2): 62-78.

Chhabra, N. (2013). "Biochemistry for Medics." Retrieved 24 Feb, 2016, from http://www.namrata.co/case-study-hart-nup-disease/tryptophan-metabolism/.

Christman, B. W., C. D. McPherson, J. H. Newman, G. A. King, G. R. Bernard, B. M. Groves and J. E. Loyd (1992). "An imbalance between the excretion of thromboxane and prostacyclin metabolites in pulmonary hypertension." N Engl J Med **327**(2): 70-75.

Cikach, F. S., Jr., A. R. Tonelli, J. Barnes, K. Paschke, J. Newman, D. Grove, L. Dababneh, S. Wang and R. A. Dweik (2014). "Breath analysis in pulmonary arterial hypertension." Chest **145**(3): 551-558.

Cloarec, O., M. E. Dumas, A. Craig, R. H. Barton, J. Trygg, J. Hudson, C. Blancher, D. Gauguier, J. C. Lindon, E. Holmes and J. Nicholson (2005). "Statistical total correlation spectroscopy: an exploratory approach for latent biomarker identification from metabolic 1H NMR data sets." Anal Chem **77**(5): 1282-1289.

Cohn, J. N. (2001). "Optimal diuretic therapy for heart failure." Am J Med **111**(7): 577.

Collaboration, C. R. P. C. H. D. G., F. Wensley, P. Gao, S. Burgess, S. Kaptoge, E. Di Angelantonio, T. Shah, J. C. Engert, R. Clarke, G. Davey-Smith, B. G. Nordestgaard, D. Saleheen, N. J. Samani, M. Sandhu, S. Anand, M. B. Pepys, L. Smeeth, J. Whittaker, J. P. Casas, S. G. Thompson, A. D. Hingorani and J. Danesh (2011). "Association between C reactive protein and coronary heart disease: mendelian randomisation analysis based on individual participant data." BMJ **342**: d548.

Condliffe, R. and L. S. Howard (2015). "Connective tissue disease-associated pulmonary arterial hypertension." F1000Prime Rep **7**: 06.

Consortium, C. A. D., P. Deloukas, S. Kanoni, C. Willenborg, M. Farrall, T. L. Assimes, J. R. Thompson, E. Ingelsson, D. Saleheen, J. Erdmann, B. A. Goldstein, K. Stirrups, I. R. Konig, J. B. Cazier, A. Johansson, A. S. Hall, J. Y. Lee, C. J. Willer, J. C. Chambers, T. Esko, L. Folkersen, A. Goel, E. Grundberg, A. S. Havulinna, W. K. Ho, J. C. Hopewell, N. Eriksson, M. E. Kleber, K. Kristiansson, P. Lundmark, L. P. Lyytikainen, S. Rafelt, D. Shungin, R. J. Strawbridge, G. Thorleifsson, E. Tikkanen, N. Van Zuydam, B. F. Voight, L. L. Waite, W. Zhang, A. Ziegler, D. Absher, D. Altshuler, A. J. Balmforth, I. Barroso, P. S. Braund, C. Burgdorf, S. Claudi-Boehm, D. Cox, M. Dimitriou, R. Do, D. Consortium, C. Consortium, A. S. Doney, N. El Mokhtari, P. Eriksson, K. Fischer, P. Fontanillas, A. Franco-Cereceda, B. Gigante, L. Groop, S. Gustafsson, J. Hager, G. Hallmans, B. G. Han, S. E. Hunt, H. M. Kang, T. Illig, T. Kessler, J. W. Knowles, G. Kolovou, J. Kuusisto, C. Langenberg, C. Langford, K. Leander, M. L. Lokki, A. Lundmark, M. I.

McCarthy, C. Meisinger, O. Melander, E. Mihailov, S. Maouche, A. D. Morris, M. Muller-Nurasyid, T. C. Mu, K. Nikus, J. F. Peden, N. W. Rayner, A. Rasheed, S. Rosinger, D. Rubin, M. P. Rumpf, A. Schafer, M. Sivananthan, C. Song, A. F. Stewart, S. T. Tan, G. Thorgeirsson, C. E. van der Schoot, P. J. Wagner, C. Wellcome Trust Case Control, G. A. Wells, P. S. Wild, T. P. Yang, P. Amouyel, D. Arveiler, H. Basart, M. Boehnke, E. Boerwinkle, P. Brambilla, F. Cambien, A. L. Cupples, U. de Faire, A. Dehghan, P. Diemert, S. E. Epstein, A. Evans, M. M. Ferrario, J. Ferrieres, D. Gauguier, A. S. Go, A. H. Goodall, V. Gudnason, S. L. Hazen, H. Holm, C. Iribarren, Y. Jang, M. Kahonen, F. Kee, H. S. Kim, N. Klopp, W. Koenig, W. Kratzer, K. Kuulasmaa, M. Laakso, R. Laaksonen, J. Y. Lee, L. Lind, W. H. Ouwehand, S. Parish, J. E. Park, N. L. Pedersen, A. Peters, T. Quertermous, D. J. Rader, V. Salomaa, E. Schadt, S. H. Shah, J. Sinisalo, K. Stark, K. Stefansson, D. A. Tregouet, J. Virtamo, L. Wallentin, N. Wareham, M. E. Zimmermann, M. S. Nieminen, C. Hengstenberg, M. S. Sandhu, T. Pastinen, A. C. Syvanen, G. K. Hovingh, G. Dedoussis, P. W. Franks, T. Lehtimaki, A. Metspalu, P. A. Zalloua, A. Siegbahn, S. Schreiber, S. Ripatti, S. S. Blankenberg, M. Perola, R. Clarke, B. O. Boehm, C. O'Donnell, M. P. Reilly, W. Marz, R. Collins, S. Kathiresan, A. Hamsten, J. S. Kooner, U. Thorsteinsdottir, J. Danesh, C. N. Palmer, R. Roberts, H. Watkins, H. Schunkert and N. J. Samani (2013). "Large-scale association analysis identifies new risk loci for coronary artery disease." Nat Genet **45**(1): 25-33.

Cool, C. D., J. S. Stewart, P. Werahera, G. J. Miller, R. L. Williams, N. F. Voelkel and R. M. Tuder (1999). "Three-dimensional reconstruction of pulmonary arteries in plexiform pulmonary hypertension using cell-specific markers. Evidence for a dynamic and heterogeneous process of pulmonary endothelial cell growth." Am J Pathol **155**(2): 411-419.

Cooper, C. J., M. J. Landzberg, T. J. Anderson, F. Charbonneau, M. A. Creager, P. Ganz and A. P. Selwyn (1996). "Role of nitric oxide in the local regulation of pulmonary vascular resistance in humans." Circulation **93**(2): 266-271.

Cotroneo, E., A. Ashek, L. Wang, J. Wharton, O. Dubois, S. Bozorgi, M. Busbridge, K. N. Alavian, M. R. Wilkins and L. Zhao (2015). "Iron homeostasis and pulmonary hypertension: iron deficiency leads to pulmonary vascular remodeling in the rat." Circ Res **116**(10): 1680-1690.

Cottrill, K. A. and S. Y. Chan (2013). "Metabolic dysfunction in pulmonary hypertension: the expanding relevance of the Warburg effect." Eur J Clin Invest **43**(8): 855-865.

Courand, P. Y., G. Pina Jomir, C. Khouatra, C. Scheiber, S. Turquier, J. C. Glerant, B. Mastroianni, B. Gentil, A. S. Blanchet-Legens, A. Dib, G. Derumeaux, M. Humbert, J. F. Mornex, J. F. Cordier and V. Cottin (2015). "Prognostic value of right ventricular ejection fraction in pulmonary arterial hypertension." Eur Respir J **45**(1): 139-149.

Cracowski, J. L., J. Labarere, J. C. Renversez, B. Degano, F. Chabot and M. Humbert (2012). "Plasma levels of high-density lipoprotein cholesterol are not associated with survival in pulmonary arterial hypertension." Am J Respir Crit Care Med **186**(1): 107; author reply 107-108.

Cramer, J. A. (2002). "Effect of partial compliance on cardiovascular medication effectiveness." Heart **88**(2): 203-206.

Cunningham, C. H., J. Y. Lau, A. P. Chen, B. J. Geraghty, W. J. Perks, I. Roifman, G. A. Wright and K. A. Connelly (2016). "Hyperpolarized 13C Metabolic MRI of the Human Heart: Initial Experience." Circ Res **119**(11): 1177-1182.

D'Alonzo, G. E., R. J. Barst, S. M. Ayres, E. H. Bergofsky, B. H. Brundage, K. M. Detre, A. P. Fishman, R. M. Goldring, B. M. Groves, J. T. Kernis and et al. (1991). "Survival in patients with primary

pulmonary hypertension. Results from a national prospective registry." Ann Intern Med **115**(5): 343-349.

D'Alto, M. and V. S. Mahadevan (2012). "Pulmonary arterial hypertension associated with congenital heart disease." Eur Respir Rev **21**(126): 328-337.

Damico, R., T. M. Kolb, L. Valera, L. Wang, T. Housten, R. J. Tedford, D. A. Kass, N. Rafaels, L. Gao, K. C. Barnes, R. L. Benza, J. L. Rand, R. Hamid, J. E. Loyd, I. M. Robbins, A. R. Hemnes, W. K. Chung, E. D. Austin, M. B. Drummond, S. C. Mathai and P. M. Hassoun (2015). "Serum endostatin is a genetically determined predictor of survival in pulmonary arterial hypertension." Am J Respir Crit Care Med **191**(2): 208-218.

Dang, C. V. (2012). "Links between metabolism and cancer." Genes Dev **26**(9): 877-890.

Dartevelle, P., E. Fadel, S. Mussot, A. Chapelier, P. Herve, M. de Perrot, J. Cerrina, F. L. Ladurie, D. Lehouerou, M. Humbert, O. Sitbon and G. Simonneau (2004). "Chronic thromboembolic pulmonary hypertension." Eur Respir J **23**(4): 637-648.

DaTorre, S. D., M. H. Creer, S. M. Pogwizd and P. B. Corr (1991). "Amphipathic lipid metabolites and their relation to arrhythmogenesis in the ischemic heart." Journal of Molecular and Cellular Cardiology **23 Suppl 1**: 11-22.

Davie, N. J., J. T. Crossno, Jr., M. G. Frid, S. E. Hofmeister, J. T. Reeves, D. M. Hyde, T. C. Carpenter, J. A. Brunetti, I. K. McNiece and K. R. Stenmark (2004). "Hypoxia-induced pulmonary artery adventitial remodeling and neovascularization: contribution of progenitor cells." Am J Physiol Lung Cell Mol Physiol **286**(4): L668-678.

de la Fuente, A., N. Bing, I. Hoeschele and P. Mendes (2004). "Discovery of meaningful associations in genomic data using partial correlation coefficients." Bioinformatics **20**(18): 3565-3574.

de Lemos, J. A., A. Rohatgi and C. R. Ayers (2015). "Applying a Big Data Approach to Biomarker Discovery: Running Before We Walk?" Circulation **132**(24): 2289-2292.

Dehaven, C. D., A. M. Evans, H. Dai and K. A. Lawton (2010). "Organization of GC/MS and LC/MS metabolomics data into chemical libraries." J Cheminform **2**(1): 9.

Deng, Z., J. H. Morse, S. L. Slager, N. Cuervo, K. J. Moore, G. Venetos, S. Kalachikov, E. Cayanis, S. G. Fischer, R. J. Barst, S. E. Hodge and J. A. Knowles (2000). "Familial primary pulmonary hypertension (gene PPH1) is caused by mutations in the bone morphogenetic protein receptor-II gene." Am J Hum Genet **67**(3): 737-744.

Diller, G. P., T. Thum, M. R. Wilkins and J. Wharton (2010). "Endothelial progenitor cells in pulmonary arterial hypertension." Trends Cardiovasc Med **20**(1): 22-29.

Doerge, R. W. (2002). "Mapping and analysis of quantitative trait loci in experimental populations." Nat Rev Genet **3**(1): 43-52.

Doran, A. K., D. D. Ivy, R. J. Barst, N. Hill, S. Murali, R. L. Benza and A. Scientific Leadership Council of the Pulmonary Hypertension (2008). "Guidelines for the prevention of central venous catheter-related blood stream infections with prostanoid therapy for pulmonary arterial hypertension." Int J Clin Pract Suppl(160): 5-9.

Dorfmuller, P., M. Humbert, F. Perros, O. Sanchez, G. Simonneau, K. M. Muller and F. Capron (2007). "Fibrous remodeling of the pulmonary venous system in pulmonary arterial hypertension associated with connective tissue diseases." Hum Pathol **38**(6): 893-902.

Draisma, H. H., R. Pool, M. Kobl, R. Jansen, A. K. Petersen, A. A. Vaarhorst, I. Yet, T. Haller, A. Demirkan, T. Esko, G. Zhu, S. Bohringer, M. Beekman, J. B. van Klinken, W. Romisch-Margl, C. Prehn, J. Adamski, A. J. de Craen, E. M. van Leeuwen, N. Amin, H. Dharuri, H. J. Westra, L. Franke, E. J. de Geus, J. J. Hottenga, G. Willemsen, A. K. Henders, G. W. Montgomery, D. R. Nyholt, J. B. Whitfield, B. W. Penninx, T. D. Spector, A. Metspalu, P. Eline Slagboom, K. W. van Dijk, P. A. t Hoen, K. Strauch, N. G. Martin, G. J. van Ommen, T. Illig, J. T. Bell, M. Mangino, K. Suhre, M. I. McCarthy, C. Gieger, A. Isaacs, C. M. van Duijn and D. I. Boomsma (2015). "Genome-wide association study identifies novel genetic variants contributing to variation in blood metabolite levels." Nat Commun **6**: 7208.

Drexel, H., F. W. Amann, K. Rentsch, C. Neuenschwander, A. Luethy, S. I. Khan and F. Follath (1992). "Relation of the level of high-density lipoprotein subfractions to the presence and extent of coronary artery disease." Am J Cardiol **70**(4): 436-440.

Dromparis, P., R. Paulin, G. Sutendra, A. C. Qi, S. Bonnet and E. D. Michelakis (2013). "Uncoupling protein 2 deficiency mimics the effects of hypoxia and endoplasmic reticulum stress on mitochondria and triggers pseudohypoxic pulmonary vascular remodeling and pulmonary hypertension." Circ Res **113**(2): 126-136.

Dumas de La Roque, E., J. P. Savineau, A. C. Metivier, M. A. Billes, J. P. Kraemer, S. Doutreleau, J. Jougon, R. Marthan, N. Moore, M. Fayon, E. E. Baulieu and C. Dromer (2012). "Dehydroepiandrosterone (DHEA) improves pulmonary hypertension in chronic obstructive pulmonary disease (COPD): a pilot study." Ann Endocrinol (Paris) **73**(1): 20-25.

Dumas, M. E. (2012). "Metabolome 2.0: quantitative genetics and network biology of metabolic phenotypes." Mol Biosyst **8**(10): 2494-2502.

Dumas, M. E., J. Kinross and J. K. Nicholson (2014). "Metabolic phenotyping and systems biology approaches to understanding metabolic syndrome and fatty liver disease." Gastroenterology **146**(1): 46-62.

Dumas, M. E., E. C. Maibaum, C. Teague, H. Ueshima, B. Zhou, J. C. Lindon, J. K. Nicholson, J. Stamler, P. Elliott, Q. Chan and E. Holmes (2006). "Assessment of analytical reproducibility of 1H NMR spectroscopy based metabonomics for large-scale epidemiological research: the INTERMAP Study." Anal Chem **78**(7): 2199-2208.

Dunn, W. B., D. I. Broadhurst, H. J. Atherton, R. Goodacre and J. L. Griffin (2011). "Systems level studies of mammalian metabolomes: the roles of mass spectrometry and nuclear magnetic resonance spectroscopy." Chem Soc Rev **40**(1): 387-426.

Dutta, A., P. Shetty, S. Bhat, Y. Ramachandra and S. Hegde (2012). "A mass spectrometric study for comparative analysis and evaluation of metabolite recovery from plasma by various solvent systems." J Biomol Tech **23**(4): 128-135.

Dweik, R. A. (2007). "The lung in the balance: arginine, methylated arginines, and nitric oxide." Am J Physiol Lung Cell Mol Physiol **292**(1): L15-17.

Eddahibi, S., M. Humbert, E. Fadel, B. Raffestin, M. Darmon, F. Capron, G. Simonneau, P. Dartevelle, M. Hamon and S. Adnot (2001). "Serotonin transporter overexpression is responsible for pulmonary artery smooth muscle hyperplasia in primary pulmonary hypertension." J Clin Invest **108**(8): 1141-1150.

Ejigu, B. A., D. Valkenborg, G. Baggerman, M. Vanaerschot, E. Witters, J. C. Dujardin, T. Burzykowski and M. Berg (2013). "Evaluation of normalization methods to pave the way towards large-scale LC-MS-based metabolomics profiling experiments." OMICS **17**(9): 473-485.

Elliott, P., J. M. Posma, Q. Chan, I. Garcia-Perez, A. Wijeyesekera, M. Bictash, T. M. Ebbels, H. Ueshima, L. Zhao, L. van Horn, M. Daviglus, J. Stamler, E. Holmes and J. K. Nicholson (2015). "Urinary metabolic signatures of human adiposity." Sci Transl Med **7**(285): 285ra262.

Evans AM1, D. C., Barrett T, Mitchell M, Milgram E. (2009). "Integrated, nontargeted ultrahigh performance liquid chromatography/electrospray ionization tandem mass spectrometry platform for the identification and relative quantification of the small-molecule complement of biological systems." Anal Chem. **81(16):6656-67**.

Evans, A. M., C. D. DeHaven, T. Barrett, M. Mitchell and E. Milgram (2009). "Integrated, nontargeted ultrahigh performance liquid chromatography/electrospray ionization tandem mass spectrometry platform for the identification and relative quantification of the small-molecule complement of biological systems." Analytical Chemistry **81**(16): 6656-6667.

Evans, J. D., B. Girerd, D. Montani, X. J. Wang, N. Galie, E. D. Austin, G. Elliott, K. Asano, E. Grunig, Y. Yan, Z. C. Jing, A. Manes, M. Palazzini, L. A. Wheeler, I. Nakayama, T. Satoh, C. Eichstaedt, K. Hinderhofer, M. Wolf, E. B. Rosenzweig, W. K. Chung, F. Soubrier, G. Simonneau, O. Sitbon, S. Graf, S. Kaptoge, E. Di Angelantonio, M. Humbert and N. W. Morrell (2016). "BMPR2 mutations and survival in pulmonary arterial hypertension: an individual participant data meta-analysis." Lancet Respir Med **4**(2): 129-137.

Everett, J. R., R. L. Loo and F. S. Pullen (2013). "Pharmacometabonomics and personalized medicine." Ann Clin Biochem **50**(Pt 6): 523-545.

Eyries, M., D. Montani, B. Girerd, C. Perret, A. Leroy, C. Lonjou, N. Chelghoum, F. Coulet, D. Bonnet, P. Dorfmuller, E. Fadel, O. Sitbon, G. Simonneau, D. A. Tregouet, M. Humbert and F. Soubrier (2014). "EIF2AK4 mutations cause pulmonary veno-occlusive disease, a recessive form of pulmonary hypertension." Nature Genetics **46**(1): 65-69.

Fang, J. C., T. DeMarco, M. M. Givertz, B. A. Borlaug, G. D. Lewis, J. E. Rame, M. Gomberg-Maitland, S. Murali, R. P. Frantz, D. McGlothlin, E. M. Horn and R. L. Benza (2012). "World Health Organization Pulmonary Hypertension group 2: pulmonary hypertension due to left heart disease in the adult--a summary statement from the Pulmonary Hypertension Council of the International Society for Heart and Lung Transplantation." J Heart Lung Transplant **31**(9): 913-933.

Fang, Y. H., L. Piao, Z. Hong, P. T. Toth, G. Marsboom, P. Bache-Wiig, J. Rehman and S. L. Archer (2012). "Therapeutic inhibition of fatty acid oxidation in right ventricular hypertrophy: exploiting Randle's cycle." J Mol Med (Berl) **90**(1): 31-43.

Farber, H. W. and J. Loscalzo (2004). "Pulmonary arterial hypertension." N Engl J Med **351**(16): 1655-1665.

Farber, H. W., D. P. Miller, A. D. Poms, D. B. Badesch, A. E. Frost, E. Muros-Le Rouzic, A. J. Romero, W. W. Benton, C. G. Elliott, M. D. McGoon and R. L. Benza (2015). "Five-Year outcomes of patients enrolled in the REVEAL Registry." Chest **148**(4): 1043-1054.

Ferrannini, E., A. Natali, S. Camastra, M. Nannipieri, A. Mari, K. P. Adam, M. V. Milburn, G. Kastenmuller, J. Adamski, T. Tuomi, V. Lyssenko, L. Groop and W. E. Gall (2013). "Early metabolic markers of the development of dysglycemia and type 2 diabetes and their physiological significance." Diabetes **62**(5): 1730-1737.

Fessel, J. P., R. Hamid, B. M. Wittmann, L. J. Robinson, T. Blackwell, Y. Tada, N. Tanabe, K. Tatsumi, A. R. Hemnes and J. D. West (2012). "Metabolomic analysis of bone morphogenetic protein

receptor type 2 mutations in human pulmonary endothelium reveals widespread metabolic reprogramming." Pulm Circ **2**(2): 201-213.

Fijalkowska, A., M. Kurzyna, A. Torbicki, G. Szewczyk, M. Florczyk, P. Pruszczyk and M. Szturmowicz (2006). "Serum N-terminal brain natriuretic peptide as a prognostic parameter in patients with pulmonary hypertension." Chest **129**(5): 1313-1321.

Fijalkowska, I., W. Xu, S. A. Comhair, A. J. Janocha, L. A. Mavrakis, B. Krishnamachary, L. Zhen, T. Mao, A. Richter, S. C. Erzurum and R. M. Tuder (2010). "Hypoxia inducible-factor1alpha regulates the metabolic shift of pulmonary hypertensive endothelial cells." Am J Pathol **176**(3): 1130-1138.

Finocchiaro, G., M. Ito and K. Tanaka (1987). "Purification and properties of short chain acyl-CoA, medium chain acyl-CoA, and isovaleryl-CoA dehydrogenases from human liver." J Biol Chem **262**(17): 7982-7989.

Flote, V. G., R. Vettukattil, T. F. Bathen, T. Egeland, A. McTiernan, H. Frydenberg, A. Husoy, S. E. Finstad, J. Lomo, O. Garred, E. Schlichting, E. A. Wist and I. Thune (2016). "Lipoprotein subfractions by nuclear magnetic resonance are associated with tumor characteristics in breast cancer." Lipids Health Dis **15**: 56.

Foletta, V. C., M. A. Lim, J. Soosairajah, A. P. Kelly, E. G. Stanley, M. Shannon, W. He, S. Das, J. Massague and O. Bernard (2003). "Direct signaling by the BMP type II receptor via the cytoskeletal regulator LIMK1." J Cell Biol **162**(6): 1089-1098.

Fourie, P. R., A. R. Coetzee and C. T. Bolliger (1992). "Pulmonary artery compliance: its role in right ventricular-arterial coupling." Cardiovasc Res **26**(9): 839-844.

Friedrich, N. (2012). "Metabolomics in diabetes research." J Endocrinol **215**(1): 29-42.

Frishman, W. H. (2007). "Importance of medication adherence in cardiovascular disease and the value of once-daily treatment regimens." Cardiol Rev **15**(5): 257-263.

Fritz, J. S., C. Blair, R. J. Oudiz, C. Dufton, H. Olschewski, D. Despain, H. Gillies and S. M. Kawut (2013). "Baseline and follow-up 6-min walk distance and brain natriuretic peptide predict 2-year mortality in pulmonary arterial hypertension." Chest **143**(2): 315-323.

Frost, A. E., R. J. Barst, M. M. Hoeper, H. J. Chang, R. P. Frantz, Y. Fukumoto, N. Galie, P. M. Hassoun, H. Klose, H. Matsubara, N. W. Morrell, A. J. Peacock, M. Pfeifer, G. Simonneau, V. F. Tapson, F. Torres, C. Dario Vizza, D. Lawrence, W. Yang, J. M. Felser, D. A. Quinn and H. A. Ghofrani (2015). "Long-term safety and efficacy of imatinib in pulmonary arterial hypertension." J Heart Lung Transplant **34**(11): 1366-1375.

Fuster, V., P. M. Steele, W. D. Edwards, B. J. Gersh, M. D. McGoon and R. L. Frye (1984). "Primary pulmonary hypertension: natural history and the importance of thrombosis." Circulation **70**(4): 580-587.

Galie, N., D. Badesch, R. Oudiz, G. Simonneau, M. D. McGoon, A. M. Keogh, A. E. Frost, D. Zwicke, R. Naeije, S. Shapiro, H. Olschewski and L. J. Rubin (2005). "Ambrisentan therapy for pulmonary arterial hypertension." J Am Coll Cardiol **46**(3): 529-535.

Galie, N., B. H. Brundage, H. A. Ghofrani, R. J. Oudiz, G. Simonneau, Z. Safdar, S. Shapiro, R. J. White, M. Chan, A. Beardsworth, L. Frumkin, R. J. Barst, H. Pulmonary Arterial and G. Response to Tadalafil Study (2009). "Tadalafil therapy for pulmonary arterial hypertension." Circulation **119**(22): 2894-2903.

Galie, N., H. A. Ghofrani, A. Torbicki, R. J. Barst, L. J. Rubin, D. Badesch, T. Fleming, T. Parpia, G. Burgess, A. Branzi, F. Grimminger, M. Kurzyna, G. Simonneau and G. Sildenafil Use in Pulmonary Arterial Hypertension Study (2005). "Sildenafil citrate therapy for pulmonary arterial hypertension." N Engl J Med **353**(20): 2148-2157.

Galie, N., M. M. Hoeper, M. Humbert, A. Torbicki, J. L. Vachiery, J. A. Barbera, M. Beghetti, P. Corris, S. Gaine, J. S. Gibbs, M. A. Gomez-Sanchez, G. Jondeau, W. Klepetko, C. Opitz, A. Peacock, L. Rubin, M. Zellweger, G. Simonneau and E. S. C. C. f. P. Guidelines (2009). "Guidelines for the diagnosis and treatment of pulmonary hypertension: the Task Force for the Diagnosis and Treatment of Pulmonary Hypertension of the European Society of Cardiology (ESC) and the European Respiratory Society (ERS), endorsed by the International Society of Heart and Lung Transplantation (ISHLT)." Eur Heart J **30**(20): 2493-2537.

Galie, N., M. Humbert, J. L. Vachiery, S. Gibbs, I. Lang, A. Torbicki, G. Simonneau, A. Peacock, A. Vonk Noordegraaf, M. Beghetti, A. Ghofrani, M. A. Gomez Sanchez, G. Hansmann, W. Klepetko, P. Lancellotti, M. Matucci, T. McDonagh, L. A. Pierard, P. T. Trindade, M. Zompatori and M. Hoeper (2015). "2015 ESC/ERS Guidelines for the diagnosis and treatment of pulmonary hypertension: The Joint Task Force for the Diagnosis and Treatment of Pulmonary Hypertension of the European Society of Cardiology (ESC) and the European Respiratory Society (ERS): Endorsed by: Association for European Paediatric and Congenital Cardiology (AEPC), International Society for Heart and Lung Transplantation (ISHLT)." European Respiratory Journal **46**(4): 903-975.

Galie, N. and N. H. Kim (2006). "Pulmonary microvascular disease in chronic thromboembolic pulmonary hypertension." Proc Am Thorac Soc **3**(7): 571-576.

Galie, N., A. Manes and A. Branzi (2004). "The endothelin system in pulmonary arterial hypertension." Cardiovasc Res **61**(2): 227-237.

Galie, N., K. Muller, A. V. Scalise and E. Grunig (2015). "PATENT PLUS: a blinded, randomised and extension study of riociguat plus sildenafil in pulmonary arterial hypertension." Eur Respir J **45**(5): 1314-1322.

Galie, N., H. Olschewski, R. J. Oudiz, F. Torres, A. Frost, H. A. Ghofrani, D. B. Badesch, M. D. McGoon, V. V. McLaughlin, E. B. Roecker, M. J. Gerber, C. Dufton, B. L. Wiens, L. J. Rubin and R. D.-B. P.-C. M. E. S. G. Ambrisentan in Pulmonary Arterial Hypertension (2008). "Ambrisentan for the treatment of pulmonary arterial hypertension: results of the ambrisentan in pulmonary arterial hypertension, randomized, double-blind, placebo-controlled, multicenter, efficacy (ARIES) study 1 and 2." Circulation **117**(23): 3010-3019.

Galie, N., L. Rubin, M. Hoeper, P. Jansa, H. Al-Hiti, G. Meyer, E. Chiossi, A. Kusic-Pajic and G. Simonneau (2008). "Treatment of patients with mildly symptomatic pulmonary arterial hypertension with bosentan (EARLY study): a double-blind, randomised controlled trial." Lancet **371**(9630): 2093-2100.

Gatzoulis, M. A., M. Beghetti, N. Galie, J. Granton, R. M. Berger, A. Lauer, E. Chiossi, M. Landzberg and B.-. Investigators (2008). "Longer-term bosentan therapy improves functional capacity in Eisenmenger syndrome: results of the BREATHE-5 open-label extension study." Int J Cardiol **127**(1): 27-32.

Gerber, J. G., N. Voelkel, A. S. Nies, I. F. McMurtry and J. T. Reeves (1980). "Moderation of hypoxic vasoconstriction by infused arachidonic acid: role of PGI2." J Appl Physiol Respir Environ Exerc Physiol **49**(1): 107-112.

Gerszten, R. E. and T. J. Wang (2008). "The search for new cardiovascular biomarkers." Nature **451**(7181): 949-952.

Ghigna, M. R., C. Guignabert, D. Montani, B. Girerd, X. Jais, L. Savale, P. Herve, V. Thomas de Montpreville, O. Mercier, O. Sitbon, F. Soubrier, E. Fadel, G. Simonneau, M. Humbert and P. Dorfmuller (2016). "BMPR2 mutation status influences bronchial vascular changes in pulmonary arterial hypertension." Eur Respir J **48**(6): 1668-1681.

Ghofrani, H. A., A. M. D'Armini, F. Grimminger, M. M. Hoeper, P. Jansa, N. H. Kim, E. Mayer, G. Simonneau, M. R. Wilkins, A. Fritsch, D. Neuser, G. Weimann, C. Wang and C.-S. Group (2013). "Riociguat for the treatment of chronic thromboembolic pulmonary hypertension." The New England journal of medicine **369**(4): 319-329.

Ghofrani, H. A., N. Galie, F. Grimminger, E. Grunig, M. Humbert, Z. C. Jing, A. M. Keogh, D. Langleben, M. O. Kilama, A. Fritsch, D. Neuser, L. J. Rubin and P.-S. Group (2013). "Riociguat for the treatment of pulmonary arterial hypertension." N Engl J Med **369**(4): 330-340.

Giaid, A. and D. Saleh (1995). "Reduced expression of endothelial nitric oxide synthase in the lungs of patients with pulmonary hypertension." N Engl J Med **333**(4): 214-221.

Gieger, C., L. Geistlinger, E. Altmaier, M. Hrabe de Angelis, F. Kronenberg, T. Meitinger, H. W. Mewes, H. E. Wichmann, K. M. Weinberger, J. Adamski, T. Illig and K. Suhre (2008). "Genetics meets metabolomics: a genome-wide association study of metabolite profiles in human serum." PLoS Genet **4**(11): e1000282.

Global Lipids Genetics, C., C. J. Willer, E. M. Schmidt, S. Sengupta, G. M. Peloso, S. Gustafsson, S. Kanoni, A. Ganna, J. Chen, M. L. Buchkovich, S. Mora, J. S. Beckmann, J. L. Bragg-Gresham, H. Y. Chang, A. Demirkan, H. M. Den Hertog, R. Do, L. A. Donnelly, G. B. Ehret, T. Esko, M. F. Feitosa, T. Ferreira, K. Fischer, P. Fontanillas, R. M. Fraser, D. F. Freitag, D. Gurdasani, K. Heikkila, E. Hypponen, A. Isaacs, A. U. Jackson, A. Johansson, T. Johnson, M. Kaakinen, J. Kettunen, M. E. Kleber, X. Li, J. Luan, L. P. Lyytikainen, P. K. Magnusson, M. Mangino, E. Mihailov, M. E. Montasser, M. Muller-Nurasyid, I. M. Nolte, J. R. O'Connell, C. D. Palmer, M. Perola, A. K. Petersen, S. Sanna, R. Saxena, S. K. Service, S. Shah, D. Shungin, C. Sidore, C. Song, R. J. Strawbridge, I. Surakka, T. Tanaka, T. M. Teslovich, G. Thorleifsson, E. G. Van den Herik, B. F. Voight, K. A. Volcik, L. L. Waite, A. Wong, Y. Wu, W. Zhang, D. Absher, G. Asiki, I. Barroso, L. F. Been, J. L. Bolton, L. L. Bonnycastle, P. Brambilla, M. S. Burnett, G. Cesana, M. Dimitriou, A. S. Doney, A. Doring, P. Elliott, S. E. Epstein, G. I. Eyjolfsson, B. Gigante, M. O. Goodarzi, H. Grallert, M. L. Gravito, C. J. Groves, G. Hallmans, A. L. Hartikainen, C. Hayward, D. Hernandez, A. A. Hicks, H. Holm, Y. J. Hung, T. Illig, M. R. Jones, P. Kaleebu, J. J. Kastelein, K. T. Khaw, E. Kim, N. Klopp, P. Komulainen, M. Kumari, C. Langenberg, T. Lehtimaki, S. Y. Lin, J. Lindstrom, R. J. Loos, F. Mach, W. L. McArdle, C. Meisinger, B. D. Mitchell, G. Muller, R. Nagaraja, N. Narisu, T. V. Nieminen, R. N. Nsubuga, I. Olafsson, K. K. Ong, A. Palotie, T. Papamarkou, C. Pomilla, A. Pouta, D. J. Rader, M. P. Reilly, P. M. Ridker, F. Rivadeneira, I. Rudan, A. Ruokonen, N. Samani, H. Scharnagl, J. Seeley, K. Silander, A. Stancakova, K. Stirrups, A. J. Swift, L. Tiret, A. G. Uitterlinden, L. J. van Pelt, S. Vedantam, N. Wainwright, C. Wijmenga, S. H. Wild, G. Willemsen, T. Wilsgaard, J. F. Wilson, E. H. Young, J. H. Zhao, L. S. Adair, D. Arveiler, T. L. Assimes, S. Bandinelli, F. Bennett, M. Bochud, B. O. Boehm, D. I. Boomsma, I. B. Borecki, S. R. Bornstein, P. Bovet, M. Burnier, H. Campbell, A. Chakravarti, J. C. Chambers, Y. D. Chen, F. S. Collins, R. S. Cooper, J. Danesh, G. Dedoussis, U. de Faire, A. B. Feranil, J. Ferrieres, L. Ferrucci, N. B. Freimer, C. Gieger, L. C. Groop, V. Gudnason, U. Gyllensten, A. Hamsten, T. B. Harris, A. Hingorani, J. N. Hirschhorn, A. Hofman, G. K. Hovingh, C. A. Hsiung, S. E. Humphries, S. C. Hunt, K. Hveem, C. Iribarren, M. R. Jarvelin, A. Jula, M. Kahonen, J. Kaprio, A. Kesaniemi, M. Kivimaki, J. S. Kooner, P. J. Koudstaal, R. M.

Krauss, D. Kuh, J. Kuusisto, K. O. Kyvik, M. Laakso, T. A. Lakka, L. Lind, C. M. Lindgren, N. G. Martin, W. Marz, M. I. McCarthy, C. A. McKenzie, P. Meneton, A. Metspalu, L. Moilanen, A. D. Morris, P. B. Munroe, I. Njolstad, N. L. Pedersen, C. Power, P. P. Pramstaller, J. F. Price, B. M. Psaty, T. Quertermous, R. Rauramaa, D. Saleheen, V. Salomaa, D. K. Sanghera, J. Saramies, P. E. Schwarz, W. H. Sheu, A. R. Shuldiner, A. Siegbahn, T. D. Spector, K. Stefansson, D. P. Strachan, B. O. Tayo, E. Tremoli, J. Tuomilehto, M. Uusitupa, C. M. van Duijn, P. Vollenweider, L. Wallentin, N. J. Wareham, J. B. Whitfield, B. H. Wolffenbuttel, J. M. Ordovas, E. Boerwinkle, C. N. Palmer, U. Thorsteinsdottir, D. I. Chasman, J. I. Rotter, P. W. Franks, S. Ripatti, L. A. Cupples, M. S. Sandhu, S. S. Rich, M. Boehnke, P. Deloukas, S. Kathiresan, K. L. Mohlke, E. Ingelsson and G. R. Abecasis (2013). "Discovery and refinement of loci associated with lipid levels." Nat Genet **45**(11): 1274-1283.

Glomset, J. A. (1968). "The plasma lecithins:cholesterol acyltransferase reaction." J Lipid Res **9**(2): 155-167.

Glomset, J. A. and J. L. Wright (1964). "Some Properties of a Cholesterol Esterifying Enzyme in Human Plasma." Biochim Biophys Acta **89**: 266-276.

Gold, L., D. Ayers, J. Bertino, C. Bock, A. Bock, E. N. Brody, J. Carter, A. B. Dalby, B. E. Eaton, T. Fitzwater, D. Flather, A. Forbes, T. Foreman, C. Fowler, B. Gawande, M. Goss, M. Gunn, S. Gupta, D. Halladay, J. Heil, J. Heilig, B. Hicke, G. Husar, N. Janjic, T. Jarvis, S. Jennings, E. Katilius, T. R. Keeney, N. Kim, T. H. Koch, S. Kraemer, L. Kroiss, N. Le, D. Levine, W. Lindsey, B. Lollo, W. Mayfield, M. Mehan, R. Mehler, S. K. Nelson, M. Nelson, D. Nieuwlandt, M. Nikrad, U. Ochsner, R. M. Ostroff, M. Otis, T. Parker, S. Pietrasiewicz, D. I. Resnicow, J. Rohloff, G. Sanders, S. Sattin, D. Schneider, B. Singer, M. Stanton, A. Sterkel, A. Stewart, S. Stratford, J. D. Vaught, M. Vrkljan, J. J. Walker, M. Watrobka, S. Waugh, A. Weiss, S. K. Wilcox, A. Wolfson, S. K. Wolk, C. Zhang and D. Zichi (2010). "Aptamer-based multiplexed proteomic technology for biomarker discovery." PLoS One **5**(12): e15004.

Gomberg-Maitland, M., R. Schulz, A. Mediratta, K. Addetia, S. Coslet, V. Thomeas, H. Gillies and R. J. Oudiz (2015). "Phase I safety study of ranolazine in pulmonary arterial hypertension." Pulm Circ **5**(4): 691-700.

Gomez-Arroyo, J., N. F. Voelkel, H. J. Bogaard and L. Taraseviciene-Stewart (2012). "Usefulness of a mouse model of reversible pulmonary arterial hypertension: be cautious, choose carefully." Am J Respir Crit Care Med **185**(12): 1326; author reply 1326-1327.

Gomez, A., D. Bialostozky, A. Zajarias, E. Santos, A. Palomar, M. L. Martinez and J. Sandoval (2001). "Right ventricular ischemia in patients with primary pulmonary hypertension." J Am Coll Cardiol **38**(4): 1137-1142.

Grosjean, H., S. Auxilien, F. Constantinesco, C. Simon, Y. Corda, H. F. Becker, D. Foiret, A. Morin, Y. X. Jin, M. Fournier and J. L. Fourrey (1996). "Enzymatic conversion of adenosine to inosine and to N1-methylinosine in transfer RNAs: a review." Biochimie **78**(6): 488-501.

Guarnieri, C. and C. Muscari (1988). "Beneficial effects of trimetazidine on mitochondrial function and superoxide production in the cardiac muscle of monocrotaline-treated rats." Biochem Pharmacol **37**(24): 4685-4688.

Guarnieri, C. and C. Muscari (1990). "Beneficial effects of trimetazidine on mitochondrial function and superoxide production in the cardiac muscle." Cardiovasc Drugs Ther **4 Suppl 4**: 814-815.

Guignabert, C., B. Raffestin, R. Benferhat, W. Raoul, P. Zadigue, D. Rideau, M. Hamon, S. Adnot and S. Eddahibi (2005). "Serotonin transporter inhibition prevents and reverses monocrotaline-induced pulmonary hypertension in rats." Circulation **111**(21): 2812-2819.

Guignabert, C., L. Tu, M. Izikki, L. Dewachter, P. Zadigue, M. Humbert, S. Adnot, E. Fadel and S. Eddahibi (2009). "Dichloroacetate treatment partially regresses established pulmonary hypertension in mice with SM22alpha-targeted overexpression of the serotonin transporter." FASEB J **23**(12): 4135-4147.

Guo, L., M. V. Milburn, J. A. Ryals, S. C. Lonergan, M. W. Mitchell, J. E. Wulff, D. C. Alexander, A. M. Evans, B. Bridgewater, L. Miller, M. L. Gonzalez-Garay and C. T. Caskey (2015). "Plasma metabolomic profiles enhance precision medicine for volunteers of normal health." Proc Natl Acad Sci U S A **112**(35): E4901-4910.

Gurtu, V. and E. D. Michelakis (2015). "Emerging therapies and future directions in pulmonary arterial hypertension." Can J Cardiol **31**(4): 489-501.

Gutierrez, G., A. Venbrux, E. Ignacio, J. Reiner, L. Chawla and A. Desai (2007). "The concentration of oxygen, lactate and glucose in the central veins, right heart, and pulmonary artery: a study in patients with pulmonary hypertension." Crit Care **11**(2): R44.

Hafiane, A. and J. Genest (2015). "High density lipoproteins: Measurement techniques and potential biomarkers of cardiovascular risk." BBA Clin **3**: 175-188.

Hall, S. M., A. A. Hislop, C. M. Pierce and S. G. Haworth (2000). "Prenatal origins of human intrapulmonary arteries: formation and smooth muscle maturation." Am J Respir Cell Mol Biol **23**(2): 194-203.

Hampl, V., J. Bibova, V. Povysilova and J. Herget (2003). "Dehydroepiandrosterone sulphate reduces chronic hypoxic pulmonary hypertension in rats." Eur Respir J **21**(5): 862-865.

Hannun, Y. A. and L. M. Obeid (2008). "Principles of bioactive lipid signalling: lessons from sphingolipids." Nature Reviews Molecular Cell Biology **9**(2): 139-150.

Hansmann, G., R. A. Wagner, S. Schellong, V. A. Perez, T. Urashima, L. Wang, A. Y. Sheikh, R. S. Suen, D. J. Stewart and M. Rabinovitch (2007). "Pulmonary arterial hypertension is linked to insulin resistance and reversed by peroxisome proliferator-activated receptor-gamma activation." Circulation **115**(10): 1275-1284.

Hao, D., M. O. Sarfaraz, F. Farshidfar, D. G. Bebb, C. Y. Lee, C. M. Card, M. David and A. M. Weljie (2016). "Temporal characterization of serum metabolite signatures in lung cancer patients undergoing treatment." Metabolomics **12**: 58.

Hartiala, J. A., W. H. Tang, Z. Wang, A. L. Crow, A. F. Stewart, R. Roberts, R. McPherson, J. Erdmann, C. Willenborg, S. L. Hazen and H. Allayee (2016). "Genome-wide association study and targeted metabolomics identifies sex-specific association of CPS1 with coronary artery disease." Nat Commun **7**: 10558.

Heresi, G. A., M. Aytekin, J. Newman, J. DiDonato and R. A. Dweik (2010). "Plasma levels of high-density lipoprotein cholesterol and outcomes in pulmonary arterial hypertension." Am J Respir Crit Care Med **182**(5): 661-668.

Herve, P., J. M. Launay, M. L. Scrobohaci, F. Brenot, G. Simonneau, P. Petitpretz, P. Poubeau, J. Cerrina, P. Duroux and L. Drouet (1995). "Increased plasma serotonin in primary pulmonary hypertension." Am J Med **99**(3): 249-254.

Hislop, A. A. and C. M. Pierce (2000). "Growth of the vascular tree." Paediatr Respir Rev **1**(4): 321-327.

Hislop, A. A., D. R. Springall, L. D. Buttery, J. S. Pollock and S. G. Haworth (1995). "Abundance of endothelial nitric oxide synthase in newborn intrapulmonary arteries." Arch Dis Child Fetal Neonatal Ed **73**(1): F17-21.

Hlatky, M. A., P. Greenland, D. K. Arnett, C. M. Ballantyne, M. H. Criqui, M. S. Elkind, A. S. Go, F. E. Harrell, Jr., Y. Hong, B. V. Howard, V. J. Howard, P. Y. Hsue, C. M. Kramer, J. P. McConnell, S. L. Normand, C. J. O'Donnell, S. C. Smith, Jr., P. W. Wilson, D. American Heart Association Expert Panel on Subclinical Atherosclerotic, F. Emerging Risk and C. the Stroke (2009). "Criteria for evaluation of novel markers of cardiovascular risk: a scientific statement from the American Heart Association." Circulation **119**(17): 2408-2416.

Hoeper, M. M., J. A. Barbera, R. N. Channick, P. M. Hassoun, I. M. Lang, A. Manes, F. J. Martinez, R. Naeije, H. Olschewski, J. Pepke-Zaba, M. M. Redfield, I. M. Robbins, R. Souza, A. Torbicki and M. McGoon (2009). "Diagnosis, assessment, and treatment of non-pulmonary arterial hypertension pulmonary hypertension." J Am Coll Cardiol **54**(1 Suppl): S85-96.

Hoeper, M. M., R. J. Barst, R. C. Bourge, J. Feldman, A. E. Frost, N. Galie, M. A. Gomez-Sanchez, F. Grimminger, E. Grunig, P. M. Hassoun, N. W. Morrell, A. J. Peacock, T. Satoh, G. Simonneau, V. F. Tapson, F. Torres, D. Lawrence, D. A. Quinn and H. A. Ghofrani (2013). "Imatinib mesylate as add-on therapy for pulmonary arterial hypertension: results of the randomized IMPRES study." Circulation **127**(10): 1128-1138.

Hoeper, M. M., H. J. Bogaard, R. Condliffe, R. Frantz, D. Khanna, M. Kurzyna, D. Langleben, A. Manes, T. Satoh, F. Torres, M. R. Wilkins and D. B. Badesch (2013). "Definitions and diagnosis of pulmonary hypertension." J Am Coll Cardiol **62**(25 Suppl): D42-50.

Hoeper, M. M. and S. J. Gibbs (2014). "The changing landscape of pulmonary arterial hypertension and implications for patient care." Eur Respir Rev **23**(134): 450-457.

Hoeper, M. M., M. Humbert, R. Souza, M. Idrees, S. M. Kawut, K. Sliwa-Hahnle, Z. C. Jing and J. S. Gibbs (2016). "A global view of pulmonary hypertension." Lancet Respir Med **4**(4): 306-322.

Hoeper, M. M., D. Huscher, H. A. Ghofrani, M. Delcroix, O. Distler, C. Schweiger, E. Grunig, G. Staehler, S. Rosenkranz, M. Halank, M. Held, C. Grohe, T. J. Lange, J. Behr, H. Klose, H. Wilkens, A. Filusch, M. Germann, R. Ewert, H. J. Seyfarth, K. M. Olsson, C. F. Opitz, S. P. Gaine, C. D. Vizza, A. Vonk-Noordegraaf, H. Kaemmerer, J. S. Gibbs and D. Pittrow (2013). "Elderly patients diagnosed with idiopathic pulmonary arterial hypertension: results from the COMPERA registry." Int J Cardiol **168**(2): 871-880.

Hoeper, M. M., M. M. Madani, N. Nakanishi, B. Meyer, S. Cebotari and L. J. Rubin (2014). "Chronic thromboembolic pulmonary hypertension." Lancet Respir Med **pii: S2213-2600(14)70089-X**(doi: 10.1016/S2213-2600(14)70089-X. [Epub ahead of print]).

Hoet, P. H. and B. Nemery (2000). "Polyamines in the lung: polyamine uptake and polyamine-linked pathological or toxicological conditions." American Journal of Physiology: Heart and Circulatory Physiology **278**(3): L417-433.

Holmes, E., J. V. Li, J. R. Marchesi and J. K. Nicholson (2012). "Gut microbiota composition and activity in relation to host metabolic phenotype and disease risk." Cell Metab **16**(5): 559-564.

Holmes, E., R. L. Loo, O. Cloarec, M. Coen, H. Tang, E. Maibaum, S. Bruce, Q. Chan, P. Elliott, J. Stamler, I. D. Wilson, J. C. Lindon and J. K. Nicholson (2007). "Detection of urinary drug metabolite (xenometabolome) signatures in molecular epidemiology studies via statistical total correlation (NMR) spectroscopy." Anal Chem **79**(7): 2629-2640.

Holmes, E., I. D. Wilson and J. K. Nicholson (2008). "Metabolic phenotyping in health and disease." Cell **134**(5): 714-717.

Holmes, M. V., F. W. Asselbergs, T. M. Palmer, F. Drenos, M. B. Lanktree, C. P. Nelson, C. E. Dale, S. Padmanabhan, C. Finan, D. I. Swerdlow, V. Tragante, E. P. van Iperen, S. Sivapalaratnam, S. Shah, C. C. Elbers, T. Shah, J. Engmann, C. Giambartolomei, J. White, D. Zabaneh, R. Sofat, S. McLachlan, U. consortium, P. A. Doevendans, A. J. Balmforth, A. S. Hall, K. E. North, B. Almoguera, R. C. Hoogeveen, M. Cushman, M. Fornage, S. R. Patel, S. Redline, D. S. Siscovick, M. Y. Tsai, K. J. Karczewski, M. H. Hofker, W. M. Verschuren, M. L. Bots, Y. T. van der Schouw, O. Melander, A. F. Dominiczak, R. Morris, Y. Ben-Shlomo, J. Price, M. Kumari, J. Baumert, A. Peters, B. Thorand, W. Koenig, T. R. Gaunt, S. E. Humphries, R. Clarke, H. Watkins, M. Farrall, J. G. Wilson, S. S. Rich, P. I. de Bakker, L. A. Lange, G. Davey Smith, A. P. Reiner, P. J. Talmud, M. Kivimaki, D. A. Lawlor, F. Dudbridge, N. J. Samani, B. J. Keating, A. D. Hingorani and J. P. Casas (2015). "Mendelian randomization of blood lipids for coronary heart disease." Eur Heart J **36**(9): 539-550.

Homma, N., T. Nagaoka, V. Karoor, M. Imamura, L. Taraseviciene-Stewart, L. A. Walker, K. A. Fagan, I. F. McMurtry and M. Oka (2008). "Involvement of RhoA/Rho kinase signaling in protection against monocrotaline-induced pulmonary hypertension in pneumonectomized rats by dehydroepiandrosterone." Am J Physiol Lung Cell Mol Physiol **295**(1): L71-78.

Hong, M. G., R. Karlsson, P. K. Magnusson, M. R. Lewis, W. Isaacs, L. S. Zheng, J. Xu, H. Gronberg, E. Ingelsson, Y. Pawitan, C. Broeckling, J. E. Prenni, F. Wiklund and J. A. Prince (2013). "A genome-wide assessment of variability in human serum metabolism." Hum Mutat **34**(3): 515-524.

Hopkins, W. E. (2005). "The remarkable right ventricle of patients with Eisenmenger syndrome." Coron Artery Dis **16**(1): 19-25.

Hopper, R. K., J. R. Moonen, I. Diebold, A. Cao, C. J. Rhodes, N. F. Tojais, J. K. Hennigs, M. Gu, L. Wang and M. Rabinovitch (2016). "In Pulmonary Arterial Hypertension, Reduced BMPR2 Promotes Endothelial-to-Mesenchymal Transition via HMGA1 and Its Target Slug." Circulation **133**(18): 1783-1794.

Hotamisligil, G. S. (2010). "Endoplasmic reticulum stress and the inflammatory basis of metabolic disease." Cell **140**(6): 900-917.

Hovingh, G. K., A. Brownlie, R. J. Bisoendial, M. P. Dube, J. H. Levels, W. Petersen, R. P. Dullaart, E. S. Stroes, A. H. Zwinderman, E. de Groot, M. R. Hayden, J. A. Kuivenhoven and J. J. Kastelein (2004). "A novel apoA-I mutation (L178P) leads to endothelial dysfunction, increased arterial wall thickness, and premature coronary artery disease." J Am Coll Cardiol **44**(7): 1429-1435.

Howard, L. S., G. M. Watson, J. Wharton, C. J. Rhodes, K. Chan, R. Khengar, P. A. Robbins, D. G. Kiely, R. Condliffe, C. A. Elliott, J. Pepke-Zaba, K. Sheares, N. W. Morrell, R. Davies, D. Ashby, J. S. Gibbs and M. R. Wilkins (2013). "Supplementation of iron in pulmonary hypertension: Rationale and design of a phase II clinical trial in idiopathic pulmonary arterial hypertension." Pulm Circ **3**(1): 100-107.

Hu, C. A., S. P. Donald, J. Yu, W. W. Lin, Z. Liu, G. Steel, C. Obie, D. Valle and J. M. Phang (2007). "Overexpression of proline oxidase induces proline-dependent and mitochondria-mediated apoptosis." Mol Cell Biochem **295**(1-2): 85-92.

Huang, N., M. Siegel, G. Kruppa and L. F. (1999). "Automation of a Fourier Transform Ion Cyclotron Resonance Mass Spectrometer for Acquisition, Analysis, and E-mailing of HighResolution Exact-Mass Electrospray Ionization Mass Spectral Data." J Am Soc Mass Spectrom **10**: 1166 –1173.

Huang, W., R. T. Yen, M. McLaurine and G. Bledsoe (1996). "Morphometry of the human pulmonary vasculature." J Appl Physiol (1985) **81**(5): 2123-2133.

Huang, Y., J. A. DiDonato, B. S. Levison, D. Schmitt, L. Li, Y. Wu, J. Buffa, T. Kim, G. S. Gerstenecker, X. Gu, C. S. Kadiyala, Z. Wang, M. K. Culley, J. E. Hazen, A. J. Didonato, X. Fu, S. Z. Berisha, D. Peng, T. T. Nguyen, S. Liang, C. C. Chuang, L. Cho, E. F. Plow, P. L. Fox, V. Gogonea, W. H. Tang, J. S. Parks, E. A. Fisher, J. D. Smith and S. L. Hazen (2014). "An abundant dysfunctional apolipoprotein A1 in human atheroma." Nat Med **20**(2): 193-203.

Human Microbiome Project, C. (2012). "A framework for human microbiome research." Nature **486**(7402): 215-221.

Humbert, M. (2010). "Pulmonary arterial hypertension and chronic thromboembolic pulmonary hypertension: pathophysiology." Eur Respir Rev **19**(115): 59-63.

Humbert, M., E. M. Lau, D. Montani, X. Jais, O. Sitbon and G. Simonneau (2014). "Advances in therapeutic interventions for patients with pulmonary arterial hypertension." Circulation **130**(24): 2189-2208.

Humbert, M., N. W. Morrell, S. L. Archer, K. R. Stenmark, M. R. MacLean, I. M. Lang, B. W. Christman, E. K. Weir, O. Eickelberg, N. F. Voelkel and M. Rabinovitch (2004). "Cellular and molecular pathobiology of pulmonary arterial hypertension." J Am Coll Cardiol **43**(12 Suppl S): 13S-24S.

Humbert, M., O. Sitbon and G. Simonneau (2004). "Treatment of pulmonary arterial hypertension." N Engl J Med **351**(14): 1425-1436.

Hurdman, J., R. Condliffe, C. A. Elliot, C. Davies, C. Hill, J. M. Wild, D. Capener, P. Sephton, N. Hamilton, I. J. Armstrong, C. Billings, A. Lawrie, I. Sabroe, M. Akil, L. O'Toole and D. G. Kiely (2012). "ASPIRE registry: assessing the Spectrum of Pulmonary hypertension Identified at a REferral centre." Eur Respir J **39**(4): 945-955.

Huston, J. H. and J. J. Ryan (2016). "The emerging role of epigenetics in pulmonary arterial hypertension: an important avenue for clinical trials (2015 Grover Conference Series)." Pulm Circ **6**(3): 274-284.

Idriss, N. K., G. Y. Lip, B. Balakrishnan, R. Jaumdally, C. J. Boos and A. D. Blann (2010). "Plasma haemoxygenase-1 in coronary artery disease. A comparison with angiogenin, matrix metalloproteinase-9, tissue inhibitor of metalloproteinase-1 and vascular endothelial growth factor." Thromb Haemost **104**(5): 1029-1037.

Ignatescu, M., K. Kostner, G. Zorn, M. Kneussl, G. Maurer, I. M. Lang and K. Huber (1998). "Plasma Lp(a) levels are increased in patients with chronic thromboembolic pulmonary hypertension." Thromb Haemost **80**(2): 231-232.

Illig, T., C. Gieger, G. Zhai, W. Romisch-Margl, R. Wang-Sattler, C. Prehn, E. Altmaier, G. Kastenmuller, B. S. Kato, H. W. Mewes, T. Meitinger, M. H. de Angelis, F. Kronenberg, N. Soranzo, H. E.

Wichmann, T. D. Spector, J. Adamski and K. Suhre (2010). "A genome-wide perspective of genetic variation in human metabolism." Nat Genet **42**(2): 137-141.

Interleukin-6 Receptor Mendelian Randomisation Analysis, C. (2012). "The interleukin-6 receptor as a target for prevention of coronary heart disease: a mendelian randomisation analysis." Lancet **379**(9822): 1214-1224.

Izikki, M., N. Hanoun, E. Marcos, L. Savale, A. M. Barlier-Mur, F. Saurini, S. Eddahibi, M. Hamon and S. Adnot (2007). "Tryptophan hydroxylase 1 knockout and tryptophan hydroxylase 2 polymorphism: effects on hypoxic pulmonary hypertension in mice." Am J Physiol Lung Cell Mol Physiol **293**(4): L1045-1052.

Jakubowski, J. A., B. G. Utterback, D. E. Mais, S. A. Hardinger, T. F. Braish, C. R. Nevill and P. L. Fuchs (1994). "Biochemical and pharmacological activity of arene-fused prostacyclin analogues on human platelets." Prostaglandins **47**(3): 189-201.

Jasiewicz, M., M. Moniuszko, D. Pawlak, M. Knapp, M. Rusak, R. Kazimierczyk, W. J. Musial, M. Dabrowska and K. A. Kaminski (2016). "Activity of the kynurenine pathway and its interplay with immunity in patients with pulmonary arterial hypertension." Heart **102**(3): 230-237.

Jeffery, T. K. and N. W. Morrell (2002). "Molecular and cellular basis of pulmonary vascular remodeling in pulmonary hypertension." Prog Cardiovasc Dis **45**(3): 173-202.

Jimenez, B., R. Mirnezami, J. Kinross, O. Cloarec, H. C. Keun, E. Holmes, R. D. Goldin, P. Ziprin, A. Darzi and J. K. Nicholson (2013). "1H HR-MAS NMR spectroscopy of tumor-induced local metabolic "field-effects" enables colorectal cancer staging and prognostication." J Proteome Res **12**(2): 959-968.

Jing, Z. C., Z. X. Yu, J. Y. Shen, B. X. Wu, K. F. Xu, X. Y. Zhu, L. Pan, Z. L. Zhang, X. Q. Liu, Y. S. Zhang, X. Jiang, N. Galie, Efficacy and G. Safety of Vardenafil in the Treatment of Pulmonary Arterial Hypertension Study (2011). "Vardenafil in pulmonary arterial hypertension: a randomized, double-blind, placebo-controlled study." Am J Respir Crit Care Med **183**(12): 1723-1729.

Johansson, J., L. A. Carlson, C. Landou and A. Hamsten (1991). "High density lipoproteins and coronary atherosclerosis. A strong inverse relation with the largest particles is confined to normotriglyceridemic patients." Arterioscler Thromb **11**(1): 174-182.

Jujo, T., S. Sakao, H. Ishibashi-Ueda, K. Ishida, A. Naito, T. Sugiura, A. Shigeta, N. Tanabe, M. Masuda and K. Tatsumi (2015). "Evaluation of the Microcirculation in Chronic Thromboembolic Pulmonary Hypertension Patients: The Impact of Pulmonary Arterial Remodeling on Postoperative and Follow-Up Pulmonary Arterial Pressure and Vascular Resistance." PLoS One **10**(8): e0133167.

Kanehisa, M., Y. Sato, M. Kawashima, M. Furumichi and M. Tanabe (2016). "KEGG as a reference resource for gene and protein annotation." Nucleic Acids Res **44**(D1): D457-462.

Kaper, T., L. L. Looger, H. Takanaga, M. Platten, L. Steinman and W. B. Frommer (2007). "Nanosensor detection of an immunoregulatory tryptophan influx/kynurenine efflux cycle." PLoS Biol **5**(10): e257.

Kastenmuller, G., J. Raffler, C. Gieger and K. Suhre (2015). "Genetics of human metabolism: an update." Hum Mol Genet **24**(R1): R93-R101.

Katajamaa, M. and M. Oresic (2005). "Processing methods for differential analysis of LC/MS profile data." BMC Bioinformatics **6**: 179.

Kelly, R. S., A. Dahlin, M. J. McGeachie, W. Qiu, J. Sordillo, E. S. Wan, A. C. Wu and J. Lasky-Su (2016). "Asthma metabolomics and the potential for integrative omics in research and the clinic." Chest **151**(2): 262-277.

Kettunen, J., A. Demirkan, P. Wurtz, H. H. Draisma, T. Haller, R. Rawal, A. Vaarhorst, A. J. Kangas, L. P. Lyytikainen, M. Pirinen, R. Pool, A. P. Sarin, P. Soininen, T. Tukiainen, Q. Wang, M. Tiainen, T. Tynkkynen, N. Amin, T. Zeller, M. Beekman, J. Deelen, K. W. van Dijk, T. Esko, J. J. Hottenga, E. M. van Leeuwen, T. Lehtimaki, E. Mihailov, R. J. Rose, A. J. de Craen, C. Gieger, M. Kahonen, M. Perola, S. Blankenberg, M. J. Savolainen, A. Verhoeven, J. Viikari, G. Willemsen, D. I. Boomsma, C. M. van Duijn, J. Eriksson, A. Jula, M. R. Jarvelin, J. Kaprio, A. Metspalu, O. Raitakari, V. Salomaa, P. E. Slagboom, M. Waldenberger, S. Ripatti and M. Ala-Korpela (2016). "Genome-wide study for circulating metabolites identifies 62 loci and reveals novel systemic effects of LPA." Nat Commun **7**: 11122.

Khogali, S. E., A. A. Harper, J. A. Lyall and M. J. Rennie (1998). "Effects of L-glutamine on post-ischaemic cardiac function: protection and rescue." J Mol Cell Cardiol **30**(4): 819-827.

Kielstein, J. T., S. M. Bode-Boger, G. Hesse, J. Martens-Lobenhoffer, A. Takacs, D. Fliser and M. M. Hoeper (2005). "Asymmetrical dimethylarginine in idiopathic pulmonary arterial hypertension." Arterioscler Thromb Vasc Biol **25**(7): 1414-1418.

Kim, N. H., M. Delcroix, D. P. Jenkins, R. Channick, P. Dartevelle, P. Jansa, I. Lang, M. M. Madani, H. Ogino, V. Pengo and E. Mayer (2013). "Chronic thromboembolic pulmonary hypertension." Journal of the American College of Cardiology **62**(25 Suppl): D92-99.

Kim, N. H. and I. M. Lang (2012). "Risk factors for chronic thromboembolic pulmonary hypertension." Eur Respir Rev **21**(123): 27-31.

Kinlay, S., T. Michel and J. A. Leopold (2016). "The Future of Vascular Biology and Medicine." Circulation **133**(25): 2603-2609.

Kirchner, S. and Z. Ignatova (2015). "Emerging roles of tRNA in adaptive translation, signalling dynamics and disease." Nature Review Genetics **16**(2): 98-112.

Klein, M. S. and J. Shearer (2016). "Metabolomics and Type 2 Diabetes: Translating Basic Research into Clinical Application." J Diabetes Res **2016**: 3898502.

Koochekpour, S., S. Majumdar, G. Azabdaftari, K. Attwood, R. Scioneaux, D. Subramani, C. Manhardt, G. D. Lorusso, S. S. Willard, H. Thompson, M. Shourideh, K. Rezaei, O. Sartor, J. L. Mohler and R. L. Vessella (2012). "Serum glutamate levels correlate with Gleason score and glutamate blockade decreases proliferation, migration, and invasion and induces apoptosis in prostate cancer cells." Clinical Cancer Research **18**(21): 5888-5901.

Kurzyna, M., M. Dabrowski, D. Bielecki, A. Fijalkowska, P. Pruszczyk, G. Opolski, J. Burakowski, M. Florczyk, W. Z. Tomkowski, L. Wawrzynska, M. Szturmowicz and A. Torbicki (2007). "Atrial septostomy in treatment of end-stage right heart failure in patients with pulmonary hypertension." Chest **131**(4): 977-983.

Labrie, F., V. Luu-The, C. Labrie and J. Simard (2001). "DHEA and its transformation into androgens and estrogens in peripheral target tissues: intracrinology." Front Neuroendocrinol **22**(3): 185-212.

Lajoie, A. C., G. Lauziere, J. C. Lega, Y. Lacasse, S. Martin, S. Simard, S. Bonnet and S. Provencher (2016). "Combination therapy versus monotherapy for pulmonary arterial hypertension: a meta-analysis." Lancet Respir Med **4**(4): 291-305.

Landt, S., K. Mordelt, I. Schwidde, J. Barinoff, S. Korlach, F. Stoblen, W. Lichtenegger, J. Sehouli and S. Kummel (2011). "Prognostic significance of the angiogenic factors angiogenin, endoglin and endostatin in cervical cancer." Anticancer Res **31**(8): 2651-2655.

Lang, I. M. and M. Madani (2014). "Update on chronic thromboembolic pulmonary hypertension." Circulation **130**(6): 508-518.

Larsen, C. M., R. B. McCully, J. G. Murphy, S. S. Kushwaha, R. P. Frantz and G. C. Kane (2016). "Usefulness of High-Density Lipoprotein Cholesterol to Predict Survival in Pulmonary Arterial Hypertension." Am J Cardiol **118**(2): 292-297.

Lau, E. M., L. Godinas, O. Sitbon, D. Montani, L. Savale, X. Jais, F. Lador, S. Gunther, D. S. Celermajer, G. Simonneau, M. Humbert, D. Chemla and P. Herve (2016). "Resting pulmonary artery pressure of 21-24 mmHg predicts abnormal exercise haemodynamics." Eur Respir J **47**(5): 1436-1444.

Lawlor, D. A., R. M. Harbord, J. A. Sterne, N. Timpson and G. Davey Smith (2008). "Mendelian randomization: using genes as instruments for making causal inferences in epidemiology." Stat Med **27**(8): 1133-1163.

Lawton, K. A., M. V. Brown, D. Alexander, Z. Li, J. E. Wulff, R. Lawson, M. Jaffa, M. V. Milburn, J. A. Ryals, R. Bowser, M. E. Cudkowicz, J. D. Berry and A. L. S. C. Northeast (2014). "Plasma metabolomic biomarker panel to distinguish patients with amyotrophic lateral sclerosis from disease mimics." Amyotrophic Lateral Sclerosis and Frontotemporal Degeneration **15**(5-6): 362-370.

Le, T. T., Y. Urasaki and G. Pizzorno (2014). "Uridine prevents fenofibrate-induced fatty liver." PLoS One **9**(1): e87179.

Lee, J., J. Park, M. S. Lim, S. J. Seong, J. J. Seo, S. M. Park, H. W. Lee and Y. R. Yoon (2012). "Quantile normalization approach for liquid chromatography-mass spectrometry-based metabolomic data from healthy human volunteers." Anal Sci **28**(8): 801-805.

Lee, S. L., W. W. Wang, J. J. Lanzillo and B. L. Fanburg (1994). "Serotonin produces both hyperplasia and hypertrophy of bovine pulmonary artery smooth muscle cells in culture." Am J Physiol **266**(1 Pt 1): L46-52.

Leslie, K. O. and M. R. Wick (2005). Practical pulmonary pathology : a diagnostic approach. Philadelphia, Churchill Livingstone.

Leuchte, H. H., C. Neurohr, R. Baumgartner, M. Holzapfel, W. Giehrl, M. Vogeser and J. Behr (2004). "Brain natriuretic peptide and exercise capacity in lung fibrosis and pulmonary hypertension." American journal of respiratory and critical care medicine **170**(4): 360-365.

Lewis, G. D. (2014). "The emerging role of metabolomics in the development of biomarkers for pulmonary hypertension and other cardiovascular diseases (2013 Grover Conference series)." Pulm Circ **4**(3): 417-423.

Lewis, G. D., L. Farrell, M. J. Wood, M. Martinovic, Z. Arany, G. C. Rowe, A. Souza, S. Cheng, E. L. McCabe, E. Yang, X. Shi, R. Deo, F. P. Roth, A. Asnani, E. P. Rhee, D. M. Systrom, M. J. Semigran, R. S. Vasan, S. A. Carr, T. J. Wang, M. S. Sabatine, C. B. Clish and R. E. Gerszten (2010). "Metabolic signatures of exercise in human plasma." Science Translational Medicine **2**(33): 33ra37.

Lewis, G. D., D. Ngo, A. R. Hemnes, L. Farrell, C. Domos, P. P. Pappagianopoulos, B. P. Dhakal, A. Souza, X. Shi, M. E. Pugh, A. Beloiartsev, S. Sinha, C. B. Clish and R. E. Gerszten (2016).

"Metabolic Profiling of Right Ventricular-Pulmonary Vascular Function Reveals Circulating Biomarkers of Pulmonary Hypertension." Journal of the American College of Cardiology **67**(2): 174-189.

Ley, R. E., P. J. Turnbaugh, S. Klein and J. I. Gordon (2006). "Microbial ecology: human gut microbes associated with obesity." Nature **444**(7122): 1022-1023.

Li, J., H. Jia, X. Cai, H. Zhong, Q. Feng, S. Sunagawa, M. Arumugam, J. R. Kultima, E. Prifti, T. Nielsen, A. S. Juncker, C. Manichanh, B. Chen, W. Zhang, F. Levenez, J. Wang, X. Xu, L. Xiao, S. Liang, D. Zhang, Z. Zhang, W. Chen, H. Zhao, J. Y. Al-Aama, S. Edris, H. Yang, J. Wang, T. Hansen, H. B. Nielsen, S. Brunak, K. Kristiansen, F. Guarner, O. Pedersen, J. Dore, S. D. Ehrlich, H. I. T. C. Meta, P. Bork, J. Wang and H. I. T. C. Meta (2014). "An integrated catalog of reference genes in the human gut microbiome." Nat Biotechnol **32**(8): 834-841.

Li, M., S. Riddle, H. Zhang, A. D'Alessandro, A. Flockton, N. J. Serkova, K. C. Hansen, R. Moldvan, B. A. McKeon, M. Frid, S. Kumar, H. Li, H. Liu, A. Caanovas, J. F. Medrano, M. G. Thomas, D. Iloska, L. Plecita-Hlavata, P. Jezek, S. Pullamsetti, M. A. Fini, K. C. El Kasmi, Q. Zhang and K. R. Stenmark (2016). "Metabolic Reprogramming Regulates the Proliferative and Inflammatory Phenotype of Adventitial Fibroblasts in Pulmonary Hypertension Through the Transcriptional Corepressor C-Terminal Binding Protein-1." Circulation **134**(15): 1105-1121.

Li, M., S. Riddle, H. Zhang, A. D'Alessandro, A. Flockton, N. J. Serkova, K. C. Hansen, R. Moldvan, B. A. McKeon, M. Frid, S. Kumar, H. Li, H. Liu, A. Canovas, J. F. Medrano, M. G. Thomas, D. Iloska, L. Plecita-Hlavata, P. Jezek, S. Pullamsetti, M. A. Fini, K. C. El Kasmi, Q. Zhang and K. R. Stenmark (2016). "Metabolic Reprogramming Regulates the Proliferative and Inflammatory Phenotype of Adventitial Fibroblasts in Pulmonary Hypertension Through the Transcriptional Co-Repressor C-terminal Binding Protein-1." Circulation **134**(15): 1105-1121.

Li, W., L. Wang, C. M. Xiong, T. Yang, Y. Zhang, Q. Gu, Y. Yang, X. H. Ni, Z. H. Liu, W. Fang and J. G. He (2015). "The Prognostic Value of 18F-FDG Uptake Ratio Between the Right and Left Ventricles in Idiopathic Pulmonary Arterial Hypertension." Clin Nucl Med **40**(11): 859-863.

Ling, Y., M. K. Johnson, D. G. Kiely, R. Condliffe, C. A. Elliot, J. S. Gibbs, L. S. Howard, J. Pepke-Zaba, K. K. Sheares, P. A. Corris, A. J. Fisher, J. L. Lordan, S. Gaine, J. G. Coghlan, S. J. Wort, M. A. Gatzoulis and A. J. Peacock (2012). "Changing demographics, epidemiology, and survival of incident pulmonary arterial hypertension: results from the pulmonary hypertension registry of the United Kingdom and Ireland." Am J Respir Crit Care Med **186**(8): 790-796.

Linsel-Nitschke, P., A. Gotz, J. Erdmann, I. Braenne, P. Braund, C. Hengstenberg, K. Stark, M. Fischer, S. Schreiber, N. E. El Mokhtari, A. Schaefer, J. Schrezenmeir, D. Rubin, A. Hinney, T. Reinehr, C. Roth, J. Ortlepp, P. Hanrath, A. S. Hall, M. Mangino, W. Lieb, C. Lamina, I. M. Heid, A. Doering, C. Gieger, A. Peters, T. Meitinger, H. E. Wichmann, I. R. Konig, A. Ziegler, F. Kronenberg, N. J. Samani, H. Schunkert, C. Wellcome Trust Case Control and C. Cardiogenics (2008). "Lifelong reduction of LDL-cholesterol related to a common variant in the LDL-receptor gene decreases the risk of coronary artery disease--a Mendelian Randomisation study." PLoS One **3**(8): e2986.

Linsel-Nitschke, P. and A. R. Tall (2005). "HDL as a target in the treatment of atherosclerotic cardiovascular disease." Nat Rev Drug Discov **4**(3): 193-205.

Liu, D. and J. S. Dillon (2002). "Dehydroepiandrosterone activates endothelial cell nitric-oxide synthase by a specific plasma membrane receptor coupled to Galpha(i2,3)." J Biol Chem **277**(24): 21379-21388.

Livshits, G., A. J. Macgregor, C. Gieger, I. Malkin, A. Moayyeri, H. Grallert, R. T. Emeny, T. Spector, G. Kastenmuller and F. M. Williams (2015). "An omics investigation into chronic widespread musculoskeletal pain reveals epiandrosterone sulfate as a potential biomarker." Pain **156**(10): 1845-1851.

Lozupone, C. A., J. I. Stombaugh, J. I. Gordon, J. K. Jansson and R. Knight (2012). "Diversity, stability and resilience of the human gut microbiota." Nature **489**(7415): 220-230.

Lusis, A. J. and J. N. Weiss (2010). "Cardiovascular networks: systems-based approaches to cardiovascular disease." Circulation **121**(1): 157-170.

Lynn, K. S., M. L. Cheng, Y. R. Chen, C. Hsu, A. Chen, T. M. Lih, H. Y. Chang, C. J. Huang, M. S. Shiao, W. H. Pan, T. Y. Sung and W. L. Hsu (2015). "Metabolite identification for mass spectrometry-based metabolomics using multiple types of correlated ion information." Anal Chem **87**(4): 2143-2151.

Lyons, T. J. and A. Basu (2012). "Biomarkers in diabetes: hemoglobin A1c, vascular and tissue markers." Transl Res **159**(4): 303-312.

Lythgoe, M. P., C. J. Rhodes, P. Ghataorhe, M. Attard, J. Wharton and M. R. Wilkins (2016). "Why drugs fail in clinical trials in pulmonary arterial hypertension, and strategies to succeed in the future." Pharmacol Ther **164**: 195-203.

Ma, L. and W. K. Chung (2014). "The genetic basis of pulmonary arterial hypertension." Human Genetics **133**(5): 471-479.

Maarman, G., S. Lecour, G. Butrous, F. Thienemann and K. Sliwa (2013). "A comprehensive review: the evolution of animal models in pulmonary hypertension research; are we there yet?" Pulm Circ **3**(4): 739-756.

Machado, R. D., O. Eickelberg, C. G. Elliott, M. W. Geraci, M. Hanaoka, J. E. Loyd, J. H. Newman, J. A. Phillips, 3rd, F. Soubrier, R. C. Trembath and W. K. Chung (2009). "Genetics and genomics of pulmonary arterial hypertension." Journal of the American College of Cardiology **54**(1 Suppl): S32-42.

Macian, F. (2005). "NFAT proteins: key regulators of T-cell development and function." Nat Rev Immunol **5**(6): 472-484.

Malik, A., U. Sharma, R. Lakshmy, R. Narang and N. R. Jagannathan (2015). "Biochemical characterization of blood plasma of coronary artery disease patients by in vitro high-resolution proton NMR spectroscopy." J Biosci **40**(1): 31-39.

Mansoor, J. K., E. S. Schelegle, C. E. Davis, W. F. Walby, W. Zhao, A. A. Aksenov, A. Pasamontes, J. Figueroa and R. Allen (2014). "Analysis of volatile compounds in exhaled breath condensate in patients with severe pulmonary arterial hypertension." PLoS One **9**(4): e95331.

Mapstone, M., A. K. Cheema, M. S. Fiandaca, X. Zhong, T. R. Mhyre, L. H. MacArthur, W. J. Hall, S. G. Fisher, D. R. Peterson, J. M. Haley, M. D. Nazar, S. A. Rich, D. J. Berlau, C. B. Peltz, M. T. Tan, C. H. Kawas and H. J. Federoff (2014). "Plasma phospholipids identify antecedent memory impairment in older adults." Nature medicine **20**(4): 415-418.

Maron, B. A., E. Hess, T. M. Maddox, A. R. Opotowsky, R. J. Tedford, T. Lahm, K. E. Joynt, D. J. Kass, T. Stephens, M. A. Stanislawski, E. R. Swenson, R. H. Goldstein, J. A. Leopold, R. T. Zamanian, J. M. Elwing, M. E. Plomondon, G. K. Grunwald, A. E. Baron, J. S. Rumsfeld and G. Choudhary (2016). "Association of Borderline Pulmonary Hypertension With Mortality and

Hospitalization in a Large Patient Cohort: Insights From the Veterans Affairs Clinical Assessment, Reporting, and Tracking Program." Circulation **133**(13): 1240-1248.

Maron, B. A. and J. A. Leopold (2014). "The role of the renin-angiotensin-aldosterone system in the pathobiology of pulmonary arterial hypertension (2013 Grover Conference series)." Pulm Circ **4**(2): 200-210.

Maron, B. A. and J. A. Leopold (2015). "Emerging Concepts in the Molecular Basis of Pulmonary Arterial Hypertension: Part II: Neurohormonal Signaling Contributes to the Pulmonary Vascular and Right Ventricular Pathophenotype of Pulmonary Arterial Hypertension." Circulation **131**(23): 2079-2091.

Marsboom, G., P. T. Toth, J. J. Ryan, Z. Hong, X. Wu, Y. H. Fang, T. Thenappan, L. Piao, H. J. Zhang, J. Pogoriler, Y. Chen, E. Morrow, E. K. Weir, J. Rehman and S. L. Archer (2012). "Dynamin-related protein 1-mediated mitochondrial mitotic fission permits hyperproliferation of vascular smooth muscle cells and offers a novel therapeutic target in pulmonary hypertension." Circ Res **110**(11): 1484-1497.

Marsboom, G., C. Wietholt, C. R. Haney, P. T. Toth, J. J. Ryan, E. Morrow, T. Thenappan, P. Bache-Wiig, L. Piao, J. Paul, C. T. Chen and S. L. Archer (2012). "Lung (1)(8)F-fluorodeoxyglucose positron emission tomography for diagnosis and monitoring of pulmonary arterial hypertension." Am J Respir Crit Care Med **185**(6): 670-679.

Masuda, M., T. Nishihira, K. Itoh, M. Mizugaki, N. Ishida and S. Mori (1993). "An immunohistochemical analysis for cancer of the esophagus using monoclonal antibodies specific for modified nucleosides." Cancer **72**(12): 3571-3578.

Matern, D. and P. Rinaldo (1993). Medium-Chain Acyl-Coenzyme A Dehydrogenase Deficiency. GeneReviews(R). R. A. Pagon, M. P. Adam, H. H. Ardinger et al. Seattle (WA).

Matsuura, F., N. Wang, W. Chen, X. C. Jiang and A. R. Tall (2006). "HDL from CETP-deficient subjects shows enhanced ability to promote cholesterol efflux from macrophages in an apoE- and ABCG1-dependent pathway." J Clin Invest **116**(5): 1435-1442.

Matthews, D. T. and A. R. Hemnes (2016). "Current concepts in the pathogenesis of chronic thromboembolic pulmonary hypertension." Pulm Circ **6**(2): 145-154.

Mayer, E., D. Jenkins, J. Lindner, A. D'Armini, J. Kloek, B. Meyns, L. B. Ilkjaer, W. Klepetko, M. Delcroix, I. Lang, J. Pepke-Zaba, G. Simonneau and P. Dartevelle (2011). "Surgical management and outcome of patients with chronic thromboembolic pulmonary hypertension: results from an international prospective registry." The Journal of thoracic and cardiovascular surgery **141**(3): 702-710.

McGarry, J. D. and N. F. Brown (1997). "The mitochondrial carnitine palmitoyltransferase system. From concept to molecular analysis." Eur J Biochem **244**(1): 1-14.

McGoon, M. D., R. L. Benza, P. Escribano-Subias, X. Jiang, D. P. Miller, A. J. Peacock, J. Pepke-Zaba, T. Pulido, S. Rich, S. Rosenkranz, S. Suissa and M. Humbert (2013). "Pulmonary arterial hypertension: epidemiology and registries." J Am Coll Cardiol **62**(25 Suppl): D51-59.

McLain, J. H., A. J. Alsterda and R. R. Arora (2016). "Cholesteryl Ester Transfer Protein Inhibitors: Trials and Tribulations." J Cardiovasc Pharmacol Ther.

McLaughlin, V. V., R. J. Oudiz, A. Frost, V. F. Tapson, S. Murali, R. N. Channick, D. B. Badesch, R. J. Barst, H. H. Hsu and L. J. Rubin (2006). "Randomized study of adding inhaled iloprost to

existing bosentan in pulmonary arterial hypertension." Am J Respir Crit Care Med **174**(11): 1257-1263.

McLaughlin, V. V., S. J. Shah, R. Souza and M. Humbert (2015). "Management of pulmonary arterial hypertension." J Am Coll Cardiol **65**(18): 1976-1997.

McLaughlin, V. V., O. Sitbon, D. B. Badesch, R. J. Barst, C. Black, N. Galie, M. Rainisio, G. Simonneau and L. J. Rubin (2005). "Survival with first-line bosentan in patients with primary pulmonary hypertension." Eur Respir J **25**(2): 244-249.

McMurtry, M. S., S. Bonnet, X. Wu, J. R. Dyck, A. Haromy, K. Hashimoto and E. D. Michelakis (2004). "Dichloroacetate prevents and reverses pulmonary hypertension by inducing pulmonary artery smooth muscle cell apoptosis." Circ Res **95**(8): 830-840.

McTaggart, F. and P. Jones (2008). "Effects of statins on high-density lipoproteins: a potential contribution to cardiovascular benefit." Cardiovasc Drugs Ther **22**(4): 321-338.

Menche, J., A. Sharma, M. Kitsak, S. D. Ghiassian, M. Vidal, J. Loscalzo and A. L. Barabasi (2015). "Disease networks. Uncovering disease-disease relationships through the incomplete interactome." Science **347**(6224): 1257601.

Menni, C., E. Fauman, I. Erte, J. R. Perry, G. Kastenmuller, S. Y. Shin, A. K. Petersen, C. Hyde, M. Psatha, K. J. Ward, W. Yuan, M. Milburn, C. N. Palmer, T. M. Frayling, J. Trimmer, J. T. Bell, C. Gieger, R. P. Mohney, M. J. Brosnan, K. Suhre, N. Soranzo and T. D. Spector (2013). "Biomarkers for type 2 diabetes and impaired fasting glucose using a nontargeted metabolomics approach." Diabetes **62**(12): 4270-4276.

Menni, C., D. Graham, G. Kastenmuller, N. H. Alharbi, S. M. Alsanos, M. McBride, M. Mangino, P. Titcombe, S. Y. Shin, M. Psatha, T. Geisendorfer, A. Huber, A. Peters, R. Wang-Sattler, T. Xu, M. J. Brosnan, J. Trimmer, C. Reichel, R. P. Mohney, N. Soranzo, M. H. Edwards, C. Cooper, A. C. Church, K. Suhre, C. Gieger, A. F. Dominiczak, T. D. Spector, S. Padmanabhan and A. M. Valdes (2015). "Metabolomic Identification of a Novel Pathway of Blood Pressure Regulation Involving Hexadecanedioate." Hypertension.

Meyburg, J., A. Schulze, D. Kohlmueller, O. Linderkamp and E. Mayatepek (2001). "Postnatal changes in neonatal acylcarnitine profile." Pediatr Res **49**(1): 125-129.

Michelakis, E. D., M. S. McMurtry, X. C. Wu, J. R. Dyck, R. Moudgil, T. A. Hopkins, G. D. Lopaschuk, L. Puttagunta, R. Waite and S. L. Archer (2002). "Dichloroacetate, a metabolic modulator, prevents and reverses chronic hypoxic pulmonary hypertension in rats: role of increased expression and activity of voltage-gated potassium channels." Circulation **105**(2): 244-250.

Michelakis, E. D., B. Thebaud, E. K. Weir and S. L. Archer (2004). "Hypoxic pulmonary vasoconstriction: redox regulation of O2-sensitive K+ channels by a mitochondrial O2-sensor in resistance artery smooth muscle cells." J Mol Cell Cardiol **37**(6): 1119-1136.

Mielniczuk, L. M., G. Chandy, D. Stewart, V. Contreras-Dominguez, H. Haddad, C. Pugliese and R. A. Davies (2012). "Worsening renal function and prognosis in pulmonary hypertension patients hospitalized for right heart failure." Congest Heart Fail **18**(3): 151-157.

Mihaleva, V. V., D. B. van Schalkwijk, A. A. de Graaf, J. van Duynhoven, F. A. van Dorsten, J. Vervoort, A. Smilde, J. A. Westerhuis and D. M. Jacobs (2014). "A systematic approach to obtain validated partial least square models for predicting lipoprotein subclasses from serum NMR spectra." Anal Chem **86**(1): 543-550.

Miller, M. J., A. D. Kennedy, A. D. Eckhart, L. C. Burrage, J. E. Wulff, L. A. Miller, M. V. Milburn, J. A. Ryals, A. L. Beaudet, Q. Sun, V. R. Sutton and S. H. Elsea (2015). "Untargeted metabolomic analysis for the clinical screening of inborn errors of metabolism." Journal of Inherited Metabolic Disease **38**(6): 1029-1039.

Miniati, M., C. Fiorillo, M. Becatti, S. Monti, M. Bottai, C. Marini, E. Grifoni, B. Formichi, C. Bauleo, C. Arcangeli, D. Poli, P. A. Nassi, R. Abbate and D. Prisco (2010). "Fibrin resistance to lysis in patients with pulmonary hypertension other than thromboembolic." Am J Respir Crit Care Med **181**(9): 992-996.

Mirnezami, R., B. Jimenez, J. V. Li, J. M. Kinross, K. Veselkov, R. D. Goldin, E. Holmes, J. K. Nicholson and A. Darzi (2014). "Rapid diagnosis and staging of colorectal cancer via high-resolution magic angle spinning nuclear magnetic resonance (HR-MAS NMR) spectroscopy of intact tissue biopsies." Ann Surg **259**(6): 1138-1149.

Mishima, E., C. Inoue, D. Saigusa, R. Inoue, K. Ito, Y. Suzuki, D. Jinno, Y. Tsukui, Y. Akamatsu, M. Araki, K. Araki, R. Shimizu, H. Shinke, T. Suzuki, Y. Takeuchi, H. Shima, Y. Akiyama, T. Toyohara, C. Suzuki, Y. Saiki, T. Tominaga, S. Miyagi, N. Kawagisihi, T. Soga, T. Ohkubo, K. Yamamura, Y. Imai, S. Masuda, V. Sabbisetti, T. Ichimura, D. B. Mount, J. V. Bonventre, S. Ito, Y. Tomioka, K. Itoh and T. Abe (2014). "Conformational change in transfer RNA is an early indicator of acute cellular damage." Journal of the American Society of Nephrology **25**(10): 2316-2326.

Misra, S. and N. S. Oliver (2015). "Utility of ketone measurement in the prevention, diagnosis and management of diabetic ketoacidosis." Diabet Med **32**(1): 14-23.

Monette, J. S., P. M. Hutchins, G. E. Ronsein, J. Wimberger, A. D. Irwin, C. Tang, J. D. Sara, B. Shao, T. Vaisar, A. Lerman and J. W. Heinecke (2016). "Patients With Coronary Endothelial Dysfunction Have Impaired Cholesterol Efflux Capacity and Reduced HDL Particle Concentration." Circ Res **119**(1): 83-90.

Moraes, D. L., W. S. Colucci and M. M. Givertz (2000). "Secondary pulmonary hypertension in chronic heart failure: the role of the endothelium in pathophysiology and management." Circulation **102**(14): 1718-1723.

Morecroft, I., Y. Dempsie, M. Bader, D. J. Walther, K. Kotnik, L. Loughlin, M. Nilsen and M. R. MacLean (2007). "Effect of tryptophan hydroxylase 1 deficiency on the development of hypoxia-induced pulmonary hypertension." Hypertension **49**(1): 232-236.

Morelli, S., M. Giordano, P. De Marzio, R. Priori, A. Sgreccia and G. Valesini (1993). "Pulmonary arterial hypertension responsive to immunosuppressive therapy in systemic lupus erythematosus." Lupus **2**(6): 367-369.

Morris, C. R., J. H. Suh, W. Hagar, S. Larkin, D. A. Bland, M. H. Steinberg, E. P. Vichinsky, M. Shigenaga, B. Ames, F. A. Kuypers and E. S. Klings (2008). "Erythrocyte glutamine depletion, altered redox environment, and pulmonary hypertension in sickle cell disease." Blood **111**(1): 402-410.

Morris, T. A. (2013). "Why acute pulmonary embolism becomes chronic thromboembolic pulmonary hypertension: clinical and genetic insights." Curr Opin Pulm Med **19**(5): 422-429.

Morris, T. A., J. J. Marsh, P. G. Chiles, W. R. Auger, P. F. Fedullo and V. L. Woods, Jr. (2006). "Fibrin derived from patients with chronic thromboembolic pulmonary hypertension is resistant to lysis." Am J Respir Crit Care Med **173**(11): 1270-1275.

Moser, K. M. and C. M. Bloor (1993). "Pulmonary vascular lesions occurring in patients with chronic major vessel thromboembolic pulmonary hypertension." Chest **103**(3): 685-692.

Mostaghel, E. A. (2014). "Beyond T and DHT - novel steroid derivatives capable of wild type androgen receptor activation." Int J Biol Sci **10**(6): 602-613.

Mueller, O., E. Chang, D. Deng, T. Franz, D. Jing, R. Kincaid, Y. Konigshofer, M. Kratzmeier, M. McNulty, H. Qian, J. Schneider, H. Schulte, U. Seedorf, X. Tian, M. Van Cleve, D. Yang and G. Assmann (2008). "PROCAM Study: risk prediction for myocardial infarction using microfluidic high-density lipoprotein (HDL) subfractionation is independent of HDL cholesterol." Clin Chem Lab Med **46**(4): 490-498.

Nagana Gowda, G. A., Y. N. Gowda and D. Raftery (2015). "Expanding the limits of human blood metabolite quantitation using NMR spectroscopy." Anal Chem **87**(1): 706-715.

Nagaya, N., T. Nishikimi, M. Uematsu, T. Satoh, S. Kyotani, F. Sakamaki, M. Kakishita, K. Fukushima, Y. Okano, N. Nakanishi, K. Miyatake and K. Kangawa (2000). "Plasma brain natriuretic peptide as a prognostic indicator in patients with primary pulmonary hypertension." Circulation **102**(8): 865-870.

Nagaya, N., M. Uematsu, H. Oya, N. Sato, F. Sakamaki, S. Kyotani, K. Ueno, N. Nakanishi, M. Yamagishi and K. Miyatake (2001). "Short-term oral administration of L-arginine improves hemodynamics and exercise capacity in patients with precapillary pulmonary hypertension." Am J Respir Crit Care Med **163**(4): 887-891.

Nagaya, N., M. Uematsu, T. Satoh, S. Kyotani, F. Sakamaki, N. Nakanishi, M. Yamagishi, T. Kunieda and K. Miyatake (1999). "Serum uric acid levels correlate with the severity and the mortality of primary pulmonary hypertension." Am J Respir Crit Care Med **160**(2): 487-492.

Newgard, C. B., J. An, J. R. Bain, M. J. Muehlbauer, R. D. Stevens, L. F. Lien, A. M. Haqq, S. H. Shah, M. Arlotto, C. A. Slentz, J. Rochon, D. Gallup, O. Ilkayeva, B. R. Wenner, W. S. Yancy, Jr., H. Eisenson, G. Musante, R. S. Surwit, D. S. Millington, M. D. Butler and L. P. Svetkey (2009). "A branched-chain amino acid-related metabolic signature that differentiates obese and lean humans and contributes to insulin resistance." Cell Metab **9**(4): 311-326.

Newman, J. H., R. C. Trembath, J. A. Morse, E. Grunig, J. E. Loyd, S. Adnot, F. Coccolo, C. Ventura, J. A. Phillips, 3rd, J. A. Knowles, B. Janssen, O. Eickelberg, S. Eddahibi, P. Herve, W. C. Nichols and G. Elliott (2004). "Genetic basis of pulmonary arterial hypertension: current understanding and future directions." J Am Coll Cardiol **43**(12 Suppl S): 33S-39S.

Nicholls, S. J., H. B. Brewer, J. J. Kastelein, K. A. Krueger, M. D. Wang, M. Shao, B. Hu, E. McErlean and S. E. Nissen (2011). "Effects of the CETP inhibitor evacetrapib administered as monotherapy or in combination with statins on HDL and LDL cholesterol: a randomized controlled trial." JAMA **306**(19): 2099-2109.

Nicholls, S. J., E. M. Tuzcu, I. Sipahi, A. W. Grasso, P. Schoenhagen, T. Hu, K. Wolski, T. Crowe, M. Y. Desai, S. L. Hazen, S. R. Kapadia and S. E. Nissen (2007). "Statins, high-density lipoprotein cholesterol, and regression of coronary atherosclerosis." JAMA **297**(5): 499-508.

Nicholson, J. K., P. J. Foxall, M. Spraul, R. D. Farrant and J. C. Lindon (1995). "750 MHz 1H and 1H-13C NMR spectroscopy of human blood plasma." Anal Chem **67**(5): 793-811.

Nicholson, J. K. and K. P. Gartland (1989). "1H NMR studies on protein binding of histidine, tyrosine and phenylalanine in blood plasma." NMR Biomed **2**(2): 77-82.

Nicholson, J. K., E. Holmes, J. M. Kinross, A. W. Darzi, Z. Takats and J. C. Lindon (2012). "Metabolic phenotyping in clinical and surgical environments." Nature **491**(7424): 384-392.

Nicholson, J. K. and J. C. Lindon (2008). "Systems biology: Metabonomics." Nature **455**(7216): 1054-1056.

Nicholson, J. K., J. C. Lindon and E. Holmes (1999). "'Metabonomics': understanding the metabolic responses of living systems to pathophysiological stimuli via multivariate statistical analysis of biological NMR spectroscopic data." Xenobiotica **29**(11): 1181-1189.

Nicholson, J. K., I. D. Wilson and J. C. Lindon (2011). "Pharmacometabonomics as an effector for personalized medicine." Pharmacogenomics **12**(1): 103-111.

Nickel, N., H. Golpon, M. Greer, L. Knudsen, K. Olsson, V. Westerkamp, T. Welte and M. M. Hoeper (2012). "The prognostic impact of follow-up assessments in patients with idiopathic pulmonary arterial hypertension." Eur Respir J **39**(3): 589-596.

Oakman, C., L. Tenori, W. M. Claudino, S. Cappadona, S. Nepi, A. Battaglia, P. Bernini, E. Zafarana, E. Saccenti, M. Fornier, P. G. Morris, L. Biganzoli, C. Luchinat, I. Bertini and A. Di Leo (2011). "Identification of a serum-detectable metabolomic fingerprint potentially correlated with the presence of micrometastatic disease in early breast cancer patients at varying risks of disease relapse by traditional prognostic methods." Ann Oncol **22**(6): 1295-1301.

Ogretmen, B. and Y. A. Hannun (2004). "Biologically active sphingolipids in cancer pathogenesis and treatment." Nat Rev Cancer **4**(8): 604-616.

Ohira, H., R. deKemp, E. Pena, R. A. Davies, D. J. Stewart, G. Chandy, V. Contreras-Dominguez, C. Dennie, B. Mc Ardle, R. Mc Klein, J. M. Renaud, J. N. DaSilva, C. Pugliese, R. Dunne, R. Beanlands and L. M. Mielniczuk (2015). "Shifts in myocardial fatty acid and glucose metabolism in pulmonary arterial hypertension: a potential mechanism for a maladaptive right ventricular response." Eur Heart J Cardiovasc Imaging.

Oikawa, M., Y. Kagaya, H. Otani, M. Sakuma, J. Demachi, J. Suzuki, T. Takahashi, J. Nawata, T. Ido, J. Watanabe and K. Shirato (2005). "Increased [18F]fluorodeoxyglucose accumulation in right ventricular free wall in patients with pulmonary hypertension and the effect of epoprostenol." J Am Coll Cardiol **45**(11): 1849-1855.

Oka, M., V. Karoor, N. Homma, T. Nagaoka, E. Sakao, S. M. Golembeski, J. Limbird, M. Imamura, S. A. Gebb, K. A. Fagan and I. F. McMurtry (2007). "Dehydroepiandrosterone upregulates soluble guanylate cyclase and inhibits hypoxic pulmonary hypertension." Cardiovasc Res **74**(3): 377-387.

Okada, K., Y. Tanaka, M. Bernstein, W. Zhang, G. A. Patterson and M. D. Botney (1997). "Pulmonary hemodynamics modify the rat pulmonary artery response to injury. A neointimal model of pulmonary hypertension." Am J Pathol **151**(4): 1019-1025.

Olson, J. W., J. E. Atkinson, A. D. Hacker, R. J. Altiere and M. N. Gillespie (1985). "Suppression of polyamine biosynthesis prevents monocrotaline-induced pulmonary edema and arterial medial thickening." Toxicology and Applied Pharmacology **81**(1): 91-99.

Olsson, K. M., M. Delcroix, H. A. Ghofrani, H. Tiede, D. Huscher, R. Speich, E. Grunig, G. Staehler, S. Rosenkranz, M. Halank, M. Held, T. J. Lange, J. Behr, H. Klose, M. Claussen, R. Ewert, C. F. Opitz, C. D. Vizza, L. Scelsi, A. Vonk-Noordegraaf, H. Kaemmerer, J. S. Gibbs, G. Coghlan, J. Pepke-Zaba, U. Schulz, M. Gorenflo, D. Pittrow and M. M. Hoeper (2014). "Anticoagulation and survival in pulmonary arterial hypertension: results from the Comparative, Prospective

Registry of Newly Initiated Therapies for Pulmonary Hypertension (COMPERA)." Circulation **129**(1): 57-65.

Olsson, K. M., A. Simon, M. Strueber, J. Hadem, O. Wiesner, J. Gottlieb, T. Fuehner, S. Fischer, G. Warnecke, C. Kuhn, A. Haverich, T. Welte and M. M. Hoeper (2010). "Extracorporeal membrane oxygenation in nonintubated patients as bridge to lung transplantation." Am J Transplant **10**(9): 2173-2178.

Omori, K. and J. Kotera (2007). "Overview of PDEs and their regulation." Circ Res **100**(3): 309-327.

Ooi, C. Y., Z. Wang, D. M. Tabima, J. C. Eickhoff and N. C. Chesler (2010). "The role of collagen in extralobar pulmonary artery stiffening in response to hypoxia-induced pulmonary hypertension." Am J Physiol Heart Circ Physiol **299**(6): H1823-1831.

Oudemans-van Straaten, H. M., R. J. Bosman, M. Treskes, H. J. van der Spoel and D. F. Zandstra (2001). "Plasma glutamine depletion and patient outcome in acute ICU admissions." Intensive Care Med **27**(1): 84-90.

Papandreou, I., R. A. Cairns, L. Fontana, A. L. Lim and N. C. Denko (2006). "HIF-1 mediates adaptation to hypoxia by actively downregulating mitochondrial oxygen consumption." Cell Metab **3**(3): 187-197.

Parikh, V. N., R. C. Jin, S. Rabello, N. Gulbahce, K. White, A. Hale, K. A. Cottrill, R. S. Shaik, A. B. Waxman, Y. Y. Zhang, B. A. Maron, J. C. Hartner, Y. Fujiwara, S. H. Orkin, K. J. Haley, A. L. Barabasi, J. Loscalzo and S. Y. Chan (2012). "MicroRNA-21 integrates pathogenic signaling to control pulmonary hypertension: results of a network bioinformatics approach." Circulation **125**(12): 1520-1532.

Paul, G. A., J. S. Gibbs, A. R. Boobis, A. Abbas and M. R. Wilkins (2005). "Bosentan decreases the plasma concentration of sildenafil when coprescribed in pulmonary hypertension." Br J Clin Pharmacol **60**(1): 107-112.

Paulin, R., P. Dromparis, G. Sutendra, V. Gurtu, S. Zervopoulos, L. Bowers, A. Haromy, L. Webster, S. Provencher, S. Bonnet and E. D. Michelakis (2014). "Sirtuin 3 deficiency is associated with inhibited mitochondrial function and pulmonary arterial hypertension in rodents and humans." Cell Metab **20**(5): 827-839.

Paulin, R., J. Meloche, M. H. Jacob, M. Bisserier, A. Courboulin and S. Bonnet (2011). "Dehydroepiandrosterone inhibits the Src/STAT3 constitutive activation in pulmonary arterial hypertension." Am J Physiol Heart Circ Physiol **301**(5): H1798-1809.

Paulin, R. and E. D. Michelakis (2014). "The metabolic theory of pulmonary arterial hypertension." Circ Res **115**(1): 148-164.

Peacock, A. J., R. Naeije, N. Galie and L. Rubin (2009). "End-points and clinical trial design in pulmonary arterial hypertension: have we made progress?" Eur Respir J **34**(1): 231-242.

Peacock, A. J., R. Naeije and L. J. Rubin (2011). Pulmonary circulation : diseases and their treatment. London, Arnold ; New York Distributed in the U.S.A. by Oxford University Press**:** xxiii, 614 p., 622 p. of plates.

Pena, M. J., A. Heinzel, P. Rossing, H. H. Parving, G. Dallmann, K. Rossing, S. Andersen, B. Mayer and H. J. Heerspink (2016). "Serum metabolites predict response to angiotensin II receptor blockers in patients with diabetes mellitus." J Transl Med **14**(1): 203.

Penning, T. M., Y. Jin, S. Steckelbroeck, T. Lanisnik Rizner and M. Lewis (2004). "Structure-function of human 3 alpha-hydroxysteroid dehydrogenases: genes and proteins." Mol Cell Endocrinol **215**(1-2): 63-72.

Perros, F., D. Montani, P. Dorfmuller, I. Durand-Gasselin, C. Tcherakian, J. Le Pavec, M. Mazmanian, E. Fadel, S. Mussot, O. Mercier, P. Herve, D. Emilie, S. Eddahibi, G. Simonneau, R. Souza and M. Humbert (2008). "Platelet-derived growth factor expression and function in idiopathic pulmonary arterial hypertension." Am J Respir Crit Care Med **178**(1): 81-88.

Petkov, V., W. Mosgoeller, R. Ziesche, M. Raderer, L. Stiebellehner, K. Vonbank, G. C. Funk, G. Hamilton, C. Novotny, B. Burian and L. H. Block (2003). "Vasoactive intestinal peptide as a new drug for treatment of primary pulmonary hypertension." J Clin Invest **111**(9): 1339-1346.

Piao, L., Y. H. Fang, V. J. Cadete, C. Wietholt, D. Urboniene, P. T. Toth, G. Marsboom, H. J. Zhang, I. Haber, J. Rehman, G. D. Lopaschuk and S. L. Archer (2010). "The inhibition of pyruvate dehydrogenase kinase improves impaired cardiac function and electrical remodeling in two models of right ventricular hypertrophy: resuscitating the hibernating right ventricle." Journal of Molecular Medicine (Berl) **88**(1): 47-60.

Piao, L., Y. H. Fang, K. Parikh, J. J. Ryan, P. T. Toth and S. L. Archer (2013). "Cardiac glutaminolysis: a maladaptive cancer metabolism pathway in the right ventricle in pulmonary hypertension." Journal of Molecular Medicine (Berl) **91**(10): 1185-1197.

Piao, L., Y. H. Fang, K. Parikh, J. J. Ryan, P. T. Toth and S. L. Archer (2013). "Cardiac glutaminolysis: a maladaptive cancer metabolism pathway in the right ventricle in pulmonary hypertension." J Mol Med (Berl) **91**(10): 1185-1197.

Piao, L., G. Marsboom and S. L. Archer (2010). "Mitochondrial metabolic adaptation in right ventricular hypertrophy and failure." J Mol Med (Berl) **88**(10): 1011-1020.

Piao, L., V. K. Sidhu, Y. H. Fang, J. J. Ryan, K. S. Parikh, Z. Hong, P. T. Toth, E. Morrow, S. Kutty, G. D. Lopaschuk and S. L. Archer (2013). "FOXO1-mediated upregulation of pyruvate dehydrogenase kinase-4 (PDK4) decreases glucose oxidation and impairs right ventricular function in pulmonary hypertension: therapeutic benefits of dichloroacetate." J Mol Med (Berl) **91**(3): 333-346.

Pirillo, A., G. D. Norata and A. L. Catapano (2013). "High-density lipoprotein subfractions--what the clinicians need to know." Cardiology **124**(2): 116-125.

Pitt, J. J. (2009). "Principles and applications of liquid chromatography-mass spectrometry in clinical biochemistry." Clin Biochem Rev **30**(1): 19-34.

Prakash, A., S. V. Sundar, Y. G. Zhu, A. Tran, J. W. Lee, C. Lowell and J. Hellman (2015). "Lung Ischemia-Reperfusion is a Sterile Inflammatory Process Influenced by Commensal Microbiota in Mice." Shock **44**(3): 272-279.

Preston, I. R., K. E. Roberts, D. P. Miller, G. P. Sen, M. Selej, W. W. Benton, N. S. Hill and H. W. Farber (2015). "Effect of Warfarin Treatment on Survival of Patients With Pulmonary Arterial Hypertension (PAH) in the Registry to Evaluate Early and Long-Term PAH Disease Management (REVEAL)." Circulation **132**(25): 2403-2411.

Prough, R., B. J. Clark and C. M. Klinge (2016). "Novel mechanisms for DHEA action." J Mol Endocrinol **56**(3): R139-155.

Psychogios, N., D. D. Hau, J. Peng, A. C. Guo, R. Mandal, S. Bouatra, I. Sinelnikov, R. Krishnamurthy, R. Eisner, B. Gautam, N. Young, J. Xia, C. Knox, E. Dong, P. Huang, Z. Hollander, T. L. Pedersen, S. R. Smith, F. Bamforth, R. Greiner, B. McManus, J. W. Newman, T. Goodfriend and D. S. Wishart (2011). "The human serum metabolome." PLoS One **6**(2): e16957.

Pullamsetti, S., L. Kiss, H. A. Ghofrani, R. Voswinckel, P. Haredza, W. Klepetko, C. Aigner, L. Fink, J. P. Muyal, N. Weissmann, F. Grimminger, W. Seeger and R. T. Schermuly (2005). "Increased levels and reduced catabolism of asymmetric and symmetric dimethylarginines in pulmonary hypertension." FASEB J **19**(9): 1175-1177.

Qiao, L., T. Nishimura, L. Shi, D. Sessions, A. Thrasher, J. R. Trudell, G. J. Berry, R. G. Pearl and P. N. Kao (2014). "Endothelial fate mapping in mice with pulmonary hypertension." Circulation **129**(6): 692-703.

Qin, J., R. Li, J. Raes, M. Arumugam, K. S. Burgdorf, C. Manichanh, T. Nielsen, N. Pons, F. Levenez, T. Yamada, D. R. Mende, J. Li, J. Xu, S. Li, D. Li, J. Cao, B. Wang, H. Liang, H. Zheng, Y. Xie, J. Tap, P. Lepage, M. Bertalan, J. M. Batto, T. Hansen, D. Le Paslier, A. Linneberg, H. B. Nielsen, E. Pelletier, P. Renault, T. Sicheritz-Ponten, K. Turner, H. Zhu, C. Yu, S. Li, M. Jian, Y. Zhou, Y. Li, X. Zhang, S. Li, N. Qin, H. Yang, J. Wang, S. Brunak, J. Dore, F. Guarner, K. Kristiansen, O. Pedersen, J. Parkhill, J. Weissenbach, H. I. T. C. Meta, P. Bork, S. D. Ehrlich and J. Wang (2010). "A human gut microbial gene catalogue established by metagenomic sequencing." Nature **464**(7285): 59-65.

Quarck, R., M. Wynants, E. Verbeken, B. Meyns and M. Delcroix (2015). "Contribution of inflammation and impaired angiogenesis to the pathobiology of chronic thromboembolic pulmonary hypertension." Eur Respir J **46**(2): 431-443.

Rabinovitch, M. (2012). "Molecular pathogenesis of pulmonary arterial hypertension." J Clin Invest **122**(12): 4306-4313.

Raffler, J., N. Friedrich, M. Arnold, T. Kacprowski, R. Rueedi, E. Altmaier, S. Bergmann, K. Budde, C. Gieger, G. Homuth, M. Pietzner, W. Romisch-Margl, K. Strauch, H. Volzke, M. Waldenberger, H. Wallaschofski, M. Nauck, U. Volker, G. Kastenmuller and K. Suhre (2015). "Genome-Wide Association Study with Targeted and Non-targeted NMR Metabolomics Identifies 15 Novel Loci of Urinary Human Metabolic Individuality." PLoS Genet **11**(9): e1005487.

Rahnavardi, M., T. D. Yan, C. Cao, M. P. Vallely, P. G. Bannon and M. K. Wilson (2011). "Pulmonary thromboendarterectomy for chronic thromboembolic pulmonary hypertension : a systematic review." Annals of Thoracic and Cardiovascular Surgery : Official Journal of the Association of Thoracic and Cardiovascular Surgeons of Asia **17**(5): 435-445.

Raina, A. and M. Humbert (2016). "Risk assessment in pulmonary arterial hypertension." Eur Respir Rev **25**(142): 390-398.

Ranchoux, B., F. Antigny, C. Rucker-Martin, A. Hautefort, C. Pechoux, H. J. Bogaard, P. Dorfmuller, S. Remy, F. Lecerf, S. Plante, S. Chat, E. Fadel, A. Houssaini, I. Anegon, S. Adnot, G. Simonneau, M. Humbert, S. Cohen-Kaminsky and F. Perros (2015). "Endothelial-to-mesenchymal transition in pulmonary hypertension." Circulation **131**(11): 1006-1018.

Randle, P. J., P. B. Garland, E. A. Newsholme and C. N. Hales (1965). "The glucose fatty acid cycle in obesity and maturity onset diabetes mellitus." Ann N Y Acad Sci **131**(1): 324-333.

Raymond, R. J., A. L. Hinderliter, P. W. Willis, D. Ralph, E. J. Caldwell, W. Williams, N. A. Ettinger, N. S. Hill, W. R. Summer, B. de Boisblanc, T. Schwartz, G. Koch, L. M. Clayton, M. M. Jobsis, J. W.

Crow and W. Long (2002). "Echocardiographic predictors of adverse outcomes in primary pulmonary hypertension." J Am Coll Cardiol **39**(7): 1214-1219.

Rehman, J. and S. L. Archer (2010). "A proposed mitochondrial-metabolic mechanism for initiation and maintenance of pulmonary arterial hypertension in fawn-hooded rats: the Warburg model of pulmonary arterial hypertension." Adv Exp Med Biol **661**: 171-185.

Remaley, A. T., G. D. Norata and A. L. Catapano (2014). "Novel concepts in HDL pharmacology." Cardiovasc Res **103**(3): 423-428.

Reuter, S. E. and A. M. Evans (2012). "Carnitine and acylcarnitines: pharmacokinetic, pharmacological and clinical aspects." Clin Pharmacokinet **51**(9): 553-572.

Rhodes, C. J., P. Ghataorhe, J. Wharton, K. C. Rue-Albrecht, C. Hadinnapola, G. Watson, M. Bleda, M. Haimel, G. Coghlan, P. A. Corris, L. S. Howard, D. G. Kiely, A. J. Peacock, J. Pepke-Zaba, M. Toshner, S. J. Wort, J. S. Gibbs, A. Lawrie, S. Graf, N. W. Morrell and M. R. Wilkins (2016). "Plasma Metabolomics Implicate Modified Transfer RNAs and Altered Bioenergetics in the Outcome of Pulmonary Arterial Hypertension." Circulation **135**(5): 460-475.

Rhodes, C. J., J. Wharton, R. A. Boon, T. Roexe, H. Tsang, B. Wojciak-Stothard, A. Chakrabarti, L. S. Howard, J. S. Gibbs, A. Lawrie, R. Condliffe, C. A. Elliot, D. G. Kiely, L. Huson, H. A. Ghofrani, H. Tiede, R. Schermuly, A. M. Zeiher, S. Dimmeler and M. R. Wilkins (2013). "Reduced microRNA-150 is associated with poor survival in pulmonary arterial hypertension." Am J Respir Crit Care Med **187**(3): 294-302.

Rhodes, C. J., J. Wharton, L. Howard, J. S. Gibbs, A. Vonk-Noordegraaf and M. R. Wilkins (2011). "Iron deficiency in pulmonary arterial hypertension: a potential therapeutic target." Eur Respir J **38**(6): 1453-1460.

Rhodes, C. J., J. Wharton, L. S. Howard, J. S. Gibbs and M. R. Wilkins (2011). "Red cell distribution width outperforms other potential circulating biomarkers in predicting survival in idiopathic pulmonary arterial hypertension." Heart **97**(13): 1054-1060.

Rich, J. D., T. Thenappan, B. Freed, A. R. Patel, R. A. Thisted, R. Childers and S. L. Archer (2013). "QTc prolongation is associated with impaired right ventricular function and predicts mortality in pulmonary hypertension." Int J Cardiol **167**(3): 669-676.

Rich, S., D. R. Dantzker, S. M. Ayres, E. H. Bergofsky, B. H. Brundage, K. M. Detre, A. P. Fishman, R. M. Goldring, B. M. Groves, S. K. Koerner and et al. (1987). "Primary pulmonary hypertension. A national prospective study." Ann Intern Med **107**(2): 216-223.

Rich, S., M. Seidlitz, E. Dodin, D. Osimani, D. Judd, D. Genthner, V. McLaughlin and G. Francis (1998). "The short-term effects of digoxin in patients with right ventricular dysfunction from pulmonary hypertension." Chest **114**(3): 787-792.

Ridker, P. M., G. Pare, A. N. Parker, R. Y. Zee, J. P. Miletich and D. I. Chasman (2009). "Polymorphism in the CETP gene region, HDL cholesterol, and risk of future myocardial infarction: Genomewide analysis among 18 245 initially healthy women from the Women's Genome Health Study." Circ Cardiovasc Genet **2**(1): 26-33.

Rosenson, R. S. (2016). "The High-Density Lipoprotein Puzzle: Why Classic Epidemiology, Genetic Epidemiology, and Clinical Trials Conflict?" Arterioscler Thromb Vasc Biol **36**(5): 777-782.

Rosenson, R. S., H. B. Brewer, Jr., B. J. Ansell, P. Barter, M. J. Chapman, J. W. Heinecke, A. Kontush, A. R. Tall and N. R. Webb (2016). "Dysfunctional HDL and atherosclerotic cardiovascular disease." Nat Rev Cardiol **13**(1): 48-60.

Rosenson, R. S., H. B. Brewer, Jr., M. J. Chapman, S. Fazio, M. M. Hussain, A. Kontush, R. M. Krauss, J. D. Otvos, A. T. Remaley and E. J. Schaefer (2011). "HDL measures, particle heterogeneity, proposed nomenclature, and relation to atherosclerotic cardiovascular events." Clin Chem **57**(3): 392-410.

Rosenson, R. S., H. B. Brewer, Jr., W. S. Davidson, Z. A. Fayad, V. Fuster, J. Goldstein, M. Hellerstein, X. C. Jiang, M. C. Phillips, D. J. Rader, A. T. Remaley, G. H. Rothblat, A. R. Tall and L. Yvan-Charvet (2012). "Cholesterol efflux and atheroprotection: advancing the concept of reverse cholesterol transport." Circulation **125**(15): 1905-1919.

Rosenzweig, E. B., D. Brodie, D. C. Abrams, C. L. Agerstrand and M. Bacchetta (2014). "Extracorporeal membrane oxygenation as a novel bridging strategy for acute right heart failure in group 1 pulmonary arterial hypertension." ASAIO J **60**(1): 129-133.

Rothman, A. M., N. D. Arnold, W. Chang, O. Watson, A. J. Swift, R. Condliffe, C. A. Elliot, D. G. Kiely, S. K. Suvarna, J. Gunn and A. Lawrie (2015). "Pulmonary artery denervation reduces pulmonary artery pressure and induces histological changes in an acute porcine model of pulmonary hypertension." Circ Cardiovasc Interv **8**(11): e002569.

Rouault, T. A. and W. H. Tong (2008). "Iron-sulfur cluster biogenesis and human disease." Trends Genet **24**(8): 398-407.

Rubin, L. J., D. B. Badesch, R. J. Barst, N. Galie, C. M. Black, A. Keogh, T. Pulido, A. Frost, S. Roux, I. Leconte, M. Landzberg and G. Simonneau (2002). "Bosentan therapy for pulmonary arterial hypertension." N Engl J Med **346**(12): 896-903.

Runo, J. R. and J. E. Loyd (2003). "Primary pulmonary hypertension." Lancet **361**(9368): 1533-1544.

Rust, S., M. Rosier, H. Funke, J. Real, Z. Amoura, J. C. Piette, J. F. Deleuze, H. B. Brewer, N. Duverger, P. Denefle and G. Assmann (1999). "Tangier disease is caused by mutations in the gene encoding ATP-binding cassette transporter 1." Nat Genet **22**(4): 352-355.

Ryan, J., A. Dasgupta, J. Huston, K. H. Chen and S. L. Archer (2015). "Mitochondrial dynamics in pulmonary arterial hypertension." J Mol Med (Berl) **93**(3): 229-242.

Ryan, J. J. and S. L. Archer (2014). "The right ventricle in pulmonary arterial hypertension: disorders of metabolism, angiogenesis and adrenergic signaling in right ventricular failure." Circ Res **115**(1): 176-188.

Ryan, J. J. and S. L. Archer (2015). "Emerging concepts in the molecular basis of pulmonary arterial hypertension: part I: metabolic plasticity and mitochondrial dynamics in the pulmonary circulation and right ventricle in pulmonary arterial hypertension." Circulation **131**(19): 1691-1702.

Ryan, J. J., G. Marsboom, Y. H. Fang, P. T. Toth, E. Morrow, N. Luo, L. Piao, Z. Hong, K. Ericson, H. J. Zhang, M. Han, C. R. Haney, C. T. Chen, W. W. Sharp and S. L. Archer (2013). "PGC1alpha-mediated mitofusin-2 deficiency in female rats and humans with pulmonary arterial hypertension." Am J Respir Crit Care Med **187**(8): 865-878.

Saccenti, E., H. C. J. Hoefsloot, A. K. Smilde, J. A. Westerhuis and M. M. W. B. Hendriks (2013). "Reflections on univariate and multivariate analysis of metabolomics data." Metabolomics **10**(3): 0.

Saikia, M. and M. Hatzoglou (2015). "The Many Virtues of tRNA-derived Stress-induced RNAs (tiRNAs): Discovering Novel Mechanisms of Stress Response and Effect on Human Health." The Journal of Biological Chemistry **290**(50): 29761-29768.

Sakao, S., H. Hao, N. Tanabe, Y. Kasahara, K. Kurosu and K. Tatsumi (2011). "Endothelial-like cells in chronic thromboembolic pulmonary hypertension: crosstalk with myofibroblast-like cells." Respir Res **12**: 109.

Sakao, S., H. Miyauchi, N. F. Voelkel, T. Sugiura, N. Tanabe, Y. Kobayashi and K. Tatsumi (2015). "Increased Right Ventricular Fatty Acid Accumulation in Chronic Thromboembolic Pulmonary Hypertension." Ann Am Thorac Soc **12**(10): 1465-1472.

Sandoval, J., J. Gaspar, T. Pulido, E. Bautista, M. L. Martinez-Guerra, M. Zeballos, A. Palomar and A. Gomez (1998). "Graded balloon dilation atrial septostomy in severe primary pulmonary hypertension. A therapeutic alternative for patients nonresponsive to vasodilator treatment." J Am Coll Cardiol **32**(2): 297-304.

Sastry, B. K., C. Narasimhan, N. K. Reddy and B. S. Raju (2004). "Clinical efficacy of sildenafil in primary pulmonary hypertension: a randomized, placebo-controlled, double-blind, crossover study." J Am Coll Cardiol **43**(7): 1149-1153.

Savai, R., S. S. Pullamsetti, J. Kolbe, E. Bieniek, R. Voswinckel, L. Fink, A. Scheed, C. Ritter, B. K. Dahal, A. Vater, S. Klussmann, H. A. Ghofrani, N. Weissmann, W. Klepetko, G. A. Banat, W. Seeger, F. Grimminger and R. T. Schermuly (2012). "Immune and inflammatory cell involvement in the pathology of idiopathic pulmonary arterial hypertension." Am J Respir Crit Care Med **186**(9): 897-908.

Schadt, E. E., S. A. Monks, T. A. Drake, A. J. Lusis, N. Che, V. Colinayo, T. G. Ruff, S. B. Milligan, J. R. Lamb, G. Cavet, P. S. Linsley, M. Mao, R. B. Stoughton and S. H. Friend (2003). "Genetics of gene expression surveyed in maize, mouse and man." Nature **422**(6929): 297-302.

Schaefer, E. J., J. R. McNamara, T. Tayler, J. A. Daly, J. A. Gleason, L. J. Seman, A. Ferrari and J. J. Rubenstein (2002). "Effects of atorvastatin on fasting and postprandial lipoprotein subclasses in coronary heart disease patients versus control subjects." Am J Cardiol **90**(7): 689-696.

Schafer, S., A. de Marvao, E. Adami, L. R. Fiedler, B. Ng, E. Khin, O. J. Rackham, S. van Heesch, C. J. Pua, M. Kui, R. Walsh, U. Tayal, S. K. Prasad, T. J. Dawes, N. S. Ko, D. Sim, L. L. Chan, C. W. Chin, F. Mazzarotto, P. J. Barton, F. Kreuchwig, D. P. de Kleijn, T. Totman, C. Biffi, N. Tee, D. Rueckert, V. Schneider, A. Faber, V. Regitz-Zagrosek, J. G. Seidman, C. E. Seidman, W. A. Linke, J. P. Kovalik, D. O'Regan, J. S. Ware, N. Hubner and S. A. Cook (2016). "Titin-truncating variants affect heart function in disease cohorts and the general population." Nat Genet **49**(1): 46-53.

Schermuly, R. T., E. Dony, H. A. Ghofrani, S. Pullamsetti, R. Savai, M. Roth, A. Sydykov, Y. J. Lai, N. Weissmann, W. Seeger and F. Grimminger (2005). "Reversal of experimental pulmonary hypertension by PDGF inhibition." J Clin Invest **115**(10): 2811-2821.

Schermuly, R. T., H. A. Ghofrani, M. R. Wilkins and F. Grimminger (2011). "Mechanisms of disease: pulmonary arterial hypertension." Nat Rev Cardiol **8**(8): 443-455.

Schicho, R., R. Shaykhutdinov, J. Ngo, A. Nazyrova, C. Schneider, R. Panaccione, G. G. Kaplan, H. J. Vogel and M. Storr (2012). "Quantitative metabolomic profiling of serum, plasma, and urine by (1)H NMR spectroscopy discriminates between patients with inflammatory bowel disease and healthy individuals." J Proteome Res **11**(6): 3344-3357.

Schooneman, M. G., F. M. Vaz, S. M. Houten and M. R. Soeters (2013). "Acylcarnitines: reflecting or inflicting insulin resistance?" Diabetes **62**(1): 1-8.

Schroeder, M. A., K. Clarke, S. Neubauer and D. J. Tyler (2011). "Hyperpolarized magnetic resonance: a novel technique for the in vivo assessment of cardiovascular disease." Circulation **124**(14): 1580-1594.

Schwartz, G. G., A. G. Olsson, M. Abt, C. M. Ballantyne, P. J. Barter, J. Brumm, B. R. Chaitman, I. M. Holme, D. Kallend, L. A. Leiter, E. Leitersdorf, J. J. McMurray, H. Mundl, S. J. Nicholls, P. K. Shah, J. C. Tardif, R. S. Wright and O. I. dal (2012). "Effects of dalcetrapib in patients with a recent acute coronary syndrome." N Engl J Med **367**(22): 2089-2099.

Scripps Center for Metabolomics and Mass Spectrometry. "What is mass spectrometry?" Retrieved 4 Nov, 2016, from https://masspec.scripps.edu/mshistory/whatisms_details.php.

Seyfarth, H. J., U. Sack, C. Gessner and H. Wirtz (2015). "Angiogenin, bFGF and VEGF: angiogenic markers in breath condensate of patients with pulmonary hypertension." Pneumologie **69**(4): 207-211.

Shah, S. H., J. R. Bain, M. J. Muehlbauer, R. D. Stevens, D. R. Crosslin, C. Haynes, J. Dungan, L. K. Newby, E. R. Hauser, G. S. Ginsburg, C. B. Newgard and W. E. Kraus (2010). "Association of a peripheral blood metabolic profile with coronary artery disease and risk of subsequent cardiovascular events." Circ Cardiovasc Genet **3**(2): 207-214.

Shah, S. H., W. E. Kraus and C. B. Newgard (2012). "Metabolomic profiling for the identification of novel biomarkers and mechanisms related to common cardiovascular diseases: form and function." Circulation **126**(9): 1110-1120.

Shah, S. J., T. Thenappan, S. Rich, L. Tian, S. L. Archer and M. Gomberg-Maitland (2008). "Association of serum creatinine with abnormal hemodynamics and mortality in pulmonary arterial hypertension." Circulation **117**(19): 2475-2483.

Shah, V. O., R. R. Townsend, H. I. Feldman, K. L. Pappan, E. Kensicki and D. L. Vander Jagt (2013). "Plasma metabolomic profiles in different stages of CKD." Clin J Am Soc Nephrol **8**(3): 363-370.

Shao, D., J. E. Park and S. J. Wort (2011). "The role of endothelin-1 in the pathogenesis of pulmonary arterial hypertension." Pharmacol Res **63**(6): 504-511.

Shapiro, R. and B. L. Vallee (1989). "Site-directed mutagenesis of histidine-13 and histidine-114 of human angiogenin. Alanine derivatives inhibit angiogenin-induced angiogenesis." Biochemistry **28**(18): 7401-7408.

Sharma, S. and S. M. Black (2009). "Carnitine Homeostasis, Mitochondrial Function, and Cardiovascular Disease." Drug Discov Today Dis Mech **6**(1-4): e31-e39.

Sharma, S., N. Sud, D. A. Wiseman, A. L. Carter, S. Kumar, Y. Hou, T. Rau, J. Wilham, C. Harmon, P. Oishi, J. R. Fineman and S. M. Black (2008). "Altered carnitine homeostasis is associated with decreased mitochondrial function and altered nitric oxide signaling in lambs with pulmonary hypertension." Am J Physiol Lung Cell Mol Physiol **294**(1): L46-56.

Sharma, S., S. Umar, F. Potus, A. Iorga, G. Wong, D. Meriwether, S. Breuils-Bonnet, D. Mai, K. Navab, D. Ross, M. Navab, S. Provencher, A. M. Fogelman, S. Bonnet, S. T. Reddy and M. Eghbali (2014). "Apolipoprotein A-I mimetic peptide 4F rescues pulmonary hypertension by inducing microRNA-193-3p." Circulation **130**(9): 776-785.

Shin, S. Y., E. B. Fauman, A. K. Petersen, J. Krumsiek, R. Santos, J. Huang, M. Arnold, I. Erte, V. Forgetta, T. P. Yang, K. Walter, C. Menni, L. Chen, L. Vasquez, A. M. Valdes, C. L. Hyde, V. Wang, D. Ziemek, P. Roberts, L. Xi, E. Grundberg, C. Multiple Tissue Human Expression

Resource, M. Waldenberger, J. B. Richards, R. P. Mohney, M. V. Milburn, S. L. John, J. Trimmer, F. J. Theis, J. P. Overington, K. Suhre, M. J. Brosnan, C. Gieger, G. Kastenmuller, T. D. Spector and N. Soranzo (2014). "An atlas of genetic influences on human blood metabolites." Nat Genet **46**(6): 543-550.

Sim, E., K. Walters and S. Boukouvala (2008). "Arylamine N-acetyltransferases: from structure to function." Drug Metab Rev **40**(3): 479-510.

Simonneau, G., R. J. Barst, N. Galie, R. Naeije, S. Rich, R. C. Bourge, A. Keogh, R. Oudiz, A. Frost, S. D. Blackburn, J. W. Crow, L. J. Rubin and G. Treprostinil Study (2002). "Continuous subcutaneous infusion of treprostinil, a prostacyclin analogue, in patients with pulmonary arterial hypertension: a double-blind, randomized, placebo-controlled trial." Am J Respir Crit Care Med **165**(6): 800-804.

Simonneau, G., M. A. Gatzoulis, I. Adatia, D. Celermajer, C. Denton, A. Ghofrani, M. A. Gomez Sanchez, R. Krishna Kumar, M. Landzberg, R. F. Machado, H. Olschewski, I. M. Robbins and R. Souza (2013). "Updated clinical classification of pulmonary hypertension." J Am Coll Cardiol **62**(25 Suppl): D34-41.

Singh, T. P., M. Rohit, A. Grover, S. Malhotra and R. Vijayvergiya (2006). "A randomized, placebo-controlled, double-blind, crossover study to evaluate the efficacy of oral sildenafil therapy in severe pulmonary artery hypertension." Am Heart J **151**(4): 851 e851-855.

Sitbon, O., M. Humbert, X. Jais, V. Ioos, A. M. Hamid, S. Provencher, G. Garcia, F. Parent, P. Herve and G. Simonneau (2005). "Long-term response to calcium channel blockers in idiopathic pulmonary arterial hypertension." Circulation **111**(23): 3105-3111.

Sitbon, O., M. Humbert, H. Nunes, F. Parent, G. Garcia, P. Herve, M. Rainisio and G. Simonneau (2002). "Long-term intravenous epoprostenol infusion in primary pulmonary hypertension: prognostic factors and survival." J Am Coll Cardiol **40**(4): 780-788.

Skoro-Sajer, N., F. Mittermayer, A. Panzenboeck, D. Bonderman, R. Sadushi, R. Hitsch, J. Jakowitsch, W. Klepetko, M. P. Kneussl, M. Wolzt and I. M. Lang (2007). "Asymmetric dimethylarginine is increased in chronic thromboembolic pulmonary hypertension." American journal of respiratory and critical care medicine **176**(11): 1154-1160.

Slotkin, W. and K. Nishikura (2013). "Adenosine-to-inosine RNA editing and human disease." Genome Medicine **5**(11): 105.

Smith, G. D. and S. Ebrahim (2004). "Mendelian randomization: prospects, potentials, and limitations." Int J Epidemiol **33**(1): 30-42.

Smith, R. J. (1990). "Glutamine metabolism and its physiologic importance." JPEN J Parenter Enteral Nutr **14**(4 Suppl): 40S-44S.

Sobolewski, A., N. Rudarakanchana, P. D. Upton, J. Yang, T. K. Crilley, R. C. Trembath and N. W. Morrell (2008). "Failure of bone morphogenetic protein receptor trafficking in pulmonary arterial hypertension: potential for rescue." Hum Mol Genet **17**(20): 3180-3190.

Song, S., S. Wang, J. Ma, L. Yao, H. Xing, L. Zhang, L. Liao and D. Zhu (2013). "Biliverdin reductase/bilirubin mediates the anti-apoptotic effect of hypoxia in pulmonary arterial smooth muscle cells through ERK1/2 pathway." Exp Cell Res **319**(13): 1973-1987.

Soubrier, F., W. K. Chung, R. Machado, E. Grunig, M. Aldred, M. Geraci, J. E. Loyd, C. G. Elliott, R. C. Trembath, J. H. Newman and M. Humbert (2013). "Genetics and genomics of pulmonary arterial hypertension." J Am Coll Cardiol **62**(25 Suppl): D13-21.

Sproule, D. M., J. Dyme, J. Coku, D. de Vinck, E. Rosenzweig, W. K. Chung and D. C. De Vivo (2008). "Pulmonary artery hypertension in a child with MELAS due to a point mutation of the mitochondrial tRNA((Leu)) gene (m.3243A>G)." Journal of Inherited Metabolic Disease **31 Suppl 3**: 497-503.

Stacher, E., B. B. Graham, J. M. Hunt, A. Gandjeva, S. D. Groshong, V. V. McLaughlin, M. Jessup, W. E. Grizzle, M. A. Aldred, C. D. Cool and R. M. Tuder (2012). "Modern age pathology of pulmonary arterial hypertension." Am J Respir Crit Care Med **186**(3): 261-272.

Stearman, R. S., A. R. Cornelius, X. Lu, D. S. Conklin, M. J. Del Rosario, A. M. Lowe, M. T. Elos, L. M. Fettig, R. E. Wong, N. Hara, J. D. Cogan, J. A. Phillips, 3rd, M. R. Taylor, B. B. Graham, R. M. Tuder, J. E. Loyd and M. W. Geraci (2014). "Functional prostacyclin synthase promoter polymorphisms. Impact in pulmonary arterial hypertension." Am J Respir Crit Care Med **189**(9): 1110-1120.

Steinberg, S. and R. Cedergren (1995). "A correlation between N2-dimethylguanosine presence and alternate tRNA conformers." RNA **1**(9): 886-891.

Stenmark, K. R., M. Frid and F. Perros (2016). "Endothelial-to-Mesenchymal Transition: An Evolving Paradigm and a Promising Therapeutic Target in PAH." Circulation **133**(18): 1734-1737.

Stenmark, K. R., E. Gerasimovskaya, R. A. Nemenoff and M. Das (2002). "Hypoxic activation of adventitial fibroblasts: role in vascular remodeling." Chest **122**(6 Suppl): 326S-334S.

Stenmark, K. R. and R. P. Mecham (1997). "Cellular and molecular mechanisms of pulmonary vascular remodeling." Annu Rev Physiol **59**: 89-144.

Stenmark, K. R., B. Meyrick, N. Galie, W. J. Mooi and I. F. McMurtry (2009). "Animal models of pulmonary arterial hypertension: the hope for etiological discovery and pharmacological cure." Am J Physiol Lung Cell Mol Physiol **297**(6): L1013-1032.

Stewart, D. J., R. D. Levy, P. Cernacek and D. Langleben (1991). "Increased plasma endothelin-1 in pulmonary hypertension: marker or mediator of disease?" Ann Intern Med **114**(6): 464-469.

Sugimura, K., Y. Fukumoto, K. Satoh, K. Nochioka, Y. Miura, T. Aoki, S. Tatebe, S. Miyamichi-Yamamoto and H. Shimokawa (2012). "Percutaneous transluminal pulmonary angioplasty markedly improves pulmonary hemodynamics and long-term prognosis in patients with chronic thromboembolic pulmonary hypertension." Circ J **76**(2): 485-488.

Suhre, K., S. Y. Shin, A. K. Petersen, R. P. Mohney, D. Meredith, B. Wagele, E. Altmaier, CardioGram, P. Deloukas, J. Erdmann, E. Grundberg, C. J. Hammond, M. H. de Angelis, G. Kastenmuller, A. Kottgen, F. Kronenberg, M. Mangino, C. Meisinger, T. Meitinger, H. W. Mewes, M. V. Milburn, C. Prehn, J. Raffler, J. S. Ried, W. Romisch-Margl, N. J. Samani, K. S. Small, H. E. Wichmann, G. Zhai, T. Illig, T. D. Spector, J. Adamski, N. Soranzo and C. Gieger (2011). "Human metabolic individuality in biomedical and pharmaceutical research." Nature **477**(7362): 54-60.

Sun, W., K. Kechris, S. Jacobson, M. B. Drummond, G. A. Hawkins, J. Yang, T. H. Chen, P. M. Quibrera, W. Anderson, R. G. Barr, P. V. Basta, E. R. Bleecker, T. Beaty, R. Casaburi, P. Castaldi, M. H. Cho, A. Comellas, J. D. Crapo, G. Criner, D. Demeo, S. A. Christenson, D. J. Couper, J. L. Curtis, C. M. Doerschuk, C. M. Freeman, N. A. Gouskova, M. K. Han, N. A. Hanania, N. N. Hansel, C. P. Hersh, E. A. Hoffman, R. J. Kaner, R. E. Kanner, E. C. Kleerup, S. Lutz, F. J. Martinez, D. A. Meyers, S. P. Peters, E. A. Regan, S. I. Rennard, M. B. Scholand, E. K. Silverman, P. G. Woodruff, W. K. O'Neal, R. P. Bowler, S. R. Group and C. O. Investigators

(2016). "Common Genetic Polymorphisms Influence Blood Biomarker Measurements in COPD." PLoS Genet **12**(8): e1006011.

Sun, X., S. Kumar, S. Sharma, S. Aggarwal, Q. Lu, C. Gross, O. Rafikova, S. G. Lee, S. Dasarathy, Y. Hou, M. L. Meadows, W. Han, Y. Su, J. R. Fineman and S. M. Black (2014). "Endothelin-1 induces a glycolytic switch in pulmonary arterial endothelial cells via the mitochondrial translocation of endothelial nitric oxide synthase." Am J Respir Cell Mol Biol **50**(6): 1084-1095.

Sun, X., S. Sharma, S. Fratz, S. Kumar, R. Rafikov, S. Aggarwal, O. Rafikova, Q. Lu, T. Burns, S. Dasarathy, J. Wright, C. Schreiber, M. Radman, J. R. Fineman and S. M. Black (2013). "Disruption of endothelial cell mitochondrial bioenergetics in lambs with increased pulmonary blood flow." Antioxid Redox Signal **18**(14): 1739-1752.

Surie, S., B. J. Bouma, R. A. Bruin-Bon, M. Hardziyenka, J. J. Kloek, M. N. Van der Plas, H. J. Reesink and P. Bresser (2011). "Time course of restoration of systolic and diastolic right ventricular function after pulmonary endarterectomy for chronic thromboembolic pulmonary hypertension." Am Heart J **161**(6): 1046-1052.

Sutendra, G., S. Bonnet, G. Rochefort, A. Haromy, K. D. Folmes, G. D. Lopaschuk, J. R. Dyck and E. D. Michelakis (2010). "Fatty acid oxidation and malonyl-CoA decarboxylase in the vascular remodeling of pulmonary hypertension." Sci Transl Med **2**(44): 44ra58.

Sutendra, G. and E. D. Michelakis (2013). "Pulmonary arterial hypertension: challenges in translational research and a vision for change." Sci Transl Med **5**(208): 208sr205.

Sutendra, G. and E. D. Michelakis (2014). "The metabolic basis of pulmonary arterial hypertension." Cell Metab **19**(4): 558-573.

Sweeney, S. R., A. Kavanaugh, A. Lodi, B. Wang, D. Boyle, S. Tiziani and M. Guma (2016). "Metabolomic profiling predicts outcome of rituximab therapy in rheumatoid arthritis." RMD Open **2**(2): e000289.

Swerdlow, D. I., K. B. Kuchenbaecker, S. Shah, R. Sofat, M. V. Holmes, J. White, J. S. Mindell, M. Kivimaki, E. J. Brunner, J. C. Whittaker, J. P. Casas and A. D. Hingorani (2016). "Selecting instruments for Mendelian randomization in the wake of genome-wide association studies." Int J Epidemiol **45**(5): 1600-1616.

Swift, A. J., S. Rajaram, M. J. Campbell, J. Hurdman, S. Thomas, D. Capener, C. Elliot, R. Condliffe, J. M. Wild and D. G. Kiely (2014). "Prognostic value of cardiovascular magnetic resonance imaging measurements corrected for age and sex in idiopathic pulmonary arterial hypertension." Circ Cardiovasc Imaging **7**(1): 100-106.

Tabima, D. M. and N. C. Chesler (2010). "The effects of vasoactivity and hypoxic pulmonary hypertension on extralobar pulmonary artery biomechanics." J Biomech **43**(10): 1864-1869.

Tachibana-Iimori, R., Y. Tabara, H. Kusuhara, K. Kohara, R. Kawamoto, J. Nakura, K. Tokunaga, I. Kondo, Y. Sugiyama and T. Miki (2004). "Effect of genetic polymorphism of OATP-C (SLCO1B1) on lipid-lowering response to HMG-CoA reductase inhibitors." Drug Metab Pharmacokinet **19**(5): 375-380.

Takeda, Y., Y. Takeda, S. Tomimoto, T. Tani, H. Narita and G. Kimura (2010). "Bilirubin as a prognostic marker in patients with pulmonary arterial hypertension." BMC Pulm Med **10**: 22.

Talati, M. H., E. L. Brittain, J. P. Fessel, N. Penner, J. Atkinson, M. Funke, C. Grueter, W. G. Jerome, M. Freeman, J. H. Newman, J. West and A. R. Hemnes (2016). "Mechanisms of Lipid

Accumulation in the Bone Morphogenic Protein Receptor 2 Mutant Right Ventricle." Am J Respir Crit Care Med **194**(6): 719-728.

Tall, A. R. (1993). "Plasma cholesteryl ester transfer protein." J Lipid Res **34**(8): 1255-1274.

Tamai, I., J. Nezu, H. Uchino, Y. Sai, A. Oku, M. Shimane and A. Tsuji (2000). "Molecular identification and characterization of novel members of the human organic anion transporter (OATP) family." Biochem Biophys Res Commun **273**(1): 251-260.

Taniguchi, M. and T. Okazaki (2014). "The role of sphingomyelin and sphingomyelin synthases in cell death, proliferation and migration-from cell and animal models to human disorders." Biochim Biophys Acta **1841**(5): 692-703.

Tantini, B., A. Manes, E. Fiumana, C. Pignatti, C. Guarnieri, R. Zannoli, A. Branzi and N. Galie (2005). "Antiproliferative effect of sildenafil on human pulmonary artery smooth muscle cells." Basic Res Cardiol **100**(2): 131-138.

Taraseviciene-Stewart, L., Y. Kasahara, L. Alger, P. Hirth, G. Mc Mahon, J. Waltenberger, N. F. Voelkel and R. M. Tuder (2001). "Inhibition of the VEGF receptor 2 combined with chronic hypoxia causes cell death-dependent pulmonary endothelial cell proliferation and severe pulmonary hypertension." FASEB J **15**(2): 427-438.

Teng, C. F., H. C. Wu, W. C. Hsieh, H. W. Tsai and I. J. Su (2015). "Activation of ATP citrate lyase by mTOR signal induces disturbed lipid metabolism in hepatitis B virus pre-S2 mutant tumorigenesis." J Virol **89**(1): 605-614.

Tennant, D. A., R. V. Duran and E. Gottlieb (2010). "Targeting metabolic transformation for cancer therapy." Nature Reviews Cancer **10**(4): 267-277.

Thenappan, T., S. J. Shah, M. Gomberg-Maitland, B. Collander, A. Vallakati, P. Shroff and S. Rich (2011). "Clinical characteristics of pulmonary hypertension in patients with heart failure and preserved ejection fraction." Circ Heart Fail **4**(3): 257-265.

Thompson, A., E. Di Angelantonio, N. Sarwar, S. Erqou, D. Saleheen, R. P. Dullaart, B. Keavney, Z. Ye and J. Danesh (2008). "Association of cholesteryl ester transfer protein genotypes with CETP mass and activity, lipid levels, and coronary risk." JAMA **299**(23): 2777-2788.

Torres, A. G., E. Batlle and L. Ribas de Pouplana (2014). "Role of tRNA modifications in human diseases." Trends in Molecular Medicine **20**(6): 306-314.

Townsley, M. I. (2012). "Structure and composition of pulmonary arteries, capillaries, and veins." Compr Physiol **2**(1): 675-709.

Tozzi, C. A., D. L. Christiansen, G. J. Poiani and D. J. Riley (1994). "Excess collagen in hypertensive pulmonary arteries decreases vascular distensibility." Am J Respir Crit Care Med **149**(5): 1317-1326.

Tuder, R. M., M. Chacon, L. Alger, J. Wang, L. Taraseviciene-Stewart, Y. Kasahara, C. D. Cool, A. E. Bishop, M. Geraci, G. L. Semenza, M. Yacoub, J. M. Polak and N. F. Voelkel (2001). "Expression of angiogenesis-related molecules in plexiform lesions in severe pulmonary hypertension: evidence for a process of disordered angiogenesis." J Pathol **195**(3): 367-374.

Tuder, R. M., C. D. Cool, M. W. Geraci, J. Wang, S. H. Abman, L. Wright, D. Badesch and N. F. Voelkel (1999). "Prostacyclin synthase expression is decreased in lungs from patients with severe pulmonary hypertension." Am J Respir Crit Care Med **159**(6): 1925-1932.

Tuder, R. M., E. Stacher, J. Robinson, R. Kumar and B. B. Graham (2013). "Pathology of pulmonary hypertension." Clin Chest Med **34**(4): 639-650.

Tyler, D. J. and S. Neubauer (2016). "Science to Practice: Hyperpolarized Metabolic MR Imaging--The Light at the End of the Tunnel for Clinical (13)C MR Spectroscopy?" Radiology **278**(3): 639-641.

Varvel, S. A., S. Voros, D. L. Thiselton, J. V. Pottala, T. Dall, G. R. Warnick, J. P. McConnell, L. Ghaedi, M. Sasinowski and T. Graham (2014). "Comprehensive biomarker testing of glycemia, insulin resistance, and beta cell function has greater sensitivity to detect diabetes risk than fasting glucose and HbA1c and is associated with improved glycemic control in clinical practice." J Cardiovasc Transl Res **7**(6): 597-606.

Vaughan, A. A., W. B. Dunn, J. W. Allwood, D. C. Wedge, F. H. Blackhall, A. D. Whetton, C. Dive and R. Goodacre (2012). "Liquid chromatography-mass spectrometry calibration transfer and metabolomics data fusion." Anal Chem **84**(22): 9848-9857.

Ventetuolo, C. E., G. L. Baird, R. G. Barr, D. A. Bluemke, J. S. Fritz, N. S. Hill, J. R. Klinger, J. A. Lima, P. Ouyang, H. I. Palevsky, A. J. Palmisciano, I. Krishnan, D. Pinder, I. R. Preston, K. E. Roberts and S. M. Kawut (2015). "Higher Estradiol and Lower Dehydroepiandrosterone-Sulfate Levels Are Associated With Pulmonary Arterial Hypertension in Men." Am J Respir Crit Care Med.

Viales, R. R., C. A. Eichstaedt, N. Ehlken, C. Fischer, M. Lichtblau, E. Grunig and K. Hinderhofer (2015). "Mutation in BMPR2 Promoter: A 'Second Hit' for Manifestation of Pulmonary Arterial Hypertension?" PLoS One **10**(7): e0133042.

Vidal, M., M. E. Cusick and A. L. Barabasi (2011). "Interactome networks and human disease." Cell **144**(6): 986-998.

Vinaixa, M., S. Samino, I. Saez, J. Duran, J. J. Guinovart and O. Yanes (2012). "A Guideline to Univariate Statistical Analysis for LC/MS-Based Untargeted Metabolomics-Derived Data." Metabolites **2**(4): 775-795.

Vlachopoulos, C., P. Xaplanteris, V. Aboyans, M. Brodmann, R. Cifkova, F. Cosentino, M. De Carlo, A. Gallino, U. Landmesser, S. Laurent, J. Lekakis, D. P. Mikhailidis, K. K. Naka, A. D. Protogerou, D. Rizzoni, A. Schmidt-Trucksass, L. Van Bortel, T. Weber, A. Yamashina, R. Zimlichman, P. Boutouyrie, J. Cockcroft, M. O'Rourke, J. B. Park, G. Schillaci, H. Sillesen and R. R. Townsend (2015). "The role of vascular biomarkers for primary and secondary prevention. A position paper from the European Society of Cardiology Working Group on peripheral circulation: Endorsed by the Association for Research into Arterial Structure and Physiology (ARTERY) Society." Atherosclerosis **241**(2): 507-532.

Voelkel, M. A., K. M. Wynne, D. B. Badesch, B. M. Groves and N. F. Voelkel (2000). "Hyperuricemia in severe pulmonary hypertension." Chest **117**(1): 19-24.

Voelkel, N. F. and H. J. Bogaard (2016). "Adding complexity to plexogenic arteriopathy." Eur Respir J **48**(6): 1553-1555.

Voight, B. F., G. M. Peloso, M. Orho-Melander, R. Frikke-Schmidt, M. Barbalic, M. K. Jensen, G. Hindy, H. Holm, E. L. Ding, T. Johnson, H. Schunkert, N. J. Samani, R. Clarke, J. C. Hopewell, J. F. Thompson, M. Li, G. Thorleifsson, C. Newton-Cheh, K. Musunuru, J. P. Pirruccello, D. Saleheen, L. Chen, A. Stewart, A. Schillert, U. Thorsteinsdottir, G. Thorgeirsson, S. Anand, J. C. Engert, T. Morgan, J. Spertus, M. Stoll, K. Berger, N. Martinelli, D. Girelli, P. P. McKeown, C. C. Patterson, S. E. Epstein, J. Devaney, M. S. Burnett, V. Mooser, S. Ripatti, I. Surakka, M.

S. Nieminen, J. Sinisalo, M. L. Lokki, M. Perola, A. Havulinna, U. de Faire, B. Gigante, E. Ingelsson, T. Zeller, P. Wild, P. I. de Bakker, O. H. Klungel, A. H. Maitland-van der Zee, B. J. Peters, A. de Boer, D. E. Grobbee, P. W. Kamphuisen, V. H. Deneer, C. C. Elbers, N. C. Onland-Moret, M. H. Hofker, C. Wijmenga, W. M. Verschuren, J. M. Boer, Y. T. van der Schouw, A. Rasheed, P. Frossard, S. Demissie, C. Willer, R. Do, J. M. Ordovas, G. R. Abecasis, M. Boehnke, K. L. Mohlke, M. J. Daly, C. Guiducci, N. P. Burtt, A. Surti, E. Gonzalez, S. Purcell, S. Gabriel, J. Marrugat, J. Peden, J. Erdmann, P. Diemert, C. Willenborg, I. R. Konig, M. Fischer, C. Hengstenberg, A. Ziegler, I. Buysschaert, D. Lambrechts, F. Van de Werf, K. A. Fox, N. E. El Mokhtari, D. Rubin, J. Schrezenmeir, S. Schreiber, A. Schafer, J. Danesh, S. Blankenberg, R. Roberts, R. McPherson, H. Watkins, A. S. Hall, K. Overvad, E. Rimm, E. Boerwinkle, A. Tybjaerg-Hansen, L. A. Cupples, M. P. Reilly, O. Melander, P. M. Mannucci, D. Ardissino, D. Siscovick, R. Elosua, K. Stefansson, C. J. O'Donnell, V. Salomaa, D. J. Rader, L. Peltonen, S. M. Schwartz, D. Altshuler and S. Kathiresan (2012). "Plasma HDL cholesterol and risk of myocardial infarction: a mendelian randomisation study." Lancet **380**(9841): 572-580.

Vonk-Noordegraaf, A., F. Haddad, K. M. Chin, P. R. Forfia, S. M. Kawut, J. Lumens, R. Naeije, J. Newman, R. J. Oudiz, S. Provencher, A. Torbicki, N. F. Voelkel and P. M. Hassoun (2013). "Right heart adaptation to pulmonary arterial hypertension: physiology and pathobiology." J Am Coll Cardiol **62**(25 Suppl): D22-33.

Vorkas, P. A., G. Isaac, A. Holmgren, E. J. Want, J. P. Shockcor, E. Holmes and M. Y. Henein (2015). "Perturbations in fatty acid metabolism and apoptosis are manifested in calcific coronary artery disease: An exploratory lipidomic study." Int J Cardiol **197**: 192-199.

W. P. Aue, E. B., and R. R. Ernst (1976). "Two-dimensional spectroscopy. Application to nuclear magnetic resonance " The Journal of Chemical Physics **64**(5): 2229-2246.

Waalkes, T. P., C. W. Gehrke, R. W. Zumwalt, S. Y. Chang, D. B. Lakings, D. C. Tormey, D. L. Ahmann and C. G. Moertel (1975). "The urinary excretion of nucleosides of ribonucleic acid by patients with advanced cancer." Cancer **36**(2): 390-398.

Wagenvoort, C. A. (1970). "The pathology of primary pulmonary hypertension." J Pathol **101**(4): Pi.

Wallace, T. M. and D. R. Matthews (2004). "Recent advances in the monitoring and management of diabetic ketoacidosis." QJM **97**(12): 773-780.

Wang, G., L. Knight, R. Ji, P. Lawrence, U. Kanaan, L. Li, A. Das, B. Cui, W. Zou, D. J. Penny and Y. Fan (2014). "Early onset severe pulmonary arterial hypertension with 'two-hit' digenic mutations in both BMPR2 and KCNA5 genes." Int J Cardiol **177**(3): e167-169.

Wang, H., W. Li, W. Zhang, K. Sun, X. Song, S. Gao, C. Zhang, R. Hui and H. Hu (2009). "Novel promoter and exon mutations of the BMPR2 gene in Chinese patients with pulmonary arterial hypertension." Eur J Hum Genet **17**(8): 1063-1069.

Wang, J. H., J. Byun and S. Pennathur (2010). "Analytical approaches to metabolomics and applications to systems biology." Semin Nephrol **30**(5): 500-511.

Wang, L., H. L. Gan, Y. Liu, S. Gu, J. Li, L. J. Guo, J. Liu, Y. Wang, Y. X. Wang, Z. F. Zhang, J. Wang and C. Wang (2013). "The distinguishing cellular features of pulmonary artery smooth muscle cells from chronic thromboembolic pulmonary hypertension patients." Exp Lung Res **39**(8): 349-358.

Wang, T. J., M. G. Larson, R. S. Vasan, S. Cheng, E. P. Rhee, E. McCabe, G. D. Lewis, C. S. Fox, P. F. Jacques, C. Fernandez, C. J. O'Donnell, S. A. Carr, V. K. Mootha, J. C. Florez, A. Souza, O.

Melander, C. B. Clish and R. E. Gerszten (2011). "Metabolite profiles and the risk of developing diabetes." Nature Medicine **17**(4): 448-453.

Wang, Z., E. Klipfell, B. J. Bennett, R. Koeth, B. S. Levison, B. Dugar, A. E. Feldstein, E. B. Britt, X. Fu, Y. M. Chung, Y. Wu, P. Schauer, J. D. Smith, H. Allayee, W. H. Tang, J. A. DiDonato, A. J. Lusis and S. L. Hazen (2011). "Gut flora metabolism of phosphatidylcholine promotes cardiovascular disease." Nature **472**(7341): 57-63.

Wanichthanarak, K., J. F. Fahrmann and D. Grapov (2015). "Genomic, Proteomic, and Metabolomic Data Integration Strategies." Biomark Insights **10**(Suppl 4): 1-6.

Want, E. J., P. Masson, F. Michopoulos, I. D. Wilson, G. Theodoridis, R. S. Plumb, J. Shockcor, N. Loftus, E. Holmes and J. K. Nicholson (2013). "Global metabolic profiling of animal and human tissues via UPLC-MS." Nat Protoc **8**(1): 17-32.

Warburg, O. H. and Kaiser Wilhelm-Institut für Biologie (Berlin). (1926). Über den Stoffwechsel der Tumoren : Arbeiten aus dem Kaiser Wilhelm-Institut für Biologie, Berlin-Dahlem. Berlin, Julius Springer.

Waxman, A., S. Y. Chen, L. Boulanger, J. A. Watson and G. Golden (2013). "Factors associated with adherence to phosphodiesterase type 5 inhibitors for the treatment of pulmonary arterial hypertension." J Med Econ **16**(2): 298-306.

Wei, C., H. Z. Li, Y. H. Wang, X. Peng, H. J. Shao, H. X. Li, S. Z. Bai, X. X. Lu, L. Y. Wu, R. Wang and C. Q. Xu (2016). "Exogenous spermine inhibits the proliferation of human pulmonary artery smooth muscle cells caused by chemically-induced hypoxia via the suppression of the ERK1/2- and PI3K/AKT-associated pathways." Int J Mol Med **37**(1): 39-46.

Weinshilboum, R. M., D. M. Otterness, I. A. Aksoy, T. C. Wood, C. Her and R. B. Raftogianis (1997). "Sulfation and sulfotransferases 1: Sulfotransferase molecular biology: cDNAs and genes." FASEB J **11**(1): 3-14.

Wharton, J., N. Davie, P. D. Upton, M. H. Yacoub, J. M. Polak and N. W. Morrell (2000). "Prostacyclin analogues differentially inhibit growth of distal and proximal human pulmonary artery smooth muscle cells." Circulation **102**(25): 3130-3136.

Wharton, J., J. W. Strange, G. M. Moller, E. J. Growcott, X. Ren, A. P. Franklyn, S. C. Phillips and M. R. Wilkins (2005). "Antiproliferative effects of phosphodiesterase type 5 inhibition in human pulmonary artery cells." Am J Respir Crit Care Med **172**(1): 105-113.

Wilkins, M. R. (2012). "Pulmonary hypertension: the science behind the disease spectrum." Eur Respir Rev **21**(123): 19-26.

Wilkins, M. R., O. Ali, W. Bradlow, J. Wharton, A. Taegtmeyer, C. J. Rhodes, H. A. Ghofrani, L. Howard, P. Nihoyannopoulos, R. H. Mohiaddin, J. S. Gibbs and G. Simvastatin Pulmonary Hypertension Trial Study (2010). "Simvastatin as a treatment for pulmonary hypertension trial." Am J Respir Crit Care Med **181**(10): 1106-1113.

Wishart, D. S., D. Tzur, C. Knox, R. Eisner, A. C. Guo, N. Young, D. Cheng, K. Jewell, D. Arndt, S. Sawhney, C. Fung, L. Nikolai, M. Lewis, M. A. Coutouly, I. Forsythe, P. Tang, S. Shrivastava, K. Jeroncic, P. Stothard, G. Amegbey, D. Block, D. D. Hau, J. Wagner, J. Miniaci, M. Clements, M. Gebremedhin, N. Guo, Y. Zhang, G. E. Duggan, G. D. Macinnis, A. M. Weljie, R. Dowlatabadi, F. Bamforth, D. Clive, R. Greiner, L. Li, T. Marrie, B. D. Sykes, H. J. Vogel and L. Querengesser (2007). "HMDB: the Human Metabolome Database." Nucleic Acids Res **35**(Database issue): D521-526.

Worley, B. and R. Powers (2013). "Multivariate Analysis in Metabolomics." Curr Metabolomics **1**(1): 92-107.

Wu, G., T. E. Haynes, H. Li and C. J. Meininger (2000). "Glutamine metabolism in endothelial cells: ornithine synthesis from glutamine via pyrroline-5-carboxylate synthase." Comp Biochem Physiol A Mol Integr Physiol **126**(1): 115-123.

Wymann, M. P. and R. Schneiter (2008). "Lipid signalling in disease." Nature Reviews Molecular Cell Biology **9**(2): 162-176.

Xia, J., I. V. Sinelnikov, B. Han and D. S. Wishart (2015). "MetaboAnalyst 3.0--making metabolomics more meaningful." Nucleic Acids Res **43**(W1): W251-257.

Xian, X., Y. Ma, D. D. Yang, W. Huang, Y. Wang, O. Mueller, E. Chang, Y. Konigshofer, M. Van-Cleve, J. Yang and G. Liu (2009). "Reduced high-density lipoprotein 2b in non-obese type 2 diabetic patients analysed by a microfluidic chip method in a case-control study." Biomarkers **14**(8): 619-623.

Xiao, J. F., B. Zhou and H. W. Ressom (2012). "Metabolite identification and quantitation in LC-MS/MS-based metabolomics." Trends Analyt Chem **32**: 1-14.

Xiao, Y., H. Christou, L. Liu, G. Visner, S. A. Mitsialis, S. Kourembanas and H. Liu (2013). "Endothelial indoleamine 2,3-dioxygenase protects against development of pulmonary hypertension." Am J Respir Crit Care Med **188**(4): 482-491.

Xu, S., J. L. Flanagan, P. A. Simmons, J. Vehige, M. D. Willcox and Q. Garrett (2010). "Transport of L-carnitine in human corneal and conjunctival epithelial cells." Mol Vis **16**: 1823-1831.

Xu, W., F. T. Kaneko, S. Zheng, S. A. Comhair, A. J. Janocha, T. Goggans, F. B. Thunnissen, C. Farver, S. L. Hazen, C. Jennings, R. A. Dweik, A. C. Arroliga and S. C. Erzurum (2004). "Increased arginase II and decreased NO synthesis in endothelial cells of patients with pulmonary arterial hypertension." FASEB J **18**(14): 1746-1748.

Xu, W., T. Koeck, A. R. Lara, D. Neumann, F. P. DiFilippo, M. Koo, A. J. Janocha, F. A. Masri, A. C. Arroliga, C. Jennings, R. A. Dweik, R. M. Tuder, D. J. Stuehr and S. C. Erzurum (2007). "Alterations of cellular bioenergetics in pulmonary artery endothelial cells." Proc Natl Acad Sci U S A **104**(4): 1342-1347.

Yamakoshi, Y., T. Kishimoto, K. Sugimura and H. Kawashima (1999). "Human prostate CYP3A5: identification of a unique 5'-untranslated sequence and characterization of purified recombinant protein." Biochem Biophys Res Commun **260**(3): 676-681.

Yang, T., M. M. Santisteban, V. Rodriguez, E. Li, N. Ahmari, J. M. Carvajal, M. Zadeh, M. Gong, Y. Qi, J. Zubcevic, B. Sahay, C. J. Pepine, M. K. Raizada and M. Mohamadzadeh (2015). "Gut dysbiosis is linked to hypertension." Hypertension **65**(6): 1331-1340.

Yano, M., K. Watanabe, T. Yamamoto, K. Ikeda, T. Senokuchi, M. Lu, T. Kadomatsu, H. Tsukano, M. Ikawa, M. Okabe, S. Yamaoka, T. Okazaki, H. Umehara, T. Gotoh, W. J. Song, K. Node, R. Taguchi, K. Yamagata and Y. Oike (2011). "Mitochondrial dysfunction and increased reactive oxygen species impair insulin secretion in sphingomyelin synthase 1-null mice." The Journal of Biological Chemistry **286**(5): 3992-4002.

Yao, X., E. M. Gordon, A. V. Barochia, A. T. Remaley and S. J. Levine (2016). "The A's Have It: Developing Apolipoprotein A-I Mimetic Peptides Into a Novel Treatment for Asthma." Chest **150**(2): 283-288.

Yao, X., E. M. Gordon, D. M. Figueroa, A. V. Barochia and S. J. Levine (2016). "Emerging Roles of Apolipoprotein E and Apolipoprotein A-I in the Pathogenesis and Treatment of Lung Disease." Am J Respir Cell Mol Biol **55**(2): 159-169.

Yates, A., W. Akanni, M. R. Amode, D. Barrell, K. Billis, D. Carvalho-Silva, C. Cummins, P. Clapham, S. Fitzgerald, L. Gil, C. G. Giron, L. Gordon, T. Hourlier, S. E. Hunt, S. H. Janacek, N. Johnson, T. Juettemann, S. Keenan, I. Lavidas, F. J. Martin, T. Maurel, W. McLaren, D. N. Murphy, R. Nag, M. Nuhn, A. Parker, M. Patricio, M. Pignatelli, M. Rahtz, H. S. Riat, D. Sheppard, K. Taylor, A. Thormann, A. Vullo, S. P. Wilder, A. Zadissa, E. Birney, J. Harrow, M. Muffato, E. Perry, M. Ruffier, G. Spudich, S. J. Trevanion, F. Cunningham, B. L. Aken, D. R. Zerbino and P. Flicek (2016). "Ensembl 2016." Nucleic Acids Res **44**(D1): D710-716.

Yeager, M. E., G. R. Halley, H. A. Golpon, N. F. Voelkel and R. M. Tuder (2001). "Microsatellite instability of endothelial cell growth and apoptosis genes within plexiform lesions in primary pulmonary hypertension." Circ Res **88**(1): E2-E11.

Yengo, L., A. Arredouani, M. Marre, R. Roussel, M. Vaxillaire, M. Falchi, A. Haoudi, J. Tichet, D. E. S. I. R. S. Group, B. Balkau, A. Bonnefond and P. Froguel (2016). "Impact of statistical models on the prediction of type 2 diabetes using non-targeted metabolomics profiling." Mol Metab **5**(10): 918-925.

Yi, E. S., H. Kim, H. Ahn, J. Strother, T. Morris, E. Masliah, L. A. Hansen, K. Park and P. J. Friedman (2000). "Distribution of obstructive intimal lesions and their cellular phenotypes in chronic pulmonary hypertension. A morphometric and immunohistochemical study." Am J Respir Crit Care Med **162**(4 Pt 1): 1577-1586.

Yuan, X. J., J. Wang, M. Juhaszova, S. P. Gaine and L. J. Rubin (1998). "Attenuated K+ channel gene transcription in primary pulmonary hypertension." Lancet **351**(9104): 726-727.

Yuhanna, I. S., Y. Zhu, B. E. Cox, L. D. Hahner, S. Osborne-Lawrence, P. Lu, Y. L. Marcel, R. G. Anderson, M. E. Mendelsohn, H. H. Hobbs and P. W. Shaul (2001). "High-density lipoprotein binding to scavenger receptor-BI activates endothelial nitric oxide synthase." Nat Med **7**(7): 853-857.

Zamanian, R. T., G. Hansmann, S. Snook, D. Lilienfeld, K. M. Rappaport, G. M. Reaven, M. Rabinovitch and R. L. Doyle (2009). "Insulin resistance in pulmonary arterial hypertension." Eur Respir J **33**(2): 318-324.

Zamzami, N., P. Marchetti, M. Castedo, T. Hirsch, S. A. Susin, B. Masse and G. Kroemer (1996). "Inhibitors of permeability transition interfere with the disruption of the mitochondrial transmembrane potential during apoptosis." FEBS Lett **384**(1): 53-57.

Zeljkovic, A., J. Vekic, V. Spasojevic-Kalimanovska, Z. Jelic-Ivanovic, N. Bogavac-Stanojevic, B. Gulan and S. Spasic (2010). "LDL and HDL subclasses in acute ischemic stroke: prediction of risk and short-term mortality." Atherosclerosis **210**(2): 548-554.

Zhai, G., A. Teumer, L. Stolk, J. R. Perry, L. Vandenput, A. D. Coviello, A. Koster, J. T. Bell, S. Bhasin, J. Eriksson, A. Eriksson, F. Ernst, L. Ferrucci, T. M. Frayling, D. Glass, E. Grundberg, R. Haring, A. K. Hedman, A. Hofman, D. P. Kiel, H. K. Kroemer, Y. Liu, K. L. Lunetta, M. Maggio, M. Lorentzon, M. Mangino, D. Melzer, I. Miljkovic, T. C. Mu, A. Nica, B. W. Penninx, R. S. Vasan, F. Rivadeneira, K. S. Small, N. Soranzo, A. G. Uitterlinden, H. Volzke, S. G. Wilson, L. Xi, W. V. Zhuang, T. B. Harris, J. M. Murabito, C. Ohlsson, A. Murray, F. H. de Jong, T. D. Spector and H. Wallaschofski (2011). "Eight common genetic variants associated with serum DHEAS levels suggest a key role in ageing mechanisms." PLoS Genet **7**(4): e1002025.

Zhang, Y., W. Zeng, S. Cheng, Z. Chen, J. Xue, Q. Wang, M. Ou and K. Cheng (2016). "Efficacy and Safety of Statins for Pulmonary Hypertension: A Meta-Analysis of Randomised Controlled Trials." Heart Lung Circ.

Zhao, Q. H., F. H. Peng, H. Wei, J. He, F. D. Chen, R. M. Di, X. Jiang, R. Jiang, Y. J. Chen, G. A. Heresi and Z. C. Jing (2012). "Serum high-density lipoprotein cholesterol levels as a prognostic indicator in patients with idiopathic pulmonary arterial hypertension." Am J Cardiol **110**(3): 433-439.

Zhao, Y., J. Peng, C. Lu, M. Hsin, M. Mura, L. Wu, L. Chu, R. Zamel, T. Machuca, T. Waddell, M. Liu, S. Keshavjee, J. Granton and M. de Perrot (2014). "Metabolomic heterogeneity of pulmonary arterial hypertension." PLoS One **9**(2): e88727.

Zhao, Y. D., L. Chu, K. Lin, E. Granton, L. Yin, J. Peng, M. Hsin, L. Wu, A. Yu, T. Waddell, S. Keshavjee, J. Granton and M. de Perrot (2015). "A Biochemical Approach to Understand the Pathogenesis of Advanced Pulmonary Arterial Hypertension: Metabolomic Profiles of Arginine, Sphingosine-1-Phosphate, and Heme of Human Lung." PLoS One **10**(8): e0134958.

Zhao, Y. D., H. Z. Yun, J. Peng, L. Yin, L. Chu, L. Wu, R. Michalek, M. Liu, S. Keshavjee, T. Waddell, J. Granton and M. de Perrot (2014). "De novo synthesize of bile acids in pulmonary arterial hypertension lung." Metabolomics **10**(6): 1169-1175.

Zharikov, S., K. Krotova, H. Hu, C. Baylis, R. J. Johnson, E. R. Block and J. Patel (2008). "Uric acid decreases NO production and increases arginase activity in cultured pulmonary artery endothelial cells." Am J Physiol Cell Physiol **295**(5): C1183-1190.

Zheng, Y., B. Yu, D. Alexander, T. A. Manolio, D. Aguilar, J. Coresh, G. Heiss, E. Boerwinkle and J. A. Nettleton (2013). "Associations between metabolomic compounds and incident heart failure among African Americans: the ARIC Study." Am J Epidemiol **178**(4): 534-542.

Appendix

Product	Company	Reference
Pure standard compounds for UPLC-MS		
2-Phenylglycine	Sigma Aldrich (Missouri, USA)	P25507-100G
L-Pipecolic acid	Sigma Aldrich (Missouri, USA)	P2519-100MG
Monobutylphthalate	Sigma Aldrich (Missouri, USA)	30751-100MG
L-(-)-Arabitol	Sigma Aldrich (Missouri, USA)	A3506-10MG
Hypotaurine	Sigma Aldrich (Missouri, USA)	H1384-10MG
N-isovalerylglycine	Sigma Aldrich (Missouri, USA)	43424-10MG
L-(+)-Arabinose	Sigma Aldrich (Missouri, USA)	A3256-10MG
5-Hydroxymethyluracil	Sigma Aldrich (Missouri, USA)	852589-1G-A
Hexadecanedioic acid	Sigma Aldrich (Missouri, USA)	177504-1G
4-Methylhippuric acid	Sigma Aldrich (Missouri, USA)	328022-1G
(R)-(+)-2-Pyrrolidone-5-carboxylic acid	Sigma Aldrich (Missouri, USA)	422614-1G
Uridine	Sigma Aldrich (Missouri, USA)	U3750-1G
L-Pyroglutamic acid	Sigma Aldrich (Missouri, USA)	83160-25G
L–(+)-α-Phenylglycine	Sigma Aldrich (Missouri, USA)	237647-25G
D-Xylulose	Sigma Aldrich (Missouri, USA)	X4625-25MG
2-pyrrolidinone	Sigma Aldrich (Missouri, USA)	240338-50G
3-Butyn-1-ol	Sigma Aldrich (Missouri, USA)	130850-5G
Cycloleucine (1-amino-1-cyclopentanecarboxylic acid)	Sigma Aldrich (Missouri, USA)	A48105-5G
2,6-Dihydroxypyridine hydrochloride	Sigma Aldrich (Missouri, USA)	D120006-5G
1,3-Dimethyluracil	Sigma Aldrich (Missouri, USA)	349801-5G
Nicotinuric acid	Sigma Aldrich (Missouri, USA)	N4751-5G
Dimethyl sulfone	Sigma Aldrich (Missouri, USA)	M81705-5G
lactose	Sigma Aldrich (Missouri, USA)	17814-1KG
Sucrose	Sigma Aldrich (Missouri, USA)	S7903-250G
1-Methyl-L-histidine	Sigma Aldrich (Missouri, USA)	67520-50MG
tyrosine	Sigma Aldrich (Missouri, USA)	T3754-50G
Trimethylamine N-oxide	Sigma Aldrich (Missouri, USA)	317594-1G
Allantoin	Sigma Aldrich (Missouri, USA)	05670-25G
arginine	Sigma Aldrich (Missouri, USA)	A5006-100G
3-Methyl-L-histidine	Sigma Aldrich (Missouri, USA)	M9005-100MG
Kynurenic acid	Sigma Aldrich (Missouri, USA)	K3375-250MG
1,7-Dimethyluric acid	Sigma Aldrich (Missouri, USA)	40407-250MG
(R)-Pantetheine	Sigma Aldrich (Missouri, USA)	16702-10MG
DL-3-Ureidoisobutyric acid	Sigma Aldrich (Missouri, USA)	74005-10MG
N-Acetyl-D-lactosamine	Sigma Aldrich (Missouri, USA)	A7791-5MG
Biliverdin hydrochloride	Sigma Aldrich (Missouri, USA)	30891-10MG
1,3-Dimethyluric acid	Sigma Aldrich (Missouri, USA)	D2889-100MG
D-(−)-Ribose	Sigma Aldrich (Missouri, USA)	R7500-10MG
D-(+)-Xylose	Sigma Aldrich (Missouri, USA)	X1500-10MG
3-hydroxybutyric acid	Sigma Aldrich (Missouri, USA)	166898-1G
N-Acetyl-L-glutamic acid	Sigma Aldrich (Missouri, USA)	855642-25G
IsoValeraldehyde	Sigma Aldrich (Missouri, USA)	146455-25ML
paraxanthine	Sigma Aldrich (Missouri, USA)	IMPC-051-03-1ML
N-Acetyl-L-methionine	Sigma Aldrich (Missouri, USA)	01310-5G
Trigonelline hydrochloride	Sigma Aldrich (Missouri, USA)	T5509-1G
NG,NG-Dimethylarginine dihydrochloride	Sigma Aldrich (Missouri, USA)	D4268-10MG
L-Methionine sulfone	Sigma Aldrich (Missouri, USA)	M0876-1G
urea	Sigma Aldrich (Missouri, USA)	U5378-100G
6-Biopterin	Sigma Aldrich (Missouri, USA)	B2517-5MG
Xylitol	Sigma Aldrich (Missouri, USA)	X3375-10MG
N-ethylmaleimide	Sigma Aldrich (Missouri, USA)	E3876-5G
Decanoylcarnitine	Sigma Aldrich (Missouri, USA)	50637-10MG
Hexanoylcarnitine	Sigma Aldrich (Missouri, USA)	07439-10MG
palmitoylcarnitine	Sigma Aldrich (Missouri, USA)	61251-10MG
octanoylcarnitine	Sigma Aldrich (Missouri, USA)	50892-10MG

Product	Company	Reference
myristoylcarnitine	Sigma Aldrich (Missouri, USA)	61367-10MG
L-Homocitrulline	Santa Cruz Biotechnology (Texas, USA)	1190-49-4-100MG
phenylacetyl-L-glutamine	Santa Cruz Biotechnology (Texas, USA)	sc-212551-50MG
1-methyladenosine	Santa Cruz Biotechnology (Texas, USA)	sc-216121-250MG
DL-Methionine sulfoxide	Santa Cruz Biotechnology (Texas, USA)	sc-257398-5G
homoarginine	Santa Cruz Biotechnology (Texas, USA)	sc-479071-5G
Acetylcarnitine (Chloride version)	Santa Cruz Biotechnology (Texas, USA)	sc-203495-100MG
N4-Acetylcytidine	Santa Cruz Biotechnology (Texas, USA)	sc-222023-25G
3-Hydroxybutyrylcarnitine Hydrochloride	Santa Cruz Biotechnology (Texas, USA)	875668-57-8-10MG
Acigosa	Enamine (New Jersey, USA)	FCH2067597-250MG
Desmosine and Isodesmosine	Elastin Products Company (Missouri, USA)	MD687-5MG
Pseudouridine	Berry and Associates (Michigan, USA)	PYA 11080-10MG
N2,N2-dimethylguanosine	Berry and Associates (Michigan, USA)	PR 3702-10MG
oleoylcarnitine	Avanti Polar Lipid (Alabama, USA)	870852-5MG
1-Methylhypoxanthine	Ambinter (Orleans, France)	Amb21864246-75MG
Hydantoin-5-propionic acid	Ambinter (Orleans, France)	Amb1063501-100MG
methylimidazoleacetate	Ambinter (Orleans, France)	Amb19944574-25G
Enzyme-linked immunosorbent assay		
Human Angiogenin Quantikine ELISA Kit	R&D systems (Abingdon, UK)	DAN00
Antibodies for immunohistochemistry		
Anti-angiogenin antibody	Sigma Aldrich (Missouri, USA)	MABC166
Anti 1-methyladenosine antibody	MBL International Corporation (Massachusetts, USA)	D345-3
Anti-pseudouridine antibody	MBL International Corporation (Massachusetts, USA)	D347-3
Histostar(Ms + Rb) (for human tissue)	MBL International Corporation (Massachusetts, USA)	8460
DAB substrate solution	MBL International Corporation (Massachusetts, USA)	8469
Targeted fluorometric assays		
Amplite™ Fluorimetric Oxaloacetate Assay Kit	Stratech Scientific Limited (Suffolk, UK), AAT Bioquest (Sunnyvale, CA, USA)	13841
The PicoProbe Acetyl CoA Assay Kit (fluorometric)	Stratech Scientific Limited (Suffolk, UK), Abcam (Cambridge, UK)	ab87546

Appendix Table 2.1 – Products purchased and reference codes. Products purchased for analysis of pure standard compounds by ultra-performance liquid chromatography mass spectrometry (UPLC-MS), Enzyme-linked immunosorbent assay experiment, immunohistochemistry and targeted fluorometric assays are shown with companies the products were purchased from and reference codes.

Peak (^{1}H shift, ppm)	Peak range (^{1}H shift, ppm)	Peaks correlated by STOCSY	2D NMR Peaks (^{13}C-^{1}H shift, ppm)	Identity
Increased in PAH versus healthy and disease controls				
2.143	2.1409-2.1442			Unknown
3.039	3.03685-3.04015	3.027-3.047, 4.04-4.05	32-35	Creatinine
3.348	3.34485-3.35145	3.33.32-3.5		Unknown
Increased in PAH versus healthy controls				
3.371	3.36355-3.37895	3.367-3.377		Unknown
2.861	2.8548-2.86635	2.853-2.865		Unknown
2.366	2.32955-2.40215	2.35-2.36		Unknown
3.581	3.57695-3.5841	3.56-3.58, 3.63-3.67, 3.787-3.81	65-69	Glycerol
3.333	3.32945-3.33605	3.328-3.336		Unknown
2.155	2.15135-2.15905	2.146-2.166, 5.08-5.10, 7.121-7.166, 7.34-7.38	24-27, 102-104, 119-121, 125-128	Paracetamol
2.061	2.05675-2.065	2.311-2.374, 2.044-2.082	Unclear	Glutamine related
3.304	3.30195-3.30635	3.302-3.309		Unknown
1.4	1.3973-1.4028	1.38-1.43		Unknown
3.567	3.5643-3.5687	3.56-3.58, 3.63-3.67, 3.787-3.81	65-69	Glycerol
2.65	2.64745-2.65295	2.5-2.55, 2.64-2.69	47-51	Citric Acid
2.188	2.1783-2.19755	0.78-0.94, 1.2-1.3, 1.4-1.6, 1.93-2, 2.17-2.2, 5.28-5.3		VLDL-4 - Phospholipids
6.926	6.92425-6.9281	6.91-6.93		Unknown
7.152	7.1448-7.15855	2.146-2.166, 5.08-5.10, 7.121-7.166, 7.34-7.38	24-27, 102-104, 119-121, 125-128	Paracetamol
2.052	2.04905-2.054	2.01-2.06		VLDL-1 - Phospholipids
7.668	7.6651-7.67005	7.6-7.68	75-77/103-105/128-130/148-150	Unknown
3.678	3.6743-3.6809	3.215-3.276, 3.373-3.578, 3.698-3.917, 5.2-5.4		Background related to glucose
6.968	6.9655-6.9699	6.96-6.97		Unknown
3.785	3.78265-3.7865	1.45-1.47, 2.07-2.16, 2.4-2.5, 3.59-3.6		Unknown
3.639	3.63745-3.64075	3.557-3.59, 3.65-3.69		Glycerol
2.32	2.31635-2.32405	1.16-1.2, 2.261-2.338, 2.369-2.42, 3.42-3.44, 4.107-4.186	47-52	3-hydroxybutyric acid
4.93	4.92885-4.93105	4.2-4.9		Unknown
5.086	5.0834-5.08945	2.146-2.166, 5.08-5.10, 7.121-7.166, 7.34-7.38	24-27, 102-104, 119-121, 125-128	Paracetamol
6.979	6.97265-6.98475	6.97-6.99		Unknown
7.734	7.7289-7.73825	7.735-7.74		Unknown
2.31	2.307-2.31305	1.16-1.2, 2.261-2.338, 2.369-2.42, 3.42-3.44, 4.107-4.186	47-52	3-hydroxybutyric acid
3.935	3.93115-3.93885	3.9-3.99		Unknown
5.757	5.74065-5.77365	5.6-5.82		Lipid region
3.62	3.61105-3.62865	2.146-2.166, 5.08-5.10, 7.121-7.166, 7.34-7.38	24-27, 102-104, 119-121, 125-128	Paracetamol
5.096	5.09165-5.101	2.146-2.166, 5.08-5.10, 7.121-7.166, 7.34-7.38	24-27, 102-104, 119-121, 125-128	Paracetamol

Peak (^{1}H shift, ppm)	Peak range (^{1}H shift, ppm)	Peaks correlated by STOCSY	2D NMR Peaks (^{13}C-^{1}H shift, ppm)	Identity
3.282	3.27885-3.2849	3.27-3.3		Unknown
4.046 *	4.04115-4.04995	3.027-3.047, 4.04-4.05	59-61	Creatinine
7.352	7.33785-7.36535	2.146-2.166, 5.08-5.10, 7.121-7.166, 7.34-7.38	24-27, 102-104, 119-121, 125-128	Paracetamol
2.104	2.10185-2.10515	1.8-1.96, 2.07-2.16, 2.38-2.48, 6.8-6.9		Unknown
2.087	2.0738-2.09965	2.084-2.095		Unknown
5.728	5.7192-5.73735	5.6-5.82		Lipid region
1.77	1.76635-1.7735	1.765-1.785		Unknown
2.41	2.40875-2.4115	1.16-1.2, 2.261-2.338, 2.369-2.42, 3.42-3.44, 4.107-4.186	47-52	3-hydroxybutyric acid
5.834	5.8281-5.8391	5.829-5.4		Unknown
Decreased in PAH versus healthy and disease controls				
0.942 *	0.89735-0.9859	0.92-1.059, 1.46-1.49	18-23	Valine
2.736	2.68155-2.7899	1.47-1.64, 1.89-2.29, 2.68-2.83, 5.23-5.37		Lipid region
3.178 *	3.1749-3.1815	3.16-3.19		Unknown
7.054	7.0502-7.05845	7.04-7.07, 7.76-7.79	141-144	1-methylhistamine
4.3	4.2782-4.32275	0.78-0.88, 1.22-1.3, 3.17-3.2		HDL3b - Phospholipids
2.442	2.44065-2.44285	2.1-2.15, 2.408-2.481, 3.74-3.8	31-37	Glutamine
2.455	2.4533-2.45605	2.1-2.15, 2.408-2.481, 3.74-3.8	31-37	Glutamine
2.466	2.46485-2.46705	2.1-2.15, 2.408-2.481, 3.74-3.8	31-37	Glutamine
Decreased in PAH versus healthy controls				
3.199	3.1859-3.21175	0.73-0.83, 3.173-3.212		HDL3a - Cholesterol
0.794	0.74555-0.8418	0.73-0.89, 3.18-3.215		HDL - Phospholipids
5.264	5.2396-5.28745	0.78-0.88, 1.22-1.3, 1.48-1.5, 5.241-5.36		HDL3a - Phospholipids
1.194	1.1916-1.196	0.73-0.84, 1.175-1.23		Lipid region
3.23	3.2211-3.2398	3.215-3.276, 3.373-3.578, 3.698-3.917, 5.2-5.4		Background related to glucose
1.448	1.43305-1.4622	1.445-1.451		Unknown
1.214	1.19985-1.22735	0.73-0.84, 1.175-1.23		HDL3a - Apo-A1
1.03	1.0255-1.03485	0.92-1.059, 1.46-1.49	18-23	Valine
1.047	1.03705-1.0563	1.045-1.05	18-23	Valine
1.906	1.88845-1.9242	1.858-1.928, 2.06-2.18, 2.42-2.48		Unknown
1.473	1.47155-1.4743	1.456-1.489		Unknown
1.182	1.1795-1.1839	0.78-0.88, 1.22-1.3, 1.48-1.5, 5.241-5.36		Lipid region
5.215	5.20715-5.22365	3.215-3.276, 3.373-3.578, 3.698-3.917, 5.2-5.4		Lipid region
1.004	0.98645-1.02165	0.92-1.059, 1.46-1.49	18-23	Valine
1.719	1.6954-1.7427	1.69-1.73, 3.008-3.028	25-32	Lysine
1.502	1.48365-1.5205	0.78-0.88, 1.22-1.3, 1.48-1.5, 5.241-5.36		Lipid region

Peak (^{1}H shift, ppm)	Peak range (^{1}H shift, ppm)	Peaks correlated by STOCSY	2D NMR Peaks (^{13}C-^{1}H shift, ppm)	Identity
1.951	1.93685-1.966	0.78-0.88, 1.22-1.3, 1.48-1.5, 5.241-5.36		Lipid region
3.02*	3.00495-3.0341	1.7-1.73, 3.008-3.028	41-43	Lysine
1.882	1.8769-1.8868	1.86-1.9, 1.701-1.752, 3-3.04	31-33	Lysine
3.25	3.24915-3.25135	3.21-3.27, 3.38-3.55, 3.69-3.9, 5.2-5.7		Background related to glucose
1.691	1.68825-1.6932	1.69-1.73, 3.008-3.028	25-32	Lysine

Appendix Table 3.1 – Identities of NMR peaks distinguishing PAH patients from healthy and disease controls. 46/71 NMR peaks which discriminate PAH from healthy controls were identified based on the NMR peak region, associated peaks from statistical total correlation spectroscopy (STOCSY) analysis, 2D 13C-1H NMR chemical shift and identities based on reference to known databases and assessment of pure standard compounds. *indicates peaks which are significantly different between PAH and CTEPH patients ($p<0.05$). HDL, high density lipoprotein; VLDL, very low density lipoprotein; Apo-A1, apolipoprotein A1.

			Discovery		Validation	
Peak, Retention Time-mass/charge (m/z) or neutral mass (n)	Platform	Identity	Hazard Ratio	Sig	Hazard Ratio	Sig
Higher value indicates mortality. Independent of established prognostic markers						
1.54_424.3423m/z	Lpos	acylcarnitine (18:2)	2.53 (1.7 - 3.77)	5.34E-06	1.46 (1.13 - 1.89)	3.39E-03
1.25_372.3112m/z	Lpos	myristoylcarnitine~	1.94 (1.29 - 2.91)	1.43E-03	1.55 (1.18 - 2.03)	1.58E-03
1.72_400.3427m/z	Lpos	palmitoylcarnitine~	2.27 (1.45 - 3.53)	3.02E-04	1.58 (1.18 - 2.13)	2.30E-03
0.55_429.3078n	Lpos	Unknown	2.4 (1.49 - 3.86)	3.22E-04	1.53 (1.16 - 2.01)	2.61E-03
0.50_461.2071m/z Δ	Lneg	Unknown	2.17 (1.3 - 3.62)	3.05E-03	1.35 (1.01 - 1.8)	4.37E-02
0.50_569.2992m/z	Lneg	Unknown	2.16 (1.33 - 3.53)	2.02E-03	1.46 (1.1 - 1.93)	8.90E-03
1.26_397.3102m/z*	Lpos	Unknown	2.13 (1.54 - 2.94)	4.22E-06	1.61 (1.15 - 2.25)	6.05E-03
1.99_452.3727m/z	Lpos	Unknown	2.04 (1.47 - 2.82)	1.62E-05	1.41 (1.11 - 1.77)	4.28E-03
1.16_396.3090m/z	Lpos	Unknown	1.96 (1.39 - 2.76)	1.38E-04	1.65 (1.21 - 2.26)	1.49E-03
0.72_456.3318m/z	Lpos	Unknown	1.94 (1.37 - 2.76)	2.13E-04	1.68 (1.23 - 2.28)	1.03E-03
0.66_611.3843m/z	Lneg	Unknown	1.94 (1.23 - 3.04)	4.03E-03	1.67 (1.15 - 2.42)	6.58E-03
1.00_484.3612m/z	Lpos	Unknown	1.92 (1.25 - 2.94)	2.71E-03	1.68 (1.19 - 2.37)	3.33E-03
1.39_318.1330m/z	Hilic	Unknown	1.92 (1.12 - 3.28)	1.68E-02	1.76 (1.23 - 2.52)	2.08E-03
0.84_458.3469m/z	Lpos	Unknown	1.91 (1.25 - 2.91)	2.70E-03	2.19 (1.34 - 3.56)	1.72E-03
1.56_448.3422m/z	Lpos	Unknown	1.77 (1.26 - 2.48)	9.73E-04	1.42 (1.19 - 1.7)	1.09E-04
0.51_428.2930m/z	Lpos	Unknown	1.77 (1.17 - 2.7)	7.39E-03	1.47 (1.12 - 1.95)	6.23E-03
0.52_501.2890n	Lpos	Unknown	1.75 (1.18 - 2.6)	5.61E-03	1.56 (1.07 - 2.26)	1.99E-02
2.35_454.3888m/z	Lpos	Unknown	1.73 (1.39 - 2.15)	9.09E-07	1.35 (1.09 - 1.68)	6.56E-03
0.49_626.2446m/z	Lneg	Unknown	1.7 (1.18 - 2.44)	4.07E-03	1.57 (1.2 - 2.04)	9.54E-04
1.07_347.2848n	Lpos	Unknown	1.7 (1.14 - 2.52)	8.77E-03	1.44 (1.07 - 1.94)	1.53E-02
1.11_217.0720m/z Δ	Hilic	Unknown	1.7 (1.02 - 2.84)	4.16E-02	1.76 (1.25 - 2.48)	1.13E-03
2.88_340.2483m/z Δ	Hilic	Unknown	1.67 (1.18 - 2.36)	3.85E-03	1.98 (1.19 - 3.29)	8.81E-03
1.92_476.3715m/z*	Lpos	Unknown	1.65 (1.23 - 2.21)	8.85E-04	1.48 (1.17 - 1.86)	9.40E-04
0.36_427.1725m/z	Lneg	Unknown	1.65 (1.12 - 2.44)	1.11E-02	1.75 (1.23 - 2.48)	1.65E-03
2.37_326.3028m/z	Lpos	Unknown	1.63 (1.09 - 2.43)	1.82E-02	1.44 (1.07 - 1.95)	1.71E-02
1.03_394.2943m/z	Lpos	Unknown	1.58 (1.16 - 2.14)	3.41E-03	1.28 (1.02 - 1.61)	3.28E-02
1.72_450.3570m/z	Lpos	Unknown	1.55 (1.2 - 2)	7.27E-04	1.39 (1.13 - 1.71)	2.06E-03
1.09_438.3197m/z Δ	Lpos	Unknown	1.5 (1.06 - 2.13)	2.16E-02	1.34 (1.03 - 1.74)	2.94E-02
1.54_194.1053m/z	Hilic	Unknown	1.45 (1.03 - 2.04)	3.26E-02	1.6 (1.22 - 2.11)	7.01E-04
6.65_747.8529m/z	Lpos	Unknown	1.36 (1.08 - 1.7)	8.07E-03	1.82 (1.22 - 2.72)	3.20E-03
Lower value indicates mortality. Independent of established prognostic markers						
4.65_751.5156n	Lpos	PC(14:0/20:5)	0.66 (0.49 - 0.89)	6.14E-03	0.59 (0.45 - 0.78)	2.34E-04
4.95_777.5321n	Lpos	PC(14:0/22:6)	0.65 (0.44 - 0.96)	3.02E-02	0.56 (0.41 - 0.77)	3.92E-04
3.30_1157.6652m/z	Hilic	Unknown	0.44 (0.24 - 0.81)	8.06E-03	0.63 (0.45 - 0.88)	6.78E-03
3.30_1137.6939m/z	Hilic	Unknown	0.47 (0.26 - 0.83)	9.25E-03	0.65 (0.43 - 0.98)	3.83E-02
4.91_828.5534m/z	Lpos	Unknown	0.49 (0.3 - 0.81)	5.80E-03	0.74 (0.57 - 0.98)	3.38E-02
6.22_866.5907m/z	Lneg	Unknown	0.53 (0.32 - 0.87)	1.32E-02	0.7 (0.54 - 0.92)	1.08E-02
3.32_1089.6842m/z	Hilic	Unknown	0.54 (0.32 - 0.91)	2.15E-02	0.59 (0.39 - 0.92)	1.84E-02
3.30_1113.6830m/z	Hilic	Unknown	0.57 (0.37 - 0.88)	1.08E-02	0.66 (0.45 - 0.97)	3.30E-02
1.91_596.3708m/z	Lpos	Unknown	0.57 (0.4 - 0.82)	2.02E-03	0.67 (0.49 - 0.93)	1.48E-02
1.35_501.3245n	Lpos	Unknown	0.58 (0.36 - 0.94)	2.81E-02	0.72 (0.53 - 0.97)	3.11E-02

			Discovery		Validation	
Peak, Retention Time-mass/charge (m/z) or neutral mass (n)	Platform	Identity	Hazard Ratio	Sig	Hazard Ratio	Sig
6.22_853.5840n Δ	Lneg	Unknown	0.58 (0.36 - 0.95)	2.99E-02	0.59 (0.43 - 0.83)	2.16E-03
9.52_881.6827m/z	Lpos	Unknown	0.6 (0.43 - 0.82)	1.61E-03	0.65 (0.44 - 0.96)	2.95E-02
6.89_480.3017m/z Δ	Lneg	Unknown	0.61 (0.38 - 0.96)	3.30E-02	0.76 (0.59 - 0.98)	3.71E-02
9.46_848.6724n	Lpos	Unknown	0.61 (0.44 - 0.84)	2.29E-03	0.45 (0.29 - 0.69)	2.45E-04
5.75_946.5393m/z Δ	Lneg	Unknown	0.62 (0.4 - 0.97)	3.53E-02	0.56 (0.42 - 0.76)	1.88E-04
8.68_661.5535m/z*	Lpos	Unknown	0.63 (0.44 - 0.88)	7.07E-03	0.59 (0.41 - 0.83)	2.83E-03
3.38_517.3198n* Δ	Hilic	Unknown	0.64 (0.41 - 1)	4.75E-02	0.61 (0.4 - 0.92)	1.81E-02
5.10_874.5109m/z Δ	Lneg	Unknown	0.64 (0.42 - 0.97)	3.47E-02	0.54 (0.38 - 0.78)	9.82E-04
4.44_702.5131m/z	Lpos	Unknown	0.64 (0.44 - 0.93)	2.04E-02	0.46 (0.3 - 0.71)	4.40E-04
9.28_937.6750m/z*	Lpos	Unknown	0.66 (0.5 - 0.88)	4.23E-03	0.47 (0.33 - 0.66)	1.73E-05
9.88_654.3897m/z*	Lneg	Unknown	0.68 (0.48 - 0.97)	3.15E-02	0.63 (0.47 - 0.86)	3.09E-03
4.96_803.5599n	Lpos	Unknown	0.71 (0.53 - 0.96)	2.60E-02	0.59 (0.42 - 0.83)	2.57E-03
Higher value indicates mortality						
2.77_398.3264m/z	Hilic	palmitoylcarnitine~	1.96 (1.27 - 3.05)	2.59E-03	1.42 (1.02 - 1.97)	3.54E-02
1.27_422.3252m/z	Lpos	Unknown	2 (1.27 - 3.15)	2.61E-03	1.3 (1.02 - 1.65)	3.62E-02
0.56_595.0086n	Lpos	Unknown	1.82 (1.19 - 2.78)	5.90E-03	1.51 (1.12 - 2.04)	7.19E-03
3.05_330.2271m/z	Hilic	Unknown	1.76 (1.13 - 2.74)	1.19E-02	1.49 (1.07 - 2.08)	1.87E-02
0.34_769.2520m/z	Lneg	Unknown	1.75 (1.08 - 2.84)	2.43E-02	1.62 (1.11 - 2.36)	1.20E-02
2.24_428.3735m/z	Lpos	Unknown	1.74 (1.28 - 2.37)	3.70E-04	1.45 (1.09 - 1.92)	1.06E-02
3.04_384.2743m/z Δ	Hilic	Unknown	1.73 (1.07 - 2.8)	2.45E-02	1.45 (1.04 - 2.03)	3.05E-02
0.70_330.2637m/z	Lpos	Unknown	1.71 (1.08 - 2.71)	2.21E-02	1.48 (1.05 - 2.07)	2.38E-02
0.89_356.2787m/z	Lpos	Unknown	1.68 (1.1 - 2.55)	1.57E-02	1.48 (1.08 - 2.02)	1.45E-02
0.50_681.3257m/z	Lneg	Unknown	1.67 (1.11 - 2.5)	1.37E-02	1.57 (1.07 - 2.28)	2.00E-02
0.89_326.2463n Δ	Lpos	Unknown	1.65 (1.06 - 2.56)	2.69E-02	1.57 (1.1 - 2.25)	1.28E-02
3.47_276.1815m/z	Hilic	Unknown	1.64 (1.04 - 2.58)	3.51E-02	1.75 (1.21 - 2.53)	2.83E-03
0.46_627.3708m/z	Lneg	Unknown	1.62 (1.08 - 2.43)	1.94E-02	1.25 (1.01 - 1.55)	3.99E-02
2.87_366.2647m/z Δ	Hilic	Unknown	1.61 (1.13 - 2.3)	9.16E-03	1.52 (1.07 - 2.15)	1.82E-02
0.97_388.3055m/z	Lpos	Unknown	1.59 (1.08 - 2.32)	1.73E-02	1.4 (1.04 - 1.87)	2.55E-02
2.79_396.3106m/z Δ	Hilic	Unknown	1.53 (1 - 2.33)	4.96E-02	1.43 (1.01 - 2)	4.17E-02
1.27_302.1275m/z	Hilic	Unknown	1.5 (1.01 - 2.23)	4.27E-02	1.54 (1.07 - 2.22)	2.16E-02
4.18_387.3218m/z*	Lneg	Unknown	1.49 (1 - 2.21)	5.00E-02	1.36 (1.02 - 1.82)	3.63E-02
0.57_642.3104n	Lneg	Unknown	1.47 (1.08 - 2)	1.57E-02	1.37 (1.03 - 1.83)	2.86E-02
0.71_284.1278m/z	Lpos	Unknown	1.45 (1.06 - 1.98)	2.07E-02	1.45 (1.06 - 1.99)	2.03E-02
2.90_327.2418n	Hilic	Unknown	1.43 (1.11 - 1.86)	6.52E-03	1.7 (1.18 - 2.46)	4.68E-03
6.66_709.5122m/z	Lpos	Unknown	1.43 (1.03 - 2)	3.34E-02	1.38 (1.03 - 1.85)	3.30E-02
1.16_209.0804n Δ	Lpos	Unknown	1.42 (1 - 2.03)	4.85E-02	1.35 (1.03 - 1.79)	3.26E-02
1.17_283.1084m/z Δ	Lpos	Unknown	1.4 (1.04 - 1.89)	2.57E-02	1.3 (1 - 1.69)	4.89E-02
1.17_299.1398m/z Δ	Lpos	Unknown	1.4 (1.01 - 1.96)	4.63E-02	1.31 (1.03 - 1.68)	2.96E-02
1.17_191.0729m/z Δ	Lpos	Unknown	1.39 (1.01 - 1.91)	4.23E-02	1.32 (1.01 - 1.72)	4.33E-02
1.39_596.2267m/z	Hilic	Unknown	1.39 (1.01 - 1.91)	4.55E-02	1.68 (1.13 - 2.51)	1.08E-02
1.17_167.0742m/z Δ	Lpos	Unknown	1.38 (1.01 - 1.9)	4.64E-02	1.34 (1.02 - 1.76)	3.42E-02
5.19_536.5038m/z	Lpos	Unknown	1.35 (1.06 - 1.72)	1.36E-02	1.6 (1.12 - 2.29)	9.87E-03

			Discovery		Validation	
Peak, Retention Time-mass/charge (m/z) or neutral mass (n)	Platform	Identity	Hazard Ratio	Sig	Hazard Ratio	Sig
7.18_747.6138n	Lpos	Unknown	1.27 (1 - 1.61)	4.81E-02	1.49 (1.06 - 2.09)	2.02E-02
Lower value indicates mortality						
9.54_824.6886n	Lpos	TG(50:5)	0.76 (0.58 - 0.99)	4.18E-02	0.34 (0.21 - 0.53)	3.16E-06
9.28_921.7065m/z	Lpos	Unknown	0.49 (0.29 - 0.84)	8.78E-03	0.47 (0.34 - 0.65)	7.10E-06
9.24_896.6939m/z*	Lpos	Unknown	0.54 (0.33 - 0.89)	1.55E-02	0.49 (0.35 - 0.69)	5.93E-05
9.09_815.6763m/z*	Lpos	Unknown	0.56 (0.36 - 0.87)	1.08E-02	0.71 (0.55 - 0.93)	1.33E-02
6.87_1840.1522m/z	Lneg	Unknown	0.57 (0.36 - 0.88)	1.25E-02	0.56 (0.38 - 0.82)	2.90E-03
6.09_607.5083m/z Δ	Lpos	Unknown	0.57 (0.36 - 0.9)	1.51E-02	0.81 (0.66 - 0.99)	4.34E-02
9.18_940.7126m/z*	Lpos	Unknown	0.57 (0.39 - 0.86)	6.63E-03	0.65 (0.49 - 0.88)	5.11E-03
5.33_1536.0987m/z	Lpos	Unknown	0.58 (0.35 - 0.97)	3.68E-02	0.61 (0.44 - 0.85)	3.31E-03
3.32_647.4386m/z	Hilic	Unknown	0.59 (0.37 - 0.95)	2.85E-02	0.69 (0.48 - 0.99)	4.26E-02
9.66_797.9016m/z*	Lpos	Unknown	0.59 (0.37 - 0.95)	2.97E-02	0.57 (0.39 - 0.84)	4.95E-03
10.11_407.2334m/z*	Lneg	Unknown	0.59 (0.38 - 0.91)	1.78E-02	0.65 (0.51 - 0.83)	6.41E-04
9.43_890.7719m/z*	Lpos	Unknown	0.59 (0.4 - 0.86)	7.07E-03	0.49 (0.33 - 0.73)	4.64E-04
10.36_526.3151m/z	Lneg	Unknown	0.6 (0.38 - 0.93)	2.29E-02	0.54 (0.38 - 0.77)	6.53E-04
10.15_612.3616m/z Δ	Lneg	Unknown	0.6 (0.39 - 0.94)	2.72E-02	0.54 (0.4 - 0.72)	3.91E-05
4.76_852.5556m/z Δ	Lpos	Unknown	0.61 (0.37 - 0.98)	4.26E-02	0.7 (0.5 - 0.96)	2.72E-02
6.02_1616.1588m/z	Lpos	Unknown	0.61 (0.38 - 0.96)	3.35E-02	0.49 (0.33 - 0.72)	2.70E-04
5.35_824.5481m/z* Δ	Lneg	Unknown	0.62 (0.39 - 0.99)	4.68E-02	0.56 (0.41 - 0.77)	3.91E-04
9.94_559.2885m/z* Δ	Lneg	Unknown	0.62 (0.39 - 0.99)	4.74E-02	0.48 (0.35 - 0.66)	6.69E-06
9.49_913.6735m/z	Lpos	Unknown	0.62 (0.42 - 0.92)	1.87E-02	0.48 (0.34 - 0.67)	2.78E-05
9.15_871.7277m/z*	Lpos	Unknown	0.62 (0.44 - 0.86)	4.66E-03	0.65 (0.48 - 0.88)	5.78E-03
9.53_883.7712m/z*	Lpos	Unknown	0.63 (0.42 - 0.95)	2.80E-02	0.56 (0.42 - 0.74)	5.23E-05
9.20_896.7181m/z*	Lpos	Unknown	0.63 (0.44 - 0.91)	1.30E-02	0.55 (0.4 - 0.77)	5.17E-04
2.98_493.3344m/z	Lneg	Unknown	0.64 (0.41 - 1.00)	4.80E-02	0.66 (0.47 - 0.91)	1.21E-02
2.97_591.3148m/z	Lneg	Unknown	0.64 (0.41 - 1.00)	4.76E-02	0.68 (0.51 - 0.9)	7.73E-03
6.87_856.6074m/z Δ	Lneg	Unknown	0.64 (0.42 - 0.98)	4.22E-02	0.54 (0.37 - 0.78)	1.05E-03
9.42_924.7143n* Δ	Lpos	Unknown	0.64 (0.43 - 0.96)	3.05E-02	0.58 (0.41 - 0.83)	2.51E-03
9.12_961.6735m/z*	Lpos	Unknown	0.64 (0.43 - 0.97)	3.38E-02	0.58 (0.41 - 0.83)	2.88E-03
9.65_909.7765m/z*	Lpos	Unknown	0.64 (0.44 - 0.92)	1.51E-02	0.65 (0.46 - 0.91)	1.14E-02
9.43_591.4996m/z*	Lpos	Unknown	0.64 (0.44 - 0.92)	1.66E-02	0.55 (0.39 - 0.79)	9.89E-04
9.27_855.7392m/z*	Lpos	Unknown	0.64 (0.44 - 0.93)	1.76E-02	0.64 (0.43 - 0.95)	2.82E-02
9.52_892.7265m/z*	Lpos	Unknown	0.64 (0.45 - 0.93)	1.85E-02	0.48 (0.34 - 0.68)	3.15E-05
9.15_896.7087m/z*	Lpos	Unknown	0.65 (0.44 - 0.94)	2.19E-02	0.55 (0.4 - 0.75)	1.90E-04
9.19_894.7164m/z*	Lpos	Unknown	0.65 (0.45 - 0.92)	1.51E-02	0.59 (0.41 - 0.85)	4.65E-03
9.15_911.7215m/z*	Lpos	Unknown	0.65 (0.47 - 0.9)	9.61E-03	0.43 (0.29 - 0.63)	1.30E-05
9.40_800.6798m/z*	Lpos	Unknown	0.66 (0.45 - 0.96)	2.94E-02	0.46 (0.3 - 0.71)	4.92E-04
4.50_802.5472m/z	Lpos	Unknown	0.66 (0.45 - 0.97)	3.31E-02	0.69 (0.5 - 0.94)	2.10E-02
9.31_890.7027m/z*	Lpos	Unknown	0.66 (0.46 - 0.94)	2.05E-02	0.5 (0.35 - 0.7)	5.70E-05
9.41_517.4254m/z*	Lpos	Unknown	0.67 (0.45 - 1.00)	4.76E-02	0.52 (0.33 - 0.82)	4.47E-03
8.89_912.7294m/z Δ	Lpos	Unknown	0.67 (0.46 - 0.97)	3.28E-02	0.73 (0.54 - 0.98)	3.90E-02
9.69_809.5145m/z*	Lneg	Unknown	0.67 (0.47 - 0.95)	2.43E-02	0.53 (0.39 - 0.73)	7.04E-05

			Discovery		Validation	
Peak, Retention Time-mass/charge (m/z) or neutral mass (n)	Platform	Identity	Hazard Ratio	Sig	Hazard Ratio	Sig
7.39_667.5347m/z* Δ	Lpos	Unknown	0.67 (0.49 - 0.92)	1.25E-02	0.66 (0.45 - 0.97)	3.43E-02
9.24_863.6698m/z*	Lpos	Unknown	0.67 (0.51 - 0.89)	5.95E-03	0.56 (0.42 - 0.76)	1.26E-04
9.38_871.6847m/z	Lpos	Unknown	0.68 (0.46 - 1.00)	4.72E-02	0.44 (0.32 - 0.62)	1.44E-06
9.54_243.2103m/z	Lpos	Unknown	0.68 (0.49 - 0.93)	1.55E-02	0.43 (0.28 - 0.65)	5.26E-05
9.37_887.6580m/z*	Lpos	Unknown	0.68 (0.49 - 0.93)	1.62E-02	0.45 (0.31 - 0.64)	1.65E-05
9.14_888.7574m/z*	Lpos	Unknown	0.68 (0.5 - 0.92)	1.13E-02	0.58 (0.41 - 0.82)	1.76E-03
8.91_694.6352m/z Δ	Lneg	Unknown	0.69 (0.48 - 1.00)	4.87E-02	0.64 (0.46 - 0.89)	8.40E-03
4.99_765.5354n	Lpos	Unknown	0.69 (0.51 - 0.93)	1.43E-02	0.74 (0.58 - 0.93)	1.03E-02
8.57_711.5682m/z*	Lpos	Unknown	0.69 (0.51 - 0.95)	2.10E-02	0.58 (0.39 - 0.86)	6.03E-03
5.33_1042.4532m/z	Lpos	Unknown	0.69 (0.52 - 0.91)	8.72E-03	0.62 (0.44 - 0.87)	5.58E-03
6.85_549.4883m/z	Lpos	Unknown	0.7 (0.49 - 0.99)	4.18E-02	0.51 (0.32 - 0.81)	4.03E-03
9.39_519.4413m/z*	Lpos	Unknown	0.7 (0.5 - 0.99)	4.21E-02	0.46 (0.29 - 0.71)	5.21E-04
8.57_664.5808n* Δ	Lpos	Unknown	0.71 (0.53 - 0.96)	2.78E-02	0.76 (0.58 - 0.98)	3.54E-02
10.20_564.3100m/z*	Lneg	Unknown	0.72 (0.53 - 0.98)	3.48E-02	0.38 (0.26 - 0.58)	3.69E-06
9.09_843.6593m/z*	Lpos	Unknown	0.72 (0.53 - 0.99)	4.12E-02	0.48 (0.33 - 0.7)	1.46E-04
6.84_339.2893m/z Δ	Lpos	Unknown	0.72 (0.53 - 0.99)	4.41E-02	0.55 (0.42 - 0.72)	1.49E-05
4.75_824.5783m/z	Lpos	Unknown	0.73 (0.55 - 0.97)	3.28E-02	0.63 (0.47 - 0.83)	1.38E-03
9.44_617.5136m/z*	Lpos	Unknown	0.76 (0.58 - 0.98)	3.26E-02	0.49 (0.34 - 0.7)	1.21E-04
3.11_367.3362m/z*	Lpos	Unknown	0.77 (0.6 - 0.98)	3.65E-02	0.64 (0.47 - 0.88)	5.40E-03
9.18_914.7584m/z*	Lpos	Unknown	0.8 (0.65 - 1.00)	4.69E-02	0.54 (0.39 - 0.74)	1.06E-04

Appendix Table 4.1 – Survival analysis of UPLC-MS peaks in PAH. 142 UPLC-MS peaks that are significantly different between PAH survivors and non-survivors in discovery and validation cohorts ($p<0.05$) are shown. Hazard ratio and significance (Sig) are shown from Cox regression analysis. 52 peaks which are also independent of established prognostic markers, NT-proBNP (N-terminal brain natriuretic peptide), 6MWD (six minute walk distance) and RDW (red cell distribution width) in the discovery cohort are shown. Metabolites marked with Δ were not significantly different in a comparison of PAH survivors and non-survivors when nine patients who had undergone transplantation were excluded in the discovery and validation cohorts ($p>0.05$). ~indicates peaks where the identity was confirmed by analysis of a pure standard compound, the remaining were confirmed by assessment of tandem MS/MS fragmentation patterns, or assessment of retention time and neutral mass. *indicates the 43 prognostic peaks which were also significantly different between PAH patients on sildenafil monotherapy defined as responders (n=18) or non-responders (n=11, defined as death or change in PAH drug therapy within 1 year) ($p<0.05$). TG, triglyceride; PC, phosphocholine.

Metabolite	Metabolic Pathway	Discovery	Validation	Validation2	PAH	BMPR2	Linear Regression		Confounder	Sub-analyses	
		PAH (19-70)	PAH	PAH2	Naïve	Mutation	HC vs PAH	HC+DC vs PAH	HC vs PAH	PAH Naïve	BMPR2
Increased PAH vs HC and DC (independent confounders)											
N-acetylaspartate (NAA)	Alanine & Aspartate	1.13	1.32	0.87	1.47	0.93	2.3E-04	4.6E-03		3.0E-09	0.46
octadecanedioate	Fatty Acid, Dicarboxylate	0.82	0.93	0.35	0.95	0.43	1.5E-02	1.3E-02		7.3E-06	0.25
3-hydroxy-3-methylglutarate	Mevalonate	0.89	1.15	0.76	1.20	0.75	3.5E-02	3.0E-02		1.6E-09	0.12
acisoga	Polyamine	1.42	1.95	1.22	1.93	1.04	1.9E-04	1.5E-02		2.7E-11	2.9E-02
N1-methylinosine	Purine, Hypo-Xanthine/Inosine	1.50	1.85	1.29	1.78	1.50	8.1E-04	2.2E-02		1.5E-13	0.48
xanthine	Purine, Hypo-Xanthine/Inosine	0.98	1.06	1.00	1.35	1.16	2.0E-07	2.8E-03		3.4E-09	0.19
N2,N2-dimethylguanosine	Purine, Guanine	1.56	2.00	1.39	1.95	1.36	1.1E-02	3.9E-02		2.2E-13	0.11
3-ureidopropionate	Pyrimidine, Uracil	0.62	1.16	0.54	1.16	0.47	1.7E-02	9.0E-04		4.0E-09	0.36
malate	TCA Cycle	1.17	1.64	1.02	1.81	1.11	8.8E-04	9.1E-03		1.5E-14	0.35
X - 12688	Unknown	1.50	1.70	1.26	1.76	0.99	4.9E-05	3.2E-02		6.4E-13	1.6E-02
X - 13737	Unknown	0.97	1.03	0.91	1.15	0.94	1.8E-02	6.1E-03		1.9E-08	0.70
X - 21796	Unknown	0.96	1.06	0.73	1.33	0.83	5.0E-03	1.3E-02		1.9E-12	0.83
Decreased PAH vs HC and DC (independent confounders)											
palmitoylcholine	Fatty Acid (Acyl Choline)	-1.33	-0.73	-1.10	-0.94	-1.35	1.7E-03	8.3E-03		3.9E-05	4.8E-02
1-arachidonoyl-GPC (20:4n6)*	Lysolipid	-1.09	-0.74	-0.81	-0.81	-1.00	1.2E-02	3.2E-02		5.9E-05	0.27
1-docosapentaenoyl-GPC (22:5n3)*	Lysolipid	-1.03	-0.80	-0.84	-0.79	-1.02	9.0E-03	6.7E-03		1.6E-05	0.23
1-linoleoyl-2-eicosapentaenoyl-GPC (18:2/20:5)*	Phospholipid	-0.81	-1.13	-0.81	-1.16	-0.77	2.4E-02	1.2E-02		3.4E-08	0.68
sphingomyelin (d18:1/20:0, d16:1/22:0)*	Sphingolipid	-1.02	-1.09	-1.05	-1.24	-0.93	1.3E-02	7.7E-03		1.2E-08	0.49

Metabolite	Metabolic Pathway	Discovery	Validation	Validation2	PAH	BMPR2	Linear Regression		Confounder	Sub-analyses	
		PAH (19-70)	PAH	PAH2	Naïve	Mutation	HC vs PAH	HC+DC vs PAH	HC vs PAH	PAH Naïve	BMPR2
sphingomyelin (d18:1/21:0, d17:1/22:0, d16:1/23:0)*	Sphingolipid	-0.89	-0.93	-0.76	-1.04	-0.83	2.7E-03	4.0E-02		1.4E-08	0.78
sphingomyelin (d18:1/22:1, d18:2/22:0, d16:1/24:1)*	Sphingolipid	-1.09	-1.16	-1.03	-1.21	-1.12	2.6E-03	7.2E-04		1.8E-07	0.95
sphingomyelin (d18:2/23:0, d18:1/23:1, d17:1/24:1)*	Sphingolipid	-0.63	-0.60	-0.54	-0.68	-0.66	4.9E-04	4.4E-02		1.0E-06	0.40
Increased PAH vs HC (independent confounders)											
oleoyl ethanolamide	Endocannabinoid	0.88	1.02	0.52	0.84	0.29	1.3E-03	2.2E-01		5.6E-05	5.4E-03
3-hydroxybutyrylcarnitine (1)	Fatty Acid (Acyl Carnitine)	0.91	0.97	0.60	1.11	0.62	6.1E-05	1.1E-01		7.3E-09	4.5E-02
3-hydroxybutyrylcarnitine (2)	Fatty Acid (Acyl Carnitine)	1.26	1.24	0.90	1.49	0.81	4.7E-03	6.8E-01		3.4E-09	3.8E-02
acetylcarnitine	Fatty Acid (Acyl Carnitine)	1.02	0.88	0.59	0.94	0.56	1.2E-02	2.9E-01		5.7E-06	3.1E-02
adipoylcarnitine	Fatty Acid (Acyl Carnitine)	1.44	1.69	1.25	1.77	1.20	4.6E-02	3.9E-01		5.8E-10	0.09
myristoleoylcarnitine*	Fatty Acid (Acyl Carnitine)	0.75	0.85	0.53	0.91	0.37	1.6E-02	4.6E-01		6.2E-05	1.0E-02
myristoylcarnitine	Fatty Acid (Acyl Carnitine)	0.81	1.06	0.60	1.07	0.44	4.1E-02	9.5E-01		9.4E-06	1.1E-02
oleoylcarnitine	Fatty Acid (Acyl Carnitine)	0.96	1.39	1.20	1.22	0.87	1.8E-02	6.7E-01		3.2E-07	0.10
palmitoleoylcarnitine*	Fatty Acid (Acyl Carnitine)	0.91	1.23	0.85	1.14	0.69	8.5E-03	8.9E-01		7.9E-07	4.1E-02
suberoylcarnitine	Fatty Acid (Acyl Carnitine)	1.40	1.61	1.23	1.66	1.03	7.1E-03	3.5E-01		1.3E-09	2.9E-02
glutamate	Glutamate	1.13	0.98	0.71	1.12	0.83	2.9E-02	1.4E-01		2.7E-07	0.98

Metabolite	Metabolic Pathway	Discovery	Validation	Validation2	PAH	BMPR2	Linear Regression		Confounder	Sub-analyses	
		PAH (19-70)	PAH	PAH2	Naïve	Mutation	HC vs PAH	HC+DC vs PAH	HC vs PAH	PAH Naïve	BMPR2
methionine sulfone	Met, Cys, SAM & Tau	1.57	1.79	1.40	1.56	1.29	3.6E-02	4.9E-01		1.8E-09	0.14
N-acetylmethionine	Met, Cys, SAM & Tau	1.08	1.27	0.60	1.30	0.80	3.3E-03	1.6E-01		1.3E-09	0.22
N-acetyltaurine	Met, Cys, SAM & Tau	1.02	1.15	0.63	1.15	0.37	1.0E-03	7.1E-02		2.7E-07	9.7E-04
N-formylmethionine	Met, Cys, SAM & Tau	1.08	1.53	0.78	1.59	0.85	4.8E-02	3.0E-01		5.8E-10	0.10
5,6-dihydrothymine	Pyrimidine, Thymine	1.33	1.37	0.62	1.38	0.71	2.0E-04	6.7E-02		1.2E-08	0.15
alpha-ketoglutarate	TCA Cycle	0.68	1.57	1.13	1.61	1.14	2.2E-02	2.4E-01		2.6E-13	1.00
fumarate	TCA Cycle	0.65	1.14	0.56	1.23	0.31	2.1E-02	9.8E-02		3.5E-16	0.28
C-glycosyltryptophan	Tryptophan	1.11	1.37	0.76	1.30	0.59	4.8E-02	3.9E-01		5.9E-07	4.7E-03
X - 12127	Unknown	0.85	1.05	0.67	1.07	0.73	1.6E-02	4.4E-01		1.6E-08	0.53
X - 12472	Unknown	1.03	1.05	0.96	1.15	0.93	3.4E-03	8.2E-01		2.5E-07	0.59
X - 12739	Unknown	1.02	1.12	0.99	1.18	0.97	2.4E-02	1.8E-01		6.8E-07	0.35
X - 12824	Unknown	0.85	1.08	0.79	1.16	0.78	2.0E-02	6.8E-01		9.5E-08	0.44
X - 17327	Unknown	0.86	0.97	0.82	1.02	0.78	2.6E-02	7.0E-01		2.4E-06	0.34
X - 21829	Unknown	0.82	1.24	0.66	1.41	0.62	2.5E-02	5.6E-01		2.4E-10	0.10
X - 24307	Unknown	0.70	1.18	0.97	1.09	0.94	6.9E-05	7.2E-02		1.2E-07	0.88
X - 24513	Unknown	1.05	1.44	0.98	1.30	0.77	2.4E-02	4.8E-01		1.4E-07	9.1E-03
X - 24527	Unknown	1.11	1.22	1.06	1.22	0.94	3.5E-02	1.9E-01		2.2E-06	0.25
X - 24678	Unknown	1.20	1.34	0.70	1.33	0.83	4.9E-03	1.2E-01		3.6E-11	0.42
X - 24766	Unknown	0.82	1.07	0.85	0.89	0.92	1.9E-02	3.9E-01		5.1E-07	0.78
Decreased PAH vs HC (independent confounders)											
asparagine	Alanine & Aspartate	-0.88	-1.00	-0.90	-1.22	-0.95	8.7E-04	8.5E-02		2.3E-07	0.64
dehydroisoandrosterone sulfate (DHEA-S)	Steroid	-1.53	-1.74	-1.77	-1.53	-1.56	2.5E-02	4.1E-01		1.3E-09	0.46
X - 23765	Unknown	-0.72	-0.90	-0.90	-1.02	-1.08	8.1E-04	2.0E-01		9.7E-07	0.15
Increased PAH vs HC											
N-acetylalanine	Alanine & Aspartate	0.76	1.15	0.66	1.04	0.50	9.9E-01	2.3E-01	Diuretics	3.2E-05	1.6E-02
N-acetylneuraminate	Aminosugar	0.93	0.88	0.47	0.76	0.28	7.4E-02	2.4E-01	Age	1.8E-04	1.0E-03
erythronate*	Aminosugar	0.71	1.16	0.59	1.10	0.37	7.1E-01	6.5E-01	Bilirubin	5.4E-06	6.0E-03

Metabolite	Metabolic Pathway	Discovery	Validation	Validation2	PAH	BMPR2	Linear Regression		Confounder	Sub-analyses	
		PAH (19-70)	PAH	PAH2	Naïve	Mutation	HC vs PAH	HC+DC vs PAH	HC vs PAH	PAH Naïve	BMPR2
N-acetylglucosamine/N-acetylgalactosamine	Aminosugar	0.72	0.95	0.58	0.62	0.54	1.0E-01	7.3E-01	Gender	1.8E-03	4.4E-02
gulonic acid*	Ascorbate & Aldarate	0.61	0.79	0.61	0.81	0.47	8.5E-01	5.3E-01	Age	4.5E-05	2.8E-02
palmitoylcarnitine	Fatty Acid (Acyl Carnitine)	0.91	1.28	0.95	1.23	0.90	6.0E-02	9.2E-01	Bilirubin	1.6E-07	0.43
malonylcarnitine	Fatty Acid Synthesis	0.56	0.94	0.48	0.96	0.57	1.3E-01	3.8E-02	Bilirubin	3.8E-09	0.53
N-acetylserine	Glycine, Serine & Threonine	1.00	1.49	0.97	1.38	0.85	5.2E-01	4.0E-01	Bilirubin	6.9E-08	0.05
N-acetylthreonine	Glycine, Serine & Threonine	0.68	0.99	0.55	1.10	0.47	6.5E-01	9.7E-01	Bilirubin	4.4E-07	2.0E-02
1-methylimidazoleacetate	Histidine	0.86	1.32	0.86	1.02	0.74	6.0E-02	9.5E-02	Age	7.9E-07	0.08
imidazole propionate	Histidine	0.84	0.99	0.79	0.98	0.84	1.4E-01	8.1E-01	Bilirubin	1.1E-07	0.54
quinolinate	Nicotinate & Nicotinamide	0.76	1.19	0.86	0.95	0.58	6.0E-01	5.0E-01	Bilirubin	1.8E-04	3.8E-02
vanillylmandelate (VMA)	Phenylalanine & Tyrosine	1.00	1.52	0.83	1.75	0.96	2.3E-01	1.5E-02	Age	6.3E-12	0.37
4-acetamidobutanoate	Polyamine	1.22	1.93	1.26	1.83	1.19	8.6E-01	7.0E-01	Bilirubin	1.0E-11	0.15
N-acetylputrescine	Polyamine	0.84	1.32	0.66	0.93	0.53	5.8E-01	6.2E-01	Bilirubin	3.0E-06	3.8E-02
N6-carbamoylthreonyl adenosine	Purine, Adenine	1.04	1.49	1.06	1.31	0.92	1.7E-01	4.5E-01	Age	8.4E-09	4.6E-02
N1-methyladenosine	Purine, Adenine	0.94	1.26	0.65	1.03	0.46	8.6E-01	1.4E-01	Bilirubin	2.4E-05	4.4E-03
N6-succinyladenosine	Purine, Adenine	0.63	0.86	0.50	0.94	0.44	1.5E-01	2.7E-01	Bilirubin	1.2E-09	2.7E-03
N4-acetylcytidine	Pyrimidine, Cytidine	1.31	1.50	1.22	1.33	1.19	2.7E-01	6.7E-01	Bilirubin	1.3E-08	0.47
orotidine	Pyrimidine, Orotate	1.07	1.27	0.96	1.27	0.83	2.8E-01	5.3E-01	Bilirubin	1.4E-08	0.08
pseudouridine	Pyrimidine, Uracil	1.22	1.66	1.17	1.68	0.97	1.5E-01	8.6E-01	Bilirubin	5.2E-11	1.4E-02
kynurenine	Tryptophan	1.00	1.37	0.77	1.44	0.68	5.6E-01	3.3E-01	Bilirubin	1.2E-08	0.07

Metabolite	Metabolic Pathway	Discovery	Validation	Validation2	PAH	BMPR2	Linear Regression		Confounder	Sub-analyses	
		PAH (19-70)	PAH	PAH2	Naïve	Mutation	HC vs PAH	HC+DC vs PAH	HC vs PAH	PAH Naïve	BMPR2
X - 12100	Unknown	1.04	1.26	0.88	1.28	0.75	1.3E-01	4.6E-01	Age	9.8E-08	0.06
X - 11564	Unknown	0.94	1.48	0.83	1.43	0.73	9.6E-01	8.8E-01	Bilirubin	3.5E-07	0.06
X - 12026	Unknown	1.58	2.01	1.36	2.20	1.26	6.9E-01	7.7E-01	Bilirubin	3.8E-12	0.07
X - 12117	Unknown	1.18	1.55	1.35	1.50	1.20	6.7E-01	3.6E-01	Bilirubin	7.7E-09	0.19
X - 15503	Unknown	1.04	1.64	1.06	1.68	1.33	6.3E-01	5.6E-02	Bilirubin	2.5E-10	0.63
X - 11429	Unknown	1.52	1.98	1.45	1.88	1.18	9.1E-02	8.4E-01	Diuretics	3.4E-10	2.0E-02
X - 21736	Unknown	1.04	1.46	0.92	1.57	0.95	2.7E-01	3.5E-01	Diuretics	1.1E-10	0.42
pro-hydroxy-pro	Urea cycle; Arginine & Proline	0.87	1.24	0.90	1.07	0.98	9.6E-01	6.9E-01	Diuretics	2.9E-06	0.95
Decreased PAH vs HC											
histidine	Histidine	-1.57	-1.89	-1.71	-1.78	-1.60	6.1E-02	8.2E-03	Prostanoids	1.2E-11	4.2E-01
1-linoleoyl-GPC (18:2)	Lysolipid	-1.22	-1.14	-1.12	-1.33	-1.10	5.8E-02	2.4E-02	Bilirubin	1.3E-07	5.2E-01
2-linoleoyl-GPC (18:2)*	Lysolipid	-1.23	-0.97	-1.09	-1.35	-1.15	9.4E-02	2.9E-02	Bilirubin	4.5E-08	9.6E-01
1-dihomo-linoleoyl-GPC (20:2)*	Lysolipid	-0.95	-0.86	-1.14	-0.98	-1.30	2.4E-01	4.3E-01	Statins	5.5E-05	1.2E-01
1-(1-enyl-palmitoyl)-2-linoleoyl-GPC (P-16:0/18:2)*	Plasmalogen	-1.06	-1.13	-0.98	-1.28	-1.08	2.3E-01	1.5E-01	PDE5 inhib	5.1E-08	9.4E-01
behenoyl sphingomyelin (d18:1/22:0)*	Sphingolipid	-0.75	-0.71	-0.92	-0.78	-0.77	1.4E-01	3.0E-02	Gender	3.6E-06	8.4E-01
4-androsten-3beta,17beta-diol disulfate (1)	Steroid	-0.87	-0.81	-1.14	-0.55	-1.06	2.4E-01	5.4E-01	Gender	4.0E-03	6.8E-01
4-androsten-3beta,17beta-diol monosulfate (1)	Steroid	-1.15	-1.30	-1.40	-1.18	-1.32	5.6E-02	3.7E-01	Gender	5.8E-07	9.3E-01
androsterone sulfate	Steroid	-1.33	-1.40	-1.40	-1.14	-1.33	1.5E-01	2.0E-01	Gender	4.6E-06	7.3E-01
epiandrosterone sulfate	Steroid	-1.42	-1.50	-1.49	-1.23	-1.40	1.3E-01	3.9E-01	Gender	1.1E-06	6.4E-01
pregn steroid monosulfate*	Steroid	-0.88	-0.93	-1.04	-0.71	-0.84	1.0E-01	6.7E-01	Gender	3.3E-04	2.6E-01
X - 23749	Unknown	-1.10	-1.05	-1.12	-0.94	-1.41	2.0E-01	2.7E-01	BMI	5.4E-05	0.02

Metabolite	Metabolic Pathway	Discovery	Validation	Validation2	PAH	BMPR2	Linear Regression		Confounder	Sub-analyses	
		PAH (19-70)	PAH	PAH2	Naïve	Mutation	HC vs PAH	HC+DC vs PAH	HC vs PAH	PAH Naïve	BMPR2
arginine	Urea cycle; Arginine & Proline	-1.05	-1.40	-1.47	-1.80	-1.32	1.1E-01	3.1E-01	DM drugs	2.1E-11	6.5E-01
homoarginine	Urea cycle; Arginine & Proline	-0.91	-1.13	-1.06	-1.11	-0.86	5.1E-02	2.1E-01	Ethnicity	4.8E-07	7.6E-02

Appendix Table 5.1 - Metabolites distinguishing PAH from healthy and disease controls. 97 metabolites that are significantly different between PAH and healthy controls in 3 cohorts ($p<7.3e-5$) are shown. Mean values are given and the data is scaled to the healthy control group. Significance from linear regression is shown (p value), and for metabolites with $p>0.05$ in PAH HC linear regression, the significant confounder is shown. Significance is also shown for Mann Whitney U test between PAH treatment naïve patients versus all HC, and PAH BMPR2 mutation versus non-mutation patients. *probable metabolite identity, but unconfirmed (see methods). PDE, phosphodiesterase; BMI, body mass index; DM drugs, antidiabetic drugs.

Metabolite	Metabolic Pathway	Discovery		Validation1	
		Hazard Ratio	Sig	Hazard Ratio	Sig
Higher value indicates mortality. Independent of established prognostic markers					
N-acetylalanine	Alanine and Aspartate	2.02 (1.22-3.36)	6.43E-03	2.08 (1.12-3.86)	2.04E-02
pimeloylcarnitine/3-methyladipoylcarnitine	Fatty Acid (Acyl Carnitine)	2.16 (1.28-3.66)	4.03E-03	2.52 (1.24-5.10)	1.04E-02
1-methylimidazoleacetate	Histidine	2.26 (1.37-3.73)	1.43E-03	1.74 (1.03-2.93)	3.93E-02
N-acetylmethionine	Methionine, Cysteine, SAM and Taurine	2.36 (1.41-3.96)	1.16E-03	2.29 (1.18-4.43)	1.44E-02
N-formylmethionine	Methionine, Cysteine, SAM and Taurine	1.79 (1.20-2.68)	4.50E-03	1.98 (1.20-3.25)	7.15E-03
4-acetamidobutanoate	Polyamine	2.20 (1.45-3.35)	2.19E-04	2.02 (1.30-3.14)	1.83E-03
N-acetylputrescine	Polyamine	1.74 (1.04-2.91)	3.54E-02	2.92 (1.51-5.66)	1.50E-03
N1-methylinosine	Purine , (Hypo)Xanthine/Inosine	2.82 (1.74-4.57)	2.42E-05	1.73 (1.09-2.77)	2.11E-02
urate	Purine , (Hypo)Xanthine/Inosine	1.61 (1.06-2.42)	2.43E-02	2.14 (1.26-3.64)	4.73E-03
N6-succinyladenosine	Purine , Adenine	3.89 (1.40-10.82)	9.18E-03	8.31 (1.94-35.54)	4.29E-03
N6-carbamoylthreonyladenosine	Purine , Adenine	3.10 (1.60-6.00)	8.04E-04	2.08 (1.08-4.00)	2.81E-02
N1-methyladenosine	Purine , Adenine	1.94 (1.25-3.01)	2.92E-03	1.93 (1.12-3.32)	1.75E-02
N2,N2-dimethylguanosine	Purine , Guanine	2.53 (1.57-4.08)	1.35E-04	1.86 (1.14-3.03)	1.25E-02
pseudouridine	Pyrimidine , Uracil	1.78 (1.07-2.94)	2.54E-02	2.75 (1.48-5.12)	1.45E-03
X - 24020 Δ	Unknown	2.47 (1.42-4.30)	1.36E-03	1.84 (1.00-3.39)	4.94E-02
X - 24513	Unknown	2.34 (1.28-4.29)	5.92E-03	2.18 (1.11-4.29)	2.34E-02
X - 12472	Unknown	2.24 (1.44-3.47)	3.11E-04	1.57 (1.00-2.46)	4.97E-02
X - 12739	Unknown	2.07 (1.41-3.04)	2.07E-04	1.56 (1.06-2.28)	2.28E-02
X - 24527	Unknown	1.85 (1.38-2.48)	4.09E-05	1.43 (1.03-1.99)	3.12E-02
X - 12688	Unknown	1.81 (1.23-2.68)	2.83E-03	2.02 (1.27-3.19)	2.80E-03
X - 24728	Unknown	1.70 (1.09-2.64)	1.96E-02	2.04 (1.09-3.79)	2.50E-02
X - 15503	Unknown	1.67 (1.11-2.52)	1.38E-02	1.51 (1.03-2.22)	3.48E-02
X - 11564	Unknown	1.62 (1.10-2.38)	1.49E-02	1.60 (1.03-2.47)	3.51E-02
X - 24411	Unknown	1.54 (1.04-2.27)	3.05E-02	2.16 (1.32-3.54)	2.17E-03
X - 11429	Unknown	1.47 (1.05-2.06)	2.65E-02	1.79 (1.18-2.71)	5.76E-03
Lower value indicates mortality. Independent of established prognostic markers					
1-eicosapentaenoyl-GPE (20:5)* Δ	Lysolipid	0.60 (0.43-0.84)	2.65E-03	0.62 (0.39-1.00)	4.98E-02

Metabolite	Metabolic Pathway	Discovery		Validation1	
		Hazard Ratio	Sig	Hazard Ratio	Sig
1-eicosapentaenoyl-GPC (20:5)*	Lysolipid	0.47 (0.31-0.73)	6.30E-04	0.50 (0.31-0.82)	6.05E-03
1-linoleoyl-2-docosahexaenoyl-GPC (18:2/22:6)*	Phospholipid	0.64 (0.46-0.89)	7.40E-03	0.65 (0.47-0.91)	1.27E-02
1-oleoyl-2-docosapentaenoyl-GPC (18:1/22:5n6)*	Phospholipid	0.64 (0.47-0.87)	4.11E-03	0.62 (0.43-0.90)	1.06E-02
1-myristoyl-2-arachidonoyl-GPC (14:0/20:4)*	Phospholipid	0.57 (0.39-0.83)	3.68E-03	0.68 (0.48-0.96)	2.66E-02
phosphatidylcholine (18:0/20:5, 16:0/22:5n6)*	Phospholipid	0.54 (0.37-0.77)	7.30E-04	0.42 (0.25-0.72)	1.44E-03
1-palmitoyl-2-eicosapentaenoyl-GPC (16:0/20:5)*	Phospholipid	0.53 (0.37-0.75)	4.11E-04	0.43 (0.26-0.74)	1.96E-03
1-linoleoyl-2-eicosapentaenoyl-GPC (18:2/20:5)*	Phospholipid	0.48 (0.33-0.70)	1.38E-04	0.60 (0.41-0.88)	8.59E-03
1-myristoyl-2-docosahexaenoyl-GPC (14:0/22:6)*	Phospholipid	0.47 (0.31-0.72)	4.84E-04	0.49 (0.29-0.81)	5.62E-03
dehydroisoandrosterone sulfate (DHEA-S)	Steroid	0.71 (0.52-0.97)	3.19E-02	0.55 (0.33-0.91)	2.06E-02
X - 24041 Δ	Unknown	0.46 (0.29-0.72)	6.88E-04	0.61 (0.38-0.99)	4.45E-02
Higher value indicates mortality					
hexadecanedioate	Fatty Acid, Dicarboxylate	1.53 (1.09-2.14)	1.40E-02	1.67 (1.16-2.41)	5.58E-03
N-acetyltaurine	Methionine, Cysteine, SAM and Taurine	1.97 (1.16-3.35)	1.19E-02	2.24 (1.13-4.43)	2.05E-02
3-hydroxy-3-methylglutarate Δ	Mevalonate	1.68 (1.03-2.74)	3.78E-02	2.08 (1.02-4.23)	4.40E-02
vanillylmandelate (VMA)	Phenylalanine and Tyrosine	1.48 (1.06-2.06)	2.02E-02	1.58 (1.06-2.34)	2.38E-02
N-acetyl-beta-alanine	Pyrimidine , Uracil	1.54 (1.08-2.21)	1.80E-02	1.65 (1.18-2.32)	3.65E-03
fumarate	TCA Cycle	1.70 (1.00-2.88)	4.97E-02	2.57 (1.09-6.06)	3.09E-02
N2,N5-diacetylornithine	Urea cycle; Arginine and Proline	2.15 (1.27-3.63)	4.37E-03	2.15 (1.13-4.09)	1.95E-02
Lower value indicates mortality					
valine	Leucine, Isoleucine and Valine	0.66 (0.49-0.89)	6.80E-03	0.68 (0.48-0.95)	2.21E-02
1-docosahexaenoyl-GPE (22:6)*	Lysolipid	0.68 (0.49-0.94)	1.86E-02	0.54 (0.34-0.85)	8.27E-03
1-dihomo-linolenoyl-GPC (20:3n3 or 6)*	Lysolipid	0.57 (0.41-0.79)	7.43E-04	0.71 (0.53-0.96)	2.82E-02
1-docosahexaenoyl-GPC (22:6)*	Lysolipid	0.54 (0.35-0.81)	3.17E-03	0.57 (0.35-0.93)	2.32E-02
phosphatidylcholine (16:0/22:5n3, 18:1/20:4)* Δ	Phospholipid	0.68 (0.48-0.96)	2.64E-02	0.59 (0.36-0.98)	4.16E-02
1-stearoyl-2-docosahexaenoyl-GPE (18:0/22:6)*	Phospholipid	0.64 (0.47-0.88)	5.99E-03	0.52 (0.32-0.85)	8.73E-03
1-palmitoleoyl-2-docosahexaenoyl-GPC (16:1/22:6)*	Phospholipid	0.62 (0.43-0.90)	1.09E-02	0.50 (0.28-0.88)	1.67E-02
1-pentadecanoyl-2-docosahexaenoyl-GPC (15:0/22:6)*	Phospholipid	0.62 (0.42-0.90)	1.30E-02	0.34 (0.17-0.68)	1.96E-03
1-stearoyl-2-docosahexaenoyl-GPC (18:0/22:6)	Phospholipid	0.60 (0.42-0.87)	7.16E-03	0.45 (0.27-0.76)	2.76E-03

Metabolite	Metabolic Pathway	Discovery		Validation1	
		Hazard Ratio	Sig	Hazard Ratio	Sig
1-stearoyl-2-docosapentaenoyl-GPC (18:0/22:5n3)*	Phospholipid	0.58 (0.41-0.82)	2.11E-03	0.50 (0.30-0.83)	8.18E-03
1-palmitoyl-2-dihomo-linolenoyl-GPC (16:0/20:3n3 or 6)*	Phospholipid	0.58 (0.38-0.88)	9.67E-03	0.54 (0.35-0.84)	6.47E-03
1-(1-enyl-stearoyl)-2-docosahexaenoyl-GPC (P-18:0/22:6)* Δ	Plasmalogen	0.56 (0.37-0.85)	6.20E-03	0.57 (0.33-0.98)	4.06E-02
1-(1-enyl-stearoyl)-2-docosahexaenoyl-GPE (P-18:0/22:6)*	Plasmalogen	0.55 (0.37-0.82)	3.45E-03	0.49 (0.27-0.91)	2.31E-02
1-(1-enyl-palmitoyl)-2-docosahexaenoyl-GPC (P-16:0/22:6)*	Plasmalogen	0.54 (0.37-0.79)	1.31E-03	0.53 (0.32-0.87)	1.30E-02
1-(1-enyl-palmitoyl)-2-docosahexaenoyl-GPE (P-16:0/22:6)* Δ	Plasmalogen	0.49 (0.34-0.71)	1.63E-04	0.47 (0.26-0.82)	8.30E-03
sphingomyelin (d18:2/14:0, d18:1/14:1)*	Sphingolipid	0.73 (0.53-1.00)	4.83E-02	0.48 (0.30-0.77)	2.36E-03
sphingomyelin (d18:1/20:0, d16:1/22:0)*	Sphingolipid	0.60 (0.41-0.87)	6.60E-03	0.57 (0.35-0.93)	2.32E-02
sphingomyelin (d18:1/22:1, d18:2/22:0, d16:1/24:1)*	Sphingolipid	0.59 (0.42-0.83)	2.51E-03	0.53 (0.33-0.85)	7.63E-03
behenoyl sphingomyelin (d18:1/22:0)*	Sphingolipid	0.42 (0.27-0.64)	5.94E-05	0.47 (0.27-0.82)	7.42E-03

Appendix Table 5.2 - Survival analysis in PAH. 62 metabolites significantly different between PAH survivors and non-survivors in discovery and validation1 cohorts ($p<0.05$) are shown. Hazard ratio and significance (Sig) is shown from Cox regression analysis. Metabolites which are also independent of established prognostic markers in the discovery cohort are also shown. Metabolites marked with Δ were not significantly different in a comparison of PAH survivors and non-survivors when six patients who had undergone transplantation were excluded in the discovery and validation1 cohorts ($p>0.05$). *probable metabolite identity, but unconfirmed (see methods). GPC, glycerophosphocholine; GPE, glycerophosphoethanolamine.

Metabolite	Metabolic Pathway	Discovery	Validation	Sub-analyses		Linear Regression		Confounder	Sub-analyses	
		CTEPH (n=82)	CTEPH (n=92)	CTED (n=13)	PE (n=28)	HC vs CTEPH	DC vs CTEPH	HC vs CTEPH	CTED vs CTEPH	PE vs CTEPH
Increased CTEPH vs HC, DC (independent confounders) and PE										
5-methylthioadenosine (MTA)	Polyamine Metabolism	1.70	1.57	1.39	0.87	2.19E-06	1.44E-02		3.76E-01	1.13E-03
acetylcarnitine	Fatty Acid Metabolism(Acyl Carnitine)	1.19	1.10	1.28	0.14	1.09E-03	2.28E-02		8.42E-01	3.10E-05
N1-methyladenosine	Purine Metabolism, Adenine containing	1.70	1.69	1.17	0.84	4.83E-05	3.20E-02		2.08E-01	1.63E-05
N1-methylinosine	Purine Metabolism, (Hypo)Xanthine/Inosine containing	1.44	1.85	1.93	0.25	1.54E-03	2.75E-03		8.61E-01	3.29E-05
N2,N2-dimethylguanosine	Purine Metabolism, Guanine containing	1.96	1.91	1.44	0.63	2.73E-04	6.59E-04		2.33E-01	4.72E-07
N-acetylmethionine	Methionine, Cysteine, SAM and Taurine Metabolism	1.29	1.21	1.06	0.55	7.06E-03	1.87E-02		3.02E-01	5.80E-06
N-formylmethionine	Methionine, Cysteine, SAM and Taurine Metabolism	1.51	1.54	1.43	0.87	3.21E-03	4.28E-02		4.96E-01	2.56E-04
X - 24527	Unknown	1.38	1.20	1.45	0.26	4.11E-02	2.25E-02		7.86E-01	1.24E-04
Increased CTEPH vs HC and DC (independent confounders)										
16-hydroxypalmitate	Fatty Acid, Monohydroxy	1.14	0.88	1.33	0.78	1.74E-04	1.28E-02		5.45E-01	3.94E-01
2-hydroxypalmitate	Fatty Acid, Monohydroxy	1.02	0.98	0.41	1.13	4.17E-05	2.04E-03		1.93E-01	2.77E-01
3-methylcytidine	Pyrimidine Metabolism, Cytidine containing	1.58	0.99	0.96	1.64	3.18E-04	5.17E-03		6.58E-01	2.31E-01
Decreased CTEPH vs HC and DC (independent confounders)										
gamma-glutamyl-epsilon-lysine	Gamma-glutamyl Amino Acid	-1.09	-0.91	-1.59	-0.92	7.11E-03	2.27E-02		2.86E-01	5.18E-01
Increased CTEPH vs HC (independent confounders)										
3-hydroxydecanoate	Fatty Acid, Monohydroxy	1.03	0.94	1.14	0.60	1.87E-02	2.08E-01		6.99E-01	1.22E-01
3-hydroxylaurate	Fatty Acid, Monohydroxy	1.03	0.94	1.14	0.52	1.09E-03	6.52E-02		8.61E-01	5.15E-02

Metabolite	Metabolic Pathway	Discovery	Validation	Sub-analyses		Linear Regression		Confounder	Sub-analyses	
		CTEPH (n=82)	CTEPH (n=92)	CTED (n=13)	PE (n=28)	HC vs CTEPH	DC vs CTEPH	HC vs CTEPH	CTED vs CTEPH	PE vs CTEPH
7-methylguanine	Purine Metabolism, Guanine containing	1.24	1.31	0.67	0.43	3.56E-02	2.29E-01		2.04E-01	2.69E-04
alpha-ketoglutarate	TCA Cycle	0.96	1.08	0.36	1.01	1.71E-02	4.47E-01		1.64E-01	1.64E-01
C-glycosyltryptophan	Tryptophan Metabolism	1.30	1.35	0.79	0.10	4.24E-02	7.33E-01		5.69E-01	1.04E-07
dimethylarginine (SDMA + ADMA)	Urea cycle; Arginine and Proline Metabolism	1.38	1.29	1.74	1.05	6.40E-03	5.10E-01		3.98E-01	5.38E-01
docosadienoate (22:2n6)	Polyunsaturated Fatty Acid (n3 and n6)	1.13	0.97	1.23	0.59	2.09E-03	9.55E-02		6.18E-01	2.88E-02
hexanoylcarnitine	Fatty Acid Metabolism(Acyl Carnitine)	0.77	0.83	0.80	0.11	1.09E-02	1.53E-01		9.94E-01	3.20E-04
kynurenine	Tryptophan Metabolism	1.21	1.40	1.16	0.36	6.67E-03	1.07E-01		8.83E-01	2.16E-05
myristoleoylcarnitine*	Fatty Acid Metabolism(Acyl Carnitine)	0.95	0.93	0.81	0.09	8.83E-03	3.04E-01		8.48E-01	2.76E-05
myristoylcarnitine	Fatty Acid Metabolism(Acyl Carnitine)	1.24	1.33	0.98	0.31	1.12E-03	4.28E-01		3.21E-01	1.09E-05
N-acetylputrescine	Polyamine Metabolism	1.19	1.12	0.55	0.97	1.54E-02	6.71E-01		1.55E-01	2.83E-01
oleoyl ethanolamide	Endocannabinoid	1.54	1.19	2.04	0.63	5.73E-05	2.99E-01		1.14E-01	1.38E-01
oleoylcarnitine	Fatty Acid Metabolism(Acyl Carnitine)	1.19	1.16	0.90	0.51	1.05E-04	2.66E-01		4.98E-01	3.81E-04
palmitoleoylcarnitine*	Fatty Acid Metabolism(Acyl Carnitine)	1.19	1.19	0.86	0.28	5.09E-04	6.76E-01		3.87E-01	1.17E-05
palmitoylcarnitine	Fatty Acid Metabolism(Acyl Carnitine)	1.37	1.31	0.72	0.49	6.16E-05	2.33E-01		9.66E-02	2.02E-04
X - 11429	Unknown	1.82	1.98	1.78	1.24	2.36E-03	8.96E-01		6.33E-01	3.01E-03
X - 12026	Unknown	2.09	1.96	1.89	0.56	1.04E-03	3.90E-01		8.23E-01	1.07E-05
X - 12100	Unknown	1.16	1.29	1.45	0.29	1.94E-03	8.64E-01		4.88E-01	8.87E-06
X - 12688	Unknown	1.50	1.39	1.55	0.71	5.73E-03	4.21E-01		9.27E-01	3.49E-03
X - 24020	Unknown	1.22	1.04	0.95	0.69	1.60E-03	1.39E-01		2.21E-01	3.09E-03
X - 24699	Unknown	1.20	1.01	1.42	0.50	1.89E-02	2.12E-01		2.07E-01	1.86E-03

Metabolite	Metabolic Pathway	Discovery	Validation	Sub-analyses		Linear Regression		Confounder	Sub-analyses	
		CTEPH (n=82)	CTEPH (n=92)	CTED (n=13)	PE (n=28)	HC vs CTEPH	DC vs CTEPH	HC vs CTEPH	CTED vs CTEPH	PE vs CTEPH
Decreased CTEPH vs HC (independent confounders)										
4-androsten-3beta,17beta-diol disulfate (1)	Steroid	-0.98	-1.02	-0.37	-0.09	3.55E-02	3.68 E-01		2.65 E-01	1.59 E-04
androsterone sulfate	Steroid	-1.24	-1.19	-0.56	0.21	4.07E-03	2.05 E-01		2.53 E-01	6.61 E-07
methionine sulfoxide	Methionine, Cysteine, SAM and Taurine Metabolism	-0.58	-0.54	-0.33	-0.09	2.57E-02	7.27 E-01		6.27 E-01	6.46 E-02
pregn steroid monosulfate*	Steroid	-0.82	-1.01	-0.75	0.38	4.17E-02	7.73 E-01		7.11 E-01	1.44 E-07
sphingomyelin (d18:1/20:0, d16:1/22:0)*	Sphingolipid Metabolism	-0.81	-0.65	-0.59	-0.09	5.19E-03	2.73 E-01		7.83 E-01	1.01 E-03
sphingomyelin (d18:1/21:0, d17:1/22:0, d16:1/23:0)*	Sphingolipid Metabolism	-0.67	-0.51	-0.02	0.13	1.30E-02	5.46 E-01		2.45 E-01	6.45 E-04
sphingomyelin (d18:1/22:1, d18:2/22:0, d16:1/24:1)*	Sphingolipid Metabolism	-0.81	-0.66	-0.28	0.03	1.72E-02	2.42 E-01		2.17 E-01	5.57 E-05
X - 23765	Unknown	-0.68	-1.01	-1.36	-0.22	3.15E-03	1.16 E-01		2.93 E-01	3.00 E-03
Increased CTEPH vs HC										
1-methylhistidine	Histidine Metabolism	0.99	1.00	0.94	0.27	5.16E-01	3.18 E-01	Cardiac glycosides	8.70 E-01	1.11 E-04
1-methylimidazoleacetate	Histidine Metabolism	0.84	0.95	0.71	-0.12	4.89E-01	5.79 E-01	ACE inhib.	7.44 E-01	1.55 E-06
3-hydroxy-3-methylglutarate	Mevalonate Metabolism	0.93	0.90	0.51	-0.35	6.64E-01	8.93 E-01	Anticoag.	3.70 E-01	8.69 E-09
3-hydroxybutyrylcarnitine (2)	Fatty Acid Metabolism(Acyl Carnitine)	1.10	1.05	1.41	0.02	1.19E-01	5.15 E-01	Iron therapy	2.32 E-01	1.56 E-08
4-acetamidobutanoate	Polyamine Metabolism	1.73	1.59	0.95	0.80	1.09E-01	9.25 E-01	Gender	3.98 E-01	3.47 E-05
erythronate*	Aminosugar Metabolism	0.95	1.12	1.32	0.58	2.70E-01	7.43 E-01	Iron therapy	4.32 E-01	3.30 E-02
fumarate	TCA Cycle	0.75	0.68	0.31	0.20	5.18E-01	9.46 E-01	Anticoag.	3.11 E-02	3.36 E-04
malate	TCA Cycle	1.38	1.34	0.39	0.33	2.30E-01	1.37 E-01	Ald. antag.	1.18 E-02	5.10 E-08
N6-carbamoylthreonyladenosine	Purine Metabolism, Adenine containing	1.34	1.45	1.57	0.79	1.00E+00	9.70 E-01	DM drugs	6.41 E-01	3.81 E-04
N-acetylalanine	Alanine and Aspartate Metabolism	1.20	1.23	1.43	0.69	9.93E-02	4.38 E-01	ERAs	5.11 E-01	2.43 E-02

Metabolite	Metabolic Pathway	Discovery	Validation	Sub-analyses		Linear Regression		Confounder	Sub-analyses	
		CTEPH (n=82)	CTEPH (n=92)	CTED (n=13)	PE (n=28)	HC vs CTEPH	DC vs CTEPH	HC vs CTEPH	CTED vs CTEPH	PE vs CTEPH
N-acetylglucosaminylasparagine	Aminosugar Metabolism	1.05	0.82	0.88	-0.17	1.69E-01	2.59E-01	Diuretics	8.58E-01	4.13E-05
N-acetylneuraminate	Aminosugar Metabolism	0.95	0.92	0.52	-0.11	5.70E-01	2.36E-01	Diuretics	1.44E-01	1.48E-07
N-acetylphenylalanine	Phenylalanine and Tyrosine Metabolism	0.92	1.02	1.03	0.26	5.92E-01	2.30E-01	Prostanoids	9.90E-01	1.18E-03
N-acetylvaline	Leucine, Isoleucine and Valine Metabolism	1.05	1.07	0.98	0.67	9.81E-02	9.51E-01	Anticoag.	6.27E-01	1.76E-02
orotidine	Pyrimidine Metabolism, Orotate containing	0.92	1.09	0.82	0.29	1.33E-01	2.88E-01	ERAs	9.49E-01	1.67E-06
pseudouridine	Pyrimidine Metabolism, Uracil containing	1.63	1.69	1.55	1.10	6.06E-02	7.86E-01	PDE inhib.	6.55E-01	1.38E-03
vanillylmandelate (VMA)	Phenylalanine and Tyrosine Metabolism	1.64	1.38	0.70	0.11	4.67E-01	1.98E-01	ERAs	1.26E-01	8.68E-08
X - 11564	Unknown	1.52	1.52	1.64	0.56	1.74E-01	5.12E-01	Anticoag.	4.47E-01	1.12E-05
X - 12117	Unknown	0.89	1.09	1.35	0.01	7.43E-01	2.81E-03	PDE inhib.	3.96E-01	1.73E-04
X - 12472	Unknown	1.04	0.95	1.16	0.20	6.16E-02	6.20E-01	Ald. antag.	6.93E-01	8.58E-05
X - 13737	Unknown	1.42	1.17	0.95	0.37	2.17E-01	1.55E-02	ACE inhib.	1.54E-01	3.31E-06
X - 15503	Unknown	1.33	1.34	0.91	0.04	1.41E-01	1.44E-01	ERAs	2.95E-01	1.66E-06
X - 22162	Unknown	0.97	1.03	0.50	0.83	1.99E-01	2.97E-01	Cardiac glycosides	2.93E-01	5.73E-01
X - 24422	Unknown	1.13	1.09	1.24	-0.02	2.68E-01	4.39E-01	Ald. antag.	4.19E-01	2.98E-05
X - 24452	Unknown	1.16	1.05	1.60	0.43	9.80E-01	9.56E-01	ERAs	2.05E-01	1.16E-03
X - 24513	Unknown	1.35	1.44	1.26	0.64	2.15E-01	2.53E-01	Anticoag.	6.99E-01	1.32E-03
Decreased CTEPH vs HC										
1-(1-enyl-palmitoyl)-2-linoleoyl-GPC (P-16:0/18:2)*	Plasmalogen	-0.76	-0.96	-1.38	0.06	5.12E-02	3.58E-01	Cardiac glycosides	2.84E-01	1.14E-04
1,2-dilinoleoyl-GPC (18:2/18:2)	Phospholipid Metabolism	-0.66	-0.64	-0.64	0.13	1.34E-01	1.72E-01	PDE inhib.	8.33E-01	7.70E-05
1-linoleoyl-2-arachidonoyl-GPC (18:2/20:4n6)*	Phospholipid Metabolism	-0.61	-0.50	-0.47	-0.06	2.38E-01	4.23E-01	Prostanoids	8.39E-01	4.01E-05
1-linoleoyl-GPC (18:2)	Lysolipid	-0.86	-0.80	-0.74	0.19	4.47E-01	2.54E-01	Ald. antag.	5.80E-01	3.17E-08
1-margaroyl-GPC (17:0)	Lysolipid	-0.65	-0.62	-0.01	0.30	3.40E-01	1.05E-01	Anticoag.	1.32E-01	2.82E-04

Metabolite	Metabolic Pathway	Discovery	Validation	Sub-analyses		Linear Regression		Confounder	Sub-analyses	
		CTEPH (n=82)	CTEPH (n=92)	CTED (n=13)	PE (n=28)	HC vs CTEPH	DC vs CTEPH	HC vs CTEPH	CTED vs CTEPH	PE vs CTEPH
1-palmitoyl-GPC (16:0)	Lysolipid	-0.86	-0.83	-0.64	-0.13	2.68E-01	1.04E-02	Iron therapy	1.62E-01	3.22E-07
1-stearoyl-GPC (18:0)	Lysolipid	-0.87	-0.78	-0.65	-0.01	1.74E-01	1.94E-01	PDE inhib.	2.59E-01	2.40E-08
arginine	Urea cycle; Arginine and Proline Metabolism	-0.84	-1.03	-0.73	-0.07	5.88E-01	8.44E-01	Prostanoids	5.45E-01	3.83E-05
behenoyl sphingomyelin (d18:1/22:0)*	Sphingolipid Metabolism	-0.59	-0.43	-0.45	0.15	6.12E-02	5.61E-01	Iron therapy	8.77E-01	7.54E-06
dehydroisoandrosterone sulfate (DHEA-S)	Steroid	-1.58	-1.54	-0.74	0.39	6.76E-02	7.08E-01	Statin	2.08E-01	1.42E-09
glycerate	Glycolysis, Gluconeogenesis, and Pyruvate Metabolism	-0.59	-0.84	-1.12	-0.47	6.62E-02	6.11E-01	Cardiac glycosides	3.64E-01	9.18E-02
histidine	Histidine Metabolism	-1.28	-1.42	-0.77	0.37	2.74E-01	4.34E-01	Cardiac glycosides	1.87E-01	1.16E-07
homoarginine	Urea cycle; Arginine and Proline Metabolism	-0.80	-1.06	-0.79	-0.07	7.38E-02	9.16E-01	BMI	5.11E-01	4.79E-04
oxalate (ethanedioate)	Ascorbate and Aldarate Metabolism	-0.42	-0.83	-0.98	-0.19	3.29E-01	1.68E-01	Age	3.68E-01	5.28E-02
palmitoylcholine	Fatty Acid Metabolism (Acyl Choline)	-0.74	-0.63	-0.81	-0.27	2.69E-01	2.50E-01	Statin	6.79E-01	1.13E-02
X - 11440	Unknown	-0.73	-0.89	-0.52	-0.12	2.81E-01	8.18E-02	CCBs	6.61E-01	7.39E-03
X - 15666	Unknown	-0.67	-1.00	-0.59	-0.48	3.91E-01	3.69E-01	Iron therapy	8.83E-01	7.01E-02
X - 24027	Unknown	-1.08	-0.86	-1.14	-1.45	1.06E-01	1.24E-01	Diuretics	6.76E-01	1.06E-02
X - 24831	Unknown	-0.82	-0.98	-0.79	-0.59	2.42E-01	2.64E-02	ERAs	9.43E-01	4.43E-02

Appendix Table 6.1 - Metabolites distinguishing CTEPH from healthy and disease controls. 87 metabolites that are significantly different between CTEPH and healthy controls in a discovery and validation cohort ($p<8.9e-5$) are shown. Mean values are given and the data is scaled to the healthy control group. Significance from linear regression is shown (p value), and for metabolites with $p>0.05$ in CTEPH HC linear regression, the significant confounder is shown. Significance is also shown for Mann Whitney U test between all CTEPH patients versus CTED and PE patients. *probable metabolite identity, but unconfirmed (see methods). DM, diabetes; GPC, glycerophosphocholine; HC, healthy controls; DC, disease controls; BMI, body mass index; CTED, chronic thromboembolic disease; PE, pulmonary embolism.